

# **Air Pollution**

edited by  
**Vanda Villanyi**

**SCIYO**

## **Air Pollution**

Edited by Vanda Villanyi

### **Published by Sciyo**

Janeza Trdine 9, 51000 Rijeka, Croatia

### **Copyright © 2010 Sciyo**

All chapters are Open Access articles distributed under the Creative Commons Non Commercial Share Alike Attribution 3.0 license, which permits to copy, distribute, transmit, and adapt the work in any medium, so long as the original work is properly cited. After this work has been published by Sciyo, authors have the right to republish it, in whole or part, in any publication of which they are the author, and to make other personal use of the work. Any republication, referencing or personal use of the work must explicitly identify the original source.

Statements and opinions expressed in the chapters are these of the individual contributors and not necessarily those of the editors or publisher. No responsibility is accepted for the accuracy of information contained in the published articles. The publisher assumes no responsibility for any damage or injury to persons or property arising out of the use of any materials, instructions, methods or ideas contained in the book.

**Publishing Process Manager** Ana Nikolic

**Technical Editor** Zeljko Debeljuh

**Cover Designer** Martina Sirotic

**Image Copyright** Aleksey Klints, 2010. Used under license from Shutterstock.com

First published September 2010

Printed in India

A free online edition of this book is available at [www.sciyo.com](http://www.sciyo.com)

Additional hard copies can be obtained from [publication@sciyo.com](mailto:publication@sciyo.com)

Air Pollution, Edited by Vanda Villanyi

p. cm.

ISBN 978-953-307-143-5

**SCIYO.COM**  
WHERE KNOWLEDGE IS FREE

**free** online editions of Sciyo  
Books, Journals and Videos can  
be found at **[www.sciyo.com](http://www.sciyo.com)**



# Contents

## **Preface VII**

- Chapter 1 **Communicating health impact of air pollution 1**  
Moshammer Hanns for the Aphekom team
- Chapter 2 **Impact of Conversion to Compact Fluorescent Lighting and other Energy Efficient Devices, on Greenhouse Gas Emissions 21**  
M. Ivanco, K. Waheer and B. W. Karney
- Chapter 3 **Importance of sources and components of particulate air pollution for cardio-pulmonary inflammatory responses 47**  
Schwarze PE, Totlandsdal AI, Herseth JI, Holme JA, Låg M, Refsnes M, Øvrevik J, Sandberg WJ and Bølling AK
- Chapter 4 **Polycyclic Aromatic Hydrocarbons in the Urban Atmosphere of Mexico City 75**  
Mugica Violeta, Torres Miguel, Salinas Erika, Gutiérrez Mirella and García Rocio
- Chapter 5 **Sources, Distribution and Toxicity of Polycyclic Aromatic Hydrocarbons (PAHs) in Particulate Matter 99**  
Byeong-Kyu Lee and Van Tuan Vu
- Chapter 6 **Air Pollutants, Their Integrated Impact on Forest Condition under Changing Climate in Lithuania 123**  
Algirdas Augustaitis
- Chapter 7 **Ozone pollution and its bioindication 153**  
Vanda Villányi, Boris Turk, Franc Batic and Zsolt Csintalan
- Chapter 8 **Biosystems for Air Protection 177**  
Krystyna Malińska and Magdalena Zabochnicka-Świątek
- Chapter 9 **Urban air pollution forecasting using artificial intelligence-based tools 195**  
Min Li and Md. Rafiul Hassan
- Chapter 10 **Artificial Neural Networks to Forecast Air Pollution 221**  
Eros Pasero and Luca Mesin

- Chapter 11 **Instrumentation and virtual library for air pollution monitoring** 241  
Marius Branzila
- Chapter 12 **Pulsed Discharge Plasma for Pollution Control** 265  
Douyan Wang, Takao Namihira and Hidenori Akiyama
- Chapter 13 **Air quality monitoring using CCD/ CMOS devices** 289  
K. L. Low, C. E. Joanna Tan, C. K. Sim, M. Z. Mat Jafri, K. Abdullah and H. S. Lim
- Chapter 14 **Novel Space Exploration Technique  
for Analysing Planetary Atmospheres** 303  
George Dekoulis
- Chapter 15 **Ambient air pollution, social inequalities and asthma exacerbation in  
Greater Strasbourg (France) metropolitan area: The PAISA study** 319  
D. Bard, O. Laurent, S. Havard, S. Deguen, G. Pedrono, L. Filleul, C. Segala, A.  
Lefranc, C. Schillinger and E. Rivière
- Chapter 16 **A new method for estimation of automobile fuel adulteration** 357  
Anil Kumar Gupta and R.K.Sharma

# Preface

Anthropogenic air pollution constitutes of many substances. Greenhouse gases absorb and reflect some of the infrared parts of solar radiation reflected from the earth surface thus causing the troposphere to be warmer. Among others, these substances are carbone-dioxide, water vapour, hydrogen oxides, nitrogen-oxides and methane. Beyond causing warming, most of these gases are poisonous to the Earth's biosphere. Besides greenhouse gases, there are a few more poisonous substances which have anthropogenic sources. Heavy metals, aromatic hydrocarbones, and dust are for example very harmful air pollutants. The problem of air pollution is very complex, and apparently this is the base of climate change on our globe. Air pollutants are also polluting the ground, waters and plantal surfaces by subsidence and aggregation.

Air pollution, as well as global warming, causes considerable biomass losses both in natural vegetations and in cultivated plants. Besides, these changes cause decrease in the quality of crops, and changes in biodiversity and species composition of natural vegetations. Climate change principally damages plant organisms, but it directly effects every member of the food chain harming animals and human beings as well.

Although the climate of the Earth is continually changing from the very beginning, anthropogenic effects, the pollution of the air by combustion and industrial activities make it change so quickly that the adaptation is very difficult for all living organisms. Researcher's role is to make this adaptation easier, to prepare humankind for new circumstances and challenges, to trace and predict the effects and, if possible, even decrease the harmfulness of these changes. In this book we provide an interdisciplinary collection of new studies and findings on the score of air pollution.

The first part consists of review-like studies, the second part contains writings that show the results of some new researches and gives a few case studies. Eventually, some astonishing new scientific innovations are introduced. For the reader we wish a pleasant and gainful time while getting acquainted with these interesting works.

Editor

**Vanda Villanyi**

*Szent István University, Institute of Botany and Ecophysiology, Gödöllő  
Hungary*



# Communicating health impact of air pollution

Moshammer Hanns for the Aphekom team<sup>1</sup>  
*Inst. Environmental Health, ZPH, Medical University of Vienna  
Austria*

## 1. Introduction

Adverse health effects of air pollution are well established mostly through epidemiological studies, although also toxicology is consistently accumulating findings as to the underlying mechanisms of these effects. Mostly, it seems, these mechanisms are not very specific: inflammatory processes and oxidative stress predominate. Some pollutants also have mutagenic properties making cancer also a plausible health endpoint of exposure to air pollution. But the long lags between exposure and final disease make epidemiological studies in this field very difficult, so direct epidemiological evidence for cancer effects of air pollution is rare. Nevertheless the few existing studies give a consistent and plausible picture. More importantly there are studies that rather than looking at ultimate disease investigate biological effects that might lead to cancer like DNA adducts or chromosome damage. So even for cancer epidemiological evidence is growing.

Several reviews have described the health effects of air pollution in more detail, namely reports by the World Health Organization (WHO 2000; 2005; 2006; 2007) and by the Health Effects Institute (HEI 2000; 2003; 2007; 2010). This chapter will not repeat these valuable and extensive summaries but is rather interested in the link between the scientific findings and policy implications. In fact policies do not deal with air pollution per se, but with specific sources of air pollution thus affecting the interests of several influential stakeholders. So from a policy perspective science is not only called to estimate the health effect of 'air pollution in general' but the health effects linked to a specific source of air pollution or more precisely a specific incremental change in pollutants production by that specific source.

Air pollution always consists of a whole range of pollutants, gaseous and particulate alike. Keeping in mind the little specificity of the air pollutants' toxicity it is not surprising that not one single pollutant alone accounts for the observed effects. Routine monitoring of air quality is usually restricted to some very few indicators (particulate mass and some gases like ozone, nitrogen oxides, sulphur oxide, and carbon monoxide). Simply because of data availability most epidemiological studies describe the association between those indicator pollutants and health risks. But that does not mean that other usually unmeasured pollutants (polycyclic aromatic hydrocarbons, volatile organic compounds, aldehydes, to name but a few) are not similarly relevant in terms of health effects. Particle mass itself is an indicator covering a whole range of particles differing in size, shape and chemical

---

<sup>1</sup> [www.aphekom.org](http://www.aphekom.org)

composition. Although the routine indicators of air quality have been shown to be generally good indicators of the overall air quality it cannot be expected that their health relevance is the same no matter what their very source is: particles from incineration processes (e.g. exhaust pipes of motor cars or industrial stacks) are certainly different from particles stemming from desert storms or from sea salt spray.

So policy is required not just to do some 'indicator variable cosmetic' but tackle those sources with the largest health relevance. Ideally it would not only be health effects of air pollutants that are mitigated by a successful policy. Take road traffic as an example: A successful policy would not only reduce air pollution but also noise, CO<sub>2</sub> and risk of accidents.

Thus source-specific effects of air pollution are one issue when science meets policy. Another equally challenging issue is the communication of scientific findings. Both health effects of air pollution and the costs of reducing air pollution are very emotional issues and science is not suited well to deal with emotions. Making things worse the talk is about 'risk' and the understanding of that word differs a lot between lay and scientific language. For a scientist 'risk' has a purely statistical meaning while a lay person is more interested in individual risk. In that case the term would include fear which is not so much associated with the statistical likelihood of an event but with (inter alia) its strangeness and severity. A 'good story' making an event more plausible in individual terms might make a risk more relevant while a perception of own control (even if misguided) will reduce the fear and thus the feeling of risk.

Even more importantly epidemiologists tend to talk about relative risks, and small relative risks indeed in the case of air pollution: Since everybody is exposed to air pollution to some extent it is not possible to describe the risk of exposure relative to non-exposure, but usually the relative risk of an incremental increase of exposure is given. Considering reasonable increases in exposure (e.g. per 10 µg/m<sup>3</sup> of fine particles, PM<sub>2.5</sub>) the incidence of some health effects might increase by a few percent or even less (depending on the averaging time of the exposure under study). For rare diseases increase in incidence (or prevalence) by a few percent is by no means much. An individual should not be deeply concerned about these additional risks, not only because these risks are small, but also because (s)he usually cannot do anything about it personally. So it might be seen as common logic that risks of that kind are usually disregarded by the general public. Nevertheless for the whole population even relatively rare diseases translate into a certain number of patients and any additional patient is an additional burden to society and the health care system, not to speak about individual hardships. These individual patients will never be proved to be caused by air pollution. The unspecific nature of the pollutants' effects makes it impossible to discern the individual causes. Nevertheless there are a number of additional cases of disease and death that could have been prevented but for the totally involuntary exposure to air pollution. Since practically everybody is exposed to air pollution also small relative risks translate into a surprisingly large number of additional 'cases'.

So science faces the task to explain small individual risks that still are relevant for society. Ideally this explanation should not end at 'air pollution per se' but should strive to discern different sources of air pollution. The latter is not only difficult because of the complex mixture of pollutants originating from each individual source but also because there is a long way from the pollution source to the population exposure where not only the chemical composition of the pollution mixture at the source must be considered but also chemical fate and distribution on its way to the noses of the people. This indeed calls for some interdisciplinary efforts.

## 2. The concepts of causality

Aristotle discerned four kinds of causes, where his term of "cause" (Greek *aitia*) had a broader meaning than today's "cause": Thus "*causa materialis*" and "*causa formalis*" describe a thing (by its material substance and its form) while the latter two "causes" are more in line with the modern meaning. It seems noteworthy that only the "*causa efficiens*" resembles the modern concept of a cause preceding the effect ("*poster hoc ergo propter hoc*") while the concept of "*causa finalis*" is usually not used in natural sciences. Nevertheless in social sciences it is well established that also goals (i.e. intended future events) strongly influence current events. Life sciences are positioned in the grey zone between natural and social sciences. Therefore it is not surprising that biological mechanisms could be described either by the concept of "*causa efficiens*" or of "*causa finalis*". While it is just and common belief that each process in life has at least one preceding cause because of the complexity of most causal chains and networks it is often more straightforward and easier to understand and memorise mechanisms that are described in relation to their intended goal. For example inflammation could be explained by describing all the cytokines and mediating substances involved or it could be described as a mechanism shaped to clean the organism from unwanted material like microbes or noxious chemicals. The latter explanation makes it easier to understand the importance but also the possible harmful effects of such a process. Often this is more relevant for an understanding that can inform reasonable intervention. Nevertheless in this paper "cause" is understood in its natural science meaning.

In formal logics simple causal chains can be constructed like "A causes B, B causes C, etc." but in real world settings causality is often more complex like "A, B, and C cause D which in turn causes E and F and prevents G and H which again in turn exact an influence on A, B or C". Thus we might have complex positive or negative feedback loops and often we even have no means to know or monitor the true underlying causes of an event but are restricted to proxy data that are only somehow related to or associated with the truly causal factor. In theory natural scientists formulate hypotheses that can be falsified. But at least in the complex world of life sciences neither "proof" nor falsification are easy tasks. More often collected data only can render hypotheses more or less plausible. As a consequence "causality" in life sciences tends to be a fuzzier term than in physics.

In their very enlightening book Rifkin & Bouwer (2008) propose the "Risk Characterisation Theatre" to illustrate risks. "If there were 1,000 people sitting in a theatre with significantly elevated cholesterol levels of 280 mg, there will be one additional death per year from coronary heart disease as compared to 1,000 people with normal cholesterol." Even more impressive is their example concerning benefits of colorectal cancer screening: "If there were 1,000 people sitting in a theatre who had colorectal cancer screening, there will be one cancer prevented over a life time as compared to 1,000 people not screened." This statement is striking considering modern theatre: were people seated there over a life time they would rather die of boredom than of colon cancer.

Apart from these entertaining examples clearly indicating that absolute risks are more relevant and meaningful to us than relative risks the authors also introduce a second term in addition to "cause". In chapter two they set out to explain the differences between "cause and effect" versus "risk factors" but in my mind they completely fail to succeed. Their first example for a "risk factor" is a "lump in the breast detected in a mammogram". This they declare to be a "risk factor" (and evidently not a cause) for breast cancer. "There is no cause and effect relationship because the presence of a lump is not always associated with cancer."

Now this is interesting! Following this line of argumentation smoking would not be causally linked with lung cancer because it does not always lead to that outcome. Or even shooting a person would not be causally linked to his or her death because a bullet not always leads to it. While I agree that a "lump in the breast" is not the cause of breast cancer (rather the other way round!) I also do not consider a lump as a risk factor, only as a symptom! In fact the authors are not very clear regarding their distinction between "cause" and "risk factor". Maybe they just have the feeling that a "cause" is a rather strong risk factor. But since they question the validity of relative risks and do not give a threshold in terms of absolute risks to discern between "cause" and "risk factor" their terminology remains obscure. Sometimes it seems they understand by "cause" an event that practically always leads to an effect but even for the examples they give this is usually not the case. Alternatively they might mean by "cause" an event that practically always precedes an effect. The typical example would be infectious diseases: Tuberculosis is always caused by mycobacteria. But in fact this statement is rather a tautology because tuberculosis is defined as being caused by mycobacteria. Tuberculosis can take many forms from acute to chronic pneumonia, inflammation of practically every body part, silent knot or scar in the lung tissue, caverns in the lung or septicaemic disease. Often only when we detect mycobacteria (or at least an immune response against these bacteria) do we diagnose tuberculosis. Pneumonia is not always caused by mycobacteria and mycobacteria not always cause pneumonia. In fact many people have been exposed to mycobacteria and only few of them have developed any kind of disease at all.

The so-called Koch's postulates<sup>2</sup> that were first proposed by Henle and then by Koch (1884) but coined as a term by Koch's pupil Loeffler are often seen as criteria of causality (Evans, 1976) and even are revoked with new emerging concepts of infectious disease (Walker et al., 2006; Falkow, 1988). But even Koch himself was aware that these were rather a description of the microbiology methods of his times and no criteria of causation. The misconception of the postulates stipulating causation indeed hindered for some time the wide acceptance of viruses as infectious agents.

Looking at the postulates without prejudice rather provokes the idea that microbiology lacks good proofs of causality at least regarding individual cases. The only fact the postulates help to establish is the ability, not the necessity of any bacterial strain to cause a certain disease.

Unfortunately with environmental epidemiology the situation is not much better (Kundi, 2006). Here the so-called "Bradford-Hill criteria"<sup>3</sup> are widely supposed to indicate causation.

---

2 Koch's postulates are:

1. The microorganism must be found in abundance in all organisms suffering from the disease, but should not be found in healthy animals.
2. The microorganism must be isolated from a diseased organism and grown in pure culture.
3. The cultured microorganism should cause disease when introduced into a healthy organism.
4. The microorganism must be reisolated from the inoculated, diseased experimental host and identified as being identical to the original specific causative agent.

3 Hill's criteria are:

1. Strength: A small association does not mean that there is not a causal effect.
2. Consistency: Consistent findings observed by different persons in different places with different samples strengthen the likelihood of an effect.

Just by calling them "criteria" makes them seem like a "check-list" (Phillips and Goodman, 2004), but this was not Bradford Hill's intention. In his seminal presentation (1965) he explicitly stated: "None of my nine viewpoints can bring indisputable evidence for or against the cause-and-effect hypothesis and none can be required sine qua non".

Comparing infectious with "environmental" diseases (like those caused by air pollution) is not so far fetched. In fact it is known that only rarely a single bacterium causes a disease. This led to postulating the "infectious dose", the minimal amount of bacteria that are necessary to trigger a disease. But microbiologists soon discovered that this is not so easy: apart from "factors of virulence" of the bacteria there are also susceptibility factors of the host. Indeed it was shown that co-exposure of bacteria and air pollutants increase the likelihood of an infectious disease: the damaged mucous membranes of the airways are more susceptible to the attack of germs. So what causes the disease? Most people would answer: "the germ, because we always find germs when there is an infection!" I could easily respond: "I checked it and I always found air pollution!"

I do not believe that finding germs establishes their causal role. What indeed does is therapeutic success: We are willing to accept those factors as "causal" which we can successfully influence. When I sit in a tram and a person besides me coughs or sneezes I automatically try to hold my breath until the germ bearing plume has settled. When I walk on the kerbside and a lorry passes by I try to do the same. Asthmatics could react to health warnings on high pollution days (Wen et al, 2009). Here the similarities between (chemical) air pollutants and infectious agents end: I have no antibiotics, no vaccination, no quarantine measures to offer to fight health effects of air pollution. It has been shown that good pharmacotherapy of asthma also mitigates exacerbations caused by air pollution (Song et al., 2009; Gilliland et al., 2009; Qian et al., 2009a; Trenga et al., 2006. But see also Quian et al., 2009b). But this is not a therapy against air pollution - it is simply good asthma therapy.

The individual doctor with her individual patient will not tackle air pollution, hence air pollution is outside her scope. But as a society we can really do something about air pollution while we are not very successful in fighting infectious agents: We have until now only conquered smallpox and polio might follow soon. In the meantime a whole bunch of new deadly viruses has been detected. Everywhere where people meet or come in contact with animals or even besides that, there is a risk of infection. Contrary to that our western civilisation was fairly successful in reducing air pollution. Indeed it was not until pollution levels were considerably reduced that epidemiologists were able to show that even low levels previously considered "safe" had in fact still an adverse effect on health.

---

3. Specificity: Causation is likely if a very specific population at a specific site and disease with no other likely explanation. The more specific an association between a factor and an effect is, the bigger the probability of a causal relationship.

4. Temporality: The effect has to occur after the cause (and if there is an expected delay between the cause and expected effect, then the effect must occur after that delay).

5. Biological gradient: Greater exposure should generally lead to greater incidence of the effect. However, in some cases, the mere presence of the factor can trigger the effect.

6. Plausibility: A plausible mechanism between cause and effect is helpful.

7. Coherence: Coherence between epidemiological and laboratory findings increases the likelihood of an effect.

8. Experimental evidence.

9. Analogy: The effect of similar factors may be considered.

I therefore hold that as a society we should more seriously consider air pollution as cause of disease. But health-policy makers usually fail to make health-policy but rather engage in disease management. Their experts usually are learned doctors (if policy-makers do indeed ask experts) who know how to treat individual disease or have studied the economy of the healthcare system. "Environment" is usually out of the scope of both.

### 3. The proof of the pudding

"The proof of the pudding is in the eating", is an old proverb. The most suggestive proof of the causal effects of air pollution on health is the beneficial effect of air pollution reduction (Renzetti et al., 2009). Be it the unintended side effect of a year long strike at a steel plant (Ghio & Delvin, 2001; Dye J et al., 2001; Pope et al., 1989) or of the short term improvements in air pollution due to a special transport scheme with restrictions of private cars during the Olympic Games in Atlanta (Friedman et al., 2001) or in Beijing (Wu et al., 2010) or during the 2002 summer Asian games in Busan (Lee et al., 2007). Even more impressive are the effects of specific measures with a lasting impact like the ban of coal sales in Dublin (Clancy et al., 2002) or in other Irish towns (Rich et al., 2009). The same holds true for the reduction of sulphur in fuels in Hong Kong (Hedley et al., 2002).

It is more difficult to show the benefit of gradually improving air quality that was seen over the last decades in many developed countries due to continuous technology improvements. A single measure that induces a significant improvement of air quality at once leads to a reduction in daily deaths. But fewer deaths in the short run will just make the age distribution of the population shift thus increasing that part of the population with the highest risk of dying. So in the long run daily death counts will not change: Everybody is bound to die exactly once. Therefore with gradually improving air quality no telling changes in daily mortality will be seen. We expect an increase in average life expectancy which indeed is the case in many countries. But two parallel trends like those of air quality and life expectancy are no proof of causal association. Indeed there are likely many causes of the increasing life expectancy and air quality is maybe not its most important cause.

It is reasonable to assume that death from air pollution will not affect all people equally. There are bound to be susceptibility factors like diabetes (Jacobs et al., 2010) but many are only partly understood by now and even include socio-economic factors (Barcelo et al., 2009). Improvements in air quality will therefore at the foremost increase the life expectancy of that group of people who are most susceptible towards air pollution. So we might expect that this group will increase in number relative to the whole population. In that case we would expect a steeper dose-response slope for air pollution and mortality with overall improving air quality. Indeed Shin et al. (2008) clearly showed this trend for Canada and nitrogen dioxide (NO<sub>2</sub>) although they failed to interpret their finding as an indication of a beneficial effect of reduced NO<sub>2</sub> levels.

### 4. Relative risks

Relative risks get increasingly criticised (Poole, 2010; Kaufman, 2010). But a high relative risk certainly is convincing. Consider a very rare disease, say, that occurs in one person only in every 100,000. Your doctor might not have seen this disease once and certainly not more often in her whole professional life. Then consider a group of people, say 500 workers in a

special industrial plant, and of these five develop this disease: one in hundred, or a relative risk of 1000:1 (1:100/1:100,000)! That does tell us something, doesn't it? There must be an exposure in this plant that poses a very strong risk factor. This is really bad news for the 500 employees. But still for them it does not mean certain doom, only a one in hundred risk. Now consider a frequent disease like arteriosclerosis. One in three might develop it. And consider an agent we are all to a higher or lesser degree exposed to, like air pollution and the relative risk is negligible! Maybe RR is 1.01 (a one percent increase) or even less. No doctor will realise when she suddenly has one percent more patients with this diagnosis among her clients: She might have seen 10 of them each day. Now she sees one more every tenth day. Yet in each population of 1000 you would have approximately 3 additional cases, and we are not talking about small groups of 1000 people only but about all citizens of your country! So with this tiny relative risk we end up with many more affected people than with the huge risk and the 5 workers at the one industrial plant.

Frequent diseases usually are frequent because they do have multiple causes. So each cause will only contribute a small percentage to the disease. This makes recognising the cause a difficult task. But if the cause is widespread it still can mean a relevant number of additional diseases. This exactly is the case with air pollution.

## 5. Duration of exposure

We are always exposed to air and the air is never free of pollutants. Hence we are always exposed to air pollution. Nevertheless it might be different if we are exposed to an episode of very high pollution for a rather short time or if we are exposed to a lower concentration for a longer period (even so that the dose, which is the concentration multiplied by time, is the same). Analysing short or long term exposures calls for different study concepts.

For short exposures and acute effects two concepts are broadly used. The first is the panel study: you select a group of volunteers that, as they live on, are exposed to ever changing concentrations of air pollutants that you are somehow able to monitor. These volunteers undergo repeated medical check-ups like lung function testing or analysis of inflammatory or cardiovascular markers. By analysing your data you can investigate the effect of short term changes of air pollution on the selected health parameters. This approach allows you a deeper insight in the influences of biological mechanisms even before the outbreak of overt disease. But when you are interested in disease outcome you must keep in mind the small relative risks you might expect. Therefore you need large numbers of people and long observation periods for meaningful statistics. This is the realm of time series studies: These can rely mostly on public data. A person that has diabetes today will likely have diabetes tomorrow. She who smokes today will likely be a smoker tomorrow. He who lives in a poor crowded area today will usually do so tomorrow. All these individual factors therefore will not confound the effects of day-to-day variation in air pollution. Therefore you can use public data like daily mortality rate or hospital admissions as a health outcome. Also daily air pollution is available from urban monitoring networks. Only factors that also change on a temporal scale can confound the association and must be taken into account: season, weather, influenza epidemics, holidays and weekends. Weather and season are very likely confounders because they both affect health and air pollution levels, but they can easily be controlled for. On weekends consistently fewer deaths are reported. This might partly be a spurious finding when deaths on Sunday are only discovered and/or reported on Monday.

But certainly there is also a true beneficial weekend effect. This is noteworthy because contrary to weather and season the weekend is not a natural phenomenon but a purely societal construct: It is the very way we organise our society that has a measurable effect on health! Maybe this information is already relevant for health policy: It does not matter so much if the final mechanism that makes workdays more dangerous is via societal stress, via noise, via air pollution (which is indeed lower on weekends), or via any other unknown route. It might be scientifically rewarding to disentangle the very contribution of air pollution. But for policy it is already important to know that "something" is wrong with the way we design our working days.

A typical outcome of time series studies on air pollution and mortality is "additional deaths per day per a certain change in air pollution concentration". For  $10 \mu\text{g}/\text{m}^3$  of fine particles (PM<sub>2.5</sub>) this is in the magnitude of approximately 1%. Cohort studies, that analyse the impact of long term air pollution exposure, produce a different outcome. To study long term exposure you cannot rely on day-to-day changes in air pollution but you must compare the health and fate of people that are continuously exposed to different levels of air pollution on average. A sensible choice would be to compare inhabitants of two (or more) cities with different average air pollution. The inhabitants of each city with certain characteristics (e.g. you could select people according to age group) are seen as a "cohort" (hence the name of the study concept), i.e. a group of people defined by common characteristics and an exposure level. Your interest lies in the fate of each cohort: do they differ in disease or mortality risk? So in mortality studies your outcome would not be (daily) counts of deaths but percentages of deaths per age-group and year, i.e. annual rates instead of daily counts. With the help of population tables you could easily translate differences of rates into differences of average life expectancy. This you cannot do with daily counts, because you do not know if a death prevented today leads to only a few additional days or to many more years of life.

Cohort studies are much more demanding than are time series analyses: When comparing different groups (cohorts) of people every characteristic that differs between the cohorts might confound the effects. So you must strive to collect as many data that are relevant to life expectancy as possible about all members of each cohort. These include age and sex, smoking behaviour, pre-existing disease status, job categories, educational and socio-economic status, and many others. And still you cannot be sure that you have covered all possible confounding factors.

This is why cohort studies are rarer than time series. Nevertheless they find stronger effects: With time series a  $10 \mu\text{g}/\text{m}^3$  change of PM<sub>2.5</sub> led to an approximately 1 % change in risk, with cohort studies this would typically be around 10%. So it is encouraging to see that when you do time series studies and you look at increasingly longer exposure periods, e.g. look at the effects of same or previous day pollutants, then at effects of average pollution over the previous 2, 3, 4 days or 1 to 4 weeks you will usually find that the longer the averaging period the stronger the effect. This does lend additional support to the stronger findings of cohort studies.

The general concept states that one must be seriously ill to acutely die from an air pollution episode. But long exposure causes additional disease thus increasing the number of people at a high risk of death. Mechanisms of disease generation involve inflammatory processes (Jacobs et al., 2010; Flamant-Hulin et al., 2010; Thompson et al., 2010; Strak et al., 2010; Hildebrandt et al., 2009; Panasevich et al., 2009; Hoffmann et al., 2009), oxidative stress (Kang et al., 2010; Sawyer et al., 2010), mutagenicity of some air pollutants, and autonomic regulation of the cardiovascular system (Franchini & Mannucci, 2009).

## 6. Source specific effects

Linking pollutants' effects to certain sources has been done by source apportionment (Sarnat et al., 2008; Watson et al., 2008; Andersen et al., 2007; Ilacqua et al., 2007; Kim & Hopke, 2007; Grahame & Hidy, 2007; Chen et al., 2007; Brook et al., 2007; Zheng et al., 2007) through chemical tracers (Moreno et al., 2009; Patel et al., 2009, Delfino et al., 2009; Lin et al., 2010; Kleeman et al., 2009; Hwang et al., 2008; John et al., 2007; Seagrave et al., 2006; Grahame & Hidy, 2004) or GIS methods (Vienneau et al., 2009; Aguilera et al., 2009), making use of dispersion models (Jacquemin et al., 2009; Kostrzewa et al., 2009), land use regression techniques (Karr et al., 2009; Su et al., 2009), Bayesian structural equation models (Nikolovet al., 2007) or principal components analysis (McNabola et al., 2009; Sanchez et al., 2008).

Not all approaches are equally convincing. Morgan et al. (2010) set out to study the effect of bushfire smoke in Sydney, Australia. In this town fine particle concentrations (PM<sub>10</sub>) are usually low and only high on bushfire days. So they performed two different time series on daily mortality: one on high pollution days, and one on "normal" days. They found that the per 10 µg/m<sup>3</sup> increase in daily deaths was stronger during "normal days" and concluded that PM<sub>10</sub> from bushfire is less harmful than the usual urban PM mix. But the not so steep slope at higher concentrations could well be due to a saturation effect that leads to a non-linear dose response curve and has nothing to do with the source of the pollutants.

Many different sources of air pollution have been investigated as causes of adverse health effects. These include, among others, municipal waste incinerators (Goria et al., 2009), residential heating (Junninen et al., 2009) and especially wood smoke (Karr et al., 2009; Naeher et al., 2007), local point sources (Karr et al., 2009) and even desert sand (Perez et al., 2008; Sandstrom & Forsberg, 2008; Shinn et al., 2003). But more than any other sources road transport has been linked to adverse health effects (Adar and Kaufman, 2007; Fan et al., 2009; Brunekreef et al., 2009; Rosenlund et al., 2009; Migliore et al., 2009; Hart et al., 2009; Delfino et al., 2009; Aguilera et al., 2009; Perez et al., 2009a; Perez et al., 2009b; Kramer et al., 2009; Kunzli et al., 2009; Tonne et al., 2009; Ranft et al., 2009; Pedersen et al., 2009; Ryan et al., 2009; Eisner et al., 2009; Gent et al., 2009; Ho et al., 2010). Only few studies (e.g. Pujades-Rodriguez et al., 2009) could not confirm this association. In these and many more studies exposure to road transport has been estimated by considering current home or school address or a history of past home addresses. For these addresses exposure was assessed using proxies like distance to next busy road, number of vehicles per day on the road next to the home, or a combination of both, or more advanced models also taking wind direction etc. into account. Various health endpoints were investigated. Therefore in spite of the impressive list of studies even for road traffic derived air pollution some more research is needed before firm conclusions as to the underlying sources and effects can be drawn and reliable dose-effect relations can be described. Regarding the sources it still is not clear which exhaust-pipe emissions are the main culprits nor to what extent other transport-related emissions including noise and mechanically generated particles like tire or brake wear or re-suspended road dust contribute to the various effects. This makes it difficult to estimate the relative impact of any specific technical measure like a filter or an innovative propulsion technique. What can be recommended clearly and without hesitation is to generally reduce road traffic in inhabited (urban) areas and/or not to place sensitive exposure groups (like children through kindergartens or schools) near busy roads.

The knowledge base is much less advanced for other sources of air pollution where there are only few studies for each specific source and exposure situation often varies fundamentally

according to specific local circumstances like meteorological conditions or the exact technical specification of the very source: not one power plant or one waste incinerator is exactly the same as the others.

## 7. The phrasing of the message

Telling policy makers and the public what to do is not easy for many reasons. First of all scientists do not want to tell others “what to do” but their first goal is to get additional funds to carry on their interesting research. Secondly, policy makers, media people, and the general public do not want to hear what scientists have to tell but what fits their current interests. Third, as we have seen above, there is still not a clear-cut message regarding specific sources and measures: Evidence based measures are bound to be based on a cost-benefit analysis. But as long as the benefits cannot be quantified for lack of source and measure specific dose-response functions we are still a far way off the mark.

Fourth, when it comes to cost-benefit statements, these are outside the narrow scope of environmental health science. Comparing benefits and costs intrinsically necessitates the monetary valuation of health benefits. But deciding on the value of reduced health risks is the task of society, not of scientists. Scientists are burdened with the task of explaining the magnitude of the risks (even including the uncertainties linked to this magnitude estimate) in an understandable, meaningful and correct way.

The European Public Health Project “Aphekom” (<http://www.aphekom.org>) set out to (among other things) clarify the public's information needs: “What would be the best metric to explain the health impact of air pollution?” was just one of the questions a panel of air pollution scientists were asked at the Aphekom symposium during the ISEE conference in Dublin (Medina et al., 2009). Death is the most emotional outcome of air pollution. So not surprisingly much of the discussion centred on the question how changes in mortality risk were best described. There is a long ongoing debate whether “number of deaths” or “changes on life expectancy” or even “disability adjusted life expectancy” would be the better metric (Brunekreef and Hoek, 2000).

At that workshop Bert Brunekreef again explained his position: *“It is methodologically more correct to express the effects in the terms of disability adjusted life years and life expectancy rather than numbers of deaths or numbers of cases. But still we tend to think that the media and the public want to hear the numbers rather than the years of life lost.*

*But when I teach about these issues I use to start my presentation with a very simple question to the audience: What matters more to you, what you're going to die from eventually or how many years you're going to live in reasonably good health? And no audience so far said that they want to know what they are going to die from, they are much more interested in how long they're going to live in a reasonably good health.”*

Christophe Declercq mostly agreed with that position: *“At the population level, the number of attributable cases by year is only an approximation. If the level of particulate matter decreases, age-specific mortality rates of the exposed population will decrease. In the long term, the age structure will change as people will live longer. This will cause the mortality rates and the number of deaths by year to increase again. Therefore, from a theoretical point of view, the gain in life expectancy is a better metric than the number of attributable cases. This is true in the long term, fifty years or so, but for the next years to come, attributable cases can still be a useful approximation if it is simpler to communicate.”*

Joel Schwartz strongly disagreed with the position that “years of life lost” is better than “number of deaths”: *“First of all, individual people would like to know how long they’re going to live but we can’t tell them that at all. We can tell them that an intervention that lowers air pollution changes average life expectancy but might not change theirs or might change it a lot more than average, so that’s not anything that we can tell them. What can we tell them, what is the product that we’re offering to sell them if society diverts some resources into pollution prevention? We can tell them that their risk goes down and there is a large and extensive literature on how people value reductions to risk. And that literature is uniformly reporting that years of life lost is not the metric that people value! The evidence of that is as strong as the evidence that cigarettes smoking causes lung cancer.*

*If years of life lost were the metric which people value reductions in risk then one would expect a roughly linear decline in the bid with the age of the participants because 80 year-olds are not going to increase their life expectancy by nearly as much as 40 year-olds by this constant 1 in 10,000 reduction in risk each year. And so that’s an empirically testable hypothesis and there was absolutely no association between what people were willing to pay and their age, in none of several studies done in the US, in Canada, in the UK.”*

Now I neither know what I would pay to get a certain percentage risk reduction nor what I would be willing to do for an additional year of life. I can understand “ten additional deaths” in a month or in a year in a certain population. I do not understand what a reduction in life expectancy by a few weeks or months means: Even if it were my personal life expectancy: I’d not so much want to know how much longer or shorter I live, but what will be the exact duration. Reducing my life expectancy by 3 weeks could mean I have to die tomorrow or in 40 years. So it is no meaningful information for me! Likewise it is not surprising that media and the public love “the numbers”. In the same workshop Marco Martuzzi gave an example that even the “wrong” numbers are nearly as good: *“We estimated the deaths attributed to air pollution for the main Italian cities and came up with unusually large numbers which activated some debate. This was quite influential at the national level and mobilized a number of people.*

*However some time later we were also invited by one of the cities. They had a heated debate regarding stricter measures for air pollution control and there was a tense situation with citizens and NGOs on one side and the local authorities on the other and we were asked to go there and present and discuss our study results. We arrived there and the situation was indeed quite tense and on the day of the event there had been headlines on the local papers saying: 50 deaths per year attributable to air pollution! In the heated discussion some said this is totally intolerable while others argued that compared to smoking this would be a very small and absolutely acceptable impact. After a while we were able to speak and to point out that they had got it wrong: it was 500, not 50 deaths per year! There was a moment of void but in the end nothing changed! The debate went on exactly the same!”*

So if the numbers really seem to be meaningless it is no wonder that Christophe Declercq argued for new aspects in communication: *“I see the problem in the translation from the population level to the individual level. When you talk to the press or to the general public, and mention a number of attributable deaths, they will ask who are the victims. But we cannot answer to this question yet. But this question is not a bad question though. We know that there are inequalities in exposure to air pollution, which is higher for example in people living in proximity to the traffic, Some studies also suggest inequalities in the health effects of air pollution, and that this differential vulnerability is linked to the social status of the exposed population. So air pollution exposure and effects contribute to social inequalities in health. We need more research in this area, but what we already know should urge us to go beyond a summary indicator of health impact of air pollution, be it*

*number of attributable cases or life expectancy. If we want to assess benefits of air pollution public policies, we should also check that the more exposed and the more vulnerable part of the population gets larger benefits in terms of air quality and health."*

Also Nino Künzli, who was one of the first to embark on the health impact assessment of air pollution (Künzli et al., 2000), warned against a too narrow look at mortality effects. But first he looked back to his seminal paper: *"The derivation and the communication of risks based on epidemiological research has a long tradition and if we take the example of smoking it has not even been much debated how we do that and how we communicate that. Such billboards are shown all over the world to communicate to people how many deaths are attributable to smoking. These numbers are simply estimates of attributable risks taking the association between smoking and death and the prevalence of smoking into account.*

*Some 10 years ago we applied these methods to answer a hot question asked by the ministers of health and environment of France, Austria and Switzerland: what is the health impact and what are the costs that can be attributed to ambient air pollution?*

*While I do not consider this my most important paper it became indeed the most cited one of all I wrote so far. And why that? Because of the numbers of attributable deaths, we estimated 40,000 attributable deaths per year due to air pollution. These numbers more than any other result in this same paper kept the world media quite busy and interested for years."*

After also discussing "years of life lost" (the more accurate metric) and "number of deaths" (the more intuitive metric) he went on with – what he called – a provocative statement: *"No matter what we use – either attributable deaths or years of life lost – we mislead and we distract from the relevant issues. Why that?*

*Let me explain this with the lifetime model of the development of chronic states, of chronic diseases which of course increase with age. Mortality – be it expressed as numbers or years – comes only at the very end after the development of all these chronic pathologies. The state of health however is what matters. It is the timing of this lifetime period that matters. It is health that matters and it is health or the reduced health that ultimately determines our life time and our life expectancy.*

*We are exposed over life time and this exposure entertains the development of chronic pathologies leading to lots of morbidities during life time and ultimately to premature death. We should invest far more in communicating that part of the air pollution related adverse effects.*

*However, to focus the risk assessment on morbidity requires an expansion of our methodologies and an in-depth discussion with economists as well who continue to attach far higher monetary value to death. Also we all know that part of this money is virtual and we know that the morbidity is far less and less completely monetized and monetization is even based on different methodologies. So we should emphasize what happens during life prior to death but how should we do this in the risk assessment framework?"*

Nino Künzli went on to discuss the combined impact of long-term and acute exposure towards air pollution: chronic exposure is known to enhance or even cause arteriosclerosis (Hoffmann et al., 2007; Künzli et al., 2005; Sun et al., 2005). And if arteriosclerosis of the coronary arteries is present acute exposures can trigger myocardial infarction (Peters et al., 2001). Similar phenomena are observed with respiratory disease: Chronic and especially early life exposure increases the prevalence of asthma (McConnell et al., 2006). And asthmatics react to acute air pollution episodes with more and more severe asthma attacks. It is still a challenge to present this combined effect of chronic and acute exposures in health impact assessments (Künzli et al., 2008). This in fact is the job of Nino Künzli's work-package in the project Aphekom.

The symposium in Dublin clearly showed the interest of the ongoing work on this issue in the Aphekom project which focuses on the need to improve the communication efforts and to fine-tune the relevant messages for the needs of the various stakeholders.

## 8. Conclusion

Adverse health effects of air pollution are well established. Experimental toxicological studies have shed light on relevant mechanisms and epidemiological data inform on the population relevance and the magnitude of the effects under realistic exposure scenarios. More recent research set out to define susceptible population subgroups. This will allow answering the question “who are the victims?” This question is of high policy relevance, but even more important is the question who the culprits are. Regarding sources there is ample evidence that proximity to road traffic poses serious health risks but other sources of air pollution including natural and industrial sources are likely equally dangerous as the average air pollution mixture on a mass concentration basis of currently used pollutants indicators (NO<sub>2</sub>, PM2.5).

Research is ongoing to better define the impact of specific pollution sources and to better understand the effects of the whole pollution mixture as compared to a “pollutant-by-pollutant” approach (Dominici et al., 2010). This is already reflected by a shift also in the policy frameworks (Greenbaum & Shaikh, 2010). Nevertheless there is still a far way to go. But gaps in current knowledge should not serve as an excuse for non-action: Where measures to improve air quality are feasible public health advantages are so striking that any cost-benefit analysis even in the light of uncertainty clearly proves that action is superior to non-action. So acting is not a question of uncertainty of benefits. In-action is caused by the difficulties in understanding health impacts and assessing these in relation to other interests that might not be as pressing, but easier to understand. Also the pressure of strong interest groups is often more successful than health concerns.

Knowledge about culprits and victims empowers science to inform policy. But communicating small relative risks that render individual preventive measures less effective but still are relevant for the whole population is still a demanding task. The public wants and deserves clear and easily understandable answers. The reality might just be a trifle too complicated for that.

## 9. References

- Adar, S.D. & Kaufman, J.D. (2007). Cardiovascular disease and air pollutants: evaluating and improving epidemiological data implicating traffic exposure, *Inhalation Toxicology*, 19, Suppl 1, 135-149, ISSN: 0895-8378
- Aguilera, I. et al. (2009). Association between GIS-based exposure to urban air pollution during pregnancy and birth weight in the INMA Sabadell Cohort, *Environmental Health Perspectives*, 117, 8, 1322-1327, ISSN: 0091-6765
- Andersen, Z.J. et al. (2007). Ambient particle source apportionment and daily hospital admissions among children and elderly in Copenhagen, *J Expo Sci Environ Epidemiol*, 17, 7, 625-636, ISSN: 1559-0631

- Barcelo, M.A. et al. (2009). Spatial variability in mortality inequalities, socioeconomic deprivation, and air pollution in small areas of the Barcelona Metropolitan Region, Spain, *Science of the Total Environment*, 407, 21, 5501-5523, ISSN: 0048-9697
- Brook, J.R. et al. (2007). Assessing sources of PM<sub>2.5</sub> in cities influenced by regional transport, *Journal of Toxicology & Environmental Health Part A*, 70, 3-4, 191-199, ISSN: 1528-7394
- Brunekreef, B. & Hoek, G. (2000), Invited Commentary - Beyond the Body Count: Air Pollution and Death, *American Journal of Epidemiology*, 151, 5, 449-451, ISSN: 0002-9262
- Brunekreef, B. et al. (2007). The Brave New World of Lives Sacrificed and Saved, Deaths Attributed and Avoided, *Epidemiology*, 18, 6, 785-788, ISSN: 1044-3983
- Brunekreef, B. et al. (2009). Effects of long-term exposure to traffic-related air pollution on respiratory and cardiovascular mortality in the Netherlands: the NLCS-AIR study, *Research Report - Health Effects Institute*, 139, 5-71, ISSN: 1041-5505
- Chen, L.W. et al. (2007). Quantifying PM<sub>2.5</sub> source contributions for the San Joaquin Valley with multivariate receptor models, *Environmental Science & Technology* 41, 8, 2818-2826, ISSN: 0013-936X
- Clancy, L. et al. (2002). Effect of air-pollution control on death rates in Dublin, Ireland: an intervention study, *Lancet*, 36, 1210-1214, ISSN: 0140-6736
- Delfino, R.J. et al. (2009). Air pollution exposures and circulating biomarkers of effect in a susceptible population: clues to potential causal component mixtures and mechanisms, *Environmental Health Perspectives* 117, 8, 1232-1238, ISSN: 00916765
- Dominici, F. et al. (2010). Protecting human health from air pollution: shifting from a single-pollutant to a multipollutant approach, *Epidemiology*, 21, 2, 187-194, ISSN: 1044-3983
- Dye, J.A. et al. (2001). Acute Pulmonary Toxicity of Particulate Matter Filter Extracts in Rats: Coherence with Epidemiologic Studies in Utah Valley Residents, *Environmental Health Perspectives*, 109, Suppl 3, 395-403, ISSN: 0091-6765
- Eisner, A.D. et al. (2009). Establishing a link between vehicular PM sources and PM measurements in urban street canyons, *Journal of Environmental Monitoring*, 11, 12, 2146-2152, ISSN: 1464-0325
- Evans, A.S. (1976). Causation and disease: the Henle-Koch postulates revisited, *Yale J Biol Med*, 49, 2, 175-195, ISSN: 0044-0086
- Falkow, S. (1988). Molecular Koch's postulates applied to microbial pathogenicity, *Rev Infect Dis*, 10, Suppl 2, S274-S276, ISSN: 0162-0886
- Fan, Z.T. et al. (2009). Acute exposure to elevated PM<sub>2.5</sub> generated by traffic and cardiopulmonary health effects in healthy older adults, *Journal of Exposure Science & Environmental Epidemiology*, 19, 5, 525-533, ISSN: 1559-0631
- Flamant-Hulin, M. et al. (2010). Air pollution and increased levels of fractional exhaled nitric oxide in children with no history of airway damage, *J Toxicol Environ Health A*, 73, 4, 272-283, ISSN: 1528-7394
- Franchini, M. & Mannucci, P.M. (2009). Particulate air pollution and cardiovascular risk: short-term and long-term effects, *Semin Thromb Hemost*, 35, 7, 665-670, ISSN: 0094-6176
- Friedman, M.S. et al. (2001). Impact of changes in transportation and commuting behaviors during the 1996 Summer Olympic Games in Atlanta on air quality and childhood asthma, *Journal of the American Medical Association*, 285, 7, 897-905, ISSN: 00987484

- Gent, J.F. et al. (2009). Symptoms and medication use in children with asthma and traffic-related sources of fine particle pollution, *Environmental Health Perspectives*, 117, 7, 1168-1174, ISSN: 00916765
- Ghio, A.J. & Delvin, R.B. (2001). Inflammatory Lung Injury after Bronchial Instillation of Air Pollution Particles, *Am J Respir Crit Care Med*, 164, 704-708, ISSN: 1073-449X
- Gilliland, F.D. et al. (2009). Outdoor air pollution, genetic susceptibility, and asthma management: opportunities for intervention to reduce the burden of asthma, *Pediatrics*, 123, Suppl 3, S168-S173, ISSN: 0031-4005
- Goria, S. et al. (2009). Risk of cancer in the vicinity of municipal solid waste incinerators: importance of using a flexible modelling strategy, *International Journal of Health Geographics*, 8, 31, ISSN: 1476-072X
- Grahame, T. & Hidy, G. (2004). Using factor analysis to attribute health impacts to particulate pollution sources, *Inhalation Toxicology*, 16, Suppl 1, 143-152, ISSN: 0895-8378
- Grahame, T. & Hidy, G.M. (2007). Pinnacles and pitfalls for source apportionment of potential health effects from airborne particle exposure, *Inhalation Toxicology*, 19, 9, 727-744, ISSN: 0895-8378
- Greenbaum, D. & Shaikh, R. (2010). Commentary: First steps toward multipollutant science for air quality decisions, *Epidemiology*, 21, 2, 187-194, ISSN: 1044-3983
- Hart, J.E. et al. (2009). Exposure to traffic pollution and increased risk of rheumatoid arthritis, *Environmental Health Perspectives*, 117, 7, 1065-1069, ISSN: 00916765
- HEI Health Effects Institute (2000). Special report: Reanalysis of the Harvard Six Cities Study and the American Cancer Society Study of Particulate Air Pollution and Mortality: <http://pubs.healtheffects.org/view.php?id=6>
- HEI Health Effects Institute (2003). Special report: Revised Analyses of Time-Series Studies of Air Pollution and Health: <http://pubs.healtheffects.org/view.php?id=4>
- Health Effects Institute (2007). Special report 16: Mobile-Source Air Toxics: A Critical Review of the Literature on Exposure and Health Effects: <http://pubs.healtheffects.org/view.php?id=282>
- Health Effects Institute (2010). Special report 17: Traffic-Related Air Pollution: A Critical Review of the Literature on Emissions, Exposure, and Health Effects: <http://pubs.healtheffects.org/view.php?id=334>
- Hedley, A.J. et al. (2002). Cardiorespiratory and all-cause mortality after restrictions on sulphur content of fuel in Hong Kong: an intervention study, *Lancet* 360: 1646-1652, ISSN: 0140-6736
- Hildebrandt, K. et al. (2009). Short-term effects of air pollution: a panel study of blood markers in patients with chronic pulmonary disease, *Particle and Fibre Toxicology*, 26, 6-25, ISSN: 1743-8977
- Hill, A.B. (1965). The environment and disease: association or causation? *Proceedings of the Royal Society of Medicine*, 58, 295-300, ISSN: 0035-9157
- Ho, C.K. et al. (2010). Traffic air pollution and risk of death from bladder cancer in Taiwan using petrol station density as a pollutant indicator, *Journal of Toxicology & Environmental Health Part A*, 73, 1, 23-32, ISSN: 1528-7394
- Hoffmann, B. et al. (2007). Residential exposure to traffic is associated with coronary arteriosclerosis, *Circulation*, 116, 489-496, ISSN: 0009-7322

- Hoffmann, B. et al. (2009). Chronic residential exposure to particulate matter air pollution and systemic inflammatory markers, *Environmental Health Perspectives*, 117, 8, 1302-1308, ISSN: 0091-6765
- Hwang, I. et al. (2008). Source apportionment and spatial distributions of coarse particles during the Regional Air Pollution Study, *Environmental Science & Technology*, 42, 10, 3524-3530, ISSN: 0013-936X
- Ilacqua, V. et al. (2007). Source apportionment of population representative samples of PM(2.5) in three European cities using structural equation modelling, *Science of the Total Environment*, 384, 1-3, 77-92, ISSN: 0048-9697
- Jacobs, L. et al. (2010). Air pollution related prothrombotic changes in persons with diabetes, *Environmental Health Perspectives*, 118, 2, 191-196, ISSN: 0091-6765
- Jacquemin, B. et al. (2009). Association between modelled traffic-related air pollution and asthma score in the ECRHS, *European Respiratory Journal*, 34, 4, 834-842, ISSN: 0903-1936
- John, K. et al. (2007). Analysis of trace elements and ions in ambient fine particulate matter at three elementary schools in Ohio, *Journal of the Air & Waste Management Association*, 57, 4, 394-406, ISSN: 1047-3289
- Junninen, H. et al. (2009). Quantifying the impact of residential heating on the urban air quality in a typical European coal combustion region, *Environmental Science & Technology*, 43, 20, 7964-7970, ISSN: 0013-936X
- Kang, X. et al. (2010). Adjuvant effects of ambient particulate matter monitored by proteomics of bronchoalveolar lavage fluid, *Proteomics*, 10, 3, 520-531, ISSN: 1615-9853
- Karr, C.J. et al. (2009). Influence of ambient air pollutant sources on clinical encounters for infant bronchiolitis, *American Journal of Respiratory & Critical Care Medicine*, 180, 10, 995-1001, ISSN: 1073-449X
- Kaufman, J.S. (2010). Toward a More Disproportionate Epidemiology, *Epidemiology*, 21, 1, 1-2, ISSN: 1044-3983
- Kim, E. & Hopke, P.K. (2007). Source identifications of airborne fine particles using positive matrix factorization and U.S. Environmental Protection Agency positive matrix factorization, *Journal of the Air & Waste Management Association*, 57, 7, 811-819, ISSN: 1047-3289
- Kleeman, M.J. et al. (2009). Source apportionment of fine (PM1.8) and ultrafine (PM0.1) airborne particulate matter during a severe winter pollution episode, *Environmental Science & Technology*, 43, 2, 272-279, ISSN: 0013-936X
- Koch, R. (1884). Die Aetiologie der Tuberkulose, *Mitt Kaiser Gesundh*, 1884, 1-88
- Kostrzewa, A. et al. (2009). Validity of a traffic air pollutant dispersion model to assess exposure to fine particles, *Environmental Research*, 109, 6, 651-656, ISSN: 0013-9351
- Krämer, U. et al. (2009). Eczema, respiratory allergies, and traffic-related air pollution in birth cohorts from small-town areas, *Journal of Dermatological Science*, 56, 2, 99-105, ISSN: 0923-1811
- Kundi, M. (2006). Causality and the Interpretation of Epidemiologic Evidence, *Environmental Health Perspectives*, 114, 969-974, ISSN: 0091-6765
- Künzli, N. et al. (2000). Public-health impact of outdoor and traffic-related air pollution: a European assessment, *Lancet*, 356, 9232, 795-801, ISSN: 0140-6736

- Künzli, N. et al. (2005). Ambient air pollution and atherosclerosis in Los Angeles, *Environmental Health Perspectives*, 113, 201-206, ISSN: 0091-6765
- Künzli, N. et al. (2008). An Attributable Risk Model for Exposures Assumed to Cause Both Chronic Disease and its Exacerbations, *Epidemiology*, 19, 2, 179-185, ISSN: 1044-3983
- Künzli, N. et al. (2009). Traffic-related air pollution correlates with adult-onset asthma among never-smokers, *Thorax*, 64, 8, 664-670, ISSN: 0040-6376
- Lee, J.T. et al. (2007). Benefits of mitigated ambient air quality due to transportation control on childhood asthma hospitalization during the 2002 summer Asian games in Busan, Korea, *Journal of the Air & Waste Management Association*, 57, 8, 968-973, , ISSN: 1047-3289
- Lin, L. et al. (2010). Review of recent advances in detection of organic markers in fine particulate matter and their use for source apportionment, *Journal of the Air & Waste Management Association*, 60, 1, 3-25, ISSN: 1047-3289
- McConnell, R. et al. (2006). Traffic, susceptibility, and childhood asthma, *Environmental Health Perspectives*, 114, 766-772, ISSN: 0091-6765
- McNabola, A. et al. (2009). A principal components analysis of the factors effecting personal exposure to air pollution in urban commuters in Dublin, Ireland, *Journal of Environmental Science & Health Part A*, 44, 12, 1219-1226, ISSN: 1093-4529
- Medina, S. et al. (2009). Communicating Air Pollution and Health Research to Stakeholders. Aphekom Symposium for the 21st ISEE Conference in Dublin, Ireland. 2009/08/26. [http://www.aphekom.org/c/document\\_library/get\\_file?uuid=9dbc8f44-6447-4a08-b81a-56b351a1f7a3&groupId=10347](http://www.aphekom.org/c/document_library/get_file?uuid=9dbc8f44-6447-4a08-b81a-56b351a1f7a3&groupId=10347)
- Migliore, E. et al. (2009). Respiratory symptoms in children living near busy roads and their relationship to vehicular traffic: results of an Italian multicenter study (SIDRIA 2), *Environmental Health: A Global Access Science Source*, 8, 27, ISSN: 1476-069X
- Moreno, T. et al. (2009). Identification of chemical tracers in the characterisation and source apportionment of inhalable inorganic airborne particles: an overview, *Biomarkers*, 14, Suppl 1, 17-22, ISSN 1354-750X
- Morgan, G. et al. (2010). Effects of Bushfire Smoke on Daily Mortality and Hospital Admissions in Sydney, Australia, *Epidemiology*, 21,1, 47-55, ISSN: 1044-3983
- Naeher, L.P. et al. (2007). Woodsmoke Health Effects: A Review, *Inhalation Toxicology*, 19, 67-106, ISSN: 0895-8378
- Nikolov, M.C. et al. (2007). An informative Bayesian structural equation model to assess source-specific health effects of air pollution, *Biostatistics*, 8, 3, 609-624, ISSN 1465-4644
- Panasevich, S. (2009). Associations of long- and short-term air pollution exposure with markers of inflammation and coagulation in a population sample, *Occup Environ Med*, 66, 11, 747-753, ISSN: 1470-7926
- Patel, M.M. et al. (2009). Ambient metals, elemental carbon, and wheeze and cough in New York City children through 24 months of age, *American Journal of Respiratory & Critical Care Medicine*, 180, 11, 1107-1113, ISSN: 1073-449X
- Pedersen, M. et al. (2009). Increased micronuclei and bulky DNA adducts in cord blood after maternal exposures to traffic-related air pollution, *Environmental Research*, 109, 8, 1012-1020, ISSN: 0013-9351

- Perez, L. et al. (2009a). Global goods movement and the local burden of childhood asthma in southern California, *American Journal of Public Health*, 99, Suppl 3, S622-628, ISSN: 0090-0036
- Perez, L. et al. (2009b). Size fractionate particulate matter, vehicle traffic, and case-specific daily mortality in Barcelona, Spain, *Environmental Science & Technology*, 43, 13, 4707-4714, ISSN: 0013-936X
- Perez, L. et al. (2008). Coarse particles from Saharan dust and daily mortality, *Epidemiology*, 19, 6, 800-807 ISSN: 1044-3983
- Peters, A. et al. (2001). Increased particulate air pollution and the triggering of myocardial infarction, *Circulation*, 103, 2810-2815, ISSN: 0009-7322
- Phillips, C.V. & Karen J.G. (2004). The missed lessons of Sir Austin Bradford Hill, *Epidemiologic Perspectives and Innovations*, 1, 3, 3, ISSN: 1742-5573
- Poole, C. (2010). On the Origin of Risk Relativism, *Epidemiology*, 21, 1, 3-9, ISSN: 1044-3983
- Pope, C.A. III. (1989). Respiratory disease associated with community air pollution and a steel mill, Utah Valley, *Am J Public Health*, 79, 623-628, ISSN: 1541-0048
- Pujades-Rodriguez, M. (2009). Effect of living close to a main road on asthma, allergy, lung function and chronic obstructive pulmonary disease, *Occupational & Environmental Medicine*, 66, 10, 679-684, ISSN: 1351-0711
- Qian, Z. et al. (2009a). Associations between air pollution and peak expiratory flow among patients with persistent asthma, *J Toxicol Environ Health A*, 72, 1, 39-46, ISSN: 1528-7394
- Qian, Z. et al. (2009b): Interaction of ambient air pollution with asthma medication on exhaled nitric oxide among asthmatics, *Arch Environ Occup Health*, 64, 3, 168-176, ISSN: 1933-8244
- Ranft, U. et al. (2009). Long-term exposure to traffic-related particulate matter impairs cognitive function in the elderly, *Environmental Research*, 109, 8, 1004-1011, ISSN: 0013-9351
- Renzetti, G. et al. (2009). Less air pollution leads to rapid reduction of airway inflammation and improved airway function in asthmatic children, *Pediatrics*, 123, 3, 1051-1058, ISSN: 0031-4005
- Rich, D. et al. (2009). Effect of Air Pollution Control on Mortality in County Cork, Ireland, *Epidemiology*, 20, 6, S69, ISSN: 1044-3983
- Rifkin, E. & Bouwer, E. (2008). *The Illusion of Certainty*, Springer, ISBN-13: 978-0-387-75165-8, New York
- Rosenlund, M. et al. (2009). Traffic-related air pollution in relation to respiratory symptoms, allergic sensitisation and lung function in schoolchildren, *Thorax*, 64, 7, 573-580, ISSN: 0040-6376
- Ryan, P.H. et al. (2009). Exposure to traffic-related particles and endotoxin during infancy is associated with wheezing at age 3 years, *American Journal of Respiratory & Critical Care Medicine*, 180, 11, 1068-1075, ISSN: 1073-449X
- Sandstrom, T. & Forsberg B. (2008). Desert dust: an unrecognized source of dangerous air pollution? *Epidemiology*, 19, 6, 808-809, ISSN: 1044-3983
- Sarnat, J.A. et al. (2008). Fine particle sources and cardiorespiratory morbidity: an application of chemical mass balance and factor analytical source-apportionment methods, *Environmental Health Perspectives*, 116, 4, 459-466, ISSN: 00916765

- Sanchez, M. et al. (2008). Source characterization of volatile organic compounds affecting the air quality in a coastal urban area of South Texas, *International Journal of Environmental Research & Public Health*, 5, 3, 130-138, ISSN: 1660-4601
- Sawyer, K. et al. (2010). The effects of ambient particulate matter on human alveolar macrophage oxidative and inflammatory responses, *J Toxicol Environ Health A*, 73, 1, 41-57, ISSN: 1528-7394
- Seagrave, J. et al. (2006). Lung toxicity of ambient particulate matter from southeastern U.S. sites with different contributing sources: relationships between composition and effects, *Environmental Health Perspectives*, 114, 9, 1387-1393, ISSN: 00916765
- Shin, H.S. et al. (2008). A Temporal, Multicity Model to Estimate the Effects of Short-Term Exposure to Ambient Air Pollution on Health, *Environmental Health Perspectives*, 116, 1147-1153, ISSN: 00916765
- Shinn, E.A. et al. (2003). Atmospheric transport of mold spores in clouds of desert dust, *Archives of Environmental Health*, 58, 8, 498-504, ISSN: 0003-9896
- Song, D.J. et al. (2009). Environmental tobacco smoke exposure does not prevent corticosteroids reducing inflammation, remodeling, and airway hyperreactivity in mice exposed to allergen, *Am J Physiol Lung Cell Mol Physiol*, 297, 2, L380-L387, ISSN: 1040-0605
- Strak, M. et al. (2010). Respiratory health effects of ultrafine and fine particle exposure in cyclists, *Occup Environ Med*, 67, 2, 118-124, ISSN: 1076-2752
- Su, J.G. (2009). Predicting traffic-related air pollution in Los Angeles using a distance decay regression selection strategy, *Environmental Research*, 109, 6, 657-670, ISSN: 0013-9351
- Sun, Q. et al. (2005). Long-term air pollution exposure and acceleration of atherosclerosis and vascular inflammation in an animal model, *Journal of the American Medical Association*, 294, 3003-3010, ISSN: 0098-7484
- Thompson, A.M. et al. (2010). Baseline Repeated Measures from Controlled Human Exposure Studies: Associations between Ambient Air Pollution Exposure and the Systemic Inflammatory Biomarkers IL-6 and Fibrinogen, *Environmental Health Perspectives*, 118, 1, 120-124, ISSN: 0091-6765
- Tonne, C. et al. (2009). Traffic particles and occurrence of acute myocardial infarction: a case-control analysis, *Occupational & Environmental Medicine*, 66, 12, 797-804, ISSN: 1351-0711
- Trenga, C.A. et al. (2006). Effect of particulate air pollution on lung function in adult and pediatric subjects in a Seattle panel study, *Chest*, 129, 6, 1614-1622, ISSN: 0012-3692
- Vienneau, D. et al. (2009). A GIS-based method for modelling air pollution exposures across Europe, *Science of the Total Environment*, 408, 2, 255-266, ISSN: 0048-9697
- Walker, L et al. (2006). Koch's postulates and infectious proteins, *Acta Neuropathol*, 112, 1, 1-4, ISSN: 0001-6322
- Watson, J.G. et al. (2008). Source apportionment: findings from the U.S. Supersites Program., *Journal of the Air & Waste Management Association*, 58, 2, 265-288, ISSN: 1047-3289
- Wen, X.J. et al. (2009). Association between media alerts of air quality index and change of outdoor activity among adult asthma in six states, BRFSS, 2005, *J Community Health*, 34, 1, 40-46, ISSN: 0094-5145

- WHO World Health Organization, Regional Office for Europe (2000). Air quality guidelines for Europe, Second edition. WHO Regional Publications, European Series, No. 91: <http://www.euro.who.int/document/e71922.pdf>
- World Health Organization, Regional Office for Europe (2005). WHO air quality guidelines. Global update 2005. Report on a Working Group meeting, Bonn, Germany, 18-20 October 2005: <http://www.euro.who.int/Document/E87950.pdf>
- WHO World Health Organization (2006). WHO Air quality guidelines for particulate matter, ozone, nitrogen dioxide and sulfur dioxide. Global update 2005. Geneva: [http://whqlibdoc.who.int/hq/2006/WHO\\_SDE\\_PHE\\_OEH\\_06.02\\_eng.pdf](http://whqlibdoc.who.int/hq/2006/WHO_SDE_PHE_OEH_06.02_eng.pdf)
- WHO World Health Organization, Regional Office for Europe (2007). Health relevance of particulate matter from various sources. Report on a WHO Workshop. Bonn, Germany, 26-27 March 2007: <http://www.euro.who.int/Document/E90672.pdf>
- Wu, S. et al. (2010). Association of Heart Rate Variability in Taxi Drivers with Marked Changes in Particulate Air Pollution in Beijing in 2008, *Environmental Health Perspectives*, 118, 1, 87-91, ISSN: 0091-6765
- Zheng, M. et al. (2007). Source apportionment of daily fine particulate matter at Jefferson Street, Atlanta, GA, during summer and winter, *Journal of the Air & Waste Management Association*, 57, 2, 228-242, ISSN: 1047-3289

# Impact of Conversion to Compact Fluorescent Lighting, and other Energy Efficient Devices, on Greenhouse Gas Emissions

M. Ivanco

*Atomic Energy of Canada Ltd.*

K. Waher

*Wardrop Engineering Inc.*

B. W. Karney

*University of Toronto*

## **Abstract**

Selecting appropriate boundaries for energy systems can be as challenging as it is important. In the case of household lighting systems, where does one draw these boundaries? Spatial boundaries for lighting should not be limited to the system that consumes the energy, but also consider the environment into which the energy flows and is used. Temporal boundaries must assess the energy system throughout its life cycle. These boundary choices can dramatically influence the analysis upon which energy strategies and policies are founded.

This study applies these considerations to the “hot” topic of whether to ban incandescent light bulbs. Unlike existing light bulb studies, the system boundaries are expanded to include the effects incandescent light bulbs have on supplementing household space heating. Moreover, a life cycle energy analysis is performed to compare impacts of energy consumption and greenhouse gas emissions for both incandescent light bulbs and compact fluorescent light bulbs. This study focuses on Canada, which not only has large seasonal variations in temperature but which has announced a ban on incandescent light bulbs.

After presenting a short history and description of incandescent light bulbs (ILBs) and compact fluorescent light bulbs (CFLBs), the notion that a ban on ILBs could alter (or even increase) greenhouse gas (GHG) emissions in certain regions of Canada are introduced. The study then applies a life cycle framework to the comparison of GHG emissions for the ILB and CFLB alternatives. Total GHG emissions for both alternatives are calculated and compared for the provinces of Canada and again a physical rebound effect sometimes occurs. Finally, the policy and decision making implications of the results are considered for each of these locations.

## 1. Introduction

While there is no question that a switch from incandescent light bulbs (ILBs) to compact fluorescent light bulbs (CFLBs) will produce comparable artificial lighting for a reduced amount of energy, it is much less clear that the switch will have a beneficial impact on greenhouse gas (GHG) emissions. Light bulbs are essentially space heaters and thus contribute to space heating and lighting, which are two of the greatest energy requirements for buildings and houses. Regions with different climates and energy sources will realize a range of environmental impacts due to a switch from ILBs to CFLBs. In this study, the impacts of substituting ILBs for CFLBs, on greenhouse gas emissions, in different regions of Canada are assessed. While most greenhouse gases are not “air pollution” in the strictest sense, since they occur in great abundance in nature, anthropogenic contributions to the environment of such gases is believed to influence not only the climate and ocean chemistry at present but may play a greater, and detrimental role, in future.

Although ILBs and CFLBs serve the same purpose, to provide light, they have different histories and properties. Humphry Davy invented the first incandescent light in 1802 after sending an electrical current through a thin strip of platinum and noticing that it produced both light and heat (Bowers, 1995). This discovery was key to the invention of our modern day ILB by Thomas Edison (Bowers, 2002). Modern ILBs consist of a filament of tungsten wire and inert gas contained within a glass bulb. The inception of CFLBs began with Alexandre Edmond Becquerel, who was the first person to put fluorescent substances in a gas discharge tube (Bowers, 2002). Although early experiments in the late 19<sup>th</sup> and early 20<sup>th</sup> centuries produced lights that varied in the colour spectrum, most were unfit for practical purposes as they did not emit white light. It wasn't until the 1920's when ultraviolet light was converted into a more uniformly white-colored light that CFLBs became a feasible alternative to ILBs. Modern CFLBs contain mercury vapour and low-pressure inert gas and are coated with a fluorescent powder to convert ultraviolet radiation into visible light.

When it comes to energy consumption for a specific light emissivity, ILBs and CFLBs have diverging properties. As many have pointed out, ILBs are essentially electric space heaters that give off a small portion of their energy (up to 10%) as light, the remainder being converted in various ways to heat energy; indeed, most of the visible light will itself ultimately become heat in the environment. CFLBs use between 20 to 25% of the power of an equivalent incandescent lamp for the same light output (Coghlan, 2007). This simple energy efficiency comparison is sometimes enough to justify using CFLBs instead of ILBs. As a result, many countries have started, or are in the process of, restricting the use of ILBs and promoting the usage of CFLBs.

On the forefront of the phasing out of ILBs for CFLBs are countries such as Brazil, Venezuela, and Australia. Brazil and Venezuela were the earliest countries to introduce legislation to phase out ILBs in 2005, while Australia is attempting to prohibit ILB use by 2010. The Canadian government has followed suit and committed to banning the sale of ILBs by 2012 (NRTEE, 2009). This topic has also garnered support from most environmental groups. The notion that using more energy efficient light bulbs is good for the environment is almost irresistible. Electricity generation is the single largest source of artificial greenhouse gas emissions, accounting for over 21% of all emissions. Hence, intuition would suggest that anything that will result in a reduction in electricity use should also reduce artificial greenhouse gas emissions.

Recent concerns over global climate change have highlighted the need to reduce our “carbon footprint.” While energy conservation is a crucial measure for accomplishing this goal, the present authors wish to detail the change in total and net GHG emissions associated with a switch from ILBs to CFLBs.

### **1.1 Switching Light Bulbs and GHG Emissions**

In Canada, the excess heat produced by interior ILBs is not entirely wasted, at least not during the cooler months between Fall to Spring. Drawing a system boundary around the common household, the light bulb emits energy in the form of light and waste heat. Both of these contribute to the space heating load during the winter months in cold climates. Therefore, electrically heated homes that replace ILBs with CFLBs will simply use additional direct electrical energy to make up for the loss in heat. Essentially, total energy savings, and subsequent impacts on global warming, for these houses could be negligible.

For residences that use other space heating systems (e.g., natural gas and oil), an increase or decrease in GHG emissions result when these homes burn larger amounts of these fuels in order to make up the additional space heating requirements caused by switching from ILBs to CFLBs. If home thermostats are left at the same temperature, the space heating system will have to work harder to supplement the loss of waste heat energy provided by the inefficient light bulbs. Depending on regional supply mix characteristics and types of household space heating, this may cause a net increase or decrease in GHG emissions for the household. The key to these impacts, to whether there is an increase or a decrease, is how the compensating electrical energy is generated, thus requiring a further expansion of the system boundaries.

In many places, a net reduction in GHG emissions will be observed. Burning fossil fuels directly to heat homes is about three times as efficient as using fossil fuels to generate electricity for the regional power grid and then distributing the electricity from that grid to heat the home. Therefore, Canadian provinces that rely heavily on fossil fuels to generate electricity and to heat homes, such as Alberta and Saskatchewan, would benefit twofold from switching from ILBs to CFLBs; energy would be saved and there would also be a reduction in GHG emissions.

In contrast, a substitution from ILBs to CFLBs would likely result in an increase in GHG emissions in provinces such as Quebec or British Columbia, where virtually 100% of the electricity generated is by non-GHG emitting technologies (i.e., hydropower), and where homes are typically heated by natural gas or oil. The overall energy consumption would be less than before, but the switch from a ‘clean’ regional electricity supply mix to a fossil-fuel generating residential space heating system would be less environmentally friendly.

But predicting the net GHG emissions due to this light bulb switch is not straightforward for all Canadian provinces. In the province of Ontario, electricity generation is provided by a variety of sources, some of which generate GHGs, such as coal and natural gas, and some of which do not, such as hydro or nuclear. In this case the situation is much more complex and the impact of a switch from ILBs to CFLBs on GHG emissions depends on what electricity generation sources are turned off, or throttled down, with the energy savings that are achieved.

But while the light bulb switch may have adverse impacts during the cold months, in the summer, the heat from incandescent light bulbs is indeed wasted and represents an extra heating load that often is removed by air conditioning. It doubly makes sense to replace

interior lights with compact fluorescent ones in the summer, across the entire country and it makes sense to replace exterior lights with fluorescent ones during all seasons. However, in Canada the summer season is approximately four months long. Therefore, it may not necessarily make sense to have a national ban on incandescent bulbs; reductions in GHG emissions for one region of the country may be cancelled out by increases in another.

## 2. Light Bulb Life Cycle Analysis Methodology

The first goal of this study is to critically analyze the life-cycle impacts of switching from ILBs to CFLBs in the following provinces of Canada: British Columbia, Alberta, Saskatchewan, Manitoba, Ontario, Quebec, New Brunswick, Nova Scotia, Prince Edward Island and Newfoundland. The framework for a comparison of GHG emissions for the ILB and CFLB scenarios requires the a model to link household life cycle energy used for space heating, space cooling and lighting with GHG emissions in order to compare the impacts of switching from ILBs to CFLBs. This is achieved in four main steps: First, energy and GHG emissions characteristics for the fabrication and disposal phases of incandescent and compact fluorescent light bulbs are estimated. Second, total energy used for household space heating, space cooling and lighting is determined using an equivalent planning period. Next, these life-cycle energy requirements are converted to GHG emission equivalents using specific energy source GHG intensities (e.g., natural gas, heating oil, and electricity) for the particular household locations. Finally, the net difference in GHG emissions due to switching from ILBs to CFLBs is compared.

The planning period of the life cycle energy analysis (LCEA) corresponds to the greater design life of the two light bulbs. System boundaries for the LCEA are specified in each life cycle phase as follows: (1) Fabrication Phase: material extraction, material production, and light bulb manufacturing; (2) Operation Phase: space heating energy, space cooling energy and lighting energy; and (3) Disposal Phase: light bulb scrapping. To simplify the model formulation, light bulb transportation energy requirements are not included within the LCEA.

The total energy expenditure of the system over the equivalent planning period can be estimated, taking into account the energy of the fabrication, operation and decommission stages. Symbolically this can be represented:

$$E = F + H + C + L + D \quad (1)$$

where:

- F = Total energy required to fabricate the bulbs,
- H = Total heat energy produced by household light bulbs during cold weather,
- C = Total heat energy produced by household light bulbs during warm weather,
- L = Total amount of energy produced in generating light, and
- D = Disposal energy required.

These terms are discussed in more detail in the following sections.

### 2.1 Fabrication and Disposal Phases

The fabrication stage includes material extraction, material production and light bulb manufacturing. Disposal involves the total energy required to scrap and deposit the light bulb. To avoid double counting and “reinventing the wheel,” unit energy requirements for the fabrication and disposal phases of a light bulb are adopted from Gydesan and Maimann (1991) (see Table 1). Gydesan and Maimann calculate the unit energy requirements for the fabrication phase by determining the material content of the light bulb and multiplying this value by the energy content found in the corresponding material. As for unit disposal energy requirements for the disposal phase, Gydesan and Maimann advise that “no quantitative calculation has been made of the energy consumption needed for scrapping the lamps, but a qualitative assessment support that it is negligible compared to the energy consumption during the operation phase.” Therefore, it is assumed that the disposal energy per bulb is equal to zero.

|                                   | ILBs | CFLBs |
|-----------------------------------|------|-------|
| Wattage Equivalency (W)           | 60   | 15    |
| Operational Lifetime (hours)      | 1000 | 8000  |
| Fabrication Energy Per Bulb (kWh) | 0.15 | 1.4   |
| Disposal Energy Per Bulb (kWh)    | 0    | 0     |

Table 1. Light Bulb Characteristics (Gydesan and Maimann, 1991).

Applying these values with the number of replacements required throughout the planning period, the total energy required in the fabrication and disposal stages can be calculated using the following formulas:

$$F = \sum_{j=1}^M e_F \tag{2}$$

$$D = \sum_{j=1}^M e_D \tag{3}$$

where, F = total energy required to fabricate the light bulbs (kWh);  $e_F$  = fabrication energy requirement per light bulb (kWh); M = number of light bulbs requiring replacement or disposal throughout the planning period; D = total energy required to dispose of the light bulbs (kWh); and  $e_D$  = disposal energy requirement per light bulb (kWh).

### 2.2 Operational Phase - Space Heating Energy

Total energy required to heat a household can be found by performing an energy balance based on conservation of energy. In a household, differences between indoor and outdoor temperatures promote heat transfer through the building envelope by conduction. In cold weather, indoor temperatures are greater than the outdoor environment. As a result, energy

is lost through the building envelope to the outdoor environment; to counteract this heat loss, heating systems such as a natural gas furnace, heating oil furnace, or electrical baseboards are installed to provide energy to maintain a constant indoor temperature. During cold days, heat wasted by inefficient light bulbs directly supplements the space heating component.

Thus, by defining the building envelope as the system boundary, a crude estimate of the annual energy required to maintain a household at a constant temperature during cold days ( $H$ ) involves subtracting the annual heat energy gains by interior lighting ( $H_L$ ) from annual building envelope heat energy loss during cold days ( $H_{BE}$ ), such that:

$$H = H_{BE} - H_L \quad (4)$$

where (4) is measured in kWh.

Average Canadian households located in different provinces vary in building size, envelope thermal resistance, and climate. These regional differences provide unique energy consumption rates for the average local household. Assuming that the majority of Canadians maintain average indoor temperatures around 18°C (Valor et. al., 2001), a common building science unit, degree-days, can be used to estimate energy losses and gains through the building envelope. Heating Degree-Days (HDD) and Cooling Degree-Days (CDD) are quantitative units that add up the differences between the mean daily temperature and the average indoor temperature of 18°C over an entire year. For example, if three average outdoor daily temperatures were 12°C, 16°C and 10°C, the total HDD for those three days would be 16 K·days (i.e., 6 + 2 + 8).

Thermal resistance of a building envelope is key to determining a household's heat loss or gain. A building envelope is effectively a membrane that separates indoor and outdoor environments whose primary function is to control heat flow through the use of thermal insulation. Regional climates make for different insulation resistance requirements (i.e. R-values). To estimate building envelope heat loss, HDD and CDD are combined with the building envelope thermal resistance and surface area by the following relationship (in kWh):

$$H_{BE} = \sum_{i=1}^n \left( \frac{A_i}{R_i} \right) HDD \quad (5)$$

where  $n$  = total number of different surface areas;  $A$  = surface area  $i$  of the building envelope area ( $m^2$ );  $R$  = building envelope surface area  $i$  thermal resistance ( $m^2 \cdot K$ )/W; and HDD = heating degree-days (K-day).

A light bulb emits all of the energy it consumes as heat or light. While the primary function of a light bulb is to provide a source of light for the resident, all of this energy supplements the space heating energy required to maintain a constant temperature within the household. Waste heat energy is emitted from the light bulb while light energy also contributes to space heating as the building walls and components absorb the light and convert it to heat. Total heat energy produced by household light bulbs during cold weather can be estimated (in kWh) as follows:

$$H_L = \alpha_H \sum_{i=1}^n 8.76 P_i t \quad (6)$$

where  $\alpha_H$  = percentage of year requiring heating;  $n$  = number of light bulbs in an average household;  $P$  = power required to operate light bulb  $i$  (W); and  $t$  = percentage of time the light bulb is turned on throughout an entire year.

### 2.3 Operational Phase - Space Cooling Energy

Total energy required to cool a household can also be found by performing an energy balance. In warm weather, high outdoor air temperatures can produce an uncomfortable indoor environment; a household air conditioning system is often installed to provide comfort for occupants by lowering the indoor air temperature.

However, in contrast to space heating energy requirements, heat energy produced by light bulbs during warm days increases the total space cooling energy required. Thus, by again defining the building envelope as the system boundary, a crude estimate of the annual energy (in kWh) required to cool a household during warm days ( $C$ ) involves adding the annual heat energy gains by interior lighting ( $C_L$ ) with annual air conditioning energy requirements ( $C_{AC}$ ), such that:

$$C = C_{AC} + C_L. \quad (7)$$

The annual energy requirements of an air conditioner are dependent on cooling degree-days, outdoor design temperatures, and energy efficiency ratings. Natural Resources Canada (2004b) uses the following formula to estimate space cooling energy requirements (in kWh):

$$C_{AC} = \frac{Q \cdot CDD}{(T_d - 18) 0.9 EER} \cdot \frac{24}{1000} \quad (8)$$

where  $Q$  = basic air conditioning cooling capacity (Btu/h);  $CDD$  = cooling degree-days (K-day);  $T_d$  = air conditioning design temperature ( $^{\circ}C$ ); and  $EER$  = air conditioning energy efficiency rating.

In summer months, the energy consumed by a light bulb will be transferred to the household and will add this energy to the space cooling load. Using the same rationale in determining equation (6) above, the total heat energy (in kWh) produced by household light bulbs during warm weather can be estimated by:

$$C_L = \alpha_L \sum_{i=1}^n 8.76 P_i t \quad (9)$$

where  $\alpha_C$  = percentage of year requiring cooling;  $n$  = number of light bulbs in an average household;  $P$  = power required to operate light bulb  $i$  (W); and  $t$  = percentage of time the light bulb is turned on.

## 2.4 Operational Phase - Lighting Energy

Energy is consumed by ILBs and CFLBs to produce visible light. The amount of electricity ( $9$  in kWh) used for home lighting ( $L$ ) is estimated using the following formula:

$$L = \sum_{i=1}^n 8.76 P_i t \quad (10)$$

where  $n$  = number of light bulbs in an average household;  $P$  = power required to operate light bulb  $i$  (W); and  $t$  = percentage of time the light bulb is turned on.

## 3. GHG Intensities

There are five main energy sources for Canadian electricity: coal, natural gas, oil, nuclear and hydroelectric. There is a small amount of wind-powered generation that is increasing in importance but at this point represents less than 1% of Canadian electricity generation. Each source has its exclusive GHG intensity (emissions per unit of electricity): coal has the highest GHG intensity; oil has about 75% of the emissions of coal; gas has about half of the coal GHG intensity; and nuclear and hydroelectric sources are assumed to be non-GHG-emitting sources. Strictly speaking there are life-cycle greenhouse gas emissions for nuclear and hydroelectric generation as well. Though there is no consensus figure on these, estimates are of the order of 10 grams of  $\text{CO}_2$  per kWh. In any event these are much lower than the additional life cycle emissions from burning of fossil fuels, which are also not considered. Only GHG emissions from operation are considered, since these are well known.

Manufacturing and disposing light bulbs requires energy. Producing this energy often involves burning fossil fuels. As a result, any light bulb produced or scrapped may produce GHG emissions. To simplify the analysis and draw from existing literature, GHG intensities used to fabricate and dispose of ILBs and CFLBs are taken from Gydesan and Maimann (1991). Although light bulbs come from different suppliers and often manufactured half-way across the globe, it is assumed for simplicity that the electricity supply mix used in their paper is common for all light bulbs used in Canada.

During the operational phase, natural gas and oil are two common forms of energy used to heat the average Canadian household. For simplicity, these GHG intensities are assumed to be constant across Canada. Space heating using electricity, on the other hand, has varied GHG intensities due to its dependence on the regional electricity supply mix. For example, Quebec will have a low level of average space heating GHG intensity primarily because it relies on electric baseboards or forced air electric furnaces for space heating.

During the operational phase of a light bulb, GHG emissions will be different for the Canadian provinces, as the electricity generation supply mix (and the corresponding GHG intensities) varies by province. For example, in the province of Alberta electricity generation is predominantly fueled by coal. Hydroelectric power is nearly the exclusive source of electricity in Quebec, and Ontario is between the two: it controls sources of hydro, coal, natural gas and a small amount of oil along with a baseline load of nuclear power to provide electricity. Average GHG intensity per region can be estimated by dividing regional GHG emissions by total electricity generated by the specific energy source (Environment Canada, 2007). As a result, Alberta has a high average GHG intensity for electricity generation while Quebec is very low and Ontario is moderate.

To assess the difference in GHG emissions involved in using ILBs and CFLBs, GHG intensities (in the form of g CO<sub>2</sub> eq/kWh) for each life-cycle phase are multiplied by corresponding fabrication, space heating, space cooling, household lighting and disposal energy requirements to estimate total GHG emissions using the following formula:

$$G = \eta_i F + \eta_i H + \eta_i C + \eta_i L + \eta_i D \tag{11}$$

where  $\eta_i$  = GHG intensity as a function of the main energy source (g CO<sub>2</sub> eq/kWh). Equation (11) is measured in g CO<sub>2</sub> equivalents.

### 4. Results

The analytical model developed above is applied to determine total life cycle energy requirements from the fabrication, operation (space heating, space cooling and lighting) and disposal phases of a light bulb within a household located in each of the provinces of Canada.

For this study, the typical design life of a CFLB is assumed to be 8000 hours (Gydesan and Maimann, 1991). The light bulbs are also assumed to operate only 4 hours per day. Using these two values, the life-cycle planning period is determined to be 5.5 years. To compare an ILB on the same timeline, the ILB is assumed to be replaced eight times throughout the planning period. Adopting the data from Gydesan and Maimann (1991), life-cycle energy requirements for the average ILB and CFLB (neglecting space heating relationships introduced earlier) fabrication and disposal stages are determined (see Table 2).

|                         | ILBs               | CFLBs              |
|-------------------------|--------------------|--------------------|
| Fabrication Stage (kWh) | 32                 | 37                 |
| Operational Phase (kWh) | Varies by Province | Varies by Province |
| Disposal Stage (kWh)    | 0                  | 0                  |

Table 2. Light Bulb Life-Cycle Energy Requirements.

Fig 1 estimates the total life cycle energy requirements throughout the entire planning period assuming only the lighting energy requirements from the operational phase. Looking at lighting energy alone, significant savings in energy consumption are realized when switching from ILBs to CFLBs.

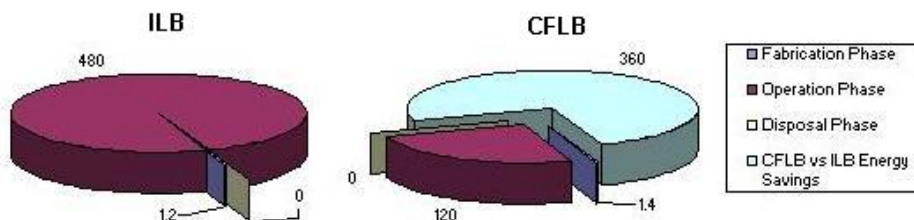


Fig. 1. Life-Cycle Energy of ILBs vs CFLBs (units in kWh).

However, the analysis that follows expands the system boundaries from their research to include space heating, cooling and total lighting energy requirements to assess the overall environmental impacts of switching from ILBs to CFLBs. Energy requirements for both ILB and CFLB scenarios, including space heating considerations, are estimated for Canadian provinces using (4) to (10). The majority of the data has been assembled from Government of Canada sources (See the Tables in Appendix A). Total operational energy estimates for ILBs and CFLBs in the average provincial household are presented in Table 3.

|   | <b>BC</b> | <b>AB</b> | <b>SK</b> | <b>MN</b> | <b>ON</b> |
|---|-----------|-----------|-----------|-----------|-----------|
| ILB Yearly Household Energy ( $E_{ILB}$ ) (kWh)   | 15,100    | 21,300    | 24,700    | 22,900    | 19,000    |
| CFLB Yearly Household Energy ( $E_{CFLB}$ ) (kWh) | 14,700    | 20,800    | 24,100    | 22,200    | 17,900    |
|   | <b>QC</b> | <b>NB</b> | <b>NS</b> | <b>PE</b> | <b>NL</b> |
| ILB Yearly Household Energy ( $E_{ILB}$ ) (kWh)   | 18,900    | 19,200    | 18,300    | 19,400    | 18,900    |
| CFLB Yearly Household Energy ( $E_{CFLB}$ ) (kWh) | 18,300    | 18,800    | 17,700    | 18,900    | 18,500    |

Table 3. Yearly Household Heating and Lighting Energy Requirements for Various Canadian Provinces.

Converting these energy requirements to GHG emissions using (11), total household GHG emissions for the selected provinces while using either ILBs or CFLBs were calculated in Table 4. Again, aggregation of data regarding regional GHG intensities came from a number of Government of Canada sources (See Tables in Appendix A).

|  | BC         | AB           | SK          | MN        | ON          |
|--|------------|--------------|-------------|-----------|-------------|
| Net GHG Emissions from the Light Bulb Switch ( $G_{net}$ ) (kt CO <sub>2</sub> eq)*                          | 1690       | -8470        | -2430       | 407       | -5460       |
| <b>Annualized Net GHG Emissions from the Light Bulb Switch (<math>G_{net}</math>) (kt CO<sub>2</sub> eq)</b> | <b>309</b> | <b>-1550</b> | <b>-443</b> | <b>74</b> | <b>-997</b> |
| Residential GHG Emissions over Planning Period (kt CO <sub>2</sub> eq)*                                      | 22100      | 40200        | 8820        | 5750      | 104000      |
| Percentage Change from Residential Emissions   | +7.7%      | -21.1%       | -27.5%      | +7.1%     | -5.2%       |
|  | QC         | NB           | NS          | PE        | NL          |
| Net GHG Emissions from the Light Bulb Switch ( $G_{net}$ ) (kt CO <sub>2</sub> eq)*                          | 1450       | -389         | -1670       | -22       | 110         |
| <b>Annualized Net GHG Emissions from the Light Bulb Switch (<math>G_{net}</math>) (kt CO<sub>2</sub> eq)</b> | <b>265</b> | <b>-71</b>   | <b>-305</b> | <b>-4</b> | <b>20</b>   |
| Residential GHG Emissions over Planning Period (kt CO <sub>2</sub> eq)*                                      | 23700      | 2850         | 5460        | 1270      | 1430        |
| Percentage Change from Residential Emissions   | +6.1%      | -13.7%       | -30.6%      | -1.7%     | +7.8%       |

\* Note: The life cycle planning period is 5.5 years

Table 4. Household Life-Cycle Heating and Lighting GHG Emissions for Various Canadian Provinces.

#### 4.1 Sensitivity Analysis

A sensitivity analysis was carried out to assess the influence of uncertain model parameters on total and net GHG emissions. Each parameter was increased and decreased by 50% in 25% increments and the model was run again with the new values to determine total and net GHG emissions due to these changes. Differences in GHG emissions between different provinces were also noted.

##### 4.1.1 Total GHG Emissions

The following parameters were found to be the most sensitive when assessing total GHG emissions:

- Percentage daily light bulb operation
- CFLB operational lifetime, and
- number of private dwellings occupied by usual residents.

The following parameters were found to have moderate sensitivity when assessing total GHG emissions:

- Average indoor wall height
- heated area
- minimum thermal resistance for the walls and floor, and
- average electricity GHG intensity

Those parameters that had the minimum impact on GHG emissions were:

- average number of household light bulbs
- minimum thermal resistance for the roof
- percentage of year requiring heating, and
- air conditioning design temperature

GHG emissions were relatively insensitive to the following parameters:

- Percentage of indoor household light bulbs
- percentage of outdoor household light bulbs
- air conditioning EER
- ILB operational lifetime
- light bulb fabrication energy
- percentage using central and portable A/C systems, and
- basic air conditioning cooling capacity

#### **4.1.2 Net GHG Emissions**

The parameters that had significant impact on net GHG emissions were:

- average number of household light bulbs
- percentage of indoor household light bulbs
- percentage daily light bulb operation
- private dwellings occupied by usual residents
- percentage of year requiring heating, and
- average electricity GHG intensity had significant sensitivity.

The percentage of outdoor household light bulbs had only moderate impact on net GHG emissions while the percentage of the year requiring cooling had only a slight impact on net GHG emissions. All other parameters were deemed to be insensitive towards net GHG emissions.

Almost all of the air conditioning parameters influenced the total and net GHG emissions for Ontario (i.e., air conditioner EER, percentage of year requiring cooling, percentage using central and portable AC systems, basic air conditioning cooling capacity, and air conditioning design temperature); the other provinces were generally insensitive to these parameters since air conditioning is not as heavily used.

## **5. Critical Reflections**

As expected, there is an overall household reduction in life-cycle energy consumption for each province when switching from ILBs to CFLBs (see Table 4). However, the energy saving is not as substantial as a first impression might have suggested. The electrical energy saved when using efficient light bulbs is generally offset to some extent by the increased space heating energy requirements. The results also indicate that the fabrication and

disposal phases of a light bulb do not have a substantial impact on the total energy consumption or GHG emissions of a light bulb (these phases generally less than 0.5% of the total life cycle energy consumption). Rather, the greatest impact is observed in the operational phase (greater than 99% of the life-cycle energy consumed by a light bulb comes from the operational phase).

Total GHG emissions caused by the light bulb “switch”, on the other hand, were strikingly different. As shown in Table 4, net GHG emissions decreased in many provincial households that switched from ILBs to CFLBs. Many provinces ‘switched’ from a high to a low GHG-emitting space heating energy source. But the marginal decrease differed for each province. For example, the decrease in Ontario was much smaller than in Alberta, even though Ontario has nearly four times the population. Meanwhile, some provinces experienced a switch in the opposite direction to that experienced by the majority of the provinces. British Columbia, Manitoba, Quebec, and Newfoundland-Labrador all experience a net increase in GHG emissions resulting from the light bulb switch.

Alberta is an example of a compelling case for making a switch from ILBs to CFLBs. The GHG intensity of electricity generation in the province is very high (861 g CO<sub>2</sub>/kWh) while the GHG intensity associated with home heating is relatively small (approximately 220 g CO<sub>2</sub>/kWh). Hence, providing partial heating for a home using inefficient ILBs is much worse for the environment in terms of GHG emissions. This same explanation can be used for households located in provinces such as Saskatchewan, New Brunswick, Nova Scotia, and PEI that also experienced a net decrease in GHG emissions.

Quebec represents the opposite extreme. In Quebec, the majority of homes are heated using electricity that has an average GHG intensity of 8 g CO<sub>2</sub>/kWh. For these homes, it makes virtually no difference to GHG emissions if interior ILBs are replaced with CFLBs in months when home heating is required. At the same time, the homes will be no less expensive to heat. Only in the summer months will Quebec’s switch from ILBs to CFLBs result in less electricity consumed and have a negligible effect on GHG emissions.

However, the situation is different for the increasing plurality of Quebec homes that are heated with oil and natural gas. The GHG intensities associated with space heating using natural gas (approximately 220 g CO<sub>2</sub>/kWh) or oil (approximately 315 g CO<sub>2</sub>/kWh) are much higher than those associated with electrical space heating; a portion of which is provided by light bulbs. In these homes, switching from ILBs to CFLBs will result in some energy savings but will also result in the use of a different mixture of energy types that have a higher overall GHG intensity. As Table 4 shows, if all homes in Quebec were required to switch from ILBs to CFLBs there would be an increase of 265,000 tonnes in CO<sub>2</sub> emissions in the province, equivalent to the annual emissions from almost 50,000 automobiles. In fact, this amount will increase in future as homes move away from electric space heating to cheaper and more efficient fossil fuel sources! Again, this same argument can be used for households located in provinces such as British Columbia, Manitoba and Newfoundland-Labrador who also experienced a net increase in GHG emissions.

In Ontario, the situation is less straightforward. The GHG intensity of electricity generation is moderate (220 g CO<sub>2</sub>/kWh) and comparable to the GHG intensity of space heating using natural gas, which is the predominant heating source in the province. A warmer climate in the summer months, compared to Quebec and Alberta, helps to tip the balance slightly in favour of switching from ILBs to CFLBs, if reduction in CO<sub>2</sub> emissions is the goal.

The opportunity for greater reduction of GHG emissions in Ontario exists but would require coordination with provincial bodies that control the electricity generation sector. Ontario has a large variety of electricity generation sources and the way that they are managed is complex. Nuclear power accounts for about 50% of Ontario's electricity generation and it is run at close to 100% output 24 hours per day providing most, but not all, of the base load electricity requirements for the province. Coal, natural gas, a small amount of oil, and hydro are used to provide the balance of base load requirements and electricity generation supplies are adjusted to meet demand, a practice the industry refers to as "load following." Wind power generation is relatively small but the grid accepts whatever energy it can provide.

In a province like Ontario it is not so much the average GHG intensity of electricity generation that matters but rather the forms of electricity generation, which are turned off with the energy saved by switching from ILBs to CFLBs. Ideally, coal generation would be turned off with the energy that is saved. At present, however, there is no regular pattern in how the Ontario electricity system responds to load changes from one day to the next, at least in terms of what forms of electricity generation are switched off. For maximum environmental benefit one would like to see hydro capacity kept constant and coal electricity generation turned off. However, most of Ontario's hydroelectric generation is not capable of 24/7 operation and many dams need to be switched off during the late evening and in the middle of the night to allow an inventory of water to build up, thus allowing them to be used to meet peak demand in the middle of the day.

In Ontario, consumers pay a fixed price for electricity depending on their usage. The largest electricity producer is the provincially owned Crown Corporation, Ontario Power Generation, and it receives a fixed price for the electricity that it generates depending on rates determined by the Ontario Energy Board, their regulating body. Many private electricity generators, most of whom run natural gas fired plants, receive the market price. Economics, therefore suggests that the best value for the taxpayer would occur if the natural gas generators were turned off in response to a reduction in demand, since this is generally the most expensive source of generation. However, this does not generally happen in isolation. At times of low demand, which can occur in the Spring and Fall periods of the year in a climate like Ontario's, hydro-electricity is sometimes used to follow electrical loads, which from a GHG emissions perspective, is the worst case scenario if the aim is to use more efficient CFLBs to reduce greenhouse gas emissions. In the absence of better information, the average GHG intensity for the provincial electricity generation grid was used in these calculations. However, it should be recognized that Ontario has potential to improve GHG emission reductions when switching from ILBs to CFLBs if this emission reduction goal is factored into operation of the diverse mix of generation facilities. In the absence of a price for carbon there are no economic drivers to encourage electrical generation utilities to manage their diverse generation sources in such a way as to turn off those that have the highest GHG emissions when electricity demand drops.

### **5.1 Sensitivity Implications**

Of the parameters that were sensitive to total GHG emissions, most of their sensitivity can be explained with common sense: the longer a light bulb operates, the greater its total GHG emissions; and with a greater number of households comes higher emissions. There is also rationale behind CFLB and ILB operational lifetime varying in sensitivity. The CFLB

operational lifetime is sensitive because the model planning period is based on this parameter. The ILB operational lifetime is insensitive due to the insignificant impact that light bulb fabrication has on the total GHG emissions throughout the planning period.

Sensitivity regarding net GHG emissions is slightly more difficult to explain. It is easy to understand that the number of household light bulbs and private dwellings occupied by usual residents will increase the marginal difference between GHG emissions associated with ILBs versus CFLBs – these parameters clearly exacerbate the net difference in GHG emissions. The percentage of indoor household light bulbs is directly related with the impacts light energy has on supplementing space heating energy during the colder months. Since space heating energy consumption is directly related to the percentage of year requiring heating, the effects a CFLB has on increasing the load of a space heating system during varying periods of ‘cold’ months may have a direct impact on net GHG emissions depending on how the electricity is generated and how the home is heated. Altering the GHG intensities involved in electricity generation for each province will also impact the net difference in GHG emissions: there are regions where electrical heating from light bulbs is effectively “switched off” and replaced with space heating energy sources other than electricity that have higher or lower GHG intensities.

As for the net GHG emissions, sensitivity involving the air-conditioning parameters are unmistakable in Ontario since it is one of the few provinces where the use of air-conditioning is prevalent.

## **5.2 Common Misconceptions**

A number of readers have an intuitive feeling that the findings from this research are just plain wrong. While many arguments against the study may be defensive “gut reactions,” two common disputes have been raised when interpreting the validity of this research: 1) the savings in electricity by switching from ILBs to CFLBs ultimately reduces fossil-fuel based electricity generation; and 2) the electricity generated in each province is fungible – electricity grids are interconnected and a savings in one area result in a decreased load in another area. Addressing both of these arguments enlightens the readers to the further intricacies discovered while modeling this light bulb “switch”. A discussion of these items follows.

### **5.2.1 “Saving electricity reduces fossil-fuel based electricity generation”**

This argument revolves around the notion that the electricity saved must be in the form of coal-fired electricity generation. But this assumption is not correct – different regions can throttle down different sources of electricity generation when experiencing a lighter load demand. It is the type of electricity generating source that is turned off with the electricity that you save by using CFLBs, specifically for each region that matters.

This point is easily illustrated. Ontario is complex and thus has no coherent pattern for throttling down generating sources in response to load reduction. For instantaneous changes, coal fired generation is generally used because it responds the fastest to demands for load increase or reduction. However, the savings one finds in switching from ILBs to CFLBs are systematic ones, more like current day to day fluctuations that are largely driven by the weather. If you look at these day to day fluctuations and compare one day to the next, between the hours of 6 PM and midnight (when people tend to use their lights),

sometimes hydroelectricity is throttled down, sometimes coal is, sometimes gas fired electricity is throttled down and sometimes all three.

Examining one month's worth of data from the Ontario Independent Electricity System Operator (IESO), from April 7th to May 8th of 2008, to see how the electricity system deals with load reductions was fascinating: nuclear generation stayed the same (as one would expect - being baseload), coal generation decreased by 43%, natural gas generation decreased by only 10% and hydro-electric generation by 47%. Using the same approach as Environment Canada (2007), this means that the incremental GHG intensity for Ontario approximately equals (if you assume that this one month stretch is representative):  $0.43 \times 900 \text{ g CO}_2/\text{kWh}$  (for coal) +  $0.10 \times 500 \text{ g CO}_2/\text{kWh}$  (for natural gas) +  $0.47 \times 0 \text{ g CO}_2/\text{kWh}$  (for Hydro) =  $437 \text{ g CO}_2/\text{kWh}$ . This incremental value, when compared to Environment Canada's (2005) Ontario GHG intensity of  $220 \text{ g CO}_2/\text{kWh}$ , would actually result in a yearly residential GHG reduction of approximately 1980 kt CO<sub>2</sub> i.e; a substantial decrease in GHG emissions for Ontario.

In Alberta, the situation is clear - reducing coal-based electricity generation is the only option and therefore the above statement remains true.

Although electricity is fungible, in Quebec, it is hard to make a compelling argument that using CFLBs will result in a coal fired electricity generating station being shut down in New Brunswick or New York State or elsewhere. The ability to transmit electricity from one jurisdiction to the next is limited by simple physics (e.g., transmission losses when transporting electricity great distances) not to mention politics (e.g., difficulties in trying to build new transmission lines). In addition, most electricity trading goes on during the day, when loads are highest, and not during the late evening when people use their home lighting the most. Understanding the incremental electricity savings and the type of electricity generation that would be subsequently throttled down is not so cut and dried as one would expect. It is complicated, which is another important point that we make in this study.

### 5.2.2 "Electricity supply is fungible"

Many arguments in favour of CFLBs have to do with the philosophical belief that reductions in load will manifest themselves in less use of fossil fuels, and this has been addressed to some extent in the previous section. There are arguments that electricity is fungible (sort of like money) - so that electricity generated by a particular source in one province can be swapped with another in an adjacent province or US state. However, understanding the electricity export/import situation in different provinces is complicated.

Many permutations involving "what ifs" are generated when including electricity exporting/importing from adjacent provinces/states. For example, one argument involves the potential export of electricity from Alberta to British Columbia if the existing demand from BC is higher than the province's generating capability. In such a case, using ILBs will cause greater GHG emissions in BC because it may have to import electricity from nearby Alberta, which is generated exclusively by fossil fuels with a high GHG intensity. But if electricity is fungible, then Alberta may also import electricity from BC. This means there is a possibility that any electricity load reduction that results from switching to CFLBs in Alberta, could result in diminished imports from BC, since that electricity will be more expensive than in-province fossil generated electricity. If that were the case then switching to CFLBs in Alberta could have no impact on GHG emissions at all in the absence of a provincial government policy

mandating the import of clean electricity from BC, even if it is more expensive. In other words, in the absence of a substantial carbon penalty, or government policy, there are no economic drivers to shut down coal fired electricity generation in response to load reduction because, whatever its faults, coal fired electricity is relatively cheap. Until such time as this happens, the greenhouse gas emission reductions that could be achieved, in switching from ILBs to CFLBs, will never come close to being realized in a country like Canada, with a relatively cold climate and relatively clean electricity generation.

## 6. Future Research

Some questions can be raised towards the validity of the unit energy requirements for the fabrication and disposal phases of a light bulb, as the values and assumptions used to estimate these values may be outdated and/or obsolete. Gydesan and Maimann (1991) indicate that their fabrication data was taken from a source dated back to 1979. At the same time, the assumption that there are no disposal phase energy requirements may be incorrect. Gydesan and Maimann (1991) explain that increased energy requirements may be needed for properly handling the mercury that remains an issue during the disposal of CFLBs. In their analysis, they assume that the light bulbs are disposed via an incinerator and that all mercury is emitted to the environment. The latter is one consequence of switching from ILBs to CFLBs that is outside of the scope of this work. ILBs can be disposed of in ordinary household waste while CFLBs require an infrastructure to manage their disposal and manage mercury pollution. In the absence of such an infrastructure and strict adherence to them, one consequence of a mandated switch from ILBs to CFLBs would be an increase in environmental mercury pollution.

Another item that may need further review is the energy and GHG emissions involved in the transportation phase. Light bulbs are also manufactured in many places across the globe – each with different local electrical generation supply mixes and varying distances to ship the light bulb from the manufacturer to the consumer. Exporting of manufactured goods from half way around the world could provide the foundation for substantial energy requirements and GHG emissions involved in the transportation phase. Additional research in this area is recommended.

Finally, additional research involving the importing/exporting of electricity across provincial, state or country boundaries in response to load changes is crucial for understanding the impact of switching from ILBs to CFLBs on GHG emissions. Bans of ILBs are largely based on the mistaken impression that the energy saving realized in switching from ILBs to CFLBs will result in the switching off of coal fired generation because of the fungible nature of electricity. This is simplistic, will only occur in some jurisdictions and is highly dependent on the nature of electricity generation available and the nature of the electricity market. Where market forces drive the dispatch of electricity generation, the electricity savings that result in switching from ILBs to CFLBs will generally result in the most expensive forms of generation being turned off first and this is usually not coal fired generation, if more expensive generation is also part of the mix.

Understanding these mechanics could have significant impacts on future decision-making and policies for Canadian homeowners and even business-owners as carbon-based currencies become popular in the future. Including this analysis is out of the scope of this study, but should be carried out before policy is executed.

## 7. Conclusions

Decisions that are made regarding the future of energy use, conservation and demand management or even the optimal blend of supply mix are interdisciplinary and complex by nature. The metrics used to evaluate the decision have to be compatible with the choices themselves and cannot be skewed towards either.

In summary, switching from ILBs to CFLBs may not always result in an environmentally friendly outcome, especially in cold climates. While the intention to reduce electricity consumption is noble, the “switch” from electrical and fossil-fuel based space heating may drive up GHG emissions in certain regions. While we agree with the paradigm of reducing overall demand, the core contribution of this research highlights the greater need to reduce demand from higher GHG intensive energy sources.

We are entering the age of carbon consequences where measuring, reporting and addressing carbon emissions will become commonplace. It is time to rethink how we use current energy supplies by eliminating fossil fuel-based energy and begin to encourage energy from sustainable sources.

If we only generated electricity in Canada by burning coal, with a GHG intensity of approximately 900 g/kWh, our model predicts that almost 14 million tonnes of CO<sub>2</sub> per year would be avoided in Canada if every household switched from using ILBs to CFLBs. However, our electricity generation is relatively clean in Canada and instead our model, together with our assumptions, predicts only a reduction of 2.7 million tonnes.

In this case, a Canadian-wide ban on ILBs is not an ideal strategy to reduce national GHG emissions. Although the ban will result in a reduction in net Canadian GHG emissions there are provinces that will see and increase in GHG emissions due to the light bulb switch (i.e., BC, MB, QC, and NL). Only certain Canadian locations would benefit most from this light bulb paradigm shift (i.e., AB, SK, ON, NB, NS, and PE); locations where the switch between space heating and lighting energy results in lower net GHG emissions.

## 8. References

- Bowers, B. (1995). “New lamps for old: the story of electric lighting”. *IEE Review*, 41(6), pp. 239-242, Nov. 1995.
- Bowers, B. (2002). "Scanning our past from London-fluorescent lighting" in *Proc. 2002 IEEE*, 90(10), Oct. 2002, pg. 1696-8
- Coghlan, A. (2007). “It's lights out for household classic.” *New Scientist*, 193(2597), pg. 26-27, Mar. 2007.
- Energy Information Agency (2007). Fuel and Energy Source Codes and Emission Coefficients. U.S. Government [Online] Available: <http://www.eia.doe.gov/oiaf/1605/factors.html>
- Environment Canada (2003a). Province-Territory Weather Winners for 70 Categories: Most heating degree days. Government of Canada, Ottawa, ON [Online]. Available: <http://www.on.ec.gc.ca/weather/winners/most-heating-e.html>
- Environment Canada (2003b). Province-Territory Weather Winners for 70 Categories: Most cooling degree days. Government of Canada, Ottawa, ON [Online] Available: <http://www.on.ec.gc.ca/weather/winners/most-cooling-e.html>

- Environment Canada (2005). Climate Data Online. Government of Canada, Ottawa, ON [Online]. Available: [http://www.climate.weatheroffice.ec.gc.ca/climateData/canada\\_e.html](http://www.climate.weatheroffice.ec.gc.ca/climateData/canada_e.html)
- Environment Canada (2006). National Inventory Report on Greenhouse Gas Sources and Sinks in Canada for 1990-2004. Government of Canada, Ottawa, ON [Online]. Available: [http://www.ec.gc.ca/pdb/ghg/inventory\\_report/2004\\_report/2004\\_report\\_e.pdf](http://www.ec.gc.ca/pdb/ghg/inventory_report/2004_report/2004_report_e.pdf)
- Environment Canada (2007). National Inventory Report on Greenhouse Gas Sources and Sinks in Canada for 1990-2005. Government of Canada, Ottawa, ON [Online]. Available: [http://www.ec.gc.ca/pdb/ghg/inventory\\_report/2004\\_report/2004\\_report\\_e.pdf](http://www.ec.gc.ca/pdb/ghg/inventory_report/2004_report/2004_report_e.pdf)
- General Electric Company (2007). Frequently Asked Questions - Compact Fluorescent. [Online]. Available: [http://www.gelighting.com/na/business\\_lighting/faqs/cfl.htm](http://www.gelighting.com/na/business_lighting/faqs/cfl.htm)
- Gydesan, A. and Maimann, D. (1991). Life Cycle analysis of integral compact fluorescent lamps versus incandescent lamps - energy and emissions. Proceedings of Right Light 1, pp. 411-417. Stockholm, Sweden.
- Haysom, J. (1998) Comparison of the Model National Energy Code of Canada for Houses 1997 with Energy-Related Requirements in Provincial Building Codes. Climate Change: Buildings Table, National Research Council, Government of Canada [Online]. Available: [http://www.nationalcodes.ca/mnech/MNECH\\_prov\\_codes\\_comparison\\_e.pdf](http://www.nationalcodes.ca/mnech/MNECH_prov_codes_comparison_e.pdf)
- National Round Table on the Environment and the Economy (2009). Response of the National Round Table on the Environment and the Economy to its Obligations under the Kyoto Protocol Implementation Act. Ottawa, ON [Online]. Available: <http://nrtee-trnee.ca/eng/publications/KPIA-2009/NRTEE-KPIA-Reponse-2009-eng.pdf>
- Natural Resources Canada (2000). 1997 Survey of Household Energy Use - Summary Report. Office of Energy Efficiency: Natural Resources Canada, Government of Canada [Online]. Available: [http://oee.nrcan.gc.ca/publications/infosource/pdfs/SHEU\\_e.pdf](http://oee.nrcan.gc.ca/publications/infosource/pdfs/SHEU_e.pdf)
- Natural Resources Canada (2004a). Basic Facts About Residential Lighting. Government of Canada, Ottawa, ON [Online]. Available: <http://www.oee.nrcan.gc.ca/residential/personal/lighting.cfm>
- Natural Resources Canada (2004b). Air Conditioning Your Home. Government of Canada, Ottawa, ON. [Online]. Available: [http://oee.nrcan.gc.ca/publications/infosource/pub/energy\\_use/air-conditioning-home2004/air-conditioning.pdf](http://oee.nrcan.gc.ca/publications/infosource/pub/energy_use/air-conditioning-home2004/air-conditioning.pdf)
- Natural Resources Canada (2004c). Heating with Oil. Government of Canada, Ottawa, ON [Online]. Available: [http://oee.nrcan.gc.ca/Publications/infosource/Pub/home/heating\\_oil\\_in\\_en.pdf](http://oee.nrcan.gc.ca/Publications/infosource/Pub/home/heating_oil_in_en.pdf)
- Natural Resources Canada (2004d). Keeping the Heat In. Government of Canada, Ottawa, ON [Online]. Available: [http://www.oee.nrcan.gc.ca/keep\\_heat\\_in/](http://www.oee.nrcan.gc.ca/keep_heat_in/)

- Natural Resources Canada (2005a). 2003 Survey of Household Energy Use – Summary Report. Government of Canada, Ottawa, ON [Online]. Available: <http://oee.nrcan.gc.ca/publications/statistics/sheu-summary/pdf/sheu-summary.pdf>
- Natural Resources Canada (2005b). EnerGuide Room Air Conditioner Directory 2004. Government of Canada, Ottawa, ON [Online]. Available: <http://oee.nrcan.gc.ca/equipment/english/page83.cfm>
- Natural Resources Canada (2006a). Table 4: Lighting Secondary Energy Use and GHG Emissions by Region – Excluding Electricity-Related Emissions. Government of Canada, Ottawa, ON [Online]. Available: [http://oee.nrcan.gc.ca/corporate/statistics/neud/dpa/tablestrends2/res\\_ca\\_4\\_e\\_3.cfm](http://oee.nrcan.gc.ca/corporate/statistics/neud/dpa/tablestrends2/res_ca_4_e_3.cfm)
- Natural Resources Canada (2006b). Energy Use Data Handbook 1990 and 1998 to 2004. Government of Canada, Ottawa, ON [Online]. Available: <http://oee.nrcan.gc.ca/Publications/statistics/handbook06/pdf/handbook06.pdf>
- Snider (2006). Home Heating and the Environment. Canadian Social Trends, Statistics Canada - Catalogue No. 11-008, Spring 2006, pg. 15-19 [Online]. Available: <http://www.statcan.ca/english/freepub/11-008-XIE/2005004/articles/9126.pdf>
- Statistics Canada (2007). Population and dwelling counts, for Canada provinces and territories, 2006 and 2001 censuses - 100% data. Government of Canada, Ottawa, ON [Online]. Available: <http://www12.statcan.ca/english/census06/data/popdwell/Table.cfm?T=101> [Accessed: August 31, 2007], Government of Canada
- Valor, E., Meneu, V., and Caselles, V. (2001). Daily Air Temperature and Electricity Load in Spain. *Journal of Applied Meteorology*, 40(8), pg. 1413-1421

## 9. Appendix A

Table I - Average Household Energy Characteristics

|  |      |
|--|------|
| Average Household Indoor Wall Height (m)                 | 2.5  |
| Average Number of Household Light Bulbs <sup>a</sup>     | 26.4 |
| Percentage of Indoor Household Light Bulbs <sup>a</sup>  | 89%  |
| Percentage of Outdoor Household Light Bulbs <sup>a</sup> | 11%  |
| Percentage Daily Light Bulb Operation                    | 17%  |
| Average Indoor Temperature <sup>b</sup> (°C)             | 18   |
| Air Conditioning EER <sup>c</sup> (Btu/h/W)              | 8.9  |

a = Natural Resources Canada (2000)

b = Base temperature to calculate HDD and CDD; and (Valor et al., 2001)

c = NRC (2006b)

Table II - Light Bulb Characteristics

|  | ILBs | CFLBs |
|--|------|-------|
| Wattage Equivalency <sup>a</sup> (W)           | 60   | 15    |
| Efficiency <sup>b</sup>                        | 0.1  | 0.3   |
| Operational Lifetime <sup>c</sup> (hours)      | 1000 | 8000  |
| Fabrication Energy Per Bulb <sup>c</sup> (kWh) | 0.15 | 1.4   |

a = Natural Resources Canada (2004a)

b = General Electric Company (2007)

c = Gydesen and Maimann (2000)

| Table III - Household Energy Characteristics for Canadian Provinces |             |             |             |             |             |             |             |         |        |             |
|---|-------------|-------------|-------------|-------------|-------------|-------------|-------------|---------|--------|-------------|
|   | BC          | AB          | SK          | MB          | ON          | QC          | NB          | NS      | PE     | NL          |
| Private Dwellings Occupied by Usual Residents <sup>u</sup>          | 1,642,715   | 1,256,192   | 387,160     | 448,766     | 4,554,251   | 3,188,713   | 295,871     | 376,829 | 53,084 | 197,245     |
| Main Heating Energy Source <sup>v</sup>                             | Natural Gas | Electricity | Electricity | Oil     | Oil    | Electricity |
| Percentage of Households Heated by Natural Gas <sup>v</sup>         | 60%         | 97%         | 89%         | 62%         | 70%         | 5%          | 0%          | 0%      | 0%     | 0%          |
| Percentage of Households Heated by Electricity <sup>v</sup>         | 32%         | 2%          | 5%          | 33%         | 18%         | 70%         | 60%         | 27%     | 0%     | 52%         |
| Percentage of Households Heated by Oil <sup>v</sup>                 | 6%          | 0%          | 3%          | 2%          | 9%          | 18%         | 22%         | 60%     | 83%    | 29%         |
| Percentage of Households Heated by Other <sup>v</sup>               | 2%          | 0%          | 0%          | 3%          | 1%          | 7%          | 17%         | 11%     | 13%    | 18%         |
| Heated Area <sup>a</sup> (m <sup>2</sup> )                          | 133         | 112         | 112         | 112         | 139         | 105         | 116         | 116     | 116    | 116         |
| Surface Area - Roof <sup>b</sup> (m <sup>2</sup> )                  | 133         | 112         | 112         | 112         | 139         | 105         | 116         | 116     | 116    | 116         |
| Surface Area - Floor <sup>b</sup> (m <sup>2</sup> )                 | 133         | 112         | 112         | 112         | 139         | 105         | 116         | 116     | 116    | 116         |
| Surface Area - Walls <sup>b</sup> (m <sup>2</sup> )                 | 115         | 106         | 106         | 106         | 118         | 102         | 108         | 108     | 108    | 108         |

| Table III - Household Energy Characteristics for Canadian Provinces |      |      |       |       |      |       |      |       |       |      |  |
|---|------|------|-------|-------|------|-------|------|-------|-------|------|--|
|   | BC   | AB   | SK    | MB    | ON   | QC    | NB   | NS    | PE    | NL   |  |
| Predominant Administrative Zone <sup>z</sup>                        | A    | B    | C     | C     | A    | B     | B    | B     | B     | B    |  |
| Minimum Thermal Resistance-Roof (m <sup>2</sup> ·K/W)               | 5.4  | 5.8  | 5.6   | 7     | 5.6  | 7     | 7    | 7     | 7     | 8.8  |  |
| Minimum Thermal Resistance-Walls <sup>c</sup> (m <sup>2</sup> ·K/W) | 2.1  | 2.1  | 2.1   | 3.1   | 2.1  | 3.1   | 3.1  | 3.1   | 3.1   | 3.1  |  |
| Minimum Thermal Resistance-Floor <sup>c</sup> (m <sup>2</sup> ·K/W) | 1.08 | 1.08 | 1.08  | 1.08  | 1.6  | 1.08  | 1.08 | 1.08  | 1.08  | 1.08 |  |
| Heating Degree Days <sup>x</sup> (K·day)                            | 2879 | 4884 | 5546  | 5717  | 3719 | 5022  | 4846 | 4403  | 4673  | 4783 |  |
| Cooling Degree Days <sup>x</sup> (K·day)                            | 49.9 | 68.8 | 184.1 | 197.4 | 436  | 121.4 | 35.2 | 118.3 | 123.5 | 55.9 |  |
| Number of HDD Days in 2007 <sup>x</sup>                             | 327  | 338  | 314   | 305   | 254  | 311   | 342  | 316   | 320   | 335  |  |
| Number of CDD Days in 2007 <sup>x</sup>                             | 36   | 27   | 47    | 58    | 111  | 54    | 22   | 47    | 43    | 29   |  |

| Table III - Household Energy Characteristics for Canadian Provinces               |       |       |       |       |       |       |       |       |       |       |
|---|-------|-------|-------|-------|-------|-------|-------|-------|-------|-------|
|   | BC    | AB    | SK    | MB    | ON    | QC    | NB    | NS    | PE    | NL    |
| Percentage of Year Requiring Heating  | 90.1% | 92.6% | 87.0% | 84.0% | 69.6% | 85.2% | 94.0% | 87.1% | 88.2% | 92.0% |
| Percentage of Year Requiring Cooling  | 9.9%  | 7.4%  | 13.0% | 16.0% | 30.4% | 14.8% | 6.0%  | 12.9% | 11.8% | 8.0%  |
| Percentage Using Central and Portable A/C Systems <sup>w</sup>                    | 16.6% | 30.2% | 30.2% | 30.2% | 73.7% | 31.1% | 7.9%  | 7.9%  | 7.9%  | 7.9%  |
| Basic Air Conditioning Cooling Capacity <sup>e</sup> (Btu/h)                      | 21900 | 19100 | 19100 | 19100 | 22700 | 17700 | 19700 | 19700 | 19700 | 19700 |
| Air Conditioning Design Temperature <sup>f</sup> (°C)                             | 25    | 29    | 32    | 31    | 30    | 29    | 26    | 27    | 26    | 24    |
| Average Electricity GHG Intensity in 2005 <sup>t</sup> (g CO <sub>2</sub> eq/kWh) | 17    | 882   | 822   | 14    | 220   | 9.1   | 394   | 771   | 252   | 31    |

a = Total floor space of a dwelling excluding the basement and the garage (NRC, 2005a)

b = Assume the heated area is 1-storey and shaped as a square.

c = MNECH (1997) and Haysom (1998), based on Administrative Region and main heating energy source.

d = Environment Canada (2005)

- e = NRC, 2005b
- f = NRC (2004b)
- h = NRC (2005a) and Snider (2006)
- t = Environment Canada (2007)
- u = Statistics Canada (2007)
- v = Snider (2006)
- w = NRC (2005a)
- x = Environment Canada (2005), based on weather stations central to population mass
- y = NRC (2005a) and Snider (2006)
- z = NRC (2004d) based on highest population concentration and Degree-Day Zones table from Chapter 1, Part 2.

Table IV - Light Bulb Life Cycle Energy Requirements

| Total Planning Period Timeline (years)  | 5.5  |       |
|---|------|-------|
|   | ILBs | CFLBs |
| Number of Replacements per Planning Period  | 8    | 1     |
| Total Energy Consumption in Fabrication Stage <sup>a</sup> (kWh)                          | 1.2  | 1.4   |
| Total Energy Consumption during Operational Phase (kWh)                                   | 480  | 120   |
| Total Energy Consumption in Disposal Stage <sup>a</sup> (kWh)                             | 0    | 0     |
| Average Light Bulb Manufacturing GHG Intensity <sup>a</sup><br>(g CO <sub>2</sub> eq/kWh) | 850  |       |

a = Gydesen and Maimann (2000)

Table V - Average Household GHG Emission Characteristics

|   |         |
|---|---------|
| Natural Gas Heat of Combustion (kJ/mol)                         | 802     |
| Molar Mass of CO <sub>2</sub> (g/mol)                           | 44      |
| Natural Gas GHG Intensity (g CO <sub>2</sub> eq/kWh)            | 198     |
| Heating Oil GHG Emissions <sup>b</sup> (g CO <sub>2</sub> eq/L) | 2680    |
| Heating Oil Energy Intensity <sup>c</sup> (MJ/L)                | 38.2    |
| Heating Oil GHG Intensity (g CO <sub>2</sub> eq/kWh)            | 253     |
| Natural Gas Furnace Efficiency <sup>d</sup>                     | 81.00%  |
| Heating Oil Efficiency <sup>d</sup>                             | 78.00%  |
| Electric Heating Efficiency <sup>d</sup>                        | 100.00% |

a = based on heat of combustion of Natural Gas when water is a vapour

a = EIA (2007)

b = NRC (2004c)

c = Mid-efficiency for Natural Gas and Oil NRC (2004c)

# Importance of sources and components of particulate air pollution for cardio-pulmonary inflammatory responses

Schwarze PE, Totlandsdal AI, Herseth JI\*, Holme JA, Låg M, Refsnes M, Øvrevik J, Sandberg WJ and Bølling AK  
*Norwegian Institute of Public Health, Oslo, Norway*  
*\*Faculty of Health Sciences, Oslo University College, Oslo, Norway*

## 1. Introduction

Particulate air pollution is regarded as a serious health problem worldwide (WHO 2005). Reductions in the levels of particulate matter (PM) have been reported to reduce the health impact of air pollution (Heinrich et al., 1999; Clancy et al., 2002; Pope, III et al., 2009). Different epidemiological studies show surprisingly little variation in the size of the risk estimates for changes in various health outcomes with increased air pollution. However, the APHEA<sup>1</sup> and NMMAPS<sup>2</sup> studies, in which associations between PM and health outcomes were investigated in many different cities, indicated some heterogeneity in the size of risk estimates (Samet et al., 2000; Samoli et al., 2005). This heterogeneity in risk estimates could at least in part be due to the contribution of specific emissions from different sources to the PM mixture. Epidemiological studies have not compared the importance of different sources, but investigations include air pollution from industry (Ghio 2004), biomass burning (Smith-Sivertsen et al., 2009) and traffic (Brunekreef et al., 2009). In addition, there are some discrepancies in epidemiological studies with respect to the importance of the various size fractions of PM. Compared to the fine PM fraction, the coarse fraction contains most of the non-combustion PM (Brunekreef and Forsberg 2005) which may have a different health impact. Experimental studies indicate that particles from different sources may have different effects. This review will focus on the effects of PM in experimental investigations, including vehicle exhaust, road dust and wood smoke particles. The importance of particle size and composition will also be addressed. The review comprises studies on humans, animals and cells in culture.

Exposure to PM has primarily been associated with morbidity and mortality due to pulmonary and cardiovascular diseases, but other organs may also be affected (WHO 2006). A key process in the development and acute exacerbations of these diseases is inflammation.

---

<sup>1</sup> APHEA: Air Pollution and Health in Europe A

<sup>2</sup> NMMAPS: National Mortality and Morbidity of Air Pollution Study

Inflammation involves a variety of cells, including migrating immune cells that may enter inflamed organs. In the lung the first line of defence includes the phagocytosing macrophages and the epithelial cells (Figure 1). These cells may release a variety of signalling molecules, such as chemokines, cytokines, leukotrienes and prostaglandins, in addition to adhesion molecules.

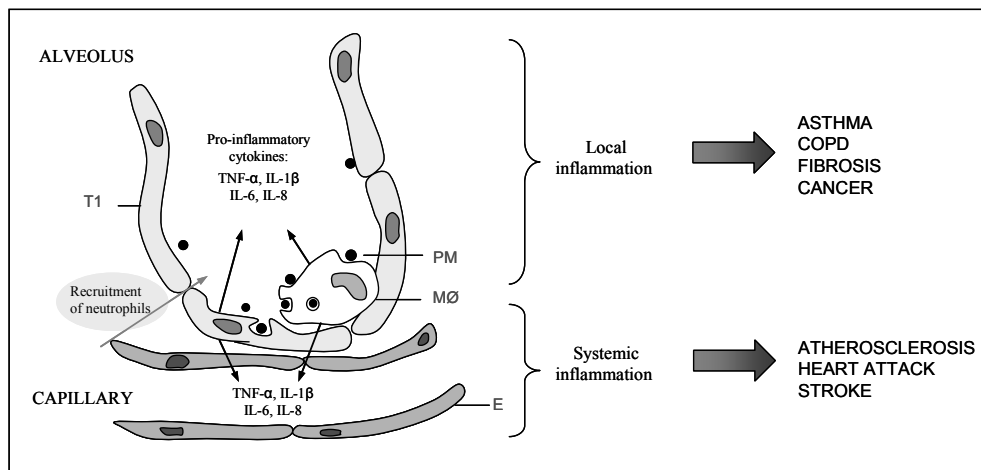


Fig. 1. Illustration of how particle-induced inflammation may affect pulmonary and cardiovascular diseases. T1 = Type 1 epithelial cell, MØ = macrophage, E = endothelial cell, PM = particulate matter (Figure from (Kocbach 2008))

Ambient particles comprise a large variety of different components, such as allergens, metals, organic compounds and microbial components. This review will focus on two groups of components commonly associated with PM, polycyclic aromatic hydrocarbons (PAH) and metals. An important question is whether particles from different sources or different components of particles trigger the release of the same signalling molecules, or whether qualitative and quantitative response differences exist. In addition to effects on the respiratory system the particles may through different mechanisms affect the cardiovascular system, to elicit or exacerbate a vascular inflammatory response. The particles or its components may also trigger cell death that *in vivo* may lead to the loss of functions or start a remodelling process of tissues. Therefore cell death will also be a part of this review, whereas DNA damage is excluded.

## 2. Traffic and wood combustion

Traffic is considered to be a major PM source in most developed countries. Emissions include particles from the tailpipe, crank case, tyre and break wear and particles generated from road pavement abrasion, sanding and resuspension (WHO 2005; Kupiainen et al., 2005; Zielinska et al., 2008; Thorpe and Harrison 2008) Combustion particles emitted from vehicles consist mainly of spherical primary carbon particles with diameters ranging from 20 to 30 nm, which tend to aggregate (Kocbach et al., 2005) (Figure 2). In contrast to larger

sized particles, like the more arbitrarily-shaped mineral particles from road wear, the small diameters of the primary carbon particles provide a relatively large surface area per mass unit. A large surface area implicates a greater potential for adsorption of various components to the particle surface, including metals, organic compounds, allergens and bacterial components like endotoxins. The contribution from residential wood combustion to ambient PM concentrations is highly dependent on the season, but in the cold season wood smoke may contribute substantially to increased levels of PM locally. Similar to combustion particles from traffic, emissions from wood stoves generally consist of aggregates of small carbon particles. However, under very poor combustion conditions spherical organic carbon particles dominate wood smoke emissions, whereas inorganic ash particles are emitted from complete high-temperature combustion (Kocbach et al., 2009). The size and composition of both traffic- and wood smoke-derived particles varies substantially in time and space, depending on the source, fuel type and post-formation processes.

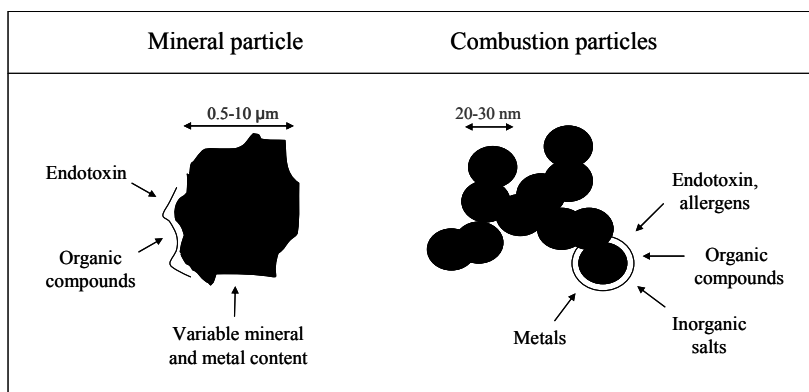


Fig. 2. Schematic figure of mineral particle from road abrasion, and combustion particles consisting mainly of aggregates of small spherical carbon particles (Figure from (Kocbach 2008))

### 2.1. Experimental studies of traffic-related particles

Experimental studies of traffic-related particles have mainly been conducted with concentrated ambient particles (CAPs) originating from motor-vehicle exhaust or collected from an urban location, and with freshly generated or sampled diesel exhaust particles (DEP). In addition, sampled road dust PM and particles of various minerals and stone types that may be found as components of road dust have been used. Studies with gasoline and biodiesel particles are emerging. Overall, this experimental research indicates that traffic-related PM may induce several changes in processes that have been linked with the development and progress of cardiopulmonary diseases. This includes increased formation of reactive oxygen species (ROS), reduction and activation of antioxidant defence, release of pro-inflammatory cytokines, increased allergy-related responses, mild though time-persistent airway inflammation, changes in autonomic nervous system regulation and changes indicative of increased risk of myocardial infarction.

### 2.1.1 Combustion particles from traffic

Most of the experimental studies on health effects of particles from tailpipe emissions have been conducted with DEP. This may be due to the fact that the PM emissions from diesel engines are greater, and thus more accessible for studies, than the PM emissions from gasoline engines. Inflammation-related changes induced by DEP in studies with human volunteers include increased levels of inflammatory markers in bronchoalveolar lavage (BAL) fluid (e.g. neutrophils, reduced levels of antioxidants, cytokines), in bronchial mucosal biopsies (e.g. cytokine expression) or in blood (e.g. platelets), increases in airway resistance, and increased number of alveolar macrophages with reduced capacity to ingest particles *in vitro* (Salvi et al., 2000; Stenfors et al., 2004; Mills et al., 2005; Tornqvist et al., 2007). An increase in the number of neutrophils in bronchial and alveolar fractions has also been detected in human volunteers exposed to CAPs (Ghio et al., 2000). Effects on the cardiopulmonary system are reported from human exposure studies using pure ultrafine (< 100 nm) carbon particles, indicating a potential of the particle core itself to induce effects. Already after 2 hours of exposure to these particles, small increases in airway resistance and reductions in carbon monoxide diffusing capacity were detected in healthy subjects, though in the absence of a detectable pulmonary inflammatory response (Pietropaoli et al., 2004). Furthermore, comparable exposure levels were associated with vascular effects, in the form of alterations in expression of adhesion molecules on blood leukocytes (Frampton et al., 2006).

Whereas the human clinical studies are limited to a few hours of observation, both short and long term effects may be studied in animals. However, most experimental studies with animals are carried out at relatively high exposure levels, limiting the usefulness of these studies compared to real life, low level, and long term exposure of humans. Using exposure levels comparable to measured ambient air concentrations, Elder and colleagues studied the effects of freshly generated vehicle exhaust emissions in old, health-compromised rats (pre-treated with LPS) in an on-road mobile laboratory (Elder et al., 2004). Both single and repeated exposures to particles significantly increased the expression of ICAM-1 on the surface of alveolar macrophages, indicative of inflammatory cell activation. Also increased plasma endothelin (Et-2) was observed, suggesting changed vascular endothelial function. Exposure to DEP is known to exacerbate allergic asthma in mouse models and exposure to DEP amplifies the allergen-induced allergic inflammation characterised by high levels of cytokines like IL-4 and IL-5 (Takano et al., 1997; Inoue et al., 2008). Moreover, exposure to diesel exhaust has been found to enhance virus-induced exacerbation of allergic inflammation in mice (Jaspers et al., 2009). Recently, Provoost and co-workers (2009) suggested that inhaled DEP modulates immune responses in the lung via stimulation of the function of pulmonary dendritic cells, known to be crucial mediators in regulation of immune responses (Provoost et al., 2010). In general, studies in animal models support findings from experimental studies with humans with regard to the potential of DEP to induce increased levels of inflammatory mediators in BAL-fluid, lung tissue and blood (Nemmar et al., 2009).

In comparison to the large amount of experimental studies conducted with DEP, only a few studies have investigated the effects of combustion particles emitted from gasoline engines. Recently, gasoline emissions were found to induce both inflammatory and vascular effects in different rodent model systems, whereas many indicators of general toxicity were not

increased, suggesting a modest health effect of the inhaled particles (McDonald et al., 2007). Intratracheally instilled diesel and gasoline PM from a range of vehicles induced similar effects on toxicity, whereas the production of the pro-inflammatory cytokine TNF was slightly higher for diesel than gasoline (Seagrave et al., 2002). The health impacts of the development of new engines and after-treatment technologies remain to be investigated. Both the application of diesel particle filters as well as using biodiesel fuel instead of diesel fuel seemed to reduce particle emissions (Rudell et al., 1999; McDonald et al., 2004). However, the few studies currently available indicate that biodiesel particles may have a greater toxic potential than diesel particles on a mass basis. For instance, biodiesel emissions induced pulmonary and systemic inflammation of similar or more severe degree than DEP in mice (de Brito et al., 2010).

*In vitro* studies have demonstrated that exposure to DEP leads to the formation of ROS and release of a range of inflammatory mediators from airway epithelial cells (Takizawa et al., 2000; Bonvallot et al., 2002). The mechanisms involved in this inflammatory response are still under investigation, but DEP has been found to trigger phosphorylation of mitogen activated protein kinases (MAPK) and activation of several transcription factors that are known to regulate pro-inflammatory mediator release, including nuclear factor  $\kappa$ B (NF $\kappa$ B), activator protein-1 (AP-1) and Stat 3, (Takizawa et al., 2000; Bonvallot et al., 2002; Cao et al., 2010). The expression of the epidermal growth factor receptor (EGFR) is also increased during DEP exposure, and EGFR is believed to play a key role in the early signalling pathways activated by DEP (Cao et al., 2010). Interestingly, all these signalling pathways are also activated in human volunteers exposed to DEP (Pourazar et al., 2005; Pourazar et al., 2008). Another possible mechanism for the DEP-induced effects was recently proposed by Jardim and co-workers, who found altered micro-RNA expression in bronchial epithelial cells after DEP exposure. Micro-RNAs are small non-coding RNAs that have been suggested to be important in maintaining the lung in a disease-free state through regulation of gene expression. The micro-RNAs affected by DEP exposure could possibly be involved in regulation of inflammatory response pathways (Jardim et al., 2009).

Although airway epithelial cells are the most commonly applied model for *in vitro* studies of DEP, a range of other mono- and co-cultures of different cell types have also been applied. DEP for instance functionally activated dendritic cells, and caused the release of a range of inflammatory mediators (Porter et al., 2007). Moreover, human bronchial epithelial cells activated by DEP induced maturation of dendritic cells via thymic stromal lymphopoietin (Bleck et al., 2008). DEP and the organic extracts of DEP have also been reported to induce apoptosis and necrotic cell death in macrophages through the generation of ROS (Hiura et al., 1999). The responses of epithelial cells to DEP seem to be amplified in the presence of monocytes (Chaudhuri et al., 2010). Such a cellular interaction has previously also been demonstrated with pure carbon particles that are commonly used as model particles for DEP (Drumm et al., 2000). With respect to cardiovascular effects of combustion particles, a co-culture model consisting of primary lung and heart cells from rats showed that soluble mediators released from lung cells after exposure to pure carbon particles induced release of inflammatory mediators from cardiac cells, supporting the hypothesis that particle-induced cardiac inflammation and disease may involve lung-derived mediators (Totlandsdal et al., 2008).

With respect to the influence of the physicochemical properties of DEP on the inflammatory responses, the importance of the organic fraction has been investigated in several studies using various solvent extracts. In human bronchial epithelial cells organic extracts of DEP induced the formation of ROS and the release of the inflammatory mediator GM-CSF to a similar extent as the native DEP, whereas the stripped carbonaceous core was less potent (Bonvallot et al., 2001; Baulig et al., 2003). Similarly, Ohtoshi and co-workers showed that DEP induced the release of GM-CSF and IL-8 from human airway epithelial cells, whereas charcoal and graphite, used as models for the carbon core of DEP, did not affect GM-CSF or IL-8 release (Ohtoshi et al., 1998). However, another study reported that DEP-induced cytotoxicity in promyelocytic cells was due to the particle core of DEP rather than the organic fraction (Matsuo et al., 2001). Taken together the *in vitro* studies conducted with DEP demonstrate that the particle core itself as well as organic compounds adsorbed to the particle surface may contribute to the inflammatory effects.

Organic extracts of DEP have been found to influence a wide variety of endpoints, including increased production and release of the chemokines IL-8 and RANTES from peripheral blood mononuclear cells (PBMCs) (Fahy et al., 1999) and oxidative stress followed by cell death in epithelial cells and macrophages (Li et al., 2002). In the latter study, epithelial cells seemed to be more susceptible to the cytotoxic effects than macrophages. DEP organic extracts also increased the IL-4 production and histamine release from human basophils (Devouassoux et al., 2002). DEP favoured Th2 cell recruitment by immune cells from allergic patients by differentially regulating the Th2-recruiting chemokine MDC and the Th1 recruiting chemokine IP-10 (Fahy et al., 2002). The specific organic compounds that account for the biological effects induced by DEP and its extracts remain to be determined. Some likely candidates have however been identified, including PAH like benzo[a]pyrene (B(a)P), phenanthrene and 1-nitropyrene (1-NP) (see paragraph on PAH) (Baulig et al., 2003). Another study fractionated organic DEP extracts into different polarity fractions and identified that the quinone-rich polar fraction was more potent than the more studied aromatic fraction (PAH) in inducing ROS and apoptotic cell death, whereas the aliphatic fraction had no effect (Xia et al., 2004).

### 2.1.2 Road dust particles

Sampled road dust particles have been observed to elicit pro-inflammatory effects in cells *in vitro* (Hetland et al., 2000; Holopainen et al., 2004; Karlsson et al., 2006). These particles, originating from road wear, sanding or resuspension of settled dust, consist mainly of crystalline or amorphous minerals. The highest concentrations of these particles occur during dry winter or spring days, particularly in countries using studded tires. Effects of mineral particles from stone often used in road pavement have been investigated in some detail in animal and cell studies to determine the importance of mineral structure or released metals (Hetland et al., 2001b; Ovrevik et al., 2005). The crystalline structure appears to be important for the toxicity of mineral particles (Guthrie, Jr. 1997; Warheit 2001), and the amorphous forms of silica are less toxic (Fubini and Hubbard 2003). It has not been possible to identify any specific mineral that explains the potential of the most toxic particles, but particles with a high content of feldspar minerals seemed to be less potent than other mineral particles (Ovrevik et al., 2005; Becher et al., 2007). Some studies indicate that particle-associated ROS does not correlate with pro-inflammatory or apoptotic responses to

mineral particles (Ovrevik et al., 2006), but that cellular ROS may be involved (Becher et al., 2007), as has been observed with combustion particles. Cellular uptake did not seem necessary for pro-inflammatory responses, but seemed to be involved in apoptosis (Refsnes et al., 2006). The pro-inflammatory responses to quartz seemed to involve to some extent the same signalling pathways as activated by carbon or other particle components, e.g. EGF-receptor and MAPK (Ovrevik et al., 2005). The importance of these pathways in pro-inflammatory responses to asbestos has been reported (Mossman et al., 2006), but has not been shown for minerals found in road dust. To what extent mineral particle-associated metals are involved in the responses is still unclear. Some studies indicate that metals are not of major importance, whereas others report that metals in mineral particles contribute to their effects (Hetland et al., 2001a; Aust et al., 2002; Ovrevik et al., 2006).

## 2.2 Residential wood combustion particles

In a human clinical study, exposure to wood smoke at levels relevant for indoor exposure in developed countries was linked with an increase in markers of inflammation and oxidative stress in the lower airways. Analyses of the blood and urine of the volunteers indicated that wood smoke exposure also was associated with systemic inflammation, blood coagulation and lipid peroxidation (Barregard et al., 2006). Preliminary data from another inhalation study showed increased levels of glutathione due to wood smoke exposure, indicating activation of the antioxidant defence, possibly due to oxidative stress (Boman et al., 2006; Jokiniemi et al., 2008). In subchronic exposure models wood smoke has been linked with modest effects on both pulmonary and systemic inflammation (Burchiel et al., 2005; Reed et al., 2006; Barrett et al., 2006). Furthermore, Ramos et al. (2009) reported that subchronic exposure to wood smoke produced pulmonary effects similar to tobacco smoke in Guinea pigs. These effects included a moderate alveolar inflammation with an influx of macrophages and neutrophils, accompanied by increased apoptosis in macrophages. In accordance with studies on particles from other sources, also wood smoke particles caused the formation of ROS, lipid peroxidation, activation of the nuclear transcription factor NF $\kappa$ B and release of the pro-inflammatory mediator TNF- $\alpha$  in macrophages (Leonard et al., 2000).

In a co-culture of monocytic and epithelial cell lines, it has been demonstrated that the organic compounds adsorbed to wood smoke particles accounted for most of the inflammatory response (Kocbach et al., 2008a). Although PAH are possible candidates for inflammatory effects of particulate matter, the content of PAHs did not seem to account for the effects induced by the organic extract in the monocytes (Kocbach et al., 2008b). In order to identify the biologically active organic compounds of organic extracts of wood smoke particles Kubatova et al. (2006) applied fractionation of organic extracts of wood smoke particles in combination with chemical analysis, and identified the mid-polarity and non-polar compounds, including oxy-PAHs, as inducers of oxidative stress in a macrophage cell line (Kubatova et al., 2006). Since the organic chemistry of wood smoke particles varies considerably with the combustion temperature, it is important to keep in mind that also other groups of organic compounds are likely to contribute to the biological effects induced by PM from different combustion conditions. Recently, it has been demonstrated that particles from different combustion conditions induced differential pro-inflammatory response patterns in a macrophage cell line. Particles from poor combustion seemed more cytotoxic than particles from more complete combustion conditions (Jalava et al., 2010). The

physicochemical properties of emitted wood smoke particles strongly depend on the combustion conditions. Further studies are needed in which the influence of combustion conditions on the biological effects of wood smoke particles is investigated (Kocbach et al., 2009).

### 2.3 Vehicle exhaust versus wood smoke particles

Relatively few studies have compared the inflammatory effects induced by traffic-derived particles and wood smoke. In a contact co-culture consisting of monocytes and pneumocytes particles from these two sources induced different response patterns. Traffic-derived particles elicited higher levels of IL-6 and IL-8 as compared to wood smoke particles, whereas wood smoke induced a greater reduction in proliferation (Kocbach et al., 2008a). Similarly, inhalation of particles from wood smoke and diesel induced to some extent different responses in rats with respect to both toxicity and inflammation, partly dependent on gender (Seagrave et al., 2005). As described above the mechanisms involved in the inflammatory responses induced by DEP seem to involve activation of EGFR, activation of MAPK and activation of different transcription factors like NF $\kappa$ B, AP-1 and Stat3. Although the mechanisms involved in the wood smoke particle-induced inflammation have been less well characterised, it seems likely that some of the same pathways may be activated. The organic fraction seems to be of importance for the inflammatory effects induced by particles from both sources, although it is likely that different organic compounds are involved. There are, however, experimental *in vivo* studies suggesting that the organic fraction is not of major importance for inflammatory effects (Gerlofs-Nijland et al., 2009; Happo et al., 2010). Little is known about how the metal content influences the inflammatory responses induced by particles from traffic and wood smoke. However, metals may contribute to the inflammatory responses, as has been shown for ambient PM (Gilmour et al., 1996; Kodavanti et al., 2008). Regardless of particle source, it should also be noticed that endotoxins adsorbed to the particle surface in the atmosphere are potent inducers of inflammatory responses, and may account for more than 70 % of the release of inflammatory mediators in various cell systems (Becker et al., 2005; Kocbach et al., 2008b). Biological components have also been shown to contribute to the inflammatory responses induced by PM in healthy volunteers (Alexis et al., 2006).

### 3. Particle size

Since the trimodal distribution of particle size in ambient air has important implications for exposure and effects in humans, the importance of size for particle-induced lung inflammatory effects has been scrutinised. Model particles with defined chemical composition as well as ambient particles from nano- to micrometer size range have been studied. The potential of different model particles to induce adverse biological responses/adverse health effects, in particular inflammation, has been assessed in various animal studies and some *in vitro* studies. Most of these studies have shown that upon instillation in animals, small-sized particles have a much greater potential to induce lung inflammation than larger particles of similar composition. However, when adjusting for the relatively larger surface area of small-sized particles compared to that of larger particles, the differences in responses have tended to disappear. Thus it has been hypothesised that particle surface area is crucial in driving pathological changes, including inflammatory

responses (Oberdorster, 1996). In support of this, Tran et al. (2000) showed that total particle surface area in the lung was the dominant metric, when quantifying the neutrophilic inflammation after exposure to different low-solubility, low-toxicity particles as TiO<sub>2</sub> and BaSO<sub>4</sub> in inhalation experiments with rats. Similar studies with ultrafine and fine carbon black or polystyrene corroborated that the smaller particles induced a much stronger lung inflammation *in vivo* or pro-inflammatory responses *in vitro* (Brown et al., 2001; Donaldson et al., 2002; Monteiller et al., 2007). These differences could also be attributed to the differences in surface area. Even with different nano-sized particles (10 to 45 nm carbon), the inflammatory potential of the particles was related to the surface area (Stoeger et al., 2006). Several studies suggest a threshold dose for the particle surface area-dependent effects (Tran et al., 2000; Stoeger et al., 2006; Monteiller et al., 2007). The surface area notion has, however, been challenged by Warheit and co-workers (Warheit et al., 2006; Warheit et al., 2007a), finding that ultrafine TiO<sub>2</sub> and quartz was not more potent than the respective fine particles, after installation in rat lungs. The authors conclude that the surface reactivity corresponded better to the responses than particle size and surface area. However, their study of TiO<sub>2</sub>-particles did not exclude that the crystallinity of the particles may be of importance. In a recent article Sager et al. (2008) suggested that the results of Warheit et al. (Warheit et al., 2007b) with TiO<sub>2</sub> particles, could be the result of insufficient dispersion of the ultrafine particles. By using a more appropriate dispersion for ultrafine TiO<sub>2</sub> particles, Sager et al. (2008) observed a much stronger response of these particles than of fine ones. However, after adjusting for surface area, the ultrafine TiO<sub>2</sub> particles were only slightly more inflammatory than the fine-sized particles. This result was not specific to TiO<sub>2</sub>, since ultrafine versus fine carbon black showed similar response patterns as TiO<sub>2</sub> (Sager and Castranova, 2009). Different *in vitro* studies with lung cells have supported a role of particle surface area for inflammatory responses. Hetland et al. (2001b) exposed human lung epithelial cells to different size fractions of quartz and observed a linear relationship between cytokine responses and particle surface area. However, mineral particle-induced apoptosis (a form of cell death) seemed mostly to depend on particle size, whereas composition and surface reactivity appeared to be more important for the pro-inflammatory potential of the particles (Schwarze et al., 2007).

Even though particle size and surface area may be important for triggering cellular responses, several studies suggest that surface reactivity may override the role of the former metrics. A study on rats exposed to well characterised particles of diesel, carbon black and silica supports the importance of surface chemistry compared to ultrafine size in biological effects (Murphy et al., 1998). The studies of Duffin et al. (2007) and Monteiller et al. (2007) support the notion on the importance of surface reactivity. Monteiller showed that similarly sized TiO<sub>2</sub> elicited greater effects compared to carbon black, but less than DQ12, a type of quartz. Furthermore, in the Monteiller study the response to TiO<sub>2</sub> exposure was greater than the response to carbon black, but less than to DQ12, indicating that surface reactivity is important in addition to surface area (Monteiller et al., 2007).

Overall, existing literature suggests that surface area is an important determinant for lung inflammation and health effects in the airway system. For low-toxicity particles the surface area might be the strongest driving force, whereas for high-toxicity particles the surface reactivity may dominate over the importance of particle surface area. Soluble factors may

modify the importance of surface reactivity. For example, the pronounced effect of the bacteria toxin LPS has been thoroughly investigated (Becker et al., 2002). Recently this response has been linked to an IL-1/inflammasome-mediated mechanism (Giamarellos-Bourboulis et al., 2009). The current state of knowledge might question the use of mass as the most appropriate metric and underlines that the surface area may be a better or additional metric, at least for low toxicity particles.

With respect to inflammation and cardiovascular effects, the importance of particle size has been much less studied. Ultrafine particles of various compositions may be translocated from the airways to the cardiovascular system (Nemmar et al., 2002). The extent to which this occurs is unclear and might be small (Kreyling et al., 2002), thus questioning the importance of direct nano-sized particle exposure for cardiovascular responses. An alternative hypothesis to translocation of ultrafine particles as a driving force for cardiovascular inflammation, states that particle-induced lung inflammation is reflected in a systemic response, which then triggers the cardiovascular system. If this were the case, the lung inflammatory response would be decisive and depend on the particle surface area and reactivity. A third possibility is that particles are carriers of metals or organic substances, which may be translocated from the lung to the cardiovascular compartment. Since small particles with large surface area could bind larger amounts of various substances, they would have a greater potential to give systemic effects than larger particles based on this hypothesis. Presently, it is unclear to what extent these different mechanisms operate eliciting cardiovascular inflammation. The studies of Totlandsdal and colleagues support an indirect mechanism, with the release of inflammatory mediators from the lung reaching the heart and initiating a pro-inflammatory response (Totlandsdal et al., 2008). Ansteinsen et al. observed that metals that may be attached to particles, have the potential to trigger cytokine release from cardiac cells (Ansteinsen et al., 2009). A fourth possibility through activation of nerve cell reactions is not discussed here.

## **4. Particle components**

Several experimental studies have attributed biological effects of combustion particles to adsorbed organic compounds and metals. Therefore this review focuses on two groups of components commonly associated with particles from traffic and residential wood smoke, PAH and metals. The content of these particle-associated components varies significantly in time and space, as it strongly depends on the type and condition of the emitting source. Biological effects of particle-associated components are commonly studied by carrying out the exposure with particle extracts prepared with various solvents (see above), which subsequently may be fractionated and analysed chemically. These studies may be further supported by studies carried out with pure particle components, administered singly as well as in combination.

### **4.1 PAH**

Following their release PAH will undergo a number of chemical modifications in the air that modify their biological properties. The type and degree of modification depends on the type and level of the chemical components available as well as the temperature and time to allow for reactions (Vione et al., 2004a; Vione et al., 2004b; Vione et al., 2006). Some of the reactions

take part directly after leaving the primary source; others take place in the atmosphere. PAH and oxy-PAH are emitted as by-products of almost every type of combustion technology in urban environments, including diesel- and petrol-fuelled motor vehicles, residential heating, fossil fuel combustion in energy and industrial processes, municipal and medical incinerators. The oxy-PAH originate from reactions between PAH and hydroxyl radicals, nitrate radicals, other organic and inorganic radicals and ozone or from photo-oxidation of PAH by singlet molecular oxygen (Andreou and Rapsomanikis 2009). However, the secondary combustion of diesel soot and associated compounds during after-treatment introduces the formation of new pollutants including various nitro-PAH. The stereo-isomers formed differ from those formed upon atmospheric nitration of PAH (Heeb et al., 2008).

Since the PAH are lipophilic, they are easily transferred to hydrophobic components of the surfactant or into the lipid layer of the cellular plasma membrane. PAH seem to induce their effects through activation of the aryl hydrocarbon receptor (AhR) and the AhR nuclear translocator (Arnt), followed by the upregulation of Cyp1A1 and 1B1. The Cyp metabolise PAH, leading to the formation of ROS and reactive metabolites that may damage macromolecules. Recent findings on single PAH indicate that, in addition, the lipophilic compounds may penetrate into the plasma membrane and change properties linked to lipid fluidity or ion transport. Single PAH may modulate the composition of plasma membrane microdomains (rafts) in a specific way, affecting inter- and/or intracellular signalling (Tekpli et al., 2010a; Tekpli et al., 2010b). This seems to cause changes in ion transport of  $K^+$  and  $Ca^{2+}$  and change intracellular pH by activating ion channels (NHE1) as well as via lysosomal rupture. However, the importance of these processes with regard to the whole mixture of organic compounds in the absence or presence of particles is not known.

Some PAH may react directly with macromolecules in tissues, whereas others are converted by enzymes into reactive metabolites within the cells. PAH may elicit pro-inflammatory effects in the lung, possibly through ROS formation (Nel et al., 2001; Xia et al., 2004). Benzo[a]pyrene (B[a]P), one of the important aromatic hydrocarbons in DEP, has been reported to elicit over-expression of keratinocyte chemo-attractant (KC), the murine functional analog of IL-8 in lung. It also triggered the recruitment of neutrophils in bronchoalveolar lavage fluids (Podechard et al., 2008). Oxygen, nitrogen radicals and reactive electrophilic metabolites of the PAH can attack or covalently bind to nucleophilic sites on cellular macromolecules within the cell. In this way several cellular macromolecules including lipids, proteins and DNA may be modified and various damage signalling pathways may be triggered. PAH that have entered cells may bind to cellular receptors such as the aryl hydrocarbon receptor (AhR) and indirectly modify the cellular response to more classical hormone receptors such as estrogen receptors (ER) and EGFR. These types of classical cellular signals are known not only to be involved in cell survival and proliferation, but also in the triggering of inflammatory responses as well as cell death pathways, much depending on the size, duration and the site of formation of the initiating signal.

PAH like B[a]P, phenanthrene and 1-nitropyrene induced similar responses as DEP extracts, when administered to epithelial cells in concentrations corresponding to DEP extracts (Baulig et al., 2003). Several other DEP related chemical compounds such as pyrene, naphthoquinone and phenanthraquinone may also affect pulmonary inflammation (Bommel

et al., 2000; Bommel et al., 2003; Xia et al., 2004; Inoue et al., 2007), but further studies are necessary to clarify their role in the adverse effects induced by DEP.

In order to understand the effect of PAH associated with PM, the effect of some of the most common PAH have often been studied singly in cell culture experiments. The bronchial epithelial cell line (BEAS-2B) released large amounts of IL-8 in response to nitro-PAH (Ovrevik et al., 2010). Nitro-PAH and their metabolite amino-PAH induced both qualitatively and quantitatively different cytokine/chemokine expression profiles. Whereas 1-nitropyrene and 3-nitrofluoranthrene elicited predominantly an IL-8 release their corresponding amines predominantly induced the release of RANTES (Ovrevik et al., 2010). It has been suggested that many inhaled environmental toxic components may trigger the release of inflammatory cytokines via an initial binding to the AhR (Wong et al., 2010). B[a]P that binds to the AhR, increased the mRNA expression and secretion of CCL1 in primary human macrophage culture. Moreover, in exposed mice the level of TCA3 (mouse ortholog of CCL1) in the lung was increased (N'diaye et al., 2006). 1-NP is known to bind to AhR, induce ROS production and activate MAPK (Asare et al., 2008) as well as NFkB (Pei et al., 2002). However, the precise roles for AhR, MAPK and NFkB in the 1-NP-induced IL-8 release are presently not clarified. ROS and nitrogen oxides are often cited as possible mediators in these reactions. Alternatively these molecules lead to a less specific activation of kinases, e.g. by inactivation of their respective phosphatases through binding or oxidizing their thiol groups. Most probably combinations of several factors are needed for the induction of cytokine responses. Often activation of the same cell signalling pathways are found to be involved in eliciting pro-inflammatory effects as well as cell death. Recent unpublished findings by our group suggest that the DNA damage induced by many of the PAH may change the inflammatory cell signalling response into cell cycle arrest, DNA damage repair or apoptotic cell death (Oya et al., personal communication). The reason why PM rich in PAH induces less cytokines than expected from 1-NP exposure alone, may be that cells interact with other PAH, giving rise to DNA damage that via p53 changes the transcriptional activity of NFkB.

## 4.2 Metals

An increasing number of studies have indicated that different transition metals may act as possible mediators of particle-induced injury and inflammation (Dreher et al., 1997; Molinelli et al., 2002; Pagan et al., 2003; Schaumann et al., 2004; Chen and Lippmann 2009). The focus has often been on transition metals such as iron (Fe), vanadium (V), nickel (Ni), chromium (Cr), copper (Cu) and zinc (Zn) on the basis of their ability to generate reactive oxygen species (ROS) in biological tissues. Most of the evidence pointing to the biological effects of metals originates from studies in animal models and cell cultures. However, in these systems pure metals have been applied in concentrations that are much higher than levels relevant for environmental exposures. Studies using PM containing multiple metals have reported effects that seem to be related to the PM metal content, despite low metal levels. However, it is difficult to determine the roles played by the individual metals in these complex PM mixtures (Chen and Lippmann 2009).

In relatively few studies human volunteers have been exposed to PM analysed for elemental composition, followed by an analysis of the extent of correlation between different metals

and biological responses. A clinical study of CAPs inhalation by Ghio et al. (2000) has been reanalyzed to determine the correlation between the nine most abundant elements and the cellular and biochemical endpoints (Huang et al., 2003). In the correlation analysis a Fe/Se/sulfate factor was associated with increased percentage of neutrophils in BAL fluid, and a Cu/Zn/V factor with increased blood fibrinogen. In another study metal-rich ambient particles PM<sub>2.5</sub> from a smelter area (Hettstedt) induced a more distinct airway inflammation and increased generation of oxidant radicals in healthy subjects as compared to samples from a non-industrialized area (Schaumann et al., 2004). PM samples with contrasting metal content collected in Utah Valley before closure, during closure and after reopening of steel mill plants have been applied in a human bronchial instillation study to investigate whether soluble components or ionizable metals could influence the biological effects. PM extracts were instilled into the bronchus of human volunteers, and phagocytic cells were obtained after 24 hours. The inflammatory response in the lungs of human volunteers was greater after exposure to aqueous extract collected before the closure and after the reopening as compared to during the shutdown of the plant (Ghio and Devlin 2001). With respect to metal content, the Zn content was 61 and 2 times higher in the aqueous extract from PM before closure as compared to the extracts from during and after reopening, respectively. In contrast, the Fe content was 5 times higher in the extract from after as compared to before the closure. Ni and V were only present in trace amounts and did not differ from year to year (Frampton et al., 1999; Dye et al., 2001; Ghio and Devlin 2001). In a clinical study using single metals rather than complex mixtures, soluble V and Cr instilled into human volunteers caused significant increases in oxidative stress, measured as 8-oxodG concentrations in lymphocytes, whereas other soluble metals (Fe, Ni, Cu and Pt) were not associated with oxidative stress (Sorensen et al., 2003).

The few *in vivo* animal studies of the response to ambient PM that investigated the contributions from specific air pollution components, either as an individual compound or as part of a mixture, may suggest that some of the PM components are more toxic than others (Chen and Lippmann 2009). For instance, inhalation of CAPs induced oxidative stress in the lung and heart of rats, but not in the liver. Using single-component regression analysis, the content of Fe, Mn, Cu and Zn was strongly associated with the oxidative stress generated in the lung, whereas Fe, Al, Si and Ti was associated with the effects observed in the heart (Gurgueira et al., 2002). Another study indicated that iron-catalyzed generation of ROS may not be a predominant mechanism of PM<sub>2.5</sub>-induced ROS formation (Shukla et al., 2000). However, inhalation of iron particles induced a decrease in total antioxidant capacity and an increase in BAL proteins and IL-1 $\alpha$  levels in rat lungs (Zhou et al., 2003). The water soluble Zn associated with PM was suggested to be one of the causal components involved in PM-induced cardiac effects in a study comparing instillation of particles with different levels of Zn, aquatic PM extracts and zinc sulphate in rats (Kodavanti et al., 2008). Moreover, the soluble fraction of an urban air particulate sample (EHC-93) induced lung cell injury and inflammation after instillation into mouse lung. Since a metal mixture containing all the metals in the sample except Zn induced minimal lung effects, Zn was suggested to be the toxic factor in the lung response (Adamson et al., 2000).

When PM collected in a smelter area (Hettstedt) with high levels of Zn, Mg, Pb, Cu, Cd and As was instilled to ovalbumin-sensitised mice it increased the allergic responses, in contrast

to PM with lower metal content collected in another area (Zerbst) in the same region (Gavett et al., 2003). However, PM from both areas significantly increased lung injury parameters and the levels of pro-inflammatory cytokines. This indicates that the metal composition of the ambient PMs may have greater influence on the allergic respiratory disease than other endpoints. The role of chemical composition of PM collected in different European cities dominated by pollution from traffic has been investigated in a study focusing on respiratory inflammation (Steenberg et al., 2006). By application of cluster analysis, in which chemical constituents of PM were clustered based on the overall response pattern in the bioassays, the cluster containing Ti, As, Cd, Zn, Pb, Hg and organics derived from several combustion processes, were primarily associated with adjuvant activity for respiratory allergy. Clusters of crustal materials (containing Ca, Al, Mg, Fe, Ba, Cu, Cr) were predominately associated with measures of inflammation and acute toxicity. Another study instilled fine PM collected in the US into rat lung, and reported that metal oxides, transition metals (Pb, Mn, Cu, Se, Zn and As), but also carbon (EC, OC) and the organic compounds hopanes and steranes, were important predictors of cytotoxic and inflammatory responses (Seagrave et al., 2006).

The extracts of Utah Valley PM with contrasting metal content have also been used *in vivo* in animal studies and in cell cultures. When aqueous extracts of the Utah PM with high metal content (open plant) were instilled in rats they induced a significant pulmonary injury and neutrophilic inflammation (Dye et al., 2001). Cu, Zn, Fe, Pb, As, Mn and Ni, could have contributed to these effects, in addition to sulfate and cationic salts. In human airway epithelial cells extracts of PM with low levels of metals (closed plant), did not induce cytotoxicity, and only generated a minimal cytokine and ROS response compared to extracts from PM collected before and after the strike with higher metal content (Frampton et al., 1999). Overall, the human epidemiological, clinical and animal toxicological studies of the Utah Valley PMs show a strong qualitative coherence, that identifies soluble metals as important components in PM related health effects.

Residual oil fly ash (ROFA) is a complex mixture of sulphate, nitrate and metals, such as Fe, V and Ni, with the majority of these metals present in high concentrations as water-soluble salts. The ROFA leachate, containing Ni and V induced lung injury (Dreher et al., 1997; Kodavanti et al., 1998). Although BAL inflammatory markers (neutrophil influx, protein leakage, etc) were similar in ROFA- and metal (Ni and V)-exposed animals, gene expression profile studies of inflammation, remodelling and stress response genes, suggest that there are more complex interactions between metal constituents than previous studies have implicated (Nadadur and Kodavanti 2002). Furthermore, Zn has also been found to be responsible component in different oil combustion emission particles (Kodavanti et al., 2002). ROFA-associated transition metals have also demonstrated immediate and delayed cardiovascular responses (Watkinson et al., 1998).

The mechanisms involved in the biological responses induced by metals relevant for PM-induced effects (Zn, V, Cu, As, Ni, Cr and Fe) have been studied in a range of lung- and heart-related cellular systems. Metals in ambient air PM may alter the intracellular redox state with subsequent modulation of the activity of several transcription factors, including NF- $\kappa$ B and AP-1 (Chen and Lippmann 2009). These factors are critical for the expression of a

variety of pro-inflammatory cytokines and adhesion proteins. Several studies suggest that MAPK such as ERK, JNK and p38 mediate metal-induced expression of inflammatory proteins in lung cells and also in cardiac cells (Samet et al., 1998; Lag et al., 2005; Kim et al., 2006; Ansteinsson et al., 2009). Furthermore, activation of MAPKs by the metals As, Cu, V and Zn have been suggested to be mediated through the EGFR (Wu et al., 1999). V and Zn seem to induce tyrosine phosphate accumulation by inhibiting protein tyrosine phosphatases and thereby also inhibiting the dephosphorylation process, whereas other mechanisms might be involved in As-induced MAPK activation (Samet et al., 1999). The mechanisms involved in the EGFR activation induced by Zn have been studied in great detail in epithelial lung cells (Samet et al., 2003; Tal et al., 2006). From the *in vitro* studies of PM the metals Zn, V, Cu and As seem more important for elucidating biological responses than for instance Fe. Although Fe induces production of ROS both *in vivo* and *in vitro*, it does not seem to play an important role for lung injury when applied in a mixture of many soluble metals, such as in ambient PM or ROFA (Chen and Lippmann 2009).

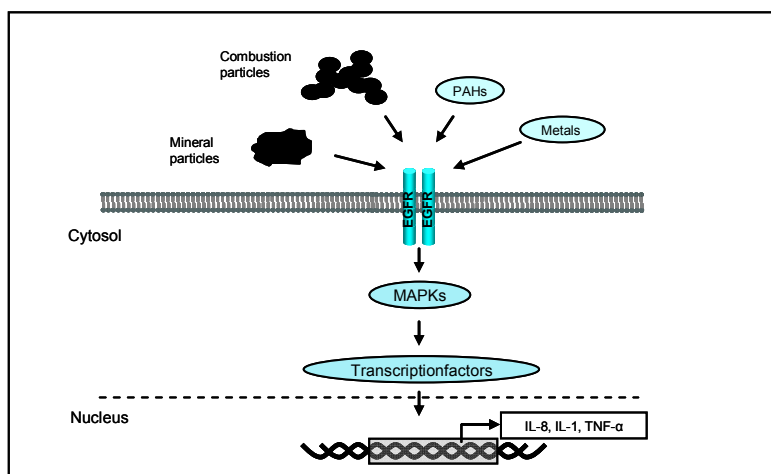


Fig. 3. Schematic figure of signalling pathways activated by particles from various sources and their components. Arrows do not necessarily indicate direct activation, but may mask involvement of other molecules, receptors etc. See text for specification of the involved MAPK and transcription factors.

## 5. Relationship between different types of particles and components with respect to pro-inflammatory responses

Identifying constituents and fractions of PM that play a critical role in eliciting health effects could provide more cost-efficient abatement strategies for the improvement of air quality. Given the relative similarity of risk estimates in epidemiological studies it is conceivable that particles of different composition might trigger similar cellular inflammatory reactions. Such a common response may be elicited through the activation of the same signalling pathways. One such pathway is the EGFR/ MAPK pathway. The activation of this pathway has been detected in bronchial epithelium of human volunteers after diesel exhaust exposure

(Pourazar et al., 2008). Similarly, this pathway has been reported to be activated after exposure of lung cells to particles or commonly occurring components of particles, including a mineral particle, a carbonaceous particle, metals and a nitro-PAH (Ovrevik et al., personal communication). The results indicate a coherence of responses of lung cells and humans exposed to particles. This mode of action is depicted in figure 3. Just how particles and their components might activate the EGFR, still needs to be elucidated.

## 6. Acknowledgements

The financial support from the Research Council of Norway (programme MILGENHEL) is gratefully acknowledged.

## 7. References

- Adamson, I. Y.; Prieditis, H.; Hedgecock, C. & Vincent, R. (2000). Zinc is the toxic factor in the lung response to an atmospheric particulate sample. *Toxicol Appl. Pharmacol.* 166, 111-119
- Alexis, N. E.; Lay, J. C.; Zeman, K.; Bennett, W. E.; Peden, D. B.; Soukup, J. M.; Devlin, R. B. & Becker, S. (2006). Biological material on inhaled coarse fraction particulate matter activates airway phagocytes in vivo in healthy volunteers. *J Allergy Clin Immunol.* 117, 1396-1403
- Andreou, G. & Rapsomanikis, S. (2009). Origins of n-alkanes, carbonyl compounds and molecular biomarkers in atmospheric fine and coarse particles of Athens, Greece. *Sci Total Environ.* 407, 5750-5760
- Ansteinsson, V.; Refsnes, M.; Skomedal, T.; Osnes, J. B.; Schiander, I. & Lag, M. (2009). Zinc- and copper-induced interleukin-6 release in primary cell cultures from rat heart. *Cardiovasc. Toxicol.* 9, 86-94
- Aust, A. E.; Ball, J. C.; Hu, A. A.; Lighty, J. S.; Smith, K. R.; Straccia, A. M.; Veranth, J. M. & Young, W. C. (2002). Particle characteristics responsible for effects on human lung epithelial cells. *Res Rep Health Eff. Inst.* 1-65
- Barregard, L.; Sallsten, G.; Gustafson, P.; Andersson, L.; Johansson, L.; Basu, S. & Stigendal, L. (2006). Experimental exposure to wood-smoke particles in healthy humans: effects on markers of inflammation, coagulation, and lipid peroxidation. *Inhal Toxicol.* 18, 845-853
- Barrett, E. G.; Henson, R. D.; Seilkop, S. K.; McDonald, J. D. & Reed, M. D. (2006). Effects of hardwood smoke exposure on allergic airway inflammation in mice. *Inhal Toxicol.* 18, 33-43
- Baulig, A.; Garlatti, M.; Bonvallot, V.; Marchand, A.; Barouki, R.; Marano, F. & Baeza-Squiban, A. (2003). Involvement of reactive oxygen species in the metabolic pathways triggered by diesel exhaust particles in human airway epithelial cells. *Am J Physiol Lung Cell Mol Physiol.* 285, L671-L679
- Becher, R.; Bucht, A.; Ovrevik, J.; Hongso, J. K.; Dahلمان, H. J.; Samuelsen, J. T. & Schwarze, P. E. (2007). Involvement of NADPH oxidase and iNOS in rodent pulmonary cytokine responses to urban air and mineral particles. *Inhal Toxicol.* 19, 645-655

- Becker, S., Fenton, M.J., & Soukup, J.M. (2002). Involvement of microbial components and toll-like receptors 2 and 4 in cytokine responses to air pollution particles. *Am J Respir Cell Mol Biol*. 27(5), 611-8.
- Becker, S.; Mundandhara, S.; Devlin, R. B. & Madden, M. (2005). Regulation of cytokine production in human alveolar macrophages and airway epithelial cells in response to ambient air pollution particles: further mechanistic studies. *Toxicol Appl. Pharmacol.* 207, 269-275
- Bleck, B.; Tse, D. B.; Curotto de Lafaille, M. A.; Zhang, F. & Reibman, J. (2008). Diesel exhaust particle-exposed human bronchial epithelial cells induce dendritic cell maturation and polarization via thymic stromal lymphopoietin. *J Clin Immunol.* 28, 147-156
- Boman, B. C., Pagels, J., Massling, A. and others 2006. Controlled human chamber exposure studies of biomass combustion aerosols. In: 7th International Aerosol Conference IAC 2006, St. Paul, Minnesota..
- Bommel, H.; Haake, M.; Luft, P.; Horejs-Hoeck, J.; Hein, H.; Bartels, J.; Schauer, C.; Poschl, U.; Kracht, M. & Duschl, A. (2003). The diesel exhaust component pyrene induces expression of IL-8 but not of eotaxin. *Int Immunopharmacol.* 3, 1371-1379
- Bommel, H.; Li-Weber, M.; Serfling, E. & Duschl, A. (2000). The environmental pollutant pyrene induces the production of IL-4. *J Allergy Clin Immunol.* 105, 796-802
- Bonvallot, V.; Baeza-Squiban, A.; Baulig, A.; Brulant, S.; Boland, S.; Muzeau, F.; Barouki, R. & Marano, F. (2001). Organic compounds from diesel exhaust particles elicit a proinflammatory response in human airway epithelial cells and induce cytochrome p450 1A1 expression. *Am J Respir. Cell Mol Biol.* 25, 515-521
- Bonvallot, V.; Baulig, A.; Boland, S.; Marano, F. & Baeza, A. (2002). Diesel exhaust particles induce an inflammatory response in airway epithelial cells: involvement of reactive oxygen species. *Biofactors.* 16, 15-17
- Brown, D. M.; Wilson, M. R.; Macnee, W.; Stone, V. & Donaldson, K. (2001). Size-dependent proinflammatory effects of ultrafine polystyrene particles: a role for surface area and oxidative stress in the enhanced activity of ultrafines. *Toxicol Appl. Pharmacol.* 175, 191-199
- Brunekreef, B.; Beelen, R.; Hoek, G.; Schouten, L.; Bausch-Goldbohm, S.; Fischer, P.; Armstrong, B.; Hughes, E.; Jerrett, M. & van den Brandt, P. (2009). Effects of long-term exposure to traffic-related air pollution on respiratory and cardiovascular mortality in the Netherlands: the NLCS-AIR study. *Res Rep Health Eff. Inst.* 5-71
- Brunekreef, B. & Forsberg, B. (2005). Epidemiological evidence of effects of coarse airborne particles on health. *Eur Respir. J.* 26, 309-318
- Burchiel, S. W.; Lauer, F. T.; Dunaway, S. L.; Zawadzki, J.; McDonald, J. D. & Reed, M. D. (2005). Hardwood smoke alters murine splenic T cell responses to mitogens following a 6-month whole body inhalation exposure. *Toxicol Appl. Pharmacol.* 202, 229-236
- Cao, D.; Bromberg, P. A. & Samet, J. M. (2010). Diesel particle-induced transcriptional expression of p21 involves activation of EGFR, Src, and Stat3. *Am J Respir. Cell Mol Biol.* 42, 88-95
- Chaudhuri, N.; Paiva, C.; Donaldson, K.; Duffin, R.; Parker, L. C. & Sabroe, I. (2010). Diesel exhaust particles override natural injury-limiting pathways in the lung. *Am J Physiol Lung Cell Mol Physiol*

- Chen, L. C. & Lippmann, M. (2009). Effects of metals within ambient air particulate matter (PM) on human health. *Inhal Toxicol.* 21, 1-31
- Clancy, L.; Goodman, P.; Sinclair, H. & Dockery, D. W. (2002). Effect of air-pollution control on death rates in Dublin, Ireland: an intervention study. *Lancet.* 360, 1210-1214
- de Brito, J. M.; Belotti, L.; Toledo, A. C.; Antonangelo, L.; Silva, F. S.; Alvim, D. S.; Andre, P. A.; Saldiva, P. H. & Rivero, D. H. (2010). Acute cardiovascular and inflammatory toxicity induced by inhalation of diesel and biodiesel exhaust particles. *Toxicol Sci*
- Devouassoux, G.; Saxon, A.; Metcalfe, D. D.; Prussin, C.; Colomb, M. G.; Brambilla, C. & Diaz-Sanchez, D. (2002). Chemical constituents of diesel exhaust particles induce IL-4 production and histamine release by human basophils. *J Allergy Clin Immunol.* 109, 847-853
- Donaldson, K.; Brown, D.; Clouter, A.; Duffin, R.; Macnee, W.; Renwick, L.; Tran, L. & Stone, V. (2002). The pulmonary toxicology of ultrafine particles. *J Aerosol Med.* 15, 213-220
- Dreher, K. L.; Jaskot, R. H.; Lehmann, J. R.; Richards, J. H.; McGee, J. K.; Ghio, A. J. & Costa, D. L. (1997). Soluble transition metals mediate residual oil fly ash induced acute lung injury. *J Toxicol Environ Health.* 50, 285-305
- Drumm, K.; Attia, D. I.; Kannt, S.; Micke, P.; Buhl, R. & Kienast, K. (2000). Soot-exposed mononuclear cells increase inflammatory cytokine mRNA expression and protein secretion in cocultured bronchial epithelial cells. *Respiration.* 67, 291-297
- Duffin, R.; Tran, L.; Brown, D.; Stone, V. & Donaldson, K. (2007). Proinflammatory effects of low-toxicity and metal nanoparticles in vivo and in vitro: highlighting the role of particle surface area and surface reactivity. *Inhal Toxicol.* 19, 849-856
- Dye, J. A.; Lehmann, J. R.; McGee, J. K.; Winsett, D. W.; Ledbetter, A. D.; Everitt, J. I.; Ghio, A. J. & Costa, D. L. (2001). Acute pulmonary toxicity of particulate matter filter extracts in rats: coherence with epidemiologic studies in Utah Valley residents. *Environ Health Perspect.* 109 Suppl 3, 395-403
- Elder, A.; Gelein, R.; Finkelstein, J.; Phipps, R.; Frampton, M.; Utell, M.; Kittelson, D. B.; Watts, W. F.; Hopke, P.; Jeong, C. H.; Kim, E.; Liu, W.; Zhao, W.; Zhuo, L.; Vincent, R.; Kumarathasan, P. & Oberdorster, G. (2004). On-road exposure to highway aerosols. 2. Exposures of aged, compromised rats. *Inhal Toxicol.* 16 Suppl 1, 41-53
- Fahy, O.; Senechal, S.; Pene, J.; Scherpereel, A.; Lassalle, P.; Tonnel, A. B.; Yssel, H.; Wallaert, B. & Tsiopoulos, A. (2002). Diesel exposure favors Th2 cell recruitment by mononuclear cells and alveolar macrophages from allergic patients by differentially regulating macrophage-derived chemokine and IFN-gamma-induced protein-10 production. *J Immunol.* 168, 5912-5919
- Fahy, O.; Tsiopoulos, A.; Hammad, H.; Pestel, J.; Tonnel, A. B. & Wallaert, B. (1999). Effects of diesel organic extracts on chemokine production by peripheral blood mononuclear cells. *J Allergy Clin Immunol.* 103, 1115-1124
- Frampton, M. W.; Ghio, A. J.; Samet, J. M.; Carson, J. L.; Carter, J. D. & Devlin, R. B. (1999). Effects of aqueous extracts of PM(10) filters from the Utah valley on human airway epithelial cells. *Am J Physiol.* 277, L960-L967
- Frampton, M. W.; Stewart, J. C.; Oberdorster, G.; Morrow, P. E.; Chalupa, D.; Pietropaoli, A. P.; Frasier, L. M.; Speers, D. M.; Cox, C.; Huang, L. S. & Utell, M. J. (2006). Inhalation of ultrafine particles alters blood leukocyte expression of adhesion molecules in humans. *Environ Health Perspect.* 114, 51-58

- Fubini, B. & Hubbard, A. (2003). Reactive oxygen species (ROS) and reactive nitrogen species (RNS) generation by silica in inflammation and fibrosis. *Free Radic. Biol Med.* 34, 1507-1516
- Gavett, S. H.; Haykal-Coates, N.; Copeland, L. B.; Heinrich, J. & Gilmour, M. I. (2003). Metal composition of ambient PM<sub>2.5</sub> influences severity of allergic airways disease in mice. *Environ Health Perspect.* 111, 1471-1477
- Gerlofs-Nijland, M. E.; Rummelhard, M.; Boere, A. J.; Leseman, D. L.; Duffin, R.; Schins, R. P.; Borm, P. J.; Sillanpaa, M.; Salonen, R. O. & Cassee, F. R. (2009). Particle induced toxicity in relation to transition metal and polycyclic aromatic hydrocarbon contents. *Environ Sci Technol.* 43, 4729-4736.
- Giamarellos-Bourboulis, E.J., Mouktaroudi, M., Bodar, E., van der Ven, J., Kullberg, B.J., Netea, M.G., & van der Meer, J.W. (2009). Crystals of monosodium urate monohydrate enhance lipopolysaccharide-induced release of interleukin 1 beta by mononuclear cells through a caspase 1-mediated process. *Ann Rheum Dis.* 68(2), 273-8.
- Ghio, A. J. (2004). Biological effects of Utah Valley ambient air particles in humans: a review. *J Aerosol Med.* 17, 157-164
- Ghio, A. J. & Devlin, R. B. (2001). Inflammatory lung injury after bronchial instillation of air pollution particles. *Am J Respir. Crit Care Med.* 164, 704-708
- Ghio, A. J.; Kim, C. & Devlin, R. B. (2000). Concentrated ambient air particles induce mild pulmonary inflammation in healthy human volunteers. *Am J Respir. Crit Care Med.* 162, 981-988
- Gilmour, P. S.; Brown, D. M.; Lindsay, T. G.; Beswick, P. H.; Macnee, W. & Donaldson, K. (1996). Adverse health effects of PM<sub>10</sub> particles: involvement of iron in generation of hydroxyl radical. *Occup Environ Med.* 53, 817-822
- Gurgueira, S. A.; Lawrence, J.; Coull, B.; Murthy, G. G. & Gonzalez-Flecha, B. (2002). Rapid increases in the steady-state concentration of reactive oxygen species in the lungs and heart after particulate air pollution inhalation. *Environ Health Perspect.* 110, 749-755
- Guthrie, G. D., Jr. (1997). Mineral properties and their contributions to particle toxicity. *Environ Health Perspect.* 105 Suppl 5, 1003-1011
- Happo, M. S.; Hirvonen, M. R.; Halinen, A. I.; Jalava, P. I.; Pennanen, A. S.; Sillanpaa, M.; Hillamo, R. & Salonen, R. O. (2010). Seasonal variation in chemical composition of size-segregated urban air particles and the inflammatory activity in the mouse lung. *Inhal Toxicol.* 22, 17-32
- Heeb, N. V.; Schmid, P.; Kohler, M.; Gujer, E.; Zennegg, M.; Wenger, D.; Wichser, A.; Ulrich, A.; Gfeller, U.; Honegger, P.; Zeyer, K.; Emmenegger, L.; Petermann, J. L.; Czerwinski, J.; Mosimann, T.; Kasper, M. & Mayer, A. (2008). Secondary effects of catalytic diesel particulate filters: conversion of PAHs versus formation of nitro-PAHs. *Environ Sci Technol.* 42, 3773-3779
- Heinrich, J.; Hoelscher, B.; Wjst, M.; Ritz, B.; Cyrys, J. & Wichmann, H. (1999). Respiratory diseases and allergies in two polluted areas in East Germany. *Environ Health Perspect.* 107, 53-62
- Hetland, R. B.; Myhre, O.; Lag, M.; Hongve, D.; Schwarze, P. E. & Refsnes, M. (2001a). Importance of soluble metals and reactive oxygen species for cytokine release induced by mineral particles. *Toxicology.* 165, 133-144

- Hetland, R. B.; Refsnes, M.; Myran, T.; Johansen, B. V.; Uthus, N. & Schwarze, P. E. (2000). Mineral and/or metal content as critical determinants of particle-induced release of IL-6 and IL-8 from A549 cells. *J Toxicol Environ Health A*. 60, 47-65
- Hetland, R. B.; Schwarze, P. E.; Johansen, B. V.; Myran, T.; Uthus, N. & Refsnes, M. (2001b). Silica-induced cytokine release from A549 cells: importance of surface area versus size. *Hum Exp Toxicol*. 20, 46-55
- Hiura, T. S.; Kaszubowski, M. P.; Li, N. & Nel, A. E. (1999). Chemicals in diesel exhaust particles generate reactive oxygen radicals and induce apoptosis in macrophages. *J Immunol*. 163, 5582-5591
- Holopainen, M.; Hirvonen, M. R.; Komulainen, H. & Klockars, M. (2004). Effect of the shape of mica particles on the production of tumor necrosis factor alpha in mouse macrophages. *Scand J Work Environ Health*. 30 Suppl 2, 91-98
- Huang, Y. C.; Ghio, A. J.; Stonehuerner, J.; McGee, J.; Carter, J. D.; Grambow, S. C. & Devlin, R. B. (2003). The role of soluble components in ambient fine particles-induced changes in human lungs and blood. *Inhal Toxicol*. 15, 327-342
- Inoue, K.; Koike, E.; Yanagisawa, R. & Takano, H. (2008). Impact of diesel exhaust particles on th2 response in the lung in asthmatic mice. *J Clin Biochem Nutr*. 43, 199-200
- Inoue, K.; Takano, H.; Hiyoshi, K.; Ichinose, T.; Sadakane, K.; Yanagisawa, R.; Tomura, S. & Kumagai, Y. (2007). Naphthoquinone enhances antigen-related airway inflammation in mice. *Eur Respir J*. 29, 259-267
- Jalava, P.; Salonen, R. O.; Nuutinen K.; Pennanen, A.; Happonen, M.; Tissari, J.; Frey, A.; Hillamo, R.; Jokiniemi, J. & Hirvonen, M. R. (2010). Effect of combustion conditions on cytotoxic and inflammatory activity of residential wood combustion particles. *Atm Environ*. In press,
- Jardim, M. J.; Fry, R. C.; Jaspers, I.; Dailey, L. & Diaz-Sanchez, D. (2009). Disruption of microRNA expression in human airway cells by diesel exhaust particles is linked to tumorigenesis-associated pathways. *Environ Health Perspect*. 117, 1745-1751
- Jaspers, I.; Sheridan, P. A.; Zhang, W.; Brighton, L. E.; Chason, K. D.; Hua, X. & Tilley, S. L. (2009). Exacerbation of allergic inflammation in mice exposed to diesel exhaust particles prior to viral infection. *Part Fibre. Toxicol*. 6, 22
- Jokiniemi, J., Hytönen, K., Tissari, J., Obernberger, I., Brunner, T., Bärnthaler, G., Friesenbichler, J., Salonen, R. O., Hirvonen, M. R., Jalava, P., Pennanen, A., Happonen, M., Vallius, M., Markkanen, P., Hartmann, H., Turwoski, P., Rossmann, P., Ellner-Schubert, T., Boman, C., Petterson, E., Wiinikka, H., Hillamo, R., Saarino, K., Frey, A., Saarikoski, S., Timonen, H., Teinilä, K., Aurela, M., Sillanpää, M., Bellmann, B., Sandström T, Sehlstedt, M., & Forsberg, B. 2008, *Biomass combustion in residential heating: particulate measurements, sampling, and physicochemical and toxicological characterisation*, University of Kuopio, Report 1/2008., Final report of the project 'Biomass-PM' funded by ERA-NET Bioenergy Programme 2007-2008., ISSN 0786-4728.
- Karlsson, H. L.; Ljungman, A. G.; Lindbom, J. & Moller, L. (2006). Comparison of genotoxic and inflammatory effects of particles generated by wood combustion, a road simulator and collected from street and subway. *Toxicol Lett*. 165, 203-211
- Kim, Y. M.; Reed, W.; Wu, W.; Bromberg, P. A.; Graves, L. M. & Samet, J. M. (2006). Zn<sup>2+</sup>-induced IL-8 expression involves AP-1, JNK, and ERK activities in human airway epithelial cells. *Am J Physiol Lung Cell Mol Physiol*. 290, L1028-L1035

- Kocbach, A. (2008). *Pro-inflammatory potential of particles from residential wood smoke and traffic: Importance of physicochemical characteristics*, PhD thesis, University of Oslo, Norway.
- Kocbach, A.; Herseth, J. I.; Lag, M.; Refsnes, M. & Schwarze, P. E. (2008a). Particles from wood smoke and traffic induce differential pro-inflammatory response patterns in co-cultures. *Toxicol Appl. Pharmacol.* 232, 317-326
- Kocbach, A.; Johansen, B. V.; Schwarze, P. E. & Namork, E. (2005). Analytical electron microscopy of combustion particles: a comparison of vehicle exhaust and residential wood smoke. *Sci Total Environ.* 346, 231-243
- Kocbach, A.; Namork, E. & Schwarze, P. E. (2008b). Pro-inflammatory potential of wood smoke and traffic-derived particles in a monocytic cell line. *Toxicology.* 247, 123-132
- Kocbach, B. A.; Pagels, J.; Yttri, K. E.; Barregard, L.; Sallsten, G.; Schwarze, P. E. & Boman, C. (2009). Health effects of residential wood smoke particles: the importance of combustion conditions and physicochemical particle properties. *Part Fibre. Toxicol.* 6, 29
- Kodavanti, U. P.; Hauser, R.; Christiani, D. C.; Meng, Z. H.; McGee, J.; Ledbetter, A.; Richards, J. & Costa, D. L. (1998). Pulmonary responses to oil fly ash particles in the rat differ by virtue of their specific soluble metals. *Toxicol Sci.* 43, 204-212
- Kodavanti, U. P.; Schladweiler, M. C.; Gilmour, P. S.; Wallenborn, J. G.; Mandavilli, B. S.; Ledbetter, A. D.; Christiani, D. C.; Runge, M. S.; Karoly, E. D.; Costa, D. L.; Peddada, S.; Jaskot, R.; Richards, J. H.; Thomas, R.; Madamanchi, N. R. & Nyska, A. (2008). The role of particulate matter-associated zinc in cardiac injury in rats. *Environ Health Perspect.* 116, 13-20
- Kodavanti, U. P.; Schladweiler, M. C.; Ledbetter, A. D.; Hauser, R.; Christiani, D. C.; Samet, J. M.; McGee, J.; Richards, J. H. & Costa, D. L. (2002). Pulmonary and systemic effects of zinc-containing emission particles in three rat strains: multiple exposure scenarios. *Toxicol Sci.* 70, 73-85
- Kreyling, W. G.; Semmler, M.; Erbe, F.; Mayer, P.; Takenaka, S.; Schulz, H.; Oberdorster, G. & Ziesenis, A. (2002). Translocation of ultrafine insoluble iridium particles from lung epithelium to extrapulmonary organs is size dependent but very low. *J Toxicol Environ Health A.* 65, 1513-1530
- Kubatova, A.; Dronen, L. C.; Picklo, M. J., Sr. & Hawthorne, S. B. (2006). Midpolarity and nonpolar wood smoke particulate matter fractions deplete glutathione in RAW 264.7 macrophages. *Chem Res Toxicol.* 19, 255-261
- Kupiainen, K. J.; Tervahattu, H.; Raisanen, M.; Makela, T.; Aurela, M. & Hillamo, R. (2005). Size and composition of airborne particles from pavement wear, tires, and traction sanding. *Environ Sci Technol.* 39, 699-706
- Lag, M.; Refsnes, M.; Lilleaas, E. M.; Holme, J. A.; Becher, R. & Schwarze, P. E. (2005). Role of mitogen activated protein kinases and protein kinase C in cadmium-induced apoptosis of primary epithelial lung cells. *Toxicology.* 211, 253-264
- Leonard, S. S.; Wang, S.; Shi, X.; Jordan, B. S.; Castranova, V. & Dubick, M. A. (2000). Wood smoke particles generate free radicals and cause lipid peroxidation, DNA damage, NFkappaB activation and TNF-alpha release in macrophages. *Toxicology.* 150, 147-157
- Li, N.; Wang, M.; Oberley, T. D.; Sempf, J. M. & Nel, A. E. (2002). Comparison of the pro-oxidative and proinflammatory effects of organic diesel exhaust particle chemicals in bronchial epithelial cells and macrophages. *J Immunol.* 169, 4531-4541

- Matsuo, M.; Uenishi, R.; Shimada, T.; Yamanaka, S.; Yabuki, M.; Utsumi, K. & Sagai, M. (2001). Diesel exhaust particle-induced cell death of human leukemic promyelocytic cells HL-60 and their variant cells HL-NR6. *Biol Pharm Bull.* 24, 357-363
- McDonald, J. D.; Harrod, K. S.; Seagrave, J.; Seilkop, S. K. & Mauderly, J. L. (2004). Effects of low sulfur fuel and a catalyzed particle trap on the composition and toxicity of diesel emissions. *Environ Health Perspect.* 112, 1307-1312
- McDonald, J. D.; Reed, M. D.; Campen, M. J.; Barrett, E. G.; Seagrave, J. & Mauderly, J. L. (2007). Health effects of inhaled gasoline engine emissions. *Inhal Toxicol.* 19 Suppl 1, 107-116
- Mills, N. L.; Tornqvist, H.; Robinson, S. D.; Gonzalez, M.; Darnley, K.; Macnee, W.; Boon, N. A.; Donaldson, K.; Blomberg, A.; Sandstrom, T. & Newby, D. E. (2005). Diesel exhaust inhalation causes vascular dysfunction and impaired endogenous fibrinolysis. *Circulation.* 112, 3930-3936
- Molinelli, A. R.; Madden, M. C.; McGee, J. K.; Stonehuerner, J. G. & Ghio, A. J. (2002). Effect of metal removal on the toxicity of airborne particulate matter from the Utah Valley. *Inhal Toxicol.* 14, 1069-1086
- Monteiller, C.; Tran, L.; Macnee, W.; Faux, S.; Jones, A.; Miller, B. & Donaldson, K. (2007). The pro-inflammatory effects of low-toxicity low-solubility particles, nanoparticles and fine particles, on epithelial cells in vitro: the role of surface area. *Occup Environ Med.* 64, 609-615
- Mossman, B. T.; Lounsbury, K. M. & Reddy, S. P. (2006). Oxidants and signaling by mitogen-activated protein kinases in lung epithelium. *Am J Respir. Cell Mol Biol.* 34, 666-669
- Murphy, S. A.; BeruBe, K. A.; Pooley, F. D. & Richards, R. J. (1998). The response of lung epithelium to well characterised fine particles. *Life Sci.* 62, 1789-1799
- N'diaye, M.; Le, F. E.; Lagadic-Gossmann, D.; Corre, S.; Gilot, D.; Lecureur, V.; Monteiro, P.; Rauch, C.; Galibert, M. D. & Fardel, O. (2006). Aryl hydrocarbon receptor- and calcium-dependent induction of the chemokine CCL1 by the environmental contaminant benzo[a]pyrene. *J Biol Chem.* 281, 19906-19915
- Nadadur, S. S. & Kodavanti, U. P. (2002). Altered gene expression profiles of rat lung in response to an emission particulate and its metal constituents. *J Toxicol Environ Health A.* 65, 1333-1350
- Nel, A. E.; Diaz-Sanchez, D. & Li, N. (2001). The role of particulate pollutants in pulmonary inflammation and asthma: evidence for the involvement of organic chemicals and oxidative stress. *Curr Opin. Pulm. Med.* 7, 20-26
- Nemmar, A.; Dhanasekaran, S.; Yasin, J.; Ba-Omar, H.; Fahim, M. A.; Kazzam, E. E. & Ali, B. H. (2009). Evaluation of the direct systemic and cardiopulmonary effects of diesel particles in spontaneously hypertensive rats. *Toxicology.* 262, 50-56
- Nemmar, A.; Hoet, P. H.; Vanquickenborne, B.; Dinsdale, D.; Thomeer, M.; Hoylaerts, M. F.; Vanbilloen, H.; Mortelmans, L. & Nemery, B. (2002). Passage of inhaled particles into the blood circulation in humans. *Circulation.* 105, 411-414
- Oberdorster, G. (1996). Significance of particle parameters in the evaluation of exposure-dose-response relationships of inhaled particles. *Inhal Toxicol.* 8 Suppl, 73-89

- Ohtoshi, T.; Takizawa, H.; Okazaki, H.; Kawasaki, S.; Takeuchi, N.; Ohta, K. & Ito, K. (1998). Diesel exhaust particles stimulate human airway epithelial cells to produce cytokines relevant to airway inflammation in vitro. *J Allergy Clin Immunol.* 101, 778-785
- Ovrevik, J.; Arlt, V. M.; Oya, E.; Nagy, E.; Mollerup, S.; Phillips, D. H.; Lag, M. & Holme, J. A. (2010). Differential effects of nitro-PAHs and amino-PAHs on cytokine and chemokine responses in human bronchial epithelial BEAS-2B cells. *Toxicol Appl. Pharmacol.* 242, 270-280
- Ovrevik, J.; Hetland, R. B.; Schins, R. P.; Myran, T. & Schwarze, P. E. (2006). Iron release and ROS generation from mineral particles are not related to cytokine release or apoptosis in exposed A549 cells. *Toxicol Lett.* 165, 31-38
- Ovrevik, J.; Myran, T.; Refsnes, M.; Lag, M.; Becher, R.; Hetland, R. B. & Schwarze, P. E. (2005). Mineral particles of varying composition induce differential chemokine release from epithelial lung cells: importance of physico-chemical characteristics. *Ann Occup Hyg.* 49, 219-231
- Pagan, I.; Costa, D. L.; McGee, J. K.; Richards, J. H. & Dye, J. A. (2003). Metals mimic airway epithelial injury induced by in vitro exposure to Utah Valley ambient particulate matter extracts. *J Toxicol Environ Health A.* 66, 1087-1112
- Podechard, N.; Lecqueur, V.; Le, F. E.; Guenon, I.; Sparfel, L.; Gilot, D.; Gordon, J. R.; Lagente, V. & Fardel, O. (2008). Interleukin-8 induction by the environmental contaminant benzo(a)pyrene is aryl hydrocarbon receptor-dependent and leads to lung inflammation. *Toxicol Lett.* 177, 130-137
- Pope, C. A., III; Ezzati, M. & Dockery, D. W. (2009). Fine-particulate air pollution and life expectancy in the United States. *N Engl J Med.* 360, 376-386
- Porter, M.; Karp, M.; Killedar, S.; Bauer, S. M.; Guo, J.; Williams, D.; Breysse, P.; Georas, S. N. & Williams, M. A. (2007). Diesel-enriched particulate matter functionally activates human dendritic cells. *Am J Respir. Cell Mol Biol.* 37, 706-719
- Pourazar, J.; Blomberg, A.; Kelly, F. J.; Davies, D. E.; Wilson, S. J.; Holgate, S. T. & Sandstrom, T. (2008). Diesel exhaust increases EGFR and phosphorylated C-terminal Tyr 1173 in the bronchial epithelium. *Part Fibre. Toxicol.* 5, 8
- Pourazar, J.; Mudway, I. S.; Samet, J. M.; Helleday, R.; Blomberg, A.; Wilson, S. J.; Frew, A. J.; Kelly, F. J. & Sandstrom, T. (2005). Diesel exhaust activates redox-sensitive transcription factors and kinases in human airways. *Am J Physiol Lung Cell Mol Physiol.* 289, L724-L730
- Provoost, S.; Maes, T.; Willart, M. A.; Joos, G. F.; Lambrecht, B. N. & Tournoy, K. G. (2010). Diesel exhaust particles stimulate adaptive immunity by acting on pulmonary dendritic cells. *J Immunol.* 184, 426-432
- Ramos, C.; Cisneros, J.; Gonzalez-Avila, G.; Becerril, C.; Ruiz, V. & Montano, M. (2009). Increase of matrix metalloproteinases in woodsmoke-induced lung emphysema in guinea pigs. *Inhal Toxicol.* 21, 119-132
- Reed, M. D.; Campen, M. J.; Gigliotti, A. P.; Harrod, K. S.; McDonald, J. D.; Seagrave, J. C.; Mauderly, J. L. & Seilkop, S. K. (2006). Health effects of subchronic exposure to environmental levels of hardwood smoke. *Inhal Toxicol.* 18, 523-539
- Refsnes, M.; Hetland, R. B.; Ovrevik, J.; Sundfor, I.; Schwarze, P. E. & Lag, M. (2006). Different particle determinants induce apoptosis and cytokine release in primary alveolar macrophage cultures. *Part Fibre. Toxicol.* 3, 10

- Rudell, B.; Blomberg, A.; Helleday, R.; Ledin, M. C.; Lundback, B.; Stjernberg, N.; Horstedt, P. & Sandstrom, T. (1999). Bronchoalveolar inflammation after exposure to diesel exhaust: comparison between unfiltered and particle trap filtered exhaust. *Occup Environ Med.* 56, 527-534
- Sager, T. M. & Castranova, V. (2009). Surface area of particle administered versus mass in determining the pulmonary toxicity of ultrafine and fine carbon black: comparison to ultrafine titanium dioxide. *Part Fibre. Toxicol.* 6, 15
- Sager, T. M.; Kommineni, C. & Castranova, V. (2008). Pulmonary response to intratracheal instillation of ultrafine versus fine titanium dioxide: role of particle surface area. *Part Fibre. Toxicol.* 5, 17
- Salvi, S. S.; Nordenhall, C.; Blomberg, A.; Rudell, B.; Pourazar, J.; Kelly, F. J.; Wilson, S.; Sandstrom, T.; Holgate, S. T. & Frew, A. J. (2000). Acute exposure to diesel exhaust increases IL-8 and GRO-alpha production in healthy human airways. *Am J Respir. Crit. Care Med.* 161, 550-557
- Samet, J. M.; Dewar, B. J.; Wu, W. & Graves, L. M. (2003). Mechanisms of Zn(2+)-induced signal initiation through the epidermal growth factor receptor. *Toxicol Appl. Pharmacol.* 191, 86-93
- Samet, J. M.; Graves, L. M.; Quay, J.; Dailey, L. A.; Devlin, R. B.; Ghio, A. J.; Wu, W.; Bromberg, P. A. & Reed, W. (1998). Activation of MAPKs in human bronchial epithelial cells exposed to metals. *Am J Physiol.* 275, L551-L558
- Samet, J. M.; Silbajoris, R.; Wu, W. & Graves, L. M. (1999). Tyrosine phosphatases as targets in metal-induced signaling in human airway epithelial cells. *Am J Respir. Cell Mol Biol.* 21, 357-364
- Samet, J. M.; Zeger, S. L.; Dominici, F.; Curriero, F.; Coursac, I.; Dockery, D. W.; Schwartz, J. & Zanobetti, A. (2000). The National Morbidity, Mortality, and Air Pollution Study. Part II: Morbidity and mortality from air pollution in the United States. *Res Rep Health Eff. Inst.* 94, 5-70
- Samoli, E.; Analitis, A.; Touloumi, G.; Schwartz, J.; Anderson, H. R.; Sunyer, J.; Bisanti, L.; Zmirou, D.; Vonk, J. M.; Pekkanen, J.; Goodman, P.; Paldy, A.; Schindler, C. & Katsouyanni, K. (2005). Estimating the exposure-response relationships between particulate matter and mortality within the APHEA multicity project. *Environ Health Perspect.* 113, 88-95
- Schaumann, F.; Borm, P. J.; Herbrich, A.; Knoch, J.; Pitz, M.; Schins, R. P.; Luettig, B.; Hohlfeld, J. M.; Heinrich, J. & Krug, N. (2004). Metal-rich ambient particles (particulate matter 2.5) cause airway inflammation in healthy subjects. *Am J Respir. Crit Care Med.* 170, 898-903
- Schwarze, P. E.; Ovreivik, J.; Hetland, R. B.; Becher, R.; Cassee, F. R.; Lag, M.; Lovik, M.; Dybing, E. & Refsnes, M. (2007). Importance of size and composition of particles for effects on cells in vitro. *Inhal Toxicol.* 19 Suppl 1, 17-22
- Seagrave, J.; McDonald, J. D.; Bedrick, E.; Edgerton, E. S.; Gigliotti, A. P.; Jansen, J. J.; Ke, L.; Naeher, L. P.; Seilkop, S. K.; Zheng, M. & Mauderly, J. L. (2006). Lung toxicity of ambient particulate matter from southeastern U.S. sites with different contributing sources: relationships between composition and effects. *Environ Health Perspect.* 114, 1387-1393

- Seagrave, J.; McDonald, J. D.; Gigliotti, A. P.; Nikula, K. J.; Seilkop, S. K.; Gurevich, M. & Mauderly, J. L. (2002). Mutagenicity and in vivo toxicity of combined particulate and semivolatile organic fractions of gasoline and diesel engine emissions. *Toxicol Sci.* 70, 212-226
- Seagrave, J.; McDonald, J. D.; Reed, M. D.; Seilkop, S. K. & Mauderly, J. L. (2005). Responses to subchronic inhalation of low concentrations of diesel exhaust and hardwood smoke measured in rat bronchoalveolar lavage fluid. *Inhal Toxicol.* 17, 657-670
- Shukla, A.; Timblin, C.; BeruBe, K.; Gordon, T.; McKinney, W.; Driscoll, K.; Vacek, P. & Mossman, B. T. (2000). Inhaled particulate matter causes expression of nuclear factor (NF)-kappaB-related genes and oxidant-dependent NF-kappaB activation in vitro. *Am J Respir. Cell Mol Biol.* 23, 182-187
- Smith-Sivertsen, T.; Diaz, E.; Pope, D.; Lie, R. T.; Diaz, A.; McCracken, J.; Bakke, P.; Arana, B.; Smith, K. R. & Bruce, N. (2009). Effect of reducing indoor air pollution on women's respiratory symptoms and lung function: the RESPIRE Randomized Trial, Guatemala. *Am J Epidemiol.* 170, 211-220
- Sorensen, M.; Autrup, H.; Moller, P.; Hertel, O.; Jensen, S. S.; Vinzents, P.; Knudsen, L. E. & Loft, S. (2003). Linking exposure to environmental pollutants with biological effects. *Mutat. Res.* 544, 255-271
- Soukup, J. M.; Ghio, A. J. & Becker, S. (2000). Soluble components of Utah Valley particulate pollution alter alveolar macrophage function in vivo and in vitro. *Inhal Toxicol.* 12, 401-414
- Steerenberg, P. A.; van, A. L.; Lovik, M.; Hetland, R. B.; Alberg, T.; Halatek, T.; Bloemen, H. J.; Rydzynski, K.; Swaen, G.; Schwarze, P.; Dybing, E. & Cassee, F. R. (2006). Relation between sources of particulate air pollution and biological effect parameters in samples from four European cities: an exploratory study. *Inhal Toxicol.* 18, 333-346
- Stenfors, N.; Nordenhäll, C.; Salvi, S. S.; Mudway, I.; Söderberg, M.; Blomberg, A.; Helleday, R.; Levin, J. O.; Holgate, S. T.; Kelly, F. J.; Frew, A. J. & Sandström, T. (2004). Different airway inflammatory responses in asthmatic and healthy humans exposed to diesel. *Eur. Respir. J.* 23, 82-86
- Stoeger, T.; Reinhard, C.; Takenaka, S.; Schroepfel, A.; Karg, E.; Ritter, B.; Heyder, J. & Schulz, H. (2006). Instillation of six different ultrafine carbon particles indicates a surface area threshold dose for acute lung inflammation in mice. *Environ Health Perspect.* 114, 328-333
- Takano, H.; Yoshikawa, T.; Ichinose, T.; Miyabara, Y.; Imaoka, K. & Sagai, M. (1997). Diesel exhaust particles enhance antigen-induced airway inflammation and local cytokine expression in mice. *Am J Respir. Crit Care Med.* 156, 36-42
- Takizawa, H.; Ohtoshi, T.; Kawasaki, S.; Abe, S.; Sugawara, I.; Nakahara, K.; Matsushima, K. & Kudoh, S. (2000). Diesel exhaust particles activate human bronchial epithelial cells to express inflammatory mediators in the airways: a review. *Respirology.* 5, 197-203
- Tal, T. L.; Graves, L. M.; Silbajoris, R.; Bromberg, P. A.; Wu, W. & Samet, J. M. (2006). Inhibition of protein tyrosine phosphatase activity mediates epidermal growth factor receptor signaling in human airway epithelial cells exposed to Zn<sup>2+</sup>. *Toxicol Appl. Pharmacol.* 214, 16-23

- Tekpli, X.; Rissel, M.; Huc, L.; Catheline, D.; Sergent, O.; Rioux, V.; Legrand, P.; Holme, J. A.; Dimanche-Boitrel, M. T. & Lagadic-Gossmann, D. (2010a). Membrane remodeling, an early event in benzo[a]pyrene-induced apoptosis. *Toxicol Appl. Pharmacol.* 243, 68-76
- Tekpli, X.; Rivedal, E.; Gorria, M.; Landvik, N. E.; Rissel, M.; Dimanche-Boitrel, M. T.; Baffet, G.; Holme, J. A. & Lagadic-Gossmann, D. (2010b). The B[a]P-increased intercellular communication via translocation of connexin-43 into gap junctions reduces apoptosis. *Toxicol Appl. Pharmacol.* 242, 231-240
- Thorpe, A. & Harrison, R. M. (2008). Sources and properties of non-exhaust particulate matter from road traffic: a review. *Sci Total Environ.* 400, 270-282
- Tornqvist, H.; Mills, N. L.; Gonzalez, M.; Miller, M. R.; Robinson, S. D.; Megson, I. L.; Macnee, W.; Donaldson, K.; Soderberg, S.; Newby, D. E.; Sandstrom, T. & Blomberg, A. (2007). Persistent endothelial dysfunction in humans after diesel exhaust inhalation. *Am J Respir. Crit Care Med.* 176, 395-400
- Totlandsdal, A. I.; Refsnes, M.; Skomedal, T.; Osnes, J. B.; Schwarze, P. E. & Lag, M. (2008). Particle-induced cytokine responses in cardiac cell cultures--the effect of particles versus soluble mediators released by particle-exposed lung cells. *Toxicol Sci.* 106, 233-241
- Tran, C. L.; Buchanan, D.; Cullen, R. T.; Searl, A.; Jones, A. D. & Donaldson, K. (2000). Inhalation of poorly soluble particles. II. Influence Of particle surface area on inflammation and clearance. *Inhal Toxicol.* 12, 1113-1126
- Vione, D.; Barra, S.; De, G. G.; De, R. M.; Gilardoni, S.; Perrone, M. G. & Pozzoli, L. (2004a). Polycyclic aromatic hydrocarbons in the atmosphere: monitoring, sources, sinks and fate. II: Sinks and fate. *Ann Chim.* 94, 257-268
- Vione, D.; Maurino, V.; Minero, C.; Lucchiarri, M. & Pelizzetti, E. (2004b). Nitration and hydroxylation of benzene in the presence of nitrite/nitrous acid in aqueous solution. *Chemosphere.* 56, 1049-1059
- Vione, D.; Maurino, V.; Minero, C.; Pelizzetti, E.; Harrison, M. A.; Olariu, R. I. & Arsene, C. (2006). Photochemical reactions in the tropospheric aqueous phase and on particulate matter. *Chem. Soc. Rev.* 35, 441-453
- Warheit, D. B. (2001). Inhaled amorphous silica particulates: what do we know about their toxicological profiles? *J Environ Pathol. Toxicol Oncol.* 20 Suppl 1, 133-141
- Warheit, D. B.; Webb, T. R.; Colvin, V. L.; Reed, K. L. & Sayes, C. M. (2007a). Pulmonary bioassay studies with nanoscale and fine-quartz particles in rats: toxicity is not dependent upon particle size but on surface characteristics. *Toxicol Sci.* 95, 270-280
- Warheit, D. B.; Webb, T. R.; Reed, K. L.; Frerichs, S. & Sayes, C. M. (2007b). Pulmonary toxicity study in rats with three forms of ultrafine-TiO<sub>2</sub> particles: differential responses related to surface properties. *Toxicology.* 230, 90-104
- Warheit, D. B.; Webb, T. R.; Sayes, C. M.; Colvin, V. L. & Reed, K. L. (2006). Pulmonary instillation studies with nanoscale TiO<sub>2</sub> rods and dots in rats: toxicity is not dependent upon particle size and surface area. *Toxicol Sci.* 91, 227-236
- Watkinson, W. P.; Campen, M. J. & Costa, D. L. (1998). Cardiac arrhythmia induction after exposure to residual oil fly ash particles in a rodent model of pulmonary hypertension. *Toxicol Sci.* 41, 209-216
- WHO (2005). Health effects of air pollution. Global Update, 2005.
- WHO (2006). Health effects of transport related air pollution.

- Wong, P. S.; Vogel, C. F.; Kokosinski, K. & Matsumura, F. (2010). Arylhydrocarbon receptor activation in NCI-H441 cells and C57BL/6 mice: possible mechanisms for lung dysfunction. *Am J Respir. Cell Mol Biol.* 42, 210-217
- Wu, W.; Graves, L. M.; Jaspers, I.; Devlin, R. B.; Reed, W. & Samet, J. M. (1999). Activation of the EGF receptor signaling pathway in human airway epithelial cells exposed to metals. *Am J Physiol.* 277, L924-L931
- Xia, T.; Korge, P.; Weiss, J. N.; Li, N.; Venkatesen, M. I.; Sioutas, C. & Nel, A. (2004). Quinones and aromatic chemical compounds in particulate matter induce mitochondrial dysfunction: implications for ultrafine particle toxicity. *Environ Health Perspect.* 112, 1347-1358
- Zhou, Y. M.; Zhong, C. Y.; Kennedy, I. M. & Pinkerton, K. E. (2003). Pulmonary responses of acute exposure to ultrafine iron particles in healthy adult rats. *Environ Toxicol.* 18, 227-235
- Zielinska, B.; Campbell, D.; Lawson, D. R.; Ireson, R. G.; Weaver, C. S.; Hesterberg, T. W.; Larson, T.; Davey, M. & Liu, L. J. (2008). Detailed characterization and profiles of crankcase and diesel particulate matter exhaust emissions using speciated organics. *Environ Sci Technol.* 42, 5661-5666



# Polycyclic Aromatic Hydrocarbons in the Urban Atmosphere of Mexico City

Mugica Violeta<sup>1</sup>, Torres Miguel<sup>1</sup>, Salinas Erika<sup>1</sup>,  
Gutiérrez Mirella<sup>1</sup> and García Rocío<sup>2</sup>

<sup>1</sup>*Universidad Autónoma Metropolitana-Azcapotzalco*

<sup>2</sup>*Universidad Nacional Autónoma de México  
México*

## 1. Introduction

Mexico City faces a severe atmospheric pollution problem, which directly affects the population's health. This problem is engraved by the geographic conditions of the city. Recent studies around the world have demonstrated an association between the presence of airborne particles and adverse effects to health (Brauer et al, 2001; de Koc et al., 2006). Significant differences exist in the chemical composition and size distribution of PM based on the wide range of sources, meteorological conditions, atmospheric chemistry, diurnal and seasonal factors. Also PM aerodynamic size has become a relevant element when studying PM toxicity due to its variable ability to penetrate the respiratory system; fine particles can reach the deep regions of the lungs, whereas coarse PM may be deposited early within the nasal-pharyngeal passages of the airways. Nevertheless, still remains an uncertainty about the physic and chemical mechanisms of these effects. Particles are composed by many different organic and inorganic species and some of these could be the main responsible of such adverse effects.

The chemical composition of the airborne particles includes inorganic species such as heavy metals and elemental and organic carbon compounds. Among these compounds, the polycyclic aromatic hydrocarbons (PAHs) are semivolatile species formed through the fusion of two or more benzene rings by a pyrolytic process during the incomplete combustion of carbonaceous materials. PAHs can be found also in the atmosphere in the vapor phase, especially those species with low molecular weight and when temperature is high.

The main anthropogenic sources of PAHs are gasoline and diesel vehicle exhaust gases, use of natural gas, LP gas and carbon, oil combustion, petroleum refining and waste incineration. Anthropogenic combustion of wood and forest fires is also important sources of PAHs (Freeman & Catell 1996). Some of these PAHs have a significant role on the mutagenic activity of airborne particles and some of them have been classified as carcinogenics for humans (IARC, 1984; Sanderson et al., 2000, NPT, 2005): benzo[a]pyrene, benzo[a]anthracene, benzo[b]fluoranthene, benzo[k]fluoranthene, chrysene, dibenzo[a]anthracene and indeno[1,2,3-cd]pyrene. PAH derivatives such as nitroPAHs, chlorinated PAHs and oxyPAHs, which can be emitted directly from anthropogenic sources

or formed in the atmosphere by secondary reactions of PAHs usually present higher mutagenic activity than their PAH parents due probably to their higher polarity (Ohura, 2007). The human health risk associate to PAHs and their derivates is higher in the urban atmospheres considering the high population's density (Harrison et al., 1996).

Mexico City lies on an elevated plateau at 2200 meters above mean sea level, with mountains on three sides, as consequence, has complex mountain and surface-driven wind flows with predominant winds from the north-northeast; in this sense, it must be remarked that most of its industries are located precisely within the northern zone (GDF, 2005). These winds transport significantly large amounts of air pollutants emitted by industries, such as uncharacterized gaseous emissions from ferrous and non-ferrous smelting and heat-treating facilities, glass manufacturers, bricks and ceramic factories, and thermoelectric power plants. Also at the north, close to Mexico City Area, there is a large oil-refining facility located in the Hidalgo State. More than four million of vehicles. The urban area of Mexico City has more than twenty millions of inhabitants, which are exposed to the emissions from 4,000,000 of vehicles and around 30,000 industries.

In the last decade, several studies have been carried out to determine the presence of PAHs in the atmosphere of Mexico City. Velasco et al. (2004), measured real time total particles' PAHs concentrations, and Marr et al. (2004, 2006) conducted studies to determine the total PAH emission factors associated to vehicles, and to understand the atmospheric PAHs transformations; nevertheless the authors did not report detailed information on individual PAHs characterization. Villalobos-Petrini et al (2006, 2007) related the mutagenic activity with atmospheric PAH's concentrations in PM<sub>10</sub> and Amador-Muñoz (2010) studied the PM size distribution of PAHs at the Southwest of Mexico City. Considering the importance of PAHs individual speciation, Mugica et al. (2010) conducted a whole year study to characterize and evaluate the seasonal behavior of PAHs in the gas phase and PM<sub>10</sub>.

The main objective of this chapter is dedicated to the review of the campaigns and studies realized in Mexico City during the last years related with the quantification and speciation of PAHs, by the group dedicated to atmospheric chemistry at the Universidad Autónoma Metropolitana-Azcapotzalco. Sampling and analysis methodologies, as well as new findings and unpublished material have been included to enrich this review.

## 2. Methodology

The U.S. Environmental Protection Agency (USEPA, 1985) has identified 16 unsubstituted PAH as priority pollutants (Figure 1).

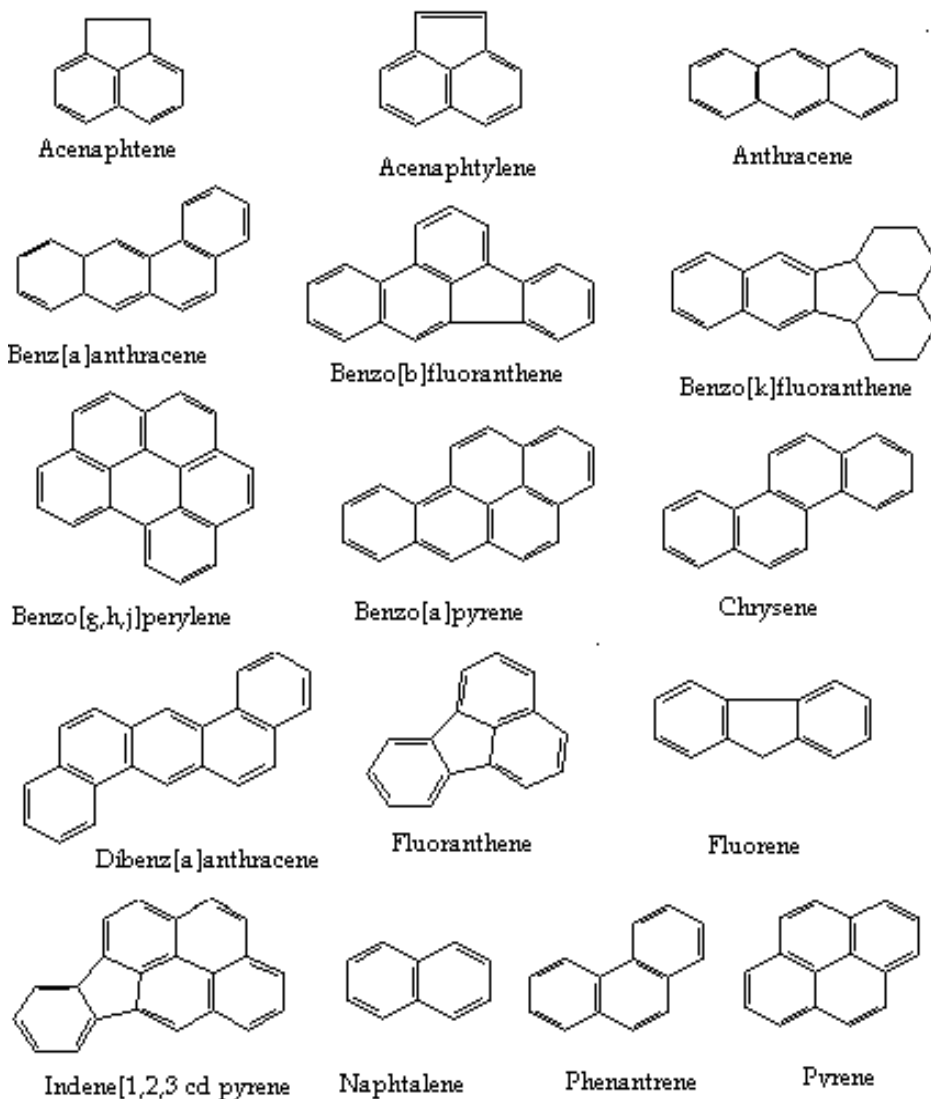


Fig. 1. Priority PAHs according to USEPA.

### 2.1 Sampling

The 2003 and 2005 sampling campaigns were carried out at the monitoring station of the Metropolitan Autonomous University, Campus Azcapotzalco (UAM-A), located at the North of the city, where the surrounding urbanization displays a mixed land occupation composed by housing and industrial areas. High volume samplers were located around six m above ground level and 230 m away from an avenue.

On the other hand, during the 2005 field campaign other three sites were selected for monitoring in order to have more information about the variation of PAHs contained in  $PM_{10}$ . These sites were the monitoring stations of Xalostoc at the Northeastern located in a huge industrial area, Merced is located close to downtown of Mexico City with many avenues with heavy and light traffic and Pedregal is located at the Southwest in a commercial and residential area. These three stations belong to the Monitoring Network of Mexico City. These places were selected since they have been representatives of other monitoring campaigns realized in Mexico City (De Vizcaya et al, 2005).

The 2006-2007 campaign was carried out from April 2006 to March 2007 within Centro de Investigación y de Estudios Avanzados (CINVESTAV, from its Spanish initials), in northern Mexico City. This site is neighboring some important state municipalities bearing intense industrial activities, and it is also surrounded by important main roads with large transit volumes, connecting northern and central regions of the metropolitan area.

In general, Mexico City climate is temperate with little humidity, namely an annual rainfall of 651.8 mm, average annual temperature of 17 °C, 3.1 m·s<sup>-1</sup> average wind velocities with prevailing northerly winds. Three seasons are recognized in Mexico City by the Monitoring System of Air Quality in Mexico City (GDF, 2005): the warm-dry season (from February to May), the rainy Season (From June to September) and the cold-dry season (from October to February).

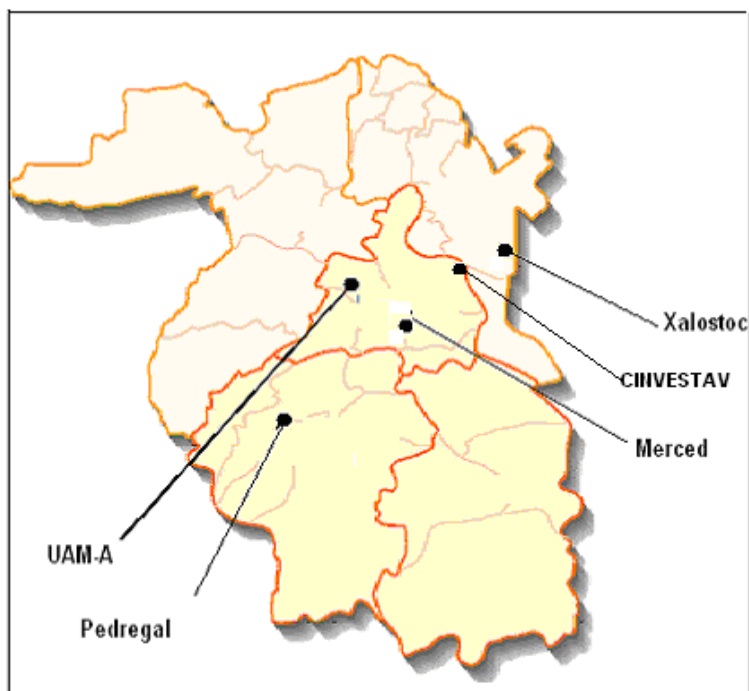


Fig. 2. Sampling Sites in the Mexico City Metropolitan Area.

Figure 2 shows the different sites where field campaigns have been performed with the aim to determine the levels of PAHs in the atmosphere of Mexico City.

The integrated 24 hr samples of PM<sub>10</sub> and PM<sub>2.5</sub> were collected every six days with the aid of Andersen and Tisch high volume samplers, using 20 x 25 cm Whatman quartz fiber filters, previously stabilized at 550°C during 24 h to remove organic matter. The vapor phase PAHs was collected into sorbent polyurethane tubes containing 50 g of XAD-4 resin located between two polyurethane foams (PUF) using a Tisch-PUF sampler. PUFs were cleaned and compress-cleaned three times using a hexane: methanol: methylene chloride (5:3:2v/v) mix, whereas the XAD-4 resin was cleaned with sonication plus water, methanol and methylene chloride rinsing. The Temperature (T), relative humidity (RH), wind speed (WS) and wind direction (WD) were obtained from the nearest monitoring station located at 2 Km of the monitoring site (Tlalnepantla) of the Automatic Monitoring Net in Mexico City (RAMA, for its Spanish initials). ([http://148.243.232.103/imecaweb/base\\_datos.htm](http://148.243.232.103/imecaweb/base_datos.htm)).

## 2.2 Extraction and analysis

PAHs were extracted from the filters and XAD4/PUFF by immersing them in an ultrasonic bath using acetonitrile/dichloromethane 1/1 v/v, for three 10 min periods. The extracts were concentrated down to 5 mL with a rotavapor followed by evaporation under purified nitrogen to near dryness and reconstituted with acetonitrile. The resulting solution was filtered to clear impurities. Finally the extracts were transferred to small amber glass vials that were sealed and stored in darkness at -18 °C until analysis.

| PAH                      | Code | MW  |
|--------------------------|------|-----|
| Naphtalene               | NAP  | 128 |
| Acenaphthylene           | ACY  | 152 |
| Acenaphtene              | ACE  | 154 |
| Fluorene                 | FLU  | 166 |
| Phenantrene              | PHE  | 178 |
| Amthracene               | ANT  | 178 |
| Fluoranthene             | FLT  | 202 |
| Pyrene                   | PYR  | 202 |
| Benz[a]anthracene        | BAA  | 228 |
| Chrysene                 | BKF  | 228 |
| Benzo[b]fluoranthene     | BBF  | 252 |
| Benzo[k]fluoranthene     | CRY  | 252 |
| Benzo[a]pyrene           | BAP  | 252 |
| Indene [1,2,3-cd] pyrene | DBA  | 276 |
| Dibenz [a,h] anthracene  | IND  | 278 |
| Benzo [ghi] perylene     | BGP  | 276 |

Table 1. Identification of quantified PAHs.

Identification and quantification was performed through GC/MS (GC model HP 6890, MS model 5973 equipped with a quadrupole mass filter and autosampler) using a 60-m 0.25 mm diameter HP-1701 capillary column (0.25 m film thickness HP). The temperature program applied was 65°C for 2 min, then 8°C/min to 320°C, held for 10 min. Fluoranthene d10 was added as internal standard according to Method TO-13A. A standard PAHs mixture was used for quantification PAHs (Table 1).

For quality control, filters and sorbent tubes were wrapped with aluminum foil and stored in the dark with refrigeration down to -18°C until sampling was to be carried out. All of the filter and PUF samples were transported to and from the field in a cooler and kept refrigerated until analysis. To address artifact contamination, a field blank for both quartz filters and PUF cartridges was collected and analyzed. As a quality control, the urban dust standard reference material (SRM 1649a) from the National Institute of Standards and Technology (NIST) was used to evaluate all PAHs mean recovery efficiency; this varied from 76% to 87.5% (ACY and BGP) from the extracted 100 ng of urban dust, subtracting of course, the field blanks filters from the sample values.

The precision and bias of the PAHs analyses were determined from quality control check samples prepared in the laboratory with fluoranthene d10 (FLUd10). Each PAH measurement was replicate eight times.

Mid-range standards (0.5 ng/L) were also run during each day of the sample analysis to verify the initial calibrations.

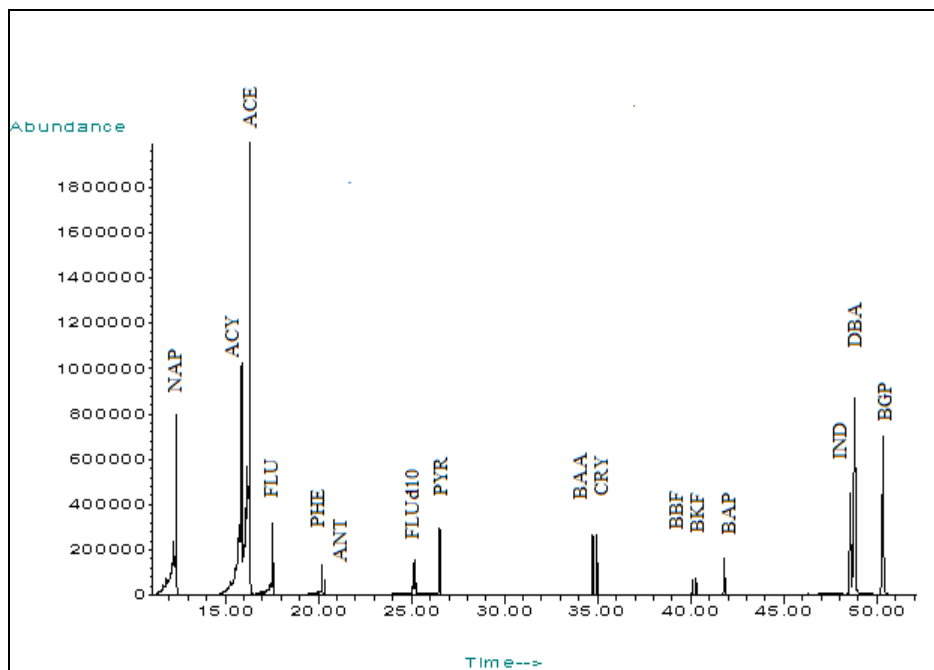


Fig. 3. Identification of PAHs by GC-MS

Precision values in percent relative standard deviation (%RSD) were: NAP (5.4), ACY (4.6), PHE (4.4), BAP (3.8), BBF (5.1), BAA (4.7), FLU (6.1), FLT (6.3), PYR (4.4), CRY (4.3), BKF (5.1), DBA (4.9), IND (4.3), and BGP (3.7). The biases in the same order were: 0.23, 2.39, -2.3, 3.4, 2.5, 2.4, -3, 0.56, 0.22, -1.24, -0.72, 1.6, -2.3, and 0.11 percent.

Figure 3 shows a typical chromatogram for individual PAH identification and quantification.

### 3. PAHs in Mexico City

In this section the most important results of the different campaigns carried out for the group of Atmospheric Chemistry of the Universidad Autónoma Metropolitana are presented and discussed.

#### 3.1 First Findings of PAH in Mexico City

The first study related to PAHs conducted at the Universidad Autónoma Metropolitana-Azcapotzalco, was carried out with the aim to standardize the sampling and PAH quantification techniques. Hi-Vol equipments (Metal Works) with fiber glass precalcinated filters were used to collect atmospheric particles, during November and December of 2003.

The results of this study showed that the average of the total sum of the 12 quantified PAHs was  $15.91 \pm 4.22$  ng/m<sup>3</sup>, with a maximum and a minimum of 20.77 and 11.04 ng/m<sup>3</sup> respectively (Figure 4); these concentrations were similar to those reported in Birmingham at the United Kingdom (Harrison et al 1996), in Naples, Italy (Caricchia et al, 1999), and Oporto and Vienna (Rocha et al, 1999).

Although naphthalene, acenaphthene, acenaphthylene and anthracene were quantified, they are not presented since during the sample manipulation, these compounds could be evaporated.

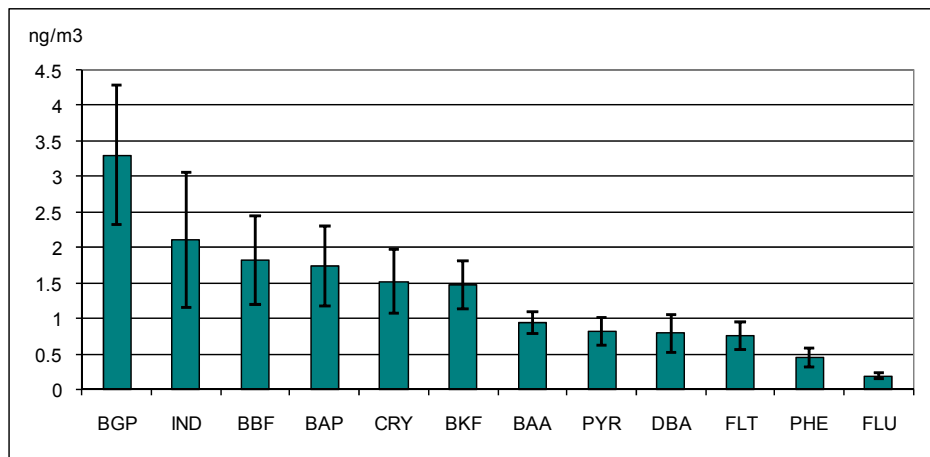


Fig. 4. PAH concentrations in PST (November and December 2003).

High molecular PAH were the most abundant species in PM. The highest concentration was presented by BGP followed by IND, BBF and BAP, which have been associated with vehicle emissions (Dichut et al, 2000). Most abundant compounds have low vapor pressures. The percentage of the seven potential carcinogenic PAHs ranged between 54 and 65% of the total PAH mixture.

It has been reported that FLT/FLT+PYR ratios below 0.40 imply the contribution of unburned petroleum and ratios between 0.40 to 0.50 suggest their emissions from the combustion of liquid fossil fuels (vehicle and crude oil), and ratios larger than 0.50 are characteristic of wood, or coal combustion (Yunker, 2002). The average ratio (0.48) obtained in this campaign is indicative of combustion of liquid fuels, such as gasoline and diesel. On the other hand, when the ratio of IND/IND+BGP is lower than 0.2 imply petroleum emissions, if the ratio ranges 0.20-0.50 imply liquid fossil fuel combustion (Yunker, 2002), as is the case again since the obtained ratio is 0.30.

### **3.2 Temporal and spatial variations of PAHs associated with particles in Mexico City**

A big field campaign was performed from February 2005 to January 2006 collecting 50 integrate samples at the UAM-A in Mexico City to determine the seasonal variation of PAHs contained in the vapor phase and in PM<sub>10</sub> (Mugica et al, 2010). On the other hand, nine samples were collected at each of the other three monitoring sites: Xalostoc, Merced and Pedregal (three samples every season) in order to know the spatial variation of PAHs associated to PM<sub>10</sub>.

The particle phase contributed with only less than 0.01 % of the total mass of PAH. High molecular PAH such as BBF, BKF, IND, DBA and BGP were found predominantly in the particle phase, whereas, as expected, light PAH of two, three and four rings, NAP, ACY, FLU and PHE were mostly in the vapor phase. Semivolatile PAH, PYR, BAA, CRY and BAP were observed in both phases.

Marr et al (2006) have reported that concentrations at different sites of the city are very variable, and this is the situation of the results found at the different locations. Figures 5, 6 and 7 show the average levels of the individual PAHs measured in PM<sub>10</sub> in the different campaigns carried out during 2003. Highest concentrations were measured at Xalostoc that is the most important industrial area in the metropolitan area of Mexico City. In this site the sum of the 12 PAHs reached up to 105 ng/m<sup>3</sup> during the dry-cold season. The lowest values were found at UAM-A, although this could be due to more samples were collected and more holidays and different meteorological conditions occurred during the campaign, in addition the University has many trees and big green areas which can capture an important proportion of atmospheric particles.

In the dry-cold season the levels of total measured PAHs were up to three fold greater than in the other seasons, and the smallest PAHs measured concentrations were in the dry-warm season. These results may be explained by the fact that during the dry-cold season, temperature inversions and calm winds, occurring very often during the fall and winter, which favors air pollutants' increase in Mexico City's atmosphere. Further, during this season the main winds come from the North where the most important industrial area is located. The highest temperature and solar radiation values occurred during the warm-dry season and the lowest values in the cold-dry season, when the solar zenith angle is around 43°. It is expected a PAHs' maximum evaporation as well as photochemical activity from PAHs to oxydated PAHs and nitro-PAHs in the months with greater actinic fluxes, which

happen at the end of winter through spring; this fact could explain the lower PAHs levels in the warm-dry season in comparison with the other seasons. The seasonal variability of PAH concentration in the atmosphere has been reported for other cities such as Los Angeles (Eiguren, 2004).

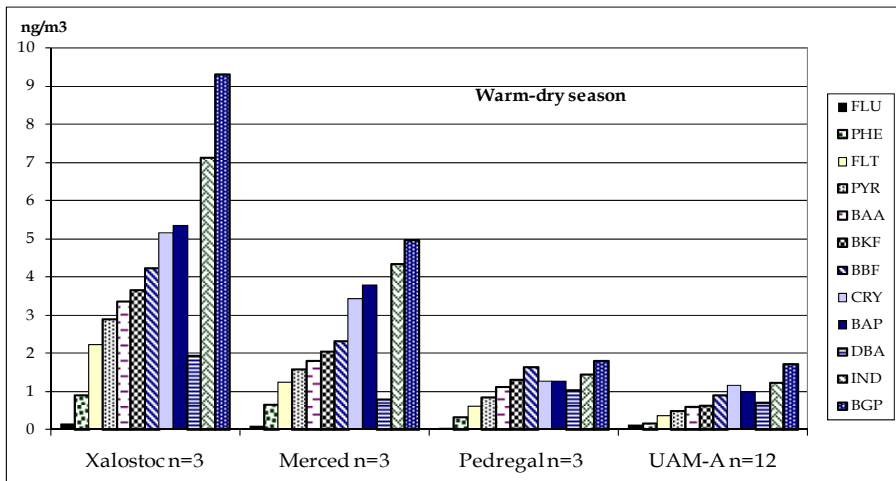


Fig. 5. Concentrations of PAHs at different locations in the warm-dry season.

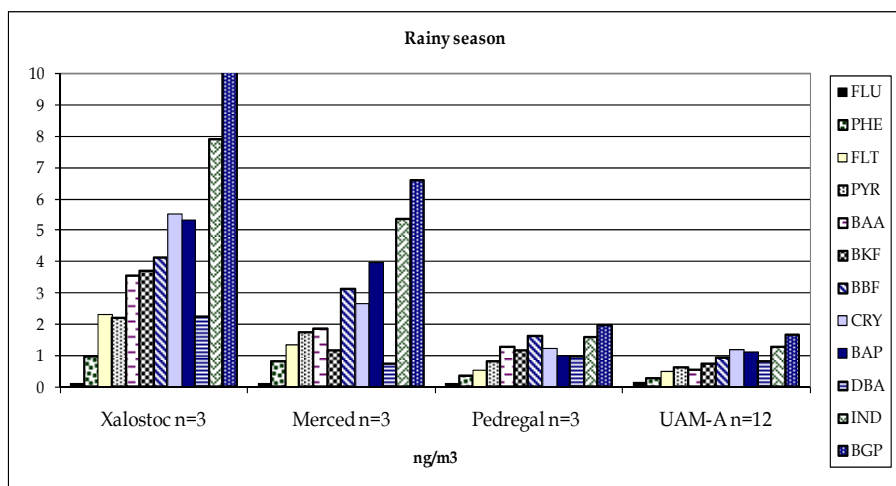


Fig. 6. Concentrations of PAHs at different locations in the rainy season.

Amador-Muñoz et al (2010) quantified in 1999 the PAH concentration at the National University of Mexico, which is located pretty close from the Pedregal site. The concentrations found in this study are a little higher to those found by these researchers although the University area has many green areas which can diminish the PM concentrations. Besides, this study is in agreement with the results reported by Guzmán-

Torres et al. (2009), where PAHs associated with PM<sub>10</sub> were determined in 2003 at two of the sites sampled in this study: Merced considered as a source site and Pedregal considered as a receptor site. In that study, was determined that higher PAH concentrations are observed during the morning from 5:00 to 13:00h, whereas the lowest concentrations were found from 13:00 to 21:00, at the two sites.

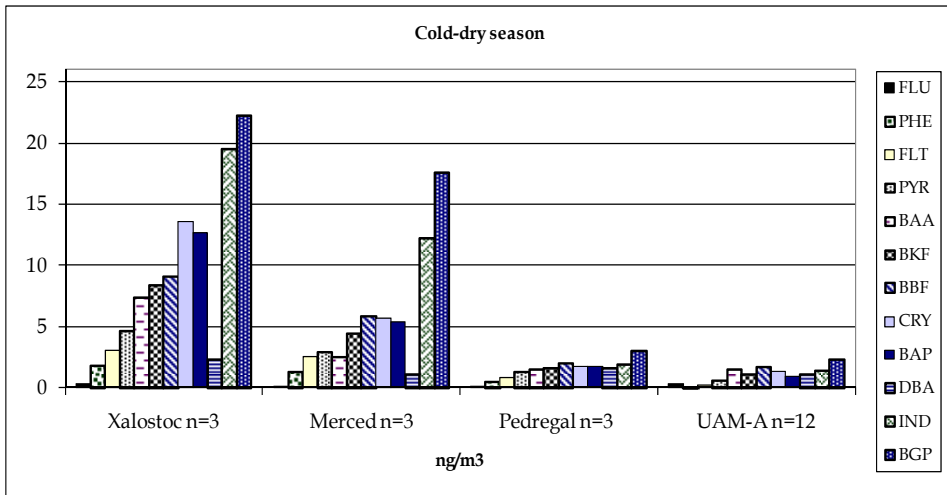


Fig. 7. Concentrations of PAHs at different locations in the cold-dry season.

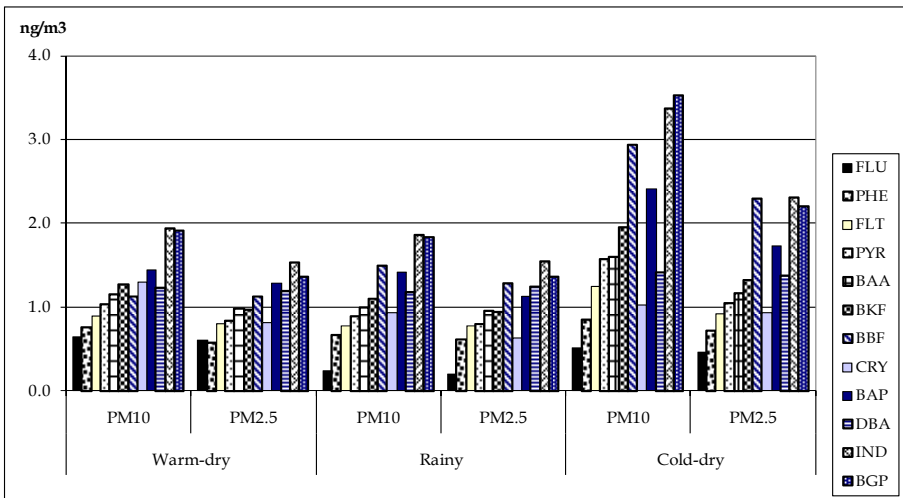


Fig. 8. Comparison of the content of PAHs in PM<sub>10</sub> and PM<sub>2.5</sub> at CINVESTAV site.

The last campaign was conducted from April 2006 to March 2007 at the CINVESTAV. In this campaign, not only were determined the PAHs contained in PM<sub>10</sub> but also in PM<sub>2.5</sub>. Figure 8 shows the comparison of the content of PAHs in both sizes of airborne particles. The

average ratio between  $PM_{2.5}/PM_{10}$  was 0.82, 0.86 and 0.74 for the warm-dry, rainy and cold-dry seasons respectively. In general, low molecular PAHs had a higher ratio than high molecular PAHs.

### 3.3 Temporal variations of PAHs in the vapour phase in Mexico City

Table 2 shows the average temperatures and relative humidity observed during 2005 in the UAM-A site. These values explain the concentrations of PAH in the vapor phase presented in the Figure 9. Due to its high abundance, naphthalene was eliminated from the graph, but its average concentrations were  $149\pm 89$ ,  $28\pm 5$  and  $78\pm 28$   $ng/m^3$ , for warm-dry, rainy and cold-dry seasons respectively.

|          | TEMPERATURE °C |     |      |      | RELATIVE HUMIDITY |      |      |      |
|----------|----------------|-----|------|------|-------------------|------|------|------|
|          | Mean           | S.D | Max  | Min  | Mean              | S:D  | Max  | Min  |
| Warm-dry | 18.5           | 5.1 | 29.9 | 8.0  | 51.0              | 16.9 | 82.9 | 19.9 |
| Rainy    | 17.6           | 3.8 | 27.3 | 11.4 | 72.0              | 13.7 | 93.4 | 40.9 |
| Cold-dry | 13.2           | 3.9 | 23.2 | 4.7  | 55.9              | 16.3 | 92.5 | 23.3 |

Table 2. Temperature and Relative Humidity in Mexico City in the three seasons

Two and three-ringed PAHs (naphtalene through anthracene), were found almost exclusively in the vapor phase. The four, five and six-ringed PAHs (FLT to BGP) were distributed in both phases.

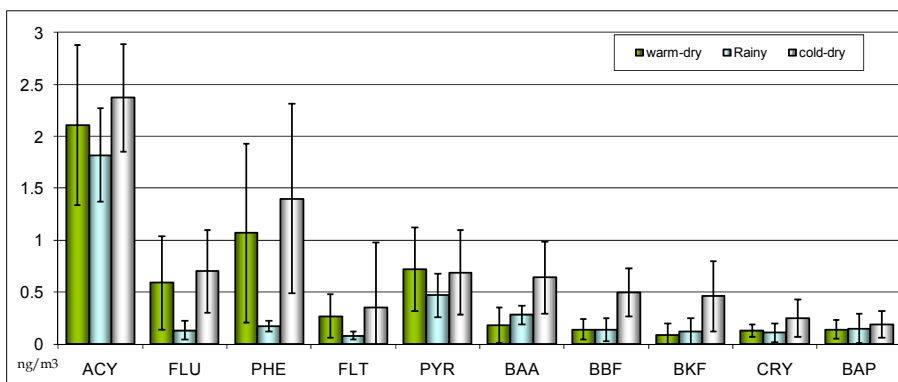


Fig. 9. Seasonal variation of PAHs in the vapor phase at UAM-A site.

The gas/particle partitioning of these compounds is affected by the physicochemical characteristics of the aerosol (chemical composition, particle size, surface area) and the ambient conditions (temperature, pressure). Table 3 shows the seasonal variability of the gas-particle partitioning through 2005 as well as their vapor pressure (USEPA, 1997). As expected, due to the elevated temperatures, the highest gas/particle ratio was attained during the dry-warm season, although the gas-partitioning ratio of most of the PAH considered was lower for the rainy season than for the dry-cold season, despite of minor

temperature during the latter, showing that other factors different from temperature have an influence on the gas-particle partitioning, such as the relative humidity and vapor pressure of PAH, among other factors as reported previously (Bae et al, 2002).

| PAH | Vapor pressure<br>KPa | Dry-warm | Rainy | Dry-cold |
|-----|-----------------------|----------|-------|----------|
| FLU | $8.7 \times 10^{-5}$  | 5.9      | 1.7   | 2.3      |
| PHE | $2.3 \times 10^{-5}$  | 13.52    | 3.12  | 5.45     |
| PYR | $3.1 \times 10^{-6}$  | 2.07     | 1.85  | 1.19     |
| FLT | $6.5 \times 10^{-7}$  | 2.28     | 0.77  | 1.4      |
| BBF | $6.7 \times 10^{-8}$  | 1.01     | 0.52  | 0.41     |
| BKF | $2.1 \times 10^{-8}$  | 0.79     | 0.57  | 0.43     |
| BAA | $1.5 \times 10^{-8}$  | 1.06     | 0.63  | 0.40     |
| CRY | $5.7 \times 10^{-10}$ | 0.54     | 0.41  | 0.18     |
| BAP | $7.3 \times 10^{-10}$ | 0.58     | 0.53  | 0.24     |

Table 3. Gas-particle partitioning of semivolatile PAH ng/m<sup>3</sup>vapor/ng/m<sup>3</sup>PM. (Mugica et al, 2010)

#### 4. Back trajectory analysis

This study was performed for the 2005 campaign although there are many similarities with the other years. Meteorological conditions varied along the year, the dry season runs from the middle of October to the beginning of May and is characterized by almost daily temperature inversions and high speed winds, producing an increase in air pollutants in the boundary layer. As often is the case, during the dry-warm season some fires were reported and the predominant high speed winds that originate from the south-east of  $5.5\text{--}10.8 \text{ m s}^{-1}$ , favored the pollutant's dispersion; consequently the PM concentrations in 2005 were lower than those registered other years, incidentally lower than in the rainy season, where winds originated mainly from the east with WS of  $1.6 \text{ a } 5.5 \text{ m s}^{-1}$ . Finally, during the dry-cold months the predominant winds came from the north and northeast, with  $0.3 \text{ to } 1.6 \text{ m s}^{-1}$ , compared with the spring and summer months, the high stability of the air mass reduced the rates of pollutant dispersion. With the aim to know the relationship between the average concentrations and wind directions, PAH were associated with the corresponding air mass back trajectories calculated by the NOAA HYSPLIT model (Hybrid Single-Particle Lagrangian Integrated Trajectory Model) (Draxler and Rolph, 2003). Air mass back trajectories were estimated for 1000 and 3000 meters above ground level. NOAA trajectories were calculated for year 2005. The 1000 MAGL (Meters above Ground Level) level was used because storm cloud bases frequently lie around 1000 MAGL. The 3000 MAGL level is about 1200 m higher than the highest mountain summit lying Mexico City; It is also close to the height of the 500 millibar (mb) isobaric surface (one of the mandatory levels in meteorological analysis).

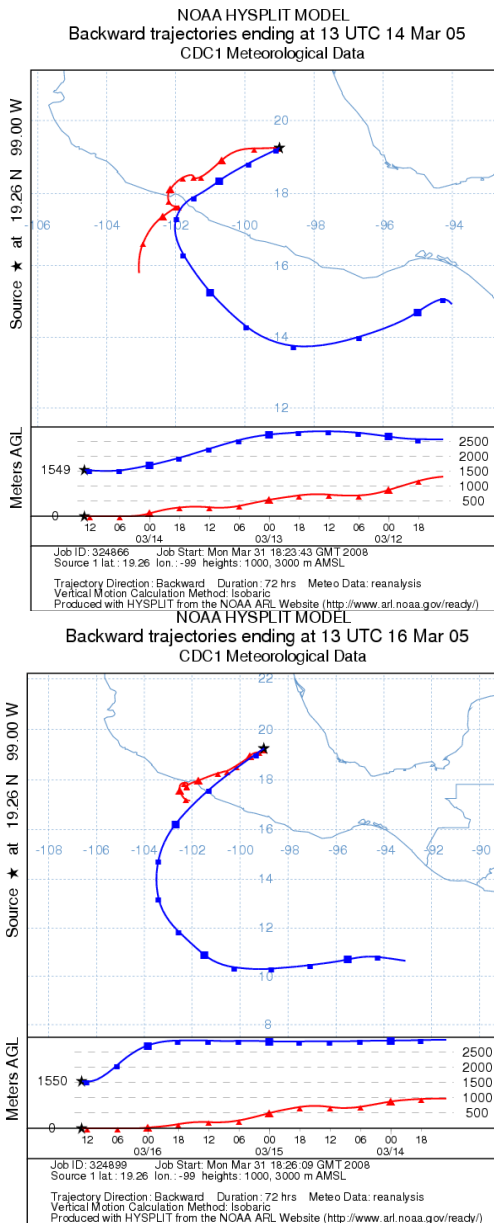


Fig. 10. Some air-mass back trajectories observed during the Dry-warm season in 2005 corresponding to 1000 and 3000 MAGL.

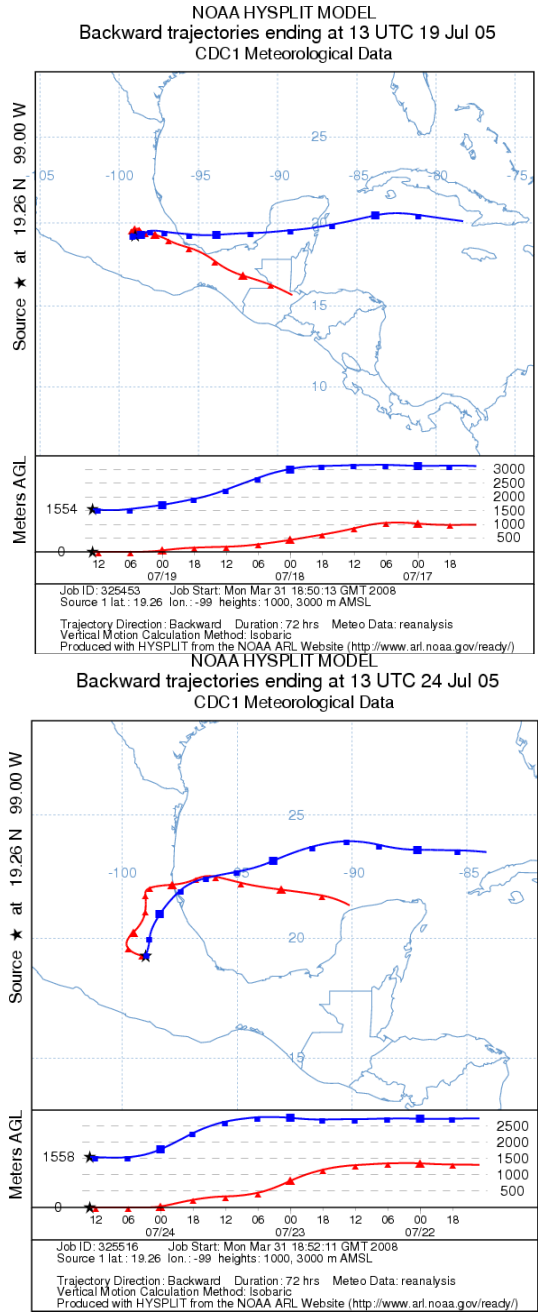


Fig. 11. Some air-mass back trajectories observed during the rainy season in 2005 corresponding to 1000 and 3000 MAGL.

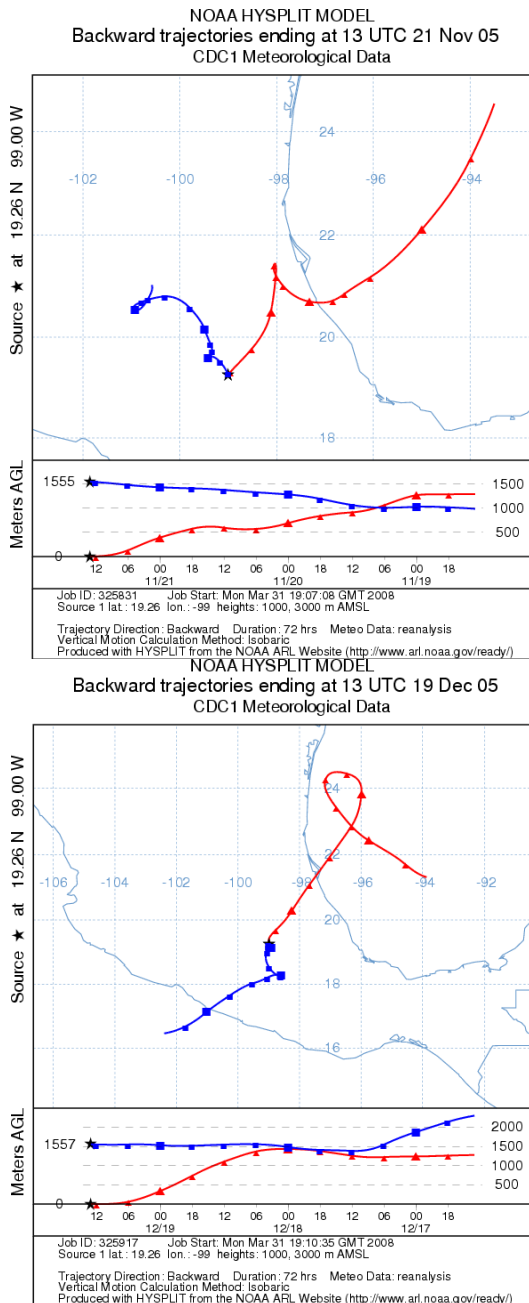


Fig. 12. Some air-mass back trajectories observed during the Dry-cold season in 2005 corresponding to 1000 and 3000 MAGL.

Figures 10, 11 and 12 show an example of six trajectories chosen at random because it would be excessive to show all the trajectories. Since Mexico City is the subject of intense anthropogenic emission sources. Figure 10 shows the air mass back trajectory analysis during the dry-warm season along 2005. Trade winds have a consistent component from the west and during this season the winds blow mostly along south and southeast. There was also a reasonably good correspondence with the physical characteristics on the sampling site. Since the University site is surrounded by intense anthropogenic emission sources, Figure 11 shows some examples of air mass back trajectories randomly selected during the rainy season when winds bear eastern directions. The average of PAH decreased in the order NAP, ACY, FLU, PYR, FLT, BAA, BAP and BGP at 1000 and 3000 MAGL.

Figure 12 shows the analysis at 3000 MAGL for the dry-cold season, where large extensions of barren soils lie. An attempt was made to associate these PAH concentrations with surface wind.

The concentration of major PAHs in PM<sub>10</sub> were presented when back trajectories indicated winds from the North and Northeast where most of the industrial areas are situated, and this, in addition to the atmospheric stability of this season explain the high concentrations of particles and total PAH found. This agree with the synoptic meteorological conditions that prevail in Central Mexico (MC) during the dry-cold; trade winds have a consistent component from the East, that is, winds blow between North and Northeast most of the time during this season.

## 5. Source identification applying statistical analysis

StatSoft 6.4 program was used to calculate Principal Component Analysis (PCA). With this analysis is possible to identify possible sources of pollutants and to validate the method applied, following the criteria described by other authors. Table 4 shows the factor loadings normalized with the VARIMAX rotation, which maximizes the variances of the squared normalized factor loadings across variables for each factor. The greater the loading of a variable the more that variable contributes to the variation accounted for the particular Factor or Principal Component (PC). In general only loadings greater than 50% are selected for PC interpretation<sup>25</sup>. This is one of the methods mostly used for source identification.

The PCA applied to PAHs, revealed three factors that explained the 72.76% of the total variance. These factors indicate their major role on the total variance, when PCA is applied through the linear combination of twelve PAHs and represent the source categories. The first factor is the most important, given the explained variance of 34.91%. The main tracers of this factor are mostly associated to low molecular weight PAHs, namely, ACY, FLU, PHE and FLT, which could be associated mainly with diesel source emissions, since Wang et al., (2007) indicated the dominance of diesel combustion with the presence of three and four ring PAHs (such as FLT and PHE), as well as with oil combustion. Large emissions from diesel could be related also with the high concentrations of CRY which has been suggested as a diesel tracer (Simcik et al. 1999; Fujita et al. 2007).

The second factor was mostly associated with high molecular weight PAHs accounting 23.66% of the total variance. CRY, BAP, BBF, BKF, IND and BGP can be related to gasoline vehicles. Some researchers have found that IND and BGP are gasoline tracers (Harrison et al, 1995; Miguel et al., 2004).

The third factor was characterized by CRY and BAP which has been related with wood burning, diesel and meat cooking (Rogge et al., 1991, Kulkani and Venkataraman, 2000).

| Variable               | 2005, 2006, 2007. PM <sub>10</sub> |              |              |
|------------------------|------------------------------------|--------------|--------------|
|                        | Factor 1                           | Factor 2     | Factor 3     |
| mass                   | 0.143                              | <b>0.603</b> | 0.304        |
| NAP                    | 0.352                              | 0.143        | <b>0.832</b> |
| ACY                    | <b>0.967</b>                       | 0.212        | 0.165        |
| FLU                    | <b>0.847</b>                       | 0.009        | 0.048        |
| PHE                    | <b>0.798</b>                       | 0.142        | 0.054        |
| FLT                    | <b>0.843</b>                       | 0.251        | 0.077        |
| PYR                    | 0.217                              | 0.187        | 0.316        |
| BAA                    | 0.233                              | 0.393        | 0.088        |
| CRY                    | <b>0.579</b>                       | <b>0.754</b> | <b>0.922</b> |
| BAP                    | <b>0.749</b>                       | <b>0.648</b> | <b>0.634</b> |
| BBF                    | 0.025                              | <b>0.792</b> | 0.212        |
| BKF                    | 0.043                              | <b>0.748</b> | 0.137        |
| IND                    | 0.085                              | <b>0.572</b> | <b>0.738</b> |
| DBA                    | 0.239                              | 0.217        | <b>0.823</b> |
| BGP                    | 0.154                              | <b>0.881</b> | 0.250        |
| % Total Variance       | 34.912                             | 23.662       | 14.183       |
| % Accumulated Variance | 35.381                             | 58.574       | 72.757       |

Table 4. Principal Component Analysis for PM<sub>10</sub> in Mexico City. Bold numbers are significant at > 0.5.

## 6. Health implications by the presence of PAHs in Mexico City

The percentage of the seven potential carcinogenic PAHs found in the TSP collected in 2003, ranged between 54 and 65% of the total PAH mixture, whereas in the campaigns conducted in 2005 the seven carcinogenic PAHs represented between 61 and 73% of the total mixture of PAHs in PM<sub>10</sub>. The carcinogenic PAHs contained in PM<sub>2.5</sub> ranged between 65 and 68% with higher percentages in the cold dry-season during 2006-2007. If we estimate the daily potential dose of carcinogenic PAHs considering an intake of 20 m<sup>3</sup> of polluted air, the average results to be between 123 ng/m<sup>3</sup> and 1460 ng/m<sup>3</sup> as can be appreciated in Table 35. These high values show that the population of Mexico City is exposed to high concentrations of potential carcinogenic species, especially those who live at the Northeast close to Xalostoc.

The European Union has proposed for the PM<sub>10</sub> fraction, a maximum permissible risk level of 1000 pg/m<sup>3</sup> of BAPEq calculated for one year calendar, to be achieved in 2010 (European directive, 2004). To calculate the inhalation unit risk for excess lung cancer over the risk posed by BAP for each of the other carcinogenic PAHs in the polluted atmosphere, the particular PAHs risk is divided by the risk of BAP to obtain their individual toxic equivalence factor /TEFs). Thus, the TEF for BAP is for definition 1.0. These TEFs can be used to estimate the relative carcinogenicity of the PAH mixture when concentrations of individual PAHs are known. The concentrations of each individual PAH are multiplied by the TEF to obtain the BAPEq values. Table 6 presents the estimated BAPEq values by site using the factors proposed by Nisbet & Lagoy factors (1992), where is evident that in all the

sites the annual average of BAPEq, which represents the carcinogenic potential of inhaled PAHs, is exceeded, especially in Xalostoc and Merced locations where the values are almost eleven and six folds higher than the proposed standard respectively. BAP alone contributes to carcinogenic potency in PM<sub>10</sub> with 63 to 71%, underlying the importance of this compound. These results suggest that the inhabitants of those municipalities could be in a high-risk category for developing cancer. Taking in account this information the policy makers could review the airborne particles regulation and consider the recommendation of a similar standard than the European Community.

| STUDY/SEASON                            | DRY-WARM SEASON<br>NG/DAY | RAINY SEASON<br>NG/DAY | COLD-DRY SEASON<br>NG/DAY |
|---|---------------------------|------------------------|---------------------------|
| PST, 2003. UAM-A                        |                           |                        | 208                       |
| PM <sub>10</sub> , 2005. UAM-A          | 123                       | 131                    | 184                       |
| PM <sub>10</sub> , 2005. Pedregal       | 180                       | 175                    | 250                       |
| PM <sub>10</sub> , 2005. Merced         | 369                       | 377                    | 748                       |
| PM <sub>10</sub> , 2005. Xalostoc       | 616                       | 647                    | 1460                      |
| PM <sub>10</sub> , 2006-2007. CINVESTAV | 190                       | 180                    | 295                       |
| PM <sub>2.5</sub> , 2006-2007 CINVESTAV | 159                       | 156                    | 223                       |

Table 5. Daily potential intake of carcinogenic PAHs at different sites and seasons in Mexico City

| PAH | Nisbet & Lagoy TEF | BAPEq in pg/m <sup>3</sup> |             |             |             |                     |
|-----|--------------------|----------------------------|-------------|-------------|-------------|---------------------|
|     |                    | XAL 2005                   | MER 2005    | PED 2005    | UAM-A 2005  | CINVESTAV 2006-2007 |
| FLU | 0.001              | 0.199                      | 0.131       | 0.097       | 0.183       | 0.465               |
| PHE | 0.001              | 1.225                      | 0.947       | 0.399       | 0.223       | 0.771               |
| FLT | 0.001              | 2.527                      | 1.728       | 0.652       | 0.367       | 0.978               |
| PYR | 0.001              | 3.247                      | 2.089       | 0.978       | 0.553       | 1.176               |
| BAA | 0.100              | 476.733                    | 207.267     | 131.567     | 90.000      | 125.682             |
| BKF | 0.100              | 523.633                    | 254.633     | 137.033     | 83.333      | 145.104             |
| BBF | 0.100              | 582.533                    | 375.967     | 177.267     | 117.333     | 186.32              |
| CRY | 0.010              | 81.000                     | 39.303      | 14.297      | 12.433      | 10.896              |
| BAP | 1.000              | 7774.333                   | 4381.000    | 1332.667    | 1000.000    | 1752.595            |
| DBA | 0.100              | 216.567                    | 87.500      | 122.633     | 86.667      | 128.355             |
| IND | 0.100              | 1151.033                   | 731.833     | 165.133     | 128.000     | 239.426             |
| BGP | 0.01               | 139.637                    | 97.173      | 22.693      | 19.033      | 24.317              |
|     |                    | <b>10953</b>               | <b>6180</b> | <b>2105</b> | <b>1538</b> | <b>2615.897</b>     |

Table 6. Toxic equivalency factors (TEFs) and calculated BAPEq from measured concentrations.

## 7. Comparison of the level of PAHs in other countries

The data for PAH concentrations in PST and PM<sub>10</sub> are lower than those measured in Shijiazhuang, China (Feng et al, 2007) and New Delhi, India (Dhruv, 2003), they are similar to those found in Seoul, Korea, Jakarta, Xiamen, China and Bangkok, Thailand (Panther et al 1999; Hong et al., 2007, Thongsanit et al., 2003), but are significantly higher than those observed in Italy (Menichini et al., 1999), London (Kendall et al., 2001), Gran Canaria (2003), Greece (Kalaitzoglou et al., 2004) and California, USA (Miguel et al., 2004).

Table 7 presents a comparison of the PAHs associated to PM<sub>2.5</sub> at different cities in the world, where it is possible observe that concentrations of PAHs in Mexico City at the CINVESTAV site are similar to those of the other Latin America city of Sao Paulo, but higher than cities in the United States and Spain.

|                      | Mexico    | USA <sup>a</sup> | USA <sup>a</sup> | Brasil <sup>b</sup> | Spain <sup>c</sup> |
|----------------------|-----------|------------------|------------------|---------------------|--------------------|
| [ng/m <sup>3</sup> ] | CINVESTAV | Lompoc/LA        | Riverside/LA     | Sao Paulo           | Valencia           |
| NAP                  | 0.629     | 0.015            | 0.007            | 0.020               | 0.13               |
| ACY                  | 0.644     | N.D.             | N.D.             | 0.090               | 0.5                |
| ACE                  | 0.488     | 0.003            | 0.001            | 0.350               | N.D.               |
| FLU                  | 0.293     | 0.008            | 0.008            | N.D.                | 0.17               |
| PHE                  | 0.739     | 0.001            | 0.027            | 0.180               | 0.33               |
| ANT                  | 0.667     | 0.002            | 0.002            | N.D.                | 0.03               |
| FLT                  | 0.858     | 0.005            | 0.024            | 0.680               | 0.37               |
| PYR                  | 0.962     | 0.006            | 0.038            | 0.520               | 0.23               |
| BAA                  | 1.081     | 0.006            | 0.020            | 0.460               | 0.29               |
| CRY                  | 1.180     | 0.008            | 0.032            | 0.510               | 0.33               |
| BBF                  | 1.831     | 0.012            | 0.056            | 1.230               | 0.48               |
| BKF                  | 0.811     | 0.006            | 0.027            | 0.760               | 0.27               |
| BAP                  | 1.483     | 0.009            | 0.047            | 0.520               | 0.32               |
| IND                  | 1.899     | 0.012            | 0.052            | 2.470               | 0.41               |
| DBA                  | 1.297     | 0.002            | 0.006            | N.D.                | 0.49               |
| BGP                  | 1.862     | 0.023            | 0.112            | 2.360               | 0.41               |

a Eiguren Fernández et al., 2004, b Bourotte et al., 2005., c Viana et al, 2008.

Table 7. Comparison of PAH associated to PM<sub>2.5</sub> in the CINVESTAV study at Mexico City with other countries.

## 8. Summary

Several studies have been carried out in Mexico City related with the presence of airborne PAHs in vapor and particle-phase. The concentration of PAHs observed are higher than those found in the United States and Europe, but lower than in the most polluted cities of China and India, and showed a great variability at different sites of the city. The most polluted locations are close to the industrial areas at the Northeast of the city where

dominant winds prevail. Most of PAHs are present in the fine fraction ( $PM_{2.5}$ ) contributing with 75 to 85% of the total mass. Seasonal variations in PAH concentrations were also observed as well as the highest concentrations in both size of particles and in the phase vapor were during the cold-dry season. High concentrations of BAP, BGP and IND indicate that the city is impacted by vehicular emissions. The levels of PAHs in the atmosphere of Mexico City are such as that constitutes a high health risk to its inhabitants. Long-term studies at several locations should be conducted to determine with a higher certainty the exposure of the population and should be considered the proposal of a standard just like in the European Union. On the other hand, results obtained showed that this is an important issue for the management of Mexico City air quality, since inhabitants of Mexico City spends more than an hour near to the roadsides.

## 9. Acknowledgements

The authors are indebted to Universidad Autónoma Metropolitana Azcapotzalco for the support to this research. Violeta Mugica, Miguel Torres, Mirella Gutiérrez and Rocío García are grateful to the SNI for the distinction of their membership and the stipend received

## 10. References

- Amador-Munoz, O., Villalobos-Pietrini, R., Agapito-Nadales, Ma.C., Munive-Colin, Z., Hernandez-Mena, L., Sanchez-Sandoval, M., Gomez-Arroyo, S., Guzman-Rincon, J. (2010). Solvent extracted organic matter and polycyclic aromatic hydrocarbons distributed in size-segregated airborne particles Atmospheric Environment, 44: p.122-130.
- Bae, S. Y., Yi, S. M., and Kim, Y. P. (2002). Temporal and Spatial Variations of the Particle Size Distribution of PAHs and their Dry Deposition Fluxes in Korea, Atmos. Environ. 34:5491-5500.
- Borja-Aburto V.H., Castillejos M., Gold D.R., Bierzwinski S., Loomis D. (1998) Mortality and ambient fine particles in southwest Mexico City, 1993-1995. Environ Health Perspective. 106: 849-55.
- Bourotte, C.; Forti, M.C.; Taniguchi, S.; Bicego, M.C.; Lotufo, P.A.; 2005. A winter study of PAHs in fine and coarse aerosols in São Paulo city, Brazil, Atmospheric Environment, 39, 3799-3811.
- Brauer M., Avila-Casado C., Fortoul T.I., Vedal S., Stevens B., Churg A. (2001) Air pollution and retained particles in the lung. Environmental Health Perspective. 109: 1039-43.
- de Kok, T.M.C.M., Driessche, H.A.L., Hogervorst, J.G.F., Briedé, J.J. (2006). Toxicological assessment of ambient and traffic-related particulate matter: A review of recent studies. Mutation Research, 613: 103-122.
- De Vizcaya-Ruiz A., Gutiérrez-Castillo ME, Uribe-Hernández M, Cebrián ME, Mugica-Alvarez V, Sepúlveda J., Rosas I, Salinas E, Martínez F, Garcia-Cuéllar C, Alfaro-Moreno E, Torres-Flores V, Osornio-Vargas A, Sioutas C, Fine P, Singh M, Geller M, Kuhn T, Eiguen-Fernandez A, Miguel A, Shiest R, Reliene R, Cho A, Patel-Coleman K, Froines J. Characterization and in vitro biological effects of concentrated particulate matter from Mexico City. Atmospheric Environment, 40. 583-592. 1352-2310.

- Dichut R., Canuel E., Gustafson K., Walker S., Edgecombe G., Gaylor M. And Macdonald E. (2000). Automotive sources of carcinogenic PAH with particulate matter in the Chesapeake Bay Region. *Environmental Science and Technology*. 34, 4535-4640.
- Eiguren-Fernández A.; Miguel H.; Froines F.; Thurairatnam S., and Avol E. (2004). Seasonal and Spatial Variation of Polycyclic Aromatic Hydrocarbons in Vapor-Phase and PM<sub>2.5</sub> in Southern California Urban and Rural Communities. *Aerosol Science and Technology*, 38:447-455.
- European directive (2004). Directive 2004/107/CE from the European Parliament, related to arsenic, cadmium, mercury, nickel and polycyclic aromatic hydrocarbons. Official Journal of the European Union, 26.1.2005, 14 pp.
- Freeman D. and Catell F. (1990) Woodburning as a Source of atmospheric Polycyclic Aromatic Hydrocarbons. *Environmental Science and Technology*; 24 , 1581-1585.
- Caricchia A. M., Chiavarini S., Pezza M. (1999). Polycyclic aromatic hydrocarbons in the urban atmosphere particulate matter in the city of Naples (Italy). *Atmospheric Environment*. 33, 3731-3738.
- Dhruv S.; Sawant A.; Uma R.; Cocker III D. (2003). Preliminary chemical characterization of particle-phase organic compounds in New Delhi, India. *Atmospheric Environment*. 37. 4317-4323.
- Draxler, R.R., Rolph, G.D., 2003. HYSPLIT (HYbrid Single-Particle Lagrangian Integrated Trajectory) Model access via NOAA ARL READY Website (<http://www.arl.noaa.gov/ready/hysplit4.html>). NOAA Air Resources Laboratory, Silver Spring, MD.
- Fujita, E.; Zielinska, B., Campbell, D.; Arnott, W.P.; Sagebiel, J.; Mazzoleni, L.; Chow, J.; Crews, W.; Snow, R.; Clark, N.; Wayne, W.S.; Lawson, D. (2007). Variations in Speciated Emissions from Spark-Ignition and Compressed-Ignition Motor Vehicles in California's South Coast Air Basin; *J. Air & Waste Manage. Assoc.*, 57, 705-720; doi: 10.3155/1047-3289.57.6.705.
- GDF. Gobierno del Distrito Federal. Informe Climatológico Ambiental en el Valle de México. 2005.
- Feng Y., Shi G. Wu J., Wang Y., Zhu T., Dai S., Pei Y. (2007). Source Analysis of Particulate-Phase Polycyclic Aromatic Hydrocarbons in an Urban Atmosphere of a Northern City in China. *J. Air & Waste Manage. Assoc.* 57:164-171.
- Guzmán-Torres, D., Eiguren-Fernández, A., Cicero-Fernández, P., Maubert-Franco, M., Retama-Hernández, A., Villegas, R.R., Miguel, A.H. (2009). Effects of meteorology on diurnal and nocturnal levels of priority polycyclic aromatic hydrocarbons and elemental and organic carbon in PM<sub>10</sub> at a source and a receptor area in Mexico City. *Atmospheric Environment*, 43: 2693-2699
- Harrison R., Smith D., Luhana L. (1996). Source apportionment of atmospheric polycyclic aromatic hydrocarbons collected from an urban location in Birmingham, U.K. *Environ. Sci. Technology*. 30, 825-832.
- Hernández, B.Y. Carreón, V. Mugica, M. Torres. (2004) Polycyclic aromatic hydrocarbons in the atmosphere of Mexico City. Proceedings of the XXIX Interamerican Conference of Sanitary and Environmental Engineering. Puerto Rico.
- Hong, H.; Yin, H.; Huang, X.; Ye, C. (2007). Seasonal Variation of PM<sub>10</sub>-Bound PAHs in the Atmosphere of Xiamen, China; *Atmos. Res.*, 85, 429-441.

- IARC, (International Agency for Research on Cancer). Polynuclear Aromatic Compound, Part 1. Chemicals, Environmental and Experimental Data. Monograph 32. Lyon. 1986.
- Kalaitzoglou, M., Terzi, E., Samara, C. (2004). Patterns and sources of particle-phase aliphatic and polycyclic aromatic hydrocarbons in urban and rural sites of western Greece. *Atmospheric Environment* 38, 2545–2560.
- Kendall, M., Hamilton, R.S., Watt, J., Williams, I.D. (2001). Characterization of selected speciated organic compounds associated with particulate matter in London. *Atmospheric Environment* 35, 2483–2495.
- Kulkarni, P. and Venkataraman, C., 2000. Atmospheric polycyclic aromatic hydrocarbons in Mumbai, India. *Atmospheric Environment*. 34, 2785-2790.
- Marr L.; Grogan L.; Wöhrnschimmel H.; Molina L; Molina M.; Smith T.; Garshick E. (2004). Vehicle Traffic as a Source of Particulate Polycyclic Aromatic Hydrocarbon Exposure in the México City Metropolitan Area. *Environ. Sci. Technol.*, 38, 2584-2592.
- Marr, L. C., Dzepina, K., Jimenez, J. L., Reisen, F., Bethel, H. L., Arey, J., Gaffney, J. S., Marley, N. A., Molina, L. T., Molina, M. J. (2006). Sources and transformations of particle-bound polycyclic aromatic hydrocarbons in Mexico City, *Atmospheric Chemistry and Physics* 6, 1733–1745.
- Menichini E. Current legislation and guidelines on PAHs in ambient air: The Italian experience. *Fresenius Environ. Bull.* 1999, 8. 512-7.
- Miguel A., Eiguren-Fernández A., Jaques P., Froines J., Gran B., Mayo P., Sioutas C. (2004). Seasonal variation of particle-size distribution of polycyclic aromatic hydrocarbons and of major aerosol species in Claremont California. *Atmospheric Environment*. 38: 3241-3251.
- Mugica V., Hernández S., Torres M., García R. (2010). Seasonal Variation of Polycyclic Aromatic Hydrocarbons Exposure Levels in Mexico City. *J. Air & Waste Manage. Assoc.* 60.
- Nisbet D. & La Goy P. (1992). Toxic equivalence factors (TEFs) for polycyclic aromatic hydrocarbons (PAHs). *Regul. Toxicol Pharmacol*, 16: 290-300.
- NTP (National Toxicology Program), 2005. Report on Carcinogens, eleventh ed. Public Health Service, US Department of Health and Human Services, Washington, DC.
- Ohura T. Environmental Behavior, Sources, and Effects of Chlorinated Polycyclic Aromatic Hydrocarbons. (2007). *The Scientific World Journal*. 372-380.
- Panther, B.C.; Hooper, M.A.; Tapper, N.J.A. (1999). Comparison of Air Particulate Matter and Associated Polycyclic Aromatic Hydrocarbons in Some Tropical and Temperate Urban Environments; *Atmos. Environ.* 33, 4087-4099.
- Rocha A., Horvath H., Oliveira J., Duarte A. (1999). Trends in alkanes and PAHs in airborne particulate matter from Oporto and Vienna: identification and comparison. (1999). *The Science of the Total Environment*. 236, 231-236.
- Rogge, W.F.; Hildemann, L.M.; Mazurek, M.A.; Cass, G.R. (1991). Sources of Fine Organic Aerosol. 1. Charbroilers and Meat Cooking Operations; *Environ. Sci. Technol.* 25, 1112-1125.
- Simcik, M.F., Eisenreich, S.J., Liroy, P.J. (1999). Source apportionment and source/sink relationships of PAHs in the coastal atmosphere of Chicago and Lake Michigan. *Atmospheric Environment*, 33, 5071–5079.

- Thongsanit P., Jinsart W., Hooper B., Hooper M., and Limpaseni W. (2003). Atmospheric Particulate Matter and Polycyclic Aromatic Hydrocarbons for PM<sub>10</sub> and Size-Segregated Samples in Bangkok. *J. Air & Waste Manage. Assoc.* 53:1490-1498
- USEPA, (U.S. Environment Protection Agency). Compendium Method TO-13. (1999). Determination of Polycyclic Aromatic Hydrocarbons in Ambient Air Using Gas Chromatographic/Mass Spectrometry (GC-MS).
- Velasco E.; Siegmann P.; Siegmann. (2004). Exploratory study of particle-bound polycyclic aromatic hydrocarbons in different environments of Mexico City. *Atmospheric Environment*. 38: 4957-4968.
- Vera-Castellano; López C. J.; Santana A. P.; Santana R. J. (2003). Polycyclic aromatic hydrocarbons in ambient air particles in the city of Las Palmas de Gran Canaria. *Environment International*, 29,475-480.
- Viana M., Querol X, Alastuey A., Ballester F., Llop S., Esplugues A., Fernández-Patier R., Garcia dos Santos S., Herce M.D. (2008). Characterising exposure to PM aerosols for an epidemiological study. *Atmospheric Environment* 42:1552-1568.
- Villalobos-Pietrini R.; Amador-Muñoz O.; Waliszewski S.; Hernández-Mena L.; Munive-Colín Z.; Gómez-Arroyo S; Bravo-Cabrera J.L; Frías-Villegas A. (2006) Mutagenicity and polycyclic aromatic hydrocarbons associated with extractable organic matter from airborne particles  $\leq 10 \mu\text{m}$  in southwest Mexico City, *Atmospheric Environment*. 2006. 40: 5845-5857.
- Villalobos-Pietrini R.; Hernández-Mena L.; Amador-Muñoz O.; Munive-Colín Z.; Bravo-Cabrera J.L.; Gómez-Arroyo S.; Frías-Villegas A.; Waliszewski S.; Ramírez-Pulido J.; Ortiz-Muñiz R. (2007). Biodirected mutagenic chemical assay of PM<sub>10</sub> extractable organic matter in southwest México City, *Mutation Research/Genetic Toxicology and Environmental Mutagenesis*. doi:10.1016/j.mrgentox.2007.07.004.
- Wang, H.-M.; Wade, T.L.; Sericano, J.L. Concentrations and Source Characterization of PAHs in Pine Needles from Korea, Mexico, and United States; *Atmos. Environment*. 2003, 37, 2259-2267.
- Yunker, M. B., Macdonald, R. W., Vingarzan, R., Mitchell, R. H., Goyette, D., and Sylvestre, S.: PAHs in the Fraser River basin: a critical appraisal of PAH ratios as indicators of PAH source and composition, *Organic Geochemistry*, 33, 489-515, 2002.



# Sources, Distribution and Toxicity of Polycyclic Aromatic Hydrocarbons (PAHs) in Particulate Matter

Byeong-Kyu Lee and Van Tuan Vu  
*Department of Civil and Environmental Engineering, University of Ulsan  
Korea*

## 1. Introduction

Polycyclic aromatic hydrocarbons (PAHs) are a group of organic compounds consisting of two or more fused aromatic rings. PAHs originate mainly from anthropogenic processes, particularly from incomplete combustion of organic fuels. PAHs are distributed widely in the atmosphere. Natural processes, such as volcanic eruptions and forest fires, also contribute to an ambient existence of PAHs. PAHs can be present in both particulate and gaseous phases, depending upon their volatility. Light molecular weight PAHs (LMW PAHs) that have two or three aromatic rings are emitted in the gaseous phase, while high molecular weight PAHs (HMW PAHs), with five or more rings, are emitted in the particulate phase. In the atmosphere, PAHs can undergo photo-degradation and react with other pollutants, such as sulfur dioxide, nitrogen oxides, and ozone.

Due to widespread sources and persistent characteristics, PAHs disperse through atmospheric transport and exist almost everywhere. Human beings are exposed to PAH mixtures in gaseous or particulate phases in ambient air. Long-term exposure to high concentrations of PAHs is associated with adverse health problems. Since some PAHs are considered carcinogens, inhalation of PAHs in particulates is a potentially serious health risk linked to an excess risk of lung cancer. Thus, studies on PAHs in particulate matter (PM), such as PM<sub>10</sub> and PM<sub>2.5</sub> in ambient air, have become attention greater focus of research in recent years.

## 2. Physical and chemical characteristics of PAHs

PAHs are a group of several hundred individual organic compounds which contain two or more aromatics rings and generally occur as complex mixtures rather than single compounds. PAHs are classified by their melting and boiling point, vapor pressure, and water solubility, depending on their structure. Table 1 shows physical and chemical characteristics of 16 priority PAHs, listed by the US EPA. Most PAHs, especially as molecular weight increases, are soluble in non-polar solvents and are barely soluble in polar water.

Most PAHs are persistent organic pollutants (POPs) in the environment. Many of them are chemically inert. However, PAHs can be photochemically decomposed under strong

ultraviolet light or sunlight, and thus some PAHs can be lost during atmospheric sampling. Also, PAHs can react with ozone, hydroxyl radicals, nitrogen and sulfur oxides, and nitric and sulfuric acids, which affect the environmental fate or conditions of PAHs.

### **3. Sources and Emission of PAHs**

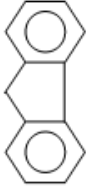
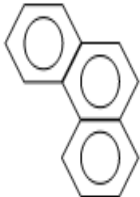
PAHs are mainly derived from anthropogenic activities related to pyrolysis and incomplete combustion of organic matter. Emission sources of PAHs affect their characterization and distribution, as well as their toxicity. In this book, the major sources of PAH emissions may be divided into four classes: stationary sources (including domestic and industrial sources), mobile emissions, agriculture activities, and natural sources.

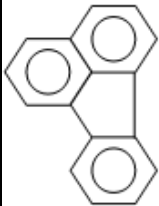
#### **3.1 Stationary sources**

##### **3.1.1 Domestic sources**

Heating and cooking are dominant domestic sources of PAHs. The burning and pyrolysis of coal, oil, gas, garbage, wood, or other organic substances are the main domestic sources. Domestic sources are important contributors to the total emissions of PAHs in the environment. Differences in climate patterns and domestic heating systems produce large geographic variations in domestic emissions. PAH emissions from these sources may be a major health concern because of their prevalence in indoor environments (Ravindra et al., 2006). According to a recent World Health Organization (WHO) report, more than 75% of people in China, India, and South East Asia and 50-75% of people in parts of South America and Africa use combustion of solid fuels, such as wood, for daily cooking.

Main indoor PAH sources are cooking and heating emissions and infiltration from outdoors. PAHs emissions from cooking account for 32.8% of total indoor PAHs (Zhu et al., 2009). LMW PAHs which originate from indoor sources are the predominant proportion of the total PAHs identified in residential non-smoking air. Toxicity of PAH mixtures from indoor sources is lower than mixtures which contain large amounts of HMW PAHs. Cigarette smoke is also a dominant source of PAHs in indoor environments. In many studies, PAHs in the indoor air of smoking residences tend to be higher than those of non-smoking residences.

| Characteristic   | Chemical formula | Chemical structure  | Molecular weight | Melting point | Boiling point | Vapor pressure             | Log Kow | Log Koc |
|--|------------------|---|------------------|---------------|---------------|----------------------------|---------|---------|
| Naphthalene<br>(naphthalin<br>Naphthaline)   | C10H8            |   | 128.17           | 80.26°C       | 218°C         | 0.087 mmHg                 | 3.29    | 2.97    |
| Acenaphthene<br>(1,8-dihydroacenaphthalene<br>1,8-ethylenenaphthalene<br>1,8-dihydroacenaphthaline<br>1,2-dihydroacenaphthylene) | C12H10           |  | 154.21           | 95°C          | 96°C          | 4.47x10 <sup>-3</sup> mmHg | 3.98    | 3.66    |
| Acenaphthylene<br>(cyclopenta(de)naphthalene)  | C12H8            |   | 152.20           | 92-93°C       | 265-275 °C    | 0.029 mmHg                 | 4.07    | 1.40    |
| Fluorene<br>(ortho-biphenylene methane<br>diphenylenemethane<br>2,2-methylene biphenyl<br>2,3-benzidene)                         | C13H10           |   | 166.2            | 116-117°C     | 295°C         | 3.2x10 <sup>-4</sup> mmHg  | 4.18    | 3.86    |
| Anthracene\<br>(anthracin<br>green oil<br>paranaphthalene)   | C14H10           |   | 178.2            | 218°C         | 340-342 °C    | 1.75x10 <sup>-6</sup> mmHg | 4.45    | 4.15    |
| Phenanthrene<br>(phenantrin)   | C14H10           |  | 178.2            | 100°C         | 340°C         | 6.8x10 <sup>-4</sup> mmHg  | 4.45    | 4.15    |

|   |   |        |         |               |                              |      |            |
|---|---|--------|---------|---------------|------------------------------|------|------------|
| Fluoranthene<br>(benzo(j,k)fluorine<br>1,2-(1,8-naphthylene)<br>benzene<br>1,2-benzacenaphthene)  |   | 202.26 | 110.8°C | 375°C         | 5.0x10 <sup>-6</sup><br>mmHg | 4.90 | 4.58       |
| Pyrene<br>(benzo(d,e,f)phenanthrene)  |   | 202.3  | 156°C   | 393-404<br>°C | 2.5x10 <sup>-6</sup><br>mmHg | 4.88 | 4.58       |
| Benzo(a)anthracene<br>(benz(a)anthracene<br>1,2-benzanthracene<br>benzo(b)phenanthrene<br>2,3-benzophenanthrene<br>Tetraphene)                        |   | 228.29 | 158°C   | 438°C         | 2.5x10 <sup>-6</sup><br>mmHg | 5.61 | 5.30       |
| Chrysene<br>(benzo(a)phenanthrene<br>1,2-benzphenanthrene)  |   | 228.28 | 254°C   | 448°C         | 6.4x10 <sup>-9</sup><br>mmHg | 5.9  | No<br>data |
| Benzo(b)fluoranthene<br>(2,3-Benzfluoranthene<br>2,3-benzofluoranthene<br>3,4-benz(e)acephenathrylene<br>3,4-benzfluoranthene<br>benz(e)fluoranthene) |  | 252.3  | 168.3°C | No data       | 5.0x10 <sup>-7</sup><br>mmHg | 6.04 | 5.74       |

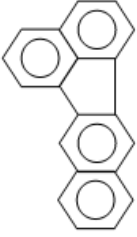
|  |   |        |                 |         |  |      |      |
|--|---|--------|-----------------|---------|--|------|------|
| Benzo(k)fluoranthene<br>(8,9-benzofluoranthene<br>11,12-benzo[k]fluoranthene<br>benzo(k)fluoranthene<br>2,3,1',8'-binaphthylene) |   | 252.3  | 215.7°C         | 480°C   | 9.59x10 <sup>-11</sup><br>mmHg               | 6.06 | 5.74 |
| C20H12   |   |        |                 |         |  |      |      |
| Benzo(a)pyrene<br>(1,2-benzopyrene<br>6,7-benzopyrene<br>B(a)P, BP<br>3,4-benzopyrene<br>benzo(d,e,f)chrysene<br>3,4-benzpyrene) |   | 252.3  | 179-179.3<br>°C | 495°C   | 5.6x10 <sup>-9</sup><br>mmHg                 | 6.06 | 6.74 |
| C20H12   |   |        |                 |         |  |      |      |
| Dibenzo(a,h)anthracene<br>(1,2,5,6-benzanthracene<br>1,2:5,6-dibenzanthracene<br>dibenzo(a,h)anthracene<br>DBA, 1,2,5,6-DBA)     |   | 278.35 | 262°C           | No data | 1x10 <sup>-10</sup><br>mmHg                  | 6.84 | 6.52 |
| C22H14   |   |        |                 |         |  |      |      |
| Benzo(g,h,i)perylene<br>(1,12-benzoperylene)   |   | 276.34 | 273°C           | 550°C   | 1.03x10 <sup>-10</sup><br>mmHg               | 6.50 | 6.20 |
| C22H12   |   |        |                 |         |  |      |      |
| Indeno(1,2,3-c,d)pyrene<br>(Indenopyrene<br>ortho-phenylene pyrene<br>1,10-(1,2-phenylene) pyrene<br>2,3-ortho-phenylene pyrene) |  | 276.3  | 163.6°C         | 530°C   | 10 <sup>-10</sup> -10 <sup>-16</sup><br>mmHg | 6.58 | 6.20 |
| C22H12   |   |        |                 |         |  |      |      |

Table 1. Physical and chemical characteristics of some popular PAHs (USEPA, 1995; ATSDR, 1995)

Liu et al. (2008) reported that coal stoves are still widely used for cooking and heating in rural North China. Total emission factors (EFs) for 15 PAHs ranged from 52.8 to 1434.8 mg/kg, depending on the drying status and compositions of raw coals used for cooking and heating. Chen et al. (2004) found a large decrease in the EFs of PAHs from residences with coal stoves that burned honeycomb coal briquettes. Emission factors of 17 PAHs and 10 genotoxic PAHs, based on a coal-weight basis were 111.65 and 18.41 mg/kg, respectively. This indicates a twenty-fold decrease in EFs, as compared to those from cooking and heating with raw coal. Oanh et al. (1999) investigated EFs from wood fuel, charcoals, and coal briquettes in a stove for domestic combustion. They found that wood fuel burning released the highest emissions of 18 PAHs and 11 genotoxic PAHs in terms of EFs, accounting for energy (mg/MJ) emission rates and based on the pollutant concentrations in smoke. Charcoal released the lowest amount of PAH emissions. On a fuel-weight basis, wood fuel burning has the same EF as coal briquette burning (110 mg/kg). However, emissions of genotoxic PAHs from wood burning were twice as high as those from charcoal burning.

### 3.1.2 Industrial sources

PAH emissions from industries are produced by burning fuels such as gas, oil, and coal. PAHs can also be emitted during the processing of raw materials like primary aluminum. Sources of PAHs include emissions from industrial activities, such as primary aluminum and coke production, petrochemical industries, rubber tire and cement manufacturing, bitumen and asphalt industries, wood preservation, commercial heat and power generation, and waste incineration.

Chen et al. (2007) studied emissions of PAHs from the pyrolysis of scrap tires. Total PAH emissions from a scrap tire plant via pyrolysis were 42.3 g/day with an EF of 4 mg/kg. To study the thermal degradation of organic materials, Fabbri et al. (2006) investigated PAH emissions from pyrolysis products. EFs of PAHs from thermal decompositions of organic materials ranged from  $0.4 \pm 0.13$  mg/g for cellulose to  $9.0 \pm 0.5$  mg/g for tyre. Yang et al. (2005) reported that EFs average 71.0 mg/g from joss paper furnaces. With applied air pollution control devices, such as adsorption towers, removal efficiencies of total PAHs are 42.5% and 11.7% for particulate and gaseous PAHs, respectively.

Yang et al. (1998) reported emissions of PAHs from various industrial stacks: a blast furnace, a basic oxygen furnace, a coke oven, an electric arc furnace, a heavy oil plant, a power plant, and a cement plant. The coke oven, electric arc furnace, and heavy oil combustor produced large amounts of HMW PAH emissions. EFs of PAHs from these industrial stacks ranged from 0.08 to 3.97 mg/kg feedstock, while EFs for BaP ranged from 1.87 to 15.5  $\mu$ g/g feedstock. The highest EFs of total PAHs and BaP were found from the combustion of heavy oils.

Recently, PAH emissions from waste incineration have been investigated in many studies. According to the Italia Agency for Environmental Protection, total EFs of PAHs ranged from 91 to 414  $\mu$ g/g of waste burned in incinerators of municipal and industrial wastes. Lee et al. (2002) estimated that EFs from two batch-type medical waste incinerators: a mechanical grate (MG-MWI) and a fixed rate (FG-MWI). EFs of total PAHs were 252 and 856 mg/kg-waste for MG-MWI and FG-MWI, respectively. EFs for medical waste incinerators were consistently much higher than those for municipal waste incinerators (871  $\mu$ g/kg-waste) operated in the same city. Air pollution control devices remove PAHs with efficiencies higher than 78% for PAHs with four or more rings, but had efficiencies lower than 5% for LMW PAHs with two or three rings.

### 3.2 Mobile sources

Mobile sources are major causes of PAH emissions in urban areas. PAHs are mainly emitted from exhaust fumes of vehicles, including automobiles, railways, ships, aircrafts, and other motor vehicles. PAH emissions from mobile sources are associated with use of diesel, coal, gasoline, oils, and lubricant oil. Exhaust emissions of PAHs from motor vehicles are formed by three mechanisms: 1) synthesis from smaller molecules and aromatic compounds in fuel; 2) storage in engine deposits and in fuel; and 3) pyrolysis of lubricant (Baek et al., 1991). One of the major influences on the production of PAHs from gasoline automobiles is the air-to-fuel ratio. It has been reported that the amount of PAHs in engine exhaust decreases with leaner mixtures (Ravindra et al., 2006).

A main contributor to PAH concentrations in road dust as well as urban areas is vehicle exhaust. Abrantes et al. (2009) reported that total emissions and toxicities of PAHs released from light-duty vehicles using ethanol fuel are less than those using gasohol. For example, in ethanol vehicles, total EFs of PAHs ranged from 11.7 to 27.4  $\mu\text{g}/\text{km}$ . In gasohol vehicles, total EFs ranged from 41.9 to 612  $\mu\text{g}/\text{km}$ . EFs for BaP toxicity equivalence varied from 11.7 to 21.8 ng TEQ/km for ethanol vehicles and from 9.84 to 4,610 ng TEQ/km for gasohol vehicles. LMW PAHs are the dominant PAHs emitted from light-duty vehicles. According to the report of PAH emissions from vehicles by Abrantes et al. (2004), total EFs of PAHs from the exhaust of light-duty diesel vehicles ranged from 1.133 to 5.801 mg/km with emissions dominated by LWM PAHs. EFs reported for heavy-duty vehicles (MSC-E, 2001) and light-duty vehicles were 11.4–82.1  $\mu\text{g}/\text{km}$  and 28.2  $\mu\text{g}/\text{km}$ , respectively.

Yang et al. (2005) reported that EFs of total PAH emissions from a 2-stroke carburetor (2-Stk/Cb), 4-stroke carburetor (4-Stk/Cb), and 4-stroke fuel injection (4-Stk/FI) motorcycles were 8.320, 5.990 and 3.390 mg/km, respectively. The EFs of total BaP equivalent are 10.8  $\mu\text{g}/\text{km}$ , indicating that most of the PAHs exhausted from the 2-Stk/Cb motorcycle are carcinogenic. Spezzano et al. (2008) reported that EFs of total PAHs (18 PAHs) ranged from 1.790 to 15.059 mg/km, and EFs of benzo(a)pyrene equivalent (BaPeq) ranged from 4.7 to 86.3  $\mu\text{g}/\text{km}$  for two-stroke 50-cm<sup>3</sup> mopeds. Two-stroke mopeds with small engines emit comparable or even more PAHs than emissions reported from gasoline- and diesel-powered passenger cars and light- and heavy-duty vehicles.

Chen et al. (2006) reported that EFs of total PAHs and total BaPeq for the UH-1H helicopter turboshaft engine (63.4 and 0.309 mg/L- fuel) are 1.65–23.4 and 1.30–7.54 times higher, respectively, than those for the motor vehicle engine, heavy-duty engine, and F101 aircraft engine. LMW PAHs are the dominant PAHs emitted from helicopter engines, accounting for 97.5% of the total PAH emissions.

Fuel type has a substantial effect on EFs and toxicity of PAHs from vehicle engines. He et al. (2010) indicated that diesel engines using diesel/biodiesel and their blends can greatly reduce total emissions of PAHs by 19.4 and 13.1%, respectively. The BaP TEQ of PAHs emitted also decreased 15% with the use of biodiesel.

### 3.3 Agricultural sources

Open burning of brushwood, straw, moorland heather, and stubble are agricultural sources of PAHs. All of these activities involve burning organic materials under suboptimum combustion conditions. Thus, it is expected that a significant amount of PAHs are produced from the open burning of biomass.

Emission factors of PAHs from wood combustion ranged from 16.4 to 1,282 mg/kg wood (Jenkins et al., 1996; Oanh et al., 1999; Schauer et al., 2001). PAH concentrations released from wood combustion depend on wood type, kiln type, and combustion temperature. 80-90% of PAHs emitted from biomass burning are LMW PAHs, including naphthalene, acenaphthylene, phenanthrene, flouranthene and pyrene.

Lu et al. (2009) reported that PAHs emitted from the open burning of rice and bean straw are influenced by combustion parameters. Total emissions of 16 PAHs from the burning of rice and bean straw varied from 9.29 to 23.6 µg/g and from 3.13 to 49.9 µg/g, respectively. PAH emissions increased with increasing temperatures from 200 to 700 °C. Maximum emissions of PAHs were observed at 40% O<sub>2</sub> content in supplied air. However, emissions of PAHs released from the open burning of rice straw negatively correlate with the moisture content in the straw.

### 3.4 Natural sources

Accidental burning of forests, woodland, and moorland due to lightning strikes are natural sources of PAHs. Furthermore, volcanic eruptions and decaying organic matter are also important natural sources, contributing to the levels of PAHs in the atmosphere. The degree of PAH production depends on meteorological conditions, such as wind, temperature, humidity, and fuel characteristics and type, such as moisture content, green wood, and seasonal wood.

### 3.5 Emission factors and inventory

Emission factors (EFs) of PAHs from different sources are given in Table 2. The EF data of PAHs are useful for estimating the amount of PAHs released from processes, including combustion, open burning, and pyrolysis. Atmospheric emission inventories of PAHs from certain sources or processes are obtained from an emission estimate using PAH EFs of various sources, using the following formula:

$$\text{Emission of PAHs} = \Sigma (\text{Activity Level}_i) \times \text{EF}_i \times \left( 1 - \frac{\text{Control Efficiency}_i}{100} \right)$$

Thus, the difference between measured values and reported or estimated values of EFs is a major limitation of PAH inventory construction. Recently, PAH emission inventories have been developed in several countries and have shown that combustion is a major source of PAHs. Combustion of biofuel contributed to 56.7% of total sixteen priority PAHs on a global basis in 2004 (Yang and Tao, 2009). Table 3 shows emission inventories of PAHs on a global scale and for some countries based on emissions in 2003 and 2004.

| Emissions source              | Emission Factor (mg/kg) | PAHs       | References           |
|-------------------------------|-------------------------|------------|----------------------|
| Wood combustion               | 16.4-1,282              | total PAHs | Schauer et al., 2001 |
| Rice burning                  | 9.29-23.6               | 16 PAHs    | Lu et al., 2009      |
| Bean burning                  | 3.13-49.9               | 16 PAHs    | -                    |
| Wood and root fuel            | 5.3-13.2                | B[a]P      | Gupta et al., 1998   |
| Two-stroke fuel-no catalyst   | 0.021                   | 6 PAHs     | Gambino et al., 2000 |
| Two-stroke fuel-with catalyst | 0.014                   | -          | -                    |
| Oil-burner-boiler combination | 0.005                   | B[a]P      | IPCS, 1998           |
| Barbecue briquettes           | 2.5-13                  | total PAHs | -                    |
| Soot open fire                | 3-240                   | B[a]P      | -                    |
| Boilers using heavy oil       | 0.013                   | total PAHs | Li et al., 1999      |
| Boilers using diesel          | 0.3                     | -          | -                    |
| Feed-stock                    | 0.077-3.970             | total PAHs | Yang et al., 1998    |
| Feed-stock                    | 0.002-0.016             | B[a]P      | -                    |
| Coal charged                  | 15                      | Total PAHs | IPCS, 1998           |
| -                             | 0.02                    | B[e]P      | -                    |
| Aluminum production           | 4.4 kg/tons             | total PAHs | -                    |
| -                             | 0.11 kg/tons            | B[a]P      | -                    |
| Bituminous coal               | 70.2                    | total PAHs | Chen et al., 2005    |
| Scrap tire pyrolysis plant    | 4                       | -          | Chen et al., 2007    |
| Honeycomb briquette           | 56.94                   | -          | Oanh et al., 1999    |
| Open burning biomass fuels    | 5-683                   | 19 PAHs    | Jenkins et al., 1996 |

Table 2. The emission factors (EFs) of PAHs from the different sources

Major emissions of PAHs in developing countries, such as China, India, Brazil, and Sudan, are associated with biomass burning, including use of biofuel and wild savanna fire. In particular, total emissions of PAHs from China and India were almost 40% of the global total emissions. However, emission features in developed countries, such as USA and UK, are quite different from those in developing countries. For example, PAH emissions in the USA are mainly associated with emissions from the use of consumer products, vehicles exhaust, and waste incinerators. The largest emissions of PAHs in UK are from traffic, followed by wood burning.

| Sources                 | Global      | USA         | China       | India       | Brazil      | Sudan       | UK          |
|-------------------------|-------------|-------------|-------------|-------------|-------------|-------------|-------------|
| Biofuel                 | 56.7        | 9.1         | 66.4        | 92.5        | 17.7        | 28.1        |             |
| Wild fire               | 17          | 3.3         |             |             | 66          |             |             |
| Savanna fire            |             |             |             |             | 4.5         | 69.7        |             |
| Firewood                |             |             |             |             |             |             | 15.5        |
| Open straw burning      |             |             | 2           | 3.2         | 1.2         |             | 4.3         |
| Consumer products       | 6.9         | 35.1        | 0.9         | 0.6         | 2.5         |             |             |
| Traffic oil             | 4.8         | 23          | 2           |             | 3           |             | 58.2        |
| Other oil               |             |             |             |             |             |             | 1.9         |
| Domestic Coal           | 3.7         |             | 10.7        | 1.3         |             |             |             |
| Industrial Coal         |             |             |             |             |             |             | 1.7         |
| Coke Industry           | 3.6         |             | 14.4        |             | 0.6         |             | 3.8         |
| Petrol refining         | 2.4         | 8.7         | 1           |             | 1.7         |             |             |
| Waste incineration      | 1.9         | 9.5         |             |             |             |             |             |
| Gasoline distribution   |             | 3           |             |             |             |             |             |
| Areospace industry      |             | 2.5         |             |             |             |             |             |
| Al electron             | 1.4         | 1.9         |             |             | 2.2         |             | 4.8         |
| Other industry          |             |             |             |             |             |             | 5.7         |
| Others                  | 1.5         | 3.9         | 2.7         | 2.3         | 0.7         | 2.2         | 5.2         |
| <b>Total (gigatons)</b> | <b>530</b>  | <b>32</b>   | <b>114</b>  | <b>90</b>   | <b>19</b>   | <b>5</b>    |             |
| <b>Year</b>             | <i>2004</i> | <i>2004</i> | <i>2004</i> | <i>2004</i> | <i>2004</i> | <i>2004</i> | <i>2003</i> |

Table 3. The emission inventories of PAHs for global and some countries (Yang & Tao, 2009)

## 4. Sampling and analytical methods

### 4.1 PAH sampling equipment

Due to the volatility of PAHs, released PAHs can be associated with the particulate and/or vapor phase. LMW PAHs are released in a vapor phase into the environment, while HMW PAHs containing five or more rings are adsorbed onto suspended particulate matter. These physical states of PAHs influence collection efficiency and selection of the sampling apparatus of PAHs. PAHs in the atmosphere are mainly collected by two sampling models: active sampling and passive sampling.

Active samplers include high-volume, low-volume, and impingement cascade samplers. A sorbent, filter, and plug are among the implements usually used to collect PAHs in the active sampling mode. Active sampling utilizes deposition or adsorption of target PAH compounds on filters or sorbent materials, through the collection of air particulates onto filters or into sorbent tubes, using a pump. PAHs accumulated on filters or sorbent materials are returned to the laboratory for analysis. In many applications, filters such as quartz fiber filters, glass fiber filters and cellulose filters are used to collect PAHs associated with particulate matter. These filters are highly vulnerable to losing the collected PAHs via

volatilization and thus precautions need to be taken to minimize the loss of LMW PAHs. For collecting gaseous PAHs, commonly used sorbents include XAD-2 resin and polyurethane foam (PUF) due to their high collection efficiencies, chemical stability, easy extractability and low cost.

However, drawbacks for active sampling include very high costs of samplers and the loss or volatilization of PAHs during the sampling and handling process. "These disadvantages can be alleviated by using passive sampling methods, which are based on free flow of analyte molecules from the sampled medium to a collecting medium as a result of differences in chemical potentials" (Caslavsky et al., 2004). Passive sampling has been widely applied for ambient monitoring over broad areas. There are many sampling devices which have been successfully used for passive sampling of PAHs. Semipermeable membrane devices (SPMDs) have been reported as the most used devices for passive sampling.

There are three basic active sampling models of PAHs associated with particulate collection equipment:

1. PUF samplers: used for sampling PAHs in both total suspended particulate (TSP) and vapor phases.
2. High-volume samplers (Tisch sampler, PQ 200 sampler): used for sampling PAHs in  $PM_{10}$  and  $PM_{2.5}$ .
3. Cascade impactor (3, 4 and 9-stages): used for sampling PAHs in different size particles.

Sampling times are restricted to 24 h to minimize degradation and loss (volatilization) of collected PAHs. Reduced sampling times and flow rates in the collection of vapor PAHs is important. The use of an annular diffusion denuder, such as an oxidant denuder, with the filter systems minimizes PAH losses during sampling.

#### **4.2 Pretreatment of air samples**

Before sampling, filters must be wrapped separately in aluminum foil and baked in a muffle furnace at a temperature of 450°C for 6 h. After sampling, they are kept under refrigeration at low temperatures to protect them from thermal degradation or loss by volatilization. Sorbents also need to be preserved carefully. XAD-2 resins and PUF plugs need to be cleaned by Soxhlet or ultrasonic methods before they are used for sampling (Lee and Lee, 2004).

#### **4.3 Extraction, concentration and analysis of PAHs**

After sampling, PAHs are extracted using organic solvents such as mixtures of n-hexane and dichloromethane. The extracted PAHs solutions need to be concentrated for analysis because PAHs are not as easily detected at low concentrations. To get sufficient detection and concentration analyses of PAHs from the collection medium, this chapter is limited to the following four major types of sample extraction techniques:

1. Soxhlet extraction
2. Ultrasonic extraction
3. Supercritical fluid extraction (SPE)
4. Accelerated solvent extraction (ASE)

Concentration methods popularly used to concentrate extracted PAH samples are rotary evaporators and K-D evaporators. For qualitative and quantitative analysis of extracted

PAHs, gas chromatography, combined with mass spectrometry (GC-MS) or high performance liquid chromatography (HPLC), are often used. Recent studies of extraction, concentration, and analysis of PAHs in particulates are summarized in Table 4.

### 5. Typical urban and rural concentrations of PAHs

In general, concentrations of total PAHs are easily affected by locational and seasonal variations. Table 5 shows concentrations of total PAHs in urban and rural areas of different regions based on a recent literature survey. Average PAH concentrations (both gaseous and particle-bound PAHs) were highest in winter and lowest in summer due to higher energy consumption for heating and engine operation of vehicles and facilities during the cold seasons. Traffic exhaust and domestic coal combustion are main contributors of PAHs in urban areas, while biomass and domestic coal combustion are the predominant PAH sources in rural areas. Sources of PAHs in both urban and rural areas can be derived from industrial areas by the transport of PAHs through the atmosphere.

Liu et al. (2008) reported that urban PAH emissions (motor vehicle and coke production) are higher than rural emissions (primarily firewood and straw burning for cooking and heating) in spring, summer, and fall. However, winter PAH emissions in rural areas were much higher than those in urban areas due to the abundance of coal, straw, and firewood burning for indoor heating in rural residences and for disposal of agricultural residues.

| Country              | Area     | $\Sigma$ PAHs | PAHs conc.<br>ng/m <sup>3</sup> | References            |
|----------------------|----------|---------------|---------------------------------|-----------------------|
| North Chinese Plain  | urban    | 10            | 870 ± 330                       | Liu et al., 2008      |
| -                    | rural    | -             | 710 ± 330                       | -                     |
| Flanders, Belgium    | rural    | 16            | 114                             | Ravindra et al., 2006 |
| Seoul, Korea         | urban    | 16            | 89 ± 74.3                       | Park et al., 2002     |
| Chicago, USA         | urban    | 16            | 13-1865                         | Li et al., 2005       |
| New Delhi, India     | urban    | 12            | 668 ± 399                       | Sharma et al., 2007   |
| -                    | -        | -             | 672 ± 388                       | -                     |
| London, UK           | urban    | 15            | 166                             | Halsal et al., 1994   |
| Cardif, UK           | urban    | 15            | 59                              | -                     |
| Campo Grande, Brazil | Campus   | 14            | 8.94-62.5                       | Poppi and Silva, 2005 |
| Tai Chung, Taiwan    | urban    | 21            | 220 ± 520                       | Fang et al., 2004     |
| -                    | rural    | -             | 831± 427                        | -                     |
| -                    | industry | -             | 1650 ±1240                      | -                     |
| Brisbane, Australia  | urban    | 16            | 0.4 - 19.73                     | Lim et al., 2005      |

Table 5. Concentration of PAHs in various cities

| <i>Analyte</i> | <i>Pretreatment method</i>  | <i>Analytical method</i> | <i>Reference</i>     |
|----------------|---|--------------------------|----------------------|
| 15-PAHs        | Soxhlet- Warm extraction method, rotary evaporation   | HPLC-FLD                 | Okuda et al., 2010   |
| 15 EPA- AHs    | RS- fluorescence detection<br>ASE extraction (hydrometric), evaporate concentration   | GC-MS                    | Li et al., 2009      |
| 16 EPA-PAHs    | Ultrasonic extraction with dichloromethane/n-hexan (1:1)<br>Nitrogen concentration  | HPLC                     | Lee and Dong, 2009   |
| 32-PAHs        | Ultrasonic extraction with methanol<br>Rotary evaporator and nitrogen concentration   | GC-MS                    | Saanio et al., 2008  |
| 20 PAHs        | Soxhlet extraction (dichloromethane, >40 cycles), column chromatography on Active silica gel. elute with mixture (n-hexan/dichloromethane =3:1) | GC-MS                    | Lee et al., 2008     |
| 16 EPA-PAHs    | Ultrasonic extraction with dichloromethane/acetone (3:1), SPE extraction<br>and concentration   | GC-MS                    | Li et al., 2007      |
| 16 EPA-PAHs    | Accelerated Solvent Extractor with dichloromethane/acetone (1:1), Turbo Vap 500 concentration, UV and fluorescence detection.                   | HPLC                     | Ravindra et al, 2006 |
| 22 PAHs        | Soxhlet extraction by dichloromethane for 8 h, evaporate concentration  | HPLC-UVD<br>HPLC-FLD     | Kameda et al., 2005  |
| 18 PAHs        | Ultrasonic extraction with dichloromethane, centrifugation, evaporate concentration   | HPLC-FLD                 | Ohura et al., 2004   |
| 16 EPA-PAHs    | Ultrasonic extraction with dichloromethane, rotary evaporation  | GC-MS                    | Gou et al., 2003     |
| 16 EPA-PAHs    | Mass selective detection HP 5972<br>Ultrasonic extraction with dichloromethane and supercritical fluid extraction<br>evaporate concentration    | GC-MS                    | Park et al., 2002    |
| 15 PAHs        | Dialysis in hexane for 48 h, silica gel/alumina column clean-up, elute with dichloromethane/hexane, GPC clean-up                                | GC-MS                    | Lohmann et al., 2001 |
| 16 EPA-PAHs    | Ultrasonic extraction with dichloromethane/acetone<br>rotary evaporation  | RP-HPLC-FLD              | Li and Ro, 2000      |

|         |  |       |                      |
|---------|--|-------|----------------------|
| 14-PAHs | Soxhlet extraction using dichloromethane, methanol, acetone<br>Nitrogen concentration, mass selective detector | GC-MS | Odabasi et al., 1999 |
|---------|--|-------|----------------------|

Table 4. Applications of pretreatment and analytical methods for PAHs in particulates

## 6. Toxicity

### 6.1 Exposure

In ambient air, human beings are exposed to PAH vapor or PAHs contained in dust and other particulate matter outdoors or indoors at the home or workplace. Sources of human exposure to PAHs include cigarette smoke, vehicle exhaust, residential heating, agriculture burning, waste incineration, and emissions from industrial processes. According to the United States Agency for Toxic Substances and Disease Registry (ATSDR), main exposures of the U.S. population to PAHs include the inhalation of tobacco smoke, wood smoke, and ambient air with PAHs from traffic emissions and consumption of food containing PAHs.

Predominant sources of PAH pollution at home include residential heating, tobacco smoking, and cooking. Vehicle emissions are also main sources of PAHs in many cities. For some people, the primary exposure to PAHs occurs in the workplace. For example, workers in a coke manufacturing factory receive high exposures to PAHs produced in their workplace.

The inhalation of air containing PAHs can lead to human exposure to PAHs. The exposure of traffic policemen to ambient PAHs is mainly from inhalation of vehicle exhaust and road dust containing PAHs. PAHs can also enter the body via food and water consumption or skin contact. PAHs are transported into all tissues of the human body containing fat. They can be stored in fat, liver and kidneys and can accumulate by repeated and long-term exposures. Smaller amounts are also stored in the spleen, adrenal glands, and ovaries.

### 6.2 Carcinogenicity and risk assessment

Air with high concentrations of PAHs causes many adverse effects on different types of organisms, including plants, birds, and mammals. Some studies reported that there is a significant positive correlation between mortality by lung cancer in humans and exposure to PAHs from exhaust from coke ovens, roofing-tar, and cigarette smoke. Some PAHs have been demonstrated to be carcinogenic in humans and experimental animals, and they are classified as carcinogenic materials by many organizations, including the United States Agency for Toxic Substances and Disease Registry (ATSDR), the International Agency for Research on Cancer (IARC), the Department of Health and Human Services (DHHS), the National Occupation Safety and Health Administration (OSHA), and the US-EPA. Table 6 shows the carcinogen classification of 17 priority PAHs by the IARC, compared to classifications by the DHHS and the US-EPA.

Table 7 shows the relative toxicity of priority PAHs selected by the US-EPA. LMW PAHs, except naphthalene, usually are associated with relatively lower toxicity (cancer risk) than HMW PAHs with 5 or 6 aromatic rings. Many toxicity studies reported that benzo[a]pyrene (BaP) has the highest carcinogenic potency with long-term persistency in the environment. Shulte et al. (1993) found a significant increase in all lung tumors and a dose-dependent increase in malignant lung tumors for mice exposed to PAH-enriched exhausts containing

0.05 or 0.09 mg/m<sup>3</sup> BaP. BaP is often used as an indicator of human exposure to PAHs, and the toxicity of other PAHs is converted into toxicity equivalency factors (TEFs) to BaP to evaluate their relative toxicities. Methods using TEFs and the BaP as a surrogate are more or less similar to each other, except for not requiring expensive monitoring. However, comparative potency methods are quite different from the previous two methods.

| PAHs                         | EPA                        | IARC                       | DHHS                     |
|------------------------------|----------------------------|----------------------------|--------------------------|
| <b>Acenaphthene</b>          |                            |                            |                          |
| <b>Acenaphthylene</b>        | <i>Not classifiable</i>    |                            |                          |
| <b>Anthanthrene</b>          | <i>Not classifiable</i>    | <i>Not classifiable</i>    |                          |
| <b>Benz(a)anthracene</b>     | <i>Probably Carcinogen</i> | <i>Probably Carcinogen</i> | <i>Animal Carcinogen</i> |
| <b>Benzo(a)pyrene</b>        | <i>Probably Carcinogen</i> | <i>Probably Carcinogen</i> | <i>Animal Carcinogen</i> |
| <b>Benzo(b)fluoranthene</b>  | <i>Probably Carcinogen</i> | <i>Possibly Carcinogen</i> | <i>Animal Carcinogen</i> |
| <b>Benzo(e)pyrene</b>        |                            | <i>Not classifiable</i>    |                          |
| <b>Benzo(ghi)perylene</b>    | <i>Not classifiable</i>    | <i>Not classifiable</i>    |                          |
| <b>Benzo(j)fluoranthene</b>  | <i>Not included</i>        | <i>Possibly Carcinogen</i> | <i>Animal Carcinogen</i> |
| <b>Benzo(k)fluoranthene</b>  | <i>Probably Carcinogen</i> | <i>Possibly Carcinogen</i> |                          |
| <b>Chrysene</b>              | <i>Probably Carcinogen</i> | <i>Not classifiable</i>    |                          |
| <b>Dibenz(ah)anthracene</b>  | <i>Probably Carcinogen</i> |                            | <i>Animal Carcinogen</i> |
| <b>Fluoranthene</b>          | <i>Not classifiable</i>    | <i>Not classifiable</i>    |                          |
| <b>Fluorene</b>              | <i>Not classifiable</i>    | <i>Not classifiable</i>    |                          |
| <b>Ideno(1,2,3-cd)pyrene</b> | <i>Probably Carcinogen</i> | <i>Possibly Carcinogen</i> | <i>Animal Carcinogen</i> |
| <b>Phenanthrene</b>          | <i>Not classifiable</i>    |                            |                          |
| <b>Pyrene</b>                | <i>Not classifiable</i>    | <i>Not classifiable</i>    |                          |

Table 6. 17 priority PAHs were classified by the IARC in comparing those by the DHHS and the US-EPA

| Route                 | Krewski <i>et al.</i> , 1989 |          | USEPA, 1993 |               | Malcom and Dobson, 1994 |          | OEHHA, 1994  |            | Kalberlah <i>et al.</i> , 1995 |          | McClure and Schoeny, 1995 |               | Muller <i>et al.</i> , MOE 1997 |            | Machala <i>et al.</i> , 2001 |          | Liao <i>et al.</i> , 2006 |               |
|-----------------------|------------------------------|----------|-------------|---------------|-------------------------|----------|--------------|------------|--------------------------------|----------|---------------------------|---------------|---------------------------------|------------|------------------------------|----------|---------------------------|---------------|
|                       | Not specified                | Multiple | Dermal      | Not specified | Inhalation              | Multiple | Subcutaneous | Inhalation | Not specified                  | Multiple | Inhalation                | Not specified | Multiple                        | Inhalation | Not specified                | Multiple | Inhalation                | Not specified |
| Acenaphthene          | 0.001                        |          |             | 0.001         |                         | 0.001    |              |            | 0.001                          |          |                           |               |                                 |            |                              |          |                           | 0.001         |
| Acenaphthylene        | 0.001                        |          |             | 0.001         |                         | 0.01     |              |            |                                |          |                           |               |                                 |            |                              |          |                           | 0.001         |
| Anthanthrene          | 0.32                         |          |             |               |                         |          |              | 0.28       |                                |          |                           |               |                                 |            |                              |          |                           | 0.001         |
| Benzo(a)anthracene    | 0.145                        | 0.1      | 0.1         | 0.1           | 0.1                     | 0.1      | 0.1          | 0.1        | 0.1                            | 0.1      | 0.1                       | 0.1           | 0.1                             | 0.1        | 0.1                          | 0.1      | 0.1                       | 0.1           |
| Benzo(a)pyrene        | 1                            | 1        | 1           | 1             | 1                       | 1        | 1            | 1          | 1                              | 1        | 1                         | 1             | 1                               | 1          | 1                            | 1        | 1                         | 1             |
| Benzo(b)fluoranthene  | 0.141                        | 0.1      | 0.1         | 0.1           | 0.1                     | 0.1      | 0.1          | 0.11       | 0.1                            | 0.1      | 0.1                       | 0.1           | 0.11                            | 0.1        | 0.1                          | 0.1      | 0.1                       | 0.1           |
| Benzo(e)pyrene        | 0.004                        |          |             | 0.01          |                         |          |              | 0          |                                |          |                           |               | 0                               |            |                              |          |                           | 0.01          |
| Benzo(ghi)perylene    | 0.022                        | 0.01     |             | 0.01          |                         | 0.01     |              | 0.012      | 0.01                           | 0.01     | 0.01                      | 0.012         | 0.012                           | 0.01       | 0.01                         | 0.01     | 0.017                     | 0.01          |
| Benzo(f)fluoranthene  |                              |          | 0.1         |               |                         | 0.1      |              | 0.045      |                                |          | 0.1                       |               | 0.045                           |            |                              |          |                           | 0.01          |
| Benzo(k)fluoranthene  | 0.061                        | 0.1      | 0.1         | 0.1           | 0.1                     | 0.1      | 0.1          | 0.037      | 0.1                            | 0.1      | 0.1                       | 0.11          | 0.037                           | 0.1        | 0.1                          | 0.1      | 0.11                      | 0.1           |
| Chrysene              | 0.0044                       | 0.01     | 0.1         | 0.01          | 0.01                    | 0.01     | 0.1          | 0.026      | 0.01                           | 0.01     | 0.17                      | 0.026         | 0.026                           | 0.017      | 0.01                         | 0.01     | 0.017                     | 0.01          |
| Coronene              |                              | 0.001    |             |               |                         |          |              | 0.012      |                                |          |                           |               | 0.012                           |            |                              |          |                           | 0.001         |
| Cyclopenta(cd)pyrene  | 0.023                        | 0.1      | 0.1         |               |                         | 0.1      |              | 0.012      | 0.1                            | 0.1      | 0.1                       | 6.9           | 0.012                           | 0.1        | 0.1                          | 0.1      | 6.9                       | 0.1           |
| Dibenzo(a,e)pyrene    |                              |          | 1           |               |                         | 1        |              | 2.9        |                                |          | 1                         | 2.9           |                                 |            |                              |          | 2.9                       | 0.1           |
| Dibenz(a,c)anthracene | 0.1                          |          |             |               |                         |          |              | 0.29       |                                |          |                           | 0.29          |                                 |            |                              |          | 0.29                      | 0.1           |
| Dibenz(ah)anthracene  | 1.11                         | 1        | 1           | 1             | 0.4                     | 1        | 1            | 2.9        | 1                              | 1        | 1                         | 2.9           | 0.89                            | 1          | 1                            | 1        | 2.9                       | 1             |
| Dibenzo(a,e)pyrene    |                              |          | 100         |               | 10                      | 100      |              | 1.4        |                                |          | 100                       | 1.4           |                                 |            |                              |          | 1.4                       | 1             |
| Dibenzo(a,h)pyrene    |                              |          | 1           |               | 10                      | 1        |              | 3.6        |                                |          | 1                         | 3.6           |                                 |            |                              |          | 3.6                       | 1             |
| Dibenzo(a,i)pyrene    |                              |          | 0.1         |               |                         | 0.1      |              | 24         |                                |          | 0.1                       | 24            |                                 |            |                              |          | 24                        | 1             |
| Dibenzo(a,l)pyrene    |                              |          |             |               | 10                      |          |              | 10         |                                |          |                           | 10            |                                 |            |                              |          | 10                        | 1             |
| Fluoranthene          | 0.001                        |          |             | 0.001         |                         | 0.01     |              | 0          |                                |          | 0.01                      | 0             |                                 |            |                              |          | 0                         | 0.001         |
| Fluorene              | 0.001                        |          |             | 0.001         |                         | 0        |              | 0.067      |                                |          | 0                         | 0.067         |                                 |            |                              |          | 0.067                     | 0.001         |
| Ideno(1,2,3-cd)pyrene | 0.232                        | 0.1      | 0.1         | 0.1           | 0.1                     | 0.1      | 0.1          | 0.31       | 0.1                            | 0.1      | 0.1                       | 0.31          | 0.1                             | 0.1        | 0.1                          | 0.1      | 0.31                      | 0.1           |

|                     |       |       |       |         |       |
|---------------------|-------|-------|-------|---------|-------|
| <b>Naphthalene</b>  | 0.001 | 0.001 | 0.001 | 0.001   | 0.001 |
| <b>Perylene</b>     |       | 0.001 |       |         | 0.001 |
| <b>Phenanthrene</b> | 0.001 | 0.001 | 0     | 0.00064 | 0.001 |
| <b>Pyrene</b>       | 0.81  | 0.001 | 0.001 | 0       | 0.001 |

Table 7. Proposed TEFs for individual PAHs (Modified from Knafla et al., 2006)

### 6.3 Toxicity equivalency factors (TEFs)

TEF evaluation is the most popular method used to identify the toxicity of PAHs. TEFs of individual PAHs have been reported by many researchers (Table 7). Toxicity equivalency concentrations (TEQs) are calculated as the product of summing up the values obtained by TEF values and concentrations of PAHs, as follows:

$$\text{TEQ} = \sum (C_i \times \text{TEF}_i)$$

Where,

TEQ: toxic equivalent concentration

$C_i$ : concentration of PAH<sub>*i*</sub>.

Petry et al. (1995) used TEFs in assessing occupational and environmental health risks associated with exposure to airborne mixtures of PAHs. They used information of the ratio between airborne concentrations of BaP equivalents to the concentrations of BaP alone, which can indicate the variation of risk for the different environments. Individual PAH-based BaP<sub>eq</sub> toxicity estimates were up to one order of magnitude higher than estimates based on BaP concentration measurements and BaP-risk from risk assessment of lung cancer related to occupational exposure (Vyskocil et al., 2004; Yanjial et al., 2007). Yajuan et al. (2008) reported that 1.73% of the cancer sufferers of Beijing inhabitants in 2007 were related to inhalation of PAHs in ambient air. There is an increasing trend of the cancer risk of residents by inhalation of ambient air containing hazardous air pollutants (HAPs), such as PAHs.

Halek et al. (2008) estimated that the annual number of lung cancer cases attributable to carcinogenic PAH compounds in 2005 was 58 persons per million. The BaP is the highest carcinogenic contributor, followed by DahA, Ind and BbF (Pufulete et al., 2004). However, DahA was suggested as a new surrogate compound to measure the toxicity of particle phase-PAHs because its toxicity is almost equal to that of BaP. While estimating the toxicity of PAHs in road dust of Ulsan, Korea, Dong and Lee (2009) found a significant correlation coefficient between TEQ and total PAH concentrations.

## 7. Introduction of Nitro-PAHs

Nitrated polycyclic aromatic hydrocarbons (N-PAHs) are an important category of derivations of PAHs and are of special interest because they include potential mutagens and carcinogens. They have been recognized as direct-acting mutagens and carcinogens to mammalian systems and are, thus, considered to have far greater toxicity than unsubstituted PAHs (Pedersen et al., 1998; Atkinson and Arey, 1994). Nitro-PAHs are formed mainly from incomplete combustion processes or by the reaction of PAH with atmospheric oxidants, such as dinitrogen pentoxide, nitrogen trioxide, and oxygen radicals in the presence of nitrogen oxides (Atkinson et al., 1990; Fan et al., 1995; Enya et al., 1997; Environmental Health Criteria-EHC, 2003).

Nitro-PAHs occur as a mixture with parent PAHs in the vapor phase or adsorbed onto particulate matter in the atmosphere. Two-ring N-PAHs, such as nitronaphthalenes, are the dominant N-PAHs in the vapor phase. However, N-PAHs, which include nitro derivatives of pyrene, fluoranthene, anthracene, chrysene, and others, tend to condense on particle surfaces because of their low vapor pressure. Atmospheric lifetimes of N-PAHs are affected

by photolysis and gas-phase reactions with hydroxyl and nitrate radicals and with ozone under atmospheric conditions. Photolysis is the dominant loss process for N-PAHs (e.g. 1-and 2-nitronaphthalene). "Particle oxidation of nitro-PAHs by ozone may be the main loss process at night" (EHC, 2003).

N-PAHs in the environment originate from direct emissions from combustion sources and nitration of unsubstituted PAHs. Main sources include vehicle exhaust (particularly diesel), industrial emissions, and domestic emissions (residential heating/cooking and wood burning), as with unsubstituted PAHs. In urban areas, N-PAH pollution is predominantly caused by diesel engine vehicle traffic and residential heating. Indoor human exposure to nitro-PAHs is from kerosene heating and use of cooking oil. Effects of N-PAHs on human health have been estimated based on the data of carcinogenic effects for 28 N-PAHs. Tokiwa et al. (1998 and 2000) reported that N-PAHs have been detected in samples of resected lung tissue from patients in Japan.

Sampling methods of nitro-PAHs are similar to those of unsubstituted PAHs. Most nitro-PAH samples are collected on sorbent (PUF) or XAD-2 resins and filters by high-volume samplers. Then, nitro-PAH samples undergo extraction, clean up, and analysis. However, there are problems which affect atmospheric sampling and measurement of N-PAHs. These issues include: 1) N-PAHs are emitted in a very complex matrix; 2) concentrations of N-PAHs are very low and only detected using highly sensitive analytical methods; and 3) formation of N-PAHs is strongly influenced by meteorological conditions, such as sunlight radiation, humidity, and concentrations of ambient contaminants, such as ozone, nitrogen oxides, and photooxidants.

## 8. References

- Aakinson, R.; Arey, J.; Zielinska, B. & Aschmann, S.M. (1990). Kinetics and nitro-products of gas-phase OH and NO<sub>3</sub> radical-initiated reactions of naphthalene, fluoranthene and pyrene. *International Journal of Chemical Kinetics*, 22., 999-1014.
- Abrantes, R.; Assunção, J.V. & Nóbrega, R.B. (2004). Emission of polycyclic aromatic hydrocarbons from light-duty diesel vehicles exhaust. *Atmospheric Environment*, 38., 1631-1640.
- Abrantes, R.; Assunção, J.V.; Pesquero, C.R.; Bruns, R.E. & Nóbrega, R.B. (2009). Emission of polycyclic aromatic hydrocarbons from gasohol and ethanol vehicles. *Atmospheric Environment*, 43., 648-654.
- Atkinson, R. & Arey, J. (1994). Atmospheric chemistry of gas-phase polycyclic aromatic hydrocarbons: formation of atmospheric mutagens. *Environmental Health Perspectives*, 102., 117-126.
- ATSDR (Agency for Toxic Substances and Disease Registry). (1995). Toxicological profile for polycyclic aromatic hydrocarbons (PAHs). US Department of Health and Human Services, Public Health Service. Atlanta, GA.  
<http://www.atsdr.cdc.gov/toxprofiles/tp69.html>.
- Australian government, 1999. Technical report No. 2: Polycyclic aromatic hydrocarbons (PAHs) in Australia. Department of the environment and heritage, Australia.
- Baek, S.; Goldstone, M.; Kirk, P.; Lester, J. & Perry, R. (1991). Phase distribution and particle size dependency of polycyclic aromatic hydrocarbons in the urban atmosphere. *Chemosphere*, 22., 503-520.

- Caslavsky, J.; Kotlarikova, P. & Benesova, K. (2004). Sampling of airborne polycyclic aromatic hydrocarbons with semipermeable membrane devices. *Environmental Chemical Letters*, 2., 89-92.
- Chen, S.; Su, B.; Chang, J.E.; Lee, W.J.; Huang, K.L.; Hsieh, L.T.; Huang, J.C.; Lin, W.J. & Lin, C.C. (2007). Emissions of polycyclic aromatic hydrocarbons (PAHs) from the pyrolysis of scrap tires. *Atmospheric Environment*, 41., 1209-1220.
- Chen, S.J.; Su, H.B.; Chang, J.E.; Lee, W.J.; Huang, K.L.; Hsieh, L.T.; Huang, Y.C.; Lin, W.Y. & Lin, C.C. (2007). Emissions of polycyclic aromatic hydrocarbons (PAHs) from the pyrolysis of scrap tires. *Atmospheric Environment*, 41., 1209-1220.
- Chen, Y.-C.; Lee, W.-J.; Uang, S.-N.; Lee, S.-H. & Tsai, P.-J. (2006). Characteristics of polycyclic aromatic hydrocarbon (PAH) emissions from a UH-1H helicopter engine and its impact on the ambient environment. *Atmospheric Environment*, 40., 7589-7597.
- Chen, Y.; Bi, X.; Mai, B.; Sheng, G. & Fu, J. (2004). Emission characterization of particulate/gaseous phases and size association for polycyclic aromatic hydrocarbons from residential coal combustion. *Fuel*, 83., 781-790.
- Cotham, W.E. & Bidleman, T.F. (1995). Polycyclic Aromatic Hydrocarbons and Polychlorinated Biphenyls in air at an urban and a rural site near Lake Michigan. *Environmental Science & Technology*, 29., 2782 - 2789.
- Dong, T.T.T. & Lee, B.K. (2009). Characteristics, toxicity, and source apportionment of polycyclic aromatic hydrocarbons (PAHs) in road dust of Ulsan, Korea. *Chemosphere*, 74., 1245-1253.
- Environmental Health Criteria (EHC) 229. (2003). Selected nitro- and nitro-oxy-polycyclic aromatic hydrocarbon. WHO Library:  
[http://whqlibdoc.who.int/ehc/WHO\\_EHC\\_229.pdf](http://whqlibdoc.who.int/ehc/WHO_EHC_229.pdf).
- European communities. (2001). Ambient air pollution by polycyclic aromatic hydrocarbons (PAHs) - Position paper.
- Fabbri, D. & Vassura, I. (2006). Evaluating emission levels of polycyclic aromatic hydrocarbons from organic materials by analytical pyrolysis. *Journal of Analytical and Applied Pyrolysis*, 75., 150-158.
- Fan, Z.; Chen, D.; Birla, P. & Kamens, R.M. (1995). Modeling of nitro-polycyclic aromatic hydrocarbon formation and decay in the atmosphere. *Atmospheric Environment*, 29., 1171-1181.
- Fang, G.C.; Chang, K.F.; Lu, C. & Bai, H. (2004). Estimation of PAHs dry deposition and BaP toxic equivalency factors (TEFs) study at urban, industry park and rural sampling sites in central Taiwan, Taichung. *Chemosphere*, 44., 787-796.
- Fang, G.C.; Wu, Y.S.; Fu, P.P.C.; Yang, I.L. & Chen, M.H. (2004). Polycyclic aromatic hydrocarbons in the ambient air of suburban and industrial regions of central Taiwan. *Chemosphere*, 54., 443-452.
- Fang, G.C.; Chang, C.N.; Wu, Y.S.; Fu, P.P.C.; Yang, I.L. & Chen, M.H. (2004). Characterization, identification of ambient air and road dust polycyclic aromatic hydrocarbons in central Taiwan, Taichung. *Science of The Total Environment*, 327., 135-146.
- Fang, G.C.; Chang, K.F.; Lu, C. & Bai, H. (2002). Toxic equivalency factors study of polycyclic aromatic hydrocarbons (PAHs) in Taichung city, Taiwan. *Toxicology and Industrial Health*, 18., 279-288.

- Fertmann, R.; Tesseraux, I.; Schümann, M. & Neus, H. (2002). Evaluation of ambient air concentrations of polycyclic aromatic hydrocarbons in Germany from 1990 to 1998. *Journal of exposure analysis and environmental epidemiology*, 12., 115-123.
- Gambino, M.; Iannaccone, S.; Prati, M.V. & Unich, A. (2000). Regulated and unregulated emissions reduction with retrofit catalytic after-treatment on small two stroke S.I. engine. *SAE Technical Paper Series 2000-01-1846*. International Spring Fuels & Lubricants Meeting & Exposition, June 19-22, Paris, France.
- Guo, H.; Lee, S.C.; Ho, K.F.; Wang, X.M. & Zou, S.C. (2003). Particle-associated polycyclic aromatic hydrocarbons in urban air of Hong Kong. *Atmospheric Environment*, 37., 5307-5317.
- Gupta, S.; Saksena, S.; Shankar, V.R. & Joshi, V. (1998). Emission factors and thermal efficiencies of cooking biofuels from developing countries. *Biomass and Bioenergy*, 14., 547-559.
- Harrison, R.M.; Smith, D.J.T. & Luhana, L. (1996). Source Apportionment of Atmospheric Polycyclic Aromatic Hydrocarbons Collected from an Urban Location in Birmingham, U.K. *Environmental Science & Technology*, 30., 825-832.
- He, C.; Ge, Y.; Tan, Y.; You, K.; Han, X. & Wang, J. (2010). Characteristics of polycyclic aromatic hydrocarbons emissions of diesel engine fueled with biodiesel and diesel. *Fuel*, In Press, Uncorrected Proof.
- IARC (International Agency for Research on Cancer), 1989. IARC monographs on the evaluation of the carcinogenic risk of chemicals to humans: occupational exposures in petroleum refining: crude oil and major petroleum fuels. Volume 45. Lyon.
- IPCS (International programme on chemical safety). (1998). <http://www.inchem.org/documents/ehc/ehc/ehc202.htm#SubSectionNumber:5.1.1>
- Jenkins, B.M.; Jones, A.D.; Turn, S.Q.; Williams, R.B. (1996). Emission factors for polycyclic aromatic hydrocarbons from biomass burning. *Environmental Science and Technology*, 30., 2462-2469.
- Kameda, Y.; Shirai, J.; Komai, T.; Nakanishi, J. & Masunaga, S. (2005). Atmospheric polycyclic aromatic hydrocarbons: size distribution, estimation of their risk and their depositions to the human respiratory tract. *Science of The Total Environment*, 340., 71-80.
- Knafla, A.; Phillipps, K.A.; Brecher, R.W.; Petrovic, S. & Richardson, M. (2006). Development of a dermal cancer slope factor for benzo[a]pyrene. *Regulatory Toxicology and Pharmacology*, 45., 159-168.
- Lee, B.K. & Lee, C.B. (2004). Development of an improved dry and wet deposition collector and the atmospheric deposition of PAHs onto Ulsan Bay, Korea. *Atmospheric Environment*, 38., 863-871.
- Lee, J.Y.; Kim, Y.P.; Kaneyasu, N.; Kumata, H. & Kang, C.H. (2008). Particulate PAHs levels at Mt. Halla site in Jeju Island, Korea: Regional background levels in northeast Asia. *Atmospheric Research*, 90., 91-98.
- Lee, W. J.; Wang, Y. F.; Lin, T. C.; Chen, Y. Y.; Lin, W. C.; Ku, C. C. & Cheng, J.T. (1995). PAH characteristics in the ambient air of traffic-source. *The Science of the Total Environment*, 159., 185-200.
- Lee, W.J.; Liow, M.C.; Tsai, P.J. & Hsieh, L.T. (2002). Emission of polycyclic aromatic hydrocarbons from medical waste incinerators. *Atmospheric Environment*, 36., 781-790

- Li, C.S. & Ro, Y.S. (2000). Indoor characteristics of polycyclic aromatic hydrocarbons in the urban atmosphere of Taipei. *Atmospheric Environment*, 34., 611-620.
- Li, C.T.; Mi, H.H.; Lee, W.J.; You, W.C. & Wang, Y.F. (1999). PAH emission from the industrial boilers. *Journal of Hazardous Material*, 169., 1-11.
- Li, K.; Li, H.; Liu, L.; Hashi, Y.; Maeda, T. & Lin, J.M. (2007). Solid-phase extraction with C30 bonded silica for analysis of polycyclic aromatic hydrocarbons in airborne particulate matters by gas chromatography-mass spectrometry. *Journal of Chromatography A*, 1154., 74-80.
- Li, Z.; Sjodin, A.; Porter, E.N.; Patterson D.G.; Needham, L.L.; Lee, S.L.; Russell, A.G. & Mulholland, J.A. (2009). Characterization of PM2.5-bound polycyclic aromatic hydrocarbons in Atlanta. *Atmospheric Environment*, 43., 5., 1043-1050.
- Lim, C.H.M.; Ayoko, G.A. & Morawska, L. (2005). Characterization of elemental and polycyclic aromatic hydrocarbon compositions of urban air in Brisbane. *Atmospheric Environment*, 39., 463-476.
- Liu, W.X.; Dou, H.; Wei, Z.W.; Chang, B.; Qui, W.X.; Liu, Y. & Shu, T. (2008). Emission characteristics of polycyclic aromatic hydrocarbons from combustion of different residential coals in North China. *Science of the total environment*, 407., 1436-1446.
- Liu, W.X.; Dou, H.; Wei, Z.W.; Chang, B.; Qui, W.X.; Liu, Y. & Shu, T. (2008). Emission characteristics of polycyclic aromatic hydrocarbons from combustion of different residential coals in North China. *Science of the total environment*, 407., 1436-1446.
- Lohmann, R.; Comgan, B.P.; Howsam, M.; Jones, K.C. & Ockenden, W.A. (2001). Further developments in the use of semipermeable membrane devices (SPMDs) as passive air samplers for persistent organic pollutants: field application in a spatial survey of PCDD/Fs and PAHs[J]. *Environmental Science and Technology*, 35., 2576- 2582.
- Lu, H.; Zhu, L. & Zhu, N. (2009). Polycyclic aromatic hydrocarbon emission from straw burning and the influence of combustion parameters. *Atmospheric Environment*, 43., 978-983.
- Oanh, N.T.K.; Reutergardh, L.B. & Dung, N.T. (1999). Emission of polycyclic aromatic hydrocarbons and particulate matter from domestic combustion of selected fuels. *Environmental Science and Technology*, 33., 2703-2709.
- Odabasi, M.; Vardar, N.; Sofuoglu, A.; Tasdemir, Y. & Holsen, T.M. (1999). Polycyclic aromatic hydrocarbons (PAHs) in Chicago air. *The Science of The Total Environment*, 227., 57-67.
- Ohura, T.; Tamagai, T.; Sugiyama, T.; Fusaya, M. & Matsushita, H. (2004). Characteristics of particle matter and associated polycyclic aromatic hydrocarbons in indoor and outdoor air in two cities in Shizuoka, Japan. *Atmospheric Environment*, 38., 2045-2054.
- Okuda, T.; Okamoto, K.; Tanaka, S.; Shen, Z.; Han, Y. & Huo, Z. (2010). Measurement and source identification of polycyclic aromatic hydrocarbons (PAHs) in the aerosol in Xi'an, China, by using automated column chromatography and applying positive matrix factorization (PMF). *Science of The Total Environment*, 408., 8., 1909-1914.
- Omar, N.Y.; Mon, T.C.; Rahman, N.A. & Abas, M.R.B. (2006). Distributions and health risks of polycyclic aromatic hydrocarbons (PAHs) in atmospheric aerosols of Kuala Lumpur, Malaysia. *Science of The Total Environment*, 369., 76-81.
- Park, S.S.; Kim, Y.J. & Kang, C.H. (2002). Atmospheric polycyclic aromatic hydrocarbons in Seoul, Korea. *Atmospheric Environment*, 36, 2917-2924.

- Pedersen, D.U.; Durant, J.L.; Penman, B.M.; Crespi, C.L.; Hemond, H.F.; Lafleur A.L. & Cass, G.R. (2004). Human-cell mutagens in respirable airborne particles in the northeastern United States. 1. Mutagenicity of fractionated samples. *Environmental Science and Technology*, 38., 682-689.
- Pedersen, D.U.; Durant, J.L.; Taghizadeh, K.; Hemond, H.F.; Lafleur A.L. & Cass, G.R. (2005). Human cell mutagens in respirable airborne particles from the Northeastern United States. 2. Quantification of mutagens and other organic compounds. *Environmental Science and Technology*, 39., 9547-9560.
- Petry, T.; Schmid, P. & Schlater, C. (1996). The use of toxic equivalency factors in assessing occupational and environmental health risk associated with exposure to airborne mixtures of polycyclic aromatic hydrocarbons (PAHs). *Chemosphere*, 32., 639-648.
- Poppi, N.R. & Silva, M.S. (2005). Polycyclic aromatic hydrocarbons and other selected organic compounds in ambient air of Campo Grande City, Brazil. *Atmospheric Environment*, 39., 2839-2850.
- Pufulete, M.; Battershill, J.; Boobis, A. & Fielder, R. (2004). Approaches to carcinogenic risk assessment for polycyclic aromatic hydrocarbons: a UK perspective. *Regulatory Toxicology and Pharmacology*, 40., 54-66.
- Ravindra, K.; Bencs, L.; Wauters, E.; de Hoog, J.; Deutsch, F.; Roekens, E.; Bleux, N.; Bergmans, P. & Van Grieken, R. (2006a). Seasonal and site specific variation in vapor and aerosol phase PAHs over Flanders (Belgium) and their relation with anthropogenic activities. *Atmospheric Environment*, 40., 771-785.
- Ravindra, K.; Sokhi, R. & Grieken, R.V. (2008). Atmospheric polycyclic aromatic hydrocarbons: Source attribution, emission factors and regulation. *Atmospheric Environment*, 42., 2895-2921.
- Ravindra, K.; Wauters, E.; Taygi, S.K.; Mor, S. & Van Grieken, R. (2006b). Assessment of air quality after the implementation of CNG as fuel in public transport in Delhi, India. *Environmental Monitoring and Assessment*, 115., 405-417
- Saarnio, K.; Sillanpää, M.; Hillamo, R.; Sandell, E.; Pennanen, A.S. & Salonen, R.O. (2008). Polycyclic aromatic hydrocarbons in size-segregated particulate matter from six urban sites in Europe. *Atmospheric Environment*, 42., 9087-9097
- Sasaki, J.; Aschmann, S.M.; Kwok, E.S.C.; Atkinson, R. & Arey, J. (1997). Products of the gas-phase OH and NO<sub>3</sub> radical-initiated reactions of naphthalene. *Environmental Science and Technology*, 31., 3173-3179.
- Schauer, J.J.; Kleeman, M.J.; Cass, G.R. & Simoneit, B.R.T. (2001). Measurement of emissions from air pollution sources, 3. C<sub>1</sub>-C<sub>29</sub> organic compounds from fireplace combustion of wood. *Environmental Science and Technology*, 35., 1716-1728.
- Sharma, H.; Jain, V.K. & Khan, Z.H. (2007). Characterization and source identification of polycyclic aromatic hydrocarbons (PAHs) in the urban environment of Delhi. *Chemosphere*, 66., 302-310.
- Sienra, M.R.; Rosazza, N.G. & Préndez, M. (2005). Polycyclic aromatic hydrocarbons and their molecular diagnostic ratios in urban atmospheric respirable particulate matter. *Atmospheric Research*, 75., 267-281.
- Spezzano, P.; Picini, P.; Cataldi, D.; Messale, F. & Manni, C. (2008). Particle- and gas-phase emissions of polycyclic aromatic hydrocarbons from two-stroke, 50-cm<sup>3</sup> mopeds. *Atmospheric Environment*, 42., 4332-4344

- Tokiwa, H. & Ohnishi, Y. (1986). Mutagenicity and carcinogenicity of nitroarenes and their sources in the environment. *Critical Reviews in Toxicology*, 17., 23–60.
- Tokiwa, H.; Nakanishi, Y.; Sera, N.; Hara, N. & Inuzuka, S. (1998). Analysis of environmental carcinogens associated with the incidence of lung cancer. *Toxicology Letters*, 99., 33–41
- US EPA. (1995). *Toxicological profile for polycyclic aromatic hydrocarbons*. US department of health and human services.
- Vasilakos, Ch.; Levi, N.; Maggos, Th.; Hatzianestis, J.; Michopoulos, J. & Helmis, C. (2007). Gas-particle concentration and characterization of sources of PAHs in the atmosphere of a suburban area in Athens, Greece. *Journal of Hazardous Materials*, 140., 45-51.
- Venkataraman, C.; Negi, G.; Sardar, S.B. & Rastogi, R. (2002). Size distributions of polycyclic aromatic hydrocarbons in aerosol emissions from biofuel combustion. *Aerosol Science*, 33., 503–518.
- Wan, X.; Chen, J.; Tian, F.; Sun, W.; Yang, F. & Saiki, K. (2006). Source apportionment of PAHs in atmospheric particulates of Dalian: Factor analysis with nonnegative constraints and emission inventory analysis. *Atmospheric Environment*, 40., 6666-6675.
- Yang, H.H.; Hsieh, L.T.; Liu, H.C. & M, H.H. (2005). Polycyclic aromatic hydrocarbon emissions from motorcycles. *Atmospheric Environment*, 39., 17-25.
- Yang, H.H.; Jung, R.C.; Wang, Y.F. & Hsieh, L.T. (2005). Polycyclic aromatic hydrocarbon emissions from joss paper furnaces. *Atmospheric Environment*, 39., 3305–3312.
- Yang, H.H.; Lee, W.J.; Chen, S.J. & Lai, S.O. (1998). PAH emission from various industrial stacks. *Journal of Hazardous Materials*, 60., 159-174.
- Zhang, Y. & Tao, X. (2009). Global atmospheric emission inventory of polycyclic aromatic hydrocarbons (PAHs) for 2004. *Atmospheric Environment*, 43., 812-819.
- Zhu, L., Lu, H.; Chen, S. & Amagai, T. (2009). Pollution level, phase distribution and source analysis of polycyclic aromatic hydrocarbons in residential air in Hangzhou. *China Journal of Hazardous Materials*, 162., 1165-1170.

# Air Pollutants, Their Integrated Impact on Forest Condition under Changing Climate in Lithuania

Algirdas Augustaitis

*Lithuanian University of Agriculture, Laboratory of Forest Monitoring  
Lithuania*

## 1. Introduction

Changes in forest ecosystems, in most cases, are related to the integrated impact of natural and anthropogenic factors, where air concentration of surface ozone, and S and N deposition play a predisposing, accompanying and locally, even a triggering role (Chappelka & Freer-Smith, 1995, Cronan & Grigal, 1995, Manion & Lachance, 1992, Schulze, 1989). These rather different effects of air pollution could be explained by the combination of direct, above-ground, impacts of O<sub>3</sub>, SO<sub>2</sub>, NO<sub>x</sub>, NH<sub>4</sub><sup>+</sup> and H<sup>+</sup> on foliage, and indirect, soil-mediated effects of acid deposition on roots, which may cause nutrient deficiencies and aggravate natural stress, such as physiological drought and the occurrence of pests and diseases (De Vries et al., 2000a). These above mentioned indirect, soil-mediated effects of air pollutants on the vitality of forests are frequently more relevant than the direct above ground effects especially in local polluted areas (Roberts et al., 1989, De Vries et al., 2000b). However, on a regional scale long range transboundary air pollution and ensuing acidification of the environment could only be detected when data of the repeated surveys for a relatively long period become available (De Vries et al., 2003a).

Ambient O<sub>3</sub> is also among the key factors resulting in spatial and temporal changes of tree crown defoliation (Reich, 1987; Guderian, 1985; Takemoto et al., 2001; Sandermann, 1996). Integrated effects of ozone with acidifying species differ significantly from the sum of their individual effects due to the complex synergistic or antagonistic interactions (Bytnerowicz et al., 2007). Therefore, the process based on plant damages due to O<sub>3</sub> exposure is still not fully clarified (Zierl, 2002; Matyssek et al., 2005), and the relationship between forest tree crown condition and O<sub>3</sub> concentrations as well as acid deposition is still not well established. O<sub>3</sub> is one of the most important and pervasive phytotoxic agents whose effects are likely to increase in future (Krupa & Manning, 1988; Hutunnen et al., 2002; Percy et al., 2003; Vingarzan, 2004). In contrast to SO<sub>2</sub>, the continuing rise in the emissions of precursor substances (NO, NO<sub>2</sub>) (Fowler, et al., 1998; Ryerson, et al., 2001) resulted in a rise in ozone concentrations (Matyssek & Innes, 1999; Coyle, et al., 2003; Fuhrer, 2000). If since the middle of the last century ozone (O<sub>3</sub>) air pollution has been recognized as a major phytotoxic agent in North America and South Europe (Smith, 1981; Schmieden & Wild, 1995; Hill, et al., 1970; Alonso, et al., 2002), then recently - in Central and Northern Europe (Utrainen & Holopainen, 2000; Muzika, et al., 2004; Karlsson, et al., 2002).

Therefore, due to the expected increase in O<sub>3</sub> concentrations (Fowler et al., 1999; Percy et al., 2003) it is necessary to determine if exposure to O<sub>3</sub> levels actually affects tree growth and crown condition in natural forests (Manning, 2005) under regional pollution load. The findings of our earlier study allowed us to make an assumption that temporal and spatial changes in pine defoliation are first of all, related to air concentrations of the acidifying compounds and their deposition meanwhile meteorological parameters only reinforce or mitigate the integrated impact of these factors (Augustaitis et al. 2003, 2005, 2007d). In this study we attempted to investigate the possible effect of natural and anthropogenic environmental factors on pine defoliation and stem growth, and quantify of O<sub>3</sub> contributions to the integrated impact of these factors.

However, in estimating the effect of air pollutants and their deposition on forest conditions, only the mean annual value of air pollutants and sum deposition over the year, or sum concentrations of ozone from April to September is usually used (Klap et al., 1997, 2000; De Vries et al., 2000a). Seasonal effects of the considered pollutants are attributed to the knowledge gaps in this area. Our earlier study showed that pine needles, which are present on trees all year round, seem to be more efficient aerosol collectors than leaves (Augustaitis et al., 2008a). Following this assumption, the negative effect of the considered contaminants, with the exception of O<sub>3</sub>, should occur during the dormant periods as well. Therefore, in the present study, we set out to see whether it is possible to detect seasonal effects of air pollutants and acid deposition on the mean defoliation of pine stands employing correlative or multiple regression analysis, and evaluate their significance in explaining the variance in mean defoliation of the pine stands.

The Integrated Monitoring Programme, which has been performed for more than 15 years in Lithuania, provides all the necessary data to identify the key environmental factors, effect character and periods when the effect of the considered contaminants is most pronounced.

To meet the objectives of the study the following studies were performed:

- an analysis of temporal and spatial variation of data on defoliation, meteorological parameters, air pollutant concentrations, including surface ozone and acid deposition;
- an analysis of variation of data on quality of soil, ground and stream waters in relation to air pollutants, their deposition and meteorological parameters;
- an estimate of the contributions of effect character to the integrated impact of air and soil mediated pollutants on tree defoliation
- an evaluation of the significance of the seasonal effects of the considered contaminants, explaining variance in mean defoliation of the pine crowns.
- an evaluation of the significance of the surface ozone concentration in the integrated effect with acidifying species, their deposition and meteorological parameters on Scots pine defoliation and stem increment reduction

The findings should increase our knowledge in the field of diagnostic and mechanistic understanding of processes occurring in ecosystem. It may help: (i) to estimate the integrated effect of environmental factors on forest ecosystem, (ii) detect peculiarities of the seasonal effects of acidifying compounds, surface ozone on pine defoliation, (iii) specify the periods when the effect of the considered contaminants is most pronounced, and (iv) predict state of forest ecosystem under the pressure of global changes.

## 2. Objects, materials and methods

In order to meet the emerged tasks the different data sets obtained in three national parks (NP), representing different Lithuanian landscape types (Aukštaitija NP - eastern part, Dzukija NP - southern part and Zemaitija NP -western part) (Fig. 1) were used. There integrated monitoring stations have been under operation since 1994.

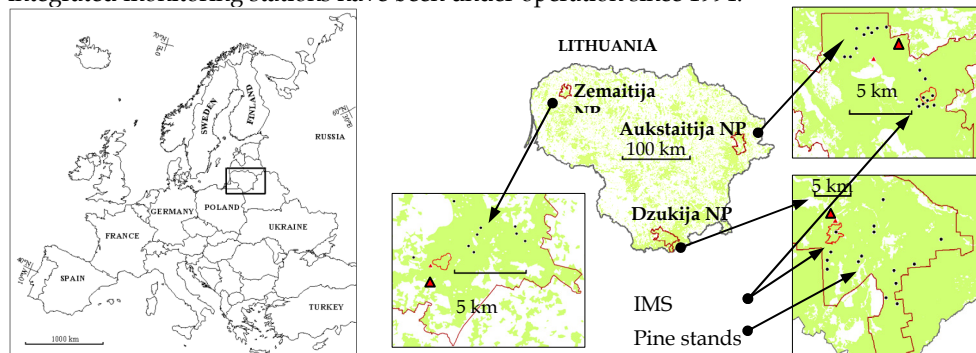


Fig. 1. Location of Aukštaitija, Dzukija and Zemaitija Integrated Monitoring Stations (▲), rivulet basins and POS in Lithuanian National Parks.

### 2.1 Objects for estimation of the direct effect of acidifying species and surface ozone

The study of direct effects of acidifying species, their deposition, surface ozone and meteorological parameters on forest health was based on annual observations of crown defoliation of more than 8,000 Scots pine (*Pinus sylvestris* L.) trees from 44 permanent observation stands (POS) between 1994 and 2007. Aukštaitija NP had 20 POS, Dzukija NP 16 POS and Zemaitija - NP 9 POS. These stands were located in the surroundings of Integrated monitoring stations (IMS) established there, and were selected according to stand maturity: 8 sapling stands (45–50 years), 10 middle aged stands (61–80 years), 10 premature stands (81–100 years), 10 mature stands (101–120 years) and 7 over mature stands >121 years).

### 2.2 Objects for estimation of the indirect effect of acidifying species

Investigations were performed on 5 vegetation plots established for intensive monitoring at IMS catchments where dendrometric parameters and crown condition of the three tree species – Scots pine (*Pinus sylvestris* L.), Norway spruce (*Picea abies* Karst.) and birch (*Betula pendula* 'Crispa' and *B. pubescens* Ehrh.) were assessed. Over the period 1994–2007 about 600 trees (pine trees– 30%, spruce – 50% and birch – 20%) in Aukštaitija NP (LT-01) on 3 intensive plots (IPs): A, B and C; in Dzukija NP (LT-02 A) about 100 trees on 1 IP (pine trees – 90%, spruce and birch – 10%), and in Zemaitija NP (LT-03 A) about 100 trees on 1 IP (pine trees – 20%, spruce – 70% and birch – 10%) were monitored annually.

### 2.3 Objects for estimation of the effect of surface ozone on pine increment

To get closer insight into the relationships between different O<sub>3</sub> indices and pine increment we chose 12 out of 44 pine permanent observation stands (POS). More than 200 trees, for which defoliation was assessed from 1994 to 2007, were chosen for the increment boring.

## 2.4 Predictor variables and methods of their estimation

The considered predictor variables were classified into 3 groups. The first group included 3 site-specific variables (forest type, soil typological groups with respect to fertility, and moisture conditions) and 5 tree and stand variables: mean tree age (A), height (H), diameter (D), basal area (BA), and stand volume (M).

The second group consisted of 10 meteorological variables (air temperature and the amount of precipitation for 8 seasons of 2 years and 2 year-long periods from September to August).

The third group of 13 variables included data on: air concentrations of sulfur dioxide (SO<sub>2</sub>), sulfate (SO<sub>4</sub><sup>2-</sup>), the sum of nitrates in aerosols and gaseous nitric acid ( $\Sigma\text{NO}_3^- = \text{NO}_3^- + \text{HNO}_3$ ), the sum of gaseous ammonia and ammonium in aerosols ( $\Sigma\text{NH}_4^+ = \text{NH}_4^+ + \text{NH}_3$ ) and surface ozone (O<sub>3</sub>); concentration of SO<sub>4</sub><sup>2-</sup>, NO<sub>3</sub><sup>-</sup>, NH<sub>4</sub><sup>+</sup> and H<sup>+</sup> in precipitation as well as their wet deposition (Sopauskiene & Jasineviciene, 2006; Girgzdiene et al., 2007).

## 2.5 Methods

**Dendrometric and health parameters of trees and stands.** Data on tree and stand parameters as well as crown defoliation were available from the permanent observation stands. A three-stage sampling pattern was used for the collection of the field material:

- (i) sampling of the research stands;
- (ii) sampling of the circular plots within each research stand;
- (iii) sampling of the trees for more detailed measurements of tree crown parameters and tree ring analysis. Each pine stand included 12 circular sample plots distributed systematically in a grid system with on average 15-20 trees on each plot, i.e., about 150-250 sample trees per stand. There, tree stem diameter was permanently measured and crown defoliation assessed for all sample trees annually. In addition three closest to the centre of sampling plot trees were sampled for measurement of crown parameters (height, diameter and length) and analysis of annual radial increment. Radial growth was assessed by measuring the width of annual rings in stem cores. Based on the ring widths the stem basal area increment (BAI) was computed.

Crown defoliation was assessed at the end of August. Forest monitoring methodology was employed to assess tree defoliation: healthy trees (defoliation up to 10%); slightly damaged trees (defoliation ranging from 11 to 25%); moderately damaged trees (defoliation 26–60%); severely damaged trees (defoliation 61–99%); dead trees (defoliation 100%) (UN-ECE, 1994).

**Soil-mediated parameters.** Glacioaquatic accumulation forms with sand, gravel and stones are typical of the Aukstaitija IMS catchment. In this area, LT-01A and LT-01B, bores No 1 and 2 for ground water (GW) studies and lysimeters for soil water (SW) collection are arranged. Soil water samples were collected at 20 cm, with a sampling period of 3–4 times per vegetation period. The surface area of the plate type lysimeter was 1000 cm<sup>2</sup>. With a decrease in altitude, these glacioaquatic accumulation forms transfer into marsh accumulation forms with organic sediments where IP LT-01C and bore No 3 are located.

The geomorphologic structure of the Dzukija IMS catchment is formed by more intensive glacioaquatic and eolian processes, than in LT-01. All 3 bores for GW collection are arranged in fine-grained sand dominated there. Soils are formed on quartz sands of eolian origin and contain no carbonates. Premature and mature pure pine stands on the haplic arenosol where lysimeters for soil water collection are arranged, dominate in the catchment.

The geomorphologic structure of LT-03 catchment of Zemaitija NP is different from that of the other stations. The marsh accumulation forms with organic sediments transfer into

limnoglacial accumulative forms and glacioaquatic accumulative sandy and hilly formations, with typical limnoglacial sand. Bores are situated on the slope of a glacioaquatic hill covered by sand stratified to a depth of more than 1.5 m with thin layers of clay loam. A spruce forest with two or more age classes and with up to a 20-30% pine mixture on albic arenosol where LT-03A, bore No 1 and lysimeters for soil water collection are arranged, dominates in the Zemaitija IMS (Augustaitis et al., 2008a).

**Air pollution and deposition.** Data on regional air concentrations of acidifying chemical species, the concentrations and fluxes of these chemical species in wet deposition and general meteorological data were obtained from the IMS established in the national parks and used for all stands located in the park. Due to a lack of funding Dzukija IMS was closed in the year 2000. Therefore, data from this region represented the period 1994–1999.

At IM stations,  $\text{SO}_2$ ,  $\text{SO}_4^{2-}$ , the sum of nitrate ( $\Sigma\text{NO}_3^- = \text{NO}_3^- + \text{HNO}_3$ ), and the sum of ammonium ( $\Sigma\text{NH}_4^+ = \text{NH}_4^+ + \text{NH}_3$ ) concentrations in the air and  $\text{H}^+$ ,  $\text{SO}_4^{2-}$ ,  $\text{NO}_3^-$  and  $\text{NH}_4^+$  concentrations in precipitation, as well as their wet deposition, were established. The air sampling was carried out at weekly intervals. The sampling equipment for  $\text{SO}_2$  and particulate sulphate consisted of a two-stage filter pack sampler with a cellulose filter (Whatman 40).  $\text{SO}_2$  was collected by retention of particles using a Whatman 40 filter impregnated with potassium hydroxide (KOH).  $\Sigma\text{NO}_3^-$  and  $\Sigma\text{NH}_4^+$  were collected using an open-face separate sampler with alkaline (KOH) and oxalic acid impregnated Whatman 40 filters, respectively (Sopauskiene & Jasineviciene, 2006).

Precipitation samples were collected in a polyethylene bulk-collector from December to March and in an automatic wet-only sampler during the remaining months. All samples were stored at 4°C until laboratory analysis. Ion chromatography using Dionex 2010i with conductivity detection was used for the chemical analysis of anions in precipitation, and in water extracts from the impregnated Whatman 40 filters.  $\text{NH}_4^+$  concentration in precipitation as well as in the extracted solutions from oxalic acid impregnated Whatman 40 filters was analysed spectrophotometrically using the indophenol blue method. The overall measurement and analytical procedures were based on a quality assurance/quality control (QA/QC) programme as described in the EMEP CCC manual for sampling, chemical analysis and quality assessment (EMEP 1977). Analytical methods were controlled through the international (EMEP and GAW) analytical intercomparisons.

**Ozone.** Ozone concentrations were measured continuously using commercial UV-absorption monitors O<sub>3</sub> 41M (Environment S.A., France) and ML9811 (Monitor Labs) with an air inlet at the height of 2.5 m above ground. The instruments were calibrated periodically every year. Hourly data on peak O<sub>3</sub> value, their annual average, and average from April through August were used in the analysis. AOT40 values, which define the potential risk of O<sub>3</sub> for vegetation (Fuhrer et al., 1997), were calculated according to the requirements of the 2002/3/EC directive. For crops, the critical level is set to 3.0 ppmh (AOT40-1); for forest trees, 10 ppmh (AOT40-2) (NABEL, 1999). Exceedance of the AOT40-2 threshold would indicate a risk of tree biomass loss of more than 10% (LRTAB, 2004).

**Meteorological parameters.** The effect of meteorological conditions on pine defoliation was analyzed for two yearlong periods from September to August. The quality of the data was assured according to the requirements of the World Meteorological Organization (WMO, 1983) and ICP IM methodology (UN-ECE, 1993). Meteorological data were collected at IM stations according to the requirements of the WMO Guidelines (1989) to ensure their comparability with the data from official weather stations and other monitoring sites.

**Statistics.** The Fisher test was employed for estimating the significance of spatial and temporal differences in changes in pollution level and tree defoliation. The integrated impact of natural and anthropogenic factors on mean defoliation of pine trees was analyzed by a multiple stress approach, using the linear multiple regression technique of "Statistica 6.0" software. The quality of the created models was assessed by determining the coefficient of determination ( $R^2$ ) and the level of statistical significance ( $p$ ). Stress factors were excluded from the regression model by a stepwise procedure based on the level of significance of each stress factor. Finally, variables with a high level of significance compiled the models. The impact of ambient  $O_3$  on pine crown defoliation and BAI was examined in a 2-step multi-regression procedure (Neiryneck & Roskams, 1999). The annual mean defoliation was regressed on site and stand predictor variables using a stepwise regression with a forward selection procedure. Then, the residual defoliation was regressed on air concentrations of acidifying compounds, their concentration in precipitation and deposition, and meteorology using the same stepwise regression procedure. The annual BAI was regressed on stand predictor variables and crown defoliation using a stepwise regression with a forward selection procedure. Then, the BAI residuals were regressed on air concentrations of acidifying compounds, their concentration in precipitation and deposition, and meteorology using the same stepwise regression procedure. Finally, the predictor variable "peak ozone concentration" was included in the created models and its contribution to the integrated impact of different combinations of natural and anthropogenic factors on pine crown defoliation and BAI was quantified.

### 3. Spatial and temporal variation of predict and response variables

#### 3.1 Air pollution and acid deposition

IMS data showed a significant decrease in pollutants until the year 2000 (Sopauskiene *et al.* 2001, Augustaitis *et al.* 2005, Sopauskiene & Jasineviciene, 2006, Augustaitis *et al.* 2007b). The air concentration of  $SO_2$  at Aukstaitija IMS decreased by 82% (from 2.73 to 0.49  $\mu\text{gS}/\text{m}^3$ ), at Zemaitija IMS by 79% (from 2.22 to 0.47  $\mu\text{gS}/\text{m}^3$ ), and at Dzukija IMS by 57% (from 3.0 to 1.3  $\mu\text{gS}/\text{m}^3$ ) (Fig. 2). Thereafter, the concentration was stable at the level of 0.5 – 1.0  $\mu\text{gS}/\text{m}^3$ . Air concentration of aerosolic  $SO_4^{2-}$  changed in a similar to  $SO_2$  air concentration pattern.

The most significant decrease in  $\Sigma\text{NH}_4^+$  air concentration lasted until 2001: 86% in LT-03 (from 8.55 to 1.15  $\mu\text{gN}/\text{m}^3$ ), 77% in LT-01 (from 4.44 to 1.02  $\mu\text{gN}/\text{m}^3$ ), and 65% in LT-02 (from 3.91 to 1.37  $\mu\text{gN}/\text{m}^3$ ). Since 2001 a stabilization of air  $\Sigma\text{NH}_4^+$  concentration at the level of 1.1 – 1.3  $\mu\text{gN}/\text{m}^3$  in both LT-01 and LT-03 was observed. Annual means of  $\Sigma\text{NO}_3^-$  concentration in the air were stable at the level of 0.5–0.7  $\mu\text{gN}/\text{m}^3$  in all stations.

Changes in annual wet deposition had a very similar pattern to that of the air. The wet deposition of sulphur for the period 1994–2000 at the Aukstaitija NP decreased by 58% (from 600 to 250  $\text{mgS}/\text{m}^2$ ), at Zemaitija by 60% (from 750 to 300  $\text{mgS}/\text{m}^2$ ), and at Dzukija by 52% (from 660 to 320  $\text{mgS}/\text{m}^2$ ). Since 2001 at LT-01, sulphur deposition further decreased to 200  $\text{mgS}/\text{m}^2$ , while at LT-03, it drastically increased again in 2002–2003 and 2007, reaching around 600  $\text{mgS}/\text{m}^2$  (Sopauskiene & Jasineviciene, 2006).

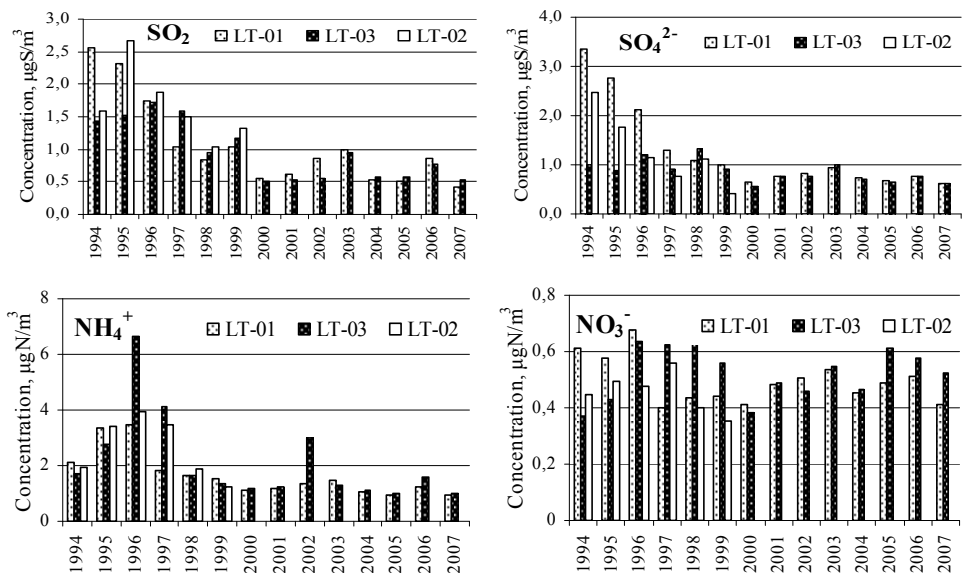


Fig. 2. Changes in the mean air concentration of the considered contaminants.

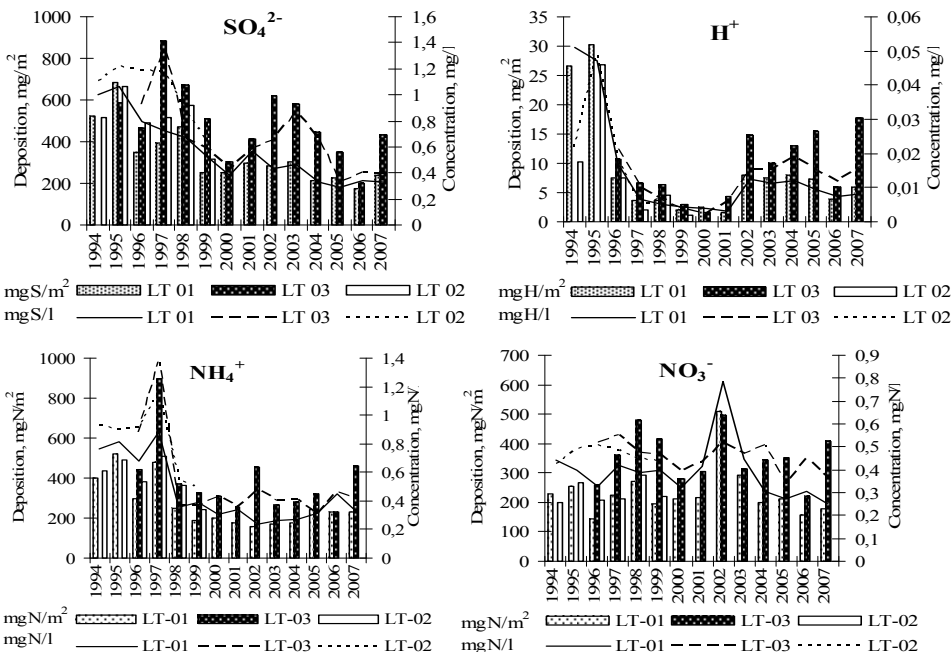


Fig. 3. Changes in acid deposition and their concentrations in precipitation (LT-01 - Aukstaitija IMS; LT-02 - Dzukija IMS; LT-03 - Zemaitija IMS)

Decreases in annual wet deposition of  $\text{NH}_4^+$  from 492 to 198  $\text{mgN/m}^2$  at LT-01 and from 537 to 303  $\text{mgN/m}^2$  at LT-03 occurred until 2001. Afterwards, a gradual increase in deposition of the contaminant was observed at all stations. Contrary to this, no significant change in wet deposition of  $\text{NO}_3^-$  was observed (Fig. 3).

Annual wet deposition values for  $\text{NO}_3^-$  ranged from 241 to 211  $\text{mgN/m}^2$  at LT-01, from 241 to 270  $\text{mgN/m}^2$  at LT-02 and from 414 to 342  $\text{mgN/m}^2$  at LT-03, with the exception of 2002, when it reached the peak. Despite this, the total N deposition since 2001 started to increase again mainly due to the increase in ammonium deposition. As a result of these changes in acidifying compounds until 2001 a more than tenfold decrease in  $\text{H}^+$  concentration in precipitation and its deposition was observed at the stations, however, since afterwards an increase especially at LT-03 was recorded. Acidity of precipitation started to increase again mainly due to repeated increase in  $\text{NH}_4^+$  deposition especially in western part of Lithuania. Therefore, even after a complete implementation of the Gothenburg Protocol and other current legislation, the effect of N deposition with commensurate adverse biological effects still remains the most relevant problem to confront in Europe as well as in the USA and Canada (Wright et al., 2005).

An analysis of the spatial pattern of regional pollution levels revealed that the Western and South-western parts of Lithuania (LT-02 and LT-03 sites) were more polluted by the considered pollutants. That was most likely related to the proximity of those regions to the major pollutant sources in Central Europe as well as to the differences in the meteorology.

### 3.2 Surface ozone

Ozone concentration data at IMS showed no clear trend in temporal changes in the annual mean, and mean values from April through August as well as in the AOT40 (Girgzdiene et al., 2007). However, decline in the peak concentrations from 215 to 125  $\mu\text{g}/\text{m}^3$  was observed until 2001 (Fig. 4). After 2001 gradual increase in both means (annual and April-August period), and peak concentrations was observed. The peak hourly  $\text{O}_3$  concentrations ranged from 125  $\mu\text{g}/\text{m}^3$  to 165  $\mu\text{g}/\text{m}^3$  during the summer period and were typical of other parts of Central Europe (Pell et al., 1999; Solberg et al., 2005; Bytnerowicz et al., 2004). In Lithuania high (more than 120  $\mu\text{g}/\text{m}^3$ ) ozone concentrations were mostly observed when air masses were transported from Western Europe. Instead of rather similar ozone concentrations at all stations (Fig. 4), AOT40 values varied more significantly due to different meteorological conditions. Ozone concentrations higher than 80  $\mu\text{g}/\text{m}^3$  were mostly observed on sunny days the number of which differed significantly in the western (LT-03) and eastern parts (LT-01) of Lithuania. The computed AOT40 values for the protection of forest at LT-01 and LT-02 ranged from 8000 to 21000  $\mu\text{g}/\text{m}^3 \text{ h}$  while at LT-03 only from 5000 to 12000  $\mu\text{g}/\text{m}^3 \text{ h}$ .

The concentration of  $\text{O}_3$  among the concentrations of the other monitored air pollutants ( $\text{SO}_2$ ,  $\Sigma\text{NO}_3^-$  and  $\Sigma\text{NH}_4^+$ ) reached the closest to critical phytotoxic level. The AOT40 value for the protection of vegetation (6000  $\mu\text{g}/\text{m}^3 \text{ per h}$ ) was exceeded at all stations for almost all considered years (Girgzdiene et al., 2007). The critical level 20000  $\mu\text{g}/\text{m}^3 \text{ per h}$  for the protection of forest was observed only at LT-01 in the year 1999. The highest peak ozone value 213  $\mu\text{g}/\text{m}^3$  was observed only in the year 1995, while higher than 160  $\mu\text{g}/\text{m}^3$  value - at the beginning of observation and recently, in the years 2002 and 2005. Peak ozone concentrations most often were observed in spring, i.e., in April and May.

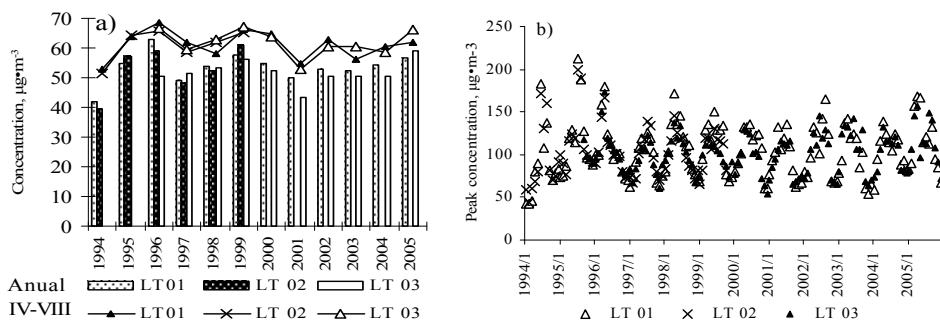


Fig. 4. Variation in ozone annual and April-August period means (a) and peak concentrations (b)

### 3.3 Soil water quality

In the period from 1994 to 1999 soil water at LT-02 was more contaminated with  $\text{SO}_4^{2-}$  and  $\text{NH}_4^+$  than in the other sites and demonstrated significant downward trends (Fig. 5):  $\text{SO}_4^{2-}$  concentration decreased by 0.79 mgS/l per year, and  $\text{NH}_4^+$  by 0.15 mgN/l per year. At LT-03 the decrease in  $\text{SO}_4^{2-}$  concentration was not so evident at 0.24 mgS/l per year. Meanwhile at LT-01,  $\text{SO}_4^{2-}$  concentration in soil water was stable at the level of 4-5 mgS/l. The decrease in  $\text{NH}_4^+$  concentration at LT-01 was at about 0.03 mgN/l per year, and at LT-03 the concentration remained stable at the level of 0.20 mgN/l. At LT-03 a downward trend in  $\text{NO}_3^-$  concentration in soil water was detected (0.013 mgN/l per year), while at LT-01 and at LT-02 it increased by 0.021 mgN/l and 0.075 mgN/l per year, respectively. The detected changes in  $\text{NO}_3^-$  concentration resulted in a significant increase in soil water pH at LT-01, by 0.1 unit per year and a decrease at LT-03, by 0.01 unit per year (Augustaitis *et al.* 2005, 2007a; 2008a). Consistently, the acidity of soil water at LT-01 decreased while at LT-03 it increased.

### 3.4 Ground water quality

Nitrate concentrations in the ground water of LT-01 had no statistically significant trends, whereas at LT-03  $\text{NO}_3^-$  concentrations in the ground water of the shallow bores showed a decreasing trend, and in the water of the deeper bores an increasing trend.  $\text{NH}_4^+$  concentration showed a trend towards decreasing in all bores of all IM stations.

$\text{SO}_4^{2-}$  concentration changes had no regular patterns at LT-01 station. The exception was the year 1996 and the last period from 2005 to 2007, when  $\text{SO}_4^{2-}$  concentration increased drastically in the third bore (near the vegetation plot LT-01 B). At LT-03  $\text{SO}_4^{2-}$  concentration changes had a tendency to decrease. The detected changes resulted in a gradual decrease of the ground water acidity at all considered depths. An exception, however, was the change in water acidity of the shallow bore at LT-03, which showed a tendency to increase.

Comparison of the means of concentrations of separate chemical components in soil and ground water of all three stations over the considered period, revealed higher concentrations of the most parameters in Dzukija (LT02), when this station was in operation. It is highly probable that this can be attributed to good infiltrational features of the continental dune sand. Since 2002, higher concentrations of the considered contaminants.

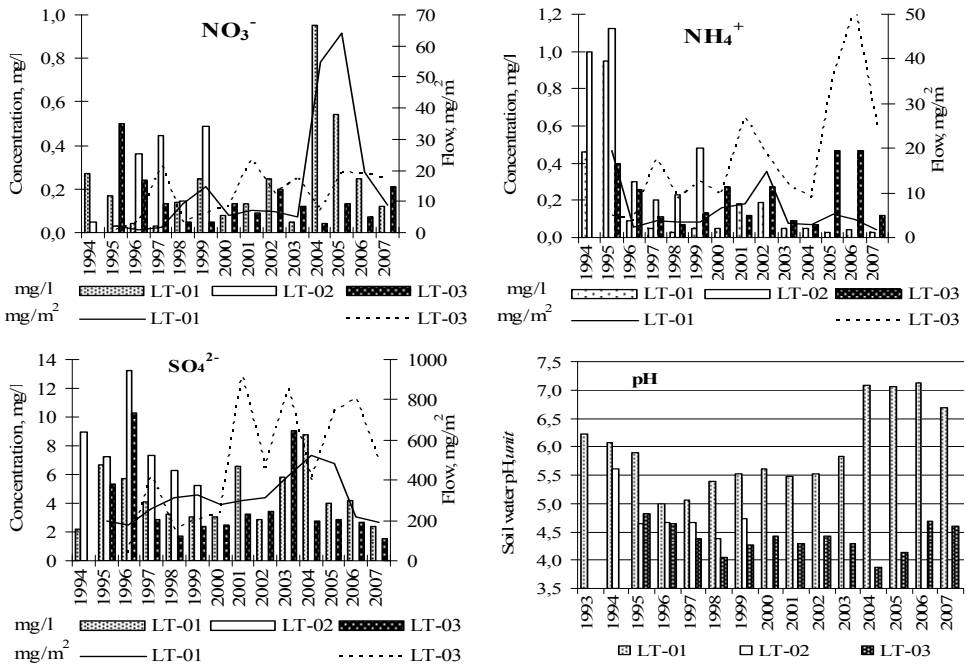


Fig. 5. Concentrations of the acidifying species in soil water and their flows at 20 cm depth. (LT-01 – Aukstaitija IMS; LT-02 – Dzukija IMS; LT-03 – Zemaitija IMS) were also observed at LT03, mainly due to higher air concentrations of the considered pollutants and their deposition (Augustaitis et al., 2005, 2008a).

### 3.5 Runoff water quality

Stream water quality and runoff of the main chemical compounds from ecosystems reliably reflect a common tendency of the chemical processes occurring in forest ecosystems. Therefore, this parameter was used in the analysis to detect the indirect effect of deposition on tree conditions. Concentrations of NO<sub>3</sub><sup>-</sup> and SO<sub>4</sub><sup>2-</sup> in the surface water had no statistically significant trends over the considered period (Fig. 6), however, since 1998 at LT-01 a significant decrease in SO<sub>4</sub><sup>2-</sup> concentration was observed. Concentration of NH<sub>4</sub><sup>+</sup> had a tendency to decrease in all stations over the entire observation period. The year 2007 was an exception, when concentration of this contaminator at LT-03 increased drastically. These detected changes resulted in a gradual decrease of surface water acidity at all sites. Despite rather similar character of the changes in NO<sub>3</sub><sup>-</sup> and NH<sub>4</sub><sup>+</sup> concentrations in runoff water, there was an evident difference in their output. Over the considered period, the output of both N compounds at LT-01 had a tendency to decrease, while at LT-03 a tendency to increase (Fig. 7). Similarly, the output of sulphur at LT-03 increased significantly while at LT-01 and LT-02, it decreased only until 2000, and afterwards some increase was observed.

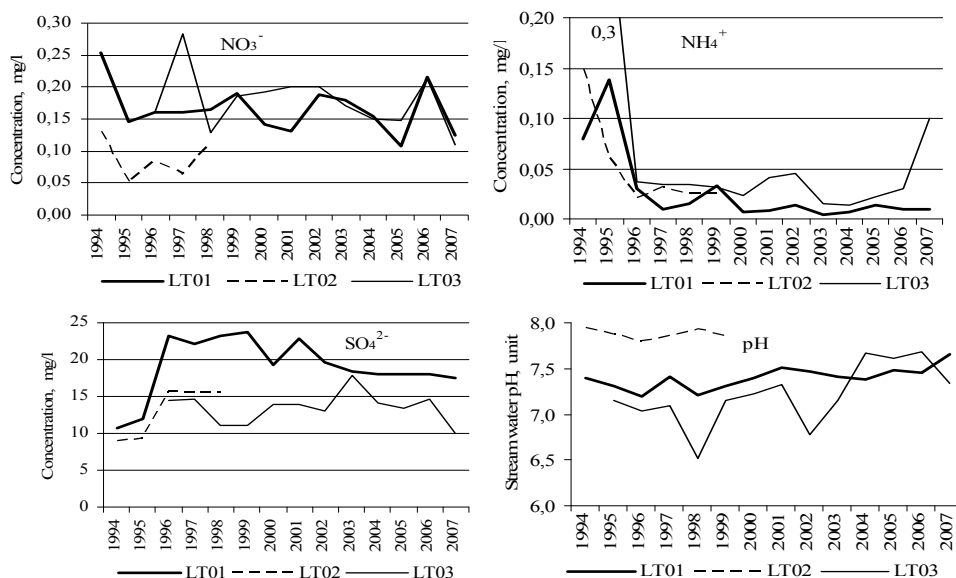


Fig. 6. Concentrations of the acidifying compounds in surface water of IM sites

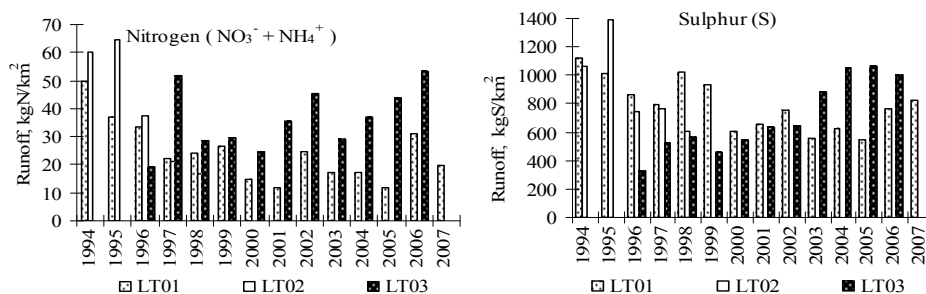


Fig. 7. Runoff of sulphur and nitrogen from the considered forest ecosystems

### 3.6 Temporal and spatial changes in meteorology

Annual amounts of precipitation did not demonstrate significant temporal tendency in NP during the 1994-2007 period meanwhile difference among them was significant ( $p < 0.05$ ). Mean annual precipitation was 930 mm at Zemaitija NP, 710 mm at Aukstaitija NP, and 650 mm at Dzukija NP (Fig. 8). The precipitation amount from October through February accounted for these differences (Augustaitis et al., 2005; 2007b; 2007d).

Mean annual temperature tended to increase between 1994 and 2007 ( $p > 0.05$ ). At Aukstaitija there was an average increase of 0.013°C per year, at Dzukija 0.061°C, and at Zemaitija 0.069°C per year. The increase was most pronounced in autumn (September-November). Mean annual temperature in Zemaitija (+6.9°C) was significantly higher than in Aukstaitija (+6.4°C), and Dzukija (+6.5°C) ( $p < 0.05$ ).

### 3.7 Tree crown defoliation

Scots pine trees in Aukstaitija NP showed the best condition as illustrated in Fig. 8. On the poorest sites (*Pinetum cladoniosum* forest type) in Dzukija NP, outbreaks of the forest pests (*Diprion pini* L. and *Ocneria monacha* L.) started in 1992 after a hot and dry vegetation period in 1991 and caused very serious crown damage. In 1996 biological insecticide Foray-48B was applied to suppress the outbreak, and recovery of the damaged Scots pine trees started. The highest level of mean defoliation of pine trees in Aukstaitija and Dzukija NPs was observed in 1995, whereas in Zemaitija NP it was observed in 1997. Afterwards, crown condition showed obvious improvement that lasted until 2005. Since this year pine defoliation started to gradually increase again. The detected temporal changes in mean defoliation of pine trees were quite common throughout most of Europe (UN-ECE, 2005; Lorenz & Mues, 2007).

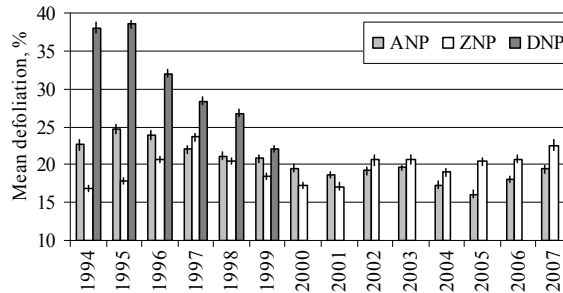


Fig. 8. Spatial and temporal changes in pine crown defoliation

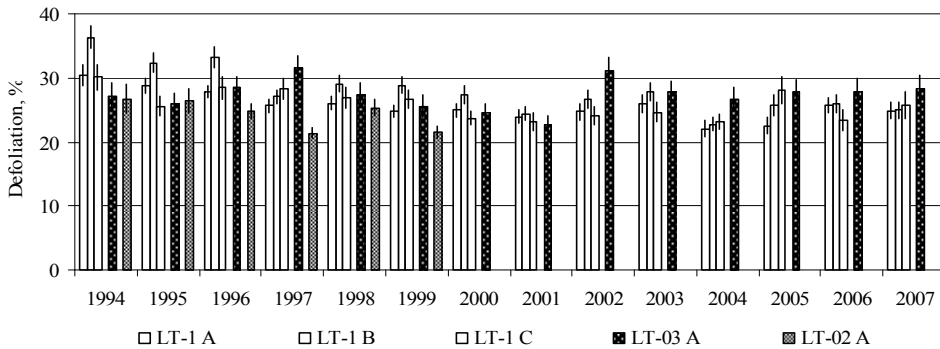


Fig. 9. Mean defoliation and standard error of estimation of the considered stands (LT-01 – Aukstaitija IMS; LT-02 – Dzukija IMS; LT-03 – Zemaitija IMS)

F test statistics indicated significant differences in mean defoliation of the prevailing tree species ( $p < 0.05$ ) among and within the intensive plots at Aukstaitija IMS (LT-01). It follows from figure 9 that from 1994 to 2004 mean defoliation of the considered tree species at the first plot, LT-01A, decreased from 30.4% to 22.1%, or at an average by 0.61% per year. At LT-01B over the same period, the decrease made from 36.2% to 22.8%, or 1.02% per year, and at LT-01C, from 30.1% to 23.2% or 0.59% per year. Over the last period (from 2005 to 2007), mean defoliation of the monitored trees increased in all plots at LT-01.

The changes in stand defoliation at LT-03A had no regular pattern. Peaks in defoliation were observed in 1997 and 2002, when they exceeded 30% (Fig. 9). During the rest of the period, defoliation fluctuated between 22% and 27%. The changes in mean defoliation at LT-02A demonstrated a significant trend towards decreasing ( $p < 0.05$ ). Between 1994 and 2001 it decreased from 26.7% to 21.6% (Augustaitis et al., 2005, 2007a; 2007b).

### 3.8 Stem radial increment of Scots pine trees

Significant temporal changes in annual stem increment were established at all sites ( $p < 0.05$ ) (Fig. 10) and reflected changes in crown defoliation (Fig. 8). Correlation coefficients between crown defoliation and stem increment ranged between  $r = -0.25$  in Zemaitija NP and  $r = -0.91$  in Dukija NP. Over the considered period increment of the pine stems in Aukstaitija NP increased by an average of 0.033 mm per year in middle aged and by 0.018 mm per year in matured stands. In contrast, in Zemaitija NP radial increments of the pine stems decreased by an average of 0.024 mm per year. Over the period from 1994 to 1999 pine stem increment increase in Dzukija NP was the most significant, by 0.178 mm per year (Fig. 10).

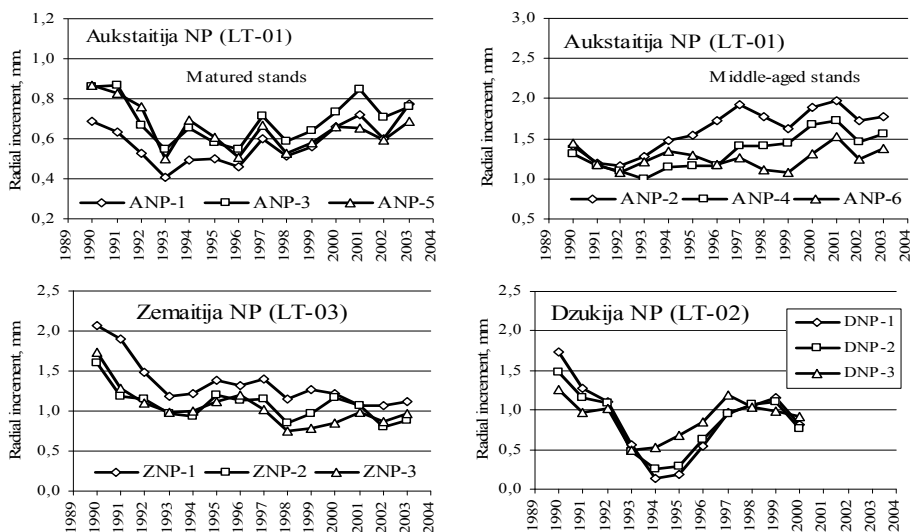


Fig. 10. Radial increment of pine trees at different sites.

## 4. Effect of predict variables on tree health and increment

### 4.1 Effect of meteorological parameters on Scots pine defoliation

Derived relationships between meteorological variables and tree defoliation showed that the correlation between pine defoliation and the amount of precipitation was generally the strongest one, followed by the correlation with air temperature. The direct correlation between pine defoliation and precipitation in September was found to be the strongest, followed by a weaker direct correlation with precipitation in the second half of the dormant period (February-April). Temporal changes in precipitation during these months (precipitation decrease) indicated improvement of pine stand conditions (lower defoliation

level). A negative correlation was established between defoliation and precipitation during the vegetation period (May-August), when the increase in precipitation should have resulted in better tree crown conditions as well (Augustaitis et al., 2010a).

The seasonal effect of monthly air temperature on pine defoliation was less significant than that of precipitation. In most cases, the effect of temperature on pine crown defoliation was negative and only higher temperatures in November-December should have resulted in better pine crown condition. The established significance of these relationships was in full agreement with the findings of the ICP Forest monitoring programme (De Vries et al., 2000a). An exceptional case, however, was the effect of the precipitation during early spring (March and May), a higher amount of which resulted in an increase in defoliation. Therefore, the hydrothermal index had no significant impact on tree crown defoliation.

An increase in both precipitation during the vegetation period and mean monthly temperature from September to December, as well as a decrease in temperature and precipitation over the rest of the dormant period, represented the conditions of climate change during the 14-year period in Lithuania, where the monitored pine stands were located. The positive effect of warmer and dryer dormant periods on tree condition is well known (Kozłowski et al., 1991), and our results confirmed that. An increase in temperature over the dormant period, particularly for the 2-month period of November and December, should have improved the condition of pine stands in Lithuania. The positive effect of more abundant precipitation over the vegetation period is well known (Makinen et al., 2003; Kahle and Spiecker, 1996). Gradual increase in temperature over vegetation, what could result in increase in surface ozone concentration should result in tree condition deterioration. Despite this, positive effects of changing climate conditions could be expected. By contrast, this process is opposite to the official scenario of climate change presented by the SRES A1 B Project (IPCC 2007), in which an increase in drought effect during the vegetation period is expected. Further investigation should allow us to check our assumptions.

#### 4.2 Effect of air pollutants and acid deposition on tree crown condition

The air concentrations of  $\text{SO}_2$  and  $\text{NH}_4^+$  as well as their wet deposition showed the strongest statistically significant relationships with temporal and spatial changes in mean defoliation of Scots pines ( $p < 0.05$ ) (Fig. 11). There was the weakest relationship between defoliation and the air concentration of  $\Sigma\text{NO}_3^-$  ( $r = 0.23$ ). The obtained results are in agreement with the ICP Forests Monitoring data (De Vries et al., 2000a, 2003; Klap et al., 2000).

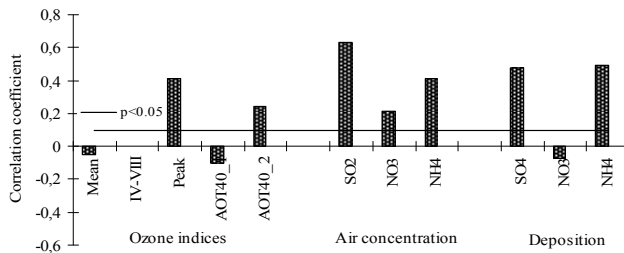


Fig. 11. Correlation coefficients of mean defoliation of pine stands and considered pollution variables in Lithuanian NPs (AOT40-1 for vegetation; AOT40-2 for forest)

Correlation coefficient between peak ozone concentration and temporal and spatial changes in mean pine defoliation was weaker. In Aukštaitija NP correlation coefficient between mean stand-wise defoliation and peak O<sub>3</sub> concentration in 13 of 22 stands was statistically significant ( $p < 0.05$ ,  $r > 0.56$ ), in Dzukija NP in 5 of 16 stands ( $r > 0.80$ ), and in Zemaitija NP - in 3 of 9 stands (Table 3). Data revealed that the changes in mean stand-wise defoliation of pines were most likely related to changes in acidifying compounds and peak concentration of ambient ozone. Significance of AOT40-2 for forest was twofold lower, meanwhile AOT40-1 for vegetation as well as other considered ozone indices were not significant ( $p > 0.05$ ).

### 4.3 Integrated effect of the considered variables on tree crown condition

A multiple regression analysis showed that 79% of the spatial and temporal variance in defoliation of the pine trees was explained by the variation in regional air pollution and meteorological, site and stand variables (Table 1). These findings suggest that the worst conditions of Scots pines which were found at Dzukija NP were not due to forest pests, alone. The poor site conditions, the higher level of pollutants, and the low precipitation amount explained together 75% of the defoliation variance of the pine trees in this park. Outbreaks of forest pests increased crown defoliation only by 7–19%, which accounted for 25% of the variance (Augustaitis et al., 2007d).

| Model      | Predictor variables (parameters) of: |      |                     |                   |                             |                          | Regression summary of model |                |      |           |
|------------|--------------------------------------|------|---------------------|-------------------|-----------------------------|--------------------------|-----------------------------|----------------|------|-----------|
|            | Stand-site                           |      | Meteorology         |                   | Pollution                   |                          | F                           | R <sup>2</sup> | p    | Std. err. |
|            | Stand                                | Site | Precipitation<br>mm | Temperature<br>°C | In air<br>µg/m <sup>3</sup> | In precipitation<br>mg/l |                             |                |      |           |
| F (4.400)  | +                                    | +    |                     |                   |                             |                          | 129.4                       | 0.564          | 0.00 | 5.2       |
| F (4.400)  | +                                    |      |                     |                   |                             |                          | 61.1                        | 0.337          | 0.00 | 6.2       |
| F (1.403)  |                                      | +    |                     |                   |                             |                          | 174.3                       | 0.301          | 0.00 | 6.5       |
| F (6.398)  |                                      |      | +                   | +                 |                             |                          | 43.0                        | 0.393          | 0.00 | 6.2       |
| F (5.399)  |                                      |      | +                   |                   |                             |                          | 48.0                        | 0.376          | 0.00 | 6.2       |
| F (3.399)  |                                      |      |                     | +                 |                             |                          | 42.2                        | 0.178          | 0.00 | 7.2       |
| F (6.398)  |                                      |      |                     |                   | +                           | +                        | 89.8                        | 0.575          | 0.00 | 5.2       |
| F (2.402)  |                                      |      |                     |                   | +                           |                          | 146.9                       | 0.422          | 0.00 | 6.0       |
| F (2.402)  |                                      |      |                     |                   |                             | +                        | 154.4                       | 0.434          | 0.00 | 5.9       |
| F (2.402)  |                                      |      |                     |                   |                             | +                        | 115.0                       | 0.364          | 0.00 | 6.3       |
| F (5.399)  |                                      |      |                     |                   | +                           | +                        | 99.8                        | 0.555          | 0.00 | 5.3       |
| F (5.399)  |                                      |      |                     |                   |                             | +                        | 84.3                        | 0.514          | 0.00 | 5.5       |
| F (5.399)  |                                      |      |                     |                   | +                           | +                        | 85.1                        | 0.516          | 0.00 | 5.5       |
| F (14.390) |                                      |      | +                   | +                 | +                           | +                        | 50.8                        | 0.646          | 0.00 | 4.8       |
| F (10.394) |                                      |      | +                   | +                 | +                           |                          | 98.9                        | 0.715          | 0.00 | 4.2       |
| F ( 8.396) |                                      |      | +                   |                   | +                           | +                        | 158.5                       | 0.762          | 0.00 | 3.8       |
| F (16.388) |                                      |      | +                   | +                 | +                           | +                        | 89.8                        | 0.787          | 0.00 | 3.7       |

Table 1. Multiple regression analysis of the impact significance of the group of predictor variables on changes in crown defoliation of Scots pine trees

Note: F(a.b) - models identified by F - test symbol with numbers of degrees of freedom: a - of the predictor variables; b - of the observations.

The group of pollution variables (air concentrations of the acidifying species, and their wet deposition) was regarded as the most relevant one. The integrated impact of these variables accounted for 58% of the variance in pine tree defoliation. A separate regression with air temperature and amount of precipitation (meteorological factors) accounted for 39%. The integrated impact of the variables from both of these groups accounted for 65% of the variance, and inclusion of stand and site parameters increased the degree of explanation by another 14% (totally 79%). Based on the obtained results we could state, that regional air pollution and acid deposition had the most significant effect on temporal and spatial changes in Scots pine crown defoliation in Lithuania.

#### 4.4 Significance of the effect character on tree defoliation

Changes detected in mean defoliation of the prevailing tree species on vegetation plots of IMS were directly related to changes in air pollutant concentrations and deposition of the acidifying compounds. An analysis of the relationships between pollution and crown defoliation of considered tree species revealed the highest susceptibility of Scots pines to the impact of air pollution by sulphur compounds ( $\text{SO}_2$  and aerosolic  $\text{SO}_4^{2-}$ ) and  $\text{SO}_4^{2-}$  and  $\text{NH}_4^+$  deposition (Fig. 12). This fully agrees with our data obtained in National parks and ICP Forest Monitoring data (Lorenz and Mues 2007, De Vries *et al.* 2000a, 2003a; UN-ECE 2005). Changes in crown defoliation of Birch were less related to changes in acidifying compounds, whereas changes in defoliation of Norway spruce were least related, mainly due to damage caused by forest pests, primarily *Ips typographus* L. (Augustaitis *et al.*, 2010b).

An analysis of possible indirect effects of the considered contaminants revealed that pine crown defoliation demonstrated the highest correlation with  $\text{NH}_4^+$  concentrations in soil and ground water, following similar with pH of soil water. The effect of these contaminants on birch defoliation was lower. Only nitrate concentrations both in ground and soil water seemed to have a positive effect on crown condition of these particular tree species. Changes in spruce crown defoliation were least related to the indirect effect of acidifying compounds. The findings have revealed that the changes in pine defoliation were most significantly related to changes in  $\text{SO}_4^{2-}$ ,  $\text{NH}_4^+$  and  $\text{NO}_3^-$  air concentrations. The effect of changes in concentrations of the considered compounds in soil and ground water on pine crown condition was remarkably lower (Table 2). However, this indirect effect increased the explanation of pine defoliation variability significantly - by 15%, up to 89%.

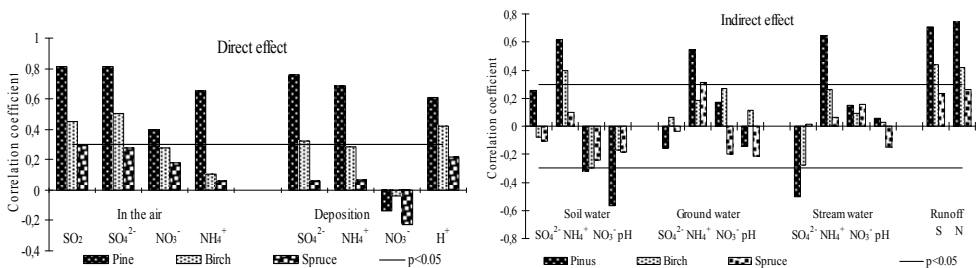


Fig. 12. Direct and indirect effect of concentrations of considered contaminants in the air, and their deposition on tree defoliation.

| Variables                  | Models, F(a,b) |       |       |       |       |       |       |        |       |       |       |       |       |       |       |       |       |       |       |       |       |   |  |
|----------------------------|----------------|-------|-------|-------|-------|-------|-------|--------|-------|-------|-------|-------|-------|-------|-------|-------|-------|-------|-------|-------|-------|---|--|
|                            | Pinus          |       |       |       |       |       |       | Spruce |       |       |       |       |       |       | Birch |       |       |       |       |       |       |   |  |
|                            | 3.43           | 2.44  | 2.44  | 3.43  | 2.44  | 5.41  | 9.37  | 1.51   | 2.50  | 2.50  | 3.49  | 2.50  | 4.48  | 5.47  | 1.54  | 2.53  | 2.53  | 3.5   | 3.52  | 4.51  | 8.47  |   |  |
| In the air: O <sub>3</sub> | +              |       |       |       |       |       | +     |        |       |       |       |       |       |       | +     |       |       |       |       |       |       | + |  |
| SO <sub>4</sub>            |                |       |       |       |       |       |       |        |       |       |       |       |       |       |       |       |       |       |       |       |       |   |  |
| SO <sub>2</sub>            | +              |       |       |       |       |       |       | +      |       |       |       |       |       |       |       |       |       |       |       |       |       |   |  |
| ΣNH <sub>4</sub>           | -              |       |       |       |       |       | +     |        |       |       |       |       |       |       |       |       |       |       |       |       |       |   |  |
| ΣNO <sub>3</sub>           |                |       |       |       |       |       |       |        |       |       |       |       |       |       |       |       |       |       |       |       |       |   |  |
| Deposition:SO <sub>4</sub> |                | +     |       |       |       |       |       |        |       |       |       |       |       |       |       |       |       |       |       |       |       |   |  |
| NH <sub>4</sub>            |                |       |       |       |       |       |       |        |       |       |       |       |       |       |       |       |       |       |       |       |       |   |  |
| NO <sub>3</sub>            |                |       |       |       |       |       |       |        |       |       |       |       |       |       |       |       |       |       |       |       |       |   |  |
| In soil water: pH          |                |       |       |       |       |       |       |        |       |       |       |       |       |       |       |       |       |       |       |       |       |   |  |
| SO <sub>4</sub>            |                |       |       |       |       |       |       |        |       |       |       |       |       |       |       |       |       |       |       |       |       |   |  |
| NH <sub>4</sub>            |                |       |       |       |       |       |       |        |       |       |       |       |       |       |       |       |       |       |       |       |       |   |  |
| NO <sub>3</sub>            |                |       |       |       |       |       |       |        |       |       |       |       |       |       |       |       |       |       |       |       |       |   |  |
| In ground water: deep      |                |       |       |       |       |       |       |        |       |       |       |       |       |       |       |       |       |       |       |       |       |   |  |
| pH                         |                |       |       |       |       |       |       |        |       |       |       |       |       |       |       |       |       |       |       |       |       |   |  |
| SO <sub>4</sub>            |                |       |       |       |       |       |       |        |       |       |       |       |       |       |       |       |       |       |       |       |       |   |  |
| NH <sub>4</sub>            |                |       |       |       |       |       |       |        |       |       |       |       |       |       |       |       |       |       |       |       |       |   |  |
| NO <sub>3</sub>            |                |       |       |       |       |       |       |        |       |       |       |       |       |       |       |       |       |       |       |       |       |   |  |
| In stream water: pH        |                |       |       |       |       |       |       |        |       |       |       |       |       |       |       |       |       |       |       |       |       |   |  |
| SO <sub>4</sub>            |                |       |       |       |       |       |       |        |       |       |       |       |       |       |       |       |       |       |       |       |       |   |  |
| NH <sub>4</sub>            |                |       |       |       |       |       |       |        |       |       |       |       |       |       |       |       |       |       |       |       |       |   |  |
| NO <sub>3</sub>            |                |       |       |       |       |       |       |        |       |       |       |       |       |       |       |       |       |       |       |       |       |   |  |
| Runoff: S                  |                |       |       |       |       |       |       |        |       |       |       |       |       |       |       |       |       |       |       |       |       |   |  |
| N                          |                |       |       |       |       |       |       |        |       |       |       |       |       |       |       |       |       |       |       |       |       |   |  |
| r <sup>2</sup> =           | 0.747          | 0.662 | 0.560 | 0.496 | 0.560 | 0.687 | 0.897 | 0.094  | 0.101 | 0.060 | 0.296 | 0.104 | 0.473 | 0.502 | 0.258 | 0.150 | 0.206 | 0.350 | 0.234 | 0.387 | 0.690 |   |  |
| p <                        | 0.000          | 0.000 | 0.000 | 0.000 | 0.000 | 0.000 | 0.000 | 0.028  | 0.071 | 0.177 | 0.001 | 0.063 | 0.000 | 0.012 | 0.000 | 0.013 | 0.002 | 0.001 | 0.001 | 0.000 | 0.000 |   |  |

Table 2. Contribution of different pollutant compounds in an integrated impact on pine, birch and spruce crown defoliation  
 Note: F(a,b) - models identified by F - test symbol. Effect on the defoliation: + - relevance; - inverse when p<0.05.

Controversial results were obtained in explaining changes in the defoliation of birch trees. The highest correlation was detected between birch defoliation and N concentration in ground water, followed closely by  $\text{NO}_3^-$  concentration in the air and  $\text{NH}_4^+$  deposition. The results revealed that the indirect effect of N compounds through soil and ground water was more significant ( $r^2=0.355$ ) than the direct effect through the air ( $r^2=0.258$ ) (Table 2).

The detected very weak relationships between spruce defoliation and considered pollutants demonstrated no regular pattern. *Ips typographus* had significant impact on vitality of spruce trees over the considered period. Due to their activity about 2 % of the monitored spruce trees died annually. Maximal value was reached in 2002 - 4.5%.

Generalizing these results, we could state that in most cases, nitrates in soil and ground water have a positive effect on crown condition as does a higher value of pH of these waters, while ammonia has a negative effect. The indirect effect of sulphur compounds was less significant. However, its concentrations in surface water and runoff, which reflect chemical processes occurring in the ecosystem, reflected changes in tree crown defoliation rather well. Nonetheless, the direct effect of air concentration was more significant for pine crown defoliation than their indirect soil-mediated effect. Needles, which are present on trees all year round, seem to be more efficient aerosol collectors than leaves what was confirmed by other authors (Blood *et al.* 1989, Rothe *et al.* 2002). To test this hypothesis, analysis of the seasonal effect of considered pollutants on pine defoliation was performed.

#### **4.5 Seasonal variation of the effect of air pollution and acid deposition on pine defoliation**

The seasonal variation in air pollutant concentrations and acid deposition resulted in different significances of the relationships of the considered pollutants and pine stand defoliation. Despite a very high seasonal variation in monthly air concentrations of  $\text{SO}_2$  ( $p<0.05$ ) and  $\text{SO}_4^{2-}$  ( $p<0.05$ ), the relationships between the considered contaminants and defoliation of pine stands did not differ significantly. Over a two year period, correlation coefficients fluctuated between 0.5 and 0.7. The findings revealed that the integrated effect of monthly values of air concentrations of sulphur compounds did not explain pine defoliation variability more significantly than their annual values. Although all possible monthly effects of this air pollutant on pine defoliation over the two year period were accounted for, the explained portion of variation in pine stand mean defoliation increased by about only 10% ( $p>0.05$ ) (Augustaitis *et al.*, 2010a).

The most stable monthly air concentrations of  $\Sigma\text{NH}_4^+$  demonstrated rather stable effects on pine crown conditions during the entire year. In contrast, insignificant seasonal variation in  $\text{NH}_4^+$  deposition demonstrated the pronounced seasonal character of  $\text{NH}_4^+$  deposition effects on pine defoliation. Correlation coefficients fluctuated between 0.1 and 0.4 during vegetation and between 0.5 and 0.8 during dormant periods.

Analysis of the relationships derived from monthly values of  $\text{NO}_3^-$  (air concentrations or deposition) and pine defoliation revealed controversial results. High variations in monthly values resulted in the highest variation of the relationships. Correlation coefficients ranged from +0.4 indicating a negative effect during the dormant period to -0.2 indicating a positive effect during the vegetation. The integrated effects of the monthly values of  $\Sigma\text{NO}_3^-$  air concentrations in comparison with its mean annual values on pine stand mean defoliation increased the explained portion of pine defoliation variance by more than two times.

The variation in seasonal O<sub>3</sub> concentrations and its effect on pine defoliation demonstrated a very similar pattern, from positive in the January to May period, to negative in the June to November period; however, this effect was not significant in most cases ( $p > 0.05$ ). Obtained results confirmed our assumption that the negative effects of acidifying compounds could occur not only during vegetation but also during the dormant period, while the negative O<sub>3</sub> effect – only in summer and autumn. This is confirmed by the current state of knowledge in this field. Finally, we could conclude that the accounting for integrated effects of the considered pollutants was generally more significant than the effect of their annual value including ozone; this should be taken into account when investigating key factors resulting in changes in tree crown defoliation (Augustaitis et al., 2010a).

## 5. Effect of surface ozone on pine tree condition

Ambient ozone (O<sub>3</sub>) is considered to be one of the most important and pervasive phytotoxic agents whose effects are likely to increase in future (Krupa and Manning, 1988; Hutunnen et al., 2002; Percy et al., 2003; Vingarzan, 2004). However, too little is known about the effect of O<sub>3</sub> on tree growth on a regional scale, where its effects may be subtle and difficult to detect (Paoletti, 2006; Percy and Ferretti, 2004) and studies often fail despite using sophisticated statistically-based approaches (Muzika et al., 2004). Therefore, in this study we attempted to quantify O<sub>3</sub> contributions to the integrated impact of environmental factors on pine defoliation and stem growth by means of multiple regression analysis.

### 5.1 Contribution of the surface ozone effect on pine crown condition increment

Correlation between pine defoliation and stand density was found to be strongest ( $r = 0.38$ ), followed by a weaker negative correlation with stand volume ( $r = -0.23$ ) and age ( $r = -0.19$ ,  $p < 0.05$ ). Significant differences in defoliation were established among stands from different sites. The highest mean defoliation ( $36.4\% \pm 1.0$ ) was recorded on *Pinetum cladoniosum* forest type, the lowest on *Pinetum vaccinosum* FT ( $19.2\% \pm 0.2$ ) and *Pinetum oxalidosum* FT ( $19.6\% \pm 1.4$ ). These data revealed that stand and site parameters had significant effect on spatial distribution of pine defoliation (Augustaitis et al., 2007b). Integrated impact of these parameters accounted for more than 60% variation in defoliation:

$$F = 11.61 + 1.378 \times A - 0.169 \times \sum G + 0.012 \times N + 1.884 \times \text{FType}; R^2 = 0.610, p < 0.05 \quad (1)$$

F - crown defoliation, %; A - stand age, years;  $\sum G$  - sum of tree basal area, m<sup>2</sup> / ha;  
N - tree number, units/ha; FType - forest type (categorical value).

In order to meet the objectives of the present study, relationships between pine defoliation and pollution and meteorology were examined after the influences of site and stand parameters had been accounted. This procedure had not considerable effect on the level of significance of the relationships between defoliation residuals and meteorology, meanwhile resulted in a decrease in significance of the relationship between defoliation residuals and acidifying compounds from 1.5 times (air concentration) to 2 times (deposition), and increase in the significance of the relationship between defoliation residuals and peak O<sub>3</sub> concentrations from 0.315 to 0.439 (Fig. 13).

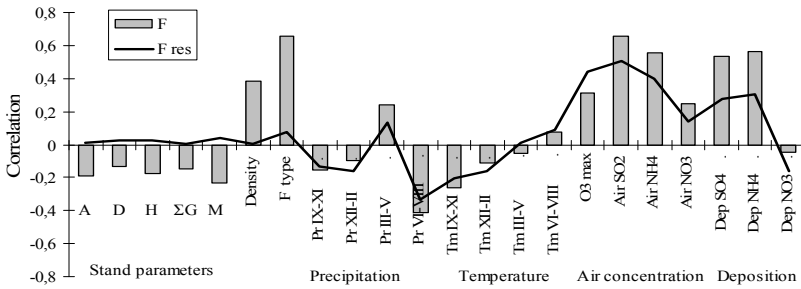


Fig. 13. Relationships between crown defoliation (F), its residuals (F\_res) and considered parameters of stand, pollution and meteorology

| Models, F(a,b)     |  | 1       | 2       | 3       | 4       | 5       | 6       | 7       | 8       | 9       |
|--------------------|--|---------|---------|---------|---------|---------|---------|---------|---------|---------|
| Variables          |  | (1.419) | (2.418) | (2.418) | (3.417) | (4.416) | (2.418) | (2.418) | (5.415) | (6.414) |
| In the air:        | SO <sub>2</sub>  | +       |         |         |         |         |         |         |         | +       |
|                    | NH <sub>4</sub> <sup>+</sup>                                 |         |         |         |         |         |         | +       |         |         |
|                    | NO <sub>3</sub> <sup>-</sup>                                 |         |         |         |         |         | +       |         |         |         |
| In precipitation:  | SO <sub>4</sub> <sup>2-</sup>                                |         | +       |         |         |         |         |         |         | +       |
|                    | NH <sub>4</sub> <sup>+</sup>                                 |         | +       |         |         |         |         |         |         |         |
|                    | NO <sub>3</sub> <sup>-</sup>                                 |         |         |         |         |         |         |         |         |         |
| Deposition:        | SO <sub>4</sub> <sup>2-</sup>                                |         |         | +       |         |         |         |         |         |         |
|                    | NH <sub>4</sub> <sup>+</sup>                                 |         |         |         |         |         |         | +       |         |         |
|                    | NO <sub>3</sub> <sup>-</sup>                                 |         |         | +       |         |         | +       |         |         |         |
| Precipitation:     | last season: IX-XI   |         |         |         |         |         |         |         |         |         |
|                    | XII-II   |         |         |         |         |         |         |         | +       | +       |
|                    | III-V  |         |         |         |         |         |         |         |         |         |
|                    | VI-VIII  |         |         |         | +       |         |         |         | +       | +       |
|                    | current season: IX-XI  |         |         |         | +       |         |         |         |         |         |
|                    | XII-II   |         |         |         |         |         |         |         |         |         |
| Temperature:       | last season: IX-XI   |         |         |         |         | +       |         |         |         |         |
|                    | XII-II   |         |         |         |         | +       |         |         | +       | +       |
|                    | III-V  |         |         |         |         |         |         |         |         |         |
|                    | VI-VIII  |         |         |         |         |         |         |         |         |         |
|                    | current season: IX-XI  |         |         |         |         | +       |         |         | +       |         |
|                    | XII-II   |         |         |         |         | +       |         |         |         |         |
| r <sup>2</sup> , % |  | 25.4    | 18.1    | 17.3    | 20.0    | 11.5    | 7.1     | 18.0    | 24.0    | 29.0    |
|                    | r <sup>2</sup> with O <sub>3</sub> effect, %                 | 27.7    | 26.1    | 23.2    | 25.7    | 22.9    | 19.5    | 25.8    | 26.7    | 29.9    |
|                    | O <sub>3</sub> effect (r <sup>2*</sup> - r <sup>2</sup> ), % | 2.4     | 8.0     | 5.9     | 5.7     | 11.4    | 12.4    | 7.8     | 2.7     | 1.0     |
|                    | O <sub>3</sub> significance: p<                              | 0.00    | 0.000   | 0.000   | 0.000   | 0.000   | 0.010   | 0.010   | 0.000   | 0.034   |

Table 3. Contribution of the ozone to integrated impact of different environmental factors on pine defoliation. Note: individual impact of O<sub>3</sub> on defoliation residual: r<sup>2</sup>=19.3% and p<0.0001.

Despite the statements that below the phytotoxic level no direct threat to vegetation from SO<sub>2</sub> (Bytnerowicz et al., 1998; Hjellbrekke, 1999) or synergetic interaction between SO<sub>2</sub> and O<sub>3</sub> could be expected (Krupa and Arndt, 1990), the presented data confirm our earlier findings that acidifying air compounds and their deposition are the key factors resulting in pine defoliation changes (Guderian, 1985; Takemoto et al., 2001). They could explain from 23–28% variance of residual defoliation of pine trees (Table 3). The effect of peak O<sub>3</sub> concentrations was less significant (19.3%), however, the presented data verified the statement that O<sub>3</sub> could reinforce their effects (Guderian, 1985; Takemoto et al., 2001). Ozone increased the explanation rate of defoliation residual variability by air concentration of acidifying species and their wet deposition by almost 3–8% (Augustaitis et al., 2007d).

Drought, especially during the vegetation period, is often mentioned as one of the key factors resulting in defoliation changes. However, there are contrary statements indicating that the effect of O<sub>3</sub> and drought might counterbalance each other (Zierl, 2002). Closed stomata protect foliage from the highest concentrations of O<sub>3</sub>. This contrary interaction could be explained by the fact that despite increase in O<sub>3</sub> concentrations from north towards south (Matyssek and Innes, 1999; Karlsson, 2002), O<sub>3</sub> exposure in northern latitudes often leads to plants becoming more susceptible to injury than in southern areas (Matyssek and Innes, 1999). Long, bright days and high humidity in air and soil are typical for the situation in large parts of the Nordic countries (Karlsson, 2002). The peak concentrations are typical in spring (Utrainen and Holopainen, 2000). Not very high air temperature, low vapor pressure deficits, and sufficient soil water supply is characteristic for this period. Therefore, in these areas, O<sub>3</sub> flux inside the leaves could be higher if compared with southern areas.

## 5.2 Contribution of the surface ozone effect on pine stem increment

Contribution of the ozone effect to the changes in residual increment was quantified after the influences of tree dendrometric parameters (age, diameter) and crown defoliation had been accounted for. Correlation between pine stem basal area increment (BAI) and crown defoliation was strongest ( $r=-0.512$ ), followed closely by positive correlation with tree diameter ( $r=0.382$ ), and a weaker negative correlation with stand age ( $r=-0.081$ ) (Fig. 14). Integrated impact of these parameters was analyzed by the means of multiregression model:

$$Zq = 7.330 - 0.189 \times F - 0.088 \times A + 0.50 \times D; R^2 = 0.795, p < 0.05 \quad (2)$$

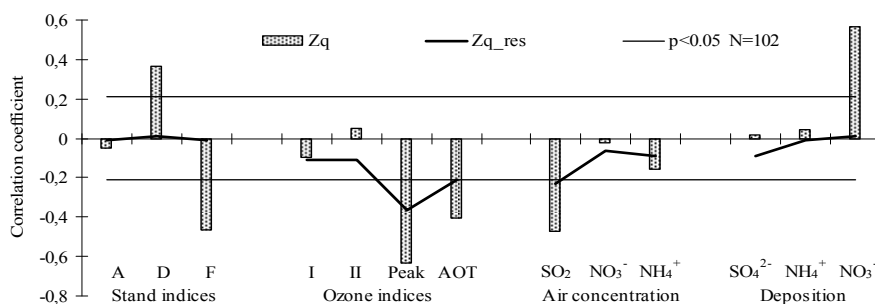


Fig. 14. Relationships between basal area increment ( $Zq$ ), its residuals ( $Zq_{res}$ ) and considered parameters of stand and pollution.

(I - mean value of ozone for April-August; II - annual mean value of ozone)

| Models, F(a,b)  | 1      | 2      | 3      | 4      | 5      | 6      | 7      | 8      | 9      |
|---|--------|--------|--------|--------|--------|--------|--------|--------|--------|
| Variables   | (3.98) | (3.98) | (3.98) | (4.97) | (4.97) | (2.99) | (4.97) | (4.97) | (8.93) |
| In the air:   |        |        |        |        |        |        |        |        |        |
| SO <sub>2</sub>   | +      |        |        | +      |        |        |        |        | -      |
| NH <sub>4</sub>   | -      |        |        |        | -      |        |        |        |        |
| NO <sub>3</sub>   | -      |        |        | +      | -      |        |        |        | +      |
| In precipitation:   |        |        |        |        |        |        |        |        |        |
| SO <sub>4</sub>   |        | -      |        |        |        |        |        |        |        |
| NH <sub>4</sub>   |        | -      |        |        | -      |        |        |        |        |
| NO <sub>3</sub>   |        | -      |        |        | -      |        |        |        |        |
| Deposition:   |        |        |        |        |        |        |        |        |        |
| SO <sub>4</sub>   |        |        | -      |        |        |        |        |        | +      |
| NH <sub>4</sub>   |        |        | -      | +      |        |        |        |        |        |
| NO <sub>3</sub>   |        |        | -      | +      |        |        |        |        | +      |
| Precipitation:  |        |        |        |        |        |        |        |        |        |
| last year:  |        |        |        |        |        |        |        |        |        |
| IX-XI   |        |        |        |        |        |        |        |        |        |
| XII-II  |        |        |        |        |        |        |        |        |        |
| current year:   |        |        |        |        |        |        |        |        |        |
| III-V   |        |        |        |        |        | -      |        | -      |        |
| VI-VIII   |        |        |        |        |        | -      |        | -      | -      |
| Temperature:  |        |        |        |        |        |        |        |        |        |
| last year:  |        |        |        |        |        |        |        |        |        |
| IX-XI   |        |        |        |        |        |        | +      | +      | +      |
| XII-II  |        |        |        |        |        |        | -      |        | -      |
| current year:   |        |        |        |        |        |        |        |        |        |
| III-V   |        |        |        |        |        |        | +      | +      |        |
| VI-VIII   |        |        |        |        |        |        | -      |        | -      |
| r <sup>2</sup> , %  | 6.3    | 0.4    | 2.5    | 18.5   | 0.7    | 0.2    | 7.7    | 10.2   | 21.7   |
| r <sup>2</sup> * with O <sub>3</sub> effect,%                 | 15.3   | 16.4   | 19.4   | 27.2   | 23.9   | 14.4   | 17.2   | 17.2   | 31.6   |
| O <sub>3</sub> effect (r <sup>2</sup> * - r <sup>2</sup> ), % | 9.0    | 16.0   | 16.9   | 8.7    | 23.2   | 14.2   | 9.5    | 7.0    | 9.9    |
| O <sub>3</sub> significance: p<                               | 0.002  | 0.000  | 0.000  | 0.001  | 0.000  | 0.000  | 0.001  | 0.005  | 0.000  |

Table 4. Contribution of ambient ozone to the integrated impact of different environmental factors on residual of pine stems basal area increment. Note: individual impact of O<sub>3</sub> on stem basal area increment residual: r<sup>2</sup>=13.3% and p<0.0002. Variables (+) - p<0.05 and (-) - p>0.05 in models.

Crown defoliation ( $F$ , %), tree age ( $A$ , years) and diameter ( $D$ , cm) accounted for 80% of spatial and temporal variability in pine stem BAI ( $Zq$ , cm<sup>2</sup>). Data on correlation analysis revealed the highest significance of the effect of peak ozone concentrations on BAI residuals ( $p < 0.001$ ) and the least - on acid deposition (Fig. 15). This procedure allowed elimination of the impact of the air concentration of the acidifying compounds and their deposition on BAI through the decrease in foliage thus verifying strong interaction of acid compounds with crown defoliation. These findings indicate a possible direct effect of ambient O<sub>3</sub> on changes in pine BAI, probably due to disturbances in CO<sub>2</sub> assimilation and carbohydrate movement within the trees. The elimination of the defoliation impact on tree increment by regression methods was a good example of an attempt to separate the effects of different pollutants, i.e., acidifying compounds and ambient O<sub>3</sub> (Table 4) (Augustaitis & Bytnerowicz, 2007d). Integrated impact of air acidifying compounds and their deposition accounted for 18.5% of variability in BAI residual. O<sub>3</sub> increased the degree of the explanation by 8.7% up to 27.2%. Integrated impact of meteorological parameters accounted for 10.2% of residuals variability, and O<sub>3</sub> increased this rate up to 17.2%. Integrated impact of air acidifying compounds, acid deposition and meteorological parameters accounted for up to 21% of variability in BAI residual. Ozone increased this rate of explanation by approximately 10% up to 31.6%.

Climate warming might have had an additional effect enhancing the phytotoxic O<sub>3</sub> effect on forest. Synergistic O<sub>3</sub> effects with high temperature and moisture stress are well known (McLoughlin & Downing, 1996). However, the statement that the effect of O<sub>3</sub> and drought might counterbalance each other (Zierl, 2002) is more significant when investigating phytotoxic O<sub>3</sub> effect on trees. Closed stomata protect foliage from the uptake of high O<sub>3</sub> concentrations into the leaves, which is typical of periods characterized by high temperature and moisture stress. Most likely therefore, the O<sub>3</sub> effect in northern latitudes (where moisture stress is less frequent) often leads to plants becoming more susceptible to injury than in southern areas, despite the increase in O<sub>3</sub> concentrations from North to South (Matyssek & Innes, 1999; Karlsson et al., 2002; Paoletti, 2006).

Data from the ICP IMS, where air pollutants have been continuously monitored offered a possibility to get closer insight into O<sub>3</sub> effect on tree growth. Peak O<sub>3</sub> concentration has more significant effect on tree defoliation and increment than other indices, such as AOT40, for vegetation and forest as well as mean O<sub>3</sub> concentrations for a vegetation period. Therefore, more thorough studies with continuous active monitors are needed, especially in the northern countries where O<sub>3</sub> concentrations seldom reach the level of toxicity. However, impact of ambient O<sub>3</sub> on native forest ecosystems could be higher than that in the southern countries where O<sub>3</sub> concentrations often exceed the phytotoxic level of the AOT index, but significant relations with tree damages fail (Paoletti, E. 2006).

Recent findings clearly show that O<sub>3</sub> exposure does not adequately characterize the potential for plant injury, because plant response is more closely related to the amount of O<sub>3</sub> absorbed into leaf tissue and modified by detoxification processes (effective flux) (Matyssek et al., 2007). Newly developed concepts based on O<sub>3</sub> flux into leaves require profound knowledge of physiological processes, e.g. of both stomatal functioning, which determines stress avoidance through the degree of opening, and of stress tolerance, which is determined by structural and physiological leaf differentiation and related capacities in primary and secondary metabolism (Paoletti et al., 2007). Therefore, a well-coordinated and enhanced international cooperation in various disciplines such as atmospheric chemistry, forestry, botany, entomology, soil science, and dendrochronology in various regions of Europe is recommended. Since climatic changes in the Baltic region manifest themselves by the earlier (up to 15 days) beginning of the growing season, when the levels of O<sub>3</sub> are high and plants have high stomatal conductance, a potential for phytotoxicity is much higher than in other parts of Europe where levels of ambient O<sub>3</sub> are higher, but frequently occurring droughts may prevent plants from taking up high levels of O<sub>3</sub>, thus reducing the risk of severe phytotoxic effects (Ferretti et al., 2007; Paoletti, 2006; Paoletti et al., 2007). In this context, the Baltic region seems to be a new and relevant European region for future studies on potential O<sub>3</sub> phytotoxicity and the evaluation of risk to temperate forest ecosystems.

Despite this, a new threat for forest ecosystem in Lithuania, changing climate, which occurs through the increase in precipitation amount during the vegetation period and mean monthly temperature from September to December, as well as a decrease in amount of precipitation during the dormant period, should mitigate the negative effect of acidifying compounds and enhance forest sustainability to unfavorable environmental factors, first of all expected increase in surface ozone concentration. Only in cases of extreme conditions such as heat and drought during the vegetation or hard frost in winter, the frequencies of which are too difficult to forecast, would not confirm our assumption.

## 6. Conclusions

The same detected character of changes in meteorology, surface ozone, acidifying species and pine defoliation, which from 1994 to 2001 changed towards decreasing of air pollution and improving of forest health, since 2001 adversely, indicated possible causative relationships among them. Air concentrations of  $\text{SO}_2$ , and  $\text{SO}_4^{2-}$  and  $\text{NH}_4^+$  deposition, as well as dormant period and vegetation precipitation and mean winter temperature were shown to be the key factors most significantly affecting changes in tree crown defoliation in Lithuania.

The acidifying compounds accounted for nearly 58% of the variance in pine defoliation. Meteorological factors increased the degree of explanation to 65%, and stand and site variables to 79%. Indirect effect of acid deposition and meteorological parameters was less pronounced, however they significantly increased explanation rate of pine crown defoliation up to 89%. Indirect effect of acidifying species on birch defoliation was more significant than the direct effect through the air on leaves what allows to state that needles, which are present on trees all year round, are more efficient aerosol collectors than leaves. The death of spruce trees due to *Ips typographus* L., prevented completion of this task.

Data revealed that  $\text{O}_3$  were among key pollutants that significantly affected tree condition in Lithuania. Correlation coefficient between temporal and spatial changes in the peak  $\text{O}_3$  concentrations and changes in mean defoliation of Scots pine trees where the AOT40 values are commonly below their phytotoxic levels was statistically significant. However, the significance was lower than it was between defoliation and the  $\text{SO}_2$  air concentration, approximately the same as between defoliation and the acidifying compounds in precipitation, acid deposition, and amount of precipitation, but considerably higher than between defoliation and mean air temperature. Contribution of peak  $\text{O}_3$  concentrations to the integrated impact of acidifying compounds and meteorological parameters on pine stem growth was found to be more significant than its contribution to the integrated impact of acidifying compounds and meteorological parameters on pine defoliation.

$\text{NH}_4^+$  air concentrations and its deposition, which show a the tendency to increase due to enhanced acidification processes in soil, with surface ozone could be the key threats to forest ecosystem in future. However, recent stable or downward tendencies in annual  $\text{SO}_2$  air concentrations,  $\text{SO}_4^{2-}$  and  $\text{NO}_3^-$  wet deposition, as well as an increase in precipitation amount over the vegetation following the increase in mean monthly temperature and decrease in precipitation from September to December, which represented the climate change condition, should mitigate negative effect of acidifying species and enhance resiliency to phytotoxic effect of surface ozone, ensuring sustainable development of Lithuanian forest under global environmental pressures.

## 7. Acknowledgements

The manuscript is supported by **Life Environment Project LIFE08 ENV/IT/000339**. Thanks are due to Dr Almantas Kliucius from the Lithuanian University of Agriculture for the help in the forest. The special thanks go to Dr Rasele Girgzdiene and Dr Dalia Sopauskiene from the Institute of Physics for providing data on environmental pollution. The author also thanks Ingrida Augustaitiene, who helped to prepare the manuscript.

## 8. References

- Alonso, R., Bytnerowicz, A. & Arbaugh, M. (2002). Vertical distribution of ozone and nitrogenous pollution in air quality class I area, the San Gorgonio Wilderness, Southern California. *TheScientificWorldJOURNAL* 2, 10-26.
- Augustaitis, A. (2003). Impact of regional pollution load on scots pine (*Pinus sylvestris* L.) tree condition. *Ekologia (Bratislava)*, 22: 30-41.
- Augustaitis, A., Augustaitiene, A., Kliucius, A., Bartkevicius, E., Mozgeris, G., Sopauskiene, D., Eitminaviciute, I., Arbaciauskas, K., Mazeikyte, R. & Bauziene, I. (2005). Impact of acidity components in the air and their deposition on biota in forest ecosystems. *Baltic Forestry*, 2, 84-93.
- Augustaitis, A., Augustaitiene, I., Kliucius, A., Mozgeris, G., Pivoras, G., Girgzdiene, R., Arbaciauskas, K., Eitminaviciute, I. & Mazeikyte, R. (2007a). Trend in ambient ozone and an attempt to detect its effect on biota in forest ecosystem. Step I of Lithuanian studies. *TheScientificWorldJOURNAL*, 7(S1), 37-46.
- Augustaitis, A., Augustaitiene, I., Kliucius, A., Girgzdiene, R. & Sopauskiene, D. (2007b). Contribution of ambient ozone to changes in Scots pine defoliation on territories under regional pollution. Step II of Lithuanian studies. *TheScientificWorldJOURNAL*, 7(S1), 47-57.
- Augustaitis, A., Augustaitiene, I., Cinga, G., Mazeika, J., Deltuvas, R., Juknys, R. & Vitas, A. (2007c). Did the ambient ozone affect stem increment of Scots pines (*Pinus sylvestris* L.) on territories under regional pollution load? Step III of Lithuanian studies. *TheScientificWorldJOURNAL*, 7(S1), 58-66.
- Augustaitis, A., Augustaitiene, I. & Deltuvas, R. (2007d). Scots pine (*Pinus sylvestris* L.) crown defoliation in relation to the acid deposition and meteorology in Lithuania. *Water, Air, and Soil Pollution*, 182, 335-348.
- Augustaitis, A., Augustaitiene, I., Kliucius, A., Pivoras, G., Bendoraičius, B., Šopauskienė, D., Jasinevičienė, D., Buzienė, I., Eitminaviciute, I., Arbačiauskas, K., Mažeikyte, R. (2008a). N deposition, balance and benefit in the forest ecosystem of main landscape types of Lithuania, *International Journal of Environmental Studies*, 65, 337-357.
- Augustaitis, A. & Bytnerowicz, A. (2008b). Contribution of ambient ozone to Scots pine defoliation and reduced growth in the Central European forests: a Lithuanian case study. *Environmental Pollution*, 155, 436-445.
- Augustaitis A., Augustaitienė I., Kliucius A., Pivoras, G., Šopauskienė D., Girgzdiene R. (2010a). The Seasonal Variability of Air Pollution Effects on Pine Conditions under Changing Climates. *European Journal of Forest Research*, (DOI 10.1007/s10342-009-0319-x).
- Augustaitis, A., Sopauskiene, D. & Bauziene, I. (2010b). Direct and Indirect Effects of Regional Air Pollution on Tree Crown Defoliation. *Baltic Forestry* (in press).
- Bytnerowicz, A., Fenn, M., Miller, P. & Arbaugh, M. (1998). Wet and dry pollutant deposition to the mixed conifer forest In *Oxidant Air Pollution Impacts in the Montane Forests of Southern California: The San Bernardino Mountains Case Study*. Miller, P.R. and McBride, J., Eds. Springer-Verlag Ecological Series, New York. Chap. 11.
- Bytnerowicz, A., Godzik, B., Grodzinska, K., Fraczek, W., Musselman, R., Manning, W., Badea, O., Popescu, F. & Fleischer, P. (2004). Ambient ozone in forests of the central and eastern European mountains. *Environment Pollution*, 130, 5-16.

- Bytnerowicz, A., Omasa, K. & Paoletti, E. (2007). Integrated effects of air pollution and climate change on forests: A northern hemisphere perspective. *Environment Pollution*, 147, 438-445.
- Chappelka, A.H. & Freer-Smith, P.H. (1995). Predisposition of trees by air pollutants to low temperatures and moisture stress. *Environmental Pollution*, 87, 105-117.
- Coyle, M., Fowler, D. & Ashmore, M. (2003). New directions: implications of increasing tropospheric background ozone concentrations for vegetation. *Atmos. Environment*, 37, 153-154.
- Cronan, C.S. & Grigal, D.F. (1995). Use of calcium/aluminium ratios as indicators of stress in forest ecosystems. *Journal of Environmental Quality*, 24, 209-226.
- De Vries, W., Klap, J. & Erisman, J.W. 2000a. Effects of environmental stress on forest crown condition in Europe. Part I: Hypotheses and approach to the study. *Water, Air, and Soil Pollution*, 119, 317-333.
- De Vries, W., Reinds, G.J., Klap, J., Leeuwen, E. & Erisman, J.W. (2000b). Effects of environmental stress on forest crown condition in Europe. Part III: estimation of critical deposition and concentration levels and their exceedances. *Water, Air, and Soil Pollution*, 119, 363-386.
- De Vries, W., Vel, E., Reinds, G. J., Deelstra, H., Klap, J. M., Leeters, E.E.J.M., Hendriks, C.M.A., Kerkvoorden, M., Landmann, G., Herkendell J., Haussmann, T. & Erisman, J. W. (2003). Intensive monitoring of forest ecosystems in Europe: 1. Objectives, set-up and evaluation strategy. *Forest ecology and management*, 174, 77-95.
- Fowler, D., Flechard, C., Skiba, U., Coyle, M., and Cape, J.N. (1998) The atmospheric budget of oxidized nitrogen and its role in ozone formation and deposition. *New Phytologist*, 139, 11-23.
- EMEP. (1977). Manual of sampling and chemical analysis, EMEP/CHEM 3/77. Norwegian Institute for Air Research.
- Fowler, D., Cape, N., Coyle, M., Flechard, C., Kuylenstierna, J., Hicks, K., Derwent, D., Johnson, C. & Stevenson, D. (1999). The global exposure of forest ecosystems to air pollution. *Water, Air, and Soil Pollution*, 116, 5-32.
- Fuhrer, J., Skärby, L. & Ashmore, M.R. (1997). Critical levels of ozone effects in Europe. *Environmental Pollution*, 97, 18-29.
- Ferretti, M., Bussotti, F., Calatayud, V., Schaub, M., Krauchi, N., Petriccione, B., Sanchez-Peña, G., Sanz, M.J. & Ulrich, E. (2007). Ozone and forests in South-Western Europe. *Environmental Pollution*, 145, 617-619.
- Fuhrer, F. (2000). Introduction to the special issue on ozone risk analysis for vegetation in Europe. *Environmental Pollution*, 109, 359-360.
- Girgzdiene, R., Bycenkiene, S. & Girgzdys, A. (2007). Variations and trends of AOT40 and ozone in the rural areas of Lithuania. *Environmental Monitoring and Assessment*, 127, (1-3), 327-335.
- Guderian, R. (1985). *Air Pollution by Photochemical Oxidants, Formation, Transport, Control and Effects on Plants*. Springer-Verlag, Berlin. 346 p.
- Hill, A.C., Heggstad, H.E., and Linzon, S.N. (1970). Ozone. In *Recognition of Air Pollution Injury to Vegetation: A Pictorial Atlas*. Jacobson, J.S. & Hill, A.C., Eds. Air Pollution Control Association, Pittsburgh, PA. B1-B6.

- IPCC. (2007). Climate change 2007. *The Physical Science Basis. Contribution of working group I to the fourth assessment report of the Intergovernmental Panel on Climate Change*. (In Solomon, S., et al. (eds.)). Cambridge University Press, Cambridge, UK and New York, NY, USA. <http://www.ipcc.ch/>
- Hjellbrekke, A.G. (1999). Ozone measurements 1997. In EMEP/CCC-Report, 2/99, 7-8.
- Hutunnen, S., Manninen, S. & Timonen, U. (2002). Ozone effects on forest vegetation in Europe. In Szaro, R.C., Bytnerowicz, A., Oszlanyi, J. (Eds.), *Effect of air pollution on forest health and biodiversity in forest of the Carpatian Mountains*. NATO Science Service, pp. 43-49.
- Kahle H.P. & Spiecker H. (1996). Adaptability of radial growth of Norway spruce to climate variations: results of a site specific dendroecological study in high elevations of the Black Forest (Germany). In Dean JS, Meko DM, Swetnam TW (Eds): *Tree Rings, Environment and Humanity: Proceedings of the International Conference: Tucson, Arizona, 17-21 May 1994*. Radiocarbon: 785-801.
- Karlsson, P.E., Tuovinen, J.-P., Simpson, D., Mikkelsen, T. & Ro-Poulsen, H. (2002). *Ozone Exposure Indices for ICP-Forest Observation Plots within the Nordic Countries*. IVL-rapport B1498. 54 p.
- Klap, J., Voshaar, J.O., Vries, W.D. & Erisman, J.W. (1997). Relation between crown condition and stress factors. In: Ch. Muller-Edzards, W. de Vries, and J.W. Erisman (eds.) *Ten Years of Monitoring Forest Condition in Europe. Studies on Temporal Development, Spatial Distribution and Impact of Natural and Anthropogenic Stress Factors*. UN-ECE pp. 277-298.
- Klap, J. M., Oude Voshaar, J. H., De Vries, W. & Erisman, J. W. (2000). Effects of Environmental Stress on Forest Crown Condition in Europe. Part IV: Statistical Analyses of Relationships. *Water, Air, and Soil Pollution*, 119, 387-420.
- Kozlovski, T.T., Kramer, P.J. & Pallardy, S.G. (1991). *The physiological ecology of woody plants*. Academic Press Inc., San Diego
- Krupa, S.V. & Arndt, U. (1990). The Hohenheim long-term experiment. Effects of ozone, sulphur dioxide and simulated acidic precipitation on tree species in a microcosm. *Environmental Pollution*, 68, 193-194.
- Krupa, S.V. & Manning, W.J. (1988). Atmospheric ozone: formation and effects on plants. *Environmental Pollution*, 50, 101-137.
- Lorenz, M. & Mues, V. (2007). Forest health status in Europe. *The ScientificWorld Journal*, 7 (S1), 22-27.
- LRTAB. (2004). LRTAB Mapping Manual. UNECE. <http://www.icpmapping.org> .
- Makinen, H., Nojd, P., Kahle, H.P., Neumann, U., Tveite, B. & Mielikainen, K. (2003). Radial growth of Norway spruce (*Picea abies* (L.) Karst.) across latitudinal and altitudinal gradients in central and northern Europe. *Forest Ecological Management*, 71, 243-259
- Manion, P.D. & Lachance, D. (1992). Forest decline concepts: an overview. In: P.D. Manion and D. Lachance (eds.), *Forest decline concepts*, St. Paul, Minnesota, USA, pp. 181-190.
- Manning, W. J. (2005). Establishing a cause and effect relationship for ambient ozone exposure and tree growth in the forest: progress and an experimental approach. *Environmental Pollution*, 137, 443-454.
- Matyssek, R. & Innes, J. L. (1999). Ozone - a risk factor for trees and forests in Europe? *Water Air Soil Pollut.* 116, 199-226.

- Matyssek, R., Wieser, G., Nunn, A.J., Löw, M., Then, C., Herbinger, K., Blumenroither, M., Jehnes, S., Reiter, I.M., Heerdt, C., Koch, N., Häberle, K.-H., Haberer, K., Werner, H., Tausz, M., Fabian, P., Rennenberg, H., Grill, D. & Oßwald, W. (2005). How sensitive are forest trees to ozone? - New research on an old issue, in: Omasa, K., Nouchi, I., De Kok, L.J. (Eds.), *Plant Responses to Air Pollution and Global Change*. Springer-Verlag, Tokyo, pp. 21-28.
- Matyssek, R., Bytnerowicz, A., Karlsson, P.-E., Paoletti, E., Sanz, M., Schaub, M. & Wieser, G. (2007). Promoting the O<sub>3</sub> flux concept for European forest trees. *Environmental Pollution*, 146, 587-607.
- McLoughlin, S.B. & Downing, D.J. (1996). Interactive effects of ambient ozone and climate measured on growth of mature loblolly pine trees. *Canadian Journal of Forest Research*, 26, 670-681.
- Muzika, R.M., Guyette, R.P., Zielonka, T. & Liebhold, A.M. (2004). The influence of O<sub>3</sub>, NO<sub>2</sub> and SO<sub>2</sub> on growth of *Picea abies* and *Fagus sylvatica* in the Carpathian Mountains. *Environmental Pollution*, 130, 65-71.
- NABEL. (1999). NABEL, Luftbelastung 1998. Herausgegeben vom Bundesamt für Umwelt, Wald und Landschaft (BUWAL), Bern. LRTAB (2004) LRTAB Mapping Manual. UNECE <http://www.icpmapping.org>.
- Neiryneck, L. & Roskams, P. (1999). Relationships between crown condition of beech (*Fagus sylvatica* L.) and through fall chemistry. *Water, Air, and Soil Pollution*, 116, 389-394.
- Paoletti, E. (2006). Impact of ozone on Mediterranean forests: A review. *Environmental Pollution*, 144, 463-474.
- Paoletti, E., Bytnerowicz, A., Andersen, C., Augustaitis, A., Ferretti, M., Grulke, N., Günthardt-Goerg, M.S., Innes, J., Johnson, D., Karnosky, D., Luangjame, J., Matyssek, R., McNulty, S., Müller-Starck, G., Musselman, R. & Percy, K. (2007). Impacts of air pollution and climate change on forest ecosystems – emerging research needs. *TheScientificWorldJOURNAL*, 7(S1), 1-8.
- Pell, E.J., Sinn, J.P., Brendley, B.W., Samuelson, L., Vinten-Johansen, C., Tien, M. & Skillman, J. (1999). Differential response of four tree species to ozone-induced acceleration of foliar senescence. *Plant, Cell and Environment*, 22, 779-790.
- Percy, K.E., Legge, A.H. & Krupa, S.W. (2003). Tropospheric ozone: a continuing threat to global forests? In: Karnosky, D.F., Percy, K.E., Chappelka, A.H., Simpson, C., Pikkariainen, J. (Eds.), *Air Pollution and Global Change and Forests in the New Millennium*. *Development in Environmental Science*, 3, 85-118.
- Percy, K.E. & Ferretti, M. (2004). Air pollution and forest health: toward new monitoring concepts. *Environmental Pollution*, 130, 113-126.
- Reich, P.B. (1987). Quantifying plant response to ozone: a unifying theory. *Tree Physiology* 3, 63-91.
- Roberts, T.M., Skeffington, R.A. & Blank, L.W. (1989). Causes of type 1 spruce decline in Europe. *Forestry* 62(3): 179-222.
- Rothe, A., Huber, C., Kreuzer, K. & Weis, W. (2002). Deposition and soil leaching in stands of Norway spruce and European Beech: Results from Höglwald research in comparison with other European case studies. *Plant Soil*, 240, 33-45.

- Ryerson, T.B., Trainer, M., Holloway, J.S., Parrish, D.D., Huey, L.G., Sueper, D.T., Frost, G.J., Donnelly, S.G., Schauffler, S., Atlas, E.S., Kustler, W.C., Goldan, P.D., Hübler, G., Meagher, J.F. & Feshenfeld, F.C. (2001). Observations of ozone formation in power plant plumes and implications for ozone control strategies. *Science*, 292, 719-723.
- Sandermann, H. J. (1996). Ozone and Plant Health. *Annual Review of Phytopathology*, 34 347-366
- Schmieden, U. & Wild, A. (1995). The contribution of ozone to forest decline. *Physiology of Plant*, 94, 371-378.
- Schulze, E.D. (1989). Air pollution and forest decline in a spruce (*Picea abies*) forest. *Science*, 244: 776-783.
- Smith, W. (1981). *Air Pollution and Forests*. Springer-Verlag, New York. 379 p.
- Solberg, S., Derwent, R.G., Hov, O., Langner, J. & Lindskog, A. (2005). European abatement of surface ozone in a global perspective. *Ambio*, 34, 47-53.
- Sopauskiene, D., Jasineviciene, D. & Stapcinskaite, S. (2001). The effect of changes in European anthropogenic emissions on the concentrations of sulphur and nitrogen components in air and precipitation in Lithuania. *Water, Air, and Soil Pollution*, 130, 517-522.
- Sopauskiene, D. & Jasineviciene, D. (2006). Changes in precipitation chemistry in Lithuania for 1981-2004. *Journal of Environmental Monitoring*, 8, 347-352.
- Takemoto, B.K., Bytnerowicz, A. & Fenn, M.E. (2001). Current and future effects of ozone and atmospheric nitrogen deposition on California's mixed conifer forests. *Forest Ecological Management*, 144, 159-173.
- UN-ECE. (1994). *Manual on methods and Criteria for Harmonised Sampling, Assessment, Monitoring and Analysis of the Effects of Air Pollution on Forests*. ICP. 178 pp.
- UN-ECE. (1993). *Manual for Integrated Monitoring Programme Phase 1993-1996*. *Environmental Report 5*. Helsinki Environmental Data Centre. National Board of Waters and the Environment.
- UN-ECE. (2005). *The Condition of Forests in Europe 2005*. Executive Report, Federal Research Centre for Forestry and Forest Products (BFH), Geneva, 34 pp.
- Utrainen, J. & Holopainen, T., 2000. Impact of increased springtime O<sub>3</sub> exposure on Scots pine (*Pinus sylvestris*) seedlings in central Finland. *Environmental Pollution*, 109, 479-487.
- Vingarzan, R. (2004). A review of surface ozone background levels and trends. *Atmospheric Environment*, 38, 3431-3442.
- WMO. (1983). *Guide of Meteorological Practices*. 2nd edition WMO-No. 100. Geneva.
- Wright, R.F., Larssen, T., Camarero, L., Cosby, B.J., Ferrier, R., Helliwell, R., Forsius, M., Jenkins, A., Kopaček, J., Moldov, F., Posch, M., Rogora, M. & Schopp, W. (2005). Recovery of acidified European surface waters. *Environment science & technology*, 1, 64-72.
- Zierl, B. (2002). Relations between crown condition and ozone and its dependence on environmental factors. *Environment Pollution*, 119, 55-68.



# Ozone pollution and its bioindication

Vanda Villányi<sup>1</sup>, Boris Turk<sup>2</sup>, Franc Batic<sup>2</sup> and Zsolt Csintalan<sup>1</sup>

<sup>1</sup>*Szent István University, Institute of Botany and Ecophysiology, Gödöllő, Hungary*

<sup>2</sup>*University of Ljubljana, Biotechnical Faculty, Department of Agronomy, Ljubljana, Slovenia*

## 1. Introduction

Triplet oxygen is a highly reactive molecule. Naturally it arises in the stratosphere, but it can as well develop through the chain reactions of photochemical smog in the troposphere. Photochemical smog occurs in highly polluted urban and industrial areas in the presence of high solar radiation. Ozone develops in the reaction of oxygen molecules with the singlet oxygen splitting off from nitrogen-oxides in the presence of UV-radiation. This reaction is quick and reversible, so the formation and degradation of ozone show steady-state balance (Crutzen et al., 1994). However, if there are hydrocarbons emitted in the atmosphere of a certain area, these will change the chemical reactions, interfering ozone to transform back to oxygen molecules. Thus, the quantity of ozone serves information about the quality and the components of photochemical smog. If nitrogen-oxides overweigh, after reacting with them, ozone dissolves again. Therefore in many cases the concentration of tropospheric ozone increases far away from the most polluted areas. Volatile organic compounds can also cause imbalance resulting ozone accumulation. Ozone and its precursors can float hundreds of kilometers from their sources and its formation often happens only during its moving with air masses. Since there are less chemical reagents by which its dissolution takes place far from the cities, the amount of ozone above cities is relatively small while passing away from urban areas this amount is gradually growing. Thus, ozone virtually originating from cities endangers natural vegetation and cultivated plants (Lorenzini and Saitanis, 2003).

Ozone effects cultivated plants in a short-term as well as in a long-term way. Visible symptoms and impairment of the photosynthetic efficiency can be named as short-term effects, while in a long term, in particular when high ozone concentrations frequently occur, it causes decrease in growth and yield, and leads to premature senescence. (Harmens et al., 2006).

The significance of ozone pollution and its effects has been clearly verified by several studies:

Ozone concentrations exceed the phytotoxic thresholds specified by the European Council all over Europe, and this amount grows by 5-20% per year (Sandermann et al., 1998).

Ozone reduces crop yield and biomass of sensitive species, and affects the crop quality (Hayes et al, 2007).

Based on the ozone levels of the year 2000, ozone induced yield losses for 23 crops in 47 European countries were estimated to be €6,7 billion per year (Holland et al., 2006).

Ozone reduces plant's Net Primary Production and the Net C Exchange thus increasing the C losses from different cropping systems; increases CO<sub>2</sub> emissions, crop nitrate loss and groundwater nitrate pollution. Several natural plant communities proved to be potentially ozone-sensitive (Mills et al., 2007). In natural ecosystems, in addition to the above mentioned effects, ozone can change the species composition causing similar changes in animal species composition as well (Fagnano and Maggio, 2008). Thus, detection of phytotoxic levels of ozone and examination of its effects on sensitive plant species is highly important in economical as well as in environmental regards.

## 2. Ozone in the troposphere

### 2.1 Formation of ozone

The short wave radiation of solar spectrum is entirely absorbed by stratospheric ozone and molecular oxygen. The infrared part of the spectrum is mostly absorbed by water vapour and carbon dioxide and some other greenhouse gases. Photochemistry in the troposphere is therefore driven by radiation with wavelengths between 300 and 600 nm (Seinfeld and Pandis, 1998).

Photooxidants are compounds formed by the oxidation processes of tropospheric gas phase chemistry. They include ozone and other compounds such as HNO<sub>3</sub>, PAN and aldehydes.

Gas phase chemistry in the troposphere (as well as in the stratosphere) includes a variety of reactions that can be viewed as the reactions of a radical reaction chain which consists of the following type of reactions:

1. Initiation reactions: Photolysis of certain molecules (ozone, HCHO, HONO, NO<sub>2</sub>), producing reactive radicals (O, OH, HO<sub>2</sub>). HO<sub>2</sub> is also converted to OH, which is very reactive, oxidizing most gaseous (reactive) compounds. Thus, OH radicals determine the oxidation capacity of the troposphere, and they are called as the „cleansing agent“ of the troposphere.
2. Propagation or radical chain: The very reactive radicals produced by the initiation reactions react with most molecules, causing sequences of radical reactions in which the same radicals are formed again, leading to a radical chain, e.g. one chlorine radical formed from one CFC<sub>3</sub> depletes not only one O<sub>3</sub> but many O<sub>3</sub> molecules since Cl is reformed by the reaction of ClO with O.
3. Termination: If two radicals react with each other, less reactive non radical species can be formed. These reactions stop the radical chain.

(The molecules formed in the termination reactions can be activated again or different radical chains can interact with each other.)

There are two (connected) types of radical chains in tropospheric gas phase chemistry:

1. The NO<sub>x</sub> radical chain includes no initiation reaction. The nitrogen oxides (NO<sub>x</sub>: NO + NO<sub>2</sub>) enter the system mainly by emissions from fuel combustion. NO<sub>2</sub> is the precursor of tropospheric ozone.
2. The members of the RO<sub>x</sub>/HO<sub>x</sub> radical chain reaction system are produced by photolysis.

These two radical chains are connected.

The radical yield of the reaction system is limited by the termination reaction which can include  $\text{RO}_2$  and/or  $\text{HO}_2$  radicals (forming peroxides), or  $\text{OH}$  and  $\text{NO}_2$  (forming  $\text{HNO}_3$ ). This latter termination reaction links the  $\text{NO}_x$  and the  $\text{RO}_x$  radical chains. This kind of termination is more important in strongly polluted air.

The oxygen atoms produced by the photolysis of  $\text{NO}_2$  react very quickly with molecular oxygen, forming ozone. Ozone in turn reacts very quickly with  $\text{NO}$  to form  $\text{NO}_2$  again. During sunlight these reactions form equilibrium called photostationary state, and this state is reached within minutes.

There is no net  $\text{O}_3$  production in the photostationary state.

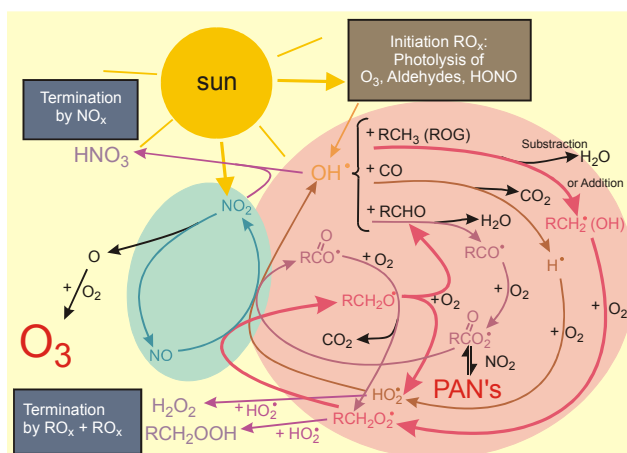
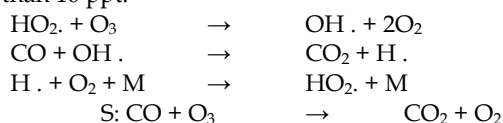


Fig 1. Overview of photochemistry in the polluted planetary boundary layer (from Staehelin et al., 2000)

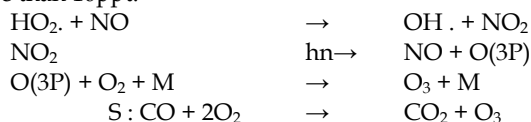
In case of very low  $\text{NO}_x$  concentrations ozone is chemically destroyed.

$\text{NO}$  less than 10 ppt:



Typically,  $\text{NO}$  concentrations need to be larger than around 10 ppt for the dominance of the reaction of  $\text{HO}_2$  with  $\text{NO}$  leading to  $\text{O}_3$ .

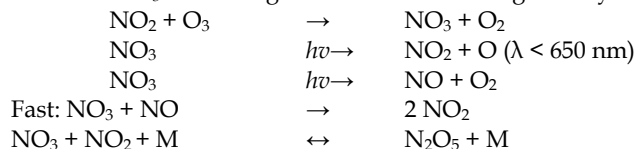
$\text{NO}$  more than 10ppt:



The dominance of the reaction channel of  $\text{HO}_2$  depends on  $\text{NO}$  as well as on  $\text{O}_3$  concentrations.

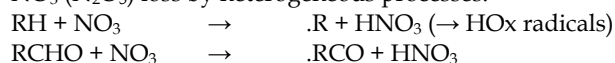
Organic chemistry in the troposphere is very complex (e.g. the reaction of alkenes with  $O_3$  is an additional source of HOx). Precursors of ozone ( $NO_x$ , Volatile Organic Compounds and CO) can be of anthropogenic or biogenic origin.

$NO_3$  is produced from reaction of  $NO_2$  with  $O_3$ . This reaction also proceeds during day, but  $NO_3$  is rapidly photolysed because of its strong absorption in the visible spectrum and therefore  $NO_3$  is not a significant oxidant during the day.



In the absence of sunlight, e.g. during night, no photolysis reactions take place. However, some gas phase oxidation still can proceed via the  $NO_3$  radical.

$NO_3$  ( $N_2O_5$ ) loss by heterogeneous processes:



During night,  $NO_3$  is a strong oxidant reacting with some organic compounds in a similar way as OH radicals, but only with specific compounds.  $NO_3$  quickly reacts with NO and  $NO_2$  which limits  $NO_3$  concentrations.

Thus, the main oxidant agent in the presence of solar radiation is OH (its concentration strongly depends on pollution level, but it is around  $10^6 \text{ cm}^{-3}$ ). In absence of solar radiation, main oxidant is  $NO_3$  (concentrations move around  $5 \times 10^8 \text{ cm}^{-3}$ ).

A few compounds (e.g. some reactive alkenes) can be oxidized by  $O_3$  (with mean concentration approximately of  $10^{12} \text{ cm}^{-3}$ ) both during day and night, but only under specific conditions.

Typical sequence of chemical regimes of an air parcel loaded by ozone precursors:

1. Photostationary state: decrease in ozone by reaction with NO.
2. VOC-limitation:  $O_3$  production increases with increasing VOC concentrations. In urban environments  $NO_2$  concentrations are usually that large that  $HNO_3$  formation dominates the reactions of OH radicals, which implies that local  $O_3$  production is small.
3. Transition regime: maximum ozone production. When  $NO_x$  concentration is decreasing steadily the mixture of organic vs.  $NO_x$  concentration passes through a state in which the ratio of ozone precursor concentration is such that local  $O_3$  production maximizes.
4.  $NO_x$ -limitation: When  $NO_x$  concentration is decreasing further, local  $O_3$  production rate becomes limited by the availability of  $NO_x$ . Such conditions usually occur in rural environments.
5. Ozone destruction

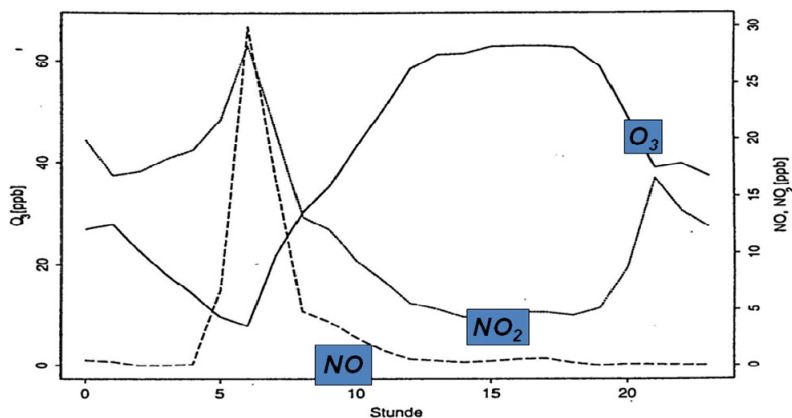


Fig. 2. Diurnal variation of trace gas concentrations at an urban site close to traffic emissions (NABEL station Dübendorf, mean of hourly mean values 18.-12. July, 1996):

- During night an inversion layer inhibits vertical mixing, and the primary air pollutants are emitted from ground below this layer.
- Ozone concentrations decrease during night because of the reaction of NO and O<sub>3</sub> and dry deposition. At this measuring site NO is steadily released from a close traffic source.
- After midnight, the reaction of NO with O<sub>3</sub> yields an increase in NO<sub>2</sub> concentration (traffic dominantly emits NO<sub>x</sub> as NO).
- Early in the morning, the close traffic emissions lead to a NO<sub>x</sub> maximum and NO increases as well (O<sub>3</sub> concentrations are very small this time).
- Later in the morning the inversion layer breaks, leading to the dilution of primary pollutants and the mixing down of O<sub>3</sub> from the layer lying above. Thus, NO<sub>x</sub> decreases while O<sub>3</sub> increases (chemical transformations are not important compared to mixing in this phase).
- Around 20h the inversion layer forms again and the destruction of O<sub>3</sub> by NO begins.

The layer above the nocturnal inversion layer is called reservoir layer. The reservoir layer (which constitutes a part of the planetary boundary layer) is decoupled from the inversion layer. In this layer, O<sub>3</sub> cannot be decomposed because NO emitted from surface is trapped below the inversion layer. Ozone (and other photooxidants) in the reservoir layer can be transported over large distances during night in summer smog episodes. Vertical mixing between the planetary boundary layer efficiently occurs during advective (smog) or convective (in summer) weather conditions.

Photocemistry of polluted air masses is exhaustively discussed by Steahelin et al., 2000.

## 2.2 Surface ozone concentrations, its measurements and trends

Ozone concentrations recorded in rural areas are higher than those in the city (Gregg et al., 2003). The main reasons of this phenomenon are the following:

- Since ozone is not a directly emitted pollutant, a considerable fraction of it is formed far away from its precursor sources.
- Nitrogen oxides leading to ozone depletion in the city's polluted atmosphere.
- In rural areas, biogenic VOCs (hydrocarbons and other organic trace gases) may contribute to ozone formation.

Daily maximum ozone values occur around midday, yearly peaks are at spring (during May) in the Northern Hemisphere while in the Mediterranean, the highest concentrations occur from June to August (Paoletti, 2006).

Sources of background O<sub>3</sub>:

- Transport from stratosphere
- Local ozone production through NO<sub>x</sub> reactions with methane above wetlands. NO<sub>x</sub> sources in this case are flashes of lightning, soil emissions and downward transport from stratosphere.
- Local ozone production through NO<sub>x</sub> reactions with biogenic VOCs.
- Long-range transport of polluted air masses.

Higher sites have atmosphere with higher ozone values, because lack of significant air mixing and higher transport of stratospheric ozone (Paoletti, 2007).

In the Northern Hemisphere, annual average ozone concentrations range between 20 and 45 ppb. By the year 2100, values are predicted to be between 42 and 84 ppb (Vingarzan, 2004).

Over the past three decades, background levels have been rising by 0.5-2% per year (Midgley et al, 2002). Although peak values are generally decreasing (Midgley et al, 2002) background values, that are increasing, have a larger impact on vegetation (Grennfelt, 2004).

Although already Schönbein, the discoverer of ozone (Schönbein 1844) developed a method in 1842 to show that O<sub>3</sub> is present in ambient air, this type of method is (quantitatively) not reliable. (At the time, mean values were about 10 ppb (Anfossi and Sandroni, 1994).) For the detection of ozone, Schönbein used impregnated papers which change color when exposed to ozone. This method was widely used in the 19th century.

From 1876 to 1911 ozone was measured by a chemical method using arsenite in the observatory of Montsouris. However, this method is susceptible to interference with sulfur dioxide and the representativeness of the measurements with respect to local influences is also questionable.

Around the end of World War II it was discovered that ozone could be produced in the troposphere by photochemical air pollution (Haagen-Smith, 1952).

In the 1930s, single measurements of O<sub>3</sub> close to Earth's surface were performed by (open path) spectroscopy. (Compared with this earlier measurements, ozone values measured at the same site in the period of 1989-1991 show more than a twofold increase.)

Chemical measurements have been widely used until the 1970s. Ozone measured by this method is also affected by interference with SO<sub>2</sub>, and therefore only background measurements are sufficient for trend analysis (Staehelin et al. 1994). This method using electrochemical detection is applied for ozone profile measurements from light balloons (ozone sondes). A network of ozone sonde stations has been operating since the late 1960s providing a unique data set to document long-term tropospheric ozone changes (e.g., Logan et al. 1994). Different sensors have been developed over time (showing systematic

differences). The quality of the data gained from old ozone sonde measurements is not reliable.

O<sub>3</sub> measurements were made in the 1950s at the Alpine village Arosa and several places in the north of the Alps. Comparison of these results with the results of measurements made in the period of 1989-1991 confirms that ozone values doubled during these 40 years all over Europe. Similar changes have been demonstrated in ozone concentrations in the marine boundary layer in the West coast of North America and Mace Head (West coast of Ireland), and at Montsouris, which is close to Paris.

This increase in background ozone concentrations in this period is probably caused by a significant increase in ozone precursor emissions in the decades following World War II.

Measurements of the European ozone sonde stations show large increases in free tropospheric ozone from the early 1970s to the 1990s (5-25% per decade during 1970-1996 Logan et al. 1994).

Today it is well known that high ozone concentrations occur all over the world.

Reliable ozone measurements can be obtained by UV absorption using the Hg emission line at 253.7 nm. This method is nowadays commonly used in ozone monitoring (e.g., Klausen et al. 2003). Data from continuous ozone measurements are available from an increasing number of stations, but that data are not every time useful for long-term trend analysis from remote sites. The method is also used to measure ozone from air planes, as well as from ships. The extended datasets provided by the MOZAIC (Measurement of Ozone and Water Vapour by Airbus In-Service Aircraft) and the earlier GASP program (Global Atmospheric Sampling Program, 1975-1979) are valuable for trend analysis.

Ozone is a precursor of OH-radical which limits the tropospheric lifetimes of many important gaseous species such as methane. Ozone is also an important greenhouse gas: its increase has significantly contributed to changes in radiative forcing. Determining this anthropogenic radiative forcing by tropospheric ozone is difficult, since its complex formation reactions need to be described by complex numerical simulations of the tropospheric ozone cycle.

To understand tropospheric ozone trends, they need to be compared with changes in anthropogenic ozone precursor emissions. Emission models rely on the description of anthropogenic activities leading to emission factors that describe the type of technology. Emissions of society depend on economy, and due to economic growth, all emission models show large increases in the period following World War II. Due to the abatement legislation, anthropogenic emissions of developed countries stabilized and decreased after the 1980s, while the emissions of developing countries still increased during the 1990s (Stahelin and Poberaj, 2008). However, different emission models show considerable differences demonstrating uncertainties in data processing.

Since 1992, ozone concentrations measured at high mountain sites in the northern extratropics, have increased further (Brönnimann et al. 2002). Since anthropogenic ozone precursor emissions have decreased in Europe and North America since the early 1990s, these increases are difficult to explain. Within the MOZAIC project ozone has been continuously measured since 1994. These measurements show a considerable increase in upper tropospheric and lower stratospheric ozone which extends over much of the northern extratropics (Thouret et al. 2006).

A similar increase in ozone concentrations has been found at Mace Head, a station at the west coast of Ireland (Simmonds et al. 2005). All measurements support that ozone trends

are most pronounced in winter. Ozone sonde measurements in Europe do not accord with the data showing these increases, possibly because limitations in data quality (Ordóñez 2006).

As discussed in the literature (Staehelin and Poberaj, 2008), different causes for this remarkable increase can be:

- effects of more frequent biomass burning
- changes in transport of air masses over the Atlantic in association with changes of the North Atlantic Oscillation (and Arctic Oscillation)
- influence of the strongly increasing emissions from South East Asia
- changes in the transport of ozone from the stratosphere

Indeed, during the 1990s, ozone substantially increased in the lowermost stratosphere at northern midlatitudes. Strong correlations have been showed between the ozone anomalies in the lowermost stratosphere and ozone concentrations measured at three European high mountain stations in the 1990s (Ordóñez et al. 2007). There are several data from all over the world, with temporal trends which are difficult to explain by changes in anthropogenic ozone precursor emissions. This temporal change in upper tropospheric ozone was similar to the changes observed in the lowermost stratosphere (Staehelin and Poberaj, 2008).

These facts suggest that long-term tropospheric ozone trends are considerably influenced by changes in ozone in the lowermost stratosphere (Tarasick et al. 2005; Ordóñez et al. 2007). Probably, there is a major contribution of an increased flux of ozone from the stratosphere to the troposphere to the 1990's increase in Europe's background ozone concentrations.

However, present chemical transport models have problems to adequately describe the influence of stratosphere-troposphere exchange.

In the tropics, upward trends were reported from long-term measurements from ship cruises over the Atlantic for 1978-2004. In the measurements of the MOSAIC project (starting in 1994), twice as large increases have been found for the free tropical troposphere over the Atlantic. In both case, these large increases were attributed to increasing fossil-fuel emissions in the Atlantic regions.

Surface-ozone measurements from Hawaii (starting in 1974) and ozone sonde measurements from Hilo (starting in 1982) show moderate increases. Data analysis provided evidence that similarly to the northern extratropics, the most probably primary cause of this increase is the change in the origin of air (Oltmans et al. 2006).

In the southern extratropics, ship measurements also show upward near-surface trends in the Southern midlatitude Atlantic region, although these trends are less pronounced than in the tropics. The only available sonde station in New Zealand shows a continued increase in the middle troposphere since 1986, which is qualitatively similar to the surface ozone increase reported from the long-term stations Cape Grim (Australia) and Cape Point (South Africa). Interestingly, the temporal evolution of surface ozone concentration at the South Pole shows a continuous decrease between the middle of the 1970s and the middle of the 1990s. This decrease is later followed by an increase (Staehelin and Poberaj, 2008).

However, according to recent studies, in the Arctic, there are special processes that evaluate ozone concentrations.

Because of the lack of available reliable long-term measurements, it seems premature to draw overall conclusions for the tropical regions as well as the southern midlatitudes (Staehelin and Poberaj, 2008).

Increases in ozone levels in the future are predicted to be larger in developing countries (Naja and Akimoto 2004; The Royal Society, 2008).

### 3. Phytotoxic effects of ozone

Current tropospheric O<sub>3</sub> concentrations are considered a toxic threat to vegetation (Ashmore, 2005).

Based on ozone emissions of the year 2000, ozone-induced crop yield loss for 23 crops was estimated to be around €6.7 billion per year (Harmens et al., 2006).

A database named OZOVEG (Ozone effects on vegetation) was established based on data collated from over 60 papers. On the grounds of this database, a model was developed that uses Ellenberg light and salinity values (Ellenberg et al., 1991) for predicting ozone sensitivity of particular species as well as of whole plant communities.

Using the European Nature Information System (EUNIS) Dry grasslands, Mesic grasslands, Seasonally-wet and wet grasslands, Woodland fringes, Alpine and subalpine grasslands and Temperate shrub heathlands were identified as potentially ozone sensitive.

Studies made to better understanding (Harmens and Mills, 2005)(Harmens et al., 2006) concluded that the response of vegetation to ozone and climate change is driven by complex interactions between several abiotic and biotic factors and making predictions is difficult (Harmens et al., 2006). There is a clear need for an approach that combines drivers when examining vegetation response to climate change. Long-term multifactorial field experiments and modelling that takes into account several climate change factors should be made.

The estimation of cause-effect relationships has to be more adequate when based on the amount of ozone entering the leaf tissues instead of being based on the amount of ozone present in ambient air (Ashmore et al., 2004).

Stomatal ozone uptake (flux-based approach) is modelled on the basis of maximum stomatal conductance values, taking into account the effects of several climatic and environmental parameters. Comparing with the concentration-based approach (Paoletti and Manning 2007), it is more precise since it includes environmental conditions that affect plant's ozone response. However, flux-based methods are species-specific, with the need of parametrisation for every particular investigated species (Paoletti et al, 2007). Considering estimations with the flux-based approach, risks are shown to be slightly lower (Baumgarten et al., 2009). Flux-based indices are considered to be more appropriate than exposure-based indices (Karlsson et al., 2009 Fredericksen et al., 1996; Karlsson et al., 2003; Matyssek et al., 2004; Pleijel et al., 2004).

The latest approach is the usage of dose-response models. This approach also needs parametrisation for certain species (Fernandez et al., 2010; Calvo et al., 2010).

The phytotoxic effect of ozone is commonly introduced through a description of stomatal behaviour based on plant's transpiration (Baldocchi et al., 1987; Meyers et al., 1998; Simpson et al., 2003). However, the contribution of non-stomatal sinks to the total ozone removal at the canopy scale can be on the order of 50% - 70%.

Also, at the shoot scale, several measurements revealed depositions exceeding the predictions based on the stomatal uptake (Rondón et al., 1993; Altimir et al., 2004) (van Hove et al., 1999). This non-stomatal deposition is a major unknown in present understanding of gas-exchange, which compiles heterogeneous chemical processes. These

processes can be reactions between ozone and Volatile Organic Compounds or nitrogen oxides emitted by the soil (Duyzer et al., 1983; Pilegaard, 2001)(Kurpius and Goldstein, 2003; Goldstein et al., 2004; Mikkelsen et al., 2000). Foliage surfaces can also sustain ozone removal through photochemical reactions or thermal decomposition of ozone on the leaf surface (Rondón et al. 1993; Coe et al. 1995; Fowler et al. 2001). Wetness of foliar surfaces and its relationship with deposition of gases has been discussed in many studies (Massman, 2004; Brewer and Smith, 1997). The foliage surface's ozone removal processes, such as scavenging reactions (in addition to stomatal uptake) are possibly controlled by several environmental factors, but it is difficult to determine the most important among these factors.

According to a study made on Scotch pine shoots and canopy in Finland (Altimir et al., 2005), ozone total deposition enhances when moist conditions occur. During moist conditions, only half of the measured ozone removal is attributable to the stomatal deposition at the shoot scale. This proportion is much higher in case of dry conditions. Among several analysed environmental factors, relative humidity was found to show the clearest correspondence with the estimated non-stomatal sink. However, this correspondence was only present when relative humidity was higher than 70%, a threshold at which surface moisture gathers at the foliage surface. This suggests that the non-stomatal sink is modulated by the foliage surface films. Moisture plays an enhancing role of ozone deposition. A part of the flux can only be explained by moisture film formation at the foliage surface. Total deposition, as well as the estimated non-stomatal deposition corresponds with *RH* rather than with temperature, at least when *RH* is over 60-70%. Thus, the portion of ozone deposition that the stomatal uptake cannot account for is related to the ambient *RH*. Possible explanation of this phenomenon is that ozone reacts with the liquid films on the foliage surface.

There is a not negligible contribution of nocturnal ozone uptake, which is often assumed to be zero during estimates of ozone uptake. Stomatal closure can be incomplete at night, even if discussing C3 plants. In addition, the enhancing effect of *RH* is more prominent at night.

According to several studies, forestal ecosystems are at risk (Paoletti, 2007 Baumgarten et al., 2009, Paoletti et al., 2007), being the thresholds of both flux-based and exposure-based O<sub>3</sub> indices are already exceeded and estimated to increase further in the future. Based on observed biomass losses and changes in ecosystem carbon-balance impairment carbon-sink strength of the forests of the Northern Hemisphere is found to be reduced by ambient ozone levels, and this reduction is predicted to be more serious in the future (Witting et al., 2009). Visible ozone injuries were observed in 55% of 67 forestal monitoring sites in an European ozone monitoring experiment (ICP Forests)(Lorenz et al., 2005). Direct ozone effects have been estimated to reduce forest productivity by 1-10% (Chappelka and Samuelson, 1998).

In a subalpine grassland ecosystem, respiration rates and gross primary production decreased under elevated O<sub>3</sub>. The 8% O<sub>3</sub> effect on GPP indicated impairment of the photosynthetic system. However, this decrease did not alter seasonal C balance. The reason is that in this ecosystem most of the biomass is in belowground, providing stable resource of new photosynthetic canopy (Volk et al., 2010).

In a long-term experiment in Lithuania, strong positive correlation was found between AOT40 (accumulated doses over 40ppb) values and defoliation of *Fraxinus excelsior* as well as the proportion of healthy individuals of several investigated tree species. The experiment

showed the deciduous tree species to be more sensitive than conifers (Girgždienė et al., 2009). Species-specific responses to ozone as well as impairment of soil nutrient balance in polluted areas affect the competition of forest ecosystems and its biodiversity (Paoletti, 2007). In general, chances of poor competitors are weakened (McDonald et al., 2002).

The risk is also present regarding cultivated crops. Not only the quantity, but the quality of crops changes as an effect of ozone pollution. Chemical composition (lignin and phenolic concentrations, protein content) in rice straw was demonstrated to change as a result of elevated ozone concentration. This changes mean reduced digestibility and feed intake, on the whole, reduced quality of this kettle feed (Frei et al., 2010).

According to Karlsson et al. (2009), ambient ozone levels cause 2%-10% reduction in growth of trees and up to 15% reduction in crop's yield in Sweden. Visible injuries on bioindicator plants were observable. The relatively large ozone impacts in spite of relatively low ozone levels in the Northern hemisphere were explained by that the humid climate promoted high ozone uptake of leaves.

The effect of ozone is similar to several other stresses, triggering ethylene emission, stress-related gene transcription and major plant defence systems such as programmed cell death (Sandermann, 1996). Ozone injury mainly occurs in the mesophyll tissue. Stomata and epidermal cells resist until the plant's total necrosis (Hill et al., 1961).

The initial effect of ozone is the destruction of cell membranes (Heath, 1980). Beyond degradation of photosynthetic membranes, ozone-induced impairment of photosynthesis is attributed to decline in carboxylation efficiency, the electrontransport system, the synthesis and activity of Rubisco (Pell et al., 1991), and changes in carbon-dioxid supply because of changed stomatal function (although the exact processes of these changes are not clearly understood) (Paoletti and Grulke, 2005).

Effects of ozone and ozone injuries are highly similar whatever the species. In the field, injuries occur after sunny periods, particularly at the light exposed parts of light exposed plants. Broadleaved trees show intervenial bronzing and stippling, reddening, stippling and bleaching. Most severe injuries are shown on palisade parenchyma cells (Vollenweider et al., 2003), that are undergoing HR-like reaction (reaction similar to Hypersensitive Reaction). The surrounding tissues show ACS (accelerated cell senescence) and OS (oxidative stress) (Pellinen et al., 1999).

Cell walls form protrusions including pectin, polyphenolic or protein material (Günthardt-Goerg, 1996; Günthardt-Goerg et al., 1996). Such symptoms also appear in shaded and asymptomatic leaves if exposed to high ozone concentrations (Vollenweider et al., 2003). The cell wall generally thickens and its thickness becomes irregular (Vollenweider et al., 2003); the formation and allocation of starch declines and also becomes irregular in symptomatic tissues (Günthardt-Goerg et al., 1998).

Symptoms of conifers are mottling and bleaching (Günthardt-Goerg and Vollenweider, 2001) that are very similar to those in broadleaved species (Dalstein et al., 2002; Vollenweider et al., 2003). The injured cells have larger vacuolium, more nucleus condensations and less and smaller chloroplasts, discrete groups of dead cells with apoptotic-like bodies. Bronzing (caused by condensed tannins) (Vollenweider et al., 2003) cannot be observed in conifer species (Günthardt-Goerg\* and Vollenweider, 2006).

Ozone most significantly affects the regulatory capacity of resource allocation, it alters source-sink balance decreasing below-ground carbon allocation (Andersen 2003). As a

defence reaction, plant's stomatal conductance is reduced when exposed to ozone. The direct reason of stomatal closure might be a reaction to an increased internal CO<sub>2</sub> concentration due to inhibited C assimilation (Paoletti and Grulke 2005). Ethylene emission and changed ion fluxes can also cause stomatal closure (Kangasjarvi et al., 2005), but it can be caused by direct O<sub>3</sub> effect on guard cells (Moldau et al., 1990).

However, above a certain concentration or after a certain time period ozone may impair stomatal control, causing sluggish stomatal response (Paoletti and Grulke 2005) and finally incomplete stomatal closure (Paoletti, 2005) which leads to lost control on transpiration. Increased nocturnal transpiration as a result of ozone exposure has been reported in several studies (Grulke et al., 2004, 2007). Ozone also increase sap-flow. Thus, in general, through its effect on stomata, ozone predisposes trees to drought stress (Paoletti, 2007).

As an ozone effect, stomatal density has been shown to increase (Paoletti and Grulke, 2005 Hetherington and Woodward, 2003) but with decreased stomatal or aperture size (Aasmaa et al., 2001; Paakkonen et al., 1997).

In trees, biomass production decreases rather through reduced leaf size and premature leaf loss than because of declined photosynthesis (Matyssek 2001).

In the Aspen-FACE experiment, where different tree species were exposed to elevated CO<sub>2</sub> contemporarily with elevated O<sub>3</sub> levels, 14%-18% decrease in growth of birch and a significant decrease of growth of maple trees were seen when exposed to both gases compared with plants grown only under elevated CO<sub>2</sub> (Karnosky et al., 2005).

Exposure to ozone affects flowering in several species (Black et al., 2000; Darbah et al., 2007).

As ozone decreases plant productivity, more CO<sub>2</sub> accumulates in the atmosphere, resulting indirect radiative forcing. This indirect effect may have larger contribution to global warming than the direct radiative forcing caused by increases in ground-level ozone concentrations (Stich et al., 2005; Paoletti, 2007).

#### 4. Bioindication of ozone

Bioindicator plant species are species with high sensitivity to ozone. This sensitivity is manifested in changes in physiological parameters, biomass reduction and the appearance of specific visible symptoms when exposed to high levels of ozone. According to the extent of these injuries, conclusions can be drawn regarding the presence (and, for some extent, the amount) of ozone in the atmosphere of the site where the plants are exposed to ambient air. In addition, ozone bioindicator plants are widely used in researches aiming to clarify plant's response to the stressor, or, in general, to oxidative stress. Reduction in biomass of sensitive clones as an effect of ozone is also a widely investigated indicative feature of biomonitoring plants.

There are a range of plants that were proved to be sufficient for demonstrate ambient ozone levels. Most important are *Nicotina Tabacum* var. Bel W 3 (applied together with the resistant Bel B clone); *Phaseolus vulgaris* var. Pinto; *Urtica urens*; *Spinacia oleracea* Var. *Monnopa* (Arndt et al. 1985); *Populus x euramericana* var. *Gelrica* (Arndt et al. 1992) as well as wheat, mallow and clover (Schafler, 1998).

Tobacco plants have been used for ozone bioindication in Europe since the early 1960's. This species is highly sensitive to ozone, chlorotic spots on its leaves appear even under O<sub>3</sub> concentrations of 40ppb. After being exposed to ozone for a relatively short time period,

large necrotic patches are formed, finally whole leaves wither (Mülleder et al., 1992). Since its oversensitivity, *Nicotiana tabacum* is only usable if applied together with another bioindicator species. Symptoms on tobacco plants soon become so expansive that no differences can be seen between extents of injuries on different individuals (Keitel, A. 1989). In spite of these disadvantages, tobacco has been used for ozone biomonitoring even in long-term experiments (Nali et al., 2006). It was demonstrated, that extent of ozone injuries on tobacco leaves is highly informative as regards the amount of ozone in ambient air (Ribas and Penuelas, 2002).

The white clover system was developed by Heagle et al. in 1995. Between 1996 and 2008 participants of the International Cooperative Programme on Effects of Air Pollution on Vegetation (ICP-Vegetation) have detected and evaluated effects of ozone on sensitive and resistant clones of *Trifolium repens* across Europe and in the USA. Initially, biomass ratio of the two clones was investigated, visible symptoms gained more attention only later (Harmens et al., 2006). Analysis of data of this long-term clover biomonitoring experiment is presented in Harmens et al. (2004) and Harmens et al. (2005).

Several individual studies were carried out using the clover system (e.g. Postiglione et al., 2000; Karlsson et al., 2002). Using the ICP-protocol, an investigation of the effect of ozone on the clover system was carried out during 1997 and 1998 at the Ruhr Valley (Köllner and Krause, 2002). Foliar injuries, protein content and biomass ratio were evaluated. This study found visible injuries on clover clones to be better bioindicator features than biomass ratio if ozone values at the experimental site are relatively low, or if the aim is to determine early ozone effects. Protein content of sensitive plants was reduced shortly after high level ozone periods.

Although visible ozone injuries are not eligible for exact quantitative estimations of ozone levels, sometimes very good relationships are shown between the extent of injuries on  $O_3$  sensitive clones and ozone doses in ambient air (Mills et al., 1999b; Ribas and Penuelas, 2002).

Since its identification as relatively ozone-sensitive species (Buse et al., 2003a), *Centaurea jacea* has been used as bioindicator. In 2002, ozone biomonitoring experiments of the ICP-Vegetation have been conducted using seeds of sensitive and resistant clones of this species (Harmens et al., 2006).

Evaluation of ozone symptoms is easier on large leaves. Thus, since 2008, the ICP-Vegetation Programme uses sensitive and resistant clones of *Phaseolus vulgaris* as a new bioindicator system. Bean lines used in this system were first reported by Reinert and Eason (2000), and tested by Burkey et al. (2005).

Although there are several ozone biomonitoring systems operating with sensitive and resistant clone pairs of bioindicator plant species, there are uncertainties in understanding physiological background of ozone sensitivity. Crous et al. (2006) studied the physiological differences between sensitive and resistant clones of widely used bioindicator clover. The experiment has represented that with the exception of chlorophyll content (which is originally higher in resistant plants), physiological parameters of the two clones differ only after ozone exposure. Ozone resulted changes in physiological parameters of the sensitive plants. While resistant clone showed no response to cumulative uptake of high ambient ozone ( $CUO_3$ ), sensitive clone reacted with decline of most investigated gas exchange parameters (e.g.: net photosynthesis and carboxylation capacity). Stomatal conductance of the two clones differed only after being exposed to ozone: after an initial increase during

lower ozone concentrations, stomatal conductance of the resistant clone significantly decreased. While maintaining higher photosynthesis, resistant clone showed higher non-photochemical quenching. This means that sensitive clone is more vulnerable to potentially generating reactive oxygen species that are harmful for cell membranes likely leading to visible symptoms. It has been concluded that the ozone resistance is based on stomatal function and the capacity of non-photochemical quenching. Physiological dysfunction may occur before visible symptoms develop (Pye, 1988; Fredericksen et al., 1996; Guidi et al., 2001).

## 5. Results of three year's Slovenian-Hungarian biomonitoring experiment

Experiments with two ozone bioindication plants (*Trifolium repens* r. cv. Regal and *Phaseolus vulgaris*) were conducted in a Slovenian and two Hungarian experimental sites.

Ljubljana (altitude: 320 m; average annual temperature: 11,4°C; yearly average precipitation: 1400 mm) is Slovenia's capital with significant public traffic.

Gödöllő (altitude: 249 m; mean annual temperature is between 9°C and 10°C; yearly average precipitation: 560 mm;) is a small town which is only 25 kilometers far from Budapest, so it must be affected by the pollutants of the capital city.

Szurdokpüspöki (altitude: 350 m; average annual temperature: 10,2°C; yearly average precipitation is 620 mm) is located in a rural environment in the Mátra mountains.

As it could be expected, Ljubljana had the lowest ozone concentrations among the three sites all over the three-year-long period between 2007 and 2009.

For planting and evaluating of ozone injuries we used the experimental protocol of the ICP-Vegetation (Hayes et al., 2006).

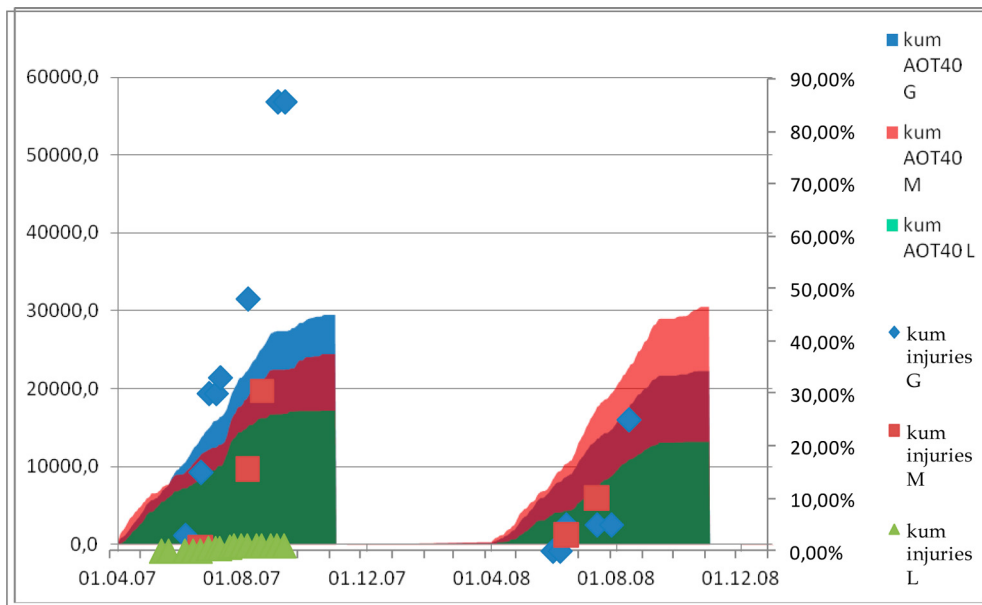


Fig 3. Two year's cumulative AOT40 values and results of ozone injury assessments on clover clones (Gödöllő-G; Mátra mountain-M; Ljubljana-L)

Ozone concentrations, ozone injuries, dry weight of clover plants and dry weight of bean's pods, number of pods were measured and evaluated.

On the base of three year's experiences in biomonitoring with the two species, we were trying to find out if bean plants were more suitable for this purpose than the clover clones.

Ozone symptoms on sensitive clover clones showed closer connection with AOT 40 values than on bean plants. Dry weight of the sensitive and resistant clones did not differ significantly; they seem to show connection with meteorological conditions rather than with ozone burden, as the dry weight of all experimental plants showed significant differences among the different sites, but these differences did not correspond with the differences in ozone values.

Neither the differences in ozone symptoms nor the dry weight of pods of ozone sensitive bean plants reflected the differences of ozone burden of the experimental sites.

Although the dry weight of pods on ozone sensitive bean strains usually remained under that on the resistant strains, this difference did not seem to have any connection with the AOT40 values. Supposedly, this is a genetic difference between the two strains in addition to but not in connection with their different reactions to ozone.

Regarding the usefulness in ozone bioindication, clover clones proved to be more valuable than bean strains. Not only had the injuries of clover clones closer connection with AOT40 values than that of the bean strains.

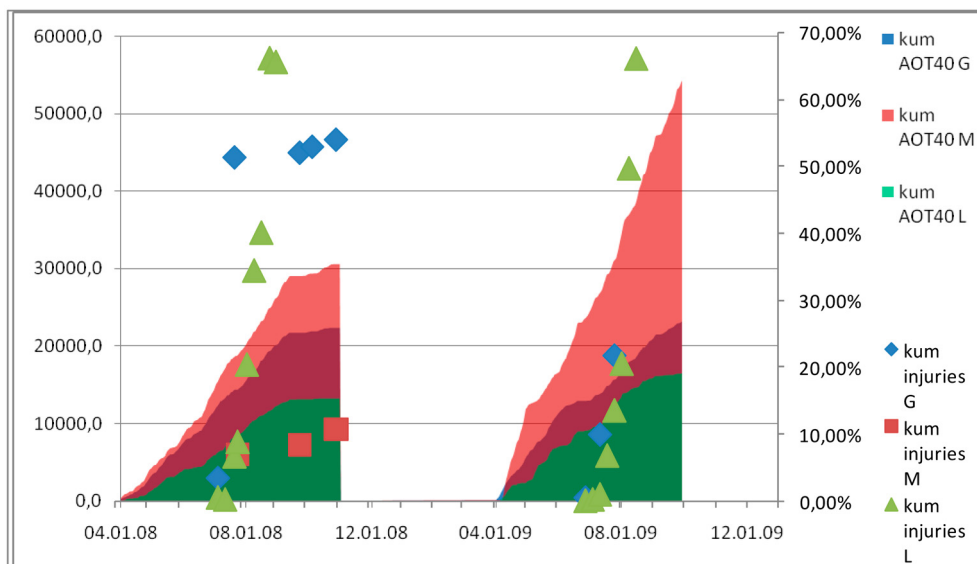


Fig 4. Two year's cumulative AOT40 values and results of ozone injury assessments on bean clones (Gödöllő-G; Mátra mountain-M; Ljubljana-L)

Comparing the bioindicator values of number of flowers on clover clones and number or dry weight of pods on bean strains, the clover clones again have appeared to be more useful. In addition, maintenance of clover clones is easier; bean plants are much more sensitive to other environmental stresses such as drought and high solar radiation which makes the experiments more complicated and their outcome more doubtful.

## 6. References

- Aasamaa K., Sober A., Rahi M. (2001): Leaf anatomical characteristics associated with shoot hydraulic conductance, stomatal conductance and stomatal sensitivity to changes of leaf water status in temperate deciduous trees, *Australian Journal of Plant Physiology* Vol 28, pp.765–74.
- Altimir N., Kolari, P., Tuovinen, J.-P., Vesala, T., Bäck, J., Suni, T., Kulmala, M. and Hari P. (2005): Foliage surface ozone deposition: a role for surface moisture? *Biogeosciences Discussions*, Vol 2, pp.1739–1793.
- Altimir, N., Tuovinen, J.-P., Vesala, T., Kulmala, M. and Hari, P. (2004): Measurements of ozone removal to Scots pine shoots: calibration of a stomatal uptake model including the non stomatal component, *Atmospheric Environment*, Vol 8, pp.2387–2398.
- Andersen, C.P. (2003): Source–sink balance and carbon allocation below ground in plants exposed to ozone, *New Phytologist* Vol 157, pp.213–28.
- Anfossi D., Sandroni S. (1994): Surface ozone at mid latitudes in the past century *Il Nuovo Cimento* Vol 17, pp.199–208.
- Arndt, U., Brausam-Schmidt, C., Geiger, B., Nobel, W. (1992): Methodische Arbeiten zur Verwendung des Pappelklons *Populus x euramericana* var. *Gelrica* als Bioindikator für Ozonbelastungen. In: Köhler, J., Arndt, U.: Bioindikatoren für Umweltbelastung – Neue Aspekte und Entwicklungen. Hohenheimer Umwelttagung–Verlag pp. 199–206.
- Arndt, U., Erhardt, W., Keitel, A., Michenfelder, K., Nobel, W., Schlüter, C. (1985): Standardisierte Exposition von pflanzlichen Reaktionsindikatoren, *Staub – Reinhaltung der Luft* Vol 45, Issue 10, pp. 481–483.
- Ashmore, M. R., Emberson, L. D., Karlson, P.-E., and Pleijel, H. (2004): A new generation of ozone 25 critical levels for the protection of vegetation in Europe, *Atmospheric Environment*, Vol 38, pp.2213–2214.
- Baldocchi, D., Hicks, B.B., and Camara, P. (1987): A canopy stomatal resistance model for gaseous deposition to vegetated surfaces, *Atmospheric Environment*, Vol 21, pp.91–101.
- Baumgarten, M., Hubera, C., Büker, P., Emberson, L., Dietrich, H-P., Nunne, A. J., Heerdtf, C., Beudertg B. and Matysseke, R. (2009): Are Bavarian Forests (southern Germany) at risk from ground-level ozone? Assessment using exposure and flux based ozone indices, *Environmental Pollution* Vol 157, Issue 7, pp. 2091–2107.
- Black, V.J., Black, C.R., Roberts, J.A., Stewart, C.A. (2000): Impact of ozone on the reproductive development of plants, *New Phytologist* Vol 147, pp.421–47.
- Brewer, C. A., and Smith, W. K. (1997): Patterns of leaf surface wetness for montane and subalpine plants, *Plant, Cell and Environment* Vol 2, pp.1–11.
- Brönnimann, S., Buchmann B., and Wanner, H. (2002): Trends in near surface ozone concentrations in Switzerland, *Atmospheric Environment*, Vol 36, pp.2841–2853.
- Burkey, K.O., Miller J.E., and Fiscus E.L. (2005): Assessment of ambient ozone effects on vegetation using snap bean as a bioindicator species, *Journal of Environmental Quality* Vol 34, pp.1081–1086
- Buse, A., Mills, G., Harmens, H., Büker, P., Hayes, F., Williams, P., Emberson, L., Cinderby, M., Ashmore, S., Holland, M. and the participants of the ICP Vegetation (2003). Air pollution and vegetation. Annual report 2002/2003

- Calvo, E., Bermejo, V., Gerosa, G., Alonso, R., Calatayud, V., Marzuoli, R. (2010): Preliminary ozone dose-response function for tomato in the Mediterranean area, in: 23rd Task Force Meeting 1 - 3 February, 2010 Tervuren, Belgium Programme&Abstracts pp.30.
- Chappelka A.H., Samuelson L. (1998): Ambient ozone effects on forest trees of the eastern United States: a review, *New Phytologist* Vol 139 pp.91-108.
- Cinderby, S., Emberson, L.D., Ashmore, M.R., Büker, P., Terry, A.C. (2005): Harmonisation of land cover mapping, in: UNECE Workshop Report "Critical levels of ozone: further applying and developing the flux-based concept", Obergurgl, Austria, 15-19 November, 2005.
- Coe, H., Gallagher, M. W., Choularton, T. W., and Dore, C. (1995): Canopy scale measurements of 25 stomatal and cuticular O<sub>3</sub> uptake by Sitka spruce, *Atmospheric Environment*, Vol 29, pp.1413-1423.
- Crous, K. Y., Vandermeiren, K., Ceulemans, R. (2006): Physiological responses to cumulative ozone uptake in two white clover (*Trifolium repens* L. cv. Regal) clones with different ozone sensitivity, *Environmental and Experimental Botany* Vol 58, pp.169-179.
- Dalstein, L., Vollenweider, P., Vas, N., Günthardt-Goerg, M.S. (2002): L'ozone et les conifères du Sud-Est de la France, *Forêt méditerranéenne* Vol 23, pp.105-116.
- Darbah J.N.T., Kubiske M.E., Nelson N., Oksanen E., Vaapavuori E., Karnosky D.F. (2007): Impacts of elevated atmospheric CO<sub>2</sub> and O<sub>3</sub> on paper birch (*Betula papyrifera*): reproductive fitness, *The Scientific World Journal* Vol 7(S1) pp.240-6.
- Duyzer, J. H., Meyer, G. M., and van Aalst, R. M. (1983): Measurements of dry deposition velocities of NO, NO<sub>2</sub> and O<sub>3</sub> and the influence of chemical reactions, *Atmospheric Environment*, Vol 7, pp.2117-2120.
- Ellenberg, H., Weber, H.E., Düll, R., Wirth, V., Werner, W., Paulissen, D. (1991): Zeigerwerte von Pflanzen in Mitteleuropa, *Scripta Geobotanica* Vol 18, pp.1-248.
- Fagnano, M., Maggio, A. (2008): Evidence of Widespread Ozone Damage to Vegetation in Europe (1990-2006) Ozone Risk Assessment for European Vegetation *Italian Journal of Agronomy* Vol 1, pp.3-5.
- Fowler, D., Flechard, C. R., Cape, J. N., Storeton-West, R. L., and Coyle, M. (2001): Measurements of ozone deposition to vegetation quantifying the flux, the stomatal and non-stomatal components, *Water, Air and Soil Pollution* Vol 1, pp. 63-74.
- Fredericksen, T.S., Skelly, J.M., Steiner, K.C., Kolb, T.E., Kouterick, K.B. (1996): Size-mediated foliar response to ozone in black cherry trees, *Environmental Pollution* Vol 91, pp.53-63.
- Frei M., Kohno Y., Makkar H.P.S., Becker K. (2010): The effect of elevated tropospheric ozone on the feeding value of rice straw in: 23rd Task Force Meeting 1 - 3 February, 2010 Tervuren, Belgium Programme&Abstracts pp.32.
- Girgždienė, R., Serafinavičiūtė, B., Stakėnas, V. and Byčėnkienė, S. (2009): Ambient Ozone Concentration and Its Impact on Forest Vegetation in Lithuania Rasa, *A Journal of the Human Environment* Vol 38, Issue 8, pp.432-436.
- Goldstein, A. H., McKay, M., Kurpius, M. R., Schade, G. W., Lee, A., Holzinger, R., and Rasmussen, R. A. (2004): Forest thinning experiment confirms ozone deposition to forest canopy is dominated by reaction with biogenic VOCs, *Geophysical Research Letters* Vol 31, L22106

- González F.I., Bermejo V., González A, de la Torre D., López A., Serra J, Elvira S., Sanz J, Gimeno B.S., Alonso R. (2010): On the application of the ozone dose-response model for wheat in southern europe in: 23rd Task Force Meeting 1 - 3 February, 2010 Tervuren, Belgium Programme&Abstracts pp.11.
- Gregg J.W., Jones C.G., Dawson T.E. (2003): Urbanization effects on tree growth in the vicinity of New York City, *Nature* Vol 424 pp.183-7.
- Grennfelt P. (2004): New directions: recent research findings may change ozone control policies, *Atmospheric Environment* Vol 38, pp.2215-6.
- Grulke N.E., Alonso R., Nguyen T., Cascio C., Dobrowolski W. (2004): Stomata open at night: implications for pollutant uptake in ponderosa pine, *Tree Physiology* Vol 24, pp.1001-1010.
- Grulke N.E., Paoletti E., Heath R.L. (2007): Chronic vs. short-term acute O<sub>3</sub> exposure effects on nocturnal transpiration in two Californian oaks, *The Scientific World Journal* Vol 7(S1), pp.134-40.
- Guidi, L., Nali, C., Lorenzini, G., Filippi, F., Soldatini, G.F. (2001): Effect of chronic ozone fumigation on the photosynthetic process of poplar clones showing different sensitivity. *Environmental Pollution* Vol 113, pp.245-254.
- Günthardt-Goerg, M.S. (1996): Different responses to ozone of tobacco, poplar, birch and alder, *Journal of Plant Physiology* Vol 148, pp.207-214.
- Günthardt-Goerg, M.S., Maurer, S., Frey, B., Matyssek, R. (1998): Birch leaves from trees grown in two fertilisation regimes: diurnal and seasonal responses to ozone. In: De Kok, L.J., Stulen, I. (Eds.), Responses of Plant Metabolism to Air Pollution and Global Change. Blackhuys Publishers, Leiden, The Netherlands, pp. 315-318.
- Günthardt-Goerg, M.S., Schmutz, P., Matyssek, R., Bucher, J.B. (1996): Leaf and stem structure of poplar (*Populus x euramericana*) as influenced by O<sub>3</sub>, NO<sub>2</sub>, their combination, and different soil N supplies, *Canadian Journal of Forest Research* Vol 26, pp.649-657.
- Günthardt-Goerg, M.S., Vollenweider, P. (2001): Diagnose von Umwelteinflüssen auf Bäume, *Schweizerische Zeitschrift für Forstwesen* Vol 152, pp.183-192.
- Günthardt-Goerg, M.S. and Vollenweider, P. (2006): Linking stress with macroscopic and microscopic leaf response in trees: New diagnostic perspectives *Environmental Pollution* xx (2006) 1-22
- Haagen-Smith A. J., 1952: Chemistry and physiology of Los-Angeles Smog, *Industrial and engineering Chemistry*, Vol 44, pp.1342-1346.
- Harmens, H., Mills, G. (2005): Review of the influences of climate change on the impacts of ozone on vegetation, The UNECE International Cooperative Programme on Vegetation
- Harmens, H., Mills, G., Emberson, L.D., Ashmore, M.R. (2007): Implications of climate change for the stomatal flux of ozone: a case study for winter wheat, *Environmental Pollution*, Vol 146 (3): pp.763-770.
- Harmens, H., Mills, G., Hayes, F., Williams, P. and the participants of the ICP Vegetation (2004): Air pollution and vegetation. Annual report 2003/2004
- Harmens, H., Mills, G., Hayes, F., Williams, P., De Temmerman, L. and the participants of ICP Vegetation (2005): Air pollution and vegetation. ICP Vegetation Annual Report 2004/2005

- Harmens, H., Mills, G., Hayes, F., Jones, L., Williams, P. and the participants of the ICP Vegetation (2006): Air Pollution and Vegetation ICP Vegetation\*Annual Report 2005/2006
- Hayes, F., Mills, G., Harmens, H., Novak, K. and Williams, P. (2006): ICP Vegetation experimental protocol for monitoring the incidences of ozone injury on vegetation
- Hayes, F., Mills, G., Harmens, H., and Norris, D. (2007): Ozone and Crop Losses 2006 (ICP Vegetation Report for Defra Contract EPG 1/3/205)
- Heagle, A.S., Miller, J.E., Chevone, B.I., Dreschel, T.W., Manning, W.J., McCool, P.M., Lynn Morrison, C., Neely, G.E., Rebbeck, J. (1995): Response of a white clover indicator system to tropospheric ozone at eight locations in the United States, *Water, Air and Soil Pollution* Vol 85, pp.1373-1378.
- Heath R.L. (1980): Initial events in injury to plants by air pollutants, *Annual Review of Plant Physiology* Vol 31, pp.395-401.
- Hetherington A.M., Woodward F.I. (2003): The role of stomata in sensing and driving environmental change, *Nature* Vol 424, pp.901-8.
- Hill, A.C., Pack, M.R., Treshow, M., Downs, R.J., Transtrum, L.G. (1961): Plant injury induced by ozone, *Phytopathology* Vol 51, pp.356-363.
- Holland, M., Kinghorn, S., Emberson, L., Cinderby, S., Ashmore, M., Mills, G., Harmens, H. (2006): Development of a framework for probabilistic assessment of the economic losses caused by ozone damage to crops in Europe, Report to Defra, contract EPG 1/3/205.
- Kangasjarvi J., Jaspers P., Kollist H. (2005): Signalling and cell death in ozone-exposed plants, *Plant, Cell and Environment* Vol 28, pp.1021-1036.
- Karlsson, G.P., Karlsson, P.E., Danielssona, H., Pleijel, H. (2003): Clover as a tool for bioindication of phytotoxic ozone – 5 years of experience from southern Sweden – consequences for theshort-term critical levels, *The Science of the Total Environment* Vol 301, pp.205-213
- Karlsson, P.E., Selldén, G., Pleijel, H. (2003): Establishing Ozone Critical Levels in: II. UNECE Workshop Report. IV report B 1523. IVL Swedish Environmental Research Institute
- Karnosky F., Pregitzer K.S., Zak D.R., Kubiske M.E., Hendrey G.R., Weinstein D. (2005): Scaling ozone responses of forest trees to the ecosystem level in a changing climate, *Plant, Cell and Environment* Vol 28, pp.965-81.
- Keitel, A. 1989. Praxiserprobte Bioindikationsverfahren – *Staub – Reinhaltung der Luft* Vol 49, pp. 29-34.
- Klausen, J., Zellweger, C., Buchmann, B. and Hofer, P. (2003): Uncertainty and bias of surface ozone measurements at selected Global Atmosphere Watch sites, *Journal of Geophysical Researches*, Vol 108(D19), pp.4622.
- Kurpius, M. R. and Goldstein, A. H. (2003): Gas-phase chemistry dominates O<sub>3</sub> loss to a forest, implying a source of aerosols and hydroxyl radicals to the atmosphere, *Geophysical Research Letters*, Vol 30(7), pp.1371.
- Logan, J.A. (1994): Trends in vertical distribution of ozone: a comparison of two analyses of ozone sonde data, *Journal of Geophysical Research*, Vol 99(D12), pp.25553-25585.
- Lorenz M., Becher G., Mues V., Fischer R., Becker R., Calatayud V. (2005): Forest Condition in Europe. Technical Report. UNECE, Geneva; pp.99

- Lorenzini, G. and Saitanis, C. (2003): Ozone: a novel plant "pathogen" in: Abiotic stresses in plants L. Sanità di Toppi and B. Pawlik Skowrońska (eds), Kluwer Academic Publishers, Netherlands, pp. 205-229.
- Massman, W. J. (1998): A review of the molecular diffusivities of H<sub>2</sub>O, CO<sub>2</sub>, CH<sub>4</sub>, CO, O<sub>3</sub>, SO<sub>2</sub>, NH<sub>3</sub>, N<sub>2</sub>O, NO, and NO<sub>2</sub> in air, O<sub>2</sub> and N<sub>2</sub> near STP, *Atmospheric Environment*, Vol 32, pp.1111-1127.
- Matyssek R. (2001): How sensitive is birch to ozone? Responses in structure and function, *Journal of Forest Science* Vol 47, pp.8-20.
- Matyssek, R., Wieser, G., Nunn, A.J., Kozovits, A.R., Reiter, I.M., Heerdt, C., Winkler, J.B., Baumgarten, M., Haberle, K.H., Grams, T.E.E., Werner, H., Fabian, P., Havranek, W.M. (2004): Comparison between AOT40 and ozone uptake in forest trees of different species, age and site conditions, *Atmospheric Environment* Vol 38, pp.2271-2281.
- McDonald E.P., Kruger E.L., Riemenschneider D.E., Isebrands J.G. (2002): Competitive status influences tree-growth responses to elevated CO<sub>2</sub> and O<sub>3</sub> in aggrading aspen stands, *Functional Ecology* Vol 16, pp.792-801.
- Meyers, T. P., Finkelstein, P. L., Clarke, J. F., Ellestad, T. G., and Sims, P. F. (1998): A multilayer model for inferring dry deposition using standard meteorological measurements, *Journal of Geophysical Research*, Vol 103, pp.22 645-22 661
- Midgley P.M., Builtjes P.J.H., Fowler D., Harrison R.M., Hewitt C.N., Noone K.J. (2002): Eurotrac-2 Synthesis and Integration Report: Towards Cleaner Air for Europe – Science, Tools and Applications. GSF, National Research Centre for Environment and Health, Munich, Germany;
- Mikkelsen, T. N., Ro-Poulsen, H., Pilegaard, K., Hovmad, M. F., Jensen, N. O., Christensen, C. S., and Hummelshøj, P. (2000): Ozone uptake by an evergreen forest canopy: temporal variation and possible mechanisms, *Environmental Pollution*, Vol 109, pp.423-429.
- Mills, G., Hayes, F., Williams, P. and Harmens, H. (2005): ICP Vegetation experimental protocol for monitoring the incidences of ozone injury on vegetation, Natural Environment Research Council pp.20
- Mills, G., Hayes, F. and Ball, G. (1999): 'ICP-Non-Wood Plants and Crops Annual Progress Report', UN/ECE, Working Group on Effects of the Convention on Long Range Transboundary Air Pollution. University of Wales, Bangor, U.K.
- Mills, G., Hayes, F., Jones, M.L.M., Cinderby, S. (2007): Identifying ozone-sensitive communities of (semi-) natural vegetation suitable for mapping exceedance of critical levels. *Environmental Pollution* Vol 146, pp.736-743.
- Moldau H., Sober J., Sober A. (1990): Differential sensitivity of stomata and mesophyll to sudden exposure of bean shoots to ozone, *Photosynthetica* Vol 24, pp.446-458.
- Müllerder, N., Gross, H., Arndt, U. (1992): Wirkungsbezogene Messung von Ozon – Ein Vergleich der Reaktion von Tabak Bel W 3 und Indigo. In: Köhler, J. – Arndt, U. Bioindikatoren für Umweltbelastung – Neue Aspekte und Entwicklungen. Hohenheimer Umwelttagung–Verlag Josef Margraf Universität Hohenheim. pp. 49-59.
- Naja, M. and Akimoto, H. (2004): Contribution of regional pollution and long-range transport to the Asian-Pacific region: analysis of log-term ozone sonde data over Japan *Journal of Geophysical Research* Vol 109

- Nali, C., Francini, A. and Lorenzini, G. (2006): Biological monitoring of ozone: the twenty-year Italian experience *Journal of Environmental Monitoring* Vol 8, pp.25–32.
- Oltmans, S.J. et al., (2006): Long-term changes in tropospheric ozone, *Atmospheric Environment* Vol 40, pp.3156–3173.
- Ordóñez, C. (2006): Trend analysis of ozone and evaluation of nitrogen dioxide satellite data in the troposphere over Europe, Doctoral thesis, 16544, ETHZ
- Paakkönen E., Holopainen T., Kaarenlampi L. (1997): Variation in ozone sensitivity of *Betula pendula* and *Betula pubescens* clones from southern and central Finland, *Environmental Pollution* Vol 95, pp.37–44.
- Paoletti E., Bytnerowicz A., Andersen C., Augustaitis A., Ferretti M., Günthardt-Goerg M.S. (2007): Impacts of air pollution and climate change on forest ecosystems – emerging research needs, *The Scientific World Journal* Vol 7(S1), pp.1–8.
- Paoletti E., Grulke N.E. (2005): Does living in elevated CO<sub>2</sub> ameliorate tree response to ozone? A review on stomatal responses, *Environmental Pollution* Vol 137, pp.483–93.
- Paoletti E., Manning W.J. (2007): Toward a biologically significant and usable standard for ozone that will also protect plants, *Environmental Pollution*, Vol 150, pp.85–95.
- Paoletti E. (2006): Impact of ozone on Mediterranean forests: a review, *Environmental Pollution* Vol 144, pp.463–74.
- Paoletti E. (2005): Ozone slows stomatal response to light variation and wounding in a Mediterranean evergreen broadleaf: *Arbutus unedo*, *Environmental Pollution* Vol 134, pp.4 39–45.
- Paoletti, E. (2007): Ozone impacts on forests CAB Reviews: Perspectives in Agriculture, Veterinary Science, Nutrition and Natural Resources Vol.2, No. 068
- Pell E.J., Schlaghaufer C.D., Arteca R.N. (1991) Ozone induced oxidative stress: mechanisms of action and reaction, *Physiologia Plantarum* Vol 100, pp.264–73.
- Pellinen, R., Palva, T., Kangasjarvi, J. (1999): Subcellular localization of ozone-induced hydrogen peroxide production in birch (*Betula pendula*) leaf cells, *Plant Journal* Vol 20, pp.349–356.
- Pilegaard, K. (2001): Air-soil exchange of NO, NO<sub>2</sub> and O<sub>3</sub> in forests, *Water, Air, Soil Pollution.: Focus*, Vol 201, pp. 79–88.
- Pleijel, H., Danielsson, H., Ojanpera, K., De Temmerman, L., Høgy, P., Badiani, M., Karlsson, P.E. (2004): Relationships between ozone exposure and yield loss in European wheat and potato—a comparison of concentration and flux-based exposure indices, *Atmospheric Environment* Vol 38, pp.2259–2269.
- Postiglione, L., Fagnano, M., Merola, G. (2000): Response to ambient ozone of two white clover (*Trifolium repens* L.cv. "Regal") clones, one resistant and one sensitive, grown in a Mediterranean environment, *Environmental Pollution* Vol 109, pp. 525–531.
- Pye, J.M. (1988): Impact of ozone on the growth and yield of trees—a review, *Journal of Environmental Quality* Vol 17, pp.347–360.
- Reinert, A., and Eason, G. (2000): Genetic control of O<sub>3</sub> sensitivity in a cross between two cultivars of snap bean, *Journal of American Society of Horticultural Science* Vol 125(2), pp.222–227.
- Ribas, A., Penuelas, J. (2003): Biomonitoring of tropospheric ozone phytotoxicity in rural Catalonia, *Atmospheric Environment* Vol 37, pp.63–71.

- Rondón, A., Johansson, C., and Granat, L. (1993): Dry deposition of nitrogen dioxide and ozone to coniferous forest, *Journal of Geophysical Research* Vol 98, pp.5159–5172.
- Sandermann J. H. (1996): Ozone and plant health, *Annual Review of Phytopathology* Vol 34, pp.347–66.
- Sandermann, H., Ernst, D., Heller, W., Langebartels, C. (1998): Ozone: An abiotic elicitor of plant defence reactions, *Trends in Plant Science* Vol. 3. pp. 47-50.
- Schafler, P. (1998): Bioindikation von Ozon in Ostösterreich eine Fallstudie. In: Forstliche Schriftenreihe Universität für Bodenkultur, Wien. Band 11.
- Schönbein, C. F. (1844): Abhandlungen der Bayrischen Akademie der Wissenschaften Naturwissenschaftlich-mathematische Klasse, München pp.257.
- Seinfeld, J. H., and Pandis, S. N. (1998): *Atmospheric Chemistry and Physics*, John Wiley and Sons, New York
- Simmonds, P.G., Manning, A.J., Derwent, R.G., Ciais, P., Ramonet, M., Kazan, V. and Ryall, D. (2005): A burning question. Can recent growth rate anomalies in the greenhouse gases be attributed to large-scale biomass burning events, *Atmospheric Environment* Vol 39, pp.2513–2517.
- Simpson, D., Tuovinen, J.-P., Emberson, L. D., and Ashmore, M. R. (2003): Characteristics of an ozone deposition module II: Sensitive analysis, *Water, Air, and Soil Pollution* Vol 143, pp.123–137, 2003.
- Sitch S., Cox P.M., Collins W.J., Huntingford C. (2007): Indirect radiative forcing of climate change through ozone effects on the landcarbon sink, *Nature* Vol 448, pp.791–4.
- Staehelin, J. andm Poberaj, C.S. (2008): Long-term Tropospheric Ozone Trends: A Critical Review in: S. Brönnimann et al. (eds.), *Climate Variability and Extremes during the Past 100 Years*.pp. 271
- Staehelin, J., Thudium,J., Bühler, R., Volz-Thomas,A and Graber,W. (1994): Surface ozone trends at Arosa (Switzerland), *Atmospheric Environment*, Vol 28, pp.75–87.
- Staehelin, J., Prévôt, A.S.H., and Barnes, J. (2000): Photochemie der Troposphäre, Handbuch der Umweltveränderungen und Ökotoxikologie, Band IA: Atmosphäre, R. Guderian, Ed., Springer Verlag, pp.207-341.
- Tarasick, D.W., Fioletov, V.E., Wardle, D.I., Kerr, J.D. and Davies,J. (2005): Changes in the vertical distribution of ozone over Canada from ozonesondes: 1980–2001. *Journal of Geophysical Research* Vol 110.
- The Royal Society (2008): Ground level ozone in the 21st century: future trends, impacts and policy implications. Science Policy Report 15/08. The Royal Society, London.
- Thouret, V., Cammas, J.-P., Sauvage, B., Athier, B., Zbinden, R. M., Nédélec, P., Simmon, P. and Karcher, F. (2006): Tropopause referenced ozone climatology and inter-annual variability (1994–2003) from MOZAIC programme. *Atmospheric Chemistry and Physics* Vol 6, pp.1033–1051.
- Van Hove, L.W.A., Bossen, M.E., de Bok, F.A.M., and Hooijmaijeres, C.A.M. (1999): The uptake of O<sub>3</sub> by poplar leaves: the impact 5 of a long-term exposure to low O<sub>3</sub>-concentrations, *Atmospheric Environment* Vol 33, pp.907–917.
- Vingarzan, R. (2004)? A review of surface O<sub>3</sub> background levels and trends, *Atmospheric Environment* Vol 38, pp.3431–3442.
- Volk, M., Obrist, D., Novak, K, Giger, R., Bassin, S. and Fuhrer, J. (2010): Subalpine grassland nee CO<sub>2</sub> fluxes indicate reduced gpp and reco at elevated ozone, but no reduction of productivity in: 23rd Task Force Meting1 - 3 February, 2010 Tervuren, Belgium Programme&Abstracts pp.26.

- Vollenweider, P., Ottiger, M., Günthardt-Goerg, M.S. (2003): Validation of leaf ozone symptoms in natural vegetation using microscopical methods, *Environmental Pollution* Vol 124, pp.101-118.
- Witting, V.E., Ainsworth, E.A., Naidu, S.L., Karnosky, D.F., Long, S.P. (2009): Quantifying the impact of current and future tropospheric ozone on tree biomass, growth, physiology and biochemistry: a quantitative meta-analysis. *Global Change Biology* Vol 15, no. 2 pp. 396-424.



# Biosystems for Air Protection

Krystyna Malińska and Magdalena Zabochnicka-Świątek  
*Częstochowa University of Technology*  
*Poland*

## 1. Introduction

With rapid development of industry and technology worldwide we are observing a gradual deterioration of the air quality. A great number of industrial processes (e.g. combustion), transportation, or even agriculture generate significant quantities of pollutants such as carbon dioxide, carbon monoxide, sulphur oxides, nitrogen oxides, volatile organic compounds (e.g. methane), ammonia, particulate matter, toxic metals (e.g. lead), odors and radioactive pollutants. These pollutants have a harmful effect on the ecosystems, human and animal health. In order to prevent from further deterioration of air there is a need for minimizing the emissions of harmful substances, performing pollution control and introducing solutions to reduce the concentrations of pollutants in the air.

Living organisms - referred to as biosystems - such as microorganisms, plants or animals in their natural habitat can respond to some changes in the air quality. Living organisms can respond to air pollutants in many ways which include e.g. accumulation of a pollutant in a tissue, visual changes on the community level, tissue injury, inhibition of growth, etc. These effects of pollutants on living organisms can be measured qualitatively and/or quantitatively. Organisms also use selected air pollutants for their growth and metabolism. Some of them have the ability to accumulate various substances and transform into less toxic. This can result in a significant decrease in the concentration of these pollutants in the air. Due to these specific properties biosystems can be used in monitoring of pollutants in the air referred to as biomonitoring. They can also allow for the reduction and removal of toxic compounds present in the air.

This chapter will provide the overview of the most common biosystems that can be used in the protection of air with the examples of practical applications, current trends and recent developments. The main focus will be placed on the characteristics of biosystems and their potentials and limitations for air protection, mechanisms and processes for accumulation and transformation of air pollutants, biomonitoring for air pollution control, and mechanisms for reduction and removal of pollutants from the air. This chapter will also present current research and future challenges in the application of biosystems for air protection.

## 2. Air pollution and quality control

### 2.1 Air pollutants

Air pollutants are referred to as gaseous, liquid and solid substances present in the atmosphere which are not the natural components of the air or any substances which are present in the atmosphere exceeding the concentrations of the air components typical for the natural composition of the air. The sources of air pollutants are natural (e.g. volcano eruptions, forest fires, pollens scattering, etc.) and anthropogenic (i.e. industrial processes, such as combustion, power generation, services also transportation, residential sources, and agriculture). Air pollutants are emitted to the atmosphere mainly from industrial processes, transportation or agriculture, and they constitute a very diverse group of substances. Generally, they are classified as primary and secondary air pollutants. The primary air pollutants are directly emitted from the source to the atmosphere (e.g. carbon dioxide, sulphur dioxide, hydrocarbons, etc.) whereas the secondary air pollutants are formed in the atmosphere due to various reactions and transformations (e.g. aerosols, nitrogen dioxide or tropospheric ozone, etc.). With view to the physical state the air pollutants can be gaseous, liquid or solid. Gaseous air pollutants include sulphur dioxide, nitrogen oxides, carbon oxide, volatile organic compounds, toxic organic compounds (polychlorinated biphenyls, polycyclic aromatic hydrocarbons, dioxins), greenhouse gases (carbon dioxide, methane), odors. Liquid substances and solid particles are also emitted to the atmosphere where they form aerosols and suspended particulate matter.

The most hazardous air pollutants include: carbon dioxide, carbon monoxide, sulphur oxides, nitrogen oxides, volatile organic compounds (e.g. methane), ammonia, particulate matter, toxic metals (e.g. lead), odors and radioactive pollutants. Sulphur dioxide is mainly produced from the combustion of sulphur-containing fossil fuels and in the atmosphere it can be oxidized to sulphurous and sulphuric acids. Also some sulphur generate from petroleum refining, production of sulphuric acid and paper (Vestreng et al., 2007). Carbon dioxide and methane are the greenhouse gases that contribute to the global warming. Carbon dioxide is generated during combustion of fossil fuels, i.e. oil, natural gas and coal, biomass and various solid waste, and also is produced from industrial processes. Methane is formed and emitted to the atmosphere from the production and transport of fossil fuels, from agriculture and landfilling of waste. Another important air pollutant on the regional as well as global scale is tropospheric ozone (Klumpp et al., 2006) which can have both a direct and indirect effect on the global warming. It is generated during photochemical reactions of  $\text{NO}_x$  and VOCs and its formation is influenced by any pollutants produced during fuel combustion. Nitrogen oxides are emitted to the atmosphere mainly from the combustion of fossil fuels (e.g. during power generation) and from transportation. Particulate matter suspended in the air is defined as a heterogeneous mixture of solid and/or liquid particles of different sizes, origin and chemical composition (Grantz et al., 2003). These particles can be generated during combustion of e.g. diesel fuel or due to churning of road dust, brake wear and also construction and agricultural activities. For the purpose of air monitoring there are two sizes of particles referred to as particulate matter with the particle size smaller than  $10\ \mu\text{m}$  (PM 10) and  $2,5\ \mu\text{m}$  (PM 2,5). Other air pollutants include heavy metals and fluoride. Heavy metals such as Cd, Cr, Co, Cu, Mn, Ni, Pb are emitted to the atmosphere from a large number of industrial processes. Fluoride is a bioelement which shows a very narrow safety margin for the environment, and therefore can pose a significant threat

towards living organisms. The main source of this air pollutant is the application of fluoropesticides which can enter the food chain. In the environment fluoride can form various compounds such as gaseous HF and SiF<sub>4</sub> which are toxic and can easily penetrate into living organisms, soluble in water salt derivatives and other fluoride compounds which are partly soluble in water (Telesiński & Śnioszek, 2009).

Not only atmospheric air is polluted with various chemical compounds. Also, the indoor air in non residential buildings (i.e. workplaces, offices, production facilities, warehouses, etc.) can be polluted with a number of substances, such as aromatic hydrocarbons (e.g. benzene, toluene, ethylbenzene, isomeric xylenes, etc.), chlorine, ozone, formaldehyde, sulphur dioxide, nitrogen dioxide and other (Ilgen et al., 2001). Generally, these indoor air pollutants are emitted from combustion processes, furniture, cleaning agents and human activity. According to the EPA about 1000 sources of indoor pollution have been identified and over 60 of them emit carcinogenic substances. In the case of indoor air pollution the most effective methods for removal or/and reduction of air pollutants are eliminating the source of indoor air pollutant emission and/or reducing the concentration of indoor air pollutant by ventilation.

Apart from already known pollutants emitted to the atmosphere there is a large and unspecified group of so called emerging pollutants. These are substances used in many areas of life, such as surfactants, pharmaceuticals, gasoline additives, steroids, hormones, etc. The effects of emerging pollutants on living organisms continuously released to air, water and soil have not been yet sufficiently investigated and thus the future consequences are difficult to predict (Rodrigues-Mozaz et al., 2005).

Air pollution causes potential threats and risk to people, animals and natural environment. The direct effects of air pollution include pulmonary deposition and absorption of inhaled chemical compounds which are hazardous to human health. The indirect effects can result from the exposure and/or uptake of food and drinking water which can contain air pollutants deposited in the environmental media (Van Leeuwen, 2002). Heavy metals can cause neurological problems and cancer in humans. According to the EEA (i.e. European Environmental Agency) in European cities during the period of 1997-2007 about 20-50% of people were exposed to particulate matter (PM<sub>10</sub>) concentration which exceeded the admissible values. During that time about 13-41% of urban population was exposed to nitrogen dioxide concentrations which also exceeded the admissible values. As for ozone it is estimated that about 14-62% Europeans in cities were exposed to the ozone concentrations which were higher than the admissible values. The urban population exposed to sulphur dioxide in European counties decreased to less than 1%. According to recent studies the exposure to airborne particulate matter and ozone may have increased the mortality rate and admissions to hospitals due to respiratory disorders, cardiovascular diseases and lung cancer (Brunekreef & Holgate, 2002). Fluoride impairs the assimilation and photosynthesis in plants. Also, particulate matter has the negative effects on plants and ecosystems which are mostly due to deposition resulting in impairing nutrient cycle, vegetation growth and ecosystem functions. Some direct effects include injury of leaf surfaces by pH (Grantz et al., 2003).

## 2.1 Control of air quality and pollution

The quality and pollution of air are controlled by continuous monitoring of atmosphere. Monitoring is a system of measuring and analyzing the parameters of air quality, and collecting, processing and publicizing the obtained data from the observation networks (e.g. automatic, manual, passive measurements.). Monitoring of air is performed on a local, regional, national and global scale. In most countries monitoring of air quality and pollution is performed through various regulatory incorporating and control-oriented programs and strategies. These programs are developed in order to provide reliable data on the occurrence and concentrations of the selected pollutants in the atmosphere. In practice, monitoring of air control and pollution requires identifying the sources of emissions, determining the scale of emissions, adapting analytical methods, determining critical emissions and evaluating the total costs. Monitoring of atmosphere poses many difficulties. Mostly, this is due to the dynamics of atmosphere which is the main medium for spreading and transporting the pollutants between different elements of the environment (i.e. air, water and soil) and the exposure of large human populations to the harmful and/or toxic air pollutants.

Monitoring of air aims at: controlling of air quality according the required standards, identifying and determining the sources and scale of emissions, determining the effects of air pollution on the environment, analyzing the processes which occur in the atmosphere. Depending on the aim, localization and scale, the quality and pollution of air is determined from the presence and concentration of the selected parameters. The essential parameters of air pollution are SO<sub>2</sub>, NO<sub>2</sub>, NO<sub>x</sub>, PM 10, PM 2,5, Pb, CO, C<sub>6</sub>H<sub>6</sub>, O<sub>3</sub> and also As, Cd, Ni in PM 10.

Monitoring of air pollution is conducted on a local, regional, national and international levels and the data on the concentration of the air pollutants is available through websites of different agencies or governmental organizations on regular basis (for Europe it is the European Environment Agency). According to recent data on the pollution of air presented by the EEA, there is a strong declining trend for the emissions of nitrogen oxides which decreased by 31% from 1990 to 2007. It is estimated that the emissions of NO<sub>x</sub> mostly came from road transport (36%), combustion for energy production (21%), use of energy for industrial purposes (15%) and other non road transport sources (16%). In the European countries the emissions of heavy metals during 1990 and 2007 also decreased. The emissions of lead, mercury and cadmium were reduced by 88%, 57% and 56%, respectively. During the last 25 years anthropogenic sulphur emissions in Europe show a steadily decreasing tendency. According to the reports from the Cooperative Programme for Monitoring and Evaluation of the Longrange Transmission of Air Pollutants in Europe (EMEP) the emissions of sulphur dioxide were reduced from 55 Tg SO<sub>2</sub> in 1980 to 15 Tg in 2004. Most European countries have reduced the emission by 60% during the period of 1990 and 2004 with the highest reductions in the sulphur emissions from combustion for energy and also transformation industries (Vestreng et al., 2007).

## 3. Biological indicators of air pollution

It has been known for a long time that many living organisms such plants, animals, fungi and bacteria are sensitive to many pollutants present in the air, soil and water. These living organisms can respond to different types of substances and the concentration. Therefore

they can be used as valuable tool for identification of the impact the air pollutants have on the natural environment. The application of living organisms for identifying and determining the impact of air pollutants on the environment requires the knowledge about the cause and effect and the exposure and response relationships. These relationships have to be defined in terms of qualitative and quantitative changes caused by a selected air pollutant to a living organism. Based on that several methods and organisms which demonstrate the ability to respond with specific and visible symptoms to air pollutants have been identified. These include:

- bioindicators (or bioindicator organisms) are organisms or a group of organisms that contain information on the quality of the environment (Markert, 2008) and refer to changes which can mainly occur at the organismic and population level (Lam & Gray, 2003),
- biomonitors are organisms that contain information on the quantitative aspects of the quality of the environment,
- bioaccumulators are organisms which demonstrate the ability to accumulate a substance or group of substances in their tissues; bioaccumulation can result from the equilibrium process of intaking/discharging a pollutant by biota from and into the surrounding environment (Batziias & Siontorou, 2007),
- biomarkers are often defined as quantitatively measurable changes in living organisms at the cellular, biochemical, molecular or physiological levels, i.e. measured in cells, body fluids, tissues or organs which were exposed to the action of pollutants; the examples of biomarkers include tanning of human skin as an effect of UV radiation, changes in morphological or histological structure of organs, such as liver or testicles (Lam & Gray, 2003; Markert, 2008); in the studies on the risk of lung cancer due to air pollution molecular alterations such as loss of heterozygosity or gene mutations are investigated as potential biomarkers (Vineis & Husgafvel-Pursiainen, 2005),
- biosensors are referred to as measuring devices which generate a response corresponding to the concentration of a selected substance or a defined group of substances through a selective biological system such as enzyme, antibody, membrane, cell or tissue to a physical transmission device (Markert, 2008); in other words, biosensors combine a response to the concentration of a selected pollutant with a measurable signal (e.g. microbial fuel cells biosensors can use microorganisms which in a response to the presence and/or concentration of given pollutant can generate electricity); these biosensors can detect a substance or a group of substances or can give information on biological effects (e.g. genotoxicity or immunotoxicity) (Batziias & Siontorou, 2007).

In terms of applied methods, biological organisms can be also classified into active and passive organisms. Active organisms are grown in laboratories and transferred into the environment whereas passive organisms (also referred to as native or in situ organisms) are already present in the environment. In terms of bioindication both types of organisms have advantages as well as some limitations. Active organisms which are transplanted into the designated area can only show accumulation of air pollutants during the selected period of study and the concentration of air pollutants may not be detectable with the commonly applied methods (Markert, 2008). Organisms transplanted into the area subjected to monitoring allow to control the range and the density of observation network.

For the purpose of biomonitoring living organisms with the potential for bioindication and bioaccumulation should also fulfill a number of requirements. They should be easily recognized and sampled, and respond quickly to changes in the environment. The cause-effect or exposure-response relationships between a pollutant sensitive organism and a pollutant itself should be clearly determined. The selected organisms should commonly occur in the area subjected to monitoring, their living requirements should not be too limited and allow for automatic and continuous monitoring of their responses. Further selection of biological indicators can be performed in view to specificity, accumulative properties and representation of a monitored site (Wolterbeek, 2002). Also, the sampling design for a monitored site should allow for statistically reliable results that can be comparable (Lam & Gray, 2003). McGeoh and Chown (1998) determined the value of species as indicators of air pollution based on the specificity and fidelity measure. This method allows to identify and determine biological indicators for a selected area or habitat types subjected to monitoring.

#### **4. Biomonitoring of air pollution**

In recent decades the increased interest in the application of biological indicators for monitoring of air pollutants is observed worldwide. Biomonitoring can be defined as the use of living organisms and/or biological materials to provide some information on a selected parameters and characteristics of the environment. It is a direct measure of a living organism's exposure to a pollutant or a group of pollutants. Biomonitoring uses sensitive or bioaccumulative organisms. This refers to the changes in the behavior of living organisms or the concentration of a pollutant in tissues (Wolterbeek, 2002; Batzias & Siontorou, 2007).

In many countries biomonitoring is strongly affected by the environmental policies, regulations and international agreements. Each country can develop and implement its own policies and programs for biomonitoring of air pollution. This however results in inconsistent programs, procedures and methodologies. Due to the fact that biomonitoring can be applied at local, regional, national or global scale, it requires further development and unification to allow for obtaining comparable and reliable results for larger geographical scales (Pirintsos & Loppi, 2008).

There are many advantages of applying biological indicators for monitoring the quality and pollution of air. One of the advantages of biomonitoring is that it provides an early warning of future effects which air pollutants can have on biosystems. Chemical analytical methods applied in monitoring do not allow for determining the direct impact of air pollution on living organisms (Lam & Gray, 2003). The application of biological indicators for monitoring of air pollution is also cost-efficient when compared to the cost of analytical methods. Possible limitations of biomonitoring may be due to the selection of a biological indicator, unpredicted changes in the environment which can affect the cause-effect relationship and make it difficult to determine the impact of a pollutant, sampling methods and also the area subjected to monitoring. The optimal solution for monitoring of air quality and pollution is the application of living organisms coupled with monitoring performed with chemical analytical methods.

The first observations of a response of living organisms to air pollutants were: the abundance of lichens and the acidification of Scandinavian lakes due to sulphur emissions in Europe (Wolterbeek, 2002). Currently, there are many species that are used for biomonitoring of various air pollutants.

Gaseous pollutants in the atmosphere such as SO<sub>2</sub>, NO<sub>2</sub>, HF or O<sub>3</sub> were initially monitored with the use of lichens which have been regarded as the long-term biomonitors of air pollution (Batzias & Siontorou, 2007). At present, many researchers investigate other plant species for biomonitoring gaseous pollutants, e.g. wheat, barley, maize, grass and tobacco (Wolterbeek, 2002). Klumpp et al. (2006) conducted research on monitoring of tropospheric ozone present in the atmosphere with the use of tobacco plant (*Nicotiana tabacum* cv. Bel-W3). The study was conducted in urban, suburban, rural and traffic exposed areas. Kumpff et al. observed the ozone-induced injury of tobacco plant mostly in suburban and rural areas. Pacheco et al. (2002) investigated olive-tree bark (*Olea europaea*) as a biological indicator for airborne trace elements. Olive-tree bark can be sampled and analyzed in a similar manner as lichens.

Biomonitoring of air polluted with heavy metals can be performed with the application of mosses. Mosses show high capacity for bioaccumulation of heavy metals due to their ability to retain particulate matter on the surface of the plant or absorb heavy metals in ionic forms (Shakya et al., 2004). Costa et al. (2002) investigated lichens as biomonitors for heavy metals in air particulate matter. However they found it difficult to establish quantitative relationship between lichens and particulate matter.

The pollution of fluoride can be monitored by various biosystems mostly plants. Plants can be affected by fluoride present in particulate matter or industrial gasses, or by direct intake of fluoride present in soil by root system. Fluoride air pollution can be monitored by gladiolous flowers which show a direct correlation between the size of necrosis of the leaves and the concentration of fluoride in the air or waste. Other bioindicators include tulips, crocuses, pines, larches, lichens and also mosses. Biomonitoring of fluoride air pollution by plants and soil organisms allow to determine the effect of fluoride on a living organism for a selected period of time (Telesiński & Śnioszek, 2009).

## 5. Removal of air pollutants with biosystems

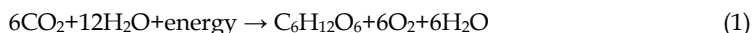
Currently, the effect of climate change is the most challenging and globally recognized threat caused by increasing emissions of greenhouse gases, predominantly by CO<sub>2</sub> (Woodward et al., 2009), and other pollutants that are emitted to the atmosphere.

Strategies for removal and/or mitigation the effects of air pollutants include: replacing fossil fuels with renewable sources of energy such as wind, solar, geothermal or nuclear energy; injecting carbon dioxide into the oceans or employing biological systems for removal of air pollutants or mitigate the effects of air pollution. Woodward et al. (2009) presented a number of biological methods for reducing carbon dioxide in the atmosphere. These methods included: reducing carbon dioxide through soil carbon sequestration based on the management of plant and decomposition processes, reducing carbon dioxide concentrations

by afforestation, reducing surface warming by increasing the albedo of crop leaves, and remediation of anthropogenic carbon dioxide by ocean biota.

Reduction in the concentration of air pollutants by various organisms strongly depends on their ability to take up selected compounds. The mechanisms for taking up selected pollutants by living organisms include: bioaccumulation which depends on the ability to store different compounds by living organisms, biomagnification which is referred to as absorption of different pollutants from nutrients through the intestines and is typical for heterotrophic organisms, and bioconcentration is a direct uptake of pollutants from the environment through tissues and organs, and is typical for plants and aquatic animals (Markert, 2008).

Reduction of air pollutants with various species is mostly based on photosynthesis. Photosynthesis is the process in green plants, algae and certain forms of bacteria by which carbohydrates are synthesized from carbon dioxide and water in the presence of chlorophyll, using light as an energy source, and releasing excess oxygen as a byproduct. Photosynthesis consists of light reactions and dark reactions. This process can be simplified in this equation:



Approximately 40% of the overall amount of carbon annually fixed on the Earth is occurring in the oceans in the process of photosynthesis by photoautotrophic organisms. Photoautotrophic organisms are able to synthesize their own food without rely on nutrients derived from other living organisms. Within the cells of plants and algae photosynthesis occurs in plastids (e.g. chloroplasts), which are membrane-bounded organelles containing photosynthetic pigments (e.g. chlorophyll). On the contrary to the photosynthetic bacteria (cyanobacteria) that do not have membrane-bounded organelles. In those organisms the process of photosynthesis occurs in the thylakoid membranes in the cytoplasm.

Currently, due to the effects of greenhouse emissions there is a tremendous interest in combining systems of reducing/mitigating the concentration/effect of greenhouse gases with biomass production for material and energy recovery. Therefore there is an increasing interest in applying algae for removal of air pollutants (mostly  $\text{CO}_2$ ,  $\text{NO}_2$ ,  $\text{SO}_2$ ).

## 6. Algae potential for removal of air pollutants

Photoautotrophic organisms like algae can absorb some of the air pollutants. Algae produce over 71% of the earth's oxygen in the process of photosynthesis. Algae belong to organisms which are able to absorb  $\text{CO}_2$ ,  $\text{NO}_2$ ,  $\text{SO}_2$  that are important nutrients for them. Moreover, addition of  $\text{CO}_2$  to algal cultures stimulates its growth. Algae can be either marine or freshwater. They have higher photosynthetic efficiencies than terrestrial plants and therefore they are more efficient capturing carbon. Algae include seaweeds and microalgae. Seaweeds are macroscopic multicellular algae that have defined tissues containing specialised cells. Microalgae are microscopic algae, many are unicellular (Packer, 2009).

Fuel source and design of the plant is responsible for the level of concentration of the CO<sub>2</sub> in flue gases. Generally, coal-fired plants having higher CO<sub>2</sub> emissions. Other constituents of the flue gases can be: oxides of nitrogen (NO<sub>x</sub>) and sulphur (SO<sub>x</sub>) and metals, such as: nickel (Ni), vanadium (V) and mercury (Hg) (Packer, 2009). Carbon dioxide and nitrogen dioxide are also released by automobiles, steel plants, cement plants, breweries and fertilizer plants. Current research indicates that algae have the potential to be able to accumulate trace metals released to the environment by biosorption and bioaccumulation processes. Wastewater could be used as microalgae nutrient and algal biomass could become, in the near future, an economic and effective material for selective recovery of heavy metals from communal and industrial wastewater or other sources (Munoz et al., 2009).

According to the literature, microalgae growth is not inhibited in a medium containing NO<sub>x</sub>. The concentration of SO<sub>x</sub> above 400 ppm resulted in the formation of sulphurous acids and impact the pH. Then, the pH of the medium can become lower than 4 that affects the productivity of the microalgae. For inhibition of fast increase of pH value it is possible to use NaOH.

Microalgae present one of the technologies for the capture of carbon dioxide emitted by industrial sources like fossil-fuelled power plants and fermentation processes, reducing CO<sub>2</sub> emissions (Usui & Ikenouchi, 1997; Benneman, 1997; Braun, 1996). Microalgae can assimilate carbon dioxide into organic material: carbohydrates, proteins and lipids that can be converted into valuable materials. One of the most important applications of algal biomass is that it can be used for production of different types of renewable biofuels, such as (Chisti, 2007): methane produced by anaerobic digestion of the algal biomass, biodiesel derived from microalgal oil, bioethanol derived from microalgal carbohydrates, photobiologically produced biohydrogen.

The algal biomass could also find application as: high-protein animal feed, food, agricultural protein-rich biofertilizer, biopolymers/bioplastics, biosorbents, medicines, cosmetics.

Optimal temperature for growing many microalgae is between 20 and 30°C and their tolerance to CO<sub>2</sub> depends on the species. For the chlorophylls and other photosynthetically active pigments the spectral quality of light is defined by absorption spectrum in the range of 400 to 700 nm.

### 6.1 Algae cultivation systems

Generally, there are two types of cultivation systems of algae: open ponds and by using enclosed photobioreactors. Photobioreactors design in a variety of configurations are currently used for algae cultivation. With reference to the investigations on CO<sub>2</sub>, many researchers observed that photobioreactors have been successfully used for producing large quantities of microalgal biomass (Molina Grima et al., 1999; Huntley & Redalje, 2006; Frac et al., 2009). The most common photobioreactors are: flat plate, thin-panel or tubular.

The diffusion of CO<sub>2</sub> from the air into the water is 0.03% that is too low for rapidly growing algae. The dissolving rate of gaseous CO<sub>2</sub> depends on temperature, pressure, bubble size, the state of saturation of the medium for CO<sub>2</sub> and the mixing. The continuous mixing is also very important in order to enhance nutrient distribution, to eliminate thermal stratification, to keep cells in suspension and to enhance light utilization efficiency (Suh & Lee, 2003). All of these parameters are connected to the types of cultivation system.

Open ponds systems for cultivation of algae can be categorized into natural waters (lakes, lagoons, ponds) and artificial ponds or containers. One of the disadvantages is that algae in

open culture system could be contaminated by predators and other fast growing heterotrophs. A typical raceway open pond system for algae cultivation is made of a closed loop recirculation channel. Circulation is provided by a paddlewheel that operates all the time to prevent sedimentation. Tubular photobioreactors and solar collectors are used for microalgal culture. For example, a tubular photobioreactor consists of an array of tubes that are usually made of plastic or glass (Chisti, 2007).

The most important advantages of enclosed photobioreactors are overcoming the problems of contamination and evaporation encountered in open ponds. Furthermore, the biomass productivity of photobioreactors is more higher than that of open pond. Algal biomass is about 30 times as concentrated as the biomass found in open pond. As a result, the harvest of biomass from photobioreactors is less expensive. Environmental control of important physico-chemical parameters (temperature, pH,  $p\text{CO}_2$ , etc.), effective sterilization of the system and easier maintenance of a monoculture are improved (Suh & Lee, 2003). However, enclosed photobioreactors are difficult to scale up.

Jorquera et al. (2010) performed comparative analyses of the energy life-cycle for production of biomass from the oil-rich microalgae *Nannochloropsis sp.*, using raceway ponds, tubular and flat plate photobioreactors in order to evaluate their feasibility. The researchers found that the use of horizontal tubular photobioreactors is not economically feasible. Furthermore, they concluded that both flat plate and raceway photobioreactors are economically feasible for mass cultivation of *Nannochloropsis sp.*

The ability of microalgae to attach to photobioreactors' walls constitutes an operational problem. Munoz et al. (2009) evaluate the potential of flat plate and a tubular photobioreactor with a an algal-bacterial biofilm, using a *Chlorella sorokiniana-Ralstonia basilensis* consortium immobilized onto the reactor walls for the treatment of industrial wastewaters. According to these researchers, the biomass immobilization maintain a high microbial activity at all operating conditions, protecting cells from pollutant toxicity and producing an effluent containing easily settleable microbial flocks. However, such type of photobioreactors have limitations that could restrict their widespread application, such as: photoinhibition in outdoors cultures, because of immobilized microalgae are constantly exposed to a high photon flux density and there is a risk of clogging due to biomass overgrowth.

Merchuk & Wu (2003) reviewed the mathematical model of the process of photosynthetic growth that integrates algal growth kinetics and fluid dynamics of the bubble column photobioreactor. Simulations carried out with the model allowed, by extrapolation, qualitative prediction of the expected behaviour of photobioreactors, such as: optimal column diameter, as a function of illuminance and gas superficial velocity in the bubble column. It also describes the dependence of photoinhibition on cell density and actual biomass decrease.

Each system has its advantages and disadvantages. In order to choose the best system the following factors such as the production costs, type of the desired products and the production quantity of the products should be considered.

## 6.2 Removal of air pollutants by algae

Flue gases from power plants are responsible for more than 7% of the total world  $\text{CO}_2$  emissions from energy use and industrial exhaust gases contains up to 15%  $\text{CO}_2$  (Mata, 2010). Chemical reaction-based approaches and the biological mitigation are the most

common CO<sub>2</sub> mitigation strategies. The capture of carbon dioxide produced by combustion of fossil fuels by amine scrubbing of the flue gases may be replaced by options such as membrane separation, molecular sieves or desiccant adsorption. The disadvantages of chemical reaction-based approaches are: energy-consuming, use costly processes, and have disposal problems of the wasted adsorbents. Furthermore, sequestration by direct injection into geologic or oceanic sinks also do not address issues of sustainability (Stuart & Hessami, 2005).

Many researchers recommend that micro-organisms capable of photosynthetic reactions may hold the key to reducing emissions in both an economically and environmentally sustainable manner. Stuart & Hessami (2005) found that a 4000 m<sup>3</sup> pond under natural daily light exposure cycles could sequester up to 2.2 ktonne of CO<sub>2</sub> per year.

Key advantages of the capture of CO<sub>2</sub> using algae are:

high purity CO<sub>2</sub> is not required for algae cultivation,  
combustion products, such as: NO<sub>x</sub> and SO<sub>x</sub> can be used as nutrients,  
the process has minimal negative impacts on the environment,  
cultivation of algae provide high value commercial products.

Chiu et al. (2008) cultured the marine microalga *Chlorella sp.* in a photobioreactor to assess biomass, lipid productivity and carbon dioxide reduction. They also determined the effects of cell density and CO<sub>2</sub> concentration on the growth of *Chlorella sp.* The researchers indicated that at CO<sub>2</sub> concentrations of 2%, 5%, 10% and 15%, the rate of CO<sub>2</sub> reduction was 0.261, 0.316, 0.466 and 0.573 g h<sup>-1</sup>, and efficiency of CO<sub>2</sub> removal was 58%, 27%, 20% and 16%, respectively. They concluded that efficiency of CO<sub>2</sub> removal was similar in the single photobioreactor and in the six-parallel photobioreactor. However, production of biomass, and production of lipid were six times greater in the six-parallel photobioreactor than those in the single photobioreactor. The researchers found that airstreams containing a high concentration of CO<sub>2</sub> (2–15%) may be introduced directly into a high-density culture of *Chlorella sp.* in a semicontinuous photobioreactor. The maximum efficiency of CO<sub>2</sub> reduction reached 58% in the culture aerated with 2% CO<sub>2</sub>. The greatest mass of CO<sub>2</sub> that was reduced (17.2 g L<sup>-1</sup> d<sup>-1</sup>) occurred at 15% CO<sub>2</sub>. The results obtained by the authors indicated that productivity and efficiency of CO<sub>2</sub> reduction did not decrease when a parallel (multiple units) photobioreactor was used.

Sung et al. (1999) determined the tolerance of *Chlorella sp.* KR-1 strain to high concentrations of CO<sub>2</sub>. The investigators observed the maximum growth at 10% CO<sub>2</sub> and a good growth rate up to 50% CO<sub>2</sub>. They indicated the feasibility of the KR-1 strain for mass cultivation using condensed stack gases.

Morais & Costa (2007) added CO<sub>2</sub> at different concentrations to cultures of the eukaryotic microalgae, *Chlorella kessleri*, *C. vulgaris* and *Scenedesmus obliquus*, and the prokaryotic cyanobacterium, *Spirulina sp.* The experiment was conducted in flasks and in a photobioreactor. The researchers found that the best kinetics and carbon fixation rate were with a vertical tubular photobioreactor. Overall, *Spirulina sp.* had the highest rates. *Spirulina sp.*, *Sc. obliquus* and *C. vulgaris* could grow with up to 18% CO<sub>2</sub>. The obtained results demonstrate that these three species could be used to mitigate the effects of CO<sub>2</sub> by reducing emissions of flue effluents.

Cheng et al. (2006) studied carbon dioxide removal from air by microalgae cultured in a membrane-photobioreactor. They found that the photosynthetic CO<sub>2</sub> fixation was strongly dependent on the concentration of CO<sub>2</sub> continuously provided during the algal growth.

Furthermore, the researchers concluded that compared to that in the ordinary photobioreactor, the CO<sub>2</sub> fixation capacity in the membrane-photobioreactor was enhanced from 80 to 260 mg L<sup>-1</sup> h<sup>-1</sup>. However, membrane modules must resolve some problems with fouling and pressure resistance to make sure that high mass transfer rates are maintained for extended periods of operation.

Jacob-Lopes et al. (2008) studied the integral method for the analysis of kinetic data to describe the removal of carbon dioxide dissolved in the aqueous phase of a tubular photobioreactor by cyanobacteria *Aphanothece microscopica Nageli*. The effects of the carbon dioxide concentration (3, 15, 25, 50 and 62%), light intensity (960, 3000, 6000, 9000 and 11,000 lux) and temperature (21.5, 25, 30, 35 and 38.5°C) were considered. The researchers indicated that sequestering CO<sub>2</sub> by way of the formation of carbonates and bicarbonates is limited by the concentration of OH<sup>-</sup> ions present in the aqueous phase of the reactors, caused by the establishment of chemical equilibrium. In case of using microalgae, the alkaline environment is provided by the action of the microbial metabolism responsible for the transport of hydroxide ions to the outside of the cell using a reaction catalysed by the enzyme carbonic anhydrase, associated with the capture of H<sup>+</sup> ions for the interior of the thylakoid membranes, resulting in the production of highly alkaline environments with consequently very efficient CO<sub>2</sub> fixation capacity.

Jacob-Lopes et al. (2010) performed laboratory experiments to study the capacity of CO<sub>2</sub> sequestration and carbon fixation into biomass during the cultivation of the cyanobacteria *Aphanothece microscopica Nageli* in refinery wastewater. The influence of the photoperiod (day/night) on the rates of CO<sub>2</sub> sequestration and O<sub>2</sub> release was also determined. Rates of CO<sub>2</sub> sequestration were measured both in the liquid and gaseous phases. The researchers found that both methodologies used are adequate for measuring CO<sub>2</sub> sequestration rates in photobioreactors.

Measurements in the gaseous phase detected a maximum CO<sub>2</sub> sequestration rate of 18.7 ± 0.5 mg/L/min and a maximum O<sub>2</sub> release rate of 16.0 ± 0.7 mg/L/min at 96 h of cultivation in the continuous illumination experiment. A strong impact on the gases exchange was observed during cultivations in intermittent light regime, since photosynthetic and heterotrophic metabolisms are occurring in the system. The operation of the system in this condition resulted in a loss of 78% and 65% on the CO<sub>2</sub> sequestration and O<sub>2</sub> release capacity, respectively. It was demonstrated that only a small fraction of the total CO<sub>2</sub> sequestered was effectively fixed into the microalgal biomass (3.1 ± 0.05% in average terms). Since the ratio between the CO<sub>2</sub> sequestration and O<sub>2</sub> release rates followed the theoretical photosynthetic value, it was possible to determine that biological sequestration routes were predominant in the photobioreactor rather than physicochemical routes. Possible biological sequestration routes include the excretion of biopolymers and the release of VOCs. These biotransformations of carbon dioxide seem to be the most important sequestration process in microalgal photobioreactors.

The rates of CO<sub>2</sub> capture by algae depends on many factors. Generally, types of photobioreactors, microalgae species and environmental control of important physicochemical parameters are the main factors influencing the process. Molecular engineering can be used to increase photosynthetic efficiency to enable increased biomass yield. There is also a need to improve temperature tolerance and reduction of photoinhibition that reduces

growth rate. Further efforts on microalgae production should also be focused on reduction costs in cultivating systems and optimization of the microalgae harvesting. Furthermore, developing an efficient oil-extraction method is also a need. The future research should also be focused on developing new technologies or improving existing ones.

## 7. Removal of air pollutants by plants

It has long been known that plants – mostly trees, shrubs and grasses– can significantly improve the quality of air in urban and rural areas by reduction and/or removal of such pollutants like sulphur dioxide, nitrogen oxides, carbon monoxide and particulates or other pollutants like airborne fluoride. The mechanism of air pollutant removal is mostly dry deposition. The gaseous and particulate pollutants are absorbed by plants through their surfaces. For example nitrogen dioxide and sulphur can be absorbed by plant tissue with carbon dioxide during photosynthesis. Then, the pollutants can be transferred and assimilated by the plant tissue. As for the particulates they can sediment on the plant surface, and then depending on the density and atmospheric conditions (i.e. wind, rainfall, etc.) they can be washed off, suspended again in the air and transported, or they can drop on the ground e.g. with the plant leaves. Due to various conditions (e.g. atmospheric conditions, vegetation) trees can have different abilities for removal air pollutants (Jim & Chen, 2008).

According to the investigations on the removal of air pollutants such as O<sub>3</sub>, PM<sub>10</sub>, NO<sub>2</sub>, SO<sub>2</sub>, CO by trees on the US urban area, the annual removal was estimated at 711,000 tones (Nowak et al., 2006). Indeed, trees can improve the quality of air by reducing or removing some air pollutants, however it has to be pointed out that some trees can emit biogenic volatile compounds (VOCs) such as monoterpene and isoprene, and in consequence they may have a negative impact on the air quality.

## 8. Removal of air pollutants in biofilters

Biofiltration is a pollution control method for removal of air pollutants, such as volatile organic compounds and also inorganic compounds (e.g. hydrogen sulfide, ammonia) from airstreams in reactors filled with solid media bed where the pollutants are absorbed/desorbed and oxidized by indigenous microorganisms. The pollutants can be converted to carbon dioxide through microbial activity due to the fact that most odorants present in airstreams from various facilities are biodegradable (Haug, 1993; Deshusses, 1997; Otten et al., 2002).

This method is suitable for treatment of polluted air streams with high volumetric rates and low concentrations of pollutants (Fazaelipoor, 2009). The advantages of biofiltration are: low costs, reliability, public acceptance and environmental friendliness. It can be performed at ambient temperature and does not generate any nitrogen oxides (Deshusses, 1997). However, the efficiency of biofiltration can be affected by excessive loading rates, poor airflow distribution through a biofilter bed, insufficient moisture in a biofilter and uneven distribution of gasses in the treated airstream (Haug, 1993).

Biofiltration occurs through many biological and physicochemical processes and depends on a number of various factors. Therefore in order to obtain high efficiencies of biofiltration the following parameters should be controlled: operating temperature (ambient 15-3540°C or for the maximum degradation rates it should be about 40°C), moisture content (about 60% w.b.), pH (7 to 8,5) air humidity (about 95%), air flow rate (less than 100 m<sup>3</sup>/h\*m<sup>2</sup>), depth of a biofilter bed (0,5 to 1,5 m high biofilters are used) (Haug, 1993; Otten et al., 2002).

Biofilters were primarily applied to control odors from wastewater treatment plants and composting facilities which emitted off-gasses from biological treatment of wastewater and organic waste. Most recently they are used for other industrial applications. The polluted airstream is humidified and then passed through a reactor column – a packed material with specific microorganisms which are immobilized on the surface of material particles – where the pollutants are degraded by microorganisms present on the surface of solid particle (Haug, 1993; Fazaelpoor, 2009). The types of biofilters can vary significantly. They can be engineered as open or close systems with various media and also multiple beds. Biofiltration media should have high surface area, air and water permeability, water holding capacity, active microbial population and low costs. The materials used for biofiltration include soil, compost, peat, bark, etc. or a mixture of various substrates. They should be biologically active, porous with the void volume about 75-90%, resistant to compaction and contain organic matter (less than 60%) as a source of nutrients (Haug, 1993). Otten et al. investigated compost and perlite mixtures used for biofiltration of butyric acid. The biofilter composed of compost and perlite media showed higher resistance to compaction and higher porosity. The removal efficiency was almost 100%. Pagans et al. (2007) applied compost as a biofilter for simultaneous removal of ammonia and volatile organic compounds emitted from a composting facility. The efficiency of ammonia and VOC removal were about 94,7% and 82%, respectively. Luo & Linsdey (2005) investigated pilot-scale biofilters for odor control at a rendering plant. As a biofiltration media they used crushed pine bark and a mixture of crushed bark and zeolite. The efficiency of odor removal was in the range of 80% to 99%.

## 9. Conclusion

Living organisms such as microorganisms, plants or animals in their natural habitat have a great potential for the protection of atmospheric air. Since many of living organisms demonstrate bioindication and/or bioaccumulation abilities, they can be employed for biomonitoring of air pollution and removal of various pollutants from the atmosphere. Biomonitoring of air pollution allows for determination of direct biological effects of air pollutants, and therefore it provides an early warning of air quality changes. Moreover, biomonitoring is cost-efficient and as such can be an alternative or complementary tool for analytical methods. Successful biomonitoring approach requires the selection of a suitable biological indicator with a known cause-effect or exposure-response relationship to various air pollutants, designing the observation network and developing a sampling method. In coming years programs for biomonitoring of air pollution will need further development in terms of environmental policies, regulations and methodologies which will assure obtaining statistically reliable data comparable on many levels, such as local, regional or international. Due to the ability to accumulate various air pollutants, many living organisms can be used to reduce the concentration of pollutants in the atmosphere or to mitigate the effects of air

pollution. In recent years, there is an increased interest in biosystems which can integrate the processes for removal of pollutants from atmosphere or industrial airstreams and production of high value products. Such systems can employ algae which are currently being extensively investigated. Industrial airstreams polluted with gaseous substances can be treated in a wide variety of biofilters which demonstrate high removal efficiencies. Plant species such as trees, shrubs or grasses can significantly reduce the exposure to air pollutants, and therefore they should be included in the architecture of urban, suburban and rural areas. As a result of gradual deterioration of air quality and the occurrence of emerging pollutants, many technologies for air protection which employ living organisms will need further development and improvement.

## 10. References

- Batzias, F. & Siontorou C.G. (2007). A novel system for environmental monitoring through a cooperative/synergistic scheme between bioindicators and biosensors. *Journal of Environmental Management*, No. 82, pp. 221-239
- Benneman, J.R. (1997). CO<sub>2</sub> mitigation with microalgae systems. *Energy Convers. Mgmt*, Vol. 38, SS475-S479
- Braun, A.R. (1996). Re-use and fixation of CO<sub>2</sub> in chemistry, algal biomass and fuel substitutions in the traffic sector. *Energy Convers. Mgmt*, Vol. 37, Nos 6-8, 1229-1234
- Brunekreef, B., Holgate, S.T. (2002). Air pollution and health. *The Lancet*, Vol. 360, pp. 1233-1242
- Cheng, L.; Zhang, L.; Chen, H. & Gao, C. (2006). Carbon dioxide removal from air by microalgae cultured in a membrane-photobioreactor. *Separation and Purification Technology*, Vol. 50, 324-32
- Chisti, Y. (2007). Biodiesel from microalgae. *Biotechnology Advances*, Vol. 25, 294-306
- Chiu, S-Y.; Kao, C-J.; Chen, C.H.; Kuan, T-C.; Ong, S-C. & Lin, C-S. (2008). Reduction of CO<sub>2</sub> by a high-density culture of *Chlorella sp.* in a semicontinuous photobioreactor. *Bioresource Technology*, Vol. 99, 3389-3396
- Costa, C.J.; Marques, A.P.; Freitas, M.C.; Reis, M.A.; Oliveira, O.R. (2002). A comparative study for results obtained using biomonitors and PM10 collectors in Sado Estuary. *Environmental Pollution*, No. 120, pp. 97-106
- Deshusses, M.A. (1997). Biological waste air treatment in biofilters. *Current Opinion In Biotechnology*, No. 8, pp. 335-339
- Fazaelipoor, M.H. (2009). Analysis of a dual liquid phase biofilter for the removal of hydrophobic organic compounds from airstreams. *Chemical Engineering Journal*, No. 147, pp. 110-116
- Fraç, M.; Jezierska-Tys, S. & Tys, J. (2009). Algi-Energia jutra (biomasa, biodiesel). *Acta Agrophysica*, Vol.13, No 3, 627-638
- Grantz, D.A.; Garner, J.H.B.; Johnson, D.W. (2003). Ecological effects of particulate matter. *Environmental International*, No. 29, pp. 213-239
- Haug, T.R. (1993). *The practical handbook of compost engineering*, Lewis Publishers, ISBN 0-87371-373-7, USA
- Huntley, M.E. & Redalje, D.G. (2006). CO<sub>2</sub> mitigation and renewable oil from photosynthetic microbes: a new appraisal. *Mitigation and adaptation strategies for global change*. Springer 2006, 1-36

- Ilgén, E.; Karfich, N.; Levsen, K.; Angerer, J.; Schneider, P.; Heinrich, J.; Wichmann, H.E.; Dunemann, L.; Begerow, J. (2001). Aromatic hydrocarbons in the atmospheric environment: Part I. Indoor versus outdoor sources, the influence of traffic. *Atmospheric Environment*, No. 35, pp. 1235-1252
- Jacob-Lopes, E.; Scoparo, C.H.G. & Franco, T.T. (2008). Rates of CO<sub>2</sub> removal by *Aphanothece microscopica Nageli* in tubular photobioreactors. *Chemical Engineering and Processing*, Vol. 47, 1371-1379
- Jacob-Lopes, E.; Scoparo, C.H.G.; Queiroz, M.I. & Franco, T.T. (2010). Biotransformations of carbon dioxide in photobioreactors. *Energy Conversion and Management*, Vol. 51, 894-900
- Jim, C.Y. & Chen, W. Y. (2008). Assessing the ecosystem service of air pollutant removal by urban trees in Guangzhou (China). *Journal of Environmental Management*, No. 88, pp. 665-676
- Jorquera, O.; Kiperstok, A.; Sales, E.A.; Embirucu, M. & Ghirardi, M.L. (2010). Comparative energy life-cycle analyses of microalgal biomass production in open ponds and photobioreactors. *Bioresource Technology*, Vol. 101, 1406-1413
- Klumpp, A.; Ansel, W.; Klumpp, G.; Vergne, P.; Sifakis, N.; Sanz, M.J.; Rasmussen, S.; Ro-Paulsen, H.; Ribas, A.; Penuelas, J.; Kambezidis, H.; Garrec, J.P.; Calataguad, V. (2006). Ozone pollution and ozone biomonitoring in European cities Part II. Ozone induced plant injury and its relationship with descriptors of ozone pollution. *Atmospheric Environment*, No. 40, pp. 7437-7448
- Lam, P.K.S. & Gray, J.S. (2003). The use of biomarkers in environmental monitoring programmes. *Marine Pollution Bulletin*, No. 46, pp. 182-186
- Luo, J. & Lindsey, S. (2005). The use of pine bark and natural zeolite as biofilter media to remove animal rendering process odours. *Bioresource Technology*, No. 97, pp. 1461-1469
- Mata, T.M.; Martins, A.A. & Caetano, N.S. (2010). Microalgae for biodiesel production and other applications: A review. *Renewable and Sustainable Energy Reviews*, Vol. 14, 217-232
- McGeoch, M.A. & Chown, S.L. (1998). Scaling up the value of bioindicators. *TREE*, Vol. 13, No.2, pp. 46-47
- Merchuk, J.C. & Wu, X. (2003). Modeling of photobioreactors: Application to bubble column simulation. *Journal of Applied Phycology*, Vol. 15, 163-169
- Merkert, B. (2008). From monitoring to integrated observation of the environment - the multi-markered bioindication concept. *Ecological Chemistry & Engineering S*, Vol. 15, No. 3, pp. 315-333
- Molina Grima, E.; Acien Fernández, F.G.; García Camacho, F. & Chisti, Y. (1999). Photobioreactors: light regime, mass transfer, and scaleup. *J. Biotechnol.*, Vol. 70, 231-47
- Morais, M.G. & Costa, J.A.V. (2007). Carbon dioxide fixation by *Chlorella kessleri*, *C. vulgaris*, *Scenedesmus obliquus* and *Spirulina sp.* Cultivated in flasks and vertical tubular photobioreactors. *Biotechnol Lett.*, Vol. 29, 1349-1352
- Munoz, R.; Kollner, C. & Guieysse, B. (2009). Biofilm photobioreactors for the treatment of industrial wastewaters. *Journal of Hazardous Materials*, Vol. 161, 29-34
- Nowak, D.J.; Crane, D.E. & Stevens, J.C. (2006). Air pollution removal by urban trees and shrubs in the United States. *Urban Forestry & Urban Greening*, Vol. 4, No. 3-4, pp. 115-123

- Otten, L.; Afzal, M.T.; Mainville, D.M. (2004). Biofiltration of odours: laboratory studies using butyric acid. *Advances in Environmental Research*, No. 8, pp. 397-409
- Pacheco, A.M.G.; Barros, L.I.C.; Freitas, M.C.; Reis, M.A.; Hipo'lito, C.; Oliveira, O.R. (2002). An evaluation of olive-tree bark for the biological monitoring of airborne trace-elements at ground level. *Environmental Pollution*, No. 120, pp. 79-86
- Packer, M. (2009). Algal capture of carbon dioxide; biomass generation as a tool for greenhouse gas mitigation with reference to New Zealand energy strategy and policy. *Energy Policy*, Vol. 37, 3428-3437
- Piritsos, S.A. & Loppi, S. (2008). Biomonitoring atmospheric pollution: the challenge of times in environmental policy on air quality. *Environmental Pollution*, No. 151, pp. 269-271
- Rodriguez-Mozaz, S.; Lopez de Alda, M.J.; Marco, M-P.; Barcel, D. (2005). Biosensors for environmental monitoring. A global perspective. *Talanta*, No. 65, pp. 291-297
- Schroeder, W. & Pesch, R. (2007). Synthesizing bioaccumulation data from the German metals in mosses surveys and relating them to ecoregions. *Science and the Total Environment*, No. 372, pp. 311-327
- Shakya, K.; Chettri, M.K.; Sawidis, T. (2004). Appraisal of some mosses for biomonitoring airborne heavy metals. *Ecoprint. An International Journal of Ecology*, Vol. 2, No. 1, pp. 35-49
- Sierra, E.; Acien, F.G.; Fernandez, J.M.; Garcia, J.L.; Gonzalez, C. & Molina, E. (2008). Characterization of a flat plate photobioreactor for the production of microalgae. *Chemical Engineering Journal*, Vol. 138, 136-147
- Stuart C. & Hessami M-A. (2005). A study of methods of carbon dioxide capture and sequestration—the sustainability of a photosynthetic bioreactor approach. *Energy Conversion and Management*, Vol. 46, 403-420
- Suh, I.S. & Lee, C-G. (2003). Photobioreactor engineering: Design and performance. *Biotechnology and Bioprocess Engineering*, Vol. 8, 313-321
- Sung, K.D.; Lee, J.S.; Shin, C.S. & Park, S.C. (1999). Isolation of a new highly CO<sub>2</sub> tolerant fresh water microalga *Chlorella sp.* KR-1. *Renewable Energy*, Vol.16, 1019-1022
- Telesiński, A. & Śnioszek, M. (2009). Bioindykatory zanieczyszczenia środowiska naturalnego fluorem. *Bromatologia i Chemia Toksykologiczna*, No. 4, pp. 1148-1154
- Usui, N. & Ikenouchi, M. (1997). The biological CO<sub>2</sub> fixation and utilization project by RITE(1) – Highly-effective photobioreactor system. *Energy Convers Mgnt.* Vol. 38, S487-S492
- Van Leeuwen, R.F.H. (2002). A European perspective on hazardous air pollutants. *Toxicology*, No. 181-182, pp. 355-359
- Vestreng, V.; Myhre, G.; Fagerli, H.; Reis, S.; Tarrason, L. (2007). Twenty-five years of continuous sulphur dioxide emission reduction in Europe. *Atmospheric Chemistry & Physics*, No. 7, pp. 3663-3681
- Vineis, P. & Husgafvel-Pursiainen, K. (2005). Air pollution and cancer: biomarkers studies in human populations. *Carcinogenesis*, Vol. 26, No. 11, pp. 1846-1855
- Wolterbeek, B. (2002). Biomonitoring of trace element air pollution: principles, possibilities and perspectives. *Environmental Pollution*, No. 120, pp. 11-21
- Woodward, F.I.; Bardegett, R.D.; Ravena J.A.; Hetherington, A.M. (2009). Biological approaches to global environment review: change, mitigation and remediation. *Current Biology*, No. 19, pp. 615-623



# Urban air pollution forecasting using artificial intelligence-based tools

Min Li<sup>1,2</sup> and Md. Rafiul Hassan<sup>1</sup>

*<sup>1</sup>Department of Computer Science and Software Engineering,  
Melbourne School of Engineering,*

*<sup>2</sup>Centre for Women's Health, Gender and Society, Melbourne School of Population Health,  
The University of Melbourne, Carlton 3010,  
Victoria, Australia*

racli@unimelb.edu.au

mrhassan@csse.unimelb.edu.au

## 1. Introduction

The detrimental effects of urban air pollution (UAP) have been represented as growing problems in recent years (Per Nafstad et al, 2004; World Health Organization). The harm represented by air pollution has been largely demonstrated from the impacts on human health and well being, such as asthma, eye irritation and even cancer (Nyberg F et al., 2000; J. Sunyer et al., 1997). Thus, the studies on specifying the pollution sources and analyzing concentrations of airborne pollutant variables are addressed sedulous attention by environmentalists and computer scientists. In order to prevent any further decline in air quality, to develop tools for air pollution control by introducing alternatives to existing practices is necessary.

Over the last decade, artificial intelligence (AI) based techniques have been proposed as alternatives to traditional statistical ones on forecasting UAP (Mikko Kolehmainen et al., 2000). Air pollution phenomena have been measured by using physical reality as the start point. And then, for example, these data traditionally has been coded into differential equations. However, these kinds of techniques have limited accuracy due to their inability to predict extreme events (Mikko Kolehmainen et al., 2000; Yilmaz Yildirim & Mahmut Bayramoglu, 2006). Comparing the traditional approaches, the models which are constructed in AI can be entirely based on these traditional measure data to forecast UAP. AI is a branch of scientific research enabling a structure to simulate intelligent behavior in computers. It is able to make a system deal with cognitive uncertainties in a manner more like human beings (Nils J. Nilsson., 1998). Thus, using AI techniques for modeling and forecasting can promote the development on UAP research.

There are several AI techniques which have been proposed as feasible and reliable ways for UAP forecasting, such as artificial neural networks (ANNs) (Harri Niska et al., 2004),

support vector machines (SVMs) (Wei-Zen Lu & Wen-Jian Wang, 2005) and fuzzy logic (FL) (Francesco Carlo Morabito & Mario Versaci, 2003). ANNs are as simplified mathematical models of brain-like systems (Dahe Jiang et al., 2004). This kind of techniques can learn the associations, functional dependencies and patterns by generalizing training data (Yilmaz Yildirim & Mahmut Bayramoglu, 2006; W. Z. Lu et al., 2002). ANNs have been used on detecting pollution sources, such as carbon monoxide (CO) (A.B.Chelani & S.Devotta, 2007; Ming Cai et al., 2009; Patricio Perez et al., 2004), particles measuring  $10\mu\text{m}$  or less ( $\text{PM}_{10}$ ) (Jef Hooyberghs et al., 2005; Patricio Perez & Jorge Reyes, 2006) and sulfur monoxide (SO) (U. Brunelli et al., 2007). Although ANN is regarded as one of the most popular AI methods on environmental researches, their inherent drawbacks (Wei-Zen Lu & Wen-Jian Wang, 2005), e.g., getting over-fitted into the training rules, can stuck in a local minima during training, poor generalization performance, determination of the appropriate network architecture, etc, impede the practical applications. The kernel-based hyper plane separation technique as SVM is another reliable and cost-effective AI technique (Wei-Zen Lu & Wen-Jian Wang, 2005) for classification and regression. For instance, it is built for predicting whether a new example belongs to one category or the other within a two categories' dataset. Although SVM has many potential problems as a new forecasting tool, there are only a few studies where SVMs has been reported to perform well by some promising results, e.g., SVM is superior to the conventional radial basis function (RBF) network in predicting air quality parameters with different time series.

Compared to other AI techniques, FL can offer a clear insight into the model for forecasting (Giorgio Corani, 2005). FL is a form of multi-valued logic to deal with reasoning that is approximate rather than precise. For example, it can be used on description of metrological impacts on UAP species (Oleg M. Pokrovsky et al., 2002; Md. Rafiul Hassan 2009; Md. Rafiul Hassan et al., 2007). However, FL suffers from the computational complexity associated with handling a large number of initially generated inappropriate rules, and thereby its interpretability is reduced (Md. Rafiul Hassan 2009).

A Hidden Markov model (HMM) is a classic approach for time series phenomena analysis and prediction. It has been widely used in the fields like DNA sequencing and speech recognition (Behzad Zamani et al. 2010). A significant hypothesis on HMM is based on the relationships between the attributes of particular data items in the dataset considered. Recently, Rafiul Hassan has developed a hybrid tool of HMM with fuzzy logic for time series forecasting (Md. Rafiul Hassan 2009; M. Maruf Hossan et al. 2008).

Contribution to the book chapter: The aim of this book chapter is to analysis the existing AI methodologies for UAP forecasting. In order to achieve this, the following approaches have been developed:

- We represented and summarized previous research on AI-based tools for UAP forecasting. This research is based on the analysis of current reliable AI methodologies which have already been used on predicting UAP.
- Based on Md. R. Hassan's previous research, we describe a HMM-FL model which combines the HMM's data pattern identification method to the generation of fuzzy logic for the prediction of UAP time series data. The dataset of testing  $\text{PM}_{10}$  was introduced for experiment and results analysis.

- We compared the AI based tools which we described on this book chapter, and analysis their results on UAP forecasting.

Organization of the book chapter: This book chapter is organized as five sections. The introduction is provided in Section 1. We have introduced our topic, 'UAP forecasting Using AI-Based Tools', and described why using AI-based tools for UAP forecasting is important in this section. The contributions to this book chapter are presented from Section 2 to Section 4. Research on AI-based tools for UAP forecasting is described in Section 2. Then, Section 3 is designed for representing HMM-FL model. We briefly introduced some related principles and algorithms firstly, such as HMM and Fuzzy rules. Then, we construct HMM-FL model for predicting UAP time series. Section 4 is on experiment and comparison analysis. Furthermore, Section 5 is the discussion and conclusion of the whole book chapter.

## 2. Previous AI-based Methodologies for UAP Forecasting

In this section, we review some of the significant AI based methodologies which has been designed for forecasting UAP. Some of them combined AI methods, such as ANN, SVM and FL, with other methods. A chronological list of the major developments is preset in Table 1.

As one of the most compromising AI methods in estimation of environmental complex air pollution problems, ANN has been used by many scientists, such as (Ulku Sahin et al., 2005) and (P. Viotti et al., 2002). In the study of Ulku Sahin et al., ANN approach was used for predicting SO<sub>2</sub> concentration in Bahcelievler region. In this paper, the results were used to compare to nonlinear regression for actual measured values (Ulku Sahin et al., 2005). By comparing maximum and minimum values of observed SO<sub>2</sub> which were predicted by ANN model and nonlinear regression respectively, the results which are from ANN are quite realistic. P. Viotti et al's paper is another good example of using KNN for forecasting air pollution time series. ANN is the main technique to predict short and middle long-term concentration levels for some of the well-known pollutants in the city of Perugia. P. Viotti et al. reported in their study that the ANN has given great results in the middle and long-term forecasting of almost all the pollutants, although the ANN forecasts appear to be worse than the 1-hour ones.

| Authors                           | Forecasting Models and techniques                           | Challenges   | Datasets   | Results/Comments  |
|-----------------------------------|---|--|--|---|
| Ulku Sahin, et al., 2005          | ANN   | Focus on modelling of SO <sub>2</sub> distribution and predicting its future concentration                                 | Meteorological variable and SO <sub>2</sub> concentrations from Istanbul-Florya meteorological station and Istanbul-Yenibosna air pollution station                  | There is an optimum correlation between input-output variables with the correlation parameter which are 0.999 and 0.528 for training and test data. |
| P. Viotti, et al., 2002           | Various ANN models  | To forecast short and middle long-term concentration levels for some of the well-known pollutants                          | Variables monitored in Perugia, particularly for the area of Fontivegge  | The ANN is able to give good results in the middle and long-term forecasting of almost all the pollutants.  |
| Wei-Zhen Lu & Wen-Jian Wang, 2005 | A support vector machine (SVM) model                        | To examine the feasibility of applying SVM to predict air pollutant levels in advancing time series                        | An air pollutant database in Hong Kong downtown area   | SVM model provides a promising alternative and advantage in time series forecast.   |
| Oleg M. Pokrovsky, et al., 2002   | FL based model  | To study the impact of meteorological factors on the evolution of air pollutant levels and to describe them quantitatively | The developed model is based on simulation of diurnal cycles of principal meteorological variables and the corresponding diurnal patterns of various air pollutants. | Fuzzy analysis is used for extreme-event prediction and it displays a very simple approach to find a solution of the state problem.                 |
| Luis A. Diaz-Robles, et al., 2008 | A hybrid model combining Box-jenkins (ARIMA) method and ANN | To improve forecast accuracy for an area with limited air quality and meteorological data.                                 | Hourly and daily time series of PM <sub>10</sub> and meteorological data during 2000-2006 at the Las Encinas monitoring station in Temuco.                           | The hybrid model was able to capture 100% and 80% of alert and pre-emergency episodes, respectively.  |

Table 1. Some Previous AI-based Methodologies for UAP Forecasting at a Glance

| Authors                                   | Forecasting Models and techniques   | Challenges   | Datasets   | Results/Comments  |
|---|---|--|--|---|
| Giorgio Corani., 2005                     | Feed-forward neural networks (FFNNs), pruned neural networks (PNNs) and lazy learning (LL)  | Prediction of ozone and PM <sub>10</sub> .   | A dataset related to ozone and PM <sub>10</sub> which are the major concern for air quality of Milan.  | Compared to the other methods which use FFNN and PNN, the LL predictor can be quickly designed, and it can be also easily kept up-to-date.                          |
| Yilmaz Yildirim & Mahmut Bayramoglu, 2006 | An adaptive neuro-fuzzy logic model   | To estimate the impact of meteorological factors on SO <sub>2</sub> and total suspended particulate matter (TSP) pollution levels.               | Datasets based on SO <sub>2</sub> and TSP detection in Zonguldak city (Turkey).  | The model forecasts satisfactorily the trends in SO <sub>2</sub> and TSP concentration levels, with performance between 75-90% and 69-80%, respectively.            |
| Mikko Kolehmainen, et al., 2000           | A model using the Self-Organizing Map (SOM) algorithm, Sammon's mapping and fuzzy distance metrics. Overlapping Multi-Layer Perceptron (MLP) models were applied to the clustered data. | By using airborne pollutant, meteorological and timing variable to develop a form of air quality modelling which can forecast urban air quality. | The data applied to the city of Kuopio during the years 1995-1997.   | The modelling of gaseous pollutants is more reliable than that of particles.  |
| M. Maruf Hossain, et al., 2008            | A hybrid approach of Hidden Markov Model (HMM) with fuzzy logic   | To model hourly air pollution at a location related to its traffic volume and meteorological variable.   | A dataset that was originally put together as part of a study on air pollution related to traffic volume and meteorological variables on a road, conducted by the Norwegian Public Roads Administration. | The HMM-Fuzzy model is effectively able to model an hourly air pollution forecasting system, compared to other common tools which are based on ANN and fuzzy logic. |

Table 1. Some Previous AI-based Methodologies for UAP Forecasting at a Glance (Continued)

Among the fewer models which are based on SVMs, Wei-Zhen Lu, et al. (Wei-Zen Lu & Wen-Jian Wang, 2005; Wei-Zen Lu et al., 2004) introduced an SVM methodology for UAP forecasting. This study examined the feasibility of applying SVM to predict air pollutant level in advancing time series based on the monitored air pollutant database in Hong Kong downtown region. In this methodology, the SVM was firstly trained by data sets selection from the original dataset. Then, the SVM were used again for forecasting the pollutant levels in different time series. Results of the comparisons in forecasting between the SVM model and classical radial basis function (RBF) network show that SVM has a better generalization performance and superior to the conventional RBF network in predicting air quality parameters.

Besides ANN and SVM, FL approach for UAP forecasting has been developed recently. For example, in Oleg M. Pokrovsky et al.'s study (Oleg M. Pokrovsky et al., 2002), a FL based method has been used to model the impact of meteorological factors on the evolution of air pollutant levels and to describe them quantitatively. The model is based on simulation of diurnal cycles of principal meteorological categories, such as wind speed and direction, and the corresponding diurnal patterns of air pollutants, such as O<sub>3</sub>. Another found from the research is that UAP phenomena can be simulated by sequences of its conservation inside some fuzzy sets and the transition from one fuzzy set to another. Thus, the development of the transition rules should be important in these kinds of cases.

Compared to above AI-based methodologies which are all used as single AI tools for UAP detection, AI-based methodologies are always combined with some other methods. Luis A. Diaz-Robles, et al. (Luis A. Diaz-Robles, et al., 2008) constructed a hybrid Box-Jenkins Time Series (ARIMA) and ANNs model to forecast particulate matter in urban areas which is the case of Temuco, Chile. Due to the inability of ARIMA to predict extreme events, the systems which based single ARIMA have limited accuracy. An improved forecasting accuracy was achieved by using the ARIMA and ANNs combined model. There is another model that predicts hourly NO<sub>x</sub> and NO<sub>2</sub> concentrations (Gardner and Dorling, 1999) and neural models for ozone concentrations (Comrie, 1997; Yi and Prytok, 1996) were constructed for UAP predicting. Most of these works have focused on comparing feed-forward neural networks with the traditional methodologies, such as the ARIMA model and linear regression.

Combination of several AI-based methodologies is another idea on UAP forecasting research. From the research of Giorgio Corani (Giorgio Corani, 2005), there are three models which have been combined for air quality prediction in Milan. They are feed-forward neural networks (FFNNs), pruned neural networks (PNNs) and lazy learning (LL). FFNN is currently recognized as state-of-the-art approach for statistical prediction of air quality, while PNNs and LL are two alternative approach derived from machine learning. They are all constructed for forecasting ozone and PM<sub>10</sub> which are the two major concerns for air pollution of Milan. From the results, it shows LL provides the best performances on indicators associated to average goodness of the prediction, such as correction, mean absolute error, etc. In addition, PNNs are superior to the other approaches in detecting the exceedances of alarm and attention thresholds.

Neuro-fuzzy methodology (S. Chiu, 1997) has been tested by many researchers for UAP prediction. Yilmaz Yildirim, et al. (Yilmaz Yildirim & Mahmut Bayramoglu, 2006) introduced an adaptive neuro-fuzzy logic method in their study. The adaptive neuro-fuzzy logic method is a hybrid of fuzzy logic and Neural-like architecture methodology. It is used to estimate the impact of meteorological factors on SO<sub>2</sub> and total suspended particulate matter (TSP) pollution levels over an urban area. The model forecasts satisfactorily the trends in SO<sub>2</sub> and TSP concentration levels, and their performance are between 75-90% and 69-80%, respectively (Yilmaz Yildirim & Mahmut Bayramoglu, 2006). Francesco Carlo Morabito et al. proposed a hybrid fuzzy neural model for predicting time series of pollutant concentration levels in urban air (Francesco Carlo Morabito, et al., 2003). Through the use of the fuzzy surface concept, the manageable model has been carried out for the reduction of the model. In order to manage the multidimensional state problem, the use of ellipsoidal rules has been tested by designing and compiling a software code.

The AI-based model which developed by Mikko Kolehmainen, et al. (Mikko Kolehmainen, et al., 2000), is a typical model which can forecast UAP for the next day using airborne pollutant, meteorological and timing variables. This model combines Self-Organising Map (SOM) algorithm, Sammon's mapping and fuzzy distance metrics. Firstly, the clusters of data were characterized by statistics. Then, several overlapping Multi-Layer Perceptron (MLP) models were used on these cluster data. After this, by using a combination of the MLP model, the actual levels for individual pollutants could be calculated.

Recently, Md. R. Hassan introduced a novel hybrid of HMM and Fuzzy Logic model to analysis time series data for UAP forecasting. This hybrid HMM-FL model has the potential to achieve high levels of performance on hourly air pollution forecasting system. This model is able to reduce complexity and simultaneously improved forecasting accuracy. Compared to other techniques, the efficiency of the HMM-FL model is higher than well-performed fuzzy rule finding methods and KNN. In order to introduce the HMM-FL model, some principles are described in the Section 3 (M. Maruf Hossain, et al., 2008).

### **3. The HMM-Fuzzy Combination Model**

#### **3.1 Preliminaries**

HMM-Fuzzy Model is combined HMM with Fuzzy Logic and Fuzzy Rule. In this section, we briefly introduce Hidden Markov Model (HMM), Fuzzy Logic (FL) and Fuzzy Rule.

##### **3.1.1 Hidden Markov Model**

A Hidden Markov Model (HMM) is a statistical model for modelling a wide range of time series data (Phil Blunsom, 2004). It is based on Markov process which is a time-varying random phenomenon for specific property holds. HMMs have been widely used in areas like speech, handwriting and gesture recognition (Lawrence R. Rabiner, 1989).

Figure 1 shows an example of a Markov process. It is a simple model for predicting air pollution. 'Clear', 'Mist' and 'Dirty' are used to represent the quality of air. 'High', 'Medium' and 'Low' are the percentage of pollutants in the air. In Markov process, 'Clear', 'Mist' and 'Dirty' are represented as states, while 'High', 'Medium' and 'Low' are index observations.

Assume the initial probability of getting 'Dirty' is 0.2. If given a sequence of observations: 'High-Low-Low', the state sequence is able to be identified as: 'Dirty-Clear-Clear'. Thus, the probability of the sequence in this case is  $0.2 \times 0.2 \times 0.3$ .

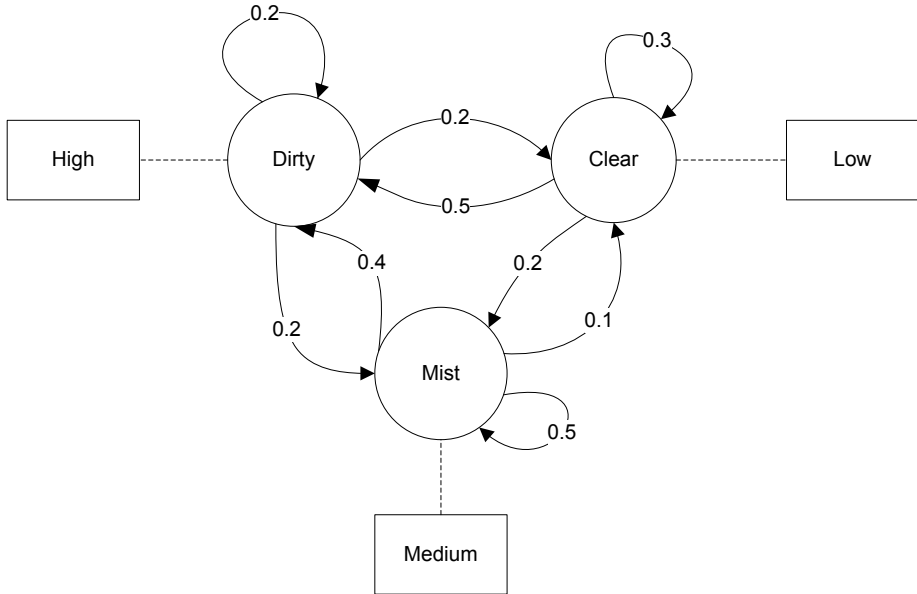


Fig. 1. Markov process example

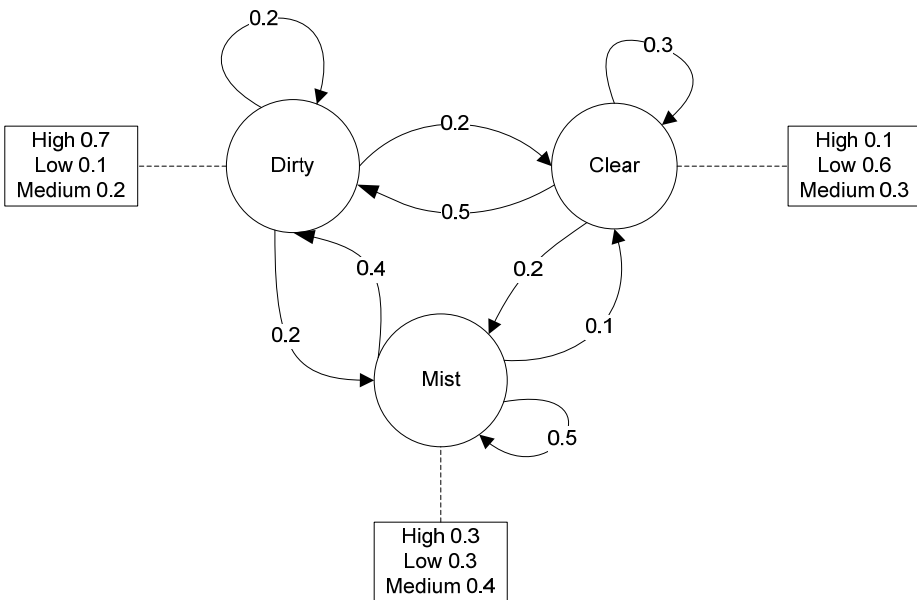


Fig. 2. Hidden Markov model example

Figure 2 depicts an example of how the previous model is able to be extended into a HMM. In this example, we could not detect exactly what state sequence ('High', 'Low' and 'Medium') is able to produce the observations ('Dirty', 'Clear' and 'Mist'). Because the state sequences are 'hidden', the state sequence that was most likely to have produced the observation could be calculated.

HMM can be described as the following equation:

$$\lambda = (A, B, \pi) \quad (1)$$

where  $\lambda$  represents HMM in equation (1).

A is a transition array, storing the probability of state  $j$  following state  $i$ . Note the state transition probabilities are independent of time:

$$A = [a_{ij}], a_{ij} = P(q_t = S_j \mid q_{t-1} = S_i) \quad (2)$$

B is the observation array, storing the probability of observation  $k$  being produced from the state  $j$ , independent of  $t$ :

$$B = [b_i(k)], b_i(k) = P(x_t = v_k \mid q_t = S_i) \quad (3)$$

$\pi$  is the initial probability array:

$$\pi = [\pi_i], \pi_i = P(q_1 = S_i). \quad (4)$$

S is our state alphabet set, and V is the observation alphabet set:

$$S = (S_1, S_2, \dots, S_N) \quad (5)$$

$$V = (V_1, V_2, \dots, V_M) \quad (6)$$

Q is defined to be a fixed state sequence of the length T, and O is the corresponding observations:

$$Q = q_1, q_2, \dots, q_T \quad (7)$$

$$O = o_1, o_2, \dots, o_T \quad (8)$$

Two assumptions are made by the model. The first, called the Markov assumption, states that the current state is dependent only on the previous state, which represents the memory of the model:

$$P(q_t \mid q_1^{t-1}) = P(q_t \mid q_{t-1}) \quad (9)$$

The independence assumption states that the output observation at time  $t$  is dependent only on the current state; it is independent of previous observations and states:

$$P(o_t | o_1^{t-1}, q_1^t) = P(o_t | q_t) \quad (10)$$

### 3.1.2 Fuzzy Logic and Fuzzy Rule

Fuzzy logic usually processes non-linear datasets by mapping input data (features) vectors into scalar output well. It is because that the fuzzy rules can be used to map the non-linear relationship between inputs and outputs. A fuzzy IF-THEN rule consists of an IF part (antecedent) and a THEN part (consequent) which can be shown as follows: (Sudhir Agarwal & Pascal Hitzler, 2005; Rouzbeh Shad et al, 2009)

**If** antecedent proposition **Then** consequent proposition

The antecedent is a combination of terms, while the consequent is exactly one term. In this standard syntax, a term is an expression of the form  $X=T$ , where  $X$  is a linguistic variable and  $T$  is one of its linguistic terms.

For example, a simple air pollution prediction that used the detection of percentage of  $PM_{10}$  in air looks like this:

IF the percentage of  $PM_{10}$  is High THEN the air is Dirty.

In this example, the linguistic variable is 'the percentage of  $PM_{10}$  is High', and its linguistic term is 'the air is Dirty'. In Hassan's paper, Takagi-Sugeno Fuzzy Model (TS) was used on predicting UAP.

A dynamic TS fuzzy model is described by a set of fuzzy "IF...THEN" rules with fuzzy sets in the antecedents and dynamic linear time-invariant systems in the consequents. A generic TS fuzzy rule can be written as follows:

$$i^{\text{th}} \text{ Rule: If } U \text{ is } M_j \text{ Then output is } (D_{j0} + D_{j1}u_1 + D_{j2}u_2 + \dots + D_{jk}u_k) \quad (11)$$

where  $U$  is the input data vector  $(u_1, u_2, \dots, u_k)$ , i.e.  $u_i \in U$ ,  $M_j$  is the set of membership functions  $M_{ji}$  for  $j^{\text{th}}$  rule, i.e.  $M_{ji} \in M_j$ ;  $M_{ji}$  is the membership function for  $i^{\text{th}}$  feature of  $j^{\text{th}}$  rule and  $D_{ji}$  represent linear parameters.

While  $(D_{j0} + D_{j1}u_1 + D_{j2}u_2 + \dots + D_{jk}u_k)$  is the output from an individual rule  $j$ , the output  $y$  from the all rules (assume  $c$  is the total number of fuzzy rules) is computed as follows:

$$\frac{\sum_{j=1}^c W_j y_j}{\sum_{j=1}^c W_j} \quad (12)$$

where,

$$W_j = \min_i M_{ji}(u) \quad (13)$$

$W_j$  represents the weight or firing strength of  $j^{\text{th}}$  rule for a data vector  $U$ , and  $M_{ji}(u)$  is the degree of membership for  $j^{\text{th}}$  rule and  $i^{\text{th}}$  feature of an attribute rule  $u$ .  $y_j$  is the output from  $j^{\text{th}}$  rule for data vector.

In fuzzy model, both the Mamdani and the TS model (Jun Young Bae et al., 2009; F. Khaber et al., 2006) can be used, because they are depending on the desired proposition and implication of the rule (Rouzbeh Shad et al., 2009). Compared to the Mamdani model which the consequent part is a fuzzy proposition, the TS model is a crisp function of the antecedent variables. Thus, TS model was used in the hybrid HMM and Fuzzy Logic model for it produces numerical output.

### 3.2 Hybrid HMM and Fuzzy Logic Model

In order to improve fuzzy rule generation, Hassan et al. have introduced a hybrid HMM and fuzzy rule generation tool (M. Maruf Hossain et al., 2008). The HMM in this model is trained using the Baum-Welch algorithm (David J.C. MacKay, 2007) and available training data vectors. There are four phrases in this model: (M. Maruf Hossain et al., 2008).

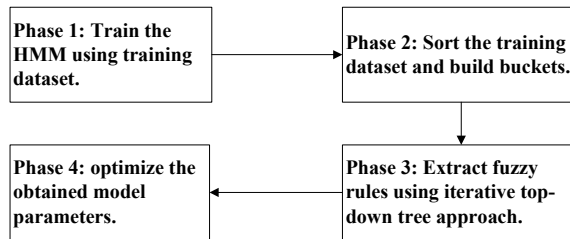


Fig. 3. The process phrases of the hmm-FL model

Firstly, an HMM is trained using the training dataset (Phrase 1) and then the training datasets are sorted and put into a number of buckets by using the HMM-log-likelihood values which are calculated in the training stage (Phrase 2). Then, a recursive divide and conquer algorithm (top-down tree approach) is used to generate a set of fuzzy rules (Phrase 3). Finally, a gradient descent method is used for further optimization of the fuzzy rule parameters (Phrase 4). The following four subsections describe more details of these four phrases respectively.

#### 3.2.1 Generating HMM-log-likelihood values

Initially, an HMM structure is built for re-estimating the parameter values of a given dataset. Each data vector is able to form a pattern. In HMM-Fuzzy model, the HMM-log-likelihood (Behzad Zamani et al., 2010) is generated from a single HMM as the first phrase. The following equations show how HMM-log-likelihood values are computed.

For a given HMM and a sequence of observation, it is common to compute  $P(O|\lambda)$ , the probability of the observation sequence. This value can be used to evaluate how well a model predicts a given observation sequence. The probability of the observations  $O$  for a specific state sequence  $Q$  is: (M. Maruf Hossain et al., 2008; Phil Blunsom, 2004)

$$P(O|Q, \lambda) = \prod_{t=1}^T P(o_t|q_t, \lambda) = b_{q_1}(o_1) \times b_{q_2}(o_2) \dots b_{q_T}(o_T) \quad (14)$$

In addition, the probability of the state sequence is:

$$P(Q|\lambda) = \pi_{q_1} a_{q_1 q_2} a_{q_2 q_3} \dots a_{q_{T-1} q_T} \quad (15)$$

By using these two equations, we can calculate the probability of the observations as:

$$P(O|\lambda) = \sum_Q P(O|Q, \lambda) P(Q|\lambda) = \sum_{q_1 \dots q_T} \pi_{q_1} b_{q_1}(o_1) a_{q_1 q_2} b_{q_2}(o_2) a_{q_2 q_3} \dots a_{q_{T-1} q_T} b_{q_T}(o_T) \quad (16)$$

The probability of the observations is known as the log-likelihood value, and it can be called the generated scalar value as well. We can accord Rabiner (Lawrence R. Rabiner, 1989)'s method to proof why the log-likelihood value can determine the similarity between two data patterns of k-dimensional vectors for sorting the data patterns: the log-likelihood value can show the probability that the vector was produced by the model, and the probability acts as an indicator for how well a given model matches a given vector. Thus, the entire vector can be transformed into related scalar log-likelihood values. For example, there are four data vectors which the log-likelihood values are  $M_1$ ,  $M_2$ ,  $M_3$  and  $M_4$  respectively. We can assume that the value of  $M_2$  and  $M_3$  are within the same tolerance level, so the data vectors that associating to  $M_2$  and  $M_3$  are similar. If the values of  $M_1$  and  $M_4$  are not close to the values of  $M_2$  and  $M_3$ , we can find out that the data vectors which corresponding to  $M_1$  and  $M_4$  are not similar to those of  $M_2$  and  $M_3$ . By using this method, we can detect that data values with similar log-likelihood values are belong to the same group.

One thing we have to mentioned is that, if we want to calculate  $P(O | \lambda)$ , the evaluation of the probability of  $O$  is allowed. However, to evaluate  $O$  directly would be exponential. A better approach is to use caching calculations which can lead to reduced complexity. The cache can be implemented as a trellis of states at each time step. The cached value (called  $\theta$ ) for each state can be calculated as a sum over all states at the previous time step. We define the forward probability variable: (Phil Blunsom, 2004)

$$\theta_t(i) = P(o_1 o_2 \dots o_t, q_t = s_i | \lambda) \quad (17)$$

The algorithm for this process is called forward algorithm which is used in HMM-FL model. The following example can explain well how HMM-log-likelihood is generated in this model.

If we want to predict the concentration of CO in the air during a certain time period for air pollution prediction, we should measure the number of cars per hour (A), wind speed (B), temperature 2 meters above the ground (C), wind direction (D) and etc. In this example, the set of predictor variable is A, B, C and D. The cached value for each state can be visualized as in Figure 4. We can use the values of these four variables to create a data vector for the particular time at each time unit. The patterns of these variables in every data vectors are assumed to appear consecutively and differently. In Hassan et al (M. Maruf Hossain et al., 2008)'s previous work, the HMM fed into these data patterns to re-estimate the parameter values, and the HMM was used as a pattern matching tool only. Once the HMM is trained well, this HMM is used to generate a log-likelihood value for every data vector in the dataset by using the forward algorithm in our project. Every data vector or pattern is able to generate one corresponding log-likelihood value. In this case, the table of the indices of data vectors and their corresponding log-likelihood values can be generated as shown in Table 2.

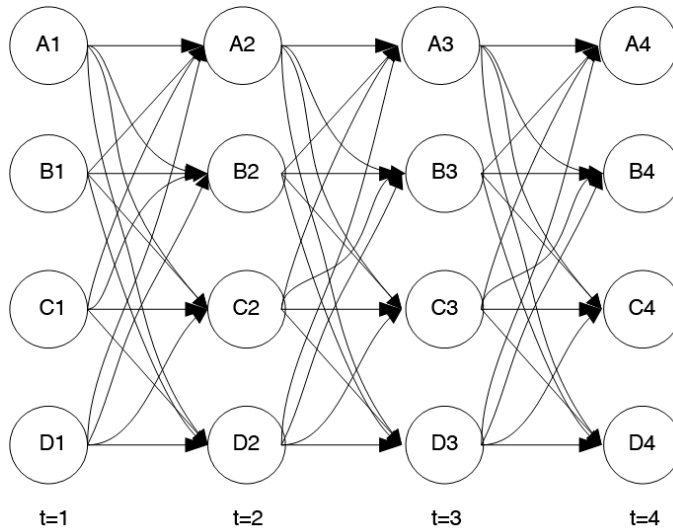


Fig. 4. A trellis algorithm example

| Data vector index i | A     | B     | C    | D     |
|---------------------|-------|-------|------|-------|
| 1                   | 8.5   | 9.25  | 8.25 | 8.25  |
| 2                   | 10.5  | 11.25 | 10   | 10.75 |
| 3                   | 8     | 9.5   | 8    | 8.5   |
| .....               |       |       |      |       |
| .....               |       |       |      |       |
| i-1                 | 10.75 | 11.5  | 10.5 | 11    |
| I                   | 10.5  | 11.25 | 9.5  | 11    |

| Data vector index i | Log-likelihood |
|---------------------|----------------|
| 1                   | -3.0090        |
| 2                   | -0.0010        |
| 3                   | -3.0080        |
| .....               |                |
| .....               |                |
| i-1                 | -0.0009        |
| I                   | -0.0008        |

Table 2. Generate log-likelihood values example

### 3.2.2 Grouping Similar Data Vectors

Grouping similar data vector is to split the range of log-likelihood values into equal sized buckets. Each bucket should contain the similar log-likelihood value of the data vectors. The fig shows there are five equal size buckets and the frequency values represents the number of similar data pattern.

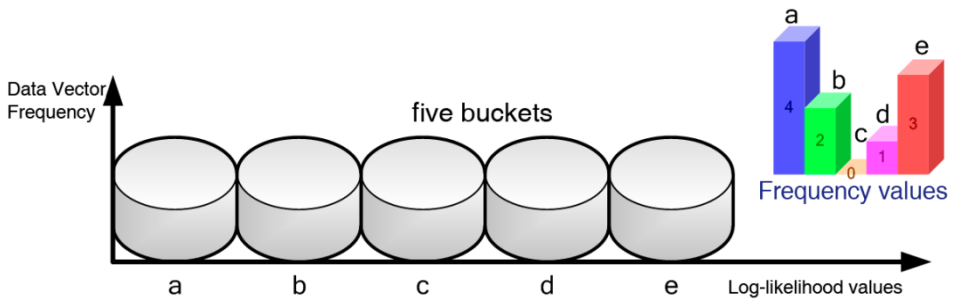


Fig. 5. Group data with similar log-likelihood values

For these buckets, each of them has a starting point and an ending point corresponding to the log-likelihood values (M. Maruf Hossain et al., 2008). The size of the bucket,  $W$ , can be used for guiding the rule extraction process. These data vectors are grouped for generating fuzzy rules and establishing the fuzzy model in the next phrase. The Figure 6 shows the pseudo-code to split the range of log-likelihood into buckets.

```
function split_values
    bucket_size = b;
    start_Range = minimum of the log-likelihood values;
    end_Range = maximum of the log-likelihood values;
    while (i < end_Range)
        bucket[j].start = i;
        bucket[j].end = i + bucket_size;
        bucket[j].data = find(log-likelihood.data >= i and log-likelihood.data < i + bucket_size)
        i = i + bucket_size;
        j = j + 1;
    end while
```

Fig. 6. The pseudo-code for split log-likelihood values into various buckets

### 3.2.3 The Fuzzy Model

The fuzzy rule extraction is a significant step in this model which after creating the buckets. (Md. Rafiul Hossain et al., 2009) In the fuzzy model, a divide and conquer (top-down tree) approach are used for the fuzzy rule generation. Initially, there is only one fuzzy rule which is generated for representing the entire input space of the training dataset. Under this circumstance, we use one global bucket to contain all the log-likelihood values of all the individual buckets. The process step is shown as Figure 7. In this process, mean squared error (MSE) is used to evaluate the performance of the developed model for the training dataset in this model.

The pseudo-code of the divide and conquer (top-down tree) approach (Joost Engelfriet, 1975) for rule extraction using buckets is shown below. Firstly, we set a threshold value  $T$ . If the prediction error for the training dataset is less than or equal to  $T$ , there should be no further

rules extracted and the algorithm is terminated. On the other hand, if the prediction error is greater than  $T$ , the input space is split into two parts with the help of the buckets produced in the second phrase. The method for splitting of the input space is to divide the total buckets into two equal parts. And then, we can create two individual rules for each of the parts. In this way, the total number of rules is increased by one. Then, we could use the extracted rule set to recalculate the training dataset. If the error threshold value is not greater than  $T$ , the buckets on the left side of the previous splitting are divided into two parts and the same process is iterated. This loop can be terminated only when the number of rules is equal to the number of buckets or the error threshold is less than or equal to  $T$ .

```

function rule_extraction

Threshold_Value = T ; (T is the desired error threshold value)
Extract only one rule using the entire training dataset
error = Calculate_Value(data,rules);
if(error>Threshold_Value)
    divide the total number of buckets into two parts and extract rules for each of
these parts;
    error = Calculate_Value(data,rules);
    left_flag = TRUE;
    right_flag = FALSE;
end if
while(error>Threshold_Value)
    if(left_flag == TRUE)
        divide the left part of buckets into two parts and extract rules for each of
these parts;
        error = Calculate_Value(data,rules);
        left_flag = FALSE;
        right_flag = TRUE;
    else
        divide the right part of buckets into two parts and extract rules for each of
these parts;
        error = Calculate_Value(data,rules);
        left_flag = TRUE;
        right_flag = FALSE;
    end if
end while
return rules

```

---

```

function error = Calculate_Value(data,rules)

simulate results by using extracted rules
error = MSE(produced_output, actual_output);
return error;

```

Fig. 7. The pseudo-code for rule extraction

In this part, the Gaussian member function is chosen for fuzzy rule extraction. As mentioned at the beginning of this section, the inference in the TS model can be further applied in this phrase. In the step of fuzzy rule extraction, there are  $k$  membership functions existed for  $k$  variables in a data pattern. We can calculate the mean value  $\mu$  and the standard deviation  $\sigma$  (Jun Young Bae et al., 2009; F. Khaber et al., 2006). Then, we could get the  $k^{\text{th}}$  membership function which is:

$$M_{ji}(u) = e^{-\frac{1}{2}(\frac{u_i - \mu_{ji}}{\sigma_{ji}})^2} \quad (18)$$

In his equation,  $M_{ji}(u)$  is the membership fuction for rule  $j$  and feature  $i$ .

### 3.2.4 Optimization of Extracted Fuzzy Rules

Gradient decent algorithm is used to optimize parameters for the extracted Fuzzy Rules in the last phrase (M. Maruf Hossain et al., 2008). In order to predict with better accuracy in the TS fuzzy model, the objective is to minimize the MSE for the training dataset. In the TS fuzzy model, every dataset has two parameters: one of them is the non-linear (premise) parameter, and the other is the linear (consequence) parameter. In our proposed model, the optimization technique ANFIS is used where a gradient decent method along with the least squared error (LSE) estimate is employed.

From the description of these four steps, we can understand how a hybrid AI-based tool is able to be used in UAP. This hybrid modeling is just like a “black box” (Mikko Kolehmainen et al., 2000) which combines HMM tools and the fuzzy model. The flowchart of the proposed model can show the main steps of this model clearly:

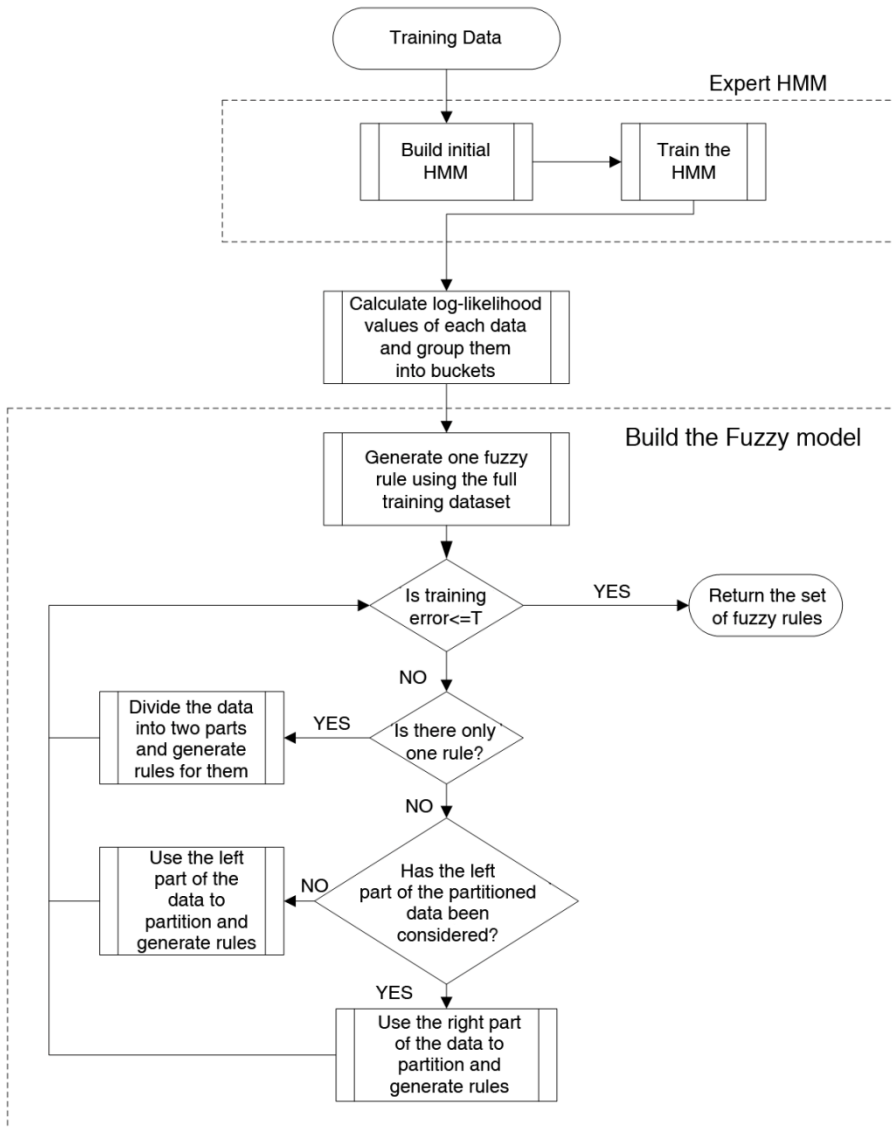


Fig. 8. The flowchart of main steps of HMM-FL model

#### 4. Experiment and Comparison

In this section, the experiment based on HMM-FL model for predicting UAP is described. And then, the comparison of all the AI-based tools for UAP forecasting which are introduced in Section 2 is analyzed as well.

#### 4.1 Experiment of HMM-FL Model

On the previous study of Md. Rafiul Hassan et al, the dataset which contains 500 observations is a good example (M. Maruf Hossain et al., 2008) on the experiment of HMM-FL model. This dataset is related to traffic volume and meteorological variables on a road, which is conducted by the Norwegian Public Roads Administration as a part of research on air pollution. It is based on the concentration of  $PM_{10}$  which was measured at Alnabru in Oslo from October 2001 to August 2003. The predictor variables of this dataset are the logarithm of (A) the number of cars per hour, (B) wind speed (m/s), (C) temperature 2 meters above the ground ( $^{\circ}C$ ), (D) the temperature deference between 25 and 2 meters above the ground ( $^{\circ}C$ ), (E) wind direction (within the range of  $0^{\circ}$  to  $360^{\circ}$ ), (F) hour of day and (G) day number as counted from 1<sup>st</sup> October, 2001. The response variable is hourly values of the logarithm of the concentration of  $PM_{10}$ . Take (B) and (C) as examples, Figure 9 shows how the dataspace is being divided by the generated rules.

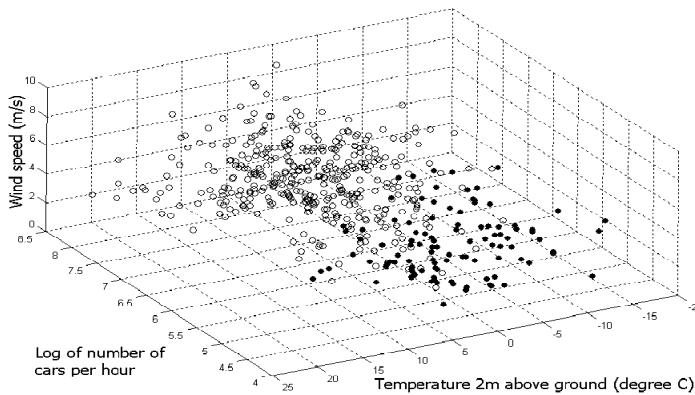


Fig. 9. Two groups in the dataspace after using HMM bucketing approach (M. Maruf Hossain et al., 2008)

In the HMM-FL model which is used on this dataset, the desired MSE was chosen to be 0.001 and the size of a bucket was 0.5. In addition, 500 epochs were chosen while executing the gradient descent algorithm for optimizing the extracted rules. In this experiment, HMM-FL model tool was executed in 10-fold cross validation. From the results, there are around  $2.9 \pm 1.3703$  rules with confidence level of 95% or over which were generated in each fold. The fuzzy rule that actually divides the dataspace which is shown in Fig. 11. and a membership function of the first attribute represented in Fig. 12 (M. Maruf Hossain et al., 2008).

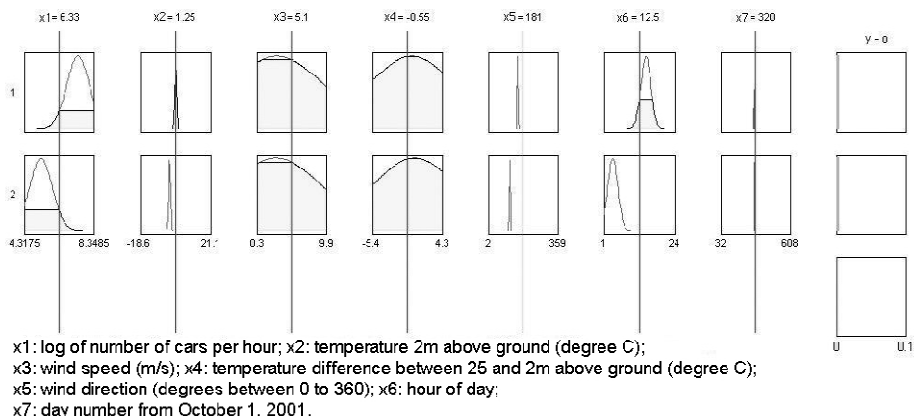


Fig. 10. Two fuzzy rules for dividing the dataspace shown in Fig. 9.

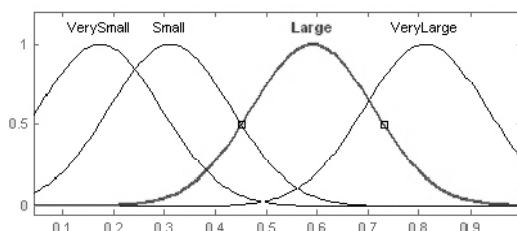


Fig. 11. Membership function of the first attribute shown in Fig. 10.

### 4.2 Results Comparison

From the comparison of the existed AI-based methodologies, we can find out that ANNs is more popular than others for predicting UAP. Ulku Sahin et al (Ulku Sahin et al., 2005) and Viotti et al (Viotti et al., 2002) introduced the ANN-based tools. In Ulku Sahin et al’s paper, they evaluated the performance by using ANN model or results to compare to other classical nonlinear methods. The correlation parameter is 0.999 and 0.528 for training and test data. P. Viotti et al also used ANNs on their UAP forecasting study. They tested various pollutants based on 48 hours and 500 hours respectively. Take Ozone as a example, they used a training set of 3500 patterns and a test set of 2300 patterns and two validation sets, 500 and 48 respectively. The number of neurons was 13 and about 10000 epochs were performed at constant learning rate of 0.3. The results for the two validations went to 0.126 (48 hours) of a relative MSE and 0.19 (500 hours) of a relative MSE. From these studies, we can see that ANNs’ behavior has always been related to non-linear statistical regression. It seems that it is naturally suited for problems that show a large dimensionality of data, such as UAP prediction system which is the task of identification for systems with a large number of state variables.

SVMs are not often used on UAP detection, but from Wei-Zhen Lu et al’s view (Wei-Zhen Lu & Wen-Jian Wang, 2005), it can also be used for regression and time series prediction and have been reported to perform well by some promising results. By comparing SVM and

radial basis function (RBF) on different months, the mean absolute error (MAE) produced by the SVM method is smaller than the ones created by the conventional RBF network in both December and June. These experiments show that SVM is superior to RBF. It is because SVM can process robust predicting performance.

The results from FL model are also promising. In Yilmaz Yildirim's research (Yilmaz Yildirim & Mahmut Bayramoglu, 2006), adaptive neuro-fuzzy logic method has been proposed on testing SO<sub>2</sub> and total suspended particular matter (TSP) pollution levels over an urban area. It shows that for SO<sub>2</sub> and TSP the model indicating acceptable forecasting limits are between 75-90% and 69-80%. It is possible to predict the air quality levels with high accuracy with a better set of training patterns in this study.

The combination of AI-based tools which contain ANNs technologies have been also used by Luis A. Diaz-Robles et al (Luis A. Diaz-Robles, et al., 2008). In this experiment, they combined ARIMA and ANNs model to improve forecast accuracy for an area with limited air quality and meteorological data. By comparison, the hybrid model had better forecasting performance than other models which were tested.

HMM-FL model is a novel hybrid AI-based model for UAP prediction. In the experiment which shows in Section 4.1, there are two other models which have been tested for comparing to HMM-FL model. They are an ANN model and a forecasting model using the subtractive clustering-based fuzzy model (S. Chiu, 1997). The ANN had 7 nodes in the input layer, 21 nodes in the hidden layer and 1 node in the output layer. The epochs and training goal were 500 and 0.001 respectively. MSE of HMM-FL model has the best results in this study, which is 0.0097 (M. Maruf Hossain et al., 2008). It shows that HMM-FL model has the potential to achieve high levels of performance on forecasting concentrations of UAP variables.

The results which come from these papers are collected and put in the Table 3. Besides MSE, in these papers, the mean absolute error (MAE) and the root mean square error (RMSE) are used as assessment indicators (Mikko Kolehmainen et al., 2000; Luis A. Diaz-Robles, et al., 2008). The MAE is used for measuring the average magnitude of the errors in a set of forecasts without considering their direction. It is usually on measuring accuracy for continuous variables. RMSE is the square root of MSE. It is a quadratic scoring rule which can measure the average magnitude. The MAE and RMSE are sometimes used together to diagnose the variation in the errors in a set of forecasts. Both of the MAE and RMSE can range from 0 to  $\infty$ . In addition, they are negatively-oriented scores which mean that lower values are better. They can be defined as follows:

$$\text{MAE} = \frac{1}{n} \sum_{i=1}^n |o_i - p_i|, \quad (19)$$

$$\text{RMSE} = \sqrt{\frac{1}{n} \sum_{i=1}^n (o_i - p_i)^2} \quad (20)$$

Where  $o_i$  is the actual values of pollutants' concentrations with  $\{i=1,2,\dots,n\}$  observations,  $n$  is the total observation number and  $p_i$  is the predicted pollutants value. The following table shows a part of results from statistic analysis.

| AUTHORS                         | NUMBER OF OBSERVED | AI-BASED TOOLS                               | THE RESPONSE VARIABLE                  | STATISTICAL PARAMETERS        | STATISTIC ANALYSIS                   |
|---------------------------------|--------------------|--|--|-------------------------------|--------------------------------------|
| M. Maruf Hossain et al. 2008    | 500                | HMM-FL model                                 | PM <sub>10</sub>                       | MSE                           | 0.0097( $\mu\text{g}^2/\text{m}^6$ ) |
| S. Chiu et al. 1997             | 500                | Fuzzy model following subtractive clustering | PM <sub>10</sub>                       | MSE                           | 0.0102( $\mu\text{g}^2/\text{m}^6$ ) |
| M. Maruf Hossain et al. 2008    | 500                | a ANN model                                  | PM <sub>10</sub>                       | MSE                           | 0.0216( $\mu\text{g}^2/\text{m}^6$ ) |
| Ulku Sahin et al. 2004          | 231                | a ANN model                                  | SO <sub>2</sub>                        | Mean absolute error (MAE)     | 0.103( $\mu\text{g}/\text{m}^3$ )    |
|                                 |                    |  |  | Root mean square error (RMSE) | 0.448( $\mu\text{g}/\text{m}^3$ )    |
| Wei-Zhen Lu et al. 2005         | 168                | SVM method                                   | Respirable suspended particulate (RSP) | MAE                           | 17.657( $\mu\text{g}/\text{m}^3$ )   |
|                                 |                    |  | NO <sub>2</sub>                        | MAE                           | 13.128( $\mu\text{g}/\text{m}^3$ )   |
|                                 |                    |  | NO <sub>x</sub>                        | MAE                           | 131.645( $\mu\text{g}/\text{m}^3$ )  |
| Luis A. Diaz-Robles et al. 2008 | 2080               | A novel hybrid model combining ARIMA and ANN | PM <sub>10</sub>                       | MAE                           | 6.74( $\mu\text{g}/\text{m}^3$ )     |
|                                 |                    |  |  | RMSE                          | 8.80( $\mu\text{g}/\text{m}^3$ )     |
| Mikko Kolehmainen et al. 2000   | --                 | A hybrid fuzzy model                         | NO <sub>2</sub>                        | RMSE                          | 12.2 ( $\mu\text{g}/\text{m}^3$ )    |
|                                 |                    |  | CO                                     | RMSE                          | 0.3 ( $\text{mg}/\text{m}^3$ )       |
|                                 |                    |  | PM <sub>10</sub>                       | RMSE                          | 11.1( $\mu\text{g}/\text{m}^3$ )     |

Table 3. The statistic analysis of AI-based tools on UAP prediction

## 5. Discussion and Conclusion

The AI techniques which are used as UAP forecasting tool can give clear and intuitive results. It is because air quality time series contains complex linear and non-linear patterns, and most methodologies cannot be used on non-linear patterns except AI techniques methodologies (Harri Niska et al., 2004; Lovro Hrust et al., 2009). Thus, combining AI

techniques, such as ANNs, SVMs and FL, with some other methods can recognize different patterns and improve the performance of UAP prediction. This book chapter represents and summarizes the current reliable researches on which AI-based tool are implemented. Although single AI technique based tools are popular and efficient, they still cannot avoid their inherent drawbacks. For example, ANNs can get over-fitted into training rules and stuck in local minima during training, SVMs is more likely to be built as the kernel-based hyper plane separation techniques than as forecasting tools, and FL suffers from the computational complexity due to its interpretability reduces. Compared to single AI-based forecasting tool, there are many models based on hybrid AI-based tools, such as a hybrid ARIMA and ANNs tool from Luis A. Diaz-Robles et al and adaptive neuro-fuzzy based modeling from Yilmaz Yildirim et al.

Combination of the HMM and Fuzzy model is a novel hybrid AI based tool that can be used on UAP forecasting (M. Maruf Hossain et al., 2008). It can improve Fuzzy model by using the HMM's data partition approach which the relationship between data features. The Markov process can be used on detecting the current event according to the immediate past event in the data patterns. In addition, the top-down tree approach can generate optimized number of fuzzy rules for the non-linear data. All of these features can make the generated fuzzy model provide a better performance.

For the UAP prediction experiment, the datasets usually contain the response variables and predictor variables. In the testing of HMM-FL model, there are 7 predictor variables used for predicting the concentration of PM<sub>10</sub>. In order to determine the efficiency of HMM-FL model, a fuzzy model which following subtractive clustering and another ANN model were tested for comparing results. By using MSE values for the evaluation, HMM-FL shows the better performance. The results represent that other techniques trained the input features as independent individuals which made complex systems. It further proves that HMM-Fuzzy model can reduce complexity and simultaneously improve the accuracy of predicting. However, a further performance can be achieved if a better weighting scheme which is used for generated fuzzy rules can be developed. In addition, larger size samples and various variables are required for further research.

## 6. References

- Per Nafstad, Lise Lund Haheim, Torbjorn Wisloff, Frederisk Gram, Bente Oftedal, Ingar Holme, Ingvar Hjermann, and Paul Leren (2004). *Urban Air Pollution and Mortality in a Cohort of Norwegian Men*. Environmental Health Perspectives, Vol. 112, No. 5.
- World Health Organization, *Urban Air Pollution with Particular Reference to Motor Vehicles*. World Health Organization Technical Report Series, No. 410.
- Nyberg F, Gustavsson P, Järup L, Bellander T, Berglind N, Jakobsson R, Pershagen G (2000). *Urban air pollution and lung cancer in Stockholm*. Epidemiology. Sep;11(5):487-95.
- J. Sunyer, C. Spix, P. Quenel, A. Ponce-de-Leon, A. Ponka, T. Barumandzadeh, G. Touloumi, L. Bacharova, B. Wojtyniak, J. Vonk, L. Bisanti, J. Schwartz, and K. Katsouyanni (1997). *Urban air pollution and emergency admissions for asthma in four European cities: the APHEA Project*. Thorax. 1997 September; 52(9): 760-765.

- Mikko Kolehmainen, Hannu Martikainen, Teri Hiltunen, and Juhani Ruuskanen (2000). *Forecasting air quality parameters using hybrid neural network modeling*. Environmental Monitoring and Assessment 65:277-286.
- Yilmaz Yildirim, Mahmut Bayramoglu (2006). *Adaptive neuro-fuzzy based modeling for prediction of air pollution daily levels in city of Zonguldak*. Chemosphere 63 1575-1582.
- Nils J. Nilsson (1998). *Artificial Intelligence: A New Synthesis*, Chapter 1. Morgan Kaufmann Publishers, Inc.
- Harri Niska, Teri Hiltunen, Ari Karppinen, Juhani Ruuskanen, and Mikko Kolehmainen (2004). *Evolving the neural network model for forecasting air pollution time series*. Engineering Applications of Artificial Intelligence 17, 159-167.
- Wei-Zen Lu, Wen-Jian Wang (2005). *Potential assessment of the "support vector machine" method in forecasting ambient air pollutant trends*. Chemosphere 59: 693-701.
- Francesco Carlo Morabito, Mario Versaci (2003). *Fuzzy neural identification and forecasting techniques to process experimental urban air pollution data*. Neural Networks 16, 493-506.
- A.B.Chelani, S.Devotta (2007). *Prediction of ambient carbon monoxide concentration using nonlinear time series analysis technique*. Transportation Research Part D 12, 596-600.
- Jef Hooyberghs, Clemens Mensink, Gerwin Dumont, Frans Fierens, Olivier Bresseur (2005). *A neural network forecast for daily average PM<sub>10</sub> concentrations in Belgium*. Atmospheric Environment 39 (2005) 3279-3289.
- U. Brunelli, V.Piazza, L.Pignato, F.Sorbello, S.Vitabile (2007). *Two-days ahead prediction of daily maximum concentrations of SO<sub>2</sub>, O<sub>3</sub>, PM<sub>10</sub>, NO<sub>2</sub>, CO in the urban area of Palermo, Italy*. Atmospheric Environment 41 (2007) 2967-2995.
- M. Maruf Hossain, Md. Rafiul Hassan, and Michael Kirley (2008). *Forecasting urban air pollution using HMM-Fuzzy Model*. PAKDD 2008, LNAI 5012, pp.572-581.
- Luis A. Diaz-Robles, Juan C. Ortega, Joshua S. Fu, Gregory D. Reed, Judith C. Chow, John G. Watson, Juan A. Moncada-Herrera (2008). *A hybrid ARIMA and artificial neural networks model to forecast particulate matter in urban areas: The case of Temuco, Chile*. Atmospheric Environment 42, 8331-8340.
- Giorgio Corani (2005). *Air quality prediction in Milan: feed-forward neural networks, pruned neural networks and lazy learning*. Ecological Modelling 185, 513-529.
- Oleg M. Pokrovsky, Roger H.F.Kwok, C.N.Ng (2002). *Fuzzy logic approach for description of meteorological impacts on urban air pollution species: a Hong Kong case study*. Computers & Geosciences 28, 119-127.
- Md. Rafiul Hassan (2009). *A combination of hidden Markov model and fuzzy model for stock market forecasting*. Neurocomputing 72, 3439-3446.
- Md. Rafiul Hassan (2007). *Hybrid HMM and Soft Computing modeling with applications to time series analysis*. Department of Computer Science and Software Engineering, the University of Melbourne, Australia.
- Joost Engelfriet (1975). *Bottom-up and Top-down tree transformations - a comparison*. Mathematical Systems Theory, Vol 9, No.3., 1975 by Springer-Verlag. New York Inc.
- Dahe Jiang, Yang Zhang, Xiang Hu, Yu Zeng, Jianguo Tan, Demin Shao (2004). *Process in developing an ANN model for air pollution index forecast*. Atmospheric Environment 38 (2004) 7055-7064. Elsevier Ltd.

- Patricio Perez, Rodrigo Palacios and Alejandro Castillo (2004). *Carbon Monoxide Concentration Forecasting in Santiago, Chile*. Journal of the air and waste management association 54:908-913. ISSN 1047-3289.
- Patricio Perez, Jorge Reyes (2006). *An integrated neural network model for PM<sub>10</sub> forecasting*. Atmospheric Environment 40 (2006) 2845-2851. Elsevier Ltd.
- Harri Niska, Teri Hiltunen, Ari Karppinen, Juhani Ruuskanen, Mikko Kolehmainen (2004). *Evolving the neural network model for forecasting air pollution time series*. Engineering Applications of Artificial Intelligence 17 (2004) 159-167. Elsevier Ltd.
- Comrie A. C. (1997). *Comparing neural networks and regression models for ozone forecasting*. Journal of Air and Waste Management Association 47, 655-663.
- Gardner M. W. Dorling S. R (1999). *Neural network modeling and prediction of hourly NO<sub>x</sub> and NO<sub>2</sub> concentrations in urban air in London*. Atmospheric Environment 33, 709-719.
- Yi J., Prybutok V. R. (1996). *A neural network model forecasting for prediction of daily maximum ozone concentration in an industrialized urban area*. Environmental Pollution 92, 349-357.
- Jun Young Bae, Youakim Badr, Ajith Abraham (2009). *A Takagi-Sugeno Fuzzy Model of a Rudimentary Angle Controller for Artillery Fire*. Institut National des Sciences Appliquees, INSA-Lyon, F-69621, France.
- F. Khaber, K. Zehar, and A. Hamzaoui (2006). *State Feedback Controller Design via Takagi-Sugeno Fuzzy Model: LMI Approach*. International Journal of Computational Intelligence 2;3. The CRESTIC laboratory, I.U.T of Troyes , University of Reims, France.
- Behzad Zamani, Ahmad Akbari, Babak NaserSharif, Mehdi Mohammadi and Azarakhsh Jalalvand (2010). *Discriminative transformation for speech features based on genetic algorithm and HMM likelihoods*. IEICE Electronic Express, Vol.7, No.4, 247-253.
- Phil Blunsom (2004). *Hidden Markov Models*. Department of Computer Science and Software Engineering, The University of Melbourne.
- Md. Rafiul Hassan, M. Maruf Hossain, Rezaul Karim Begg, Kotagiri Ramamohanarao, Yos Morsi (2009). *Breast-Cancer identification using HMM-Fuzzy approach*. Computers in Biology and Medicine. October 2009.
- Ulku Sahin, Osman N. Ucan, Cuma Bayat and Namik Ozturun (2005). *Modeling of SO<sub>2</sub> distribution in Istanbul using artificial neural networks*. Environmental Modeling and Assessment (2005) 10: 135-142. Springer.
- Lovro Hrust, Zvezdana Bencetic Klaic, Josip Krizan, Oleg Antonic, Predrag Hercog (2009). *Neural network forecasting of air pollutants hourly concentrations using optimized temporal averages of meteorological variables and pollutant concentrations*. Atmospheric Environment 43 (2009) 5588-6696. Elsevier Ltd.
- P. Viotti, G. Liuti, P. Di Genova (2002). *Atmospheric urban pollution: applications of an artificial neural network (ANN) to the city of Perugia*. Ecological Modelling 148 (2002) 27-46. Elsevier Science B.V.
- Wei-Zhen Lu, Wen-Jian Wang, Xie-Kang Wang, Sui-Hang Yan, and Joseph C. Lam (2004). *Potential assessment of a neural network model with PCA/RBF approach for forecasting pollutant trends in Mong Kok urban air, Hong Kong*. Environmental Research 96 (2004) 79-87. 2003 Elsevier Inc.

- Ming Cai, Yafeng Yin, Min Xie (2009). *Prediction of hourly air pollutant concentrations near urban arterials using artificial neural network approach*. Transportation Research Part D 14 (2009) 32-41. 2008 Elsevier Ltd.
- W. Z. Lu, W. J. Wang, X.K. Wang, Z. B. Xu and A. T. Leung (2002). *Using improved neural network model to analyze RSP, NOx and NO2 levels in urban air in Mong Kok, Hong Kong*. Environmental Monitoring and assessment 87: 235-254, 2003. Kluwer Academic Publisher. Netherlands.
- Rouzbeh Shad, Mohammad Saadi Mesgari, Aliakbar Abkar, Arefeh Shad (2009). *Predicting air pollution using fuzzy genetic linear membership kriging in GIS*. Computer ,Environment and Urban System 33(2009) 472-481. 2009 Elsevier Ltd.
- Matthew J. Beal, Zoubin Ghahramani, Carl Edward Rasmussen (2002). *The Infinite Hidden Markov Model*. Gatsby Computational Neuroscience Unit University College, London. 17 Queen Square, London WC1N 3AR, England.
- Lawrence R. Rabiner (1989). *A tutorial on Hidden Markov Models and selected applications in speech recognition*. Proceedings of the IEEE, Vol.77, No.2, Debruary 1989.
- Sudhir Agarwal and Pascal Hitzler (2005). *Modeling Fuzzy Rules with Description Logics*. Institute of Applied Informatics and Formal Description Methods. (AIFB), University of Karlsruhe (TH), Germany.
- S. Chiu (1997). *Extracting Fuzzy Rules from Data for Function Approximation and Pattern Classification*. Chapter 9 in Fuzzy Information Engineering: A guided Tour of Applications. Ed: D. Dubois, H. Prade, and R. Yager, John Wiley & Sons, 1997.
- David J. C. MacKay (1997). *Ensemble Learning for Hidden Markov Models*. Cavendish Laboratory, Cambridge CB3, DHE, UK.



# Artificial Neural Networks to Forecast Air Pollution

Eros Pasero and Luca Mesin

*Dipartimento di Elettronica, Politecnico di Torino  
Italy*

## 1. Introduction

European laws concerning urban and suburban air pollution requires the analysis and implementation of automatic operating procedures in order to prevent the risk for the principal air pollutants to be above alarm thresholds (e.g. the Directive 2002/3/EC for ozone or the Directive 99/30/CE for the particulate matter with an aerodynamic diameter of up to 10  $\mu\text{m}$ , called  $\text{PM}_{10}$ ). As an example of European initiative to support the investigation of air pollution forecast, the COST Action ES0602 (Towards a European Network on Chemical Weather Forecasting and Information Systems) provides a forum for standardizing and benchmarking approaches in data exchange and multi-model capabilities for air quality forecast and (near) real-time information systems in Europe, allowing information exchange between meteorological services, environmental agencies, and international initiatives. Similar efforts are also proposed by the National Oceanic and Atmospheric Administration (NOAA) in partnership with the United States Environmental Protection Agency (EPA), which are developing an operational, nationwide Air Quality Forecasting (AQF) system.

Critical air pollution events frequently occur where the geographical and meteorological conditions do not permit an easy circulation of air and a large part of the population moves frequently between distant places of a city. These events require drastic measures such as the closing of the schools and factories and the restriction of vehicular traffic. Indeed, many epidemiological studies have consistently shown an association between particulate air pollution and cardiovascular (Brook et al., 2007) and respiratory (Pope et al., 1991) diseases. The forecasting of such phenomena with up to two days in advance would allow taking more efficient countermeasures to safeguard citizens' health.

Air pollution is highly correlated with meteorological variables (Cogliani, 2001). Indeed, pollutants are usually entrapped into the planetary boundary layer (PBL), which is the lowest part of the atmosphere and has behaviour directly influenced by its contact with the ground. It responds to surface forcing in a timescale of an hour or less. In this layer, physical quantities such as flow velocity, temperature, moisture and pollutants display rapid fluctuations (turbulence) and vertical mixing is strong.

Different automatic procedures have been developed to forecast the time evolution of the concentration of air pollutants, using also meteorological data. Mathematical models of the

advection (the transport due to the wind) and the pollutant reactions have been proposed. For example, the European Monitoring and Evaluation Programme (EMEP) model was devoted to the assessment of the formation of ground level ozone, persistent organic pollutants, heavy metals and particulate matters; the European Air Pollution Dispersion (EURAD) model simulates the physical, chemical and dynamical processes which control emission, production, transport and deposition of atmospheric trace species, providing concentrations of these trace species in the troposphere over Europe and their removal from the atmosphere by wet and dry deposition (Hass et al., 1995; Memmesheimer et al., 1997); the Long-Term Ozone Simulation (LOTOS) model simulates the 3D chemistry transport of air pollution in the lower troposphere, and was used for the investigation of different air pollutions, e.g. total PM<sub>10</sub> (Manders et al. 2009) and trace metals (Denier van der Gon et al., 2008). Forecasting the diffusion of the cloud of ash caused by the eruption of a volcano in Iceland on April 14<sup>th</sup> 2010 is finding great attention recently. Airports have been blocked and disruptions to flight from and towards destinations affected by the cloud have already been experienced. Moreover, a threatening effect on European economy is expected. The statistical relationships between weather conditions and ambient air pollution concentrations suggest using multivariate linear regression models. But pollution-weather relationships are typically complex and have nonlinear properties that might be better captured by neural networks.

Real time and low cost local forecasting can be performed on the basis of the analysis of a few time series recorded by sensors measuring meteorological data and air pollution concentrations. In this chapter, we are concerned with specific methods to perform this kind of local prediction methods, which are generally based on the following steps:

- a) Information detection through specific sensors and sampled at a sufficient high frequency (above Nyquist limit).
- b) Pre-processing of raw time series data (e.g. noise reduction), event detection, extraction of optimal features for subsequent analysis.
- c) Selection of a model representing the dynamics of the process under investigation.
- d) Choice of optimal parameters of the model in order to minimize a cost function measuring the error in forecasting the data of interest.
- e) Validation of the prediction, which guides the selection of the model.

Steps c)-e) are usually iterated in order to optimize the modelling representation of the process under study. Possibly, also feature selection, i.e. step b), may require an iterative optimization in light of the validation step e).

Important data for air pollution forecast are the concentration of the principal air pollutants (Sulphur Dioxide SO<sub>2</sub>, Nitrogen Dioxide NO<sub>2</sub>, Nitrogen Oxides NO<sub>x</sub>, Carbon Monoxide CO, Ozone O<sub>3</sub> and Particulate Matter PM<sub>10</sub>) and meteorological parameters (air temperature, relative humidity, wind velocity and direction, atmospheric pressure, solar radiation and rain). We provide an example of application based on data measured every hour by a station located in the urban area of the city of Goteborg, Sweden (Goteborgs Stad Miljo). The aim of the analysis is the medium-term forecasting of the air pollutants mean and maximum values by means of meteorological actual and forecasted data. In all the cases in which we can assume that the air pollutants emission and dispersion processes are stationary, it is possible to solve this problem by means of statistical learning algorithms that do not require the use of an explicit prediction model. The definition of a prognostic dispersion model is necessary when the stationarity conditions are not verified. It may happen for example

when it is needed to forecast the evolution of air pollutant concentration due to a large variation of the emission of a source or to the presence of a new source, or when it is needed to evaluate a prediction in an area where no measurement points are available. In this case using neural networks to forecast pollution can give a little improvement, with a performance better than regression models for daily prediction.

The best subset of features that are going to be used as the input to the forecasting tool should be selected. The potential benefits of the features selection process are many: facilitating data visualization and understanding, reducing the measurement and storage requirements, reducing training and utilization times, defying the curse of dimensionality to improve prediction or classification performance. It is important to stress that the selection of the best subset of features useful for the design of a good predictor is not equivalent to the problem of ranking all the potentially relevant features. In fact the problem of features ranking is sub-optimum with respect to features selection especially if some features are redundant or unnecessary. On the contrary a subset of variables useful for the prediction can count out a certain number of relevant features because they are redundant (Guyon and Elisseeff, 2003). Depending on the way the searching phase is combined with the prediction, there are three main classes of feature selection algorithms.

1. Filters are defined as feature selection algorithms using a performance metric based entirely on the training data, without reference to the prediction algorithm for which the features are to be selected. In the application discussed in this chapter, features selection was performed using a filter. More precisely a selection algorithm with backward eliminations was used. The criterion used to eliminate the features is based on the notion of relative entropy (also known as the Kullback-Leibler divergence), inferred by the information theory.
2. Wrapper algorithms include the prediction algorithm in the performance metric. The name is derived from the notion that the feature selection algorithm is inextricable from the end prediction system, and is wrapped around it.
3. Embedded methods perform the selection of the features during the training procedure and are specific of the particular learning algorithm.

The Artificial Neural Networks (Multi-layer perceptrons and Support Vector Machines) have been often used as a prognostic tool for air pollution (Benvenuto and Marani, 2000; Perez et al., 2000; Božnar et al., 2004; Cecchetti et al., 2004; Slini et al., 2006).

ANNs are interesting for classification and regression purposes due to their universal approximation property and their fast training (if sequential training based on backpropagation is adopted). The performances of different network architectures in air quality forecasting were compared in (Kolehmainen et al., 2001). Self-organizing maps (implementing a form of competitive learning in which a neural network learns the structure of the data) were compared to Multi-layer Perceptrons (MLP, dealt with in the following), investigating the effect of removing periodic components of the time series. The best forecast estimates were achieved by directly applying a MLP network to the original data, indicating that a combination of a periodic regression and the neural algorithms does not give any advantage over a direct application of neural algorithms. Prediction of concentration of PM<sub>10</sub> in Thessaloniki was investigated in (Slini et al., 2006) comparing linear regression, Classification And Regression Trees (CART) analysis (i.e., a binary recursive partitioning technique splitting the data into two groups, resulting in a binary tree, whose terminal nodes represent distinct classes or categories of data), principal component

analysis (introduced in Section 2) and the more sophisticated ANNs approach. Ozone forecasting in Athens was performed in (Karatzas et al., 2008), again using ANNs. Another approach in forecasting air pollutant was proposed in (Marra et al., 2003), by the use of a combination of the theories of ANN and time delay embedding of a chaotic dynamical system (Kantz & Schreiber, 1997).

Support Vector Machines (SVMs) are another type of statistical learning-artificial neural network technique, based on the computational learning theory, which face the problem of minimization of the structural risk (Vapnik, 1995). An online method based on an SVM model was introduced in (Wang et al., 2008) to predict air pollutant levels in a time series of monitored air pollutant in Hong Kong downtown area.

Even if we refer to MLP and SVM approaches as black-box methods, in as much as they are not based on an explicit model, they have generalization capabilities that make possible their application to not-stationary situations.

The combination of the predictions of a set of models to improve the final prediction represents an important research topic, known in the literature as stacking. A general formalism that describes such a technique can be found in (Wolpert, 1992). This approach consists of iterating a procedure that combines measurements data and data which are obtained by means of prediction algorithms, in order to use them all as the input to a new prediction algorithm. This technique was used in (Canu and Rakotomamonjy, 2001), where the prediction of the ozone maximum concentration 24 hours in advance, for the urban area of Lyon (France), was implemented by means of a set of non-linear models identified by different SVMs. The choice of the proper model was based on the meteorological conditions (geopotential label). The forecasting of ozone mean concentration for a specific day was carried out, for each model, taking as input variables the maximum ozone concentration and the maximum value of the air temperature observed on the previous day together with the maximum forecasted value of the air temperature for that specific day.

In this chapter, the theory of time series prediction by MLP and SVM is briefly introduced, providing an example of application to air pollutant concentration. The following sections are devoted to the illustration of methods for the selection of features (Section 2), the introduction of MLPs and SVMs (Section 3), the description of a specific application to air pollution forecast (Section 4) and the discussion of some conclusions (Section 5).

## 2. Feature Selection

The first step of the analysis was the selection of the most useful features for the prediction of each of the targets relative to the air-pollutants concentrations. To avoid overfitting to the data, a neural network is usually trained on a subset of inputs and outputs to determine weights, and subsequently validated on the remaining (quasi-independent) data to measure the accuracy of predictions. The database considered for the specific application discussed in Section 4 was based on meteorological and air pollutant information sampled for the time period 01/04÷10/05. For each air pollutant, the target was chosen to be the mean value over 24 hours, measured every 4 hours (corresponding to 6 daily intervals a day). The complete set of features on which was made the selection, for each of the available parameters (air pollutants, air temperature, relative humidity, atmospheric pressure, solar radiation, rain, wind speed and direction), consisted of the maximum and minimum values and the daily averages of the previous three days to which the measurement hour and the reference to the

week day were added. Thus the initial set of features, for each air-pollutant, included 130 features. From this analysis an opposite set of data was excluded; such a set was used as the test set.

Popular methods for feature extraction from a large amount of data usually require the selection of a few features providing different and complementary information. Different techniques have been proposed to individuate the minimum number of features that preserve the maximum amount of variance or of information contained in the data.

Principal Component Analysis (PCA), also known as Karhunen-Loeve or Hotelling transform, provides de-correlated features (Haykin, 1999). The components with maximum energy are usually selected, whereas those with low energy are neglected. A useful property of PCA is that it preserves the power of observations, removes any linear dependencies between the reconstructed signal components and reconstructs the signal components with maximum possible energies (under the constraint of power preservation and de-correlation of the signal components). Thus, PCA is frequently used for a lossless data compression.

PCA determines the amount of redundancy in the data  $\mathbf{x}$  measured by the cross-correlation between the different measures and estimates a linear transformation  $W$  (whitening matrix), which reduces this redundancy to a minimum. The matrix  $W$  is further assumed to have a unit norm, so that the total power of the observations  $\mathbf{x}$  is preserved.

The first principal component is the direction of maximum variance in the data. The other components are obtained iteratively searching for the directions of maximum variance in the space of data orthogonal to the subspace spanned by already reconstructed principle directions

$$\mathbf{w}_1 = \arg \max_{\|\mathbf{w}\|=1} E \left[ \left( \mathbf{w}^T \mathbf{x} \right)^2 \right] \quad \mathbf{w}_k = \arg \max_{\|\mathbf{w}\|=1} E \left[ \left( \mathbf{w}^T \left( \mathbf{x} - \sum_{i=1}^{k-1} (\mathbf{w}_i^T \mathbf{x}) \mathbf{w}_i \right) \right)^2 \right] \quad (1)$$

The algebraic method for the computation of principal components is based on the correlation matrix of data

$$\hat{\mathbf{R}}_{\mathbf{xx}} = \begin{bmatrix} r_{11} & \cdots & r_{1m} \\ \vdots & \ddots & \vdots \\ r_{m1} & \cdots & r_{mm} \end{bmatrix} \quad (2)$$

where  $r_{ij}$  is the correlation between the  $i^{\text{th}}$  and the  $j^{\text{th}}$  data. Note that  $\hat{\mathbf{R}}_{\mathbf{xx}}$  is real, positive, and symmetric. Thus, it has positive eigenvalues and orthogonal eigenvectors. Each eigenvector is a principal component, with energy indicated by the corresponding eigenvalue.

Independent Component Analysis (ICA) determines features which are statistically independent. It works only if data (up possibly to one component) are not distributed as Gaussian variables. ICA preserves the information contained in the data and, at the same time, minimizes the mutual information of estimated features (mutual information is the information that the samples of the data have on each other's). Thus, also ICA is useful in data compression, usually allowing higher compression rates than PCA.

ICA, like as PCA, performs a linear transformation between the data and the features to be determined. Central limit theorem guarantees that a linear combination of independent non-Gaussian random variables has a distribution that is "closer" to a Gaussian than the distribution of any individual variable. This implies that the samples of the vector of data  $x(t)$  are "more Gaussian" than the samples of the vector of features  $s(t)$  that are assumed to be non Gaussian and linearly related to the measured data  $x(t)$ . Thus, the feature estimation can be based on minimization of Gaussianity of reconstructed features with respect to the possible linear transformation of the measurements  $x(t)$ . All that we need is a measure of (non) Gaussianity, which is used as an objective function by a given numerical optimization technique. Many different measures of Gaussianity have been proposed. Some examples are the followings.

1. Kurtosis of a zero-mean random variable  $v$  is defined as

$$K(v) = E[v^4] - 3E[v^2]^2 \quad (3)$$

where  $E[\cdot]$  stands for mathematical expectation, so that it is based on 4<sup>th</sup> order statistics. Kurtosis of a Gaussian variable is 0. For most non-Gaussian distributions, kurtosis is non-zero (positive for supergaussian variables, which have a spiky distribution, or negative for subgaussian variables, which have a flat distribution).

2. Negentropy is defined as the difference between the entropy of the considered random variable and that of a Gaussian variable with the same covariance matrix. It vanishes for Gaussian distributed variables and is positive for all other distributions. From a theoretical point of view, negentropy is the best estimator of Gaussianity (in the sense of minimal mean square error of the estimators), but has a high computational cost as it is based on estimation of probability density function of unknown random variables. For this reason, it is often approximated by  $k^{\text{th}}$  order statistics, where  $k$  is the order of approximation (Hyvarinen, 1998).
3. Mutual Information between  $M$  random variables is defined as

$$I(y_1, \dots, y_m) = \sum_{i=1}^m H(y_i) - H(\mathbf{y}) \quad (4)$$

where  $\mathbf{y} = [y_1, \dots, y_m]$  is a  $M$ -dimensional random vector, and the information entropy is defined as

$$H(\mathbf{y}) = \sum_{i=1}^m -P(\mathbf{y} = \mathbf{a}_i) \log P(\mathbf{y} = \mathbf{a}_i) \quad (5)$$

Mutual information is always nonnegative, and equals zero only when variables  $y_1, \dots, y_m$  are independent. Maximization of negentropy is equivalent to minimization of mutual information (Hyvarinen & Oja, 2000).

For the specific application provided below, the algorithm proposed in (Koller and Sahami, 1996) was used to select an optimal subset of features. The mutual information of the features is minimized, in line with ICA approach. Indicate the set of structural features as

$F = (F_1, F_2, \dots, F_N)$ ; the set of the chosen targets is  $Q = (Q_1, Q_2, \dots, Q_M)$ . For each assignment of values  $f = (f_1, f_2, \dots, f_N)$  to  $F$ , we have a probability distribution  $P(Q | F = f)$  on the different possible classes,  $Q$ . We want to select an optimal subset  $G$  of  $F$  which fully determines the appropriate classification. We can use a probability distribution to model the classification function. More precisely, for each assignment of values  $g = (g_1, g_2, \dots, g_p)$  to  $G$  we have a probability distribution  $P(Q | G = g)$  on the different possible classes,  $Q$ . Given an instance  $f = (f_1, f_2, \dots, f_N)$  of  $F$ , let  $f_G$  be the projection of  $f$  onto the variables in  $G$ . The goal of the Koller-Sahami algorithm is to select  $G$  so that the probability distribution  $P(Q | F = f)$  is as close as possible to the probability distribution  $P(Q | G = f_G)$ .

To select  $G$ , the algorithm uses a backward elimination procedure, where at each step the feature  $F_i$  which has the best Markov blanket approximation  $M_i$  is eliminated (Pearl, 1988). A subset  $M_i$  of  $F$  which does not contain  $F_i$  is a Markov blanket for  $F_i$  if it contains all the information provided by  $F_i$ . This means that  $F_i$  is a feature that can be excluded if the Markov blanket  $M_i$  is already available, as  $F_i$  does not provide any additional information with respect to what included in  $M_i$

$$P(Q | M_i, F_i) = P(Q | M_i). \tag{6}$$

In order to measure how close  $M_i$  is to being a Markov blanket for  $F_i$ , the Kullback-Leibler divergence (Hyvarinen, 1999) was considered. The Kullback-Leibler divergence can be seen as a measure of a distance between probability density functions, as it is nonnegative and vanishes if and only if the two probability densities under study are equal. In the specific case under consideration, we have

$$\delta_G(F_i | M_i) = \sum_{f_{M_i}, f_i} P(M_i = f_{M_i}, F_i = f_i) \cdot \sum_{Q_i \in Q} P(Q_i | M_i = f_{M_i}, F_i = f_i) \cdot \log \frac{P(Q_i | M_i = f_{M_i}, F_i = f_i)}{P(Q_i | M_i = f_{M_i})} \tag{7}$$

The computational complexity of this algorithm is exponential only in the size of the Markov blanket, which is small. For the above reason we could quickly estimate the probability distributions  $P(Q_i | M_i = f_{M_i}, F_i = f_i)$  and  $P(Q_i | M_i = f_{M_i})$  for each assignment of values  $f_{M_i}$  and  $f_i$  to  $M_i$  and  $F_i$ , respectively.

A final problem in computing Eq. (7) is the estimation of the probability density functions from the data. Different methods have been proposed to estimate an unobservable underlying probability density function, based on observed data. The density function to be estimated is the distribution of a large population, whereas the data can be considered as a random sample from that population. Parametric methods are based on a model of density function which is fit to the data by selecting optimal values of its parameters. Other methods are based on a rescaled histogram. For our specific application, the estimate of the probability density was made by using the kernel density estimation or Parzen method (Parzen, 1962; Costa et al., 2003). It is a non-parametric way of estimating the probability density function extrapolating the data to the entire population. If  $x_1, x_2, \dots, x_n \sim f$  is an independent and identically distributed sample of a random variable, then the kernel density approximation of its probability density function is

$$\hat{f}(x) = \frac{1}{nh} \sum_{i=1}^n K\left(\frac{x-x_i}{h}\right) \quad (8)$$

where the kernel  $K$  was assumed Gaussian and  $h$  is the kernel bandwidth. The result is a sort of smoothed histogram for which, rather than summing the number of observations found within bins, small "bumps" (determined by the kernel function) are placed at each observation.

Koller-Sahami algorithm was applied to the selection of the best subset of features useful for the prediction of the average daily concentration of PM<sub>10</sub> in the city of Goteborg. In fact from the data it was observed that this concentration was often above the limit value for the safeguard of human health (50 µg/m<sup>3</sup>). The best subset of 16 features turned out to be the followings.

1. Average concentration of PM<sub>10</sub> on the previous day.
2. Maximum hourly value of the ozone concentration one, two and three days in advance.
3. Maximum hourly value of the air temperature one, two and three days in advance.
4. Maximum hourly value of the solar radiation one, two and three days in advance.
5. Minimum hourly value of SO<sub>2</sub> one and two days in advance.
6. Average concentration of the relative humidity on the previous day.
7. Maximum and minimum hourly value of the relative humidity on the previous day.
8. Average value of the air temperature three days in advance.

The results can be explained considering that PM<sub>10</sub> is partly primary, directly emitted in the atmosphere, and partly secondary, that is produced by chemical/physical transformations that involve different substances as SO<sub>x</sub>, NO<sub>x</sub>, COVs, NH<sub>3</sub> at specific meteorological conditions (see the "Quaderno Tecnico ARPA" quoted in the Reference section).

### 3. Introduction to Artificial Neural Networks: Multi Layer Perceptrons and Support Vector Machines

#### 3.1 Multi Layer Perceptrons (MLP)

MLPs are biologically inspired neural models consisting of a complex network of interconnections between basic computational units, called neurons. They found applications in complex tasks like patterns recognition and regression of non linear functions. A single neuron processes multiple inputs applying an activation function on a linear combination of the inputs

$$y_i = \varphi_i \left( \sum_{j=1}^N w_{ij} x_j + b_i \right) \quad (9)$$

where  $\{x_j\}$  is the set of inputs,  $w_{ij}$  is the synaptic weight connecting the  $j^{\text{th}}$  input to the  $i^{\text{th}}$  neuron,  $b_i$  is a bias,  $\varphi_i(\cdot)$  is the activation function, and  $y_i$  is the output of the  $i^{\text{th}}$  neuron considered. Fig. 1A shows a neuron. The activation function is usually non linear, with a sigmoid shape (e.g., logistic or hyperbolic tangent function).

A simple network having the universal approximation property (i.e., the capability of approximating a non linear map as precisely as needed, by increasing the number of parameters) is the feedforward MLP with a single hidden layer, shown in Fig. 1B (for the case of single output, in which we are interested).

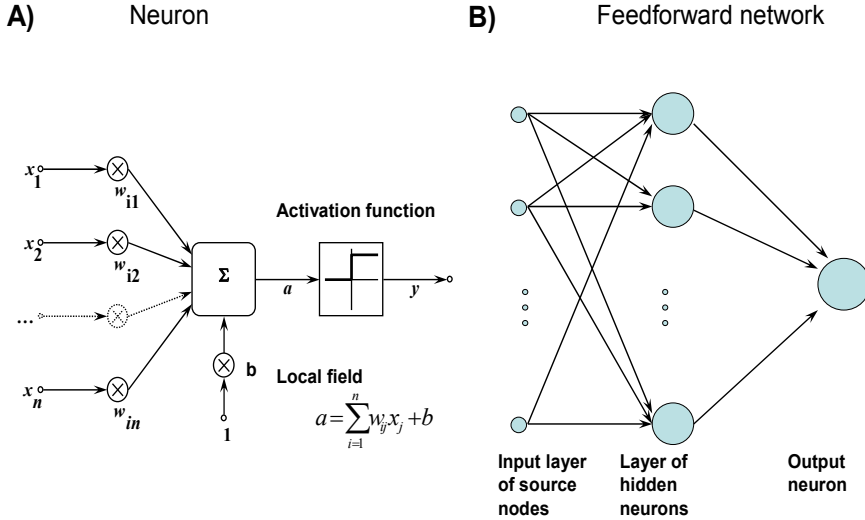


Fig. 1. A) Sketchy representation of an artificial neuron. B) Example of feedforward neural network, with a single hidden layer and a single output neuron.

A MLP may learn a task based on a training set, which is a collection of pairs  $\{\bar{x}_k, d_k\}$ , where  $\bar{x}_k$  is an input vector and  $d_k$  is the corresponding desired output. The parameters of the network (synaptic weights and bias) can be chosen optimally in order to minimize a cost function which measures the error in mapping the training input vectors to the desired outputs. Different methods were investigated to avoid to be entrapped in a local minimum. Different cost functions have also been proposed to speed up the convergence of the optimization, to introduce a-priori information on the non linear map to be learned or to lower the computational and memory load. For example, the cost function could be computed for each sample of the training set sequentially for each step of iteration of the optimization algorithm (sequential mode) instead of defining the total cost, based on the whole training set (batch mode). A MLP is usually trained by updating the weights in the direction of the gradient of the cost function. The most popular algorithm is backpropagation, which is a stochastic (i.e., sequential mode) gradient descent algorithm for which the errors (and therefore the learning) propagate backward from the output nodes to the inner nodes.

The Levenberg-Marquardt algorithm (Marquardt, 1963) was used in this study to predict air pollution dynamics for the application described in Section 4. It is an iterative algorithm to estimate the vector of synaptic weights  $\bar{w}$  (a single output neuron is considered) of the model (9), minimising the sum of the squares of the deviation between the predicted and the target values

$$E(\bar{w}) = \sum_{i=1}^N (d_i - y(\bar{x}_i, \bar{w}))^2 \quad (10)$$

where a batch mode is considered in (10). In each iteration step, the synaptic weights are updated  $\bar{w} \rightarrow \bar{w} + \bar{\delta}$ . In order to estimate the update vector  $\bar{\delta}$ , the output of the network is approximated by the linearization

$$y(\bar{x}_i, \bar{w} + \bar{\delta}) \approx y(\bar{x}_i, \bar{w}) + J_i \bar{\delta} \quad (11)$$

where  $J_i$  is the gradient

$$J_i = \frac{\partial y(\bar{x}_i, \bar{w})}{\partial \bar{w}} \quad (12)$$

Correspondingly, the square error can be approximated by

$$E(\bar{w} + \bar{\delta}) \approx \sum_{i=1}^N (d_i - y(\bar{x}_i, \bar{w}) - J_i \bar{\delta})^2 = \|\bar{d} - y(\bar{x}, \bar{w}) - J\bar{\delta}\|^2 \quad (13)$$

The choice of update  $\bar{\delta}$  minimizing (13) is obtained by pseudoinversion of the matrix  $J$

$$\bar{\delta}_{opt} = (J^T J)^{-1} J^T (\bar{d} - y(\bar{x}, \bar{w})) \quad (14)$$

Levenberg suggested introducing a regularization term (damping factor  $\lambda$ )

$$(J^T J + \lambda I) \bar{\delta}_{opt} = J^T (\bar{d} - y(\bar{x}, \bar{w})) \quad (15)$$

If reduction of the square error  $E$  is rapid, a smaller damping can be used, bringing the algorithm closer to the Gauss-Newton algorithm, whereas if the iteration gives insufficient reduction in the residual,  $\lambda$  can be increased, giving a step closer to the gradient descent direction (indeed the gradient of the error is  $-2(J^T (\bar{d} - y(\bar{x}, \bar{w})))^T$ ). To avoid slow convergence in the direction of small gradients, Marquardt suggested scaling each component of the gradient according to the curvature so that there is larger movement along the directions where the gradient is smaller

$$(J^T J + \lambda \text{diag}(J^T J)) \bar{\delta}_{opt} = J^T (\bar{d} - y(\bar{x}, \bar{w})) \quad (16)$$

where  $J^T J$  was considered as an approximation of the Hessian matrix of the approximating function  $y(\bar{x}, \bar{w})$ .

For prediction purposes, time is introduced in the structure of the neural network. For one step ahead prediction, the desired output  $d_n$  at time step  $n$  is a correct prediction of the value attained by the time series at time  $n+1$

$$y_n = \hat{x}_{n+1} = \varphi(\bar{w} \cdot \bar{x} + b) \quad (17)$$

where the vector of regressors  $\vec{x}$  includes information available up to the time step  $n$ . A number of delayed values of the time series up to time step  $n$  can be used together with additional data from other measures (non linear autoregressive with exogenous inputs model, NARX; Sjöberg et al., 1994). Such values may also be filtered (e.g., using a FIR filter). More generally, interesting features extracted from the data using one of the methods described in Section 2 may be used. Moreover, previous outputs of the network (i.e., predicted values of the states/features) may be used (non linear output error model, NOE). This means introducing a recursive path connecting the output of the network to the input. Other recursive topologies have also been proposed, e.g. a connection between the hidden layer and the input (e.g. the simple recurrent networks introduced by Elman, connecting the state of the network defined by the hidden neurons to the input layer; Haykin, 1999).

### 3.2 Support Vector Machines (SVM)

Kernel-based techniques (such as support vector machines, Bayes point machines, kernel principal component analysis, and Gaussian processes) represent a major development in machine learning algorithms. Support vector machines (SVM) are a group of supervised learning methods that can be applied to classification or regression. They were first introduced to separate optimally two linearly separable classes. As shown in Fig. 2A, the two sets of points (filled and unfilled points belonging to two different classes), also interpretable as two dimensional vectors, may be separated by a line (in the case of multidimensional vectors, a separation hyperplane is required). Multiple solutions are possible. We consider optimal the solution that maximizes the margin, i.e. the width that the boundary could be increased by before hitting a datapoint, which is also the distance between the two vectors (called support vectors and indicated with  $x^+$  and  $x^-$  in Fig. 2B) belonging to each of the two classes placed closest to the separation line.

The problem can be stated as: given the training pairs  $\{x_i, y_i = \pm 1\}$  (where the vectors  $x_i$  are associated to the class +1 or to -1 indicated by the corresponding value of  $y_i$ ), find the line  $\vec{w} \cdot \vec{x} + b = 0$  separating the two classes, which can be obtained by imposing

$$y_i(w x_i + b) \geq 1 \quad (18)$$

where the vector sign was dropped (as in Fig. 2) to simplify notation and we considered that the parameters  $w$  and  $b$  can be scaled in order that for the support vectors we have  $w x^+ + b = 1$  and  $w x^- + b = -1$ . From these conditions, the margin is given by

$$M = \frac{2}{|w|} \quad (19)$$

so that the following constrained optimization problem can be stated

$$\text{Minimize } \Phi(w) = \frac{1}{2} w^T w \quad \text{subject to } y_i(w x_i + b) \geq 1 \quad (20)$$

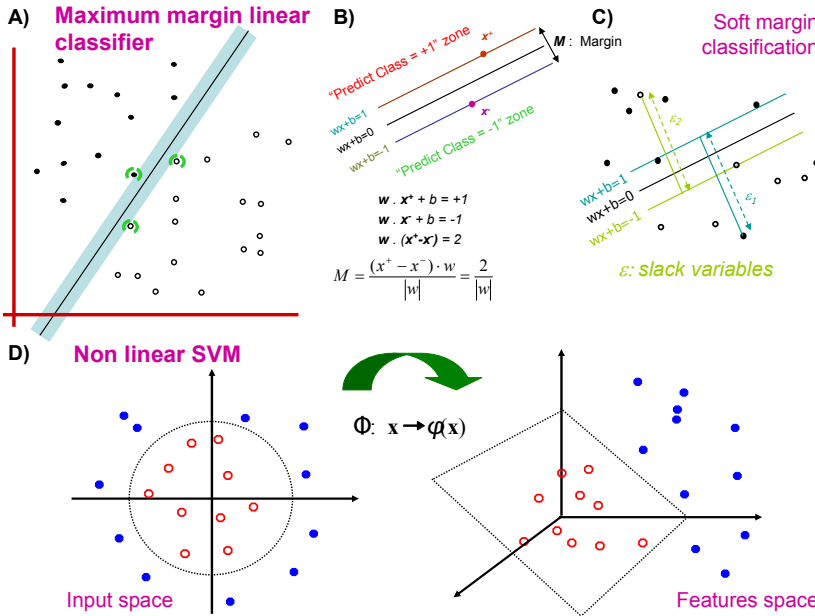


Fig. 2. Sketchy representation of support vector machines. Linear classification problems, with A), B) hard or C) soft margins. D) Non linear classification.

The problem can be solved by determining the saddle point of the Lagrangian

$$J(w, b, \alpha) = \frac{1}{2} w^T w - \sum_{i=1}^N \alpha_i [y_i (w x_i + b) - 1] \tag{21}$$

by minimizing  $J(w, b, \alpha)$  with respect to  $w$ ,  $b$  and maximizing with respect to the non negative Lagrange multipliers  $\alpha_i$  (Haykin, 1999). Determining the stationary points of the Lagrangian, only some  $\alpha_i, i=1, \dots, m$  are non vanishing and indicate that the corresponding  $x_i$  are support vectors. The corresponding constraint is said to be active, which means that the equality sign in the inequality constraint in problem (20) is attained. The following classifying function is obtained

$$f(\vec{x}) = \vec{w} \cdot \vec{x} + b \quad \text{where} \quad \vec{w} = \sum_{i=1}^m \alpha_i y_i \vec{x}_i, \quad b = y_k - \vec{w} \cdot \vec{x}_k \quad \text{for an arbitrary support vector } \vec{x}_k \tag{22}$$

A generalization is required to apply SVMs to the case of not linearly separable classes. Suppose that two linearly separable classes are corrupted by additive noise that determines the jump of the optimal separation line by a few outliers, as shown in Fig. 2C. A soft margin is introduced to allow for misclassification of a few datapoints. The distance from the

misclassified points to the separation line (slack variables) is penalized by adding a regularization term to the cost function to be minimized and weakening the constraint of the optimization problem

$$\text{Minimize } \Phi'(w) = \frac{1}{2} w^T w + C \sum_{i=1}^s \varepsilon_i \quad \text{subject to } y_i(wx_i + b) \geq 1 - \varepsilon_i, \varepsilon_i \geq 0 \quad (23)$$

where  $C$  is the regularization parameter to be selected by the user to give the proper weight to the misclassifications and  $\varepsilon_i$  are the slack variables.

If the two classes are non linearly intermixed, introducing slack variables is not sufficient. An additional method is to map the input space into a feature space in which linear separation is feasible (Fig. 2D)

$$x \in \mathbb{R}^N \rightarrow \varphi(x) \in \mathbb{R}^F \quad (24)$$

Cover's theorem (Haykin, 1999) indicates that the probability of getting linear separability is high if the function mapping the input space into the feature space is non linear and if the feature space has a high dimension (much larger than the input space,  $F \gg N$ ). The linear classification is performed in the feature space as before, obtaining the following classification map which resembles the equivalent expression (22) obtained for the linearly separable classes

$$f(\vec{x}) = \vec{w} \cdot \varphi(\vec{x}) + b \quad \text{where } \vec{w} = \sum_{i=1}^m \alpha_i y_i \varphi(\vec{x}_i), b = y_k - \vec{w} \cdot \varphi(\vec{x}_k) \quad (25)$$

where slack variables were not included for simplicity. Comparing the linear and the non linear separation problems, the following inner-product kernel appears

$$K(\vec{x}_i, \vec{x}) = \varphi(\vec{x}_i) \cdot \varphi(\vec{x}) \quad (26)$$

which allows writing the classification map as

$$f(\vec{x}) = \sum_{i=1}^m \alpha_i y_i K(\vec{x}_i, \vec{x}) + b \quad (27)$$

Different kernels have been applied (Gaussian, polynomial, sigmoidal), with parameters to be chosen in order to optimize the classification performance.

A straightforward generalization to multi-class separation is possible, by solving multiple two-class problems.

Moreover, SVMs may be applied to solve regression problems, which are of interest in the case of air pollution prediction. The following  $\varepsilon$ -insensitive loss function is introduced to quantify the error in approximating a desired response  $d$  using a SVM with output  $y$

$$L_\varepsilon(d, y) = \begin{cases} |d - y| - \varepsilon & \text{if } |d - y| \geq \varepsilon \\ 0 & \text{otherwise} \end{cases} \quad (28)$$

The following non linear regression model

$$d = f(x) \quad (29)$$

is optimized on the basis of a training set  $\{\bar{x}_k, d_k\}$ . The estimate of  $d$  is expressed as the linear combination of a set of non linear basis functions

$$y = \sum_{i=0}^N w_i \varphi_i(\bar{x}) + b = \bar{w} \cdot \bar{\varphi}(\bar{x}) + b \quad (30)$$

The weight vector and the bias are chosen in order to minimize the empirical risk

$$R_{emp} = \frac{1}{N} \sum_{i=1}^N L_\varepsilon(d_i, y_i) \quad (31)$$

The problem can be recast in terms of the formulism of SVM, by introducing two sets of non negative slack variables and writing the following constrained optimization problem

$$\text{Minimize } \Phi(w) = \frac{1}{2} w^T w + C \sum_{i=1}^s \hat{\varepsilon}_i + \tilde{\varepsilon}_i \quad \text{subject to } \begin{cases} d_i - \bar{w} \cdot \bar{\varphi}(x_i) - b \leq \varepsilon + \hat{\varepsilon}_i \\ d_i - \bar{w} \cdot \bar{\varphi}(x_i) - b \geq \varepsilon + \tilde{\varepsilon}_i \end{cases} \quad (32)$$

#### 4. Forecasting when the Concentrations are above the Limit Values for the Protection of Human Health

A set of feedforward neural networks with the same topology was used. Each network had three layers with 1 neuron in the output layer and a certain number of neurons in the hidden layer (varying in a range between 3 and 20). The hyperbolic tangent function was used as activation function. The backpropagation rule (Werbos, 1974) was used to adjust the weights of each network and the Levenberg-Marquardt algorithm (Marquardt, 1963) to proceed smoothly between the extremes of the inverse-Hessian (or Gauss-Newton) method and the steepest descent method. The Matlab Neural Network Toolbox (Demuth and Beale, 2005) was used to implement the neural networks.

An SVM with an  $\varepsilon$ -insensitive loss function (Vapnik, 1995) was also used. A Gaussian kernel function was considered. The principal parameters of the SVM were the regularized constant  $C$  determining the trade-off between the training error and model flatness, the width value  $\sigma$  of the Gaussian kernel, and the width  $\varepsilon$  of the tube around the solution. The SVM performance was optimized choosing the proper values for such parameters. An active set method (Fletcher, 1987) was used as optimization algorithm for the training of the SVM.

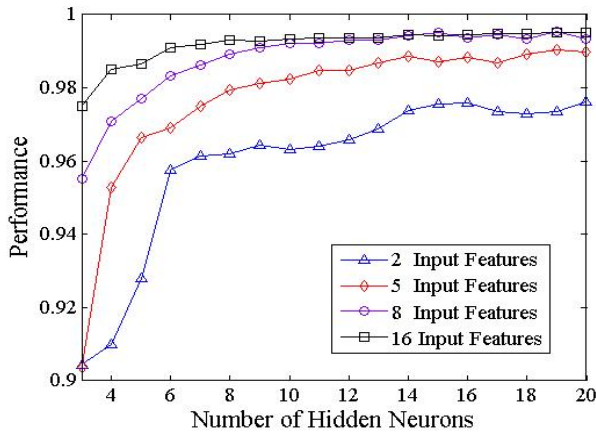


Fig. 3. Performance of the MLP as a function of the number of input Features (samples below the threshold).

The neural networks were trained on a representative subset of the data used for the features selection algorithm. A subset of the first two years of data was used: a measurement sample every three samples after leaving out one sample out of five of the original data. In this way the computational time of the adopted machine-learning algorithms was reduced while obtaining a subset of data as representative as that used for the features selection. In fact such a subset included a sufficient number of all the 6 daily intervals in which the measurement data were divided by our analysis. The test set consisted of the data not used for the features selection algorithm. Since the number of the training samples above the maximum threshold for the  $PM_{10}$  concentration was much lower than the number of samples under such threshold, the training of the networks was performed weighting more the kind of samples present a fewer number of times.

As we can see from Fig. 3 and Fig. 4 the MLP performance, both for the samples under the threshold and for the samples above the threshold, increased when the number of input features increased. More precisely the performance increased meaningfully from 2 to 8 input features and tended to flatten when the size of the input vector was greater than 8.

The best subset of 8 features was the following:

1. Average concentration of  $PM_{10}$  on the previous day.
2. Maximum hourly value of the ozone concentration one, two and three days in advance.
3. Maximum hourly value of the air temperature on the previous day.
4. Maximum hourly value of the solar radiation one, two and three days in advance.

Selecting as input to the MLP such a set of 8 features, the best results could be obtained with a neural network having 18 neurons in the hidden layer. In Table 1 are displayed the results obtained with 5115 samples of days under the threshold and 61 samples of days above the threshold. It can be noted that the probability to have a false alarm is really low (0.82%) while the capability to forecast when the concentrations are above the threshold is about 80%.

Different assignment for SVM parameters  $\epsilon$ ,  $\sigma$  and  $C$ , were tried in order to find the optimum configuration with the highest performance.

| Samples             | Correct Forecasting | Incorrect Forecasting |
|---------------------|---------------------|-----------------------|
| Below the threshold | 5073                | 42                    |
| Above the threshold | 48                  | 13                    |

Table 1. MLP performance.

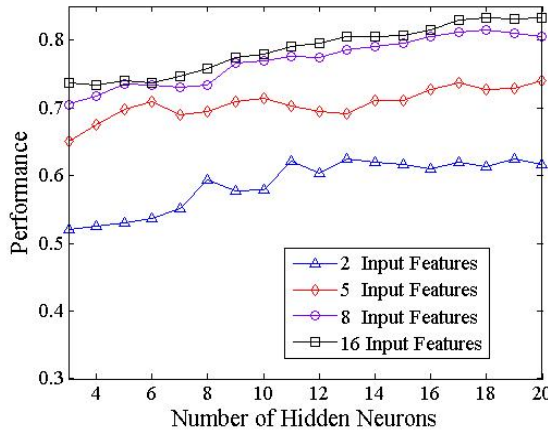


Fig. 4. Performance of the MLP as a function of the number of input Features (samples above the threshold).

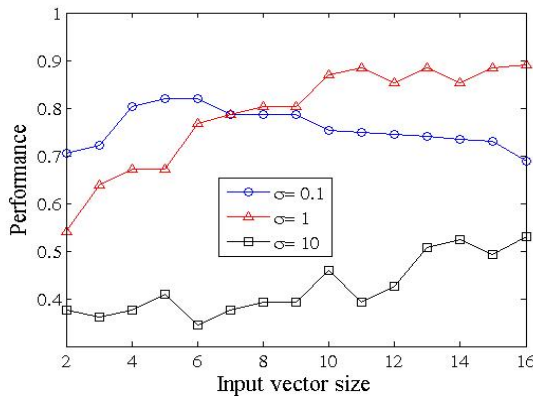


Fig. 5. Performances of the SVM as a function of  $\sigma$  ( $\epsilon=0.001$  and  $C=1000$ ), samples below the threshold.

As we can see from Fig. 5, when  $\epsilon$  and  $C$  were kept constant ( $\epsilon=0.001$  and  $C=1000$ ), the SVM performances referring to samples above the threshold, for a high number of input features, depended on  $\sigma$  and reached a maximum when  $\sigma=1$ , corresponding to an optimum trade-off between SVM generalization capability (large values of  $\sigma$ ) and model accuracy with respect to the training data (small values of  $\sigma$ ). The value of  $\sigma$  corresponding to this trade-off

decreased to 0.1 for lower values of the input vector size (Fig. 5) and for samples below the threshold (Fig. 6), reflecting the fact that the generalization capability was less important when the training set was more representative.

When  $\sigma$  and  $C$  were kept constant (Fig. 7:  $\sigma=1$  and  $C=1000$ ; Fig. 8:  $\sigma=0.1$  and  $C=1000$ ), the best performances were achieved when  $\epsilon$  was close to 0 and the allowed training error was minimized. From this observation, by abductive reasoning we could conclude that the input noise level was low. In accordance with such behaviour the performance of the network improved when the parameter  $C$  increased from 1 to 1000. Since the results tended to flatten for values of  $C$  greater than 1000, the parameter  $C$  was set equal to 1000. The best performance of the SVM corresponding to  $\epsilon=0.001$ ,  $\sigma=0.1$  and  $C=1000$  was achieved using as input features the best subset of 8 features previously defined. The probability to have a false alarm was really low (0.13%) while the capability to forecast when the concentrations were above the threshold was about 80%. The best performance of the SVM corresponding to  $\epsilon=0.001$ ,  $\sigma=1$  and  $C=1000$  was achieved using as input features the best subset of 11 features.

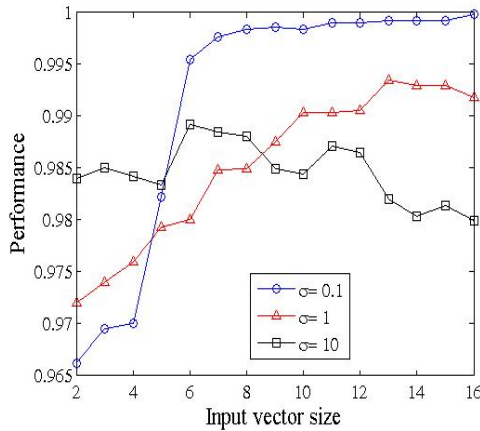


Fig. 6. Performances of the SVM as a function of  $\sigma$  ( $\epsilon=0.001$  and  $C=1000$ ), samples below the threshold.

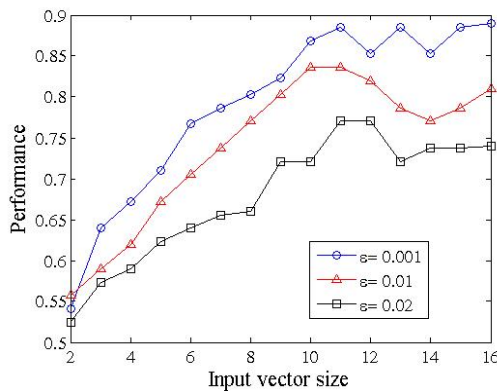


Fig. 7. Performances of the SVM as a function of  $\epsilon$  ( $\sigma=1$  and  $C=1000$ ), samples above the threshold

In this case the probability to have a false alarm was higher than in the previous one (0.96%) but the capability to forecast when the concentrations were above the threshold was nearly 90%.

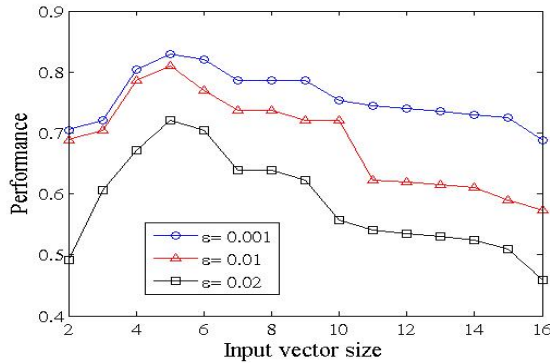


Fig. 8. Performances of the SVM as a function of  $\epsilon$  ( $\sigma=0.1$  and  $C=1000$ ), samples above the threshold.

## 5. Discussion and Conclusion

This chapter provides an introduction to non-linear methods for the prediction of the concentration of air pollutants. We focused on the selection of features and the modelling and processing techniques based on the theory of Artificial Neural Networks, using Multi Layer Perceptrons and Support Vector Machines.

Joint measurements of meteorological data and pollutants concentrations is useful in order to increase the number of parameters to be studied for the construction of mathematical air quality forecasting models and hence to improve forecast performances. Weather variables have a non-linear relationship with air quality, which can be captured by non-linear models such as Multi Layer Perceptrons and Support Vector Machines.

Our analysis carries on the work already developed by the NeMeFo (Neural Meteo Forecasting) research project for meteorological data short-term forecasting (Pasero et al., 2004). The application provided in Section 4 illustrates how the theoretical methods for feature selection (Section 2) and data modelling (Section 3) can be implemented for the solution of a specific problem of air pollution forecast. The principal causes of air pollution are identified and the best subset of features (meteorological data and air pollutants concentrations) for each air pollutant is selected in order to predict its medium-term concentration (in particular for the  $PM_{10}$ ). The selection of the best subset of features was implemented by means of a backward selection algorithm which is based on the information theory notion of relative entropy. Multi Layer Perceptrons and Support Vector Machines constitute some of the most wide-spread statistical data-learning techniques to develop data-driven models. Their use is shown for the prediction problem considered.

In conclusion, the final aim of this research is the implementation of a prognostic tool able to reduce the risk for the air pollutants concentrations to be above the alarm thresholds fixed by the law. The detection of meteorological and air pollutant data, the automatic selection of optimal descriptors of such data and the use of Multi Layer Perceptrons and Support Vector Machines are proposed as an efficient strategy to perform an accurate prediction of the time evolution of air pollutant concentration.

## Acknowledgement

We are deeply indebted to Fiammetta Orione for his infinite patience reviewing our work, to Walter Moniaci, Giovanni Raimondo, Suela Ruffa and Alfonso Montuori for their interesting comments and suggestions.

This work was partly funded by AWIS (Airport Winter Information System), Bando Regione Piemonte per la ricerca industriale per l'anno 2006.

## 6. References

- Benvenuto, F. & Marani A. (2000). Neural networks for environmental problems: data quality control and air pollution nowcasting, *Global NEST: The International Journal* Vol. 2, No. 3, pp. 281-292, Nov. 2000.
- Božnar, M. Z.; Mlakar, P. J. & Grašič, B. (2004). Neural Networks Based Ozone Forecasting, *Proceeding of 9th Int. Conf. on Harmonisation within Atmospheric Dispersion Modelling for Regulatory Purposes*, June 1-4, 2004, Garmisch-Partenkirchen, Germany.
- Brook, R.D.; Rajagopalan, S.; Jerrett, M.; Burnett, R.T.; Kaufman, J.D.; Miller, K. A. & Sheppard, L. (2007). Air Pollution and Cardiovascular Events. *NEJM* Vol. 356, pp. 2104-2106.
- Canu, S. & Rakotomamonjy, A. (2001). Ozone peak and pollution forecasting using Support Vectors, *IFAC Workshop on environmental modelling*, Yokohama, 2001.
- Cecchetti, M.; Corani, G & Guariso, G. (2004). Artificial Neural Networks Prediction of PM<sub>10</sub> in the Milan Area, *Proc. of IEMSS 2004*, University of Osnabrück, Germany, 14-17 June 2004.
- Cogliani, E. (2001). Air pollution forecast in cities by an air pollution index highly correlated with meteorological variables, *Atm. Env.*, Vol. 35, No. 16, pp. 2871-2877.
- Costa, M.; Moniaci, W. & Pasero, E. (2003). INFO: an artificial neural system to forecast ice formation on the road, *Proceedings of IEEE International Symposium on Computational Intelligence for Measurement Systems and Applications*, pp. 216-221, 29-31 July 2003.
- Demuth, H. & Beale, M. (2005). *Neural Network Toolbox User's Guide*, The MathWorks, Inc., 2005.
- Denier van der Gon, H.A.C.; J.H.J. Hulskotte, A.J.H.; Visschedijk, M. & Schaap, M. (2007). A revised estimate of copper emissions from road transport in UNECE Europe and its impact on predicted copper concentrations, *Atmos. Env.*, Vol. 41, pp. 8697-8710.
- Fletcher, R. (1987). *Practical Methods of Optimization*, John Wiley & Sons, NY, 2nd ed.
- Goteborgs Stad Miljo, <http://www.miljo.goteborg.se/luftnet/>.
- Guyon, I. & Elisseeff, A. (2003). An introduction to variable and feature selection, *The Journal of Machine Learning Research*, Vol. 3, pp. 1157-1182, January 2003.
- Hass, H.; Jakobs, H.J. & Memmesheimer, M. (1995). Analysis of a regional model (EURAD) near surface gas concentration predictions using observations from networks, *Meteorol. Atmos. Phys.* Vol. 57, pp. 173-200.
- Haykin, S. (1999). *Neural Networks: A Comprehensive Foundation*, Prentice Hall.
- Hyvarinen, A. (1998). New approximations of differential entropy for independent component analysis and projection pursuit, *Advances in Neural Information Processing Systems*, Vol. 10, pp. 273-279. MIT press.
- Hyvarinen, A. (1999). Survey on Independent Component Analysis, *Neural Computing Surveys*, Vol. 2, pp. 94-128.

- Hyvarinen A. & Oja, E. (2000). Independent Component Analysis: Algorithm and applications, *Neural Networks*, Vol. 13(4-5), pp. 411-430.
- Kantz, H. & Schreiber, T. (1997). *Nonlinear Time Series Analysis*, Cambridge University Press.
- Karatzas, K.D.; Papadourakis, G. & Kyriakidis, I. (2008). Understanding and forecasting atmospheric quality parameters with the aid of ANNs, *Proceedings of the International Joint Conference on Neural Networks, IJCNN 2008*, Hong Kong, China, June 1-6, 2008, pp. 2580-2587.
- Koller, D. & Sahami, M. (1996). Toward optimal feature selection, *Proceedings of 13th International Conference on Machine Learning (ICML)*, , pp. 284-292, July 1996, Bari, Italy.
- Manders, A.M.M.; Schaap, M. & Hoogerbrugge, R. (2009). Testing the capability of the chemistry transport model LOTOS-EUROS to forecast PM<sub>10</sub> levels in the Netherlands, *Atmos. Env.*, Vol. 43, No. 26, pp. 4050-4059.
- Marquardt, D. (1963). An algorithm for least squares estimation of nonlinear parameters, *SIAM J. Appl. Math.*, Vol. 11, pp. 431-441, 1963.
- Marra, S.; Morabito, F.C. & Versaci M. (2003). Neural Networks and Cao's Method: a novel approach for air pollutants time series forecasting, *IEEE-INNS International Joint Conference on Neural Networks*, July 20-24, Portland, Oregon.
- Memmesheimer, M.; Ebel, A. & Roemer, M. (1997). Budget calculations for ozone and its precursors: seasonal and episodic features based on model simulations, *J. Atmos. Chem.* Vol. 28, pp. 283-317.
- Parzen, E. (1962). On Estimation of a Probability Density Function and Mode, *Annals of Math. Statistics*, Vol. 33, pp. 1065-1076, Sept. 1962.
- Pasero, E.; Moniaci, W.; Meindl, T. & Montuori, A. (2004). NEMEF0: NEural MEteorological Forecast, *Proceedings of SIRWEC 2004*, 12th International Road Weather Conference, Bingen.
- Pearl, J. (1988). *Probabilistic Reasoning in Intelligent Systems*, Morgan Kaufmann, San Mateo, CA, 1988.
- Perez, P.; Trier, A. & Reyes, J. (2000). Prediction of PM<sub>2.5</sub> concentrations several hours in advance using neural networks in Santiago, Chile, *Atmospheric Environment*, Vol. 34, pp. 1189-1196, ISSN.
- Pope, C.A.; Dockery, D.W., Spengler J.D. & Raizenne, M.E. (1991). Respiratory health and PM<sub>10</sub> pollution: A daily time series analysis. *Am Rev Respir Dis* Vol. 144, pp. 668-74.
- Quaderno Tecnico ARPA (Emilia Romagna) - SMR n°10-2002.
- Sjöberg, J.; Hjalmeron, H. & L. Ljung (1994). Neural Networks in System Identification. Preprints 10<sup>th</sup> IFAC symposium on SYSID, Copenhagen, Denmark. Vol.2, pp. 49-71.
- Slini, T.; Kaprara, A.; Karatzas, K. & Moussiopoulos, N. (2006). PM<sub>10</sub> forecasting for Thessaloniki, Greece, *Environmental Modelling & Software*, Vol. 21, No. 4, pp. 559-565, April 2006.
- Vapnik, V. (1995). *The Nature of Statistical Learning Theory*, New York, Springer-Verlag.
- Werbos, P. (1974). Beyond regression: New tools for Prediction and Analysis in the Behavioural Sciences, Ph.D. Dissertation, *Committee on Appl. Math.*, Harvard Univ. Cambridge, MA, Nov. 1974.
- Wang, W.; Men, C. & Lu, W. (2008). Online prediction model based on support vector machine, *Neurocomputing*, Vol. 71, No. 4-6, pp. 550-558.
- Wolpert, D. (1992). Stacked generalization, *Neural Networks*, Vol. 5, pp. 241-259, ISSN.

# Instrumentation and virtual library for air pollution monitoring

Marius Branzila  
*Technical University Gh. Asachi of Iasi  
Romania*

## 1. Abstract

In this work a data acquisition board (DAQB) with data transfer by serial port and the associated virtual library included into LabVIEW software are presented. The DAQB developed around a National Semiconductor LM 12458 device, have the capability to perform tasks that diminish the host processor work and is capable to communicate with the host computer by using a set of drivers associated. Highly integrated device circuit that has into it the most components of the board, facility in data handling, good metrological performance and a very low cost are the benefits of the proposed system. Using the LabView environment, we have realized a virtual instrument able to get from the prototype data acquisition board for environmental monitoring parameters the information about air pollution factors like CO, H<sub>2</sub>S, SO<sub>2</sub>, NO, NO<sub>2</sub> etc. In order to get effective information about those factors and the monitoring points, this intelligent measurement system, compound from portable computer, and gas detector. This system can be used to map the information about the air pollution factors dispersion in order to answer to the needs of residential and industrial areas expansion.

## 2. Introduction

The modern microcomputer technology has made it relatively simple to install, configure, and start up a high-performance data acquisition system. Experienced users will be happy to know that many of the problems encountered a few years ago are gone. New users will never realize how difficult it once was to bring up a data acquisition system. These same technology advances have made it even more difficult than ever to select among the many options. The hardware decisions facing a user today require a great deal of study, analysis, and consideration. Every system will work, but some are better than others for each particular application.

Most data acquisition hardware is compatible with most popular industrial software, or it comes with a software package of its own. Virtually all these data acquisition devices and systems have the same basic specifications and options on their data sheets: signal conditioning, number of analog input channels, sampling rate, resolution, accuracy etc.

The most DAS's used in instrumentation are made it by National Instrument, including the software. These boards are plug-in types on ISA or PCI slots of the computers. In this case they will be affected by electromagnetic field. The manufacturer has to take special protection measures that increase the device costs.

Taking in consideration all this facts, we have developed a DAQB with data transfer by serial port. A set of drivers and functions specially designed to by access in LabVIEW functions palette we have made.

The EU-funded conference on "Environment, Health, Safety: a challenge for measurements", held in Paris in June 2001, recognized the need to improve the performance of environmental measurement systems and their harmonization at EU level, to foster the dialogue between the providers of measurement methods and the users of measurement results, and to prepare the base - by establishing special communication tools - for the integration of research expertise and resources of environmental monitoring across Europe. The concept presented herein aims to respond to this actual challenge by combining the latest software trends with the newest hardware concepts in environmental monitoring, towards providing reliable measurement results and representative environmental indicators, evaluating trends and quantifying the achieved results in order to manage the potential environmental risk in compliance with European legislation and local particularities.

In the actual development stage of the Romanian residential and industrial areas, the society demands more accurate and elaborated information in every domain. One of great interest is the air pollution filed. Over the last years, the clime changes have made the old prevision for dispersion of the air pollution around the industrial areas no longer accurate.

The atmospheric environment needs to be examined in consideration of the following three phenomena: global warming, ozone-layer depletion, air pollution.

Among these three, global warming is the most critical in terms of environmental conservation. Global warming is a result of greenhouse-gas emissions; therefore, to prevent it, greenhouse-gas emissions must be reduced. A major greenhouse gas is carbon dioxide (CO<sub>2</sub>). Therefore, reducing energy use, or saving energy, is the most effective way to help prevent global warming. There are some other gases that have a considerable influence on global warming. The first step to cutting the emissions of these gases as another environmental conservation measure is to monitor them in order to find a way to control them.

For this purpose, a new concept of performing high-speed data acquisition based on remote sensors, and an accurate transmission and processing of the meteorological parameters towards obtaining useful data for the users was developed in connection with the centre services. New methods of interconnecting hardware and dedicated software support were successfully implemented in order to increase the quality and precision of measurements.

In the same time, the Web concept itself is changing the way the measurements are made available and the results are distributed/communicated. Many different options are occurring as regards reports publishing, data sharing, and remotely controlling the applications. The LabVIEW environment was incorporated in centre concept towards creating a unique and powerful distributed application, combining together different measurement nodes and multiple users into a unique measurement controlling system, in order to integrate and revolutionize the fundamental architecture of actual PC-based measurement solutions.

The main objective of this work is to realize an intelligent system for environmental quality control and monitoring based on specialized sensors that are connected in a unit system.

### 3. System architecture

The hardware of environmental quality monitoring systems (sensors, conditioning circuits, acquisition and communication) must usually be complemented with processing blocks to perform different tasks associated to one-dimensional or multi-dimensional data that flow on the system measurement channels.

The architecture is composed as follows: the specialized sensors, detection circuit, a prototype data acquisition board, PC-host. Using all this hardware we are able to perform a study for Taguchi-type gas sensors.

Intelligent system achievement which is dedicated for particular application is not easy. It presume a selection of chemical sensors area which provide a large information quantity and complex algorithms development for signal processing.

The developed environmental monitoring systems (EMS), that use a prototype data acquisition board, perform different tasks like: multi-sensors/multi-point measurement, continuum real-time monitoring, across limits warnings, save data etc.

Air quality parameters can be monitories, from interested areas like public places, enterprises etc. The desktop PC and LabVIEW software have the following functions:

- DAQB control,
- Data processing and results display,
- Data storage and data administration
- User warning,
- Analysis and decision etc.

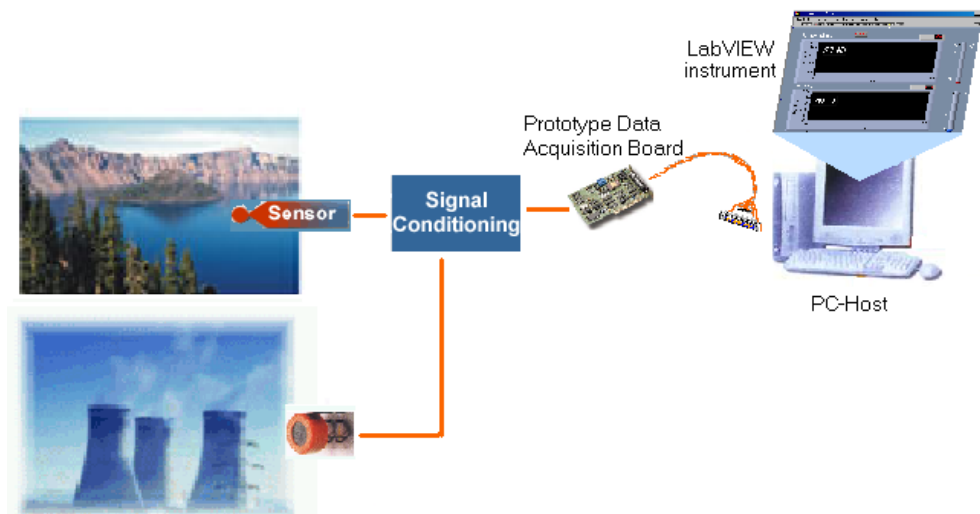


Fig. 1. System architecture.

### 3.1 Data acquisition system

The data acquisition system is a low cost board realized around the chip LM12H458 that is an integrated DAS and offers a self-calibrating 12-bit signed A/D converter with choice of single ended, fully differential, or mixed inputs, with on-chip differential reference, 8-input analog multiplexer, sample-and-hold, an impressive, flexible programmable logic system and a choice of speed/power combinations. The programmable logic has the circuitry to perform a number of tasks on its own, freeing the host processor for other tasks. This logic includes:

1. An instruction RAM that allows the DAS to function on its own (after being programmed by the host processor) with programmable acquisition time, input selection, 8-bit or 12-bit conversion mode.
2. Limit registers for comparison of the inputs against high and low limits in the "watchdog" mode.
3. A 32-word FIFO register to store conversion results until read by the host.
4. Interrupt control logic with interrupt generation for 8 different conditions.
5. A 16-bit timer register.
6. Circuitry to synchronize signal acquisition with external events.
7. A parallel microprocessor/microcontroller interface with selectable 8-bit or 16-bit data access.

The board can be used to develop both software and hardware. Since the parallel port is limited to 8-bit bidirectional data transfers, the BW pin is tied high for 8-bit access. Multiplexed address/data bus architecture was used. The circuit operates on a single +5V supply derived from the external supply using an LM7805 regulator or from USB port. This greatly attenuates noise that may be present on the computer's power supply lines.

Digital and analog supply pins are connected together to the same supply voltage but they need separate, multiple bypass capacitors. Multiple capacitors on the supply pins and the reference inputs ensure a low impedance bypass path over a wide frequency range.

All digital interface control signals (/RD, /WR, ALE, /INT, /CS), data lines (DB0-DB7), address lines (A0-A4) connections are made through the microcontroller pins ports.

All analog signals applied to, or received by, the input multiplexer (IN0-IN7),  $V_{REF+}$ ,  $V_{REF-}$ ,  $V_{REFOUT}$ , and the SYNC signal input/output are applied through a connector on the rear side of the board.

The voltage applied to  $V_{REF-}$  is GND and  $V_{REF+}$  is selected using a jumper. This jumper selects between the LM12H458 internal reference output,  $V_{REFOUT}$ , and the voltage applied to the corresponding pin applies it to the LM12H458  $V_{REF+}$  input.

A SYNC push button is available on the DAQB. With signal SYNC configured as an input, it is possible to synchronize the start of a conversion to an external event. This is useful in applications such as digital signal processing (DSP) where the exact timing of conversions is important.

Because the LM12H458 is so versatile, working with them may appear to be an overwhelming task. However, gaining a basic understanding of the device will prove to be fairly easy and using it to be as easy as programming the host microprocessor or microcontroller (AT90S8515).

The DAS is designed to be controlled by a processor, but the DAS functionality off loads most of the data acquisition burden from the processor, resulting in a great reduction of software and processor overhead. The processor downloads a set of operational instructions

to the DAS RAM and registers, and then issues a start command to the DAS, which performs conversions and/or comparisons as indicated by the instructions, loading conversion results into the FIFO, while the processor is free to do other chores, or can be idled, if not needed.

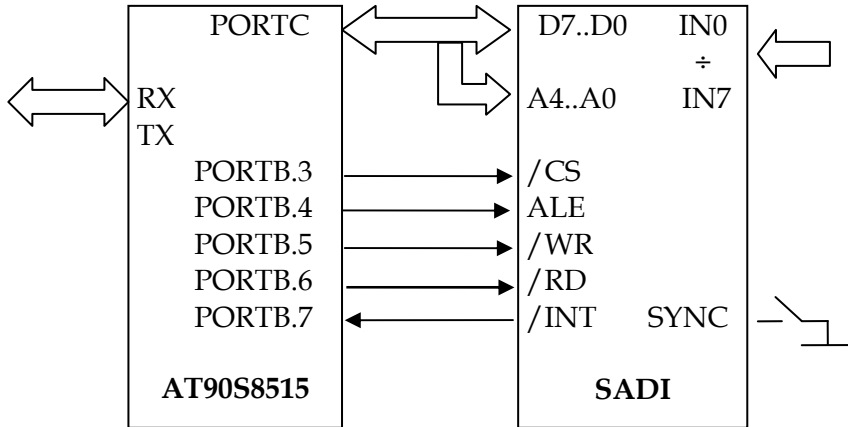


Fig. 2. The DAQB architecture design.

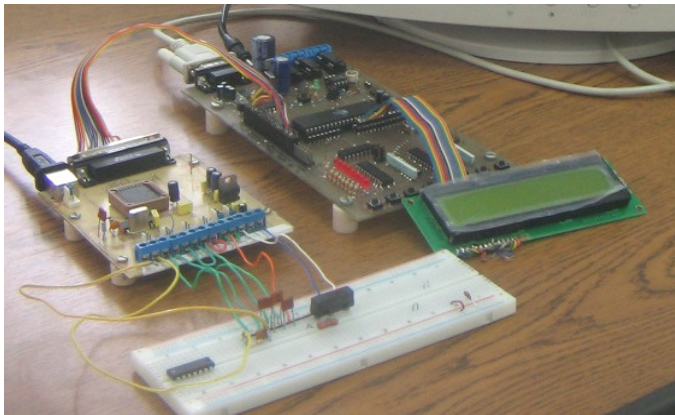


Fig. 3. The hardware picture.

After the DAS starts operating, the processor may respond to interrupts from the DAS, or it may interrogate the DAS at any time.

The architecture design and the hardware picture are presented in figures 2 and 3.

The main features of our DAQB are: 4 full-differential channels, 12 + sign ADC resolution, 100 ksamples acquisition rate, 20 ksamples transfer rate, 1 LSB linearity, 0,5 LSB accuracy, auto-zero and full calibration procedures,  $\pm 5V$  input voltage span, 30 mW power dissipation. In Table 1 we present the obtained results using the new DAQB and different apparatus.

| Nr. | GEN DC<br>[V] | New<br>DAQB<br>[V] | KEITHLEY<br>2000<br>[V] | METERMAN<br>38XR<br>[V] |
|-----|---------------|--------------------|-------------------------|-------------------------|
| 1   | 0.010         | 0.0117             | 0.0116                  | 0.0114                  |
| 2   | 0.020         | 0.0218             | 0.0216                  | 0.0213                  |
| 3   | 0.040         | 0.0425             | 0.0418                  | 0.0414                  |
| 4   | 0.060         | 0.0621             | 0.0618                  | 0.0615                  |
| 5   | 0.080         | 0.0825             | 0.0819                  | 0.0816                  |
| 6   | 0.100         | 0.0102             | 0.1018                  | 0.1015                  |
| 7   | 0.500         | 0.0505             | 0.5036                  | 0.5034                  |
| 8   | 1.000         | 1.0100             | 1.0060                  | 1,0020                  |
| 9   | 1.500         | 1.5130             | 1.5070                  | 1,5040                  |
| 10  | 1.700         | 1.7150             | 1.7080                  | 1,7050                  |
| 11  | 2.000         | 2.0180             | 2.0090                  | 2,0060                  |
| 12  | 2.200         | 2.2190             | 2.2100                  | 2,2070                  |
| 13  | 2.400         | 2.4220             | 2.4110                  | 2,4070                  |
| 14  | 2.500         | 2.4994             | 2.5120                  | 2,5090                  |

Table 1. Comparative results obtained using new DAQB and different apparatus.

DAQB presented have the capability to perform tasks that diminish the host processor work and is capable to communicate with the host computer by using a set of drivers associated in LabVIEW software. The novelty of the system mostly consists in the drivers and functions associated that are gathered into a library easily accessed by LabVIEW and assure the flexibility and the portability of the system. One of the performances consist in the fact that you can plug-in the DAQB to the running host computer externally.

DAQB is simple, versatile, flexible, cheap, high-speed digital data acquisition system that combined with LabVIEW software, become a very useful measurement instrument.

### 3.2 The sensors module

The sensitive elements included in analyzed environment are metal oxide semiconductor mainly composed of SnO<sub>2</sub> and are tied to the EMS. These elements are heated at a suitable operating temperature by a built-in heater. Exposure of the sensor to a vapour produces a large change in its electrical resistance. In fresh air the sensor resistance is high. When a combustible gas such as propane, methane etc. comes in contact with the sensor surface, the sensor resistance decreases in accordance with the present gas concentration (Fig. 4.a). Semiconductor gas sensors based on SnO<sub>2</sub> are widely used as safety monitors for detecting most combustible and pollution gases. However, most of the commercial gas sensors are not selective enough to detect a single chemical species in a gaseous mixture. It is desirable that a single sensor should be able to selectively detect several kinds of gases.

Recently, new methods have been proposed for chemical sensing that utilizes the analysis of the stochastic component of the sensor signal in Taguchi type sensors. It has been shown that even a single sensor may be sufficient for realizing a powerful electronic nose.

One of the problems appearing when we use sensitive elements like metal oxide semiconductor (SnO<sub>2</sub>) is the temperature and humidity dependence of sensibility characteristic.

In this case the influences of physical environmental parameters must be compensated.

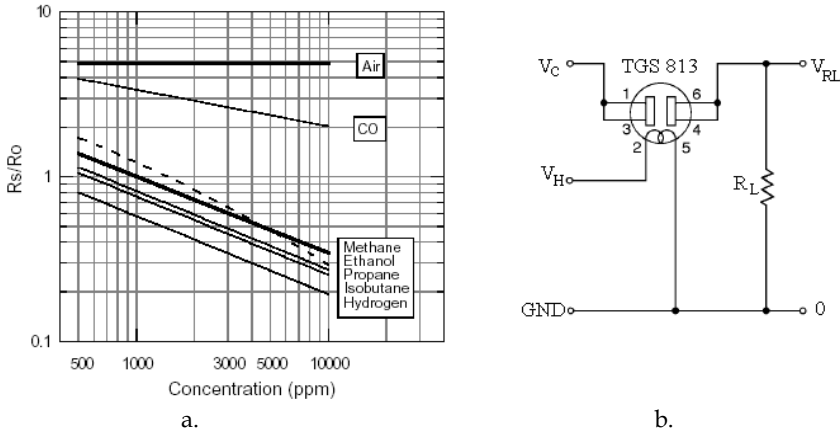


Fig. 4. Sensitivity characteristics and detection circuit for a Figarosensor.

The signal conditioning circuits (Fig. 4.b) associated with Figaro gas sensors (TGS813, TGS 822), have the function to convert  $\Delta R_s$  variation of sensor resistance in  $\Delta V$  variation of voltage.

The change in the sensor resistance is obtained as the change of the output voltage across the load resistor ( $R_L$ ) in series with the sensor resistance ( $R_s$ ). The constant 5V output of the data acquisition board is available for the heater of the sensor ( $V_H$ ) and for the detecting circuit ( $V_C$ ). The relationship between  $R_s$  and  $V_{RL}$  is expressed by the following equation.

$$R_s = \frac{V_C - V_{R_L}}{V_{R_L}} \cdot R_L \quad [\Omega] \quad (1)$$

The interaction of the chemical with the surface and bulk of the sensor induces spontaneous fluctuations. Recently, new methods have been proposed for chemical sensing that utilizes the analysis of the stochastic component of the sensor signal in Taguchi type sensors. It has been shown that even a single sensor may be sufficient for realizing a powerful electronic nose. However, there are no studies of the power spectrum in different types of commercial gas sensors under different gas atmospheres. This paper studies the stochastic signal in commercial semiconductor gas sensors measured under different atmospheres.

A unique gas detection block is used for both architectures of the system. It contains an array of five sensors and the corresponding detection circuits (Fig. 5).

To detect hydrogen sulfide ( $H_2S$ ), ammonia ( $NH_3$ ) and combustible gases we use Taguchi type gas sensors produced by Figaro Co. The detection principle of TGS sensors is based on chemical adsorption and desorption of gases on the sensor surface. The sensing element is a tin dioxide ( $SnO_2$ ) semiconductor that is heated at a suitable operating temperature by a built-in heater. In the presence of a detectable gas, the sensor conductivity increases

depending on the gas concentration in the air. A simple electrical circuit converts the change in the sensor resistance to an output voltage, which corresponds to the gas concentration.

TGS 813 sensor has a good sensitivity to a wide range of combustible gases for concentrations from several ppm to over 10,000 ppm. Because of poor sensor selectivity, it is used only to detect the presence of some flammable gases in the environment (methane, ethanol, isobutane, and hydrogen).

TGS 825 and TGS 826 sensors have good sensitivity and selectivity to H<sub>2</sub>S and NH<sub>3</sub>, respectively. The relationship of sensor resistance to gas concentration is non-linear within the practical range of gas concentration (from several ppm to 100 ppm). In the data processing part, two artificial neural networks approximate the sensitivity characteristics of these sensors for the continual measurement of H<sub>2</sub>S and NH<sub>3</sub> concentration.

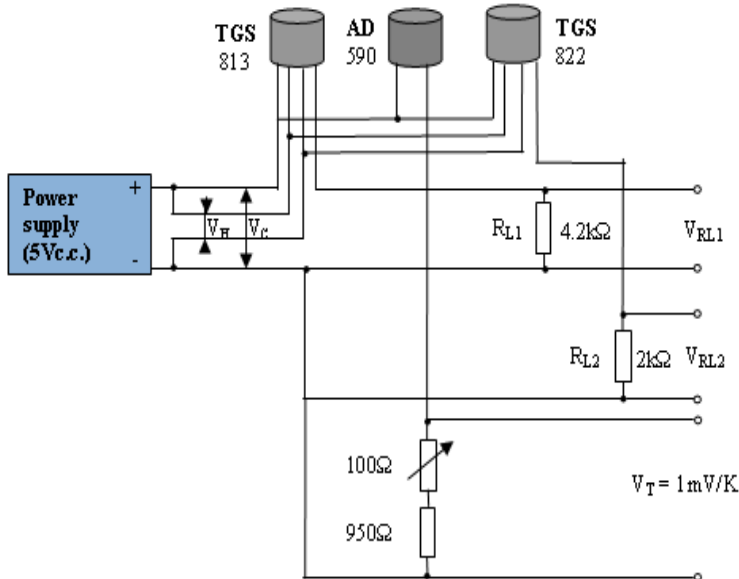


Fig. 5. The signal conditioning circuit.

### 3.3 Driver and LabVIEW library

Using LabVIEW software that has the capability to communicate with the serial port by Inport-Output functions, a driver for this data acquisition board was made it. We created two basic functions Write.vi (Scrie.vi) and Read.vi (Citeste.vi) which are the main functions when communicate with DAQB. The Write and Read functions are used for writing and reading into/from DAS registers.

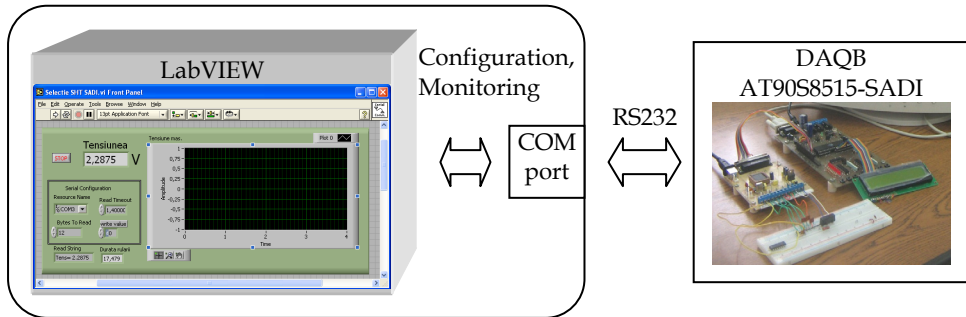


Fig. 6. Configuration and monitoring architecture.

Based on functions Write and Read others complex functions are developed and consists in multiple writing and reading operations into and from the board registers using the basic functions. Each is responsible with specific procedures in the board operation. The functions of the virtual library in LabVIEW environment include:

1. One Push One Channel (acquisition with external start conversion),
2. One Push Multi Channel (acquisition with external start conversion),
3. One Scan One Channel (acquisition without external start conversion),
4. One Scan Multi Channel (acquisition without external start conversion),
5. Waveform multi channel acquisition by interruption,
6. Watchdog/One Push –one channel and acquisition
7. Watchdog/One Push –one channel without acquisition
8. Watchdog/One Push –multi channel and acquisition,
9. Watchdog/One Push –multi channel without acquisition,
10. Watchdog/One Scan –one channel and acquisition,
11. Watchdog/One Scan –one channel without acquisition,
12. Watchdog/One Scan –multi channel and acquisition),
13. Watchdog/One Scan –multi channel without acquisition,
14. Watchdog/Waveform –without acquisition for one channel,
15. Watchdog and alarm without acquisition multi channel.

For LabVIEW, the functions are constituted as sub-VIs that are included into a separate acquisition subpalette, part of the main function palette. The main function palette of the DAQB is LPT-DAS and palette includes other subpalettes:

1. Analog Input,
2. Calibration and Configuration,
3. Timer,
4. Signal Condit.,
5. Wachdog.

In figure 7, subpalettes of Analog Input and Wachdog are presented.

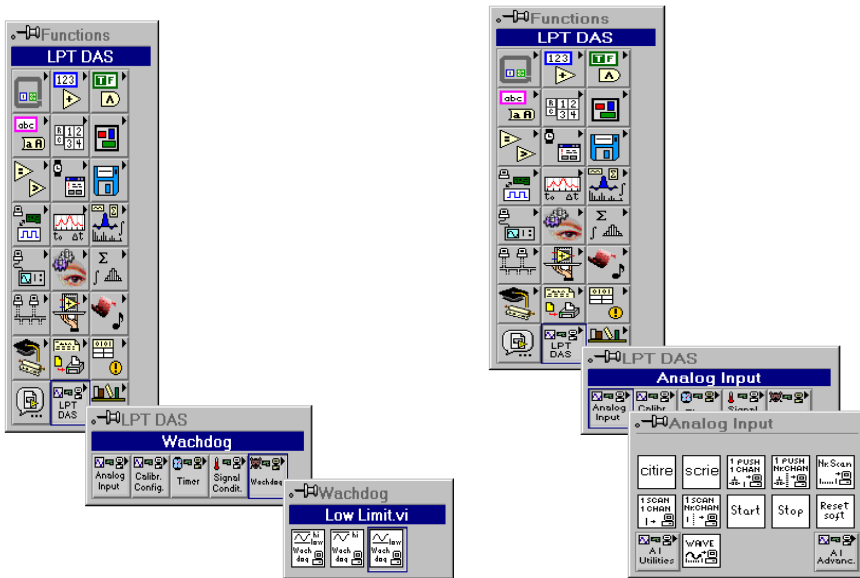


Fig. 7. The functions palette used for communicating with the new DAQB.

The Analog Input subpalette functions contain other two subpalette functions and simple functions like Write, Read, Start, Stop or Reset (internal sequencer).

Wachdog subpalette contains three functions: Low Limit, High Limit and Low & High Limit.

No conversion is performed in the watchdog mode, but the DAS samples the selected input(s) and compares it/them with values of the low and high limits stored in the instruction RAM. This comparison is done with a voltage comparator with one comparator input being the selected multiplexer input (pair) and the other input being the appropriate tap on the internal capacitive ladder of the converter. This tap is selected by a programmed value in the instruction register. If the input voltage is outside of the user defined and programmed minimum/maximum limits, an interrupt can be generated to indicate a fault condition, and the host processor could then service that interrupt, taking the appropriate action.

The flow diagram of the Watchdog One Channel without Acquisition.vi function will be presented. It consists in multiple writing and one final reading operation into and from the board registers. First, the reset operation has to be performed by selecting RAM section 0(RP=00) and write 0002H to CONFIGURATION register. Next, is loading instruction to INSTRUCTION RAM (set the utilized channel, the reference to ground or to other channel and the load impedance threshold. Afterwards, select the RAM section 1(RP=01) and write 0100H to CONFIGURATION register. In this moment it is possible to write the Superior Limit. Afterwards, select the RAM section 2(RP=10, write 0200H to CONFIGURATION register) and write the Inferior Limit. Start the DAS conversion by setting D0 of CONFIGURATION register high. Read the results of conversion from the Limit Status.

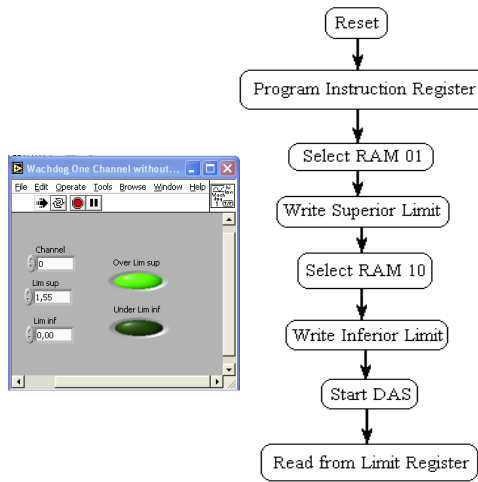


Fig. 8. The flow chart of the Watchdog One Channel without Acquisition.vi.

The Limit Status Register is likewise cleared whenever (Limit Status Register) is read or a device reset is issued.

#### 4. Virtual instrument

The virtual instrument is the main part of the monitoring system and, in the same time, the human interface, providing parameters control (Fig.8). The main functions of the VI are:

1. SADI programming and communication control using Nr.Scan function from the specific functions palette.
2. data processing after data reading from SADI analog input channels
3. environmental temperature calculus starting from the analog input voltage(CH2)  $V_T$ .

$$T = V_T \cdot 1000 - 273,15 \text{ [}^\circ\text{C]} \quad (2)$$

4. sensors resistance calculus starting from  $CH_0$  and  $CH_1$  read voltages ( $V_{RL1}$  and  $V_{RL2}$ ):

$$R_s = \frac{V_C \times R_L}{V_{RL}} - R_L \text{ [}\Omega\text{]} \quad (3)$$

5. Mean pollutant concentration calculus for a user presetting time interval (ppm/30min, ppm/8h, ppm/24h) for pollution level testing.
6. Pollution agent concentration limits exceeding verify for knowing the immediate effects fort health, lighting and voice user warning
7. Decrease the environmental temperature influence using a compensation subVI
8. Data base saving.

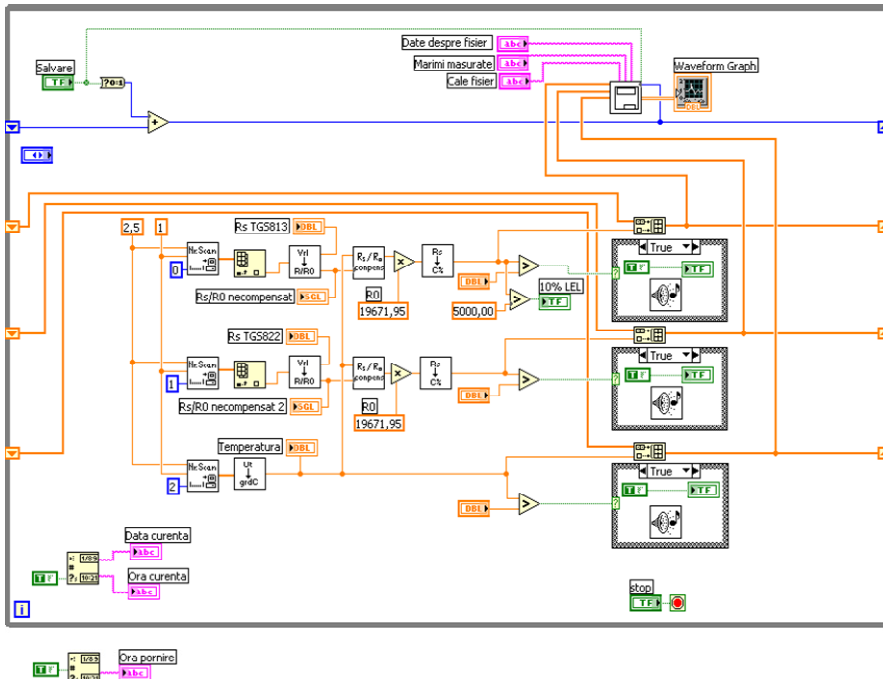
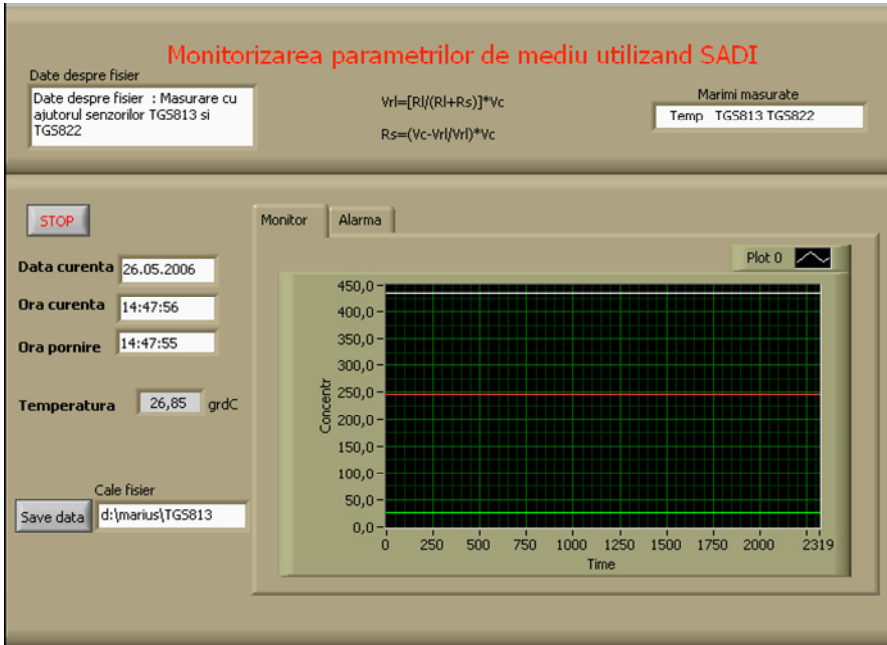


Fig. 8. Front panel and diagram of VI environmental monitoring system.

Admitting that the temperature and humidity have a great influence to Taguchi sensor resistance we have to make a compensation of the effect very utile when the system is used for outside. Knowing the  $R_S/R_0=f(T)$  dependency characteristic of the sensors and the temperature from AD590 temperature sensor the VI realize a temperature compensation by parts.

At 65% relative humidity, a characteristic linearization is made on the next intervals:  $-10^{\circ}\text{C} \div 20^{\circ}\text{C}$ ,  $20^{\circ}\text{C} \div 30^{\circ}\text{C}$ ,  $30^{\circ}\text{C} \div 40^{\circ}\text{C}$ . A slope determination for the three straight lines is done and for each temperature values is established the compensation factor. The main sub-VI's are:

1. *Nr.Scan* do the samples acquisition from an analog input channel.

2. *Vrl to RpeR0.vi* do the determination of  $R_S/R_0$

3. *Compens\_term.vi* realizes the compensation of temperature influence on sensor resistance (TGS). The VI inputs are: current temperature ( $^{\circ}\text{C}$ ) and measured value of  $R_S/R_0$ . The VI output is  $R_S/R_0$  value after thermo-compensation. The compensation of temperature influence is realized by equation implementation of linear variation  $R_S/R_0=f(T)$  on temperature interval previously mentioned.

4. *R to Concentratie.vi* determine the methane concentration based on sensor measured resistance using the next equation:

$$G_s = S_0 \cdot C^b \quad (4)$$

where,

$G_s=1/R_S$  is the sensor conductivity at certain methane concentration C.

$S_0$ , b - constants determinate for two concentration ( $C_1=1000$  ppm,  $C_2=3000$  ppm) when we know the value of sensor resistance. At VI input is applied the sensor resistance ( $R_S$ ) after the thermal effect compensation obtaining to the output the calculated value of concentration.

5. *Tens to grdC.vi* give the temperature dependence on input voltage of analogical channel 2 (1m/K).

However, in some situation is necessary the identification (recognize) of some gases compound with different smells using complex chemical analyzes.

If the imitation of tactile, additive and visual human senses and there implementation in tele-transmitting automat systems is well known in the literature, the smell sense was ignored. They are many applications where so called electronic nose may detect what is difficult or impossible for human or animal nose (for example, toxic waste identification, combustible mixture analyze, industrial emission monitoring, noninvasive medical analyzes, verification of food qualities, drugs detecting, mine and explosive detecting).

Intelligent system achievement which is dedicated for particular application is not easy. It presumes a selection of chemical sensors area which provide a large information quantity and complex algorithms development for signal processing.

## 5. Web E-Nose System

For ages, the human nose has been an important tool in assessing the quality of many products, food products being good examples. While all others parts of production processes, including these of the food industry, were getting more and more automated,

there was still no “objective” means for using the “subjective” information confined in the smell of products. This changed in 1982, when Persaud and Dodd introduced the concept of an electronic nose. They proposed a system, comprising an array of essentially non-selective sensors and an appropriate pattern recognition system, often called “e-nose”.

The task of an electronic nose is to identify an odorant sample and perhaps to estimate its concentration. The E-Nose consists of two main components: an array of gas sensors, and a pattern-recognition algorithm. Electronic odour sensing systems can include a combination of hardware components such as sensors, electronics, pumps, fans, air conditioners and flow controllers, and software for hardware observation and data processing. The gas sensors most commonly used in electronic noses are based on metal oxide semiconductor and conducting polymer techniques. Metal oxide sensors were first produced in Japan in the 1960s for use in gas alarms and depend on an alteration in conductance caused by contact with the odour and the reaction that result.

The proposed Web E-Nose consists of three main components: an array of gas sensors, a pattern-recognition algorithm and an Ethernet module with a static IP.

We developed a simple and original WebE-Nose prototype to test pattern recognition techniques that are necessary for building remote electronic nose systems.

Gas sensors tend to have very broad selectivity, responding to many different substances. This is a disadvantage in most applications, but in the electronic nose, it is an advantage. Although every sensor in an array may respond to a given chemical, these responses will usually be different.

Sensor array “sniffs” the vapors from a sample and provides a set of measurements. The pattern-recognizer compares the pattern of the measurements to stored patterns for known materials (Branzila M 2007).

The implemented Web E-Nose system consists in three main components (Fig. 11):

1. a gas sensors array,
2. the pattern recognition algorithm, and
3. Ethernet with IP static module.

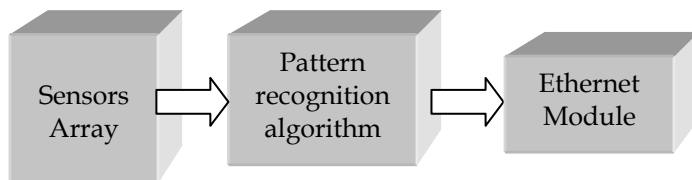


Fig. 9. Main components of the Web E-Nose.

The initial experiment was performed with a number of low selectivity gas sensors – calibrated to identify a threshold value of the most important polluting gases occurring in the atmosphere, combined with SHT11 humidity and temperature sensor, allowing immediate temperature and humidity compensation. The sensor array was also trained to recognize, by different sets of measurements, the hazard patterns for different polluting factors acting in the monitored area, as well as identify accidental patterns of polluting factors with external causes. The Ethernet module, having a static IP, give the possibility to share, over the World Wide Web, information’s about “remote polluters and potential

effects, hazard level etc." with a clear identification of the instrument and area. Finally, the result of Web E-Nose expertise may be visualized either as a code image of a given combination of volatile compounds, or may offer a review of the concentrations of individual molecule species detected in a complex environment (Fig. 10).

The response of the sensor array is numerically converted using a prototype data acquisition system SADI (integrated data acquisition system). This response is registered by microcontroller as "case pattern", compared and classified with the ones predefined within the training library. The microcontroller, playing the role of Web E-Nose "brain", communicates with SADI or with IP-Static module server by a serial interface.

Hence, the most important function of the Web E-Nose system consists in detecting and evaluating toxic gases or mixtures at minimum threshold quantities, especially those odourless to human senses. The information, acquired by the gas sensor arrays and rough calibrated by SHT11 temperature and humidity sensor, is subject of further processing for pattern recognition and transmission to the decision block by RS232 protocol to the Ethernet server.

The Web E-Nose system has five sequential stages: pre-processing, feature extraction, classification, decision making and decision transmission to the network. The decision making, based on pattern recognition, is assisted by a neural network with both training and extraction functions.

It goes without saying that the Web E-Nose system was not projected to substitute human capability of detecting hazardous situations by "smelling". In addition, the exquisite sensitivity of the dog's nose for sniffing out odours associated to drugs or other hazardous vapours has not yet been matched by currently designed E-nose.

But the system is well suited for repetitive and accurate measurements, and provided not to be affected by saturation, a common disadvantage of natural smelling senses.

Our human nose is elegant, sensitive, and self-repairing, but the Web-E-Nose sensors do not fatigue or get the "flu". Further, the Web-E-Nose can be sent to detect toxic and otherwise hazardous situations that humans may wish to avoid. Sensors can detect toxic CO, which is odorless to humans. And humans are not well suited for repetitive or boring tasks that are better left to machines. No wonder the E-Nose is sometimes referred to as a "sniffer".

However, the human nose is still preferred for many situations like the selection of a fine wine or to determine the off-odor of recycled plastics. In addition, the exquisite sensitivity of the dog's nose for sniffing out drugs or contraband at an airport is legendary already. These skills have not yet been matched by any currently designed E-Nose.

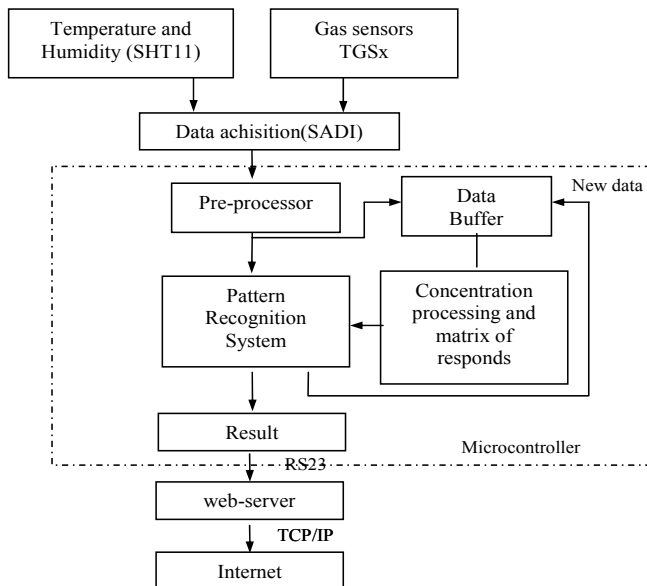


Fig. 10. Web E-Nose communication architecture.

## 6. Instrumentation and virtual laboratory

The Web concept itself is changing the way the measurements are made available and the results are distributed/communicated. Many different options are occurring as regards reports publishing, data sharing, and remotely controlling the applications.

The low-cost availability of new communication tools based on Internet is opening more and more horizons to remote teaching. Interactive on-line tutorials based on World Wide Web (WWW) sites now can be followed directly on the web site. The hardware of monitoring systems (sensors, conditioning circuits, acquisition and communication) must usually be complemented with processing blocks to perform different tasks associated to one-dimensional or multi-dimensional data that flow on the system measurement channels.

The recent wide diffusion of (i) easy-to-use software tools for the implementation of Graphical User Interfaces (GUIs); and (ii) communication-oriented instrumentation, often provided with Ethernet interface, in addition to the more traditional GPIB and RS-232 ones, can be particularly exploited in the field of measurement teaching. It is well known, in fact, that for a better understanding of the teaching issues in such a field, the students have to practice with real instrumentation. The computer-based simulations are often inadequate to assure a good experience in that direction. The tools mentioned above give the possibility of accessing real measurement instrumentation from a remote location, such as the students' homes (Arpaia P& Daponte P 1996, 1997, 2000). Moreover, it could be possible to repeat the same experience many times in order to make all students able to operate the measuring instrumentation without devoting expert technicians to such activity for many days [11-15]. In measurement teaching, the great increase of students on the one hand, and the reduced number of technicians on the other, greatly requires the possibility of accessing real

measurement instrumentation for remote experiments (Donciu C, 2001), (Donciu C & Rapuano C, 2002).

In electrical and electronic measurement courses, particularly, these problems become more severe as consequences of the more sophisticated and expensive apparatus now available which makes it difficult to keep the technical staff up-to-date, and the necessity for repeating the same experience many times in order to make all students able to operate the measuring instrumentation.

There are two basic options when it comes to atmospheric monitoring: use of portable gas detectors or use of fixed detection systems. Portable monitors are battery-operated, transportable devices worn by the person using it and generally can detect only few gases at a time. There are places where many potentially hazardous gases can be permanently present: refineries, chemical plants, gas production plants, laboratories, mines, a.s.o. In these cases, a fixed system placed in the area where leaks of potentially dangerous gases likely to occur may provide general continuous monitoring.

The objective of our research is the development of compact fixed systems for real-time monitoring of the air contaminants, suited for gas leak detection, environmental control, worker protection or other industrial applications. In the first stage, we have designed a system capable to detect only several combustible gases, using a Web E-Nose. The monitoring of more air pollutants increases the system complexity.

Our system performs the following main functions: detection of combustible gases (methane, ethanol, isobutane, hydrogen) and concentration measurement of toxic gases (carbon monoxide, hydrogen sulfide, ammonia). The system provides an alarm when the concentration of detected gases in the air reaches a dangerous level: % LEL (Lower Explosive Limit) - for combustible gases, TLV/TWA (Threshold Limit Value/Time Weighted Average), IDHL (Immediately Dangerous to Life or Health) - for toxic gases.

It can be very useful in the new society information to create a Virtual Laboratory for a remote teaching [3-4].

An adaptive architecture based on web server application is proposed, in order to increase the performance of the server that hosts a dedicated Web site, and customize the Web site in a manner that emphasizes the interests of the clients. The most virtual laboratories normally provide access either to one remote application, or accept only one user at a time. The system presented below provide a multitask connection, with possible variants for remote education. In this way, two parts compose the architecture of the system:

- client user that uses a client computer and
- measurement provider who disposes the server with the web site of the virtual laboratory.

The users will be able to perform the lab work, controlling the applications and accessing the virtual library. Number of users connected in the same time is unlimited.

The LabVIEW environment was incorporated in centre concept towards creating a unique and powerful distributed application, combining together different measurement nodes and multiple users into a unique measurement controlling system, in order to integrate and revolutionize the fundamental architecture of actual PC-based measurement solutions. All communication software is designed under LabVIEW graphical programming language.

In the figure 11 is presented the main web page of application

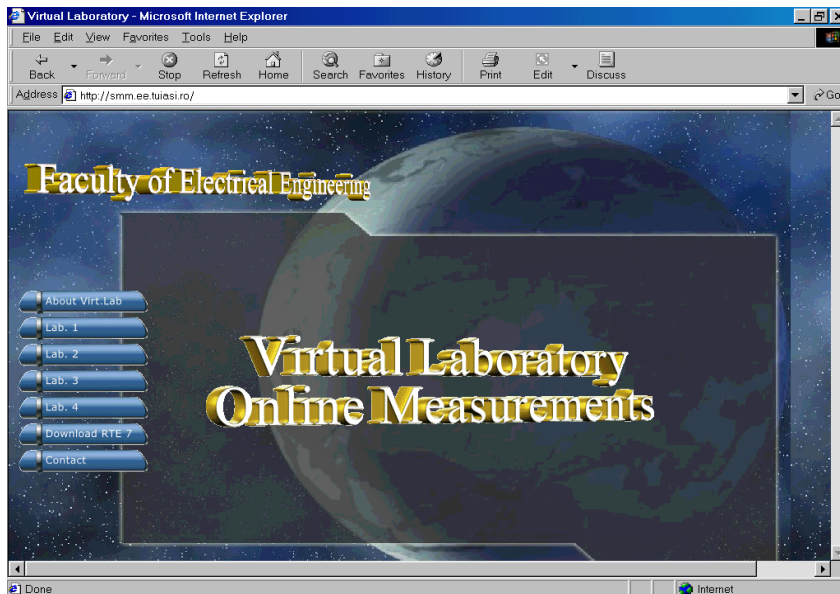


Fig. 11. The main web page of Virtual Laboratory.

## 7. Instrumentation and next generation Grid

The Grid technologies are introduced to build e-Learning environments for engineering education. Service-oriented Grids open new fields of applications, the Learning Grids. The learning services concept based on a learning model and their deployment through Grid technologies are excellent means to integrate virtual laboratories into e-Learning environments for engineering education. Examples from a virtual laboratory demonstrate the advantages of a Grid.

Remote or virtual laboratories with real or simulated experiments are becoming accepted in the engineering community for providing distance education and for augmenting traditional laboratories. Students have to modify instruments for a better understanding of the principle on which the plant operates. They even have to set their own conditions. From a pedagogical point of view, in this kind of environments the student has an active and central role in the learning process. Learning activities are inherently aimed at aiding the construction of knowledge and skills in the student, rather than the memorization of information. In keeping the student at the centre of the learning process, personalization and individualization become relevant aspects to be supported by technologies through the creation of the right context. The students can learn through direct experiences. So, the question remains - how do we provide better means for e-Learning environments combined with virtual laboratories while maintaining or improving the quality of learning by new information and communication technologies. A Learning Grid can contribute to the achievement of these objectives through the definition of the learning services concept and their deployment through Grid technologies.

Grids yield significant benefits to applications. A Grid is considered as a collection of clustered computational machines, the nodes. In order to have a powerful supercomputer by a Grid the computational problem has to be split into slices and assigned to these nodes. Each node processes its slice individually and after the completion of its slice the results are put back together. Grid nodes do not need to be placed in one geographic location; moreover, machines collaborating in the Grid may have different architectures and operating systems. It is obvious that these nodes need to communicate with each other based on some standards. Therefore a vital topic of security is involved for the interchange of data between nodes. Depending on the application the data should be kept confidential and protected from undesired external changes. Also other issues must be addressed, e.g. redundancy of nodes, quality of service and scalability.

The Grid is applicable only for tasks that can be easily split into smaller slices and that do not require the characteristics of a real-time challenge. In order to reduce the complexity of a Grid, a special layer is introduced that is for gluing the nodes on a logical level. This layer of software sandwiched between the operating system and the applications is commonly called middleware. During recent years a new approach for building Grids has emerged. Instead of perceiving the Grid nodes only as computational elements of an infrastructure they became providers of services. This shift, from strict computational capabilities to service suppliers, opens new fields of applications for Grids. The nodes, instead of only delivering their computational and storage capacity, are now regarded as providers of particular services. They may be parts of some code existing in multiple instances allowing the parallelization of the execution of an application. This new Grid philosophy allows perceiving it in analogy to the commonly known concept of power grids, where the consumer is not aware where and how the power is exactly produced. The consumer only receives the final product with a defined quality.

Figure 12 presents basic interactions between elements of a service-oriented Grid. Services published into a Grid Registry are queried and when discovered then instantiated depending on the user request. Mainly for sake of efficiency the client's communication with the service is direct but may also be virtualized.

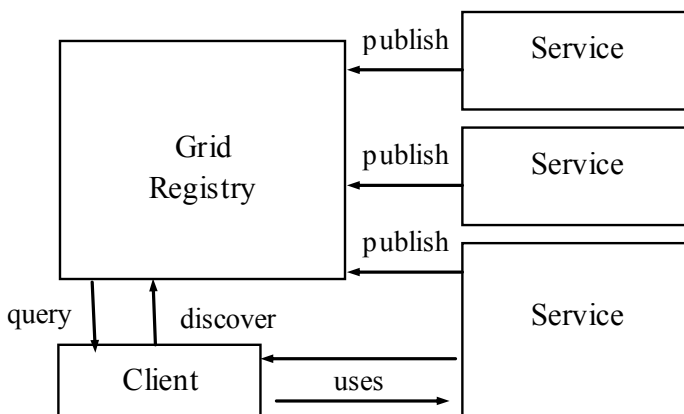


Fig. 12. Structure of a service-oriented Grid environment.

The main functionalities delivered by the middleware of a service-oriented Grid are:

1. Location – allows the determination, whether the required service exists and at which locations it is accessible
2. Instantiation – allows the instantiation of the service on that host, which matches the capabilities required for the service running with a given quality of service.
3. Orchestration – allows the dynamical composition of more complex services.

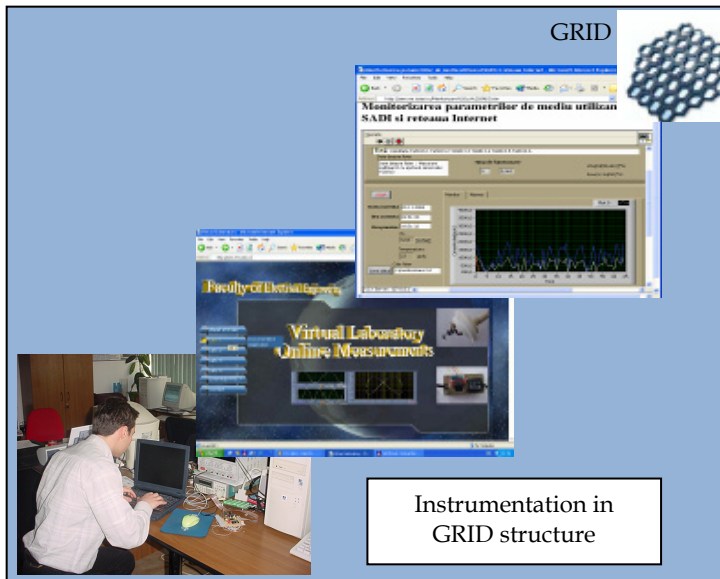


Fig. 13. From real world instruments to Grid structure, through Virtual Laboratory.

Learning Grids contribute to the achievement of the objectives given in the introductory chapter to this article through the definition of the learning services concept and their deployment through Grid technologies. Learning services will be consumed in dynamic virtual communities based on communications and collaborations where learners, through direct experiences, create and share their knowledge in a contextualized and personalized way.

This way of learning using grid resources can become now more open to learners in the engineering domain. The application of Grid technologies in education is of course a much wider topic than presented in this article and by the practical example of a virtual control laboratory. Nonetheless the most important aspects of utilizing service-oriented Grids in distance learning for control education are presented.

## 8. Conclusion

The presented system constitutes a versatile, flexible, cheap, high-speed digital data acquisition system that combined with LabView software give the possibility to easily monitoring the environmental parameters. They are many applications where the system can be used like: toxic waste identification, combustible mixture analyze, industrial emission

monitoring, non-invasive medical analyzes, verification of food qualities, drugs detecting, mine and explosive detecting.

This system can be adapted for an intelligent electronic nose with data transfer directly through the internet. I named Web E-Nose.

The Internet continues to become more integrated into our daily lives. This is particularly true for scientists and engineers, because designers of development systems view the Internet as a cost-effective worldwide standard for distributing data.

The paper presents the architecture of a versatile, flexible, cost efficient, high-speed measurement centre, based on remote instrumentation, and having as final purposes the monitoring of the air quality and the advertising of the air pollution. On the other hand the E-Medicine becomes a very interesting domain for physicians and bioengineers. That for the purposed system can be very useful tool for them.

In many locations a basic infrastructure to evaluate the E-Medicine already exists, but a unitary concept of an E-Medicine centre can be used to deliver services of comparable or higher quality, at a clear lower cost and a higher speed and reliability.

The Web-E-Nose system was tested, and provided to be well suited for repetitive and accurate measurements, without being affected by saturation. But the successful implementation of such Web E-Nose concepts for air pollution evaluation at larger scales will require a careful examination of all costs, either direct or indirect, and should demonstrate its societal benefit over time.

The remote and distributed measurement system developed as environmental centre may be also particularized as virtual laboratory for on-line environmental monitoring, helping the formation of well trained specialists in the domain.

The Web E-Nose is a tool that may be used for safety, quality, or process monitoring, accomplishing in a few minutes procedures that may presently require days to complete.

The system performs good and fast measurement, processing and transmission of the odors. It is very useful in the new society information to create a Virtual Laboratory for a remote teaching or to get information about gas mixtures or odours from a remote site.

The application of Grid technologies in education is of course a much wider topic than presented in this article and by the practical example of a virtual control laboratory. Nonetheless the most important aspects of utilizing service-oriented Grids in distance learning for control education are presented.

## 9. References

- Arpaia P., Daponte P. (2000), A measurement laboratory on geographic network for remote test experiments, *IEEE Trans. on Instrumentation and Measurement*, vol. 49, No. 5, Oct. 2000, pp. 992-997.
- Arpaia P., Daponte P. (1997) Ethernet application perspectives for distributed measurement systems, *Proc. of XIV IMEKO World Congress*, June 1997, Tampere, Finland, vol. IVA, pp. 13-18.
- Arpaia P., Daponte P. (1996) A distributed laboratory based on object-oriented systems, *Measurement*, vol. 19, No. 3/4, Nov.-Dec. 1996, pp. 207-215.

- Bertocco M., Cappellazzo S., A. Carullo, M. Parvis, A. Vallan, "Virtual environment for fast development of distributed measurement applications", Proc. of IEEE International Workshop on Virtual and Intelligent Measurement Systems, VIMS 2001, Budapest, Hungary, May 2001, pp. 57-60.
- Branzila M., and Co., A complex system for environmental monitoring with a prototype data acquisition board, IMEKO 2004 - 13th International Symposium on Measurements for Research and Industry Applications - 9th Workshop on ADC Modelling and Testing files, Athens - Greece, ISBN 960-254-645-X, pp.428-430
- Branzila M.C, and Co., Virtual Library Included in LabVIEW Environment for a New DAS with Data Transfer by LPT, IMEKO 2005 - 14th International Symposium on New Technologies in Measurement and Instrumentation and 10th Workshop on ADC Modelling and Testing, 12-15 September 2005, Gdynia/Jurata Poland, ISBN 83-89786-37-0, pp.535-540
- Branzila M., Alexandru C.I., Donciu C., Cretu M., Design and Analysis of a proposed Web Electronic Nose (WebE-Nose), EPE 2007 12th-14 th Oct, IAȘI - ROMÂNIA Buletinul IPI, Tomul LII(LIV), Fasc. 5
- Branzila, M., Alexandru, C., Donciu, C., Virtual environmental measurement center based on remote instrumentation, Environmental Engineering And Management Journal, Vol. 6, pp. 517-520, nov-dec 2007
- Branzila M. (2008) Intelligent system for monitoring of exhaust gas from hybrid vehicle, Intelligent Systems, 2008. IS '08, 4th International IEEE Conference, Volume 1, 6-8 Sept. 2008, Varna, Bulgaria, Page(s):5-2 - 5-5, ISBN: 978-1-4244-1739-1
- Branzila M. (2008) New DAQB and associated virtual library included in LabVIEW for environmental parameters monitoring, VECIMS 2008 IEEE Conference, 14-16 July 2008, Istanbul, page(s): 121-124, ISBN: 978-1-4244-1927-2, INSPEC Accession Number: 10156672
- Branzila M. (2007), Virtual environmental measurement center based on remote instrumentation, ENVIRONMENTAL ENGINEERING AND MANAGEMENT JOURNAL, Volume: 6, Issue: 6, pp. 517-520
- Branzila M. (2007) Virtual meteorological center, International Journal of Online Engineering, Vol. 3, No. 4 , 2007, pp. 45-480
- Branzila M. (2006) Design and Analysis of a proposed Web Electronic Nose (WebE-Nose), IAȘI - ROMÂNIA Buletinul Institutului Politehnic din Iasi, Tomul LII(LIV), Fasc. 5, 2006, ISSN 1223-8139, pp.971-976
- Carlosena A., Cabeza R. (1977), A course on instrumentation: the signal processing approach, Proc. of IEEE IMTC-97, Ottawa, Canada, May 1997, pp. 1326-1331.
- Donciu C., Petrescu M., Branzila M.C., Cantemir L., Cretu M., Prototype For A Distributed Measurement System, 4th International Conference On Electromechanical And Power Systems, September 26-27, Chisinau, Moldova, pp187-188, 2003
- Donciu, C., Temneanu, M., Branzila, M., Sustainable irrigation based on intelligent optimization of nutrients applications, Environmental Engineering And Management Journal, Vol. 6, pp. 537-540, nov-dec 2007
- Donciu, C., Temneanu, M., Branzila, M., Urban traffic pollution reduction using an intelligent video semaphoring system, Environmental Engineering And Management Journal, Vol. 6, pp. 563-566, nov-dec 2007

- Donciu C, Cretu M. (2001) "Communication in Virtual Instrumentation", Management of technological changes, Iasi, Romania, pp 69-74
- Donciu C, Rapuano S. (2002) A Remote Inter-University System for Measurement Teaching 12th IMEKO TC4 International Symposium, Zagreb, Croatia, pp 420-424
- Dyer S.A., Dyer R.A. (1977) Emphasizing the interdependence of topics in required undergraduate electrical engineering courses: a case study, Proc. of IEEE IMTC-97, Ottawa, Canada, May 1997, pp. 1320-1325.
- Hancock N.H. (1977), I&M in the 21st century engineering curriculum-a direction for change, Proc. of IEEE IMTC-97, Ottawa, Canada, May 1997, pp. 1326-1331.
- Keller P.E., Kouzes R.T., and Kangas L.J., "Three Neural Network Based Sensor Systems for Environmental Monitoring," IEEE Electro 94 Conference Proceedings, pp. 377-382, IEEE Press, Piscataway, NJ, USA, 1994
- Keller P.E. (1996), Electronic Noses and Their Applications, Proceedings of the World Congress on Neural Networks'96, pp. 928-931, Lawrence Erlbaum Associates Inc., Mahwah, NJ, USA, 1996.
- Schreiner C., Branzila M. (2006), Air quality and pollution mapping system, using remote measurements and GPS technology, Global NEST Journal, Vol 8, No 3, ISSN 1790-7632, pp 315-323, 2006



# Pulsed Discharge Plasma for Pollution Control

Douyan Wang, Takao Namihira and Hidenori Akiyama  
*Kumamoto University  
Japan*

## 1. Nonthermal Plasma for Air Pollution Control

Air pollution caused by emission of a pollutant produced by a variety of sources must be substantially reduced as mandated by recent national legislations and international agreements. In recent years, several techniques have been used to remove pollutants from air, with various degrees of success. Nonthermal plasmas, in which the mean energy of electrons is substantially higher than that of the ions and the neutrals, offer a major advantage in reducing the energy requirements to remove the pollutants [1], [2]. The application of a short-duration pulsed power to a gaseous gap at an atmospheric pressure results in the production of nonthermal plasma.

Acid rain is partly produced by emissions of nitrogen oxides such as nitric oxide (NO) and nitrogen dioxide (NO<sub>2</sub>) originating from fossil fuels burning in thermal power stations, motor vehicles, and other industrial processes such as steel production and chemical plants [3]-[8]. Nonthermal plasmas for removal of NO<sub>x</sub> have been produced using an electron beam [9], [10], a dielectric barrier discharge [6], [11], and a pulsed corona discharge [8], [12]-[24] at various energy effectiveness. Nevertheless, energy loss occurs in each plasma processing system which cannot be neglected. For an electron beam system, it has been reported that only 26% of the input energy can be transferred to the plasma due to losses in the vacuum interface [25]. In a dielectric barrier discharge system, the input energy is largely consumed by the dielectric barrier and gas heating and cooling. Consequently, only 20% of the primary energy is transmitted into the plasma [26]. In a pulsed discharge, the input energy is mainly consumed in the pulse forming circuit, and the impedance mismatching between the generator and discharge electrode gap results in further energy loss. Approximately 30% of primary energy can be transmitted into the plasma [27]. In order to improve the energy efficiency of plasma processing system, the effect of the pulse duration on NO removal concentration was studied. The results showed the pulse duration of the applied voltage has a strong influence on the energy efficiency of the removal of pollutants [28], [29], shorter pulse duration is required to reach cost effective NO removal. Consequently, a detailed understanding of the development of streamer discharge using very short duration pulses is important for practical applications. Here it should be noted that NO<sub>2</sub> can be converted to ammonium nitrate (NH<sub>4</sub>NO<sub>3</sub>) by adding ammonia (NH<sub>3</sub>) into the treatment gas, and NH<sub>4</sub>NO<sub>3</sub> can be used to make fertilizer. Therefore, the major discussion is focused on removal of NO. The mechanism of NO removal is resulted from the plasma enhanced chemical reactions. The energy input into the discharge resulted in a

larger number of collisions between electrons and the neutrals and produce the radicals such as O and N according to [30],



as well as other reactions [31], which then remove NO via the following reactions [32]:



where M is a third body, which can be said  $N_2$  or  $O_2$ . The reaction rate of  $K_1=6.9 \times 10^{-32} \text{ cm}^6/\text{s}$  [33] and



with a reaction rate of  $K_2=5.9 \times 10^{-11} \text{ cm}^3/\text{s}$  [34].

## 2. Observation of Pulsed Streamer Discharge and the Generation of Nano-seconds Pulsed Streamer Discharge

### 2.1 Methods and procedure

The most effective condition of streamer discharges might be obtained from investigating the streamer propagation across the electrodes gap, the electrode impedance, and gas temperature of the discharges. Under this purpose, the emission from pulsed streamer discharges in coaxial electrodes geometry at 0.1 MPa of air pressure was observed with the intensified charge-coupled display (ICCD) camera having a high-speed gate, a streak camera, and a spectrometer depending on the desired measurement.

The process of the streamer propagation can be obtained by taking framing and streak images with the camera system. Fig. 1 shows a schematic diagram of the experimental apparatus used to observe the positive and negative pulsed streamer discharges. A three-staged Blumlein line generator with a pulse duration of 100 ns was used as a pulsed power generator [35]. The generator was charged either at positive or negative voltages by a dc high voltage source. A coaxial cylindrical reactor was utilized as a discharge electrode to observe pulsed streamer discharges. For each test, a positive or negative polarity voltage from the generator was applied to the central rod electrode.

The electrode impedance can be calculated from the applied voltage and discharge current through the electrode gap waveforms.

When an electrical discharge is initiated from the electrode, a large amount of excited species can be generated by electron impact processes. These active species contribute to the plasma-enhanced chemical reactions which can lead to decomposition of pollutant gases and ozone generation. Measurement of gas temperature is one of the important factors to understand the plasma reaction process, because it is an important parameter in gas reactions and is expected to be higher than the room temperature in the active region of streamers [36]. Measurement of the band spectra of second positive system of nitrogen

molecule is one of the methods to examine the rotational temperatures of the  $C^3\Pi_u$  and  $B^3\Pi_g$  states by optical emission spectroscopy. Thus, the rotational temperature, which is assumed to be close to the gas temperature, can be determined by fitting the calculated spectrum with that measured experimentally [37].

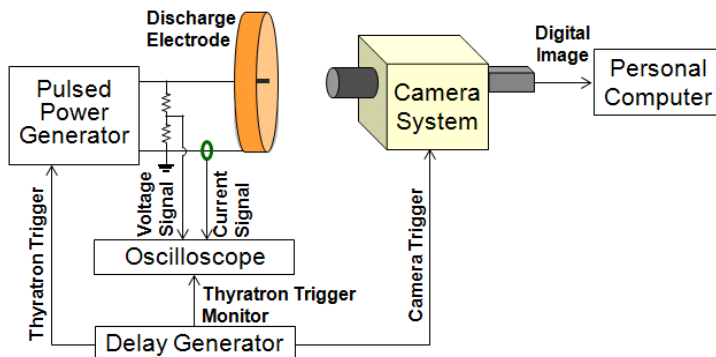


Fig. 1. Schematic diagram of the experimental apparatus used to observe the positive and negative pulsed streamer discharges. A rod made of stainless steel, 0.5 mm in diameter and 10 mm in length, was placed concentrically in a copper cylinder, 76 mm in diameter.

## 2.2 Observation of general pulsed streamer discharge (Pulse duration of 100 ns with 25 ns rise and fall time)

In a rod-to-cylinder coaxial electrode, the positive streamer discharge propagate straight in the radial direction from the coaxial electrode because the interactions between the electric fields near the neighboring streamer heads are the same at somewhere in the coaxial electrode geometry. The streamer heads are associated with a higher density of ionization due to the high electric field therein, and subsequently enhanced recombination, which is followed by increased light emission [35] (Fig.2, Fig.3). In positive pulsed streamer discharge, the emission at the vicinity of the rod electrode is observed 10-15ns after pulsed voltage application. The streamer heads were generated in the vicinity of the central electrode and then propagated toward the ground cylinder electrode. After full development of the streamer heads between the electrodes, the discharge phase transformed to a glow-like discharge with a large flow of current in the plasma channel produced by the streamer propagation. Finally, the glow-like discharge finished at the end of the applied pulsed voltage [35], [38] (Fig.3, Fig.4(a)). Therefore, two stages of the discharge can be clearly defined during the pulsed discharge. The first one is the 'streamer discharge', which means the phase of streamer heads propagation between electrodes. The other is the 'glow-like discharge' that follows the streamer discharge. Here it should be mentioned that in some publications, the track of the streamer head which propagates from the central rod electrode to the outer cylinder electrode is called as 'primary streamer', and the subsequent streamer head that started from the central electrode at 30 ~ 35 ns (Fig.3, Fig.4(a)) and disappeared at the middle of the electrodes gap is called a 'secondary streamer'. In negative pulsed streamer discharge, the negative streamer head initiates in the vicinity of the central rod electrode and then propagates toward the cylinder wall electrode. After fully development of the streamer head across the electrode gap (time at the peak applied

voltage), the discharge mode changed from a streamer to a glow-like discharge with a large discharge current, same as the positive one. It should be mentioned that discharge emission recorded near the surface of the rod electrode after the negative streamer head left the central rod is due to the surrounding photoionization and then the heat of the rod electrode surface. The propagation velocity of the streamer heads at certain time,  $v_{streamer}$ , can be given by

$$v_{streamer} = \frac{\Delta L}{\Delta t} \quad (5)$$

where  $\Delta L$  and  $\Delta t$  are the developed distance and time progress for its propagation from the streak images (Fig.4), respectively. The velocity of positive streamer is the same at certain applied voltage for different charging voltages, and the velocity increases with increasing applied voltage to the rod electrode. This may be due to the applied voltage to the rod electrode having a strong influence on the motion of the streamer head since there is a higher conductivity plasma channel between the rod and streamer head. The velocity of a negative streamer is approximately half that of positive streamers and also increases by increasing the absolute value of the applied voltage to the rod electrode. The propagation velocity of the streamer heads was 0.1 ~ 1.9 mm/ns for a positive peak applied voltage of 15 ~ 60 kV and 0.1 ~ 1.2 mm/ns for a negative peak applied voltage -28 ~ -93 kV, respectively. The electric field for streamer onset was constant at 15 kV for all different applied voltages in positive streamers. Likewise, the applied voltage at streamer onset was -25 kV for negative streamers. The electric field on the surface of the rod electrode before discharge initiation,  $E_0$ , were 12 and 20 MV/m, respectively.  $E_0$  is given by

$$E_0 = \frac{|V_{applied}|}{r \ln \frac{r_2}{r_1}} \quad (6)$$

where  $|V_{applied}|$ ,  $r$ ,  $r_1$ , and  $r_2$  are the absolute value of the applied voltage to the rod electrode, the distance from the center of the rod electrode, the radius of the rod electrode, and the inner radius of the cylinder electrode, respectively [35], [38].

The electrode impedance calculated from the applied voltage and discharge current through the electrode gap waveforms was about 13 k $\Omega$  in the streamer discharge phase and then dropped to 2 k $\Omega$  during glow-like discharge (Fig. 6(b)). Generally, impedance match between a power generator and a reactor is an important factor to improve higher energy transfer efficiency of the plasma processing system. This dramatic change of the electrode gap impedance during the discharge propagation makes it difficult to impedance match between the power generator and reactor.

Time dependence of the gas temperature around the central rod in a coaxial electrode geometry during a 100 ns pulsed discharge is shown in Fig. 7. The gas temperature remained about 300 K in the streamer discharge phase, and subsequently increased by about 150 K during the glow-like discharge. The temperature rise indicates thermal loss during the plasma reaction process that would lower gas treatment efficiency.

From those points of view, it is clear that a large energy loss occurred in the glow-like discharge phase. Therefore, to improve energy efficiency of a pulsed discharge, a system should be developed for an ideal discharge which ends before it shifts to the glow-like phase. This can be achieved by designing a pulsed power generator with short pulse duration.

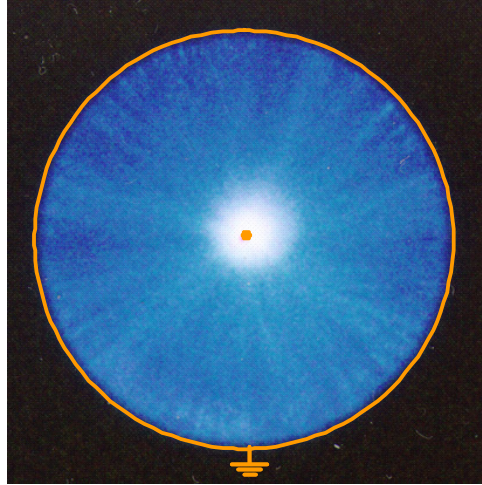


Fig. 2. Typical still image of a single positive pulsed streamer discharge taken from the axial direction in a coaxial electrode.

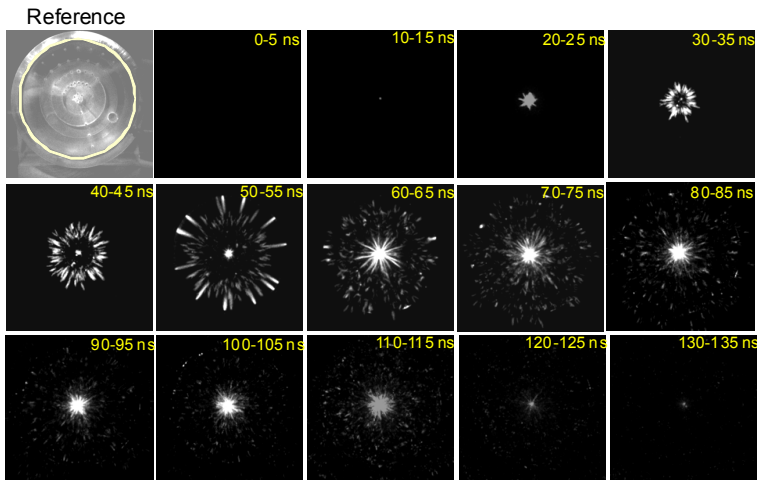
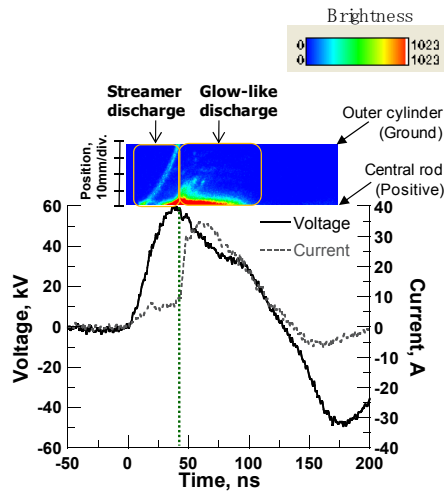
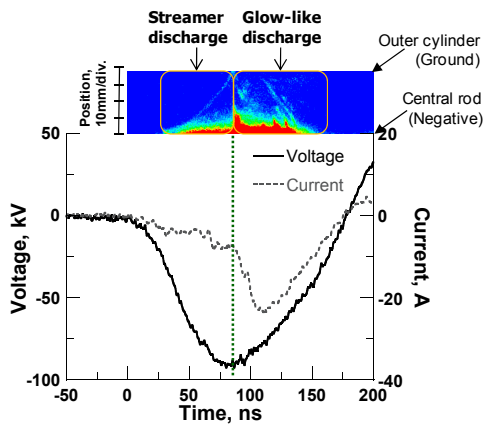


Fig. 3. Images of light emissions from positive pulsed streamer discharges as a function of time after initiation of the discharge current. Peak voltage: 72 kV. 100 ns of pulse duration. Outer cylinder diameter: 76 mm. The bright areas of the framing images show the position of the streamer heads during the exposure time of 5 ns.



(a) Positive pulsed streamer discharge at 30 kV charging voltage.



(b) Negative pulsed streamer discharge at -30 kV charging voltage.

Fig. 4. Typical applied voltage and discharge current in the electrode gap, and streak image for the generator with 100 ns of pulse duration. Voltage was measured using a voltage divider, discharge current through the electrodes was measured using a current transformer. The vertical direction of the streak image corresponds to the position within the electrode gap. The bottom and top ends of the streak image correspond to the central rod and the surface of the grounded cylinder, respectively. The horizontal direction indicates time progression. The sweep time for one frame of exposure was fixed at 200 ns.

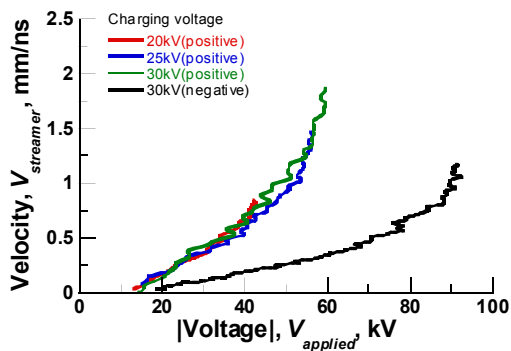
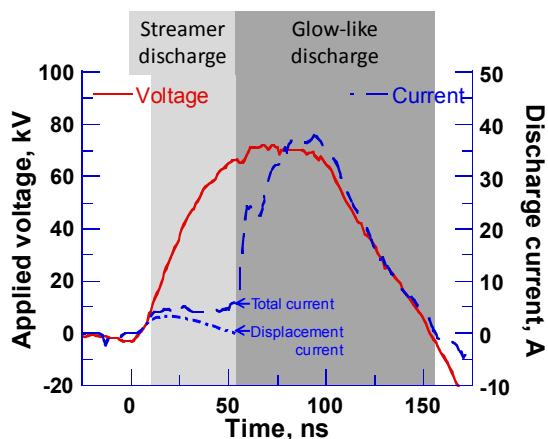
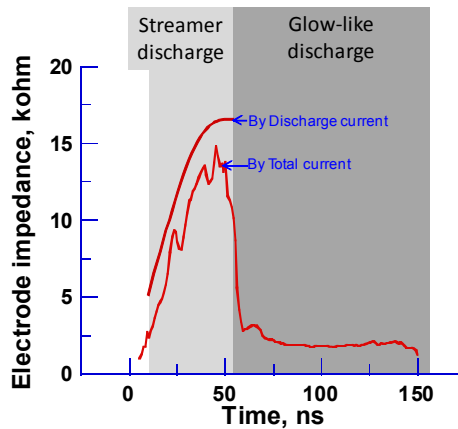


Fig. 5. Dependence of the velocity of the streamer heads on the applied voltage to the rod electrode for both positive and negative pulsed streamer discharge cases. 100 ns of pulse duration.



(a) applied voltage and discharge current through the electrode gap. 100 ns of pulse duration. Displacement current was calculated from  $(C_{reactor} \times dV_i/dt)$  where  $C_{reactor}$  is the capacitance of the reactor and  $V_i$  is the voltage from the waveform.



(b) Electrode gap impedance calculated from Fig. 6 (a).

Fig. 6. Change of electrode impedance during 100 ns discharge propagation process.

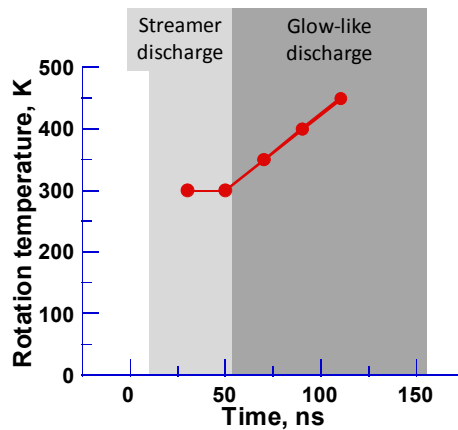


Fig. 7. Time dependence of the gas temperature around the central rod in a coaxial electrode geometry during a 100 ns pulsed discharge.

### 3. Generation of Nano-seconds Pulsed Streamer Discharge (Pulse duration of 5 ns with 2.5 ns rise and fall time)

A nano-seconds pulsed power generator (NS-PG) having a pulse duration of 5 ns and maximum applied voltage of 100 kV was developed by Namihira et al. in early 2000s [39]. The generator consists of a coaxial high-pressure spark gap switch (SGS) as a low inductance self-closing switch, a triaxial Blumlein as a pulse-forming line, and a voltage transmission line which transmit energy from the triaxial Blumlein line to the load. The SGS was filled with SF<sub>6</sub> gas, and the output voltage from the generator is regulated by varying the pressure of the SF<sub>6</sub> gas. Gap distance of the SGS was fixed. The triaxial Blumlein consists of an inner

rod conductor, a middle cylinder conductor, and an outer cylinder conductor. The inner, the middle, and the outer conductors of the triaxial Blumlein were concentric. The triaxial Blumlein and the transmission line were filled with silicone oil as an insulation and dielectric medium. For operation of the NS-PG, the middle conductor of the triaxial Blumlein was charged through a charging port that was connected to a pulsed charging circuit. The pulsed charging circuit consists of a dc source, a charging resistor, a capacitor, a thyatron switch, and a pulse transformer. The outer conductor was grounded. A capacitive voltage divider was mounted on the transmission line to measure output voltage of the NS-PG. The discharge current through the electrode was measured using a current monitor which was located after the transmission line. Polarity of the NS-PG output voltage could be controlled as either positive or negative by changing the polarity of output of the pulse transformer in the charging circuit. Typical applied voltage and current waveforms with an impedance matched resistive load are shown in Fig.8. The rise and fall times, and the pulse width are approximately 2.5 ns and 5 ns for both polarities.

Framing images and streak images of the discharge phenomena caused by the NS-PG are shown in Fig. 9 and Fig. 10, respectively. In case of positive pulsed streamer discharge, the streamer heads were generated near the central rod electrode and then propagated toward the grounded cylinder electrode in all radial direction of the coaxial electrode. The time duration of the streamer discharge was within 6 ns. At around 5 ns, emission from a secondary streamer discharge was observed in the vicinity of the central rod electrode. This is attributed to the strong electric field at the rod. Finally, emission from the pulsed discharge disappeared at around 7ns, and the glow-like discharge phase was not observed. Similar propagation process of a discharge can be confirmed from the negative pulsed discharge. The average propagation velocity of the streamer heads calculated by equation (5) was 6.1 ~ 7.0 mm/ns for a positive peak applied voltage of 67 ~ 93 kV and 6.0 ~ 8.0 mm/ns for a negative peak applied voltage -67 ~ -80 kV, respectively. The average velocity of the streamer heads slightly increased at higher applied voltages but showed no significant difference between positive and negative voltage polarities. Since the propagation velocity of the streamer heads is 0.1 ~ 1.2mm/ns for a 100 ns pulsed discharge, five times faster velocity is observed with the NS-PG (Fig.11). The streamer head always has the largest electric field in the electrode gap, and it is known streamer heads with higher value electric fields have a faster propagation velocity [40]. Therefore, it is understood that the faster propagation velocity of the streamer head means that the streamer head has more energetic electrons and higher energy. Consequently, the electron energy generated by nano-seconds pulsed discharge is higher than that of a general pulsed discharge [41], [42]. Here it should be mentioned that the voltage rise time (defined between 10 to 90%) was 25 ns for a 100 ns general pulsed discharge and 2.5 ns for the 5 ns nano-seconds pulsed discharge. Therefore, the faster propagation velocity of streamer head might be affected by the faster voltage rise time. The dependence of the propagation velocity of the streamer heads on the voltage rise time was studied by controlling the winding ratio of the pulse transformer (PT) that connected after the pulse generator. The dependence of the velocity of the streamer heads on the applied voltage to the rod electrode for different voltage rise time is shown in Fig. 12. From Fig.12, the propagation velocity of the streamer heads for 1:3 is approximately one and a half times faster than that of 3:9 PT winding ratio at the same applied voltage. Hence, the reason of the faster propagation velocity resulted in the nano-seconds pulsed discharge is due to the faster voltage rise time in comparison of the general

pulsed discharge [43]. Another interesting phenomenon of the nano-seconds pulsed discharge is the polarity dependence of the streamer propagation velocity. Generally, the velocity of a streamer head is faster for positive voltage application. In case of 100 ns pulsed discharges, the velocity for a negative streamer was approximately half that of a positive streamer. However, no significant difference was observed in the nano-seconds discharge by NS-PG for different polarities.

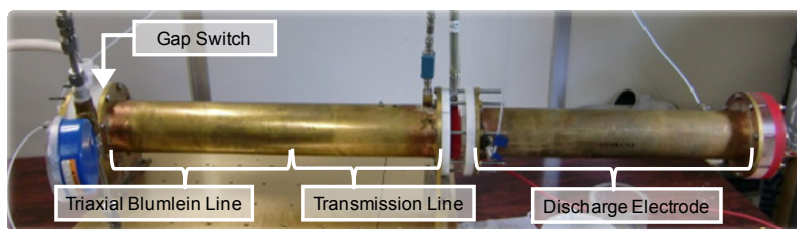
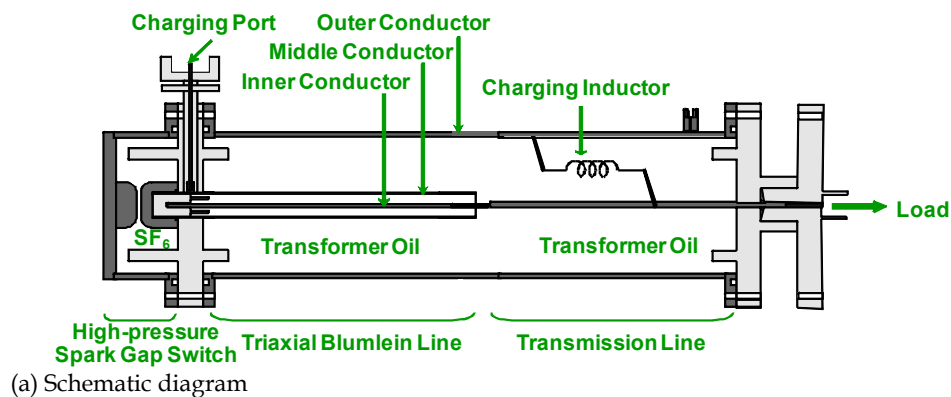


Fig. 8. Schematic diagram (a) and a still image (b) of the nano-seconds pulsed generator having pulse duration of 5 ns.

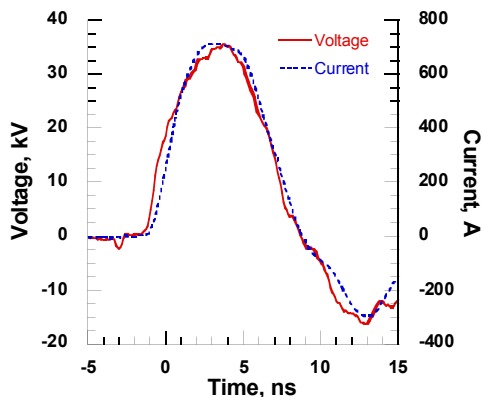


Fig. 8. Typical applied voltage and current waveforms for the nano-seconds pulsed generator with 5 ns of pulse duration. Load is impedance matched non-inductive resistor.

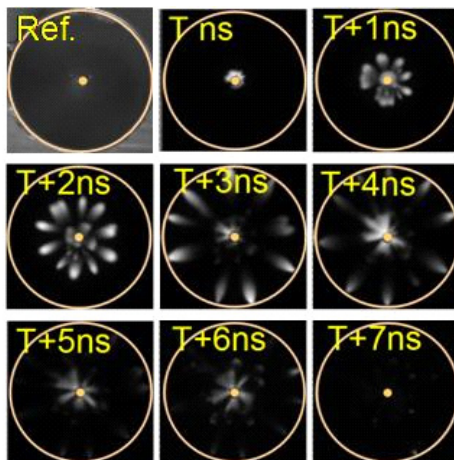
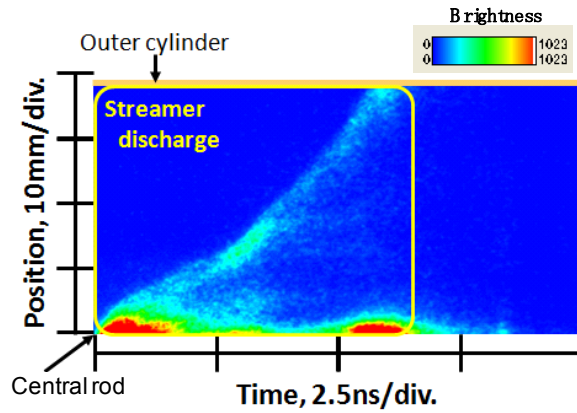
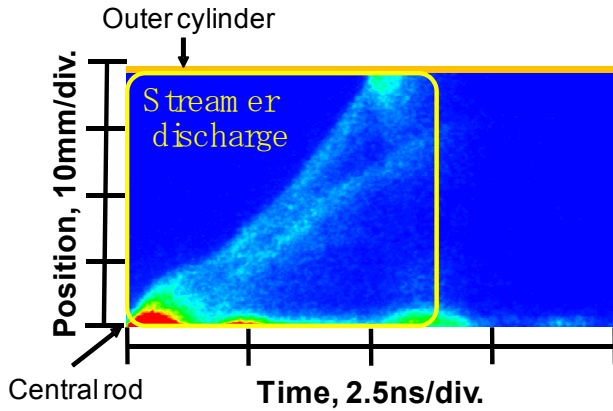


Fig. 9. Images of light emissions from positive pulsed streamer discharges as a function of time after initiation of the discharge current. Peak voltage: 100 kV. 5 ns of pulse duration. Outer cylinder diameter: 76 mm. The bright areas of the framing images show the position of the streamer heads during the exposure time of 200 ps.



(a) Positive polarity. Peak voltage: 93 kV.



(b) Negative polarity. Peak voltage: -80 kV.

Fig. 10. Streak images for the nano-seconds pulsed generator with 5 ns of pulse duration. The vertical direction of the streak image corresponds to the position within the electrode gap. The bottom and top ends of the streak image correspond to the central rod and the surface of the grounded cylinder, respectively. The horizontal direction indicates time progression. The sweep time for one frame of exposure was fixed at 10 ns.

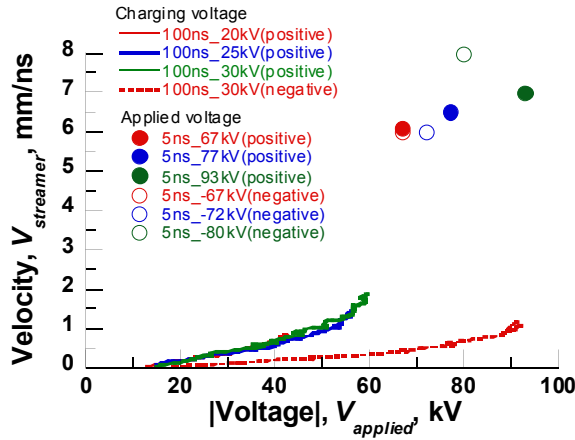


Fig. 11. Dependence of the velocity of the streamer heads on the applied voltage to the rod electrode for both positive and negative streamer discharge cases. (Comparison between general pulsed discharge and nano-seconds pulsed discharge)

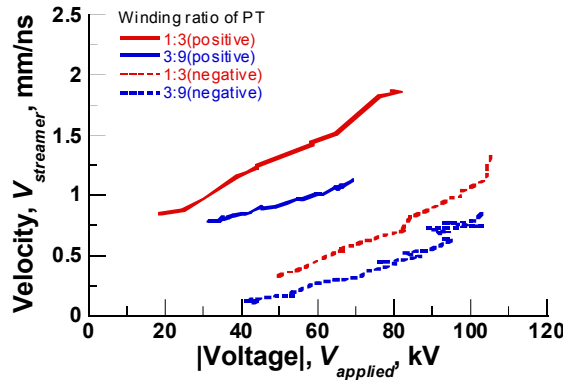


Fig. 12. Dependence of the velocity of the streamer heads on the applied voltage to the rod electrode for different voltage rise time. A three-staged Blumlein line generator with pulse duration of 200 ns was used to generate pulsed discharges. The voltage rise time was controlled by changing the winding ratio of the pulse transformer (PT) which connected after the Blumlein line generator. The winding ratio of primary to secondary windings of the PT was designed as 1:3 or 3:9. 30 kV of charging voltage.

#### 4. Comparison of General Pulsed Streamer Discharge and the Nano-seconds Pulsed Streamer Discharge

A comparison of the discharge characteristics are shown in Table 1. In general, streamer and glow-like discharges were observed in a pulsed discharge with a 100 ns pulse duration. In the glow-like discharge phase, a change of the electrode gap impedance and rise of the gas temperature occurred. Those factors could induce energy loss in the plasma processing

system for gas treatment. On the other hand, the discharge propagation finished before it shifted to the glow-like discharge phase in case of a nano-seconds pulsed discharge. The pulse duration of the NS-PG was approximately 5 ns with over 90 kV of peak applied voltage. The streamer propagation velocity by NS-PG is about five times faster than that of the general pulsed discharge, and has little difference between positive and negative voltage polarities. These results might be due to the very fast voltage rise and fall time of NS-PG. Because the electron energy in the streamer head generated by NS-PG is thought to be relatively high, the plasma-enhanced chemical reactions for gas decomposition and generation are expected to be more effective. Therefore, the energy transfer efficiency from the charging circuit to discharge reactor can be estimated to be higher than that of a general pulsed discharge. It can be concluded that a nano-seconds pulsed discharge is a promising method as a non-thermal plasma processing technique.

|  | General pulsed streamer discharge |                          | Nano-seconds pulsed streamer discharge                       |
|--|-----------------------------------|--------------------------|--|
| Voltage rise time  | 25 ns                             |                          | 2.5 ns   |
| Voltage fall time  | 25 ns                             |                          | 2.5 ns   |
| Pulse duration   | 100 ns                            |                          | 5 ns   |
| Discharge phase  | Streamer                          | Glow-like                | Streamer   |
| Propagation velocity of streamer heads ( $V_{\text{applied-peak}}$ ) | 0.1 ~ 1.2 mm/ns (10 ~ 60 kV)      | -                        | 6.1 ~ 7.0 mm/ns (67 ~ 93kV)<br>6.0 ~ 8.0 mm/ns (-67 ~ -80kV) |
| Electrode impedance  | 5 ~ 17 k $\Omega$ (L = 10 mm)     | 2 k $\Omega$ (L = 10 mm) | 0.3 k $\Omega$ (L = 200 mm)                                  |

Table 1. A comparison of the discharge characteristics between general pulsed streamer discharge and nano-seconds pulsed streamer discharge.

## 5. Characterization Map of NO Removal for Different Discharge Methods

Characteristic map of NO removal based on different discharge methods is given in Fig. 13. [44]. Comparison of nano-seconds pulsed discharge, dielectric barrier discharge (DBD) and pulsed corona discharge are displayed under the same condition of 200 ppm of initial NO concentration. NO removal ratio,  $NO_R$  in %, and removal efficiency,  $NO_E$  in mol/kWh, are given by equation (7) and (8):

$$NO_R = \frac{NO_i - NO_f}{NO_i} \times 100 \quad (7)$$

$$NO_E = \frac{G \times \frac{1}{22.4} [\text{mol/l}] \times NO_R \times 60 [\text{min/h}]}{f \times E \times 10^3} \quad (8)$$

where  $NO_i$  (in ppm),  $NO_f$  (in ppm),  $G$  (l/min),  $f$  (pps) and  $E$  (J/pulse) are the initial and the final concentrations of NO in the exhaust gas, gas flow rate, pulse repetition rate and input energy into discharge electrode per pulse ( $\int VIdt$ ), respectively.

The characterization map is based on input energy to discharge electrode. In Fig. 13, the right-upper region identifies the better performance of NO removal method. Nano-seconds pulsed discharge shows the best energy efficiency than other discharge methods.

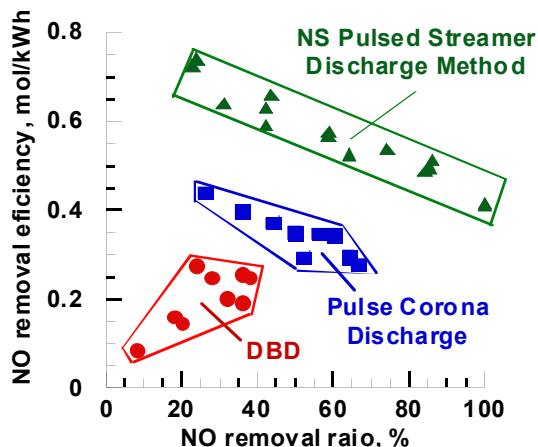


Fig. 13. Characteristic map of NO removal based on different discharge methods under the same condition of 200 ppm of initial NO concentration.

## 6. Ozone Generation

Ozone is known as a powerful oxidizing agent, far better than chlorine, which exists in nature. It is also a gas that does not generate by products since ozone decays to ordinary diatomic oxygen. Wide interests are focused on ozone generation studies for practical applications such as treatment of drinking and waste water, air purification, decoloration, bactericide and sterilization of food products etc [45], [46]. Recently, the medical usage of ozone has been widely studied in Europe, mainly in the fields of internal medicine, pediatrics, obstetrics and gynecology, and otorhinology [47]. Therefore, much attention has been paid for developing an energy-efficient ozonizer. However, ozone is an unstable agent which decays into oxygen at high concentrations, so that on-site production of ozone is desired. Several methods are available for ozone production: UV, electrolysis, and discharge method [48]. The leading method is the dielectric barrier discharge (DBD) which has been studied extensively using ac applied voltages. Several studies of ozone production using corona discharges incorporating dielectric barriers have been reported. However, the relatively long time duration of the applied voltage of a DBD leads to energy loss since not only electrons but also ions are accelerated, which generate heating losses during ozone production. Moreover, cooling systems are required for the dielectric materials resulting in further energy loss. Therefore, pulsed discharges, as distinguished without dielectric materials and only accelerated electrons, have been studied for ozone production in recent years.

### 6.1. Ozone Generation Using Pulsed Discharges

Pulsed discharges having different pulse duration, 50, 100, and 150 ns, were applied for ozone generation experiments (Fig. 14). The results showed that pulsed discharge with shorter duration has higher energy efficiency of ozone generation. This is because that the glow-like discharge resulted in the longer pulsed power has negative influences for ozone generation; ozone molecules attach low energy electron, typically 0 ~ 2.5 eV [49]-[51], during the glow-like discharge phase of the pulsed discharge, so that the ozone molecules were dissociated by the attachment of the low energy electrons. Here, it should be mentioned that the energetic electron during the streamer discharge phase is around 5 ~ 10 eV [52].

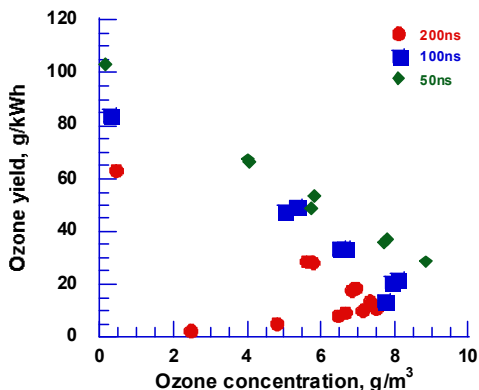


Fig. 14. Characteristic map of ozone generation based on different pulse duration under same positive applied voltages. Dry air was fed into the ozone generation at 1.0 l/min of gas flow rate was fixed at 273 K and 0.1 MPa.

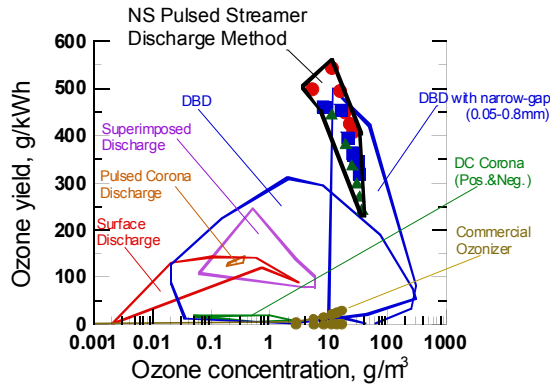
### 6.2. Characterization Maps of Ozonizers Based on Different Discharge Methods

Characterization maps of ozonizers based on different discharge methods (nano-seconds pulsed discharge, DBD, DBD with narrow-gap, surface discharge, pulsed corona discharge, DC corona, superimposed discharge methods and a commercial ozonizer) were presented with oxygen-fed and air-fed cases (Fig. 15) [53]-[72]. The production yield of ozone,  $\eta$  in g/kWh, was determined from

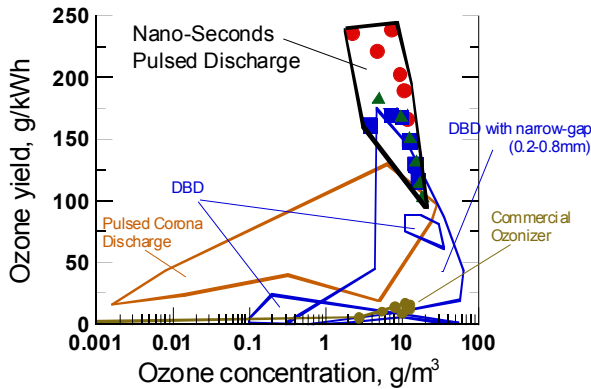
$$\eta = \frac{c \cdot r \cdot 60}{f \cdot E} \quad (9)$$

where  $c$  is the concentration of ozone (in g/Nm<sup>3</sup>),  $r$  is the gas flow rate in the discharge reactor (in l/min),  $f$  is the pulse repetition rate (in pps, pulses/second) and  $E$  is the input energy to the reactor per pulse (J/pulse). It should be noted that 0.048 kg of ozone is equivalent to 1 mol and 22.4 L at 1.01×10<sup>5</sup> Pa and 273 K. Equation (9) can also give the yield in mol/kWh by dividing  $\eta$  (g/kWh) by 48. The concentration of ozone can be given in ppm by multiplying  $c$  (g/Nm<sup>3</sup>) by 467. In Fig. 15, the right-upper region identifies the better performance of an ozonizer. It should be noted that the ozone yield resulting from the commercial ozonizer was evaluated from the plug-in energy while the others were

examined using the discharge energy. The nano-seconds pulsed discharge showed the highest ozone yield in the characterization maps for both the oxygen-fed and air-fed cases, where the highest ozone yield were 544 and 239 g/kWh in the oxygen-fed and air-fed cases, respectively. A summary of the characteristics map of ozonizer based on the different discharge methods (Fig. 15) is shown in Table 2 [73].



(a) Oxygen-fed



(b) Air-fed

Fig. 15. Characteristics map of ozonizers based on different discharge methods.

| Discharge method              | Oxygen-fed              |   | Air-fed                 |   |
|-------------------------------|-------------------------|---|-------------------------|---|
|                               | Max. ozone yield, g/kWh | Available ozone concentration, g/m <sup>3</sup> | Max. ozone yield, g/kWh | Available ozone concentration, g/m <sup>3</sup> |
| Nano-Seconds Pulsed Discharge | 544                     | 4.9 ~ 36.5                                      | 239                     | 2.2 ~ 18.3                                      |
| DC Corona                     | 19                      | 0.05 ~ 2  | -                       | -   |
| Pulsed Corona Discharge       | 145                     | 0.1 ~ 0.3                                       | 130                     | 0.001 ~ 28                                      |
| Surface Discharge             | 143                     | 0.002 ~ 3                                       | -                       | -   |
| DBD                           | 310                     | 0.02 ~ 299                                      | 88                      | 0.1 ~ 55  |

|   |      |          |     |          |
|---|------|----------|-----|----------|
| DBD with narrow-gap   | 500  | 10 ~ 300 | 175 | 0.3 ~ 62 |
| Superimposed Discharge  | 138  | 0.06 ~ 6 | -   | -        |
| Commercial ozonizer   | 30.5 | ~16      | ~17 | ~10      |
| Commercial ozonizer<br>(System evaluation, with plug-in energy) | 1.9  | ~16      | -   | -        |

Table 2. Summary of the characteristics map of ozonizer based on different discharge methods.

## 7. Conclusion

A discharge with pulse duration of 100 ns, the general pulsed streamer discharge, shows two discharge phases: a streamer discharge which initiates in the vicinity of the central electrode and propagates toward the outer electrode; and a glow-like discharge which is generated after full development of the streamer discharge. It was also observed that the plasma impedance was different for the streamer and the glow-like discharges. Moreover, a rise of the gas temperature occurred during the glow-like discharge phase. These factors could induce energy losses due to the impedance mismatching between the pulsed power generator and discharge reactor, with gas thermalization of plasma-enhanced chemical reactions during gas treatment. On the other hand, the discharge with pulse duration of 5 ns, nano-seconds pulsed streamer discharge, indicates that the discharge history finishes before it shifts to the glow-like discharge phase. Consequently, the impedance matching between the power generator and discharge reactor can be improved and the gas heating problem can be minimized. It can be concluded that a nano-seconds pulsed discharge is a promising method as a non-thermal plasma processing technique [74], [75].

## 8. References

- [1] Penetrante, B. M. & Schultheis, S. E., (1993). Nonthermal plasma techniques for pollution control, *Fundamentals and Supporting Technologies*, pt. A, 1-393, Springer-Verlag, New York
- [2] Penetrante, B. M. & Schultheis, S. E., (1993). Nonthermal plasma techniques for pollution control, *Electron Beam and Electrical Discharge Processing*, pt. B, 1-397, Springer-Verlag, New York
- [3] Urashima, K.; Chang, J.-S.; Park, J.-Y.; Lee, D.-C.; Chakrabarti, A. & Ito, T. (1998). Reduction of NO from natural gas combustion flue gases by corona discharge radical injection techniques, *IEEE Trans. Indust. Appl.*, Vol. 34, 934-939
- [4] Penetrante, B. M. (1993). Pollution control applications of pulsed power technology, *Proceedings of 9th IEEE Int. Pulsed Power Conf.*, pp. 1-5, Albuquerque, NM, USA
- [5] Gallimberti, I. (1988). Impulse corona simulation for flue gas treatment, *Pure Appl. Chem.*, Vol. 60, 663-674
- [6] Urashima, K.; Chang, J.-S. & Ito, T. (1997). Reduction of NO from combustion flue gases by superimposed barrier discharge plasma reactors, *IEEE Trans. Indust. Appl.*, Vol. 33, 879-886
- [7] Bhasavanich, D.; Ashby, S.; Deeney, C. & Schlitt, L. (1993). Flue gas irradiation using pulsed corona and pulsed electron beam technology, *Proceedings of 9th IEEE Int. Pulsed Power Conf.*, pp. 441-444, Albuquerque, NM, USA

- [8] Chang, J.-S.; Looy, P. C.; Nagai, K.; Yoshioka, T.; Aoki, S. & Maezawa, A. (1996). Preliminary pilot plant tests of a corona discharge-electron beam hybrid combustion flue gas cleaning system, *IEEE Trans. Indust. Appl.*, Vol. 32, 131-137
- [9] Penetrante, B. M.; Hsiao, M. C.; Bardsley, J. N.; Merritt, B. T.; Vogtlin, G. E.; Wallman, P. H.; Kuthi, A.; Burkhart, C. P. & Bayless, R. J. (1995). Electron beam and pulsed corona processing of volatile organic compounds and nitrogen oxides, *Proceedings of 10th IEEE Int. Pulsed Power Conf.*, 144-149, Albuquerque, NM, USA
- [10] Penetrante, B. M. (1997). Removal of NO from diesel generator exhaust by pulsed electron beams, *Proceedings of 11th IEEE Int. Pulsed Power Conf.*, 91-96, Baltimore, MD, USA
- [11] Rosocha, L.; Anderson, G. K.; Bechtold, L. A.; Coogan, J. J.; Heck, H. G.; Kang, M.; McCulla, M.; M. Tennant, M. & Wantuck, P. J. (1993). Treatment of hazardous organic wastes using silent discharge plasmas, In: *Non-Thermal Plasma Techniques for Pollution Control*, Penetrante, B. M. & Schultheis S. E. (Ed.), pt. B, 281-308, Springer-Verlag, New York
- [12] Masuda, S. (1988). Pulse corona induced plasma chemical process: A horizon of new plasma chemical technologies, *Pure Appl. Chem.*, Vol. 60, 727-731
- [13] Akiyama, H.; Kawamura, K.; Takeshita, T.; Katsuki, S.; Maeda, S.; Tsukamoto, S. & Murata, M. (1995). Removal of NO using discharges by pulsed power, *Proceedings of 10th IEEE Int. Pulsed Power Conf.*, pp. 133-137, Albuquerque, NM, USA
- [14] Dinelli, G.; Civitano, L. & Rea, M. (1990). Industrial experiments on pulse corona simultaneous removal of NO and SO from flue gas, *IEEE Trans. Indust. Appl.*, Vol. 26, 535-541
- [15] Chang, J.-S.; Lawless, P. A. & Yamamoto, T. (1991). Corona discharge processes, *IEEE Trans. Plasma Sci.*, Vol. 19, 1152-1166
- [16] Heesch, E. J. M. Van; Smulders, H. W. M.; Paasen, S. V. B. Van; Blom, P. P. M.; Gompel, F. M. Van; Staring, A. J. P. M. & Ptasinski, K. J. (1997). Pulsed corona for gas and water treatment, *Proceedings of 11th IEEE Int. Pulsed Power Conf.*, pp. 103-108, Baltimore, MD, USA
- [17] Clements, J. S.; Mizuno, A.; Finney, W. C. & Davis, R. H. (1989). Combined removal of SO<sub>2</sub>, NO<sub>x</sub> and fly ash from simulated flue gas using pulsed streamer corona, *IEEE Trans. Indust. Appl.*, Vol. 25, 62-69
- [18] Masuda S. & Nakao, H. (1995). Control of NO by positive and negative pulsed corona discharges, *IEEE Trans. Indust. Appl.*, Vol. 26, 374-383
- [19] Mizuno, A.; Shimizu, K.; Chakrabarti, A.; Dascalescu, L. & Furuta, S. (1995). NO removal process using pulsed discharge plasma, *IEEE Trans. Indust. Appl.*, Vol. 31, 957-963
- [20] Akiyama, H. (1995). Pollution control by pulsed power, *Proceedings of 1995 Int. Power Electron. Conf.*, 1397-1400, Yokohama, Kanagawa, Japan
- [21] Tsukamoto, S.; Namihira, T.; Wang, D.; Katsuki, S.; Akiyama, H.; Nakashima, E.; Sato, A.; Uchida, Y. & Koike, M. (1999). NO<sub>x</sub> and SO<sub>2</sub> removal by pulsed power at a thermal power plant, *Proceedings of 12th IEEE Int. Pulsed Power Conf.*, Monterey, CA, USA
- [22] Masuda S. & Nakao, H. (1990). Control of NO<sub>x</sub> by positive and negative pulse corona discharges, *IEEE Trans. Indust. Appl.*, Vol. 26, 374-383

- [23] Tsukamoto, S.; Namihira, T.; Wang, D.; Katsuki, S.; Akiyama, H.; Nakashima, E.; Sato, A.; Uchida, Y. & Koike, M. (1999). Pollution control of actual flue gas using pulsed power at a thermal power plant (in Japanese), *Trans. IEEJ*, Vol. 119-A, 984-989
- [24] Namihira, T.; Wang, D.; Tsukamoto, S.; Katsuki, S. & Akiyama, H. (1999). Effect of gas composition for NO<sub>x</sub> removal using pulsed power (in Japanese), *Trans. IEEJ*, Vol. 119-A, 1190-1195
- [25] Hirota, K.; Sakai, H.; Washio M. & Kojima, T. (2004). Application of Electron Beams for the Treatment of VOC Streams, *Ind. Eng. Chem. Res.*, Vol. 43, 1185-1191
- [26] Nozaki, T.; Miyazaki, Y.; Unno, Y. & Okazaki, K. (2001). Energy distribution and heat transfer mechanism in atmospheric pressure non-equilibrium plasmas, *Journal of Physics D: Applied Physics*, Vol. 34, No. 23, 3383-3390
- [27] Wang, D.; Namihira, T.; Fujiya, K.; Katsuki S. & Akiyama, H. (2004). The reactor design for diesel exhaust control using a magnetic pulse compressor, *IEEE Transactions on Plasma Science*, Vol. 32, No. 5, 2038-2044
- [28] Namihira, T.; Tsukamoto, S.; Wang, D.; Katsuki, S.; Hackam, R.; Akiyama, H.; Uchida, Y. & Koike, M. (2000). Improvement of NO removal efficiency using short width pulsed power, *IEEE Trans. Plasma Sci.*, Vol. 28, 434-442
- [29] Puchkarev V. & Gundersen, M. (1997). Energy efficient plasma processing of gaseous emission using a short pulse discharge, *Appl. Phys. Lett.*, Vol. 71, No. 23, 3364-3366
- [30] Penetrante, B. M. (1993). Plasma chemistry and power consumption in nonthermal de-NO<sub>x</sub>, In: *Nonthermal Plasma Techniques for Pollution Control*, Penetrante B. M. & Schultheis, S. E. (Ed.), pt. A, 65-90, Springer-Verlag, 1993, New York
- [31] Penetrante B. M. & Schultheis, S. E. (1993). Nonthermal plasma techniques for pollution control, *Fundamentals and Supporting Technologies*, pt. A, 1-393, Springer-Verlag, New York
- [32] Hackam R. & Akiyama, H. (2000). Air pollution control by electrical discharges, *IEEE Trans. Dielect. Elect. Insulation*, Vol. 7, 654-683
- [33] Urashima K. & Chang, J. S. (1997) The effect of ammonia injection rate and discharge power on the reduction of NO from combustion flue gas by superimposing barrier discharge reactors, *J. Adv. Oxid. Technol.*, Vol. 2, 286-293
- [34] Urashima, K.; Chang, J. S. & Ito, T. (1997). Reduction of NO from combustion flue gases by superimposed barrier discharge plasma reactions, *IEEE Trans. Ind. Applicat.*, Vol. 33, 879-886
- [35] Namihira, T.; Wang, D.; Katsuki, S.; Hackam R. & Akiyama, H. (2003). Propagation velocity of pulsed streamer discharges in atmospheric air, *IEEE Transactions on Plasma Science*, Vol.31, No.5, 1091-1094
- [36] Tochikubo F. & Teich, T. H. (2000). Optical Emission from a Pulsed Corona Discharge and Its Associated Reactions, *Jpn. J. Appl. Phys.*, Vol. 39, 1343-1350
- [37] Sakamoto, T.; Matsuura, H. & Akatsuka, H. (2007). Spectroscopic study on the vibrational populations of N<sub>2</sub> C<sup>3</sup>Π and B<sup>3</sup>Π states in a microwave nitrogen discharge, *Journal of Applied Physics*, Vol.101, 023307-1-7
- [38] Wang, D.; Jikuya, M.; Yoshida, S.; Namihira, T.; Katsuki, S. & Akiyama, H. (2007). Positive- and Negative-Pulsed Streamer Discharges Generated by a 100-ns Pulsed Power in Atmospheric Air, *IEEE Transactions on Plasma Science*, Vol.35, No.4, 1098-1103

- [39] Wang, D.; Namihira, T.; Katsuki S. & Akiyama, H. (2004). Ultra-short pulse generator for environmental control, *Proceedings of 15th International Conference on Gas Discharges and Their Applications*, Vol.2, pp. 709-712, Toulouse, France
- [40] Tochikubo F. & Arai, H. (2002). Numerical Simulation of Streamer propagation and Radical Reaction in Positive Corona Discharge in  $N_2/NO$  and  $N_2/O_2/NO$ , *Jpn. J. Appl. Phys.*, Vol. 41, 844-852
- [41] Wang, D.; Namihira T. & Akiyama, H. (2009). Pulsed discharge plasma generated by nano-seconds pulsed power in atmospheric air, *Proceedings of 17th IEEE International Pulsed Power Conference*, Washington, DC, USA
- [42] Wang, D; Okada, S; Matsumoto, T; Namihira, T & Akiyama, H. (2010). Pulsed Discharge Induced by Nanosecond Pulsed Power in Atmospheric Air, *IEEE Transactions on Plasma Science*, in press
- [43] Wang, D; Namihira, T; Matsumoto, T; Okada, S & Akiyama, H. (2010). Different Discharge Phenomena Between General and Nano-Seconds Pulsed Discharges, *Proceedings of The seventh International Symposium on Non-Thermal Plasma Technology*, X-5, John's, Newfoundland, Canada
- [44] Kim, Y. (2004). Experimental and Numerical Analysis of Streamers in Pulsed Corona and Dielectric Barrier Discharges, *IEEE Transactions on plasma science*, Vol.32, No. 1
- [45] Kogelschatz, U.; Eliasson B. & Hirth, M. (1987). Ozone generation from oxygen and air: Discharge physics and reaction mechanisms, *Ozone: Science & Engineering*, Vol. 9, 367-377
- [46] Eliasson, B.; Hirth, M. & Kogelschatz, U. (1987). Ozone synthesis from oxygen in dielectric barrier discharges, *J. Phys. D, Appl. Phys.*, Vol. 20, 1421-1437
- [47] Viebahn-Haensler, R. (2002). The Use of Ozone in Medicine, *Medicina Biologica*, 4th edition
- [48] Sugimoto, H. (1996). *Basis and applications of ozone (in Japanese)*, Korin
- [49] Tegeeder, P.; Kendall, P.A.; Penno, M.; Mason N.J. & Illenberger, E. (2001). Electron stimulated desorption of O- and O<sub>2</sub>- from condensed ozone: Possible implications for the heterogeneous photochemistry of stratospheric O<sub>3</sub>, *Physical Chemistry chemical Physics*, Vol.3, 2625-2629
- [50] Walker, I.C.; Gingell, J.M.; Mason N.J. & Marston, G. (1996). Dissociative electron attachment (DEA) in ozone 0-10eV, *Journal of Physics B: Atomic, Molecular and Optical Physics*, Vol.29, 4749-4759
- [51] Kuzumoto, M. (1998). Extremely narrow discharge gap ozone generator, *Journal of Plasma and Fusion Research*, Vol.74, No.10, 1144-1150
- [52] Kanazawa, S. (2008). Dynamics and structure of ignition process in plasmas, *Journal of Plasma Fusion Research*, Vol.84, No.6, 348-355
- [53] Kuzumoto, M. (1998). Extremely narrow discharge gap ozone generator, *Journal of Plasma and Fusion Research*, Vol. 74, No. 10, 1144-1150
- [54] Pietsch, G. J; Gibalov, V. I. (1998). Dielectric barrier discharge and ozone synthesis, *Pure & Appl. Chem.*, Vol. 70, No. 6, 1169-1174
- [55] AHN, H. S.; Hayashi, N.; Ihara, S. & Yamabe, C. (2003). Ozone generation characteristics by superimposed discharge in oxygen-fed ozonizer, *Jpn. J. Appl. Phys.*, Vol. 42, Part 1, No. 10, 6578-6583

- [56] Kimura, T.; Hattori, Y. & Oda, A. (2004). Ozone production efficiency of atmospheric dielectric barrier discharge of oxygen using time-modulated power supply, *Japanese Journal of Applied Physics*, Vol. 43. No. 11A, 7689-7692
- [57] Golota, V. I.; Zvavada, L. M.; Kadolin, B. B.; Paschenko, I. A.; Pugach, S. G.; Taran, G. V. & Yakovlev, A. V. (2004). Pulsed discharge for ozone synthesis, *Proceedings of XV International Conference on Gas Discharge and their Applications*, Toulouse, France
- [58] Simek, M. & Clupek, M. (2002). Efficiency of ozone production by pulsed positive corona discharge in synthetic air, *Journal of Physics D: Applied Physics*, Vol. 35, 1171-1175
- [59] Takaki, K.; Hatanaka, Y.; Arima, K.; Mukaigawa, S. & Fujikawara, T. (2009). Influence of electrode configuration on ozone synthesis and microdischarge property in dielectric barrier discharge reactor, *Vacuum*, 83, 128-132
- [60] Fang, Z.; Qiu, Y.; Sun, Y.; Wang, H. & Edmund, K. (2008). Experimental study on discharge characteristics and ozone generation of dielectric barrier discharge in a cylinder-cylinder reactor and a wire-cylinder reactor, *Journal of Electrostatics*, 66, 421-426
- [61] Takayama, M.; Ebihara, K.; Stryczewska, H.; Ikegami, T.; Gyoutoku, Y.; Kubo, K. & Tachibana, M. (2006). Ozone generation by dielectric barrier discharge for soil sterilization, *Thin Solid Films*, 506-507, 396-399
- [62] Park, S.L.; Moon, J. D.; Lee, S. H. & Shin, S. Y. (2006). Effective ozone generation utilizing a meshed-plate electrode in a dielectric-barrier discharge type ozone generator, *Journal of Electrostatics*, 64, 275-282
- [63] Jung, J. S. & Moon, J. D. (2008). Corona discharge and ozone generation characteristics of a wire-plate discharge system with glass-fiber layer, *Journal of Electrostatics*, 66, 335-341
- [64] Sung, Y. M. & Sakoda, T. (2005). Optimum conditions for ozone formation in a micro dielectric barrier discharge, *Surface & Coatings Technology*, 197, 148-153
- [65] Yamamoto, M.; Ehara, Y.; Kishida, H. & Itho, T. (1997). Ozone generation using three-phase asymmetrical system, *Proceedings of 6th Annual Conference on ozone Science and Technology in Japan*, pp. 63-65
- [66] Kitayama, J. & Kuzumoto, M. (1997). Theoretical and experimental study on ozone generation characteristics of an oxygen-fed ozone generator in silent discharge, *Journal of Physics. D: Applied Physics*, 30, 2453-2461
- [67] Kitayama, J. & Kuzumoto, M. (1999). Analysis of ozone generation from air in silent discharge", *Journal of Physics D: Applied Physics*, 32, 3032-3040
- [68] Stryczewska, H. D.; Ebihara, K.; Takayama, M.; Gyoutoku, Y. & Tachibana, M. (2005). Non-thermal plasma-based technology for soil treatment, *Plasma Processes and Polymers*, 2, 238-245
- [69] Toyofuku, M.; Ohtsu, Y. & Fujita, H. (2004). High ozone generation with a high-dielectric-constant material, *Japanese Journal of Applied Physics*, Vol. 43, No. 7A, 4368-4372
- [70] Kuzumoto, M.; Tabata, Y. & Shiono, S. (1997). Development of a very narrow discharge gap ozone generator -Generation of high concentration ozone up to 20 wt% for pulp bleaching-, *Kami Pa Gikyoushi/Japan Tappi Journal*, 51(2), 345-350

- [71] Zhang, Z.; Bai, X.; Bai, M.; Yang, B. & Zhou, X. (2003). An ozone generator of miniaturization and modularization with the narrow discharge gap, *Plasma Chemistry and Plasma Processing*, 23(3), 559-568
- [72] Itoh, H.; Teranishi, K. & Shimomura, N. (2008). Ozone yield efficiency of piezoelectric transformer-based ozone generator, *Proceedings of 18th Annual Conference on ozone Science and Technology in Japan*, pp. 149-152
- [73] Wang, D.; Namihira, T.; Katsuki S. & Akiyama, H. (2010). Development of Higher Yield Ozonizer Based on Nano-Seconds Pulsed Discharge, *Journal of Advanced Oxidation Technologies*, Vol.13, No.1, 71-78
- [74] Namihira, T.; Wang, D & Akiyama, H. (2009). Pulsed power technology for pollution control, *Physica Polonica A*, Vol.115, No.6, 953-955
- [75] Namihira, T.; Wang, D.; Matsumoto, T.; Okada, S. & Akiyama, H. (2009). Introduction of nano-seconds pulsed discharge plasma and its applications (in Japanese), *IEEJ Transactions on Fundamentals and Materials*, Vol.129, No.1, 7-14



# Air quality monitoring using CCD/ CMOS devices

K. L. Low, C. E. Joanna Tan, C. K. Sim,  
M. Z. Mat Jafri, K. Abdullah and H. S. Lim  
*Universiti Sains Malaysia  
Penang, Malaysia*

## 1. Introduction

The atmosphere, which makes up the largest fraction of the biosphere, is a dynamic system that continuously absorbs a wide range of solids, liquids as well as gases from both natural and man-made sources (M. Rao, *Air Pollution*, 1989).

The environmental pollution such as the air pollution is a common global issue especially in Malaysia. We encounter haze problem every year. This is due to the open burning after the harvest season in the country and also from the neighboring country. The worst of these events caused Malaysia to declare an emergency in 1997 for Kuching, Sarawak, and in 2005 for Port Klang and the district of Kuala Selangor. Air pollution was defined as “the presence in the outdoor atmosphere of one or more contaminants, such as dust, fumes, gas, mist, odor, smoke or vapor in quantities of characteristics, and of duration, such as to be injurious to human, plant, or property, or which unreasonably interferes with the comfortable enjoyment of life and property” (Lawrence K. Wang *et.al.*, 2004), is not a recent phenomenon.

Air pollution affects human health and reduces the quality of our land and water. We cannot escape from it, even in our own homes. In particular, environmental pollution is a persistent problem in Malaysia. Atmosphere contains various sizes of particles. Light is absorbed when sunlight penetrates through the atmospheric layer. This is because aerosol reduces 10% of light intensity when light reaches the earth surface. Air quality data is an important formula for monitoring and managing the environment. Air pollution can cause death, impair health, reduce visibility, bring about vast economic losses and contribute to the general deterioration of both our cities and country-side. It can also cause intangible losses to historical monuments such as the Taj Mahal which is believed to be badly affected by air pollution (M. Rao, 1989).

Air pollution also means different things to different people. To the householder it may be an eye irritation and soiled clothing, to the farmer damaged vegetation, to the pilot dangerously reduced visibility and to industries problems of process control and public relations (M. Rao, 1989).

Generally, human activities also cause some mankind sources to air pollution for instance cooking, invented heating appliances and pets often make important contribution to expose and induce monotonous accumulation of pollutants. Road traffic, however, generally provides the major source of ambient particulate pollution.

Remote sensing techniques have been widely used for environmental pollution application such as water quality (Dekker *et.al.*, 2002, Doxaran *et. al.*, 2002 and Tassan, S. 1997) and air pollution (Ung, *et.al.*, 2001b). Several studies had shown the relationships between satellite data and air pollution concentration (Ung *et al.*, 2001a; Weber, *et.al.*, 2001). Other researchers used satellite data in such environment atmospheric studies such as NOAA-14 AVHRR (Asmala Ahmad and Mazlan Hashim, 2002) and TM Landsat (Weber, *et.al.*, 2001). But the main drawback of satellite images is the difficulty in obtaining cloud-free scenes especially at the Equatorial region. This problem can be overcome by using airborne images. In fact, air quality can be measured using ground instrument such as air samplers. But these instruments are quite expensive and a limited number of stations are available in each area. So, they cannot provide a good spatial distribution of the air pollutant readings over a city.

The objective of this study is to test the potential of using remote sensing and digital image processing techniques for air quality measurements. The digital images were captured using a normal CCTV and webcam. We used visible digital CCTV and webcam imageries for this purposed. This study tested a normal CCTV and webcam for air quality detection. This CCTV and webcam captured images in visible wavelengths. In situ PM<sub>10</sub> data were collected simultaneously with the acquired digital imageries. This corresponding data were used for algorithm regression analysis. This study showed the feasibility of using the digital camera for the determination of PM<sub>10</sub>. An algorithm was developed based on the atmospheric characteristic in the visible bands. The development of the algorithm was developed base on the aerosol characteristics in the atmosphere.

### **1.1 The measurement of air quality - Air Quality Index (AQI)**

The Air Quality Index (AQI) (also known as Air Pollution Index (API) or Pollutant Standard Index (PSI)) is a tool developed by EPA to provide people with timely and easy to understand information on local air quality and whether it poses a health concern. The air quality index is shown in Figure 1. It provides a simple system that can be used throughout the country for reporting levels of major pollutants regulated under the Clean Air Act, including ground-level ozone and particulate matter.

The AQI converts measured pollutant concentration to a number on scale of 0-500. The higher the index value is, the greater the health concern. For most of the criteria pollutants, the AQI valued of 100 corresponds to the National Ambient Air Quality Standard established for the pollutant under the Clean Air Act. This is the level that EPA has determined to be generally protective of human health (Scott Hedges, 2002).

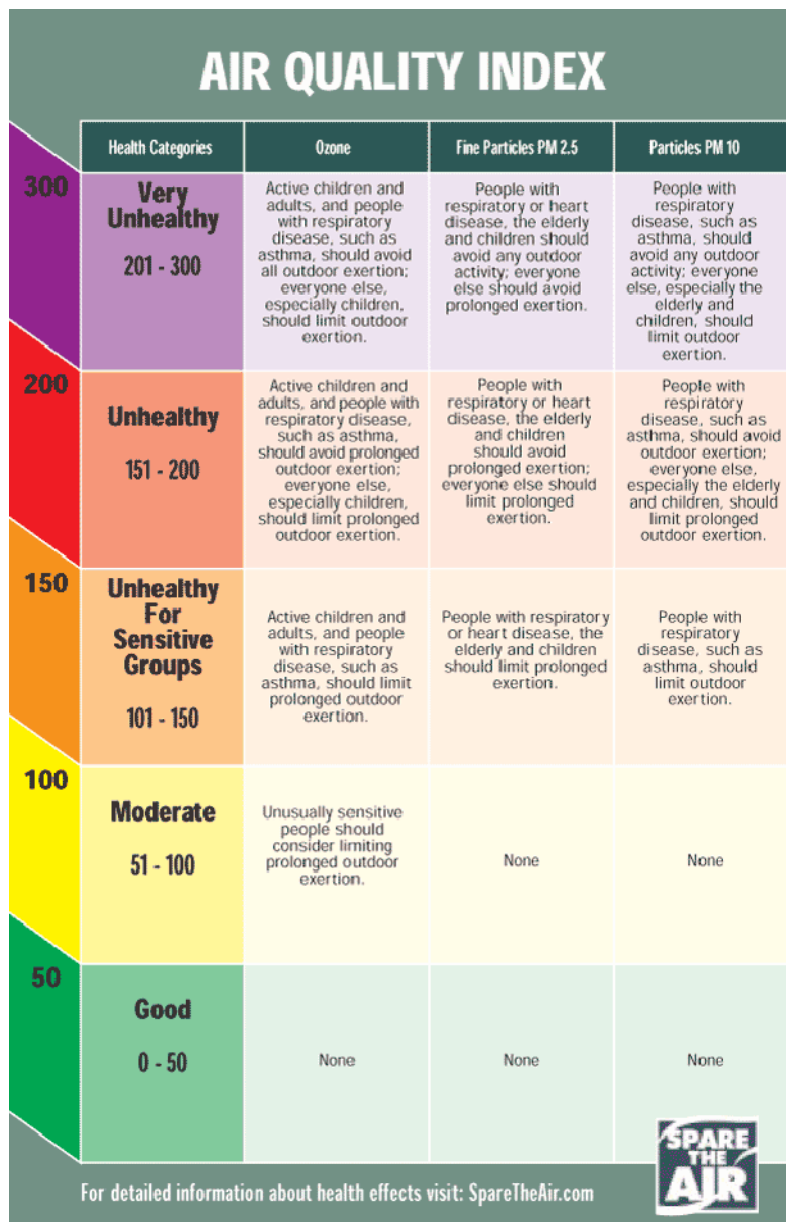


Fig. 1. Air Quality Index (SpareTheAir.com)

## 1.2 The root cause and new invention of Air Quality Monitoring CCD/CMOS Devices

Air pollution is one of the most important environmental problems. In Malaysia, the country encounters the haze problem almost every year. It is due to the illegal open burning activities after each harvesting season in the country as well as in the neighbouring country. The worst cases of air pollution lead to the emergency declarations at Kuching, Sarawak in 1997, and at Port Klang as well as the district of Kuala Selangor in 2005. The declarations were made when the Air Quality Index (AQI) which is also known as Air Pollution Index (API) or Pollutant Standard Index (PSI) values reached dangerous levels. Haze contains different sizes of pollutants. They are harmful and dangerous to human being as they can affect our respiratory system as well as cause death. However, with human naked eyes, it is hard to measure the air quality or the particle concentration in air to take prevention steps especially to those having respiratory problem patients. Therefore, a new method which is cheap and simple but effective to detect air pollution is introduced in this chapter to monitor the air quality.

The advance development in CCD/ CMOS devices such as CCTV and webcam enables us to capture images in real time and also in digital format. Digital camera is then calibrated with irradiance.

The calibrated digital camera coefficients are

$$y_1 = 0.0004x_1 + 0.0612 \quad (1)$$

$$y_2 = 0.0006x_2 + 0.0398 \quad (2)$$

$$y_3 = 0.0005x_3 + 0.0511 \quad (3)$$

where

$y_1$  = irradiance for red band ( $\text{Wm}^{-2} \text{nm}^{-1}$ )

$y_2$  = irradiance for green band ( $\text{Wm}^{-2} \text{nm}^{-1}$ )

$y_3$  = irradiance for blue band ( $\text{Wm}^{-2} \text{nm}^{-1}$ )

$x_1$  = digital number for red band

$x_2$  = digital number for green band

$x_3$  = digital number for blue band

After that, the irradiance values were converted into reflectance values for each band by using equation (4). Each reflectance value represents,  $\rho_T$  the total reflectance value of digital images. This equation requires the sun radiation value on the surface transmittance detected by spectroradiometer. The parameter depends on factors such as atmosphere and sun position.

$$R_{um} = \frac{\pi L(\lambda)}{E_s(\lambda)} \quad (4)$$

where

$L(\lambda)$  = sun radiation ( $\text{Wm}^{-2}\text{sr}^{-1}\mu\text{m}^{-1}$ )

$E_s(\lambda)$  = radiation of sunlight on the surface measured by the spectroradiometer. ( $\text{Wm}^{-2}\mu\text{m}^{-1}$ )

Then, an algorithm was developed based on the relationship between the atmospheric reflectance and the corresponding air quality. The captured images were separated into three bands namely red, green and blue and their digital number values were determined. A special transformation was then performed to the data. Ground PM10 measurements were taken by using DustTrak™ meter. The algorithm was calibrated using a regression analysis. The proposed algorithm produced a high correlation coefficient (R) and low root-mean-square error (RMS) between the measured and produced PM10. The analysis was carried

out using data collected by a webcam (K. L. Low, 2007) and Penang Bridge CCTV system. (K. L. Low, 2006, 2007, 2007)

### 2. Methodology

In this study a modification was made to the model developed by Ahmad and Hashim (1997). Skylight is an indirect radiation, which occurs when the radiation from the sun being scattered by elements within the air pollutant column. It is not a direct radiation, which is dominated by pixels on the reference surface. Figure 2 shows electromagnetic radiation path propagating from the sun towards the digital camera penetrating through the air pollutant column (Source: Modified after Ahmad and Hashim, 1997).

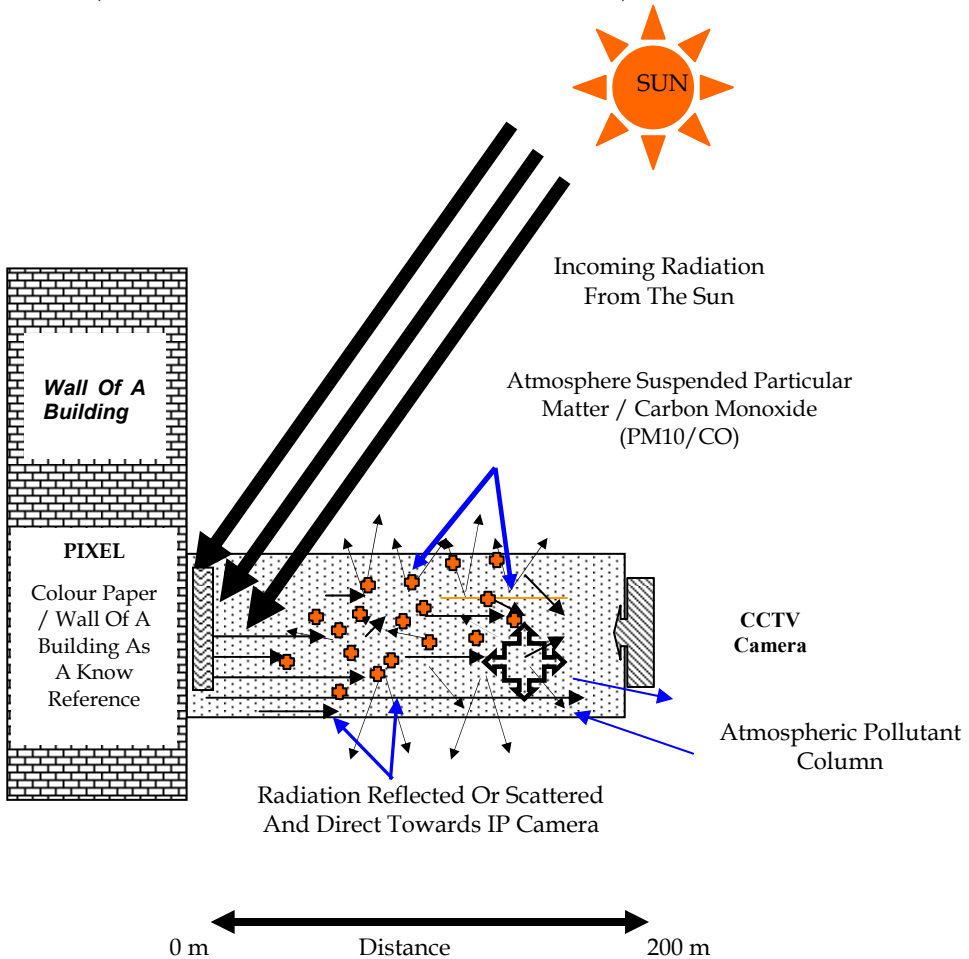


Fig. 2. The skylight parameter model (Source: Modified after Ahmad and Hashim, 1997)

The modified model is described by:

$$R_s - R_r = R_a \quad (5)$$

where  $R_s$  = reflectance recorded by IP camera sensor,  $R_r$  = reflectance from the known reference and  $R_a$  = reflectance from atmospheric scattering.

## 2.1 Algorithm Model

The atmospheric reflectance due to molecule,  $R_r$ , is given by (Liu, et al., 1996)

$$R_r = \frac{\tau_r P_r(\Theta)}{4\mu_s \mu_v} \quad (6)$$

where  $\tau_r$  = Aerosol optical thickness (Molecule),  $P_r(\Theta)$  = Rayleigh scattering phase function,  $\mu_v$  = Cosine of viewing angle and  $\mu_s$  = Cosine of solar zenith angle. We assume that the atmospheric reflectance due to particle,  $R_a$ , is also linear with the  $\tau_a$  [King, et al., (1999) and Fukushima, et al., (2000)]. This assumption is valid because Liu, et al., (1996) also found the linear relationship between both aerosol and molecule scattering.

$$R_a = \frac{\tau_a P_a(\Theta)}{4\mu_s \mu_v} \quad (7)$$

where  $\tau_a$  = Aerosol optical thickness (aerosol) and  $P_a(\Theta)$  = Aerosol scattering phase function. Atmospheric reflectance is the sum of the particle reflectance and molecule reflectance,  $R_{atm}$  (Vermote, et al., 1997).

$$R_{atm} = R_a + R_r \quad (8)$$

where  $R_{atm}$  = atmospheric reflectance,  $R_a$  = particle reflectance and  $R_r$  = molecule reflectance.

$$R_{atm} = \left[ \frac{\tau_a P_a(\Theta)}{4\mu_s \mu_v} + \frac{\tau_r P_r(\Theta)}{4\mu_s \mu_v} \right]$$

$$R_{atm} = \frac{1}{4\mu_s \mu_v} [\tau_a P_a(\Theta) + \tau_r P_r(\Theta)] \quad (9)$$

The optical depth is given by Camagni and Sandroni, (1983), as in equation (10). From the equation, we rewrite the optical depth for particle and molecule as equation (11) and (12)

$$\tau = \sigma \rho s \quad (10)$$

where  $\tau$  = optical depth,  $\sigma$  = absorption and  $s$  = finite path

$$\tau = \tau_a + \tau_r \quad (\text{Camagni and Sandroni, 1983})$$

$$\tau_r = \sigma_r \rho_r s \quad (11)$$

$$\tau_p = \sigma_p \rho_p s \quad (12)$$

Equations (11) and (12) are substituted into equation (9). The result was extended to a three bands algorithm as equation (13). From the equation we found that PM10 was linearly related to the reflectance for band 1 and band 2. This algorithm was generated based on the linear relationship between  $\tau$  and reflectance. Retalis et al., (2003), also found that the PM10 was linearly related to the  $\tau$  and the correlation coefficient for linear was better than exponential in their study (overall). This means that reflectance was linear with the PM10. In order to simplify the data processing, the air quality concentration was used in our analysis instead of using density,  $\rho$ , values.

$$\begin{aligned}
 R_{atm} &= \frac{1}{4\mu_s\mu_v} [\sigma_a \rho_a s P_a(\Theta) + \sigma_r \rho_r s P_r(\Theta)] \\
 R_{atm} &= \frac{S}{4\mu_s\mu_v} [\sigma_a \rho_a P_a(\Theta) + \sigma_r \rho_r P_r(\Theta)] \\
 R_{atm}(\lambda_1) &= \frac{S}{4\mu_s\mu_v} [\sigma_a(\lambda_1) P P_a(\Theta, \lambda_1) + \sigma_r(\lambda_1) G P_r(\Theta, \lambda_1)] \\
 R_{atm}(\lambda_2) &= \frac{S}{4\mu_s\mu_v} [\sigma_a(\lambda_2) P P_a(\Theta, \lambda_2) + \sigma_r(\lambda_2) G P_r(\Theta, \lambda_2)] \\
 P &= a_0 R_{atm}(\lambda_1) + a_1 R_{atm}(\lambda_2)
 \end{aligned} \tag{13}$$

where  $P$  = Particle concentration (PM10),  $G$  = Molecule concentration,  $R_{atm_i}$  = Atmospheric reflectance,  $i = 1, 2$  and  $3$  are the band number and  $a_j$  = algorithm coefficients,  $j = 0, 1, 2, \dots$  are then empirically determined.

### 3. Applications

#### 3.1 WebCAM

##### 3.1.1 Study area

The study area is Universiti Sains Malaysia, Penang Island, Malaysia. It is located at longitude of  $100^{\circ} 17.864'$  and latitude of  $5^{\circ} 21.528'$ . The university campus is situated in the northeast district of Penang island (Figure 3).

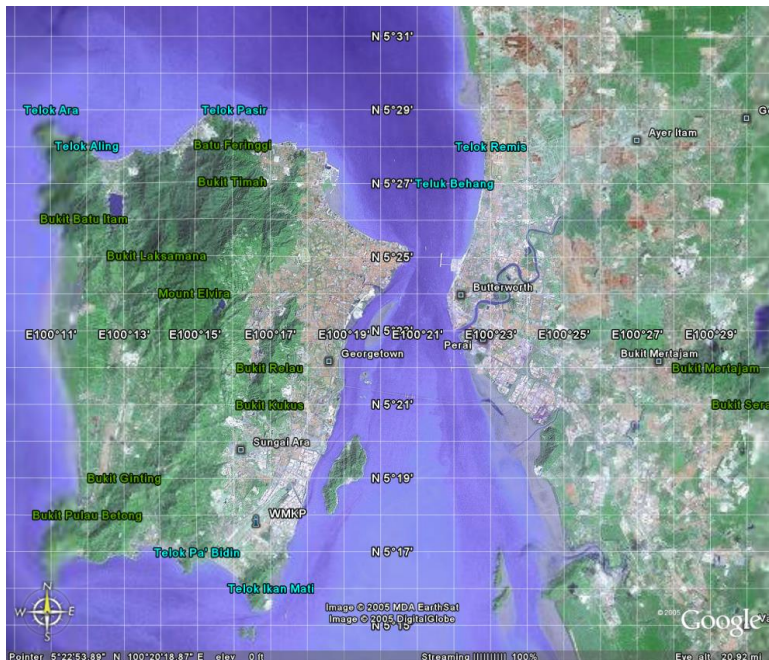


Fig. 3. Study area

### 3.1.2 Methodology

The digital images were captured during a period from 9.00am to 6pm. The images were captured at half an hour interval and simultaneously with the air quality data measurement. The sample image is shown in Figure 4. The digital number values of the images were extracted and converted into irradiance values using equations (1), (2) and (3) and then converted into reflectance values using equation (4) for each visible band.



Fig. 4. The image captured by using webcam

After that, the reflectance recorded by the web cam was subtracted by the reflectance of a known surface feature (equation(5)) and we obtained the reflectance caused by the atmospheric components. The relationship between the atmospheric reflectance and the corresponding air quality data was determined by using a regression analysis. For the proposed regression model, the correlation coefficient,  $R$ , and the root-mean-square deviation,  $RMS$ , were noted. The proposed equation is shown in equation(14). The proposed algorithm produced the correlation coefficient of 0.7320 between the predicted and the measured  $PM_{10}$  values and  $RMS$  value of  $18.7137 \text{ mg/m}^3$ . With the present data set, the  $R$  and  $RMS$  values produced by the proposed algorithm for  $PM_{10}$  is shown in Figure 5.

$$PM_{10} = -484.8459y_1 + 3249.8387y_2 - 741.5425y_3 - 1374.4198 \quad (14)$$

where  $y_1$  = irradiance for red band ( $\text{Wm}^{-2} \text{ nm}^{-1}$ )

$y_2$  = irradiance for green band ( $\text{Wm}^{-2} \text{ nm}^{-1}$ )

$y_3$  = irradiance for blue band ( $\text{Wm}^{-2} \text{ nm}^{-1}$ )

$PM_{10}$  = particulate matter  $10\mu\text{g}/\text{m}^3$

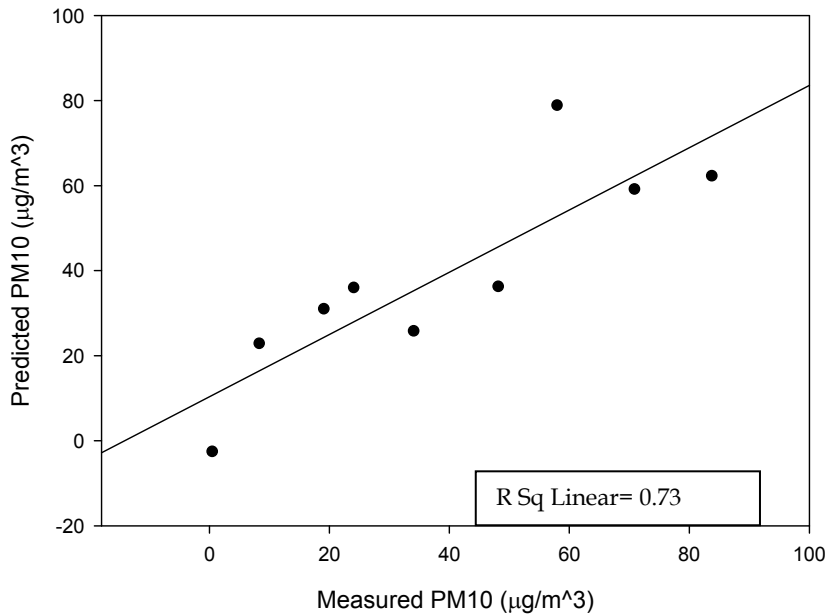


Fig. 5. Correlation coefficient measured and estimated PM10 ( $\text{mg}/\text{m}^3$ ) value for calibration analysis

## 3.2 Penang bridge CCTV

### 3.2.1 Study Area

There are 8 CCTV cameras installed at 8 different places on Penang Bridge and as shown in Figure 6. The purpose of the camera system is to monitor the flow of traffic on the Penang Bridge. The access of data from the cameras is open for public and is available on <http://pbcam.blogspot.com>. Not all of the 8 cameras could be used for the air quality study. The camera that we used was Cam 3 because the scenes captured by this camera contained the most number of vegetation pixels. It is suitable to be used as reference target.

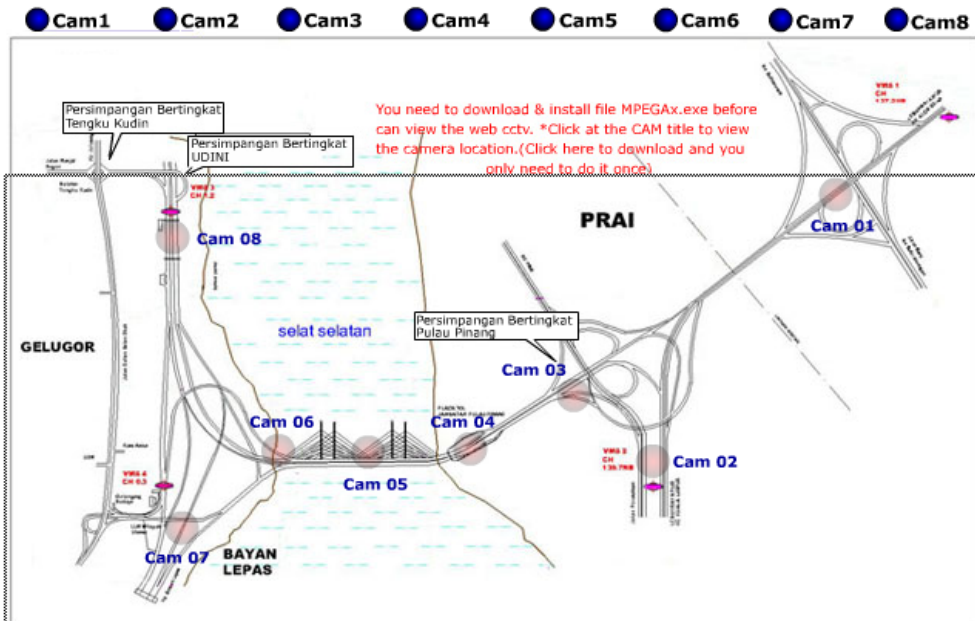


Fig. 6. Locations of the CCTV along the Penang Bridge.

### 3.2.2 Methodology

The CCTV camera Cam 7 is located at Bayan Lepas interchange to Penang Bridge (Penang Island). It captured digital images of Penang Bridge (Figure 6). We used green vegetation as our reference target. The camera was at about  $90^\circ$  with the plane of the reference target. Our reference targets are images of green vegetation canopies located at near and at a kilometer away from the camera. The data were captured from 9.00am until 5.00pm at every 1 hour interval. The example image is shown in Figure 7. All image-processing tasks were carried out using PCI Geomatica version 9.1.8 digital image processing software at the School Of Physics, University Sains Malaysia (USM). A program was written by using Microsoft Visual Basic 6.0 to download still images from the camera over the internet automatically and implement the newly developed algorithm. The digital images were separated into three bands (red, green and blue). The DN values were extracted and converted into irradiance values using equation (1), (2) and (3), and then converted into reflectance values using equation (4) for each visible bands.



Fig. 7. The digital image used in this study.

After that, the reflectance recorded by the IP camera was subtracted by the reflectance of the known surface (equation (5)) and we obtained the reflectance caused by the atmospheric components. The relationship between the atmospheric reflectance and the corresponding air quality data for the pollutant was carried out using regression analysis. For the proposed regression model, the correlation coefficient,  $R$ , and the root-mean-square deviation,  $RMS$ , were noted. The proposed algorithm is shown in equation(15). The proposed algorithm produced the highest correlation coefficient of 0.7650 between the predicted and the measured  $PM_{10}$  values and lowest  $RMS$  value of  $0.0070 \text{ mg/m}^3$ . Red and green bands are considered in this algorithm model because it produced the highest correlation coefficient. With the present data set, the  $R$  and  $RMS$  values produced by the proposed algorithm for  $PM_{10}$  is shown in Figure 8.

$$PM_{10} = 0.3664y_1 - 0.3728y_2 - 0.0547 \quad (15)$$

where  $y_1$  = irradiance for red band ( $Wm^{-2} nm^{-1}$ )

$y_2$  = irradiance for green band ( $Wm^{-2} nm^{-1}$ )

$PM_{10}$  = particulate matter  $10mg/m^3$

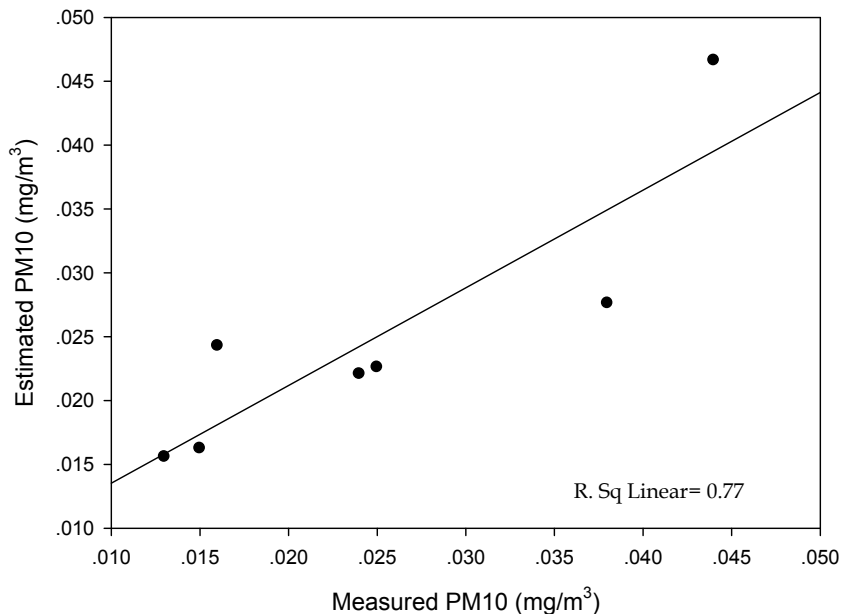


Fig. 8. Correlation coefficient of the measured and estimated PM10 (mg/m<sup>3</sup>) value for calibration analysis

#### 4. Conclusion

In this chapter, we showed a method for measuring of the air quality index by using the CCD/CMOS sensor. We showed two examples to obtain index values by using webcam and CCTV. Both devices provided a high correlation between the measured and estimated PM10. So, the imaging method is capable to measure PM10 values in the environment. Further application can be conducted using different devices.

#### 5. Acknowledgements

This project was carried out using a USM short term grants. We would like to thank the technical staff who participated in this project. Thanks are extended to USM for support and encouragement.

#### 6. Reference

Ahmad, A and Hashim, M., 1997, Determination of Haze from Satellite Remotely Sensed Data: Some Preliminary Results, [Online] available: <http://www.gisdevelopment.net/aars/acrs/1997/ps3/ps3011.shtml>.

- Camagni, P. and Sandroni, S., 1983, Optical Remote sensing of air pollution, Joint Research Centre, Ispra, Italy, Elsevier Science Publishing Company Inc.
- Dekker, A. G., Vos, R. J. and Peters, S. W. M. (2002). *Analytical algorithms for lakes water TSM estimation for retrospective analyses of TM dan SPOT sensor data*. International Journal of Remote Sensing, 23(1), 15–35.
- Doxaran, D., Froidefond, J. M., Lavender, S. and Castaing, P. (2002). *Spectral signature of highly turbid waters application with SPOT data to quantify suspended particulate matter concentrations*. Remote Sensing of Environment, 81, 149–161.
- Fukushima, H., Toratani, M., Yamamiya, S. and Mitomi, Y., 2000, Atmospheric correction algorithm for ADEOS/OCTS ocean color data: performance comparison based on ship and buoy measurements. Adv. Space Res, Vol. 25, No. 5, 1015-1024.
- King, M. D., Kaufman, Y. J., Tanre, D. dan Nakajima, T., 1999, Remote sensing of tropospheric aerosol from space: past, present and future, Bulletin of the American Meteorological society, 2229-2259.
- Lawrence K.Wang, Norman C. Pereira, Yung-Tse Hung, Air pollution control engineering, 2004
- Liu, C. H., Chen, A. J. and Liu, G. R., 1996, An image-based retrieval algorithm of aerosol characteristics and surface reflectance for satellite images, International Journal Of Remote Sensing, 17 (17), 3477-3500.
- M. Rao, H.V.N. Rao, Air Pollution, McGraw Hill, 1989
- Retalis, A., Sifakis, N., Grosso, N., Paronis, D. and Sarigiannis, D., Aerosol optical thickness retrieval from AVHRR images over the Athens urban area, [Online] available: [http://sat2.space.noa.gr/rsensing/documents/IGARSS2003\\_AVHRR\\_Retalisetal\\_web.pdf](http://sat2.space.noa.gr/rsensing/documents/IGARSS2003_AVHRR_Retalisetal_web.pdf). SpareTheAir.com
- Scott Hodges, Planning and implementing a real-time air pollution monitoring and outreach Program for Your Community, 2002.
- Tassan, S. (1997). A numerical model for the detection of sediment concentration in stratified river plumes using Thematic Mapper data. International Journal of Remote Sensing, 18(12), 2699–2705.
- Ung, A., Weber, C., Perron, G., Hirsch, J., Kleinpeter, J., Wald, L. and Ranchin, T., 2001a. Air Pollution Mapping Over A City - Virtual Stations And Morphological Indicators. Proceedings of 10<sup>th</sup> International Symposium "Transport and Air Pollution" September 17 - 19, 2001 - Boulder, Colorado USA.
- Ung, A., Wald, L., Ranchin, T., Weber, C., Hirsch, J., Perron, G. and Kleinpeter, J., 2001b., Satellite data for Air Pollution Mapping Over A City- Virtual Stations, Proceeding of the 21<sup>th</sup> EARSeL Symposium, Observing Our Environment From Space: New Solutions For A New Millenium, Paris, France, 14 - 16 May 2001, Gerard Begni Editor, A., A., Balkema, Lisse, Abingdon, Exton (PA), Tokyo, pp. 147 - 151,
- Vermote, E., Tanre, D., Deuze, J. L., Herman, M. and Morcrette, J. J., 1997, Second Simulation of the satellite signal in the solar spectrum (6S),

- Weber, C., Hirsch, J., Perron, G., Kleinpeter, J., Ranchin, T., Ung, A. and Wald, L. 2001. Urban Morphology, Remote Sensing and Pollutants Distribution: An Application To The City of Strasbourg, France. International Union of Air Pollution Prevention and Environmental Protection Associations (IUAPPA) Symposium and Korean Society for Atmospheric Environment (KOSAE) Symposium, 12<sup>th</sup> World Clean Air & Environment Congress, Greening the New Millennium, 26 - 31 August 2001, Seoul, Korea.
- K. L. Low, C.J. Wong, H. S. Lim, M. Z. MatJafri, K. Abdullah, Siti Munirah bt Azmi and Nurharin bt Che Mohamed Nor, 2006, Air Quality Monitoring Along Penang Bridge Over Internet Through Surveillance Camera, International Conference on Space Technology and Geo-informatics 2006.
- K. L. Low, H. S. Lim, M. Z. MatJafri, K. Abdullah, H. G. Ng and C. J. Wong, Evaluation Of CCTV Camera Images For PM10 Monitoring, National Conference on Environment & Community Development 2007.
- K. L. Low, H. S. Lim, M. Z. MatJafri, K. Abdullah, C. J. Wong, *"Real Time Pm10 Concentration Monitoring On Penang Bridge By Using Traffic Monitoring CCTV"*, SPIE 2007.
- K. L. Low, H. S. Lim, M. Z. MatJafri, K. Abdullah, C. J. Wong, H. G. Ng, "Air Quality Monitoring Using Webcam", ECOMOD 2007.

# Novel Space Exploration Technique for Analysing Planetary Atmospheres

George Dekoullis

*Space Plasma Environment and Radio Science Group, Lancaster University  
United Kingdom*

## 1. Introduction

Spaceborne instrumentations impose strict design specifications for accurate and high-resolution magnetic field, ultraviolet, X-ray and stray light imaging power planetary measurements. Similar measurements can also be studied at suborbital altitudes. The various Space industries have expressed an interest over the recent years in providing capable suborbital instruments to complement current spaceborne activities. For instance, increasing the spatial resolution of a suborbital remote sensing instrument assists in better comprehending an in-situ measurement.

The various costs of employing cleanroom procedures, space qualification, launch and operation are in some cases reduced or eliminated. Costs associated to maintenance and upgrades are seriatim being reduced. High-resolution measurements rely on the design of noise-free, electromagnetic compatibility proof, multi-frequency, multi-bandwidth, multi-dynamic range and multi-integration time instrumentations. The frequency range of operation is selected to complement the bandwidths of spaceborne systems, in order to extend the limits of the various observations. In-situ data time-stamping, real-time clock support and geographical position ensure synchronisation to other networked data sets. Performing parametric alterations in run-time or automatic event-driven astrophysical observations demand programmable and dynamically reconfigurable instrumentations.

This chapter discusses the implementation of such specifications and presents the latest scientific results obtained from a novel radio interferometer system designed for galactic and extragalactic astrophysical studies. The system quantifies the planetary atmospheric layers' absorption of the energised galactic particle rays. The measurements are filtered from the Cosmic Microwave Background (CMB) and other last scattering surface cosmological emissions, which are post-processed independently.

Accurate right ascension and declination coordinates have determined the accuracy of measurements over existing radio interferometer systems. This is due to the strict specifications set early in the design process. The power and flexibility in terms of the available digital signal processing capacity is a virtue of the implemented hardware configuration. Heliospheric-driven events are sensed yielding to scientifically post-processed data products. The instrumentation is based in an all-digital reconfigurable

system architecture that satisfied the demands for various planetary atmospheric measurements.

The system is constantly being enriched by research results from an ongoing collaboration with NASA's Jet Propulsion Laboratory (JPL) on a different project for future missions. The presented system is complementary to existing and under development state-of-the-art systems, such as, interferometers, scalar/vector magnetometers etc. The system is a point of reference for seriatim high-resolution Deep Space missions with landing probes to Mars, Titan or Europa.

## 2. Space Observations

The CMB is the blackbody radiation left over from the Big Bang and has been the major source of scientific observations about the origin, geometry and constituents of the Universe for over 40 years. Blackbody radiation is emitted by an isothermal object that absorbs all incident radiation. The resulting radiation spectrum and the power received at a planet's surface, excluding frequency dependent atmospheric attenuation effects, depend on its temperature and can be calculated using the Planck function.

A large number of observations of the intensity of the CMB radiation have been made over the whole spectrum of available frequencies ranging from 0.5 MHz (Reber & Ellis, 1956) up to 10 THz (Braine & Hughes, 1999). Measurements have been made using spaceborne and suborbital experiments. Suborbital experiments include rocket-borne, balloon-borne (Mather et al., 1974) and ground-based instrumentations. Only a small percentage of the information available in the CMB has been captured to date.

The COsmic Background Explorer (COBE) mission was NASA's first CMB mission, outperforming any previous suborbital measurements in return-science. COBE was launched in 1989 and performed full sky observations until 1993. The spacecraft carried the Far-InfraRed Absolute Spectrophotometer (FIRAS) to search for radiation distortions, the Differential Microwave Radiometer (DMR) to study anisotropies and the Diffuse Infrared Background Experiment (DIBRE) (Kelsall et al., 1998).

The captured data proved that the CMB exhibits no deviations from a blackbody spectrum and the non-dipole anisotropy was determined. The absence of distortion from the spectrum and the detection of non-dipole anisotropy indicated that the large-scale geometry of the Universe must have been generated by dark matter gravitational forces. The gravitational forces were created during the first picosecond after the Big Bang. The anisotropy in sky power measurements indicated the interrelation between the seriatim evolved, although distant in time, Big Bang Nucleogenesis and Recombination eras. The two eras are separated by a factor of  $10^{6.7}$  in cosmic scale.

NASA's currently active Wilkinson Microwave Anisotropy Probe (WMAP) mission was launched in 2001 to assist in establishing the initial conditions that existed at recombination (Bennett et al., 2003). Before recombination, ordinary matter was associated to photons, and structures like clusters of galaxies could not grow. After recombination, the clusters were able to expand and the measured data specify parameters related to the gravitational potential and density fluctuations at recombination. Knowledge of the initial conditions allows accurate determination of the behavior of the matter between the recombination era and now. Full sky observations occur in five frequency bands in the range 20-94 GHz, while the spacecraft is in an L2 orbit.

The European Space Agency (ESA) Planck mission to be launched in October 2008 is the third space mission after COBE and WMAP to study the anisotropies of the CMB radiation by scanning the whole sky at least twice. Planck will be placed in an L2 orbit. The spacecraft is equipped with the Low Frequency Instrument (LFI) and the High Frequency Instrument (HFI) to cover the frequency ranges 30-100 GHz and 100-857 GHz, respectively. Both instruments exhibit wide angular resolutions: 1980 arcsec at 30 GHz for the LFI being progressively improved to 300 arcsec at 857 GHz for the HFI. The angular resolution of the DMR was in the range of  $\approx 7^\circ$ . The LFI is an improved microwave radiometer, compared to DMR and WMAP, for the study of background anisotropies. The sensitivity of the HFI at the lower edge of the spectrum is close to the fundamental limit set by the photon statistics of the CMB itself (Lamarre et al., 2003).

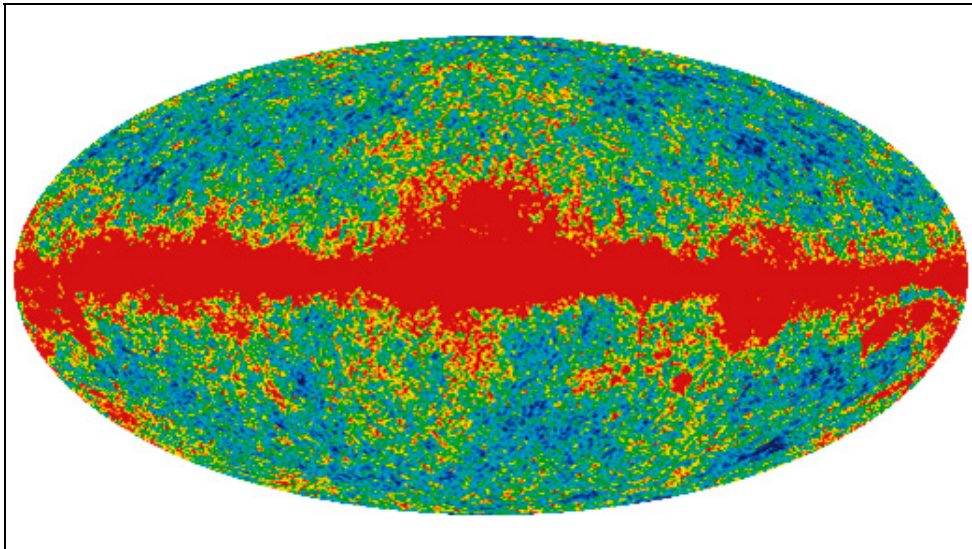


Fig. 1. WMAP sky map in Galactic coordinates in Ka band (NASA/WMAP Science Team).

Planck's observations would contribute significantly to measurements of fundamental cosmological parameters, such as the cold dark matter and baryon densities, with a maximum error of 1%. This would be possible, since hundreds of more points than COBE or WMAP on the angular CMB spectrum would be determined to allow a consistent check. An example of a five year temperature map at the Ka band for the WMAP is in Fig. 1 (Hinsaw et al., 2008). Similarly, measurements of space physics parameters at energies larger than  $10^{15}$  GeV are not possible with any suborbital experiment.

However, the demands for capable suborbital and especially ground-based facilities have increased over the recent years. Costs associated with cleanroom procedures, space qualification, launch and operation are avoided. Low-cost ground instrumentations are easier to maintain and upgrade. Frequency ranges outside the bands of spaceborne instruments increase the range of scientific observations.

### 3. Wide-Beam Radio Interferometers Observing Attenuation

The CMB is the major source of the sky brightness at centimetre wavelengths. This corresponds to a temperature of 2.728 K and it is used to derive the brightness intensity of many other wavelengths in the near region (Wilson, 1979). Passive suborbital radio interferometers observing the sky at long radio wavelengths measure much brighter intensity than from the cosmic background alone. The corresponding effective temperature is  $>10,000$  K at 33 MHz.

This radiation is due to highly energetic Galactic electrons, which radiate predominantly at those wavelengths. Their spectrum is different to the spectrum of the blackbody, safely assumed for the calculation of the different near-centimetre wavelengths cases, since the derivations do not include any radiation processes (Thomson et al., 2001). This is because radiation used to equipose matter at an early cosmic evolution stage, and maintained its spectrum in any seriatim expansion and cooling stages.

Superimposed on the CMB radiation is any induced noise from the interferometer system itself. Including the emissions from the different radio stars at the frequency of observation, the system is still presented with very low-power levels to be measured. Some of these radio sources have angular sizes of several arcsec to be measured using narrow-beam radio interferometers at higher frequencies. Imaging systems use wide-beam antennas to deliberately exhibit resolution in the range of  $\approx 11^\circ$  /beam to cover wider sky areas. The strongest of these sources could be detected, if more directional antenna phased-array systems are built with higher spatial resolution for resolving the acquired power measurements. Introducing higher power gain systems is not an option, due to the passive nature of the systems.

In phased-array systems two strong radio sources are additionally superimposed on the background radiation. Due to the diurnal Earth's rotation first the extragalactic source Cygnus A and, then, the supernova remnant Cassiopeia A pass through the antenna-array field-of-view. Cygnus A radio galaxy is one of the strongest radio sky sources. The youngest supernova remnant in the Galaxy (300 years old) Cassiopeia A is the brightest radio source (Bell et al., 1975), although its emission is progressively decreasing.

The background radiation is attenuated as it passes through a planet's atmosphere. The amount of attenuation is mainly dependent to the frequency of observation. The order of the planet's idiomorphic magnetic field discriminates amongst the different atmospheric layers. The energy deposition mechanisms at different atmospheric altitudes, due to the solar wind's burst radiation and the precipitation of highly energetic particles, attenuate the background radiation before reaching the planet's surface. For Earth, the amount of attenuation is related to the activity of the complex solar wind-magnetospheric-ionospheric plasma environment. The vast three dimensional area of the solar-terrestrial plasma environment, still, has been partially sampled despite the numerous in-situ and suborbital observations. PLANCK will experience the streaming solar wind, magnetosheath, magnetospheric lobes and auroral tail plasmas in an L2 orbit, while the halo orbit places the spacecraft in the magnetosheath for long periods of time.



Fig. 2. Northern hemisphere survey of wide-beam systems.

At atmospheric altitudes where electron motion is collision-dominated, the partial release of the CMB radiation energy to heat through electron collisions signifies attenuation (Stoker et al., 1997). Atmospheric attenuation measurements depend on the frequency, geographic position, altitude, heliospheric activity and plasma ionisation mechanisms. Although solar wind radiation dominates planetary plasma ionisation during daytime, especially for the planets of the inner solar system, galactic energetic particles with energies between up to one hundred KeV sustain plasma density, ionisation and attenuation to a seasonal periodic level during night time.

Typically low-noise and sensitive receivers are used equipped with calibration circuits. Amplitude and, in some systems, phase, is measured of the received background wavefront. A single vertical antenna with the main lobe in the direction of local zenith can form a wide-beam system. The background radiation attenuation varies according to the Earth rotation, but remains constant for a repeated local sidereal time. Wide-beam systems with a single antenna above a ground plane have been reported to operate at frequencies of 16.6, 20, 20.5, 21.3, 25, 27.6, 29.7, 29.9, 30, 32, 32.4, 35, 38.2 and 51.4 MHz and bandwidths of 15 to 250 KHz (Abdu et al., 1967). At frequencies below 20 MHz the background radiation can be attenuated completely by the magnetospheric plasma without reaching Earth's surface. For frequencies over 50 MHz, the atmospheric attenuation is virtually un-differentiable from the CMB.

Known systems located in the northern and southern hemispheres are marked with red in Fig. 2 and 3, respectively. The antenna is usually a wide-beam design of a vertical three element Yagi, two parallel horizontal dipoles or a circularly polarised cross-dipole with a

beam-width in the region of  $60^\circ$ . Circularly polarised cross-dipole antennas receive both vertically and horizontally polarised transmitted radio signals. They are insensitive to plane polarisation variation due to the ionospheric Faraday rotation effect and are also used in L-band space observations (Le Vine & Abraham, 2004).

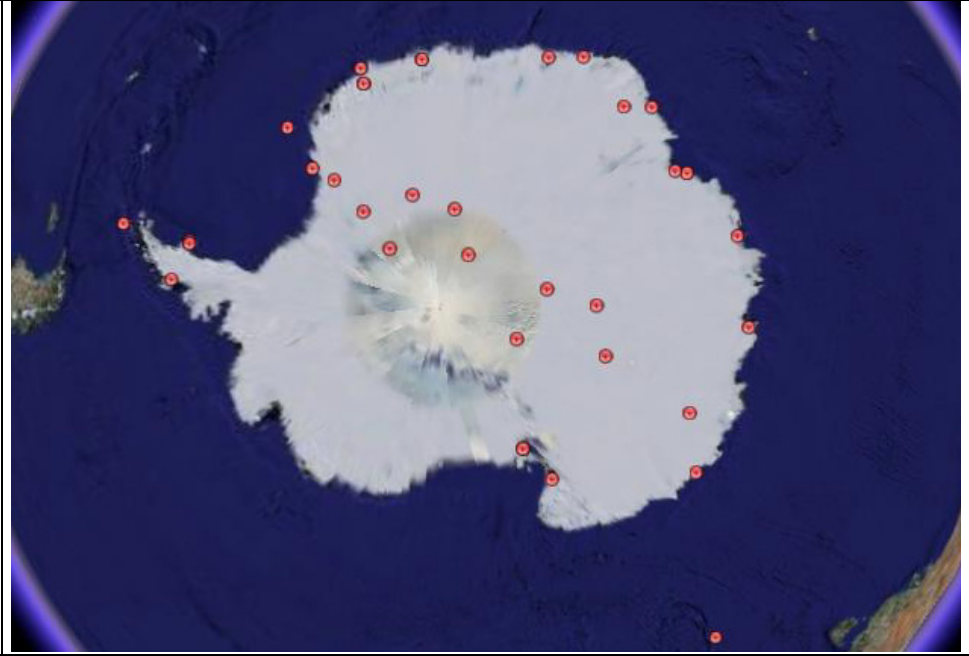


Fig. 3. Southern hemisphere survey of wide-beam systems.

Most of the systems installed in both northern and southern hemispheres have been built upon the principle of operation described in (Haldoupis et al., 1982). The design is based on the implementation of a feedback control loop to stabilise the output power, as shown in Fig. 4. The receiver continuously adjusts the noise source to match the power signal received by the antenna. A servo-controlled noise diode is typically used. The receiver input alternates between the antenna input and calibration noise source at a frequency rate of 583 Hz. The switching frequency is derived from a local oscillator. The difference between the antenna power and the noise diode signal is detected as a squarewave at 583 Hz. The squarewave is amplified and detected by the phase detector.

The output voltage of the detector is proportional to the mismatching and its polarity depends on the strongest signal. The output voltage is being used to adjust the power of the noise diode, in order to match the noise power of the antenna. The resulting difference is zero. The power of the noise diode is proportional to the current passing through it and the received power signal of the antenna is measured on a linear scale by recording the diode current.

The frequency of operation is typically determined as a function of geographical position and can vary according to the expected attenuation. At high-latitudes, and especially to

regions close to the polar cap, many systems have been operated at 27.6 MHz, since the corresponding attenuation is high. At lower geographical latitudes, 18 and 20 MHz have been traditionally used (Pinto & Gonzalez, 1989). Most of the recently installed systems, either at the northern or southern hemispheres, operate at 30 MHz.

The systems have been based upon the standard dual-stage superheterodyne receiver architecture. To avoid radio-wave interference at these frequencies, a swept-frequency and minimum-signal-detector scheme has been implemented. The first-stage local oscillator varies the frequency in 100 KHz steps every 40 s. The triangular frequency sweep is achieved by mechanically adjusting a capacitor determining the frequency of the first oscillator.

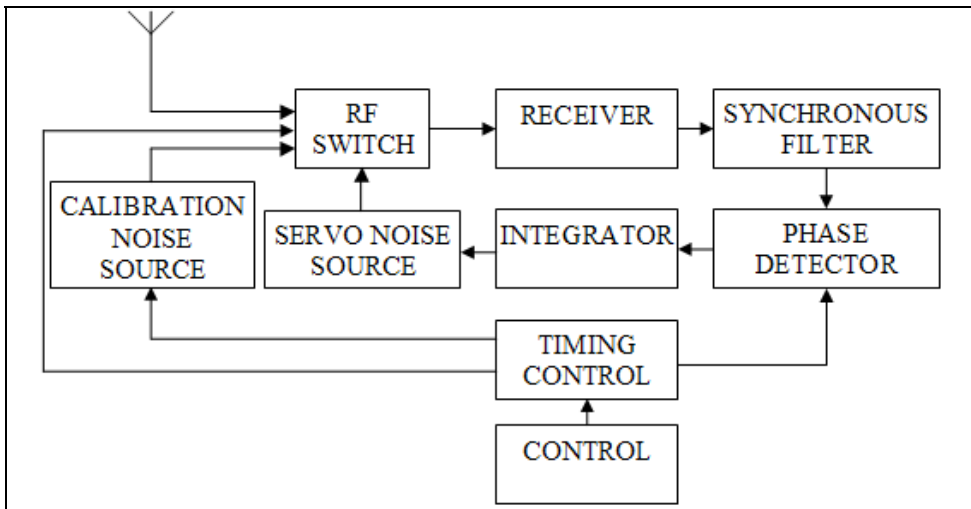


Fig. 4. Typical wide-beam system architecture.

Modern system architectures and digital signal processing technologies have carefully been considered and the optimum has been selected (Pui-In et al., 2007). The proposed system architecture mainly eliminates the classical analogue feedback control loop, exhibits an improvement in the overall performance by at least 9 dB and introduces state-of-the-art features and specifications into this field of science. The signal processing accuracy is increased. The scientific post-processing of the data also yields to more stable results.

#### 4. Novel Wide-Beam Radio Interferometer

The new wide-beam system has been designed in a modular hardware and software manner, so that the high-speed field programmable gate array (FPGA) and host instrumentation are independent of the antenna type being used. In order to validate the advanced specifications set at the beginning of the project, a circularly polarised crossed-dipole antenna was designed, tuned to 38.2 MHz.

The system is capable of processing CMB emissions up to 60 MHz by electronically switching to the appropriate channel. Although attenuation measurements have been typically performed tuned to a single operating frequency in the range 25-50 MHz, the

system provides systematic coverage of CMB attenuation for a wide range of observations and environments. The power stabilising loop of Fig. 4 has been removed. The system is continuously monitoring the antenna input and exhibits improvement of 3 dB, in terms of power levels.

|                         |  |
|-------------------------|--|
| Frequency               | 1 - 60 MHz                                 |
| Bandwidth               | 5 KHz - 1 MHz                              |
| Noise figure            | 3.05 dB                                    |
| Sampling resolution     | 14 bits                                    |
| Dynamic range           | < 175 dB                                   |
| Radiation protection    | < SRE IV                                   |
| Integration time        | 1 ms - 22 m                                |
| Tx losses               | 0 dB                                       |
| ISA                     | > 300                                      |
| Timekeeping             | GPS (UTC) & RTC                            |
| GPS Recovery            | Automatic                                  |
| Onboard storage         | < 144 h                                    |
| Interfaces              | RS-232, USB 2.0, 10/100 Mbps Fast Ethernet |
| Attenuation calculation | Automatic                                  |
| Calibration             | Automatic                                  |

Table 1. Specifications

The system amplifies the broadband input up to 60 MHz by 31.7 dB. The signal is further bandpass filtered to 1 MHz. The FPGA-controlled and custom-built digital amplifier (DA) takes into account the current Space Physics event being measured and adjusts the gain to a known level suitable for the analogue-to-digital converter (ADC) to detect. The ADC samples at 2.5 times the selected input. Investigation was made whether the signal can be processed at RF by the FPGA. The implementation results indicated that 400 clock cycles are required to produce the first result, excessive amount of hardware resources and raises the system cost significantly.

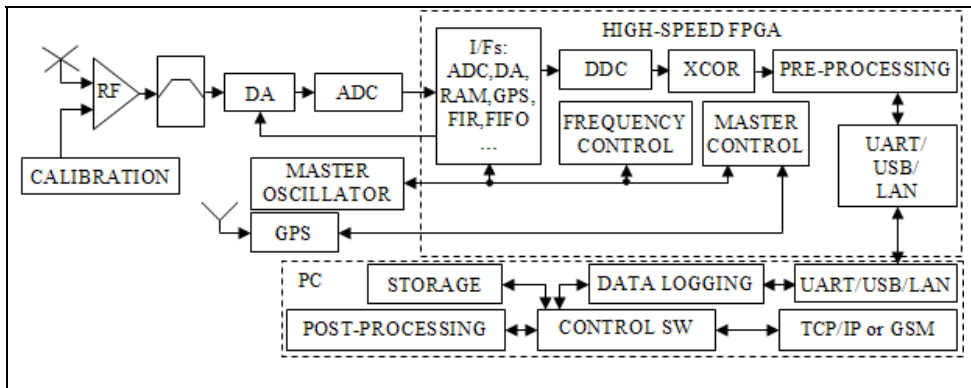


Fig. 5. All-digital system architecture.

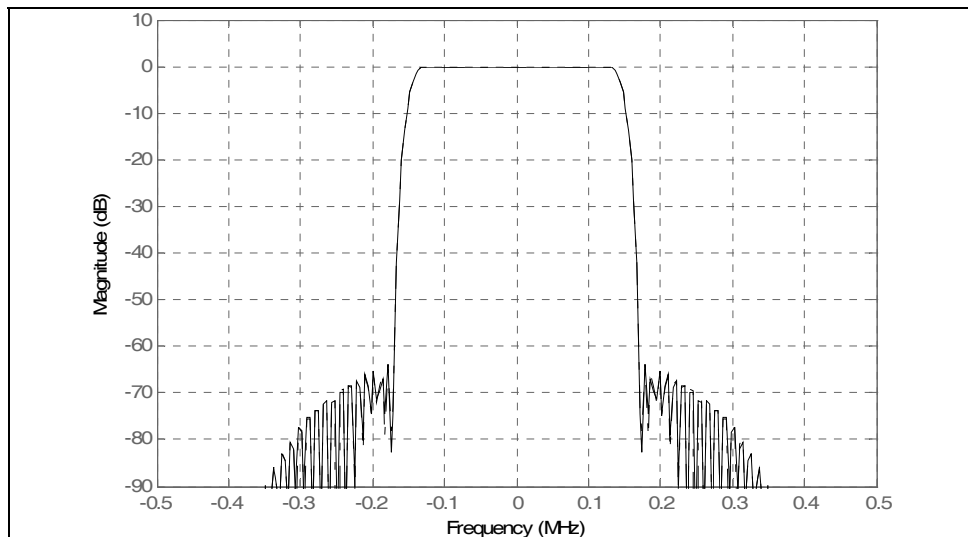


Fig. 6. DDC frequency response for a bandwidth of 250 KHz.

The FPGA-embedded digital-down-converter (DDC) converts the signal to baseband, reduces the data rate by a factor of 256 and extracts the in-phase (I) and quadrature (Q) components of the signal. The signal is low-pass filtered to the desired bandwidth. Fig. 6 demonstrates performance for a bandwidth of 250 KHz. The power results are integrated for a default 1 s and logged for post-processing. The programmable GPS receiver provides the pulse-per-second (PPS) signal, universal time (UT) for timestamping and geographic position for the theoretical calculation of the CMB radiation attenuation. A real-time clock (RTC) scheme has been implemented to allow the system's auto-recovery from loss of synchronisation. The system automatically computes attenuation by comparing the measured with the theoretical values.

The major new specifications introduced into this field of science are in Table 1. Most of the parameters are either reprogrammable or set via reconfiguration of the system. The new all-digital system architecture is presented in the block diagram of Fig. 5.

## 5. Scientific Results

The distributed FPGA data can be accessed by privileged PC hosts via the selected interface. The data are stored for post-processing. Data logging, programming and reconfiguration of the system favoured the usage of the 10/100 Mbps fast Ethernet interface during all phases of the testing. Using default settings and integration of the power results for 1 s, each sidereal day is represented by 86,164 UTC timestamped data values. The integrated power results are converted to dBm. The post-processing algorithms used are compatible with other networked data sets used by the SPEARS group at Lancaster University. Theoretical quiet day curves (QDCs) are derived knowing the CMB emissions, antenna radiation pattern and geographical location.

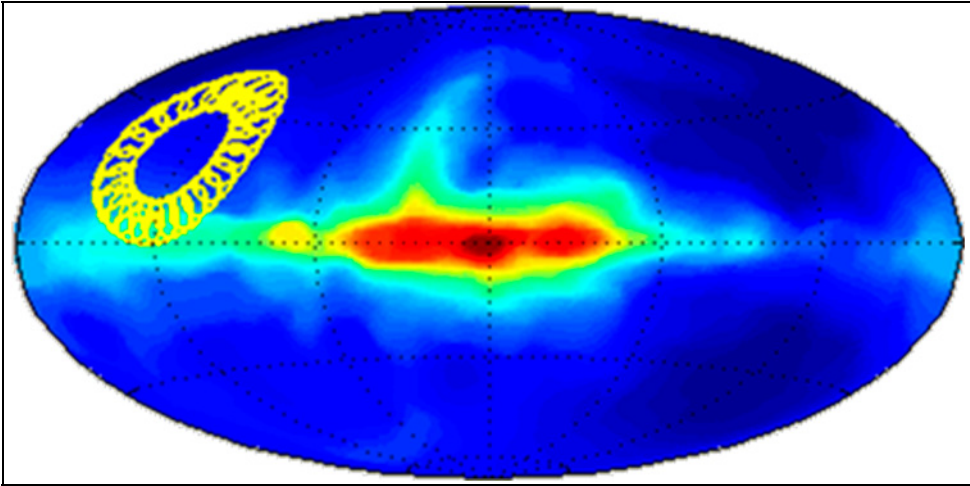


Fig. 7. Right ascension scanning of the Galactic plane within a sidereal day at 38.2 MHz.

A sky map in Galactic coordinates has been produced in Fig. 7 at 38.2 MHz. The cross-dipole antenna's field-of-view is projected at an altitude of 90 km, as shown in Fig. 8. CMB radiation attenuation is maximised at this altitude for the Earth environment. Similar results can be produced for any antenna type, knowing the current geographical position. The comparison between the experimental and theoretical CMB emissions for a quiet sidereal day is in Fig. 9. The corresponding attenuation is minimum and less than 0.1 dB, as shown in Fig. 10.

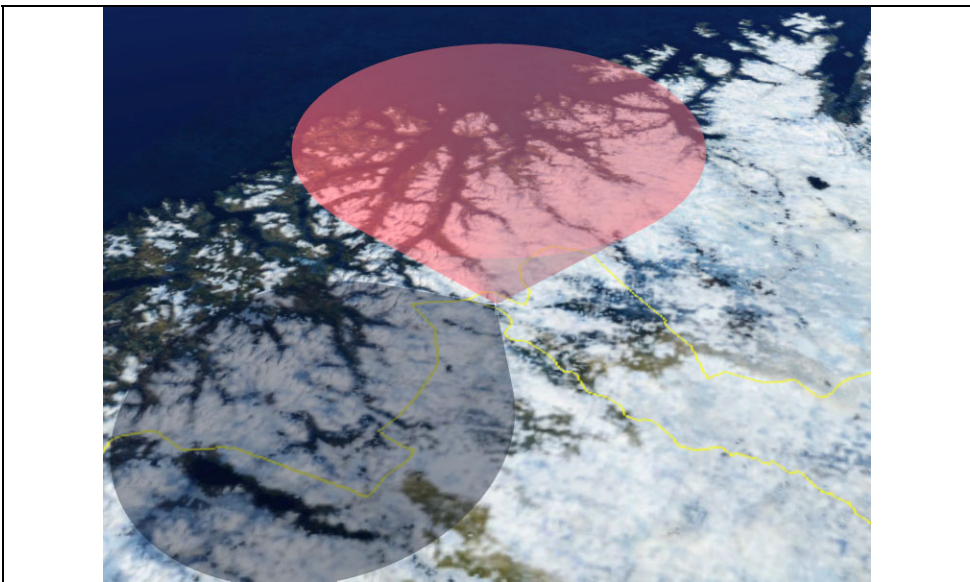


Fig. 8. System's field of view projected at 90 km altitude.

For Earth and Mars, attenuation  $A$ , is calculated in dB by solving the integral of eq. (1) and (2), respectively (Hargreaves, 1995; Rzhiga, 2005).

$$A = 1.14 \times 10^5 \int dy \frac{n(y)}{v_c(y)} C_{5/2} \left( \frac{\omega \pm \Omega(y)}{v_c(y)} \right) \tag{1}$$

$$A = 4.62 \times 10^4 \int dy \frac{1.5n(y)v_c(y)}{(1.5v_c(y))^2 + \omega^2} \tag{2}$$

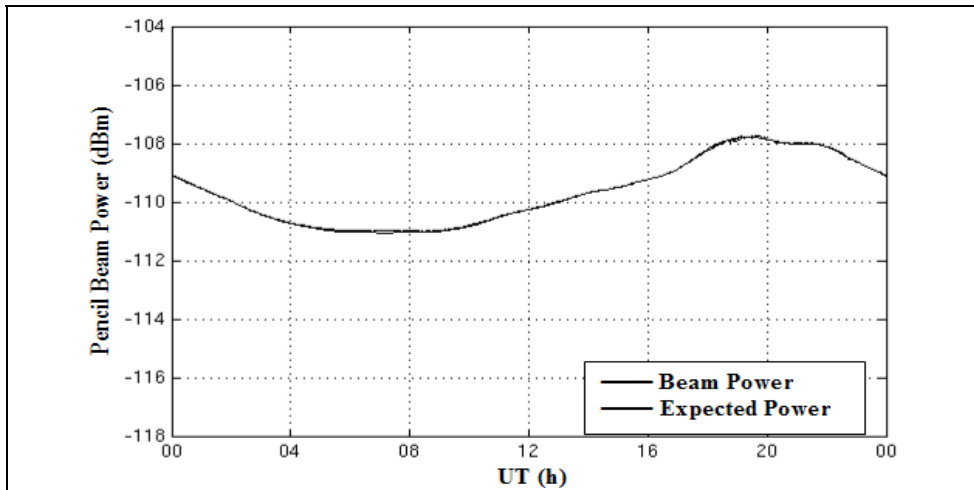


Fig. 9. Comparison between the received (RX) and expected (QDC) background emissions over a quiet sidereal day.

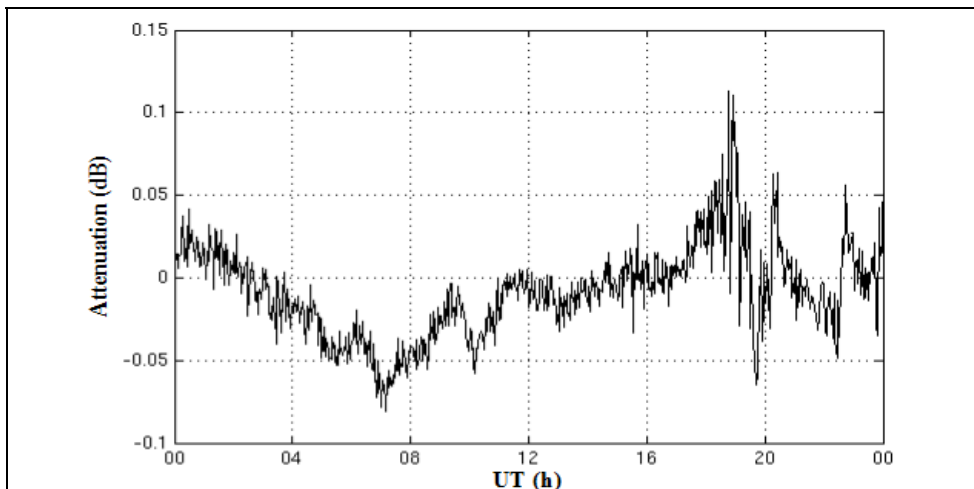


Fig. 10. Background attenuation for a quiet sidereal day.

where,  $y$  is the altitude variation of the electron-neutral momentum transfer collision frequency,  $v_c(y)$  and electron plasma density,  $n(y)$ , while  $\omega$  is the system's angular frequency of observation,  $C_{5/2}$  the semiconductor integral and  $\Omega(y)$  the electron gyrofrequency. The instrument is being used to study a variety of heliospheric events as being measured on the planet's surface. For instance, abrupt solar flares cause sudden attenuation events detectable at medium and high frequencies, as in Fig. 11. The corresponding sudden attenuation is in Fig. 12.

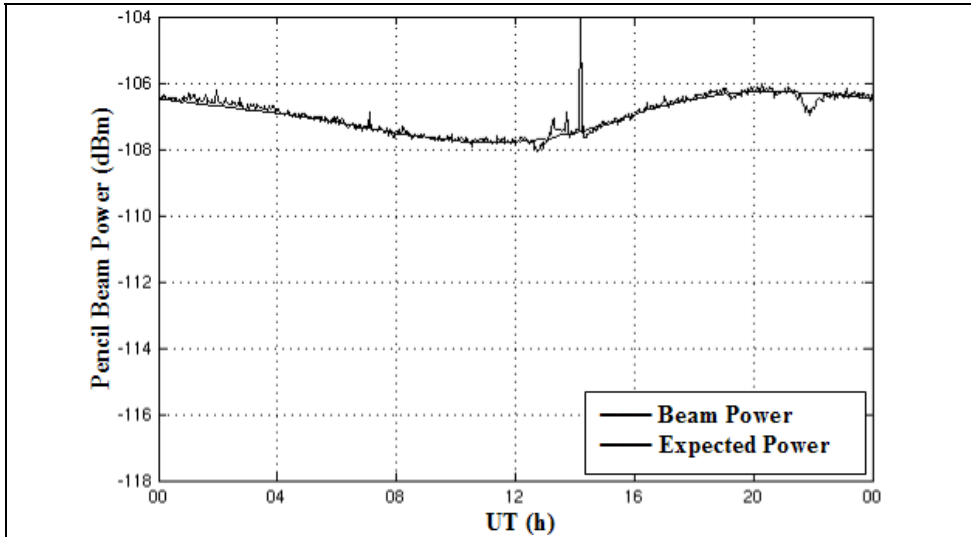


Fig. 11. Abrupt solar flare.

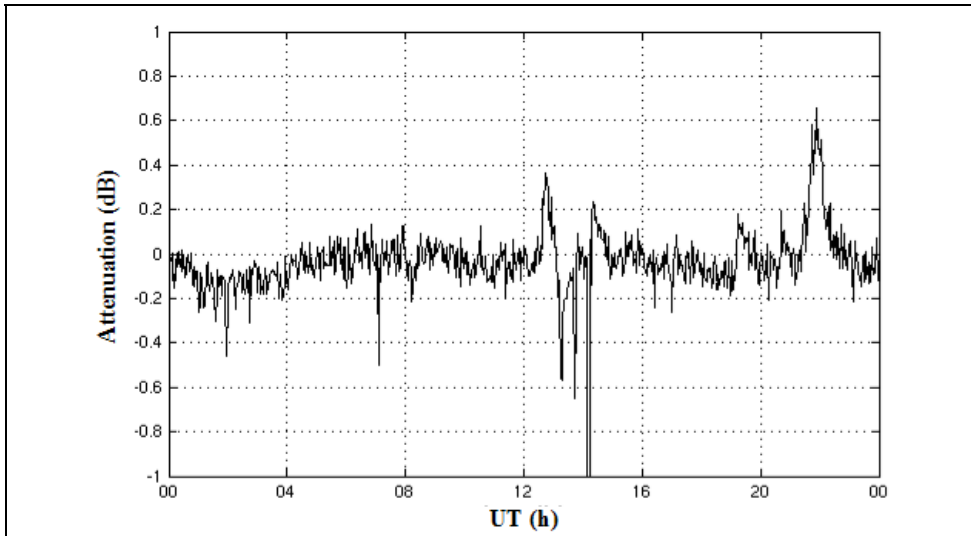


Fig. 12. Sudden attenuation, coinciding with a sub-flare which evolved into a flare.

The event coincided with a sub-flare, which evolved into a flare from SGR 1900+14 in Fig. 13 and 14.

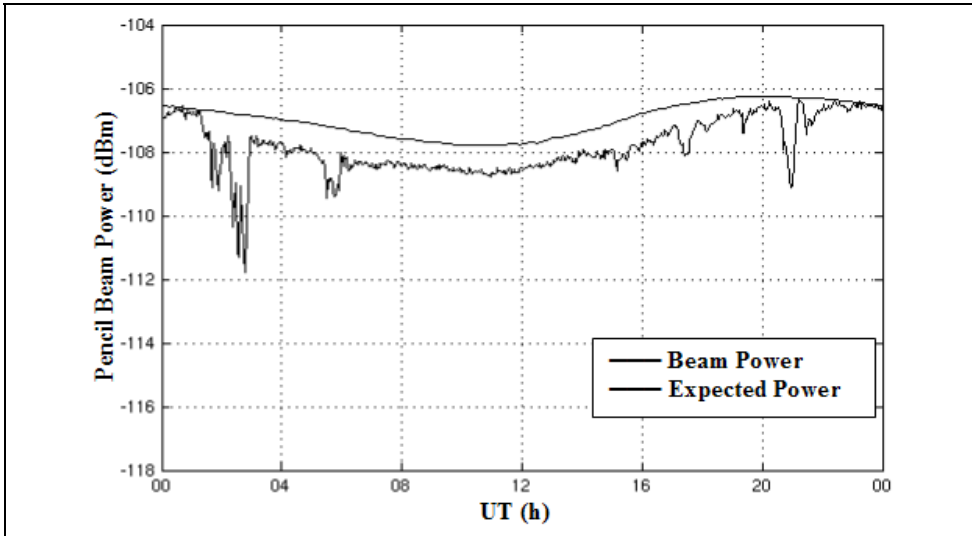


Fig. 13. Solar flare from SGR 1900+14 followed by X-ray afterglows.

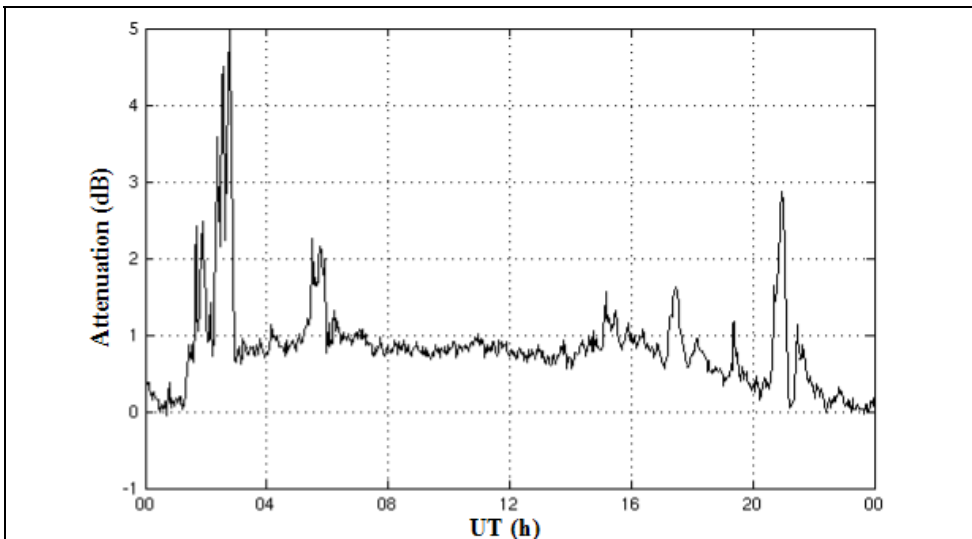


Fig. 14. Strong attenuation, due to the solar flare and afterglows from SGR 1900+14.

Solar activity is categorised in five taxonomies. Level 1 corresponds to less than five unexpected quiet regions. Less than ten class C sub-flares are usually expected, each corresponding to an X-ray blow with peak flux of 1 to 10 angstrom. The transmitted power

is  $<10$  mW/m<sup>2</sup>. At level 2, less than ten unexpected quiet regions are observed and class C sub-flares are expected. At level 3, solar eruptive regions are observed. The radiation is of class M, with a peak flux of 1-10 angstrom and the power is  $>10$  and  $<100$  mW/m<sup>2</sup>. At level 4, the active solar regions are responsible for sudden attenuation events. Class M X-ray events can be accompanied by either one or two chromospheric flares. Level 5 involves the highest activity. Protons can be produced in a region on the sun. Class X X-ray burst and several chromospheric flares can occur. Class X X-ray bursts are transmissions over 100 mW/m<sup>2</sup>.

Solar radio emissions form four categories. Category I is within 50-300 MHz. Many narrowband, short in period bursts occur. Category II starts at 300 MHz and progressively reduces to 10 MHz. Category II emissions are slightly associated with large solar flares. They consist more of an indication that a shock wave is moving through the solar atmosphere, 676 km/s in Fig. 15. The results of Fig. 15 and 16 are measured at the local plasma frequency, while its harmonics can also be detected. The radiation is similar to that generating the category III bursts.

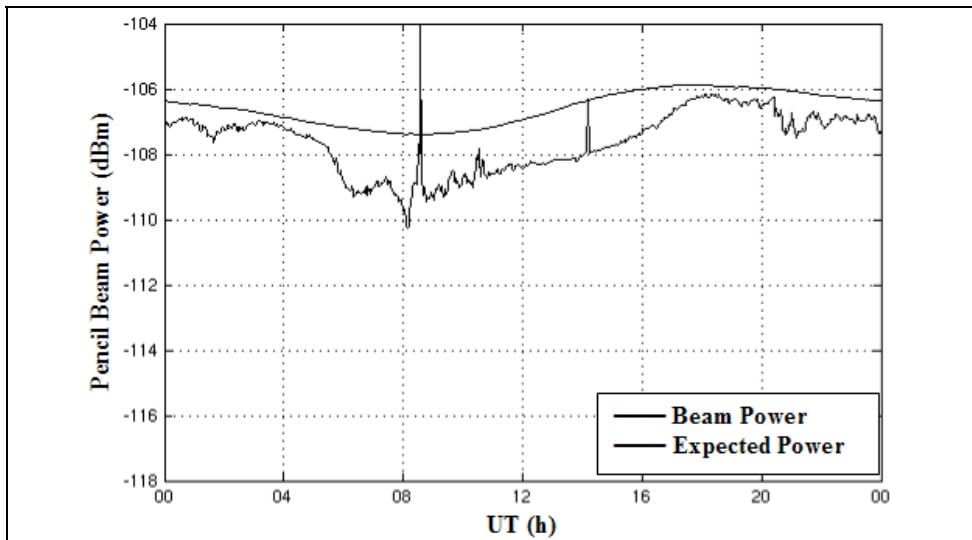


Fig. 15. Category II solar radio emission observed throughout the instrument's operating frequencies.

Two types of shock waves produce the category II radiation. The coronal shocks generate metric bursts and the coronal mass ejection (CME) driven shocks generate interplanetary bursts [15]. Metric category II bursts are related to flares and usually nullify before reaching the high corona. Their relation to Ha Moreton waves verifies that they are generated by blast coronal waves. Moreton waves leave the flare region with speeds in the range of few hundred km/s, e.g. 676 km/s, up to a thousand km/s in other data. Chromospheric trace of magnetohydrodynamic coronal waves generates these bursts.

Category III consists of narrowband bursts that sweep within seconds from decimeter to decameter wavelengths (0.5 to 500 MHz). This category consists of a group of solar

emissions and is a measure of the complex solar active region activity. Category IV is within 30-300 MHz and only broadband bursts occur. These bursts may be associated with major flares 10 to 20 minutes after the flare maximum, and can last for hours.

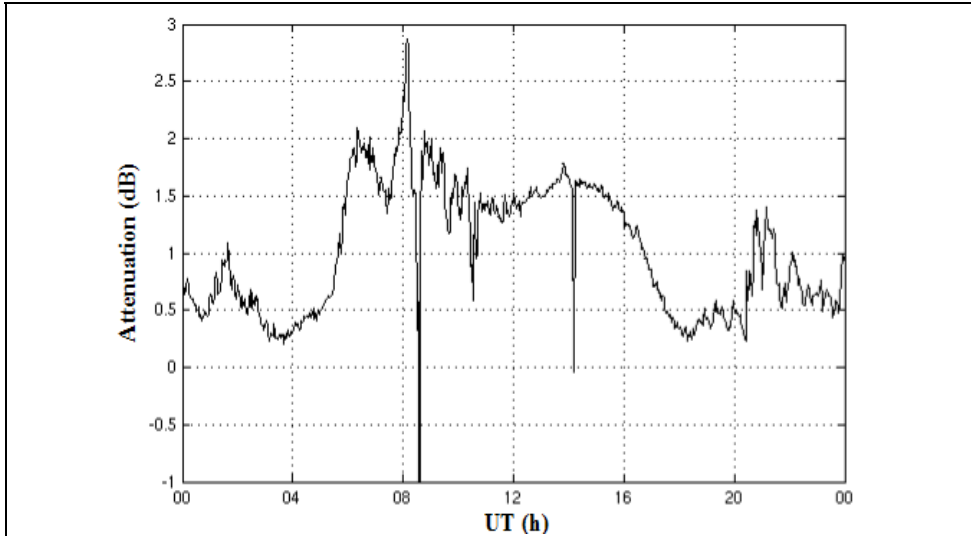


Fig. 16. Characteristic signature on the attenuation results for category II solar radio emissions.

Solar radio emission observations occur during daytime, as in Fig. 15 and 16. They correspond to an increase in the experimental power results. The increased received power is responsible for the large negative attenuation. The emissions' intensity raises concerns to the operation of spaceborne and ground-based instrumentations. The new system automatically adjusts its dynamic range to fully measure the solar radio emissions of categories I - IV. Current and future planetary missions' return-science data would assist in expanding the calculations to other planets and moons.

## 6. Conclusion

The chapter presents a new reconfigurable wide-beam radio interferometer system for analysing planetary atmospheres. The system operates at frequencies, where the ionisation of the planetary plasma regions induces strong attenuation. For Earth, the attenuation is undistinguishable from the CMB at frequencies over 50 MHz. The system introduces a set of advanced specifications to this field of science, previously unseen in similar suborbital experiments. The reprogrammable dynamic range of the system expedites signal conditioning to known gain levels to detect Space Physics events. The all-digital architecture facilitates flexible remote control over the numerous programmable or reconfigurable digital functional blocks and external hardware interfaces for fast prototyping of future experiments. The system acts as a pathfinder for future space exploration missions to Luna, Mars, Titan or Europa.

## 7. References

- Abdu, M. A.; Degaonkar, S. S. & Ramanathan, K. R. (1967). Attenuation of galactic noise at 25 MHz and 21.3 MHz in the ionosphere over Ahmedabad during 1957-1964. *Journal of Geophysical Research*, Vol. 72, No. 1, 1574-1554
- Bell, A. R.; Gull, S. F. & Kenderdine, S. (1975). New radio map of Cassiopeia A at 5 GHz. *Nature*, Vol. 257, 463-465
- Bennett, C. L. et al. (2003). The microwave anisotropy probe mission. *Journal of Astrophysics*, Vol. 583, 1-23
- Braine, J. & Hughes, D. H. (1999). The 10 GHz-10 THz spectrum of a normal spiral galaxy. *Journal of Astronomy and Astrophysics*, Vol. 344, No. 1, 779-786
- Haldoupis, C. I. et al. (1982). Radar auroral observations during a burst of irregular magnetic pulsations. *Journal of Geophysics*, Vol. 87, No. A3, 1541-1550
- Hargreaves, J. K. (1995) *The solar-terrestrial environment*, Cambridge University Press
- Hinsaw, G. et al. (2008). Five-year microwave anisotropy probe (WMAP) observations: data processing, sky maps, & basic results. *Journal of Astrophysics*, Vol. x, xx-xx
- Kelsall, T. et al. (1998). The COBE diffuse infrared background experiment search for the cosmic infrared background. II. model of the interplanetary dust cloud. *Journal of Astrophysics*, Vol. 508, No. 1, 44-73
- Lamarre, J. M. et al. (2003). Planck high-frequency instrument. *Proceedings SPIE 4850*, pp. 730-739
- Le Vine, D. M. & Abraham, S. (2004). Galactic noise and passive microwave remote sensing from space at L-band. *IEEE Transactions of Geoscience and Remote Sensing*, Vol. 42, No. 1, 119-129
- Mather, J. C.; Richards, P. L. & Woody, D. P. (1974). Balloon-based measurements of the cosmic background radiation. *IEEE Transactions of Microwave Theory and Technology*, Vol. 22, No. 12, 1046-1048
- Pinto, J. O. & Gonzalez, W. D. (1989). Energetic electron precipitation at the South Atlantic magnetic anomaly: a review. *Journal of Atmospheric and Terrestrial Physics*, Vol. 51, No. 5, 351-365
- Pui-In, M.; Seng-Pan, U. & Martins, R. P. (2007). Transceiver architecture selection: review, state-of-the-art survey and case study. *IEEE Circuits and Systems Magazine*, Vol. 7, No. 2, 6-25
- Reber, G. & Ellis, G. R. (1956). Cosmic radio-frequency radiation near one megacycle. *Journal of Geophysical Research*, Vol. 61, No. 1, 1-10
- Rzhiga, O. N. (2005). Distortions of the low frequency signal by Martian ionosphere at vertical propagation. *IEEE Transactions of Antennas and Propagation*, Vol. 53, No. 12, 4083-4088
- Thomson, A. R.; Moran, J. M. & Swenson, G. W. Jr. (2001). *Interferometry and synthesis in radio astronomy*, Wiley-Interscience
- Stoker, P. H. et al. (1997). Cosmic radio noise absorption related to structures in aurora luminosity. *Journal of Geophysical Research*, Vol. 102, No. A4, 7439-7447
- Wilson, R. W. (1979). The cosmic microwave background radiation. *Revision of Modern Physics*, Vol. 51, No. 3, 433-446

# Ambient air pollution, social inequalities and asthma exacerbation in Greater Strasbourg (France) metropolitan area: The PAISA study

D. Bard<sup>1</sup>, O. Laurent<sup>1,2</sup>, S. Havard<sup>1,3</sup>, S. Deguen<sup>1</sup>, G. Pedrono<sup>4</sup>, L. Filleul<sup>5</sup>,  
C. Segala<sup>4</sup>, A. Lefranc<sup>6</sup>, C. Schillinger<sup>7</sup> and E. Rivière<sup>7</sup>

<sup>1</sup>*Département d'Epidémiologie et de Recherche Clinique, École des Hautes Études en Santé  
Publique, Rennes*

<sup>2</sup>*LEPID, Institut de Radioprotection et de Sécurité Nucléaire, Fontenay aux Roses*

<sup>3</sup>*INSERM U 707, Paris*

<sup>4</sup>*SEPIA-santé, Baud*

<sup>5</sup>*CIRE Aquitaine, Institut national de Veille Sanitaire, Bordeaux*

<sup>6</sup>*DSE, Institut national de Veille Sanitaire, Saint Maurice*

<sup>7</sup>*Association pour la Surveillance et l'Etude de la Pollution Atmosphérique en Alsace,  
Schiltigheim*

## 1. Introduction

The socio-economic status (SES) of populations has an influence on the incidence or mortality rates of numerous health outcomes, among which respiratory diseases (Prescott et al., 2003; Ellison-Loschmann et al., 2007). Considering asthma, the possible contribution of SES to overall prevalence –regardless of asthma severity–, remains controversial in industrialized countries. Several studies indicate that allergic asthma is more prevalent in more well-off populations whereas the non-allergic forms of asthma are more common in the deprived ones (Cesaroni et al., 2003; Blanc et al., 2006). On the other hand, severe asthma whatever its etiology appears to be more frequent in the latter populations, as compared to the more affluent (Basagana et al., 2004). Risk factors for exacerbations (*e.g.*, passive smoking (Wright Subramanian, 2007), psychosocial stress (Gold & Wright, 2005), cockroach allergens (Kitch et al., 2000), and suboptimal compliance with anti-inflammatory medication (Gottlieb et al., 1995)) are generally more common among people with asthma and low SES than their better-off counterparts. These observations support the hypothesis that some factors more present in deprived populations contribute to asthma exacerbation (Mielck et al., 1996).

One candidate factor is ambient air pollution, a well-demonstrated risk factor for asthma (Samet & Krewski, 2007). Epidemiologic studies report short-term associations (latency of several hours to several days) between exposure to air pollutants (particulate matter, nitrogen dioxide [NO<sub>2</sub>], sulfur dioxide, and ozone [O<sub>3</sub>]) and various asthma attack indicators routinely available: hospitalization (Sunyer et al., 1997), emergency department (ED) visits (Romeo et al., 2006), calls to mobile emergency medical service networks (Medina

et al., 1997) and visits to doctors' offices for asthma attacks (Hajat et al., 1999). Associations are also reported with indicators measured directly in individuals with asthma: respiratory symptoms and consumption of short-acting  $\beta$ -agonist (SABA) drugs (von Klot et al., 2002; Schildcrout et al., 2006).

It should be stressed that in such studies, be they time series (Sunyer et al., 1997), case-crossover (Jalaludin et al., 2008), or panel (Ward & Ayres, 2004; Romeo et al., 2006) studies, investigators average citywide ambient pollutant concentrations for estimating exposure, although these concentrations often vary spatially and strongly within cities (Jerrett et al., 2005a), with few exceptions (Tolbert et al., 2000; Neidell, 2004; Erbas et al., 2005). Failure to consider these spatial variations at the sub-city level can lead to exposure misclassification and resulting bias (Jerrett et al., 2005a). Conversely, taking these spatial variations into account in studying the relations between air pollution and health would allow more rigorous measurement of the magnitude of these relations (Jerrett et al., 2005a). Another problem inherent in ecologic studies is spatial autocorrelation, which expresses the non-independence of geographic observations (Haynes et al., 2001). With very rare exceptions (Jerrett et al., 2001; Buzzelli et al., 2003), studies of environmental equity do not consider this phenomenon, although it is essential to avoid violating the hypotheses that underlie the application of statistical models, and may thus lead to erroneous conclusions about associations.

Another key issue is identification of the populations most susceptible to air pollution and the precise measurement of exposure-response relations in these subsets (Maynard et al., 2003; Samet & Krewski, 2007). Several studies show that some specific populations, such as children, the elderly, and people with chronic diseases, including people with diabetes and chronic obstructive pulmonary disease, are more susceptible to air pollution than the general population (Annesi-Maesano et al., 2003; Samet & Krewski, 2007). Some suspect that socioeconomic deprivation influences the relations between air pollution and health (O'Neill et al., 2003). Many investigators have tested this hypothesis with regard to mortality, and their overall results suggest the existence of larger relative risks for more deprived populations (Laurent et al., 2007). Substantially fewer researchers have tested this hypothesis with regard to asthma attacks (Norris et al., 1999; Lin et al., 2004; Neidell, 2004), and the few that have done so have considered socioeconomic indicators measured at resolutions ranging from the individual level (Neidell, 2004; Kim et al., 2007) to the level of geographic residence areas of various sizes (Nauenberg & Basu, 1999; Norris et al., 1999; Lin et al., 2004; Son et al., 2006; Kim et al., 2007). Whether or not a socioeconomic indicator is an effect modifier, however, may well depend on the resolution at which it is measured (Laurent et al., 2007). To our knowledge, only two studies have tested the influence of socioeconomic indicators measured at the level of small areas (Canadian enumeration areas (Lin et al., 2004) and US zip codes (Neidell, 2004) on the short-term relations between air pollution and asthma attacks. Disadvantaged people may be more susceptible to asthma attacks when they face additional environmental insults, such as ambient air pollution (Maynard et al., 2003). Nonetheless, the few studies (Nauenberg & Basu, 1999; Annesi-Maesano et al., 2003; Maynard et al., 2003; O'Neill et al., 2003; Lin et al., 2004; Laurent et al., 2007) that have tested this hypothesis have produced divergent results. This may be because the distribution according to SES of factors modulating the relations between air pollution and asthma morbidity differs between the study settings or because of lack of statistical power.

In the absence of individual data, which are not generally routinely available, ecological (or contextual) measures of SES are frequently used to describe health inequalities. Although some epidemiological studies are based on only one socioeconomic indicator (income, educational level, or occupation), *e.g.* (Kunst et al., 1998; Finkelstein et al., 2003), SES is usually recognized as complex and multidimensional, integrating different components that may be either material (*e.g.*, housing conditions, income, or occupation), social (*e.g.*, social position or isolation, or family support) or both (Folwell, 1995; Braveman et al., 2005).

Area-based deprivation indices for the measurement of the economic or social disadvantages of urban areas were proposed in the 1980s (Townsend, 1987). Initially designed for health care planning and resource allocation, they have been recently used to evaluate and analyse health inequalities (Carstairs, 1995; Niggebrugge et al., 2005; Eibner Sturm, 2006). These measures, including Townsend's, Carstairs', and Jarman's indices, as well as the more recent Index of Multiple Deprivation, combine contextual indicators such as unemployment rate or proportions of overcrowded or of non-owner-occupied households (Jarman, 1983; Townsend et al., 1988; Carstairs & Morris, 1991; DETR, 2000). Since the end of the 1990s, numerous other area-based deprivation indices have emerged – in the United States (Singh, 2003; Eibner & Sturm, 2006; Messer et al., 2006), Canada (Pampalon & Raymond, 2000), New Zealand (Salmond et al., 1998), Japan (Fukuda et al., 2007), Italy (Tello et al., 2005), Spain (Benach & Yasui, 1999), and Belgium (Lorant, 2000).

Hospitalizations or emergency department visits reflect severe asthma exacerbation episodes. As to increase sensitivity, alternative indicators integrating less severe events may be used, such as telephone calls to medical services or asthma exacerbation specific drugs.

Naureckas et al. (Naureckas et al., 2005) showed that SABA sales are valuable indicators of asthma morbidity and its temporal variability. These sales are especially good predictors of the risk of emergency department visits and hospitalization for asthma attacks in the days immediately afterwards (Naureckas et al., 2005). Moreover, they generally reflect less severe morbidity states than those requiring emergency department visits or hospitalizations and are therefore very sensitive indicators. Finally, they are very common, likely to involve large numbers of individuals, even within small geographic units and short observation periods (Pitard et al., 2004; Naureckas et al., 2005). While SABA drugs are the treatment of choice for asthma attacks (Global Initiative for Asthma, 2007), they are also prescribed for acute exacerbation of chronic obstructive pulmonary disorders (COPD) (Urbano & Pascual, 2005). Nevertheless, this disease is rare in people less than 40 years old (Viegi et al., 2007); within this age group, SABA prescriptions and sales are therefore very specific for asthma attacks.

The PAISA study objectives were to investigate the short-term relations between air pollution estimated at the level of small geographic areas and asthma attacks and to test the influence of socioeconomic deprivation, also measured at this level, on these relations. Two different, although related, indicators were tested, that is *i*) calls for emergency services for asthma exacerbation and *ii*) SABA drugs deliveries.

## 2. Methods

### 2.1 Setting and statistical unit

The setting of our study was the Strasbourg metropolitan area (SMA), gathering municipalities (316 km<sup>2</sup>) with a population of about 450,000 inhabitants located in the Bas-Rhin district (or 'département', an administrative subdivision) in the Alsace region of North-

Eastern France. The statistical small-area unit used was the French census residential block (Ilots Regroupés pour l'Information Statistique-IRIS), a submunicipal division devised by the National Institute for Statistics and Economic Studies (INSEE). This unit is the smallest geographic area in France for which socioeconomic and demographic information from the national census is available. It is, in terms of population size, intermediate between US census tracts (about 4,000 inhabitants) and US census block groups (about 1,000 inhabitants) with an average number of inhabitants of 2,000. The division of neighborhoods into census blocks takes into account the physical obstacles that may break up urban landscapes (important traffic arteries, bodies of water, green spaces, etc.) and aims to maximize their homogeneity in population size, socioeconomic characteristics, land use and zoning. The SMA is subdivided into 190 blocks, with areas ranging from 0.05 km<sup>2</sup> to 19.6 km<sup>2</sup> (median values of 0.45 km<sup>2</sup> for the entire SMA and 0.29 km<sup>2</sup> for the city center). Fifteen blocks covering a very small population (250 people, altogether 0.2 percent of the total population) were removed from the study because of confidentiality rules in force in France.

## 2.2 Socioeconomic Status Indicator

The demographic and socioeconomic data come from the 1999 national population census, conducted by INSEE. The census database is structured into different domains, including employment, family and household, educational level, housing, immigration status, and income; together these regroup a collection of very diverse quantitative variables, such as proportions of unemployed people, foreigners, blue-collar workers, households without cars, people aged 15 years or older with general or vocational maturity certificates, etc. Accordingly, we selected 52 variables from the available data, endeavoring to apply theoretical concepts of deprivation (Krieger et al., 1997), relying on the indicators most often used in the literature (Morris & Carstairs, 1991; Pampalon & Raymond, 2000; Challier & Viel, 2001; Jordan et al., 2004), and using the same definitions as INSEE most often uses in its studies. All but 2 of the 52 variables were proportions (the exceptions were mean number of people per room and median income per consumption unit). Some variables, intentionally redundant, were introduced into the analysis to determine statistically the most discriminating for characterizing deprivation (*e.g.*, unemployment among total labor force, among men, among women).

### *Constructing the index*

We developed the socioeconomic deprivation index by principal component analysis (PCA) of the 52 variables. All variables were first standardized (*i.e.* centered and reduced) to remove the influence of different units of measure and thus to give them the same weight in the analysis. This statistical technique permits the synthesis of information contained in a great number of variables by constructing new and independent synthetic variables - the principal components. These new variables are linear combinations of some of the initial variables, defined by a maximum variance. The principal advantage of this method is that it makes it possible to consider relations between the variables, by attributing to each a weight that takes the relations into account (that is, treating them as coefficients of the linear combinations).

In our study, to facilitate the use of the deprivation index in a public health context, we chose to construct a single index for all the blocks to maximizing the variance of the first principal component. Several consecutive PCA were thus performed to conserve only the variables most strongly correlated with the first component and contributing most to its

construction. If two redundant variables were conserved, only the one most closely correlated with the first component was finally retained (and in each case, that turned out to be the variable not stratified by sex). Finally, this first component, used as our socioeconomic deprivation index, was calculated for each block, as the linear combination of the final variables retained.

To obtain the most discriminant cartographic representation of socioeconomic disparities, the blocks were grouped into five classes of index values, approximately equivalent to the quintiles (Beguín & Pumain, 1994). The first class comprised the least deprived blocks and the fifth the most deprived blocks. The choropleth mapping of the index was performed with the Geographic Information System ArcView™ v. 9.1 (ESRI Inc., Redlands, CA, USA).

#### *Index validity*

According to Coste et al. (1995) (Coste et al., 1995), several criteria make it possible to judge the validity of composite measurement scales (in our case, a socioeconomic deprivation index), in particular, its content validity and its construct validity (Ferமானian, 1996).

Content validity is assessed by the extent to which the items composing the scale or index are relevant to and representative of all of the possible items that can describe the phenomenon measured. To select the initial subset of variables for analysis, we carefully ensured that each census domain (income, job, housing, family and household, etc.) was represented by at least one variable, and again at the end we verified this representativeness for all of the final variables.

Construct validity verifies that from a theoretical point of view the instrument is associated with the concept it is supposed to measure. It tests the relations between the index variables, both internally (factorial validity and internal consistency) and externally (convergent validity), and thus identifies more precisely the real meaning of the concept measured by the indicator. The internal validity of our index was estimated with the results of the PCA and Cronbach's alpha coefficient. This coefficient judges how the variables retained by the PCA measure a one-dimensional concept – here, socioeconomic deprivation. The closer the coefficient value is to one, the better the verification that the index variables are homogenous. The convergent validity was tested using Pearson's correlation coefficients with the most widely used British indices (those of Carstairs and Townsend) (Townsend et al., 1988; Carstairs & Morris, 1991). These indices combine four variables, three common to both: (1) proportion of unemployed, (2) proportion of households without a car, and (3) proportion of over-crowded households. Townsend's index also includes the concept of rental versus owner-occupied housing (proportion of non-owner-occupied housing) while Carstairs' index considers a variable related to the household head's place in the British social scale (proportion of households in which the householder belongs to social classes 4 or 5). These indices were compiled at the census block level by adapting or translating some British variables when they had no direct correspondence in the French census database (for example, the variable "proportion of households in which the householder belongs to social class 4 or 5" was translated for the French census database as "the proportion of blue-collar workers").

#### *Index reliability*

To test the robustness of our index, the same methodological procedure as that used for the SMA (the same 52 initial variables, same algorithm decision for the final choice of variables, the same tests of validity) was conducted for another French metropolitan area at the

resolution of the census block - the Lille metropolitan area (LMA). The LMA was selected because its demographic and socioeconomic characteristics are quite distinct from those of the SMA (*e.g.*, 489 census blocks for a total population around 1,100,000 inhabitants). The objective of this stage was to demonstrate that similar results could be obtained in a different part of France and to show that the variables selected for the construction of the index were independent of the study area and characterized socioeconomic level in as discriminating a manner as possible.

#### *Application*

Census blocks were divided into five deprivation categories according to their index value; the first category comprised the most privileged blocks and the fifth the most deprived ones. More details can be found in (Havard et al., 2008).

#### **Calls to emergency medical services for asthma exacerbation**

The two mobile emergency and healthcare networks operating in the SMA (Service d'Aide Médicale d'Urgence (SAMU) and SOS Médecins) provided data about emergency telephone calls made to physicians for asthma attacks. The Bas-Rhin emergency medical services unit (SAMU 67) is a public service that coordinates pre-hospital emergency medical services. SOS Médecins of Strasbourg is a private service providing emergency general medical care. We included each call regarding an asthma attack that reached either SAMU or SOS Médecins from January 1, 2000, to December 31, 2005. The two databases were merged, duplicates being excluded. Each call was geo-coded to the census block where the patient was located at the time of the call, based on the postal address. Only 2 percent of the calls could not be geocoded; they were excluded from the analysis.

#### **SABA sales**

The data about SABA sales to people living in the SMA during 2004 came from four health insurance funds: the regional union of health insurance funds (Union Régionale des Caisses d'Assurance Maladie [URCAM], for salaried workers and very low-income families), agricultural social insurance fund (Mutualité Sociale Agricole [MSA], for farmers and similar workers), the fund for self-employed workers (Régime Social des Indépendants [RSI]), and the Lorraine students' insurance fund (Mutuelle Générale des Etudiants de Lorraine [MGEL]). These funds cover >90% of the local population (Com-Ruelle et al.). In 2004, these funds either paid or reimbursed (fully or partially) all SABA sales prescribed by a physician. All records of SABA sales in pharmacies were extracted from the databases of these four insurance funds by requests for code R3A4 of the European Pharmaceutical Market Research Association nomenclature (Tollier et al., 2005). The following information was furnished for each sale: date, age group (0 to 9, 10 to 19, 20 to 39 years), sex, and census block of residence of the person for which SABA were prescribed. All sales were combined into a single file for analysis.

#### **Ambient air pollution**

Hourly ambient concentrations of particulate matter less than 10  $\mu\text{m}$  in aerodynamic diameter ( $\text{PM}_{10}$ ), nitrogen dioxide, sulfur dioxide, and ozone were modeled by the local air quality monitoring association (Association pour la Surveillance et l'Etude de la Pollution Atmosphérique en Alsace, Schiltigheim) for each block during the entire study period (Bard et al., 2007). Modeling was conducted with Atmospheric Dispersion Modeling System (ADMS-Urban), a deterministic Gaussian dispersion model (McHugh et al., 1997) that integrates emissions inventories, meteorological data (wind direction and speed, temperature and cloudiness, supplied by Météo France, the French meteorological service), and background

pollution measurements as input parameters. A limitation of the model was the estimation of Monin-Obukhov length from cloudiness measurements, but the correlation coefficients for the modeled and effectively measured ambient concentrations were 0.73 for PM<sub>10</sub>, 0.87 for nitrogen dioxide, 0.84 for ozone. However, this correlation was only 0.06 for sulfur dioxide. Therefore, sulfur dioxide was no longer considered in the analyses.

### **Potential confounders**

Daily meteorological variables (temperature, atmospheric pressure, and relative humidity) were obtained from Météo France, and daily pollen counts were obtained from the National Network of Aerobiological Surveillance (Thibaudon, 2004). Weekly influenza case counts came from the Sentinelles network (Flahault et al., 2006) of the National Institute of Health and Medical Research.

### **Statistical analyses**

As some census blocks featured a relatively small population size, yielding unstable rates, we carried out an empirical Bayesian smoothing using STIS™ software (Space Time Intelligence System 2007 (Ann Arbor, MI, USA: Terraseer), except for drug sales, where smoothing was not warranted in view of the much greater number of events per census block (Marshall, 1991). Positive and statistically significant spatial autocorrelations were found for our SES index (Moran's I = 0.54,  $p < 0.01$ ), rates and standardized incidence ratios (SIR) for asthma calls (I from 0.67 to 0.77 according to age group,  $p < 0.01$ ). Associations between SES and health event rates or SIR were quantified by Pearson's correlation test and their significance assessed using a modified Student's t-test as proposed by Clifford et al., (Clifford et al., 1989) as to accounting for spatial autocorrelation of neighboring census blocks variables.

Associations between asthma calls and air pollution were assessed with case-crossover models (Maclure & Mittelman, 1991), which are similar to case-control models, except that in the former, the subjects serve as both cases and controls, depending on when they are considered. The subject serves as a case on the day of the health event and a control on days without any health event. Control days were defined according to a monthly time-stratified design (Janes et al., 2005). For an asthma call occurring on a given weekday (*e.g.*, Monday), control days were chosen as the same days of the week throughout the rest of the month (thus, three or four days; here, the other Mondays of the month). Conditional logistic regression was employed for analyses. The statistical significance of the odds ratios was tested by means of a two-sided  $\chi^2$  test at the 5 percent level.

### *Base models*

We first analyzed all calls or SABA sale, without differentiating them according to socioeconomic deprivation. Associations between health events and ambient air pollution concentrations modeled by census block were estimated, adjusting for holidays, meteorological variables (daily maximum temperature, maximum atmospheric pressure, and mean relative humidity), influenza epidemics, and pollen counts.

We tested the influence of air pollution indicators averaged on the day of the call (lag 0) and then averaged on the day of the call and the 1-5 previous days (lag 0-1 to 0-5) or up to 10 days in the case of SABA sales. The daily air pollution indicator considered for PM<sub>10</sub>, nitrogen dioxide, and sulfur dioxide was the 24-hour average concentration, and for ozone it was the maximum daily value of the 8-hour moving average. The analysis for ozone considered only health events occurring between April 1 and September 30 of each year, because of the very low concentrations of this pollutant in winter.

These associations were assessed for cases of all ages and then for groups of cases aged 0–19, 20–64, and >64 years, except for SABA sales (below 40). These groups were defined according to the guidelines of the French Data Protection Authority, to ensure the confidentiality of the health data geocoded by census blocks.

#### *Testing the influence of deprivation*

Interactions with socioeconomic deprivation were tested for the lag times for which the strongest associations were observed in the basic models.

Deprivation was introduced first as a discrete variable. The SMA population was divided into five strata with contrasting deprivation levels, according to the quintiles of the distribution of the deprivation index. An odds ratio for the relation between asthma calls and pollution was estimated for each stratum. The heterogeneity of the odds ratios between these strata was assessed by means of a two-sided  $\chi^2$  test at the 5 percent level (Atkinson et al., 2001). These analyses were conducted for the same age groups as in the base models.

In an alternative method, deprivation was introduced as a continuous variable. For that purpose, a case-crossover model was constructed for each of the 174 census blocks in which asthma calls occurred during the study period. The models did not converge in the census blocks with fewer than 11 asthma calls. These census blocks were treated as follows. Those adjoining neighboring census blocks of a similar deprivation level (differences of deprivation index values less than one 10th of the deprivation index scale) were merged with them. The deprivation index value attributed to each newly created geographic unit was the mean of the deprivation index values from the merged blocks, weighted by their respective population counts. Census blocks ( $n = 26$ ) that bordered no neighboring census block of a similar deprivation level (differences of deprivation index values one 10th or more of the deprivation index scale) were excluded from these analyses.

The heterogeneity of the odds ratios estimated in the 136 geographic units so defined was assessed as described above (Atkinson et al., 2001). The influence of the deprivation level of the geographic units on the odds ratios was tested by linear regression (weighted by the inverse of the variance of these odds ratios) in both fixed- and random-effects models. These analyses were conducted for  $PM_{10}$ , nitrogen dioxide, and sulfur dioxide for cases of all ages but were not feasible for ozone (April–September) and specific age groups, because of the small numbers of calls in most census blocks.

All analyses were carried out using SAS statistical software v 9.1 and 8.2 (SAS Institute, Cary, NC, USA).

### **3. Results**

#### **3.1 Socioeconomic Status Indicator**

Our deprivation index was defined by the PCA as the first principal component, which explained 66% of the total variance of the model, while the second explained only 17%. The impossibility of drawing any residual structure from the second component justifies the conclusion that all of the discriminating information useful for characterizing socioeconomic deprivation was in fact captured by the first component. Our index is composed of 19 socioeconomic variables that describe different dimensions of socioeconomic deprivation. Seventeen can be qualified as primarily material variables and only two directly refer to social dimension of the deprivation (that is, single-parent family and foreign population). Although several of the variables retained belong to the same domain, we consider that they

provide complementary information for characterizing the deprivation. Our index opposes the concepts of material and, to a lesser extent, social deprivation (it is significantly and positively correlated with variables relative to unemployment, immigration, social isolation, household overcrowding, low educational level, and low income) to those of well-being and economic comfort (it is significantly and negatively correlated with variables relative to job stability, high educational level, better living conditions, and high income). Moreover, these variables had differing relative influences in the construction of the index (*e.g.*, proportion of unemployed people contributed to 6.72% of the variance and the percentage of households without cars to only 3.91%).

Table I presents the mean values of the index and of the 19 variables by deprivation class. The first class (C1) is characterized by the lowest mean index value and includes the most privileged blocks, defined by the best living conditions (low percentages of the variables describing socioeconomic deprivation and high percentages of variables illustrating material comfort). At the other end, the fifth class (C5) is characterized by the highest mean index value and includes the most deprived blocks. The blocks of this class are characterized by more socioeconomic deprivation, a greater cumulative lack of material and social resources (the highest percentages of variables describing deprivation and the lowest percentages of variables related to positive living conditions). For example, on average, only 1.28% of homes in the C1 blocks were low income subsidized housing while this percentage exceeded 75% for the C5 blocks.

**Table I. Deprivation Index and mean values of its 19 variables, according to deprivation categories<sup>a</sup>**

| Variables  | Census domain           | Deprivation categories |        |        |        |       |
|--|-------------------------|------------------------|--------|--------|--------|-------|
|  |                         | C1                     | C2     | C3     | C4     | C5    |
| Blue collar workers in the labor force                                     | Job                     | 17.40                  | 15.80  | 17.20  | 21.70  | 36.40 |
| Primary residences that are houses or farms                                | Housing                 | 61.40                  | 28.60  | 7.10   | 5.80   | 3.60  |
| Primary residences that are multiple dwelling units                        | Housing                 | 37.10                  | 69.50  | 90.20  | 90.90  | 95.10 |
| Households without a car   | Housing                 | 8.80                   | 16.00  | 27.60  | 35.80  | 36.50 |
| Households with $\geq 2$ cars  | Housing                 | 48.90                  | 32.40  | 18.90  | 14.90  | 14.00 |
| People with insecure jobs in the labor force                               | Job                     | 8.30                   | 10.40  | 13.70  | 16.90  | 17.40 |
| People aged $\geq 15$ yrs with general or vocational maturity certificates | Education               | 13.30                  | 12.20  | 11.90  | 9.50   | 6.60  |
| People aged $\geq 15$ yrs with at least a lower postsecondary education    | Education               | 10.90                  | 10.30  | 10.30  | 8.10   | 3.50  |
| People aged $> 15$ yrs with no more than a completed elementary education  | Education               | 9.80                   | 9.80   | 10.80  | 16.20  | 33.50 |
| Non owner-occupied primary residences                                      | Housing                 | 28.20                  | 48.90  | 72.10  | 80.30  | 91.30 |
| People with stable jobs in the labor force                                 | Job                     | 76.40                  | 72.00  | 68.20  | 63.10  | 54.90 |
| Subsidized housing among all primary residences                            | Housing                 | 1.30                   | 6.80   | 9.30   | 27.30  | 75.60 |
| Single-parent families   | Families and households | 7.70                   | 10.30  | 13.20  | 15.70  | 23.60 |
| Median income/consumption unit (in Euros/yr) <sup>c</sup>                  | Income                  | 19,977                 | 19,819 | 17,120 | 14,270 | 8,402 |
| Primary residences with more than 1 person/room                            | Housing                 | 3.20                   | 4.30   | 5.90   | 7.90   | 21.40 |
| Foreigners in the population   | Immigration status      | 3.20                   | 6.20   | 7.90   | 12.30  | 22.0  |
| Mean no. people/room <sup>c</sup>  | Housing                 | 0.60                   | 0.60   | 0.64   | 0.69   | 0.86  |
| Unemployed people in the labor force                                       | Job                     | 5.30                   | 7.50   | 10.20  | 13.50  | 24.20 |
| People unemployed $> 1$ yr in the labor force                              | Job                     | 2.40                   | 3.20   | 4.40   | 5.80   | 11.70 |
| Deprivation index  | --                      | 1.09                   | 1.75   | 2.25   | 2.67   | 3.44  |

<sup>a</sup>All variables are percentages (%), unless otherwise stated; *p* value for trend < 0.01 for all variables. <sup>b</sup>C1 is the least deprived category, C5 is the most. <sup>c</sup>Not a percentage.

Conversely, nearly 50% of the households in C1 blocks had two cars or more compared with 14% for the C5 blocks (Table I).

Our index thus demonstrates the existence of a socio-economic gradient in the SMA, along which we observe a progressive degradation of level and quality of life between the first and fifth classes ( $p < 0.01$ ). The different variables used to construct the index sometimes vary significantly in the same direction as the gradient, and sometimes in the opposite direction (Table I), depending on the aspect (positive or negative) of SES that they express ( $p < 0.01$ ).

This gradient appears clearly in the cartographic representation (Figure 1). The most affluent blocks are located on the outskirts of the study area and constitute a peri-urban ring around Strasbourg. These are principally blocks with a relatively low population, comprising rural municipalities. Conversely, socioeconomic deprivation is accentuated as we approach Strasbourg and reaches its maximum at the centre of the metropolitan area. The most disadvantaged blocks are principally those in Strasbourg and the inner suburbs with a relatively high population and comprising the urban municipalities.

#### *Validity tests*

**Content validity.** The 19 variables retained cover all of the census domains and thus insure that our index has fully integrated the multiple socioeconomic aspects of deprivation (Table I).

**Construct validity.** The high Cronbach's  $\alpha$  coefficient (0.92) supports the hypothesis that these variables measure a one-dimensional concept - socioeconomic deprivation. Convergent validity is verified by very high correlation coefficients with the indices of both Townsend (0.97;  $p < 0.01$ ) and Carstairs (0.96;  $p < 0.01$ ).

#### *Reliability*

Following the same process, 20 variables were retained for Lille metropolitan area, 18 of them were the same as for SMA and they explained the same proportion of variance (66%). Only three variables differed between the two indices: the percentages of the self-employed and of foreign immigrants were retained only for the Lille index and the percentage of blue-collar workers only for Strasbourg. Mapping the index for LMA again illustrates the strong spatial heterogeneity of SES between urban centers and outer suburbs. Finally, as for Strasbourg, all the tests of the index conclusively demonstrated its validity (*i.e.*, the Lille index had a high Cronbach's  $\alpha$  coefficient and was very highly correlated with both British indices; data not shown).

#### **Calls to emergency medical services for asthma exacerbation**

There were 4,682 calls for asthma (SAMU and SOS Médecins combined) and 1,173 SAMU-confirmed asthma cases (from 1,578 calls given to SAMU - some but not all initially reported to be for asthma). Cases finally diagnosed as asthma by participating physicians were treated as such in our analyses, regardless of the initial reason for call. We observed no trend in the annual number of health events.

Figure 2 shows the results of empirical Bayesian smoothing of calls for asthma exacerbation SIRs.

Maps of ambient air pollutant concentrations averaged by census block across the SMA (for the period 2000–2005) appear on figure 3.

As expected for a small-area study, high and statistically significant spatial autocorrelation was found for the deprivation index ( $I = 0.54$ ,  $p < 0.01$ ) and for health event indicators (Table II). These are mapped respectively in figures 4 and 5.

The age-specific rates and SIRs of calls for asthma increased from the least towards the most deprived blocks (Figure 4). Elevated ( $R \geq 0.65$ ,  $p < 0.01$ ) correlations were observed between the deprivation index and both the SIRs and rates of calls for the groups aged 20 years or older (Table II). Correlations were lower but still statistically significant for the younger groups.

Results were similar for SAMU-confirmed asthma cases (Table II). Correlations with the deprivation index were elevated ( $R \approx 0.62-0.63$ ,  $p < 0.01$ ) for those aged 20 years or older, and lower (but still significant) for the younger groups.

Table III presents the distribution of asthma calls and air pollutant concentrations for the entire SMA and for the five socioeconomic deprivation strata. Overall, there were 4,677 usable asthma calls made during the study period. As we previously reported, the numbers of calls increased from the least deprived stratum to the most deprived, despite their similar population denominators.

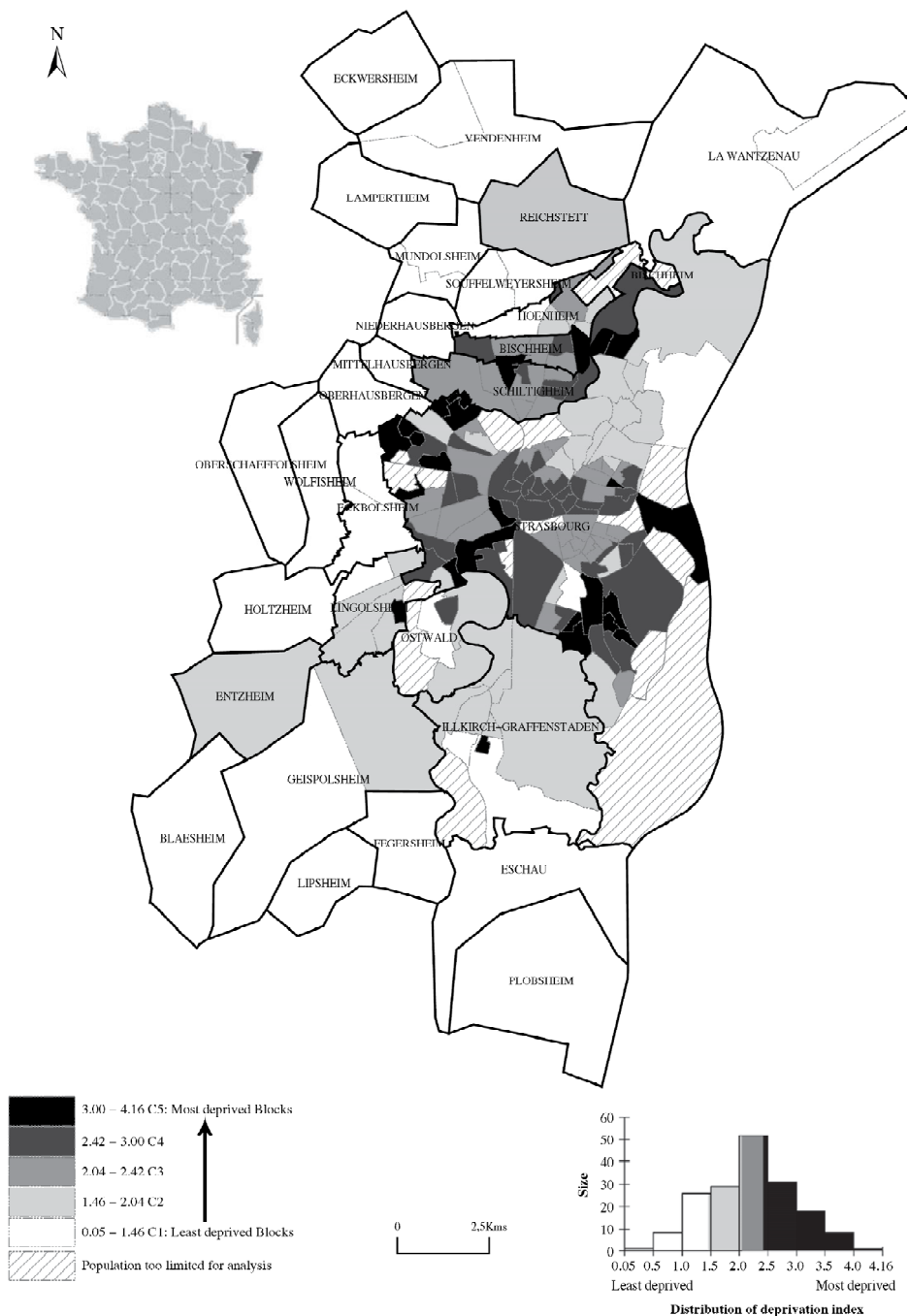


Fig. 1. Mapping deprivation in the Strasbourg (France) Metropolitan Area.

Table II. Summary of health data for the Strasbourg metropolitan area and their correlations with deprivation index

| Age group of calls | All calls for asthma           |                |                                   |               | Asthma cases confirmed by SAMU     |                                |                               |                                   |               |                                    |                   |                   |
|--------------------|--------------------------------|----------------|-----------------------------------|---------------|------------------------------------|--------------------------------|-------------------------------|-----------------------------------|---------------|------------------------------------|-------------------|-------------------|
|                    | Mean number of calls per block | % of all calls | Annual rate per 1,000 inhabitants | Moran's index | Correlation with deprivation index | Mean number of cases per block | % of all SAMU-confirmed cases | Annual rate per 1,000 inhabitants | Moran's index | Correlation with deprivation index |                   |                   |
| 0-9                | 539                            | 3.1            | 11.5                              | 1.760         | 0.67 <sup>s</sup>                  | 0.52 <sup>†</sup>              | 135                           | 0.8                               | 11.5          | 0.437                              | 0.71 <sup>s</sup> | 0.26 <sup>†</sup> |
| 10-19              | 416                            | 2.4            | 8.8                               | 1.208         | 0.74 <sup>s</sup>                  | 0.47 <sup>†</sup>              | 120                           | 0.7                               | 10.2          | 0.349                              | 0.68 <sup>s</sup> | 0.20 <sup>†</sup> |
| 20-39              | 951                            | 5.4            | 20.3                              | 1.037         | 0.75 <sup>s</sup>                  | 0.65 <sup>†</sup>              | 249                           | 1.4                               | 21.2          | 0.272                              | 0.64 <sup>s</sup> | 0.63 <sup>†</sup> |
| 40-64              | 1138                           | 6.5            | 24.3                              | 1.464         | 0.70 <sup>s</sup>                  | 0.70 <sup>†</sup>              | 377                           | 2.11                              | 32.1          | 0.485                              | 0.71 <sup>s</sup> | 0.62 <sup>†</sup> |
| 65 +               | 1637                           | 9.3            | 35                                | 4.589         | 0.75 <sup>s</sup>                  | 0.68 <sup>†</sup>              | 292                           | 1.7                               | 24.9          | 0.819                              | 0.66 <sup>s</sup> | 0.63 <sup>†</sup> |
| Total*             | 4682                           | 26.8           | 100                               | 1.752         | 0.77 <sup>s</sup>                  | 0.77 <sup>†</sup>              | 1173                          | 6.7                               | 100           | 0.442                              | 0.73 <sup>s</sup> | 0.66 <sup>†</sup> |

\* Moran's index and correlations with SES index calculated for the age-standardised incidence ratio (SIR)

<sup>s</sup> $p < 0.01$ , estimated by a standard *t*-test

<sup>†</sup>  $p < 0.01$  estimated by Clifford, Richardson and Hémon's test

<sup>#</sup>  $p < 0.05$  estimated by Clifford, Richardson and Hémon's test

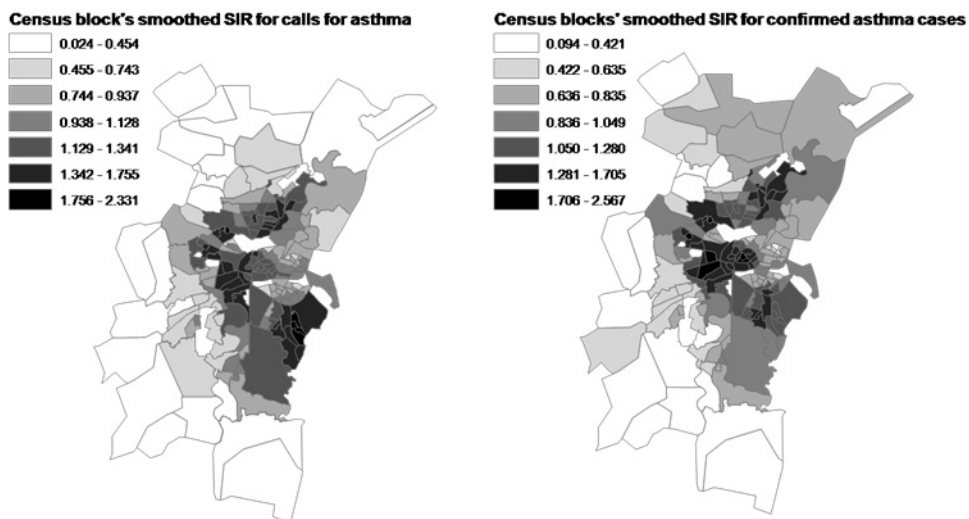


Fig. 2. Maps of age-standardized incidence ratios of emergency calls for asthma and of SAMU-confirmed asthma cases, across Strasbourg Metropolitan Area's census blocks

Table III. Distribution of population, asthma calls and air pollutant concentrations (Strasbourg Metropolitan Area, 2000-2005)

| Deprivation stratum † | Population | Calls, all ages | Calls, age 0-19 | Calls, age 19-64 | Calls, age over 64 | PM <sub>10</sub> ‡ | SO <sub>2</sub> ‡ | NO <sub>2</sub> ‡ | O <sub>3</sub> § |
|-----------------------|------------|-----------------|-----------------|------------------|--------------------|--------------------|-------------------|-------------------|------------------|
| Stratum 1             | 80,917     | 313             | 70              | 125              | 118                | 21                 | 7.6               | 30.2              | 63.4             |
| Stratum 2             | 92,534     | 784             | 159             | 300              | 325                | 22.1               | 8.6               | 35                | 58.6             |
| Stratum 3             | 93,392     | 959             | 169             | 384              | 406                | 23.2               | 9.6               | 39                | 55               |
| Stratum 4             | 105,367    | 1,243           | 226             | 574              | 443                | 23                 | 9.3               | 38.3              | 55.5             |
| Stratum 5             | 74 695     | 1,378           | 330             | 703              | 345                | 22.5               | 8.8               | 35.7              | 58               |
| Overall               | 446,905    | 4,677           | 954             | 2,086            | 1,637              | 22.6               | 8.9               | 36.0              | 57.7             |

† Stratum 1 is the least deprived, and stratum 5 the most deprived

‡ PM<sub>10</sub>, particulate matter less than 10 micrometers in aerodynamic diameter; NO<sub>2</sub>, nitrogen dioxide; SO<sub>2</sub>, sulfur dioxide. Concentrations for these three pollutants are averaged for period 2000-2005, in microgram per cubic meter

§ O<sub>3</sub>, ozone. Numbers reported are maximum 8-hour daily concentrations, averaged for summer months (April 1 to September 30) of period 2000-2005, in microgram per cubic meter

### *Base models*

Figure 5 shows the odds ratios for the relations between asthma calls (all ages) and pollutant concentrations averaged on the day of the call (lag 0) and the previous 1–5 days (lag 0–1 to lag 0–5). The highest positive associations were observed for lag 0–1 for PM<sub>10</sub> (for a 10- $\mu\text{g} \times \text{m}^3$  increase, odds ratio (OR) = 1.035, 95 percent confidence interval (CI): 0.997, 1.075) and sulfur dioxide (OR = 1.056, 95 percent CI: 0.979, 1.139) and for lag 0 for nitrogen dioxide (OR = 1.025, 95 percent CI: 0.990, 1.062). The association for PM<sub>10</sub> approached statistical significance ( $p = 0.07$ ). For ozone, no association was observed (OR = 0.998, 95 percent CI: 0.965, 1.032).

Table IV presents the results of analyses by age group for these same lags. For PM<sub>10</sub> (lag 0–1), associations were stronger for people younger than age 20 years and older than age 64 years as compared with people of all ages. For nitrogen dioxide (lag 0), higher odds ratios were observed in people over age 64 years than in people of all ages. For ozone, positive associations were observed only in persons older than 64 years.

### *Testing the influence of deprivation*

**Deprivation as a discrete variable.** Figure 6 presents the odds ratios for the five deprivation strata among people of all ages. The odds ratios show no clear trend according to deprivation level for any pollutant. We detected no heterogeneity of the odds ratios between strata. No clear trends by deprivation were observed in specific age groups (Figure 7).

**Deprivation as a continuous variable.** Significant heterogeneity ( $p < 0.05$ ) was detected between the odds ratios estimated for the 136 geographic units for each of the three pollutants considered (PM<sub>10</sub>, and nitrogen dioxide). Heterogeneity remained significant after we discarded the highest and lowest 5 percent of the odds ratios in the distribution. Negative linear regression coefficients (table V) suggested that the values of the odds ratios for these pollutants tended to decrease slightly from the least deprived geographic units to the most deprived (Figure 8). The associations between the odds ratios and deprivation were not significant, however, regardless of the pollutant or the model (fixed or random effects).

### **SABA sales**

Table VI presents the distribution of SABA sales and ambient pollutant concentrations for the entire SMA and for the five socioeconomically different strata. In 2004, SABA drugs were dispensed on 15,121 separate occasions for subjects aged 0 to 39 years. The number of sales per inhabitant slightly increased from the least to the most deprived stratum (Bard et al., 2007). The mean ambient pollutant concentrations over the study period were 20.8  $\mu\text{g}/\text{m}^3$  for PM<sub>10</sub> (range, 1.2 to 106.3  $\mu\text{g}/\text{m}^3$ ), 35.0  $\mu\text{g}/\text{m}^3$  for nitrogen dioxide (range, 6.4 to 84.3  $\mu\text{g}/\text{m}^3$ ), and 58.7  $\mu\text{g}/\text{m}^3$  for ozone (range, 2.6 to 220.0  $\mu\text{g}/\text{m}^3$ ).

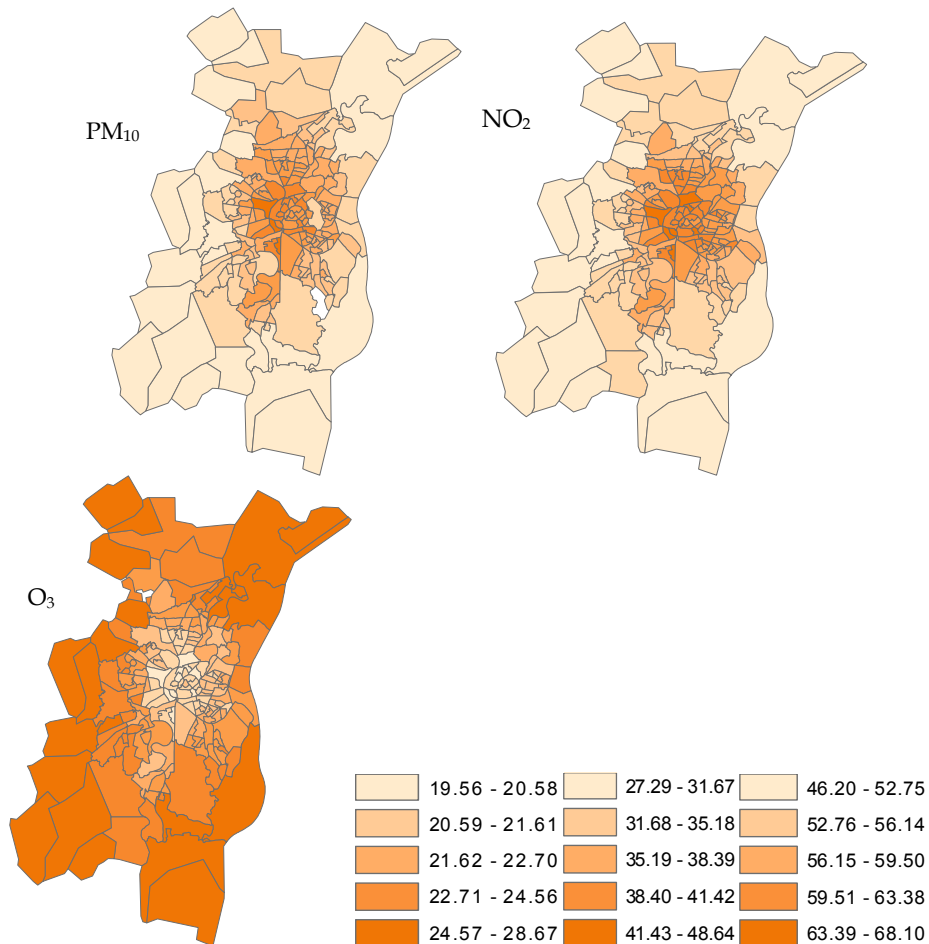


**Fig. 3.** Maps of ambient air pollutant concentrations ( $\mu\text{g}/\text{m}^3$ ) averaged by census block across the Strasbourg Metropolitan Area (2000–2005)

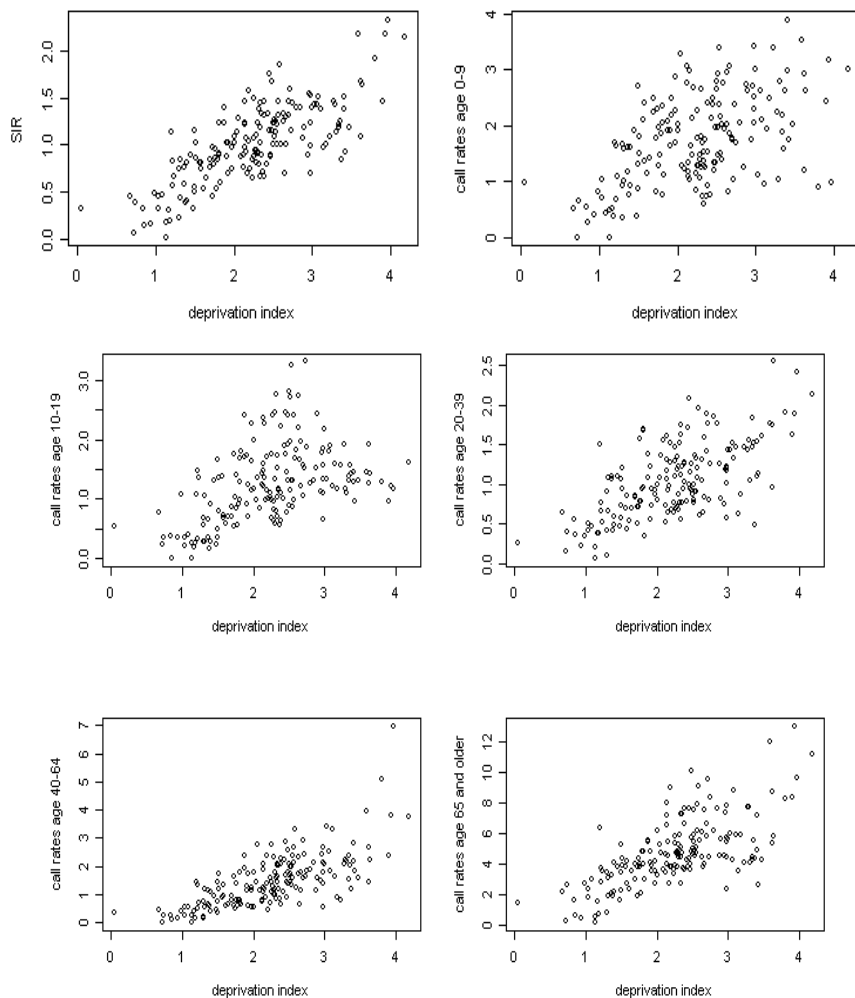


**Fig. 4.** Scatterplots of the rates of emergency calls for asthma according to deprivation of census blocks, for different age groups (on the left, the most privileged census blocks, on the right the most disadvantaged ones). SIR: Standardized Incidence Ratio

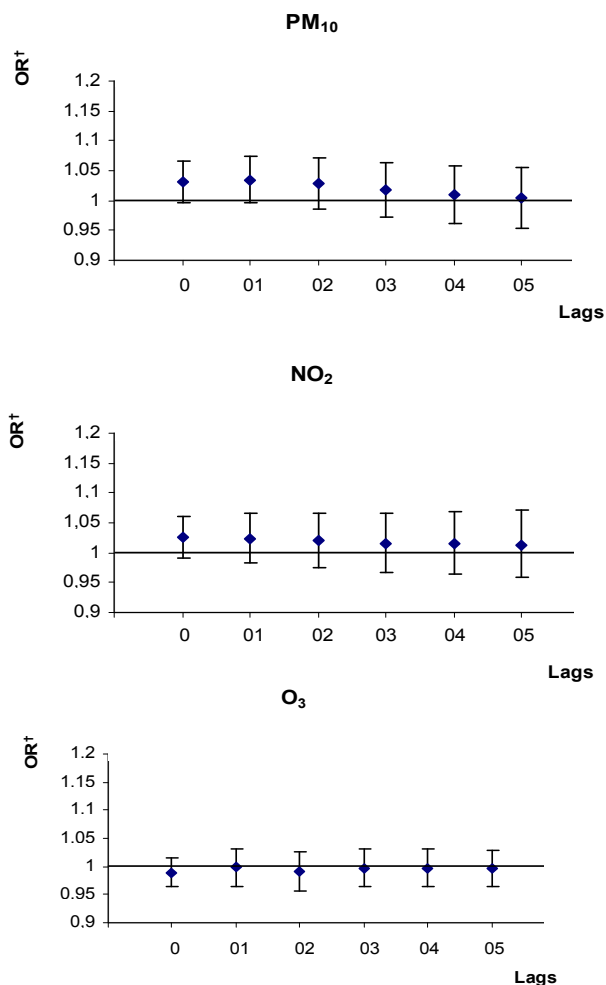


**Fig. 5. Odds ratios between asthma calls and pollutant concentrations\*, for various lag times (Strasbourg Metropolitan Area, 2000-2005)**

\* PM<sub>10</sub>, particulate matter less than 10 micrometers in aerodynamic diameter; NO<sub>2</sub>, nitrogen dioxide; O<sub>3</sub>, ozone.

† Odds ratios reported for a 10 µg.m<sup>-3</sup> increase in pollutant concentrations, adjusted for temperature, relative humidity, atmospheric pressure, holidays, influenza epidemics and pollen counts. Lag 0 is for pollutant concentrations averaged on the day of the call, lag 01 for pollutant concentrations averaged on the day of the call and the previous one, and so on.

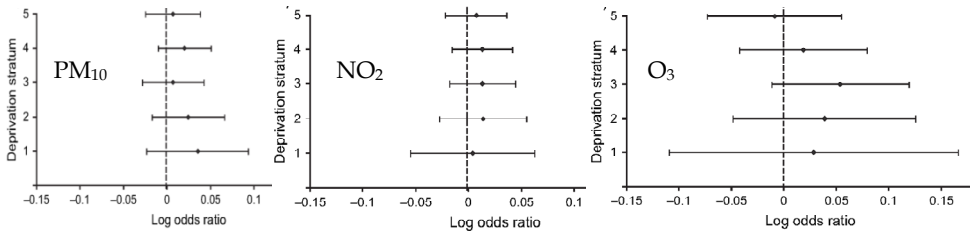


**Fig. 6.** Log odds ratio for emergency asthma calls per 10  $\mu\text{g}/\text{m}^3$  increase in ambient pollutant concentrations, according to stratum of socioeconomic deprivation, Strasbourg, France, 2000–2005. Stratum 1 was the least deprived, and stratum 5 was the most deprived. PM<sub>10</sub>: particulate matter less than 10  $\mu\text{m}$  in aerodynamic diameter; NO<sub>2</sub>: nitrogen dioxide; O<sub>3</sub>: ozone. Bars, 95% confidence interval.

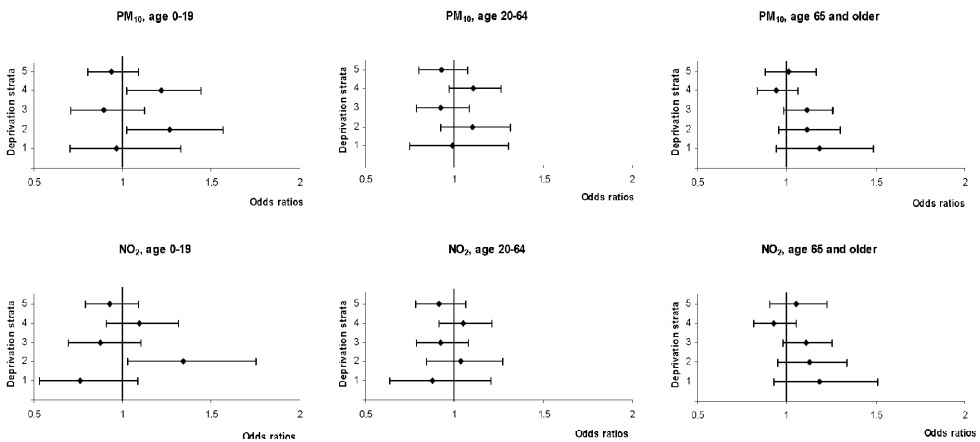


**Fig. 7.** Odds ratios between asthma calls and pollutants\*, for five strata of deprivation levels† and different age groups (Strasbourg Metropolitan Area, 2000–2005)

\* PM<sub>10</sub>, particulate matter less than 10 micrometers in aerodynamic diameter; NO<sub>2</sub>, nitrogen dioxide; O<sub>3</sub>, ozone. Odds ratios reported for a 10  $\mu\text{g}/\text{m}^3$  increase in pollutant concentrations, adjusted for temperature, relative humidity, atmospheric pressure, holidays, influenza epidemics and pollen counts

† Stratum 1 is the least deprived, and stratum 5 is the most

#### Base model

Figure 9 presents the odds ratios for the individual lags for subjects aged 0 to 39 years. For all three pollutants, odds ratios greater than one were observed for lags from 4 to 10 days. For PM<sub>10</sub> and nitrogen dioxide, most of the odds ratios were statistically significant ( $p < 0.05$ ) for lags from 5 to 10 days. For a lag of 2 days, odds ratios significantly lower than one were observed for all three pollutants. The structure of the lags reported in Figure 9 did not change when the analyses were stratified by smaller age subgroups (0 to 19 years, 20 to 39 years). No association was observed between SABA sales and the mean pollutant concentrations of the day of the sale and the 1 to 10 preceding days (lags 0 to 1 to 0 to 10).

On the basis of the associations reported in Figure 9, the lags kept for the subsequent analyses were lag 4 to 7 (mean concentrations of days 4, 5, 6, and 7 for PM<sub>10</sub>, lag 4 to 10 for nitrogen dioxide, and lag 4 to 6 for ozone). A 10 µg/m<sup>3</sup> increase in ambient concentrations of PM<sub>10</sub>, nitrogen dioxide, and ozone for these lags was associated with increases of 7.5% (95% CI, 4 to 11.2%), 8.4% (95% CI, 5 to 11.9%), and 1 (95% CI, - 0.3 to 2.2%), respectively, in SABA sales.

#### *Testing the influence of deprivation*

Figure 10 presents the odds ratios for the five different socioeconomic strata for the optimal lags mentioned above for all subjects aged 0 to 39 years. We observed no trend toward an increase or decrease of these odds ratios according to SES or when we stratified the analyses by smaller age subgroups (0 to 19 years, 20 to 39 years).

## **4. Discussion**

### **4.1 Socioeconomic Status Indicator**

From available census variables, we developed and validated a new French socioeconomic deprivation index at the census block level. Working at this resolution ensures a better homogeneity of the residents' characteristics. As a result, it is possible to better identify and measure with greater precision their relation with the health events observed. Available French census data combines material and, to a lesser extent, social aspects of deprivation, with no indication of a possible association with the health events to which it may be associated. In this study, it allowed to identify a socioeconomic gradient in the utilization of mobile emergency medical services for asthma attacks in the SMA (Laurent et al., 2008). This scale has also been shown to be robust (validity criterion) and reproducible for another French metropolitan area with different socioeconomic characteristics.

**Table IV. Odds ratios between asthma calls and pollutant concentrations for different age groups and for selected lag times (Strasbourg Metropolitan Area, 2000-2005)**

| Lag †              | All ages      |                          |              |               | Age 0-19                 |              |               |                          | Age 20-64    |               |                          |              | Age 64 +      |                          |    |  |
|--------------------|---------------|--------------------------|--------------|---------------|--------------------------|--------------|---------------|--------------------------|--------------|---------------|--------------------------|--------------|---------------|--------------------------|----|--|
|                    | Odds ratios § | 95% confidence intervals | p#           | Odds ratios § | 95% confidence intervals | p#           | Odds ratios § | 95% confidence intervals | p#           | Odds ratios § | 95% confidence intervals | p#           | Odds ratios § | 95% confidence intervals | p# |  |
| PM <sub>10</sub> * | 0-1           | 1.035                    | 0.997, 1.075 | 0.07          | 1.047                    | 0.961, 1.141 | 0.29          | 1.020                    | 0.964, 1.079 | 0.49          | 1.049                    | 0.985, 1.116 | 0.14          |                          |    |  |
| NO <sub>2</sub> *  | 0             | 1.025                    | 0.990, 1.062 | 0.16          | 1.003                    | 0.926, 1.086 | 0.94          | 1.015                    | 0.964, 1.070 | 0.57          | 1.050                    | 0.990, 1.113 | 0.10          |                          |    |  |
| SO <sub>2</sub> *  | 0-1           | 1.056                    | 0.979, 1.139 | 0.15          | 1.122                    | 0.945, 1.334 | 0.19          | 0.990                    | 0.882, 1.112 | 0.87          | 1.102                    | 0.975, 1.245 | 0.12          |                          |    |  |
| O <sub>3</sub> †   | 0-1           | 0.998                    | 0.965, 1.032 | 0.90          | 0.966                    | 0.891, 1.048 | 0.40          | 0.997                    | 0.949, 1.047 | 0.90          | 1.015                    | 0.960, 1.074 | 0.59          |                          |    |  |

\* PM<sub>10</sub>, particulate matter less than 10 micrometers in aerodynamic diameter; NO<sub>2</sub>, nitrogen dioxide.

† O<sub>3</sub>, ozone. Study period extending from April 1 to September 30 of each year

‡ Lag 0 is for pollutant concentrations averaged on the day of the call, lag 01 for pollutant concentrations averaged on the day of the call and the previous one.

§ Odds ratios reported for a 10 µg·m<sup>-3</sup> increase in pollutant concentrations, adjusted for temperature, relative humidity, atmospheric pressure, holidays, influenza epidemics and pollen counts

# Estimated by a two-sided χ<sup>2</sup> test

**Table V. Influence of deprivation introduced as a continuous variable on the relations between pollutants and asthma calls (Strasbourg Metropolitan Area, 2000-2005)**

|   |                      | Dependent variables: odds ratios between pollutants and asthma calls |                            |                             |
|---|----------------------|--|----------------------------|-----------------------------|
|   |                      | NO <sub>2</sub> †  | SO <sub>2</sub> †          | PM <sub>10</sub> †          |
| Independent variable: deprivation index | Fixed effects model  | -0.00272, <i>p</i> =0.49 ‡   | -0.01032, <i>p</i> =0.18 ‡ | -0.00244, <i>p</i> = 0.48 ‡ |
|   | Random effects model | -0.00284, <i>p</i> =0.48 ‡   | -0.01052, <i>p</i> =0.18 ‡ | -0.00249, <i>p</i> =0.47 ‡  |

† Odds ratios reported for a 10 µg.m<sup>-3</sup> increase in pollutant concentrations, adjusted for temperature, relative humidity, atmospheric pressure, holidays, influenza epidemics and pollen counts. PM<sub>10</sub>, particulate matter less than 10 micrometers in aerodynamic diameter; NO<sub>2</sub>, nitrogen dioxide.

‡ Beta coefficients for regression of the values of the odds ratios on the deprivation index. Statistical significance was estimated by a two-sided χ<sup>2</sup> test

Nonetheless, the strength of the correlations observed with the British indices by Townsend and Carstairs (correlations greater than 0.95 for both) suggest that we might have simply used them in our study, rather than constructing our own index. Indeed, their indices are more straightforward to use than ours (unweighted sum of standardized variables) and require fewer variables for their construction (4 compared with 19 in ours). However, they rely exclusively on purely material indicators, thus missing the social dimension of deprivation. The direct use of the British indices in a French setting is also limited by several factors. Firstly, these indices use data from the British census that do not correspond directly to French census items and for which an adaptation or translation is required (for example, the variable “proportion of households in which the householder belongs to social class 4 or 5” considered by Carstairs must be translated as “the proportion of blue-collar workers” for use in the French census database). Secondly, they were developed at a specific geographical level (enumeration district or ward) that is not equivalent to the French census block in terms of population size and socioeconomic characteristics. The effects of these adaptations (*i.e.*, variable definitions and geographical units) on the associations observed with health events have never, as far as we know, been assessed and do not encourage their use in our context. A last limitation of these indices is their inability to take into account differences between rural and urban areas because they include in their composition only variables specific to urban conditions (Gilthorpe & Wilson, 2003). The use in our study of the Index of Multiple Deprivation, constructed especially to overcome this weakness (Jordan et al., 2004) should therefore be a useful option. The French census data do not, however, lend themselves to the use of this index, for its composition includes 33 variables, many of which were either unavailable or could not be transposed from the census data. Our index thus appears to be a good alternative to the existing British indices: it is simpler to implement than the Index of Multiple Deprivation (19 compared with 33 variables, no weighting, etc.) and at the same time it overcomes the principal limitations of Carstairs and Townsend’s indices, that is, it is validated at the resolution of census blocks and able to contrast deprived urban and advantaged rural areas in our study. This study nonetheless has its own

limitations, the first of which is the need to acknowledge that one size does not fit all (Braveman et al., 2005). Our index is a comprehensive and composite measure of SES and was constructed independently of the health events to which it might be associated. It includes variables related to education, income, occupation, etc. and in that respect is a better indicator than a single variable taken in isolation to describe SES as a whole.

Characterizing in more detail the social component of deprivation, both at the individual level and accounting for neighborhood influences would allow shedding more light on the complex and intricate relationships between socioeconomic characteristics and the health impact of exposure to environmental stressors. Nonetheless, in the absence of individual data, ecological studies of this type remain necessary and useful for a better understanding of the interactions between socioeconomic factors and health.

#### **Calls to emergency medical services for asthma exacerbation**

Emergency calls for asthma attacks were positively, although not significantly, associated with concentrations of PM<sub>10</sub>, and nitrogen dioxide modeled by census blocks. No association was observed for ozone. Overall, associations were higher among people younger than 20 years and older than 64 years. Socioeconomic deprivation measured by census block did not appear to influence these relations.

The daily exposure estimates we used were modeled for small areas and are geographically more precise than those usually employed to study short-term relations between air pollution and health. Compared with ambient concentrations averaged citywide, our exposure estimate likely reduced ecological biases (Jerrett et al., 2005b). Practically, the exposure measurement attributed to each subject was the concentration estimated for the census block where each patient was when the emergency network was called. However, we do not actually know whether the patients were in the same block in the hours to days preceding the call, and this fact obviously determines the extent to which our exposure measurement adequately reflects subjects' true exposure.

This point matters mainly for subjects who are frequently away from the neighborhood they live in -principally in the 20-64 year-old age group, globally characterized by mobility and autonomy, and who work for a living (often outside the neighborhood of residence). Conversely, in general the elderly rarely commute out of their neighborhoods of residence and when they do so, they generally go shorter distances (Benlahrech et al., 2001). Children also have more limited mobility than people aged 20-64 years (Agence de l'Environnement et de la Maîtrise de l'Energie/Institut de Radioprotection et de Sûreté Nucléaire, 2003) and generally attend the schools closest to their homes.

These points support the idea that our exposure measurement is more accurate for people aged younger than 20 and older than 64 years. These subjects are more likely to have called the emergency networks from their neighborhood of residence (and thus be geocoded in it). Moreover, for these subjects, the measurement of air pollution in the neighborhood of residence is more likely to provide an adequate reflection of exposure integrated over the days preceding the call than for more mobile subjects.

The ranges of the associations we found for the base models were similar to those reported by other studies of emergency calls (Medina et al., 1997) and visits to hospital emergency departments (Galan et al., 2003) for asthma. Above all, the associations observed for PM<sub>10</sub> were very close to those reported by two meta-analyses of the associations between this pollutant and asthma symptoms (Weinmayr et al., 2010; Kunzli et al., 2000).

Small-area deprivation (introduced either as a discrete or as continuous variable) did not appear to influence the relations between ambient air pollution and asthma attacks. Of the six previous studies that investigated the influence of socioeconomic indicators on these relations (Nauenberg & Basu, 1999; Norris et al., 1999; Lin et al., 2004; Neidell, 2004; Son et al., 2006; Kim et al., 2007), five reported higher relative risks for populations with less advantageous socioeconomic characteristics (Nauenberg & Basu, 1999; Lin et al., 2004; Neidell, 2004; Lee et al., 2006; Kim et al., 2007). However, one of these studies found evidence of interaction according to the ecological socioeconomic indicator considered, and no interaction with the individual indicator (Kim et al., 2007). The sixth study reported slightly higher relative risks for the most deprived populations (Norris et al., 1999). Nevertheless, formal comparison of the results of these studies is difficult, as they focused on socioeconomic indicators measured at very heterogeneous resolutions (Laurent et al., 2007).

Three of these studies focused on socioeconomic indicators measured at very coarse geographic resolutions. Lee et al (Lee et al., 2006) and Kim et al (Kim et al., 2007) focused on *Gu* neighborhoods (of around 400,000 inhabitants) in the city of Seoul (Korea), for children aged 0-15 (Lee et al., 2006) and people of all ages, respectively (Kim et al., 2007). Overall, these studies reported higher relative risks between PM<sub>10</sub>, SO<sub>2</sub>, and NO<sub>2</sub> concentrations and asthma hospitalizations in the most deprived *Gu*. Norris et al, in Seattle (Washington, USA) (Norris et al., 1999) studied associations between the same pollutants and visits to emergency departments for asthma in children aged 0-18. They reported slightly lower relative risks for residents of the inner city, that is, the most deprived areas.

Two other studies focused on individual socioeconomic indicators in people of all ages. Kim et al (Lee et al., 2006), in Seoul (Korea) found that associations between PM<sub>10</sub> and visits to emergency departments for asthma did not vary according to the annual amount of taxes paid to the national health insurance system. In contrast, Nauenberg and Basu, in Los Angeles (USA), found that effects of PM<sub>10</sub> were greater in people with a less favorable health insurance status (Nauenberg & Basu, 1999).

Last, two studies focused on socioeconomic indicators measured by small areas. Neidell (Neidell, 2004) observed that carbon monoxide and ozone had a greater effect on asthma hospitalizations of Californian children aged 3-18 in ZIP codes characterized by lower educational attainment. This study, however, estimated associations between asthma hospitalizations and air pollutants on the basis of monthly indicators, which are inadequate to study short-term relations between these factors. Lin et al studied children aged 6-12 years in Vancouver (Canada) (Lin et al., 2004) and reported higher associations between nitrogen dioxide, sulfur dioxide and hospitalization for asthma in enumeration areas with lower household income levels.

The study by Lin et al (Lin et al., 2004) is the most comparable in design to ours, but reports somewhat different results. The reasons for this are unclear. Pollutant concentrations were very similar in the two settings. Although the studies used different types of exposure measurements (pollutant concentrations averaged citywide for Lin et al (Lin et al., 2004) and modeled by census blocks in ours), this difference does not explain the variation in findings. Indeed, alternative analysis in the SMA with citywide average exposure measurements did not noticeably change our results about interactions with deprivation. Lack of statistical power appears to be a plausible explanation for the difference between our results and those of Lin et al. For comparable age groups (0-20 versus 6-12) we had one quarter the number of health events to analyze.

Another point is that findings of interaction with deprivation are not necessarily transposable from one setting to another. If small-area deprivation does exert an influence on the relations between air pollution and asthma attacks, it would most likely be mediated through "third" factors that in some (but perhaps not in all) settings would be distributed unequally according to deprivation. Previous studies report that several factors thought to strengthen the associations between air pollution and asthma attacks are more present in deprived than in well-off neighborhoods. Among these are the prevalence of (both active and passive) smoking (Diez-Roux et al., 2003), psychosocial stress (Gold & Wright, 2005), unhealthy eating habits (Diez-Roux et al., 1999), amounts of indoor allergens (Kitch et al., 2000), inadequate compliance with anti-inflammatory medication (Gottlieb et al., 1995) and (a plausible result of the factors mentioned above) a higher ratio of severe to moderate forms of asthma among subjects with asthma (Basagana et al., 2004). Nevertheless, the distribution of these factors according to small-area deprivation may differ between study settings, due, for instance, to differences in climate (affecting allergen proliferation), social and cultural characteristics of local populations (influencing, among other things, eating and smoking habits) or effectiveness of health systems (influencing prescription of and compliance with anti-inflammatory medication).

Moreover, although we observed no interactions with small-area deprivation in the SMA, this does not rule out the existence here of interactions by socioeconomic factors measured at other resolutions (individual, household, geographic areas more or less fine than the French census block), as the study by Kim et al clearly illustrates (Kim et al., 2007). The use of multilevel models, which make it possible to assess more precisely the influence of factors (e.g. socioeconomic characteristics) measured at different resolutions, would be useful in studying this question further (O'Neill et al., 2003).

#### **SABA sales**

We observed positive associations between ambient concentrations of atmospheric pollutants and SABA sales for subjects < 40 years old. These are expressed with latency periods of 4 to 10 days and do not tend to increase or decrease according to SES.

This study is the first to examine the relations between exposure to urban air pollution and SABA sales. The use of this indicator, obtained from the four primary French health insurance funds, allowed us to cover > 90% of the local population and to capture the entire range of SES in the SMA. People not covered by these funds are mainly employees of various sectors once publicly owned (railway, electricity, gas), with jobs ranging from manual workers to administrators and mainly in the middle classes. The large number of SABA sales allowed us to measure their associations with air pollution modeled by small areas. This resolution is particularly pertinent for studying this risk factor because its spatial distribution varies strongly within urban areas (Laurent et al., 2008). These large numbers also allowed us to test the existence of interactions by neighborhood SES with satisfactory statistical power. The event analyzed is the patient's purchase of one (or sometimes more) box of drugs, and not a quantity of active ingredient delivered or really inhaled. Naureckas et al. (Naureckas et al., 2005) nonetheless showed that this indicator is a good predictor of the risk of emergency department visits and of hospitalization for asthma attacks in the days immediately afterwards. These purchases generally reflect asthma morbidity less severe than that requiring hospitalization or emergency treatment (Naureckas et al., 2005). A large portion of SABA sales anticipate the respiratory disorders the drugs are intended to treat. These sales, which need not be associated in time with asthma, add some "noise" to the data. Noise is standard in ecologic studies of the

short-term health effects of air pollution because of the influence of unmeasured competing factors (other than air pollution) on the temporal distribution of the health outcomes studied. Nevertheless, if the signal-to-noise ratio is sufficiently high, the effect specifically due to air pollution can be observed. In our study, despite the additional noise due to anticipatory sales, this ratio appears to be high enough to detect statistically significant associations. These associations are consistent with those reported by most panel studies (von Klot et al., 2002; Romeo et al., 2006; Schildcrout et al., 2006) that have investigated the relation between air pollution and SABA consumption.

The associations observed involved latency periods of 4 to 10 days, an order of magnitude similar to the delayed responses observed in two earlier temporal ecologic studies of the relation between air pollution and drug sales mucolytic and antitussive agents (Zeghnoun et al., 1999) "cough and cold preparations," and all types of anti-COPD/asthma drugs (Pitard et al., 2004). This is probably because the latency periods between exposure to air pollution and drug purchases result from a mixed process involving both pathophysiological response and management of medicine supplies. The literature (von Klot et al., 2002; Rabinovitch et al., 2006; Romeo et al., 2006; Schildcrout et al., 2006) shows that in people with asthma, air pollution induces respiratory disorders expressed by increased SABA consumption, with low latency periods (several hours 34 to several days (von Klot et al., 2002; Schildcrout et al., 2006)). This increased consumption requires a successive -but not necessarily immediate- replenishment of the SABA supply. Several days of delay, possibly marked by a return to a normal rhythm of use, may pass before the purchase, which may explain the particularly long lags (up to 10 days) observed. For lag 2, we observed odds ratios significantly less than one. Several authors, in other settings and with different methods, report similar findings. Zeghnoun et al. (Zeghnoun et al., 1999) also observed low associations for lag 2, especially for mucolytic and antitussive drugs. Moreover, in a panel study of SABA consumption, Rabinovitch et al. (Rabinovitch et al., 2006) also observed relative risks less than one for the same lag. Von Klot et al. (von Klot et al., 2002) report comparable observations specifically for lag 1. No satisfactory explanation has yet been found for these observations.

SES did not influence the relation between SABA sales and ambient air pollution. This is consistent with the results appearing above for an indicator of more severe asthma morbidity, interventions of mobile emergency medical services for asthma attacks (Laurent et al., 2008).

In conclusion, emergency calls for asthma attacks SABA sales for children, adolescents and young adults were positively (not significantly for the former, but significantly for SABA sales) associated with  $PM_{10}$ ,  $NO_2$  but not  $O_3$  concentrations modeled by small areas. Small area deprivation did not influence these associations. Nonetheless, discrepancies between our results on emergency calls and those of the study of Lin et al (Lin et al., 2004) emphasize the need to investigate this question further in other study settings. Similarly, the observations we made regarding SABA sales do not rule out the possibility that SES might be an interaction factor in other settings, for the distribution according to SES of other factors that might modulate the relations between air pollution and asthma morbidity may well differ between countries or even cities. The results on SABA are consistent with those of panels of asthma patients and their SABA consumption, although expressed here with longer time lags. Our results support the usefulness of SABA sales for the analysis of relations between asthma morbidity and air pollution.

## 5. Acknowledgments

The authors thank all the organizations that kindly provided the data used in these analyses: URCAM Alsace (especially Benoit Wollbrett), RSI Alsace (especially Katia Bischoff), MSA Alsace (especially Hervé Hunold), MGEL (especially Gérard Rey), Météo France, National Network of Aerobiologic Surveillance, and the INSERM Sentinelles Network. The authors also thank Professor Frédéric de Blay for providing opinion as a specialist in pulmonary medicine, and Dr. Fabienne Wachet for providing expertise on drug supply and repayment systems. Finally, the authors thank Jo Ann Cahn for editorial assistance. These studies were made possible by the grant ANR SEST 0057 05 from the French National Research Agency (ANR).

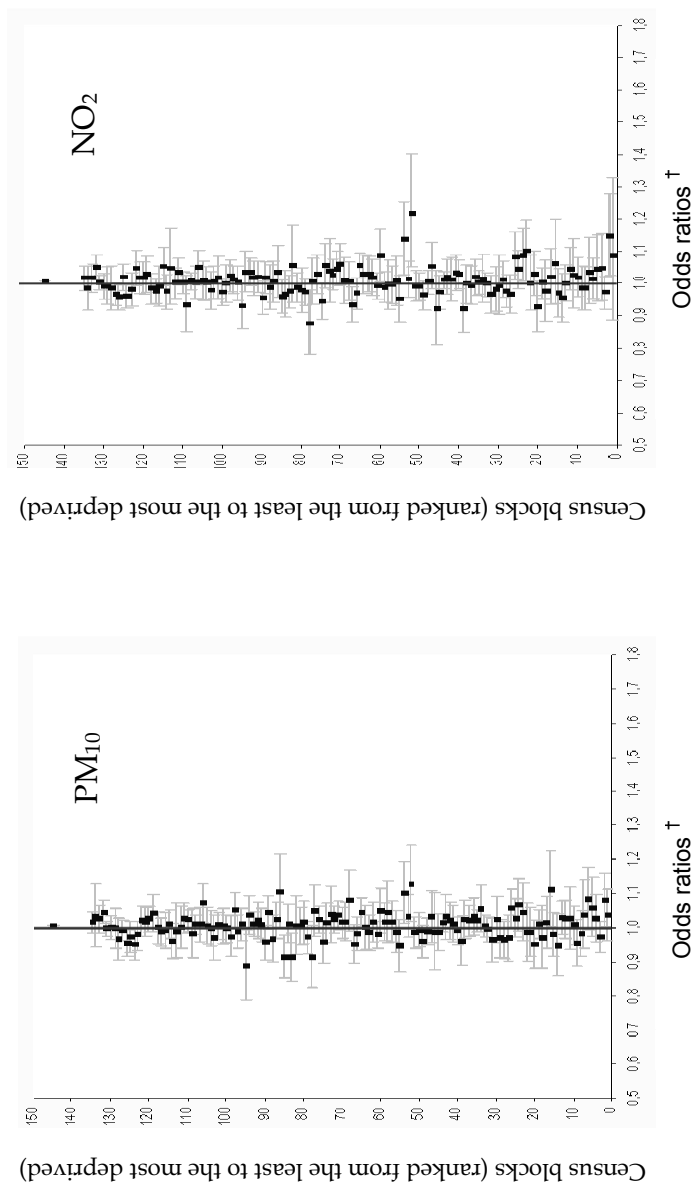


**Fig. 8. Odds ratios between asthma calls and pollutants in the 136 statistical units retained, ranked according to deprivation (from the least deprived on the bottom to the most deprived at the top). Strasbourg Metropolitan Area, 2000-2005**  
†Odds ratios reported for a 1  $\mu\text{g}\cdot\text{m}^{-3}$  increase in pollutant concentrations (for the sake of figure visibility), adjusted for temperature, relative humidity, atmospheric pressure, holidays, influenza epidemics and pollen counts. PM<sub>10</sub>, particulate matter less than 10 micrometers in aerodynamic diameter; NO<sub>2</sub>: nitrogen dioxide

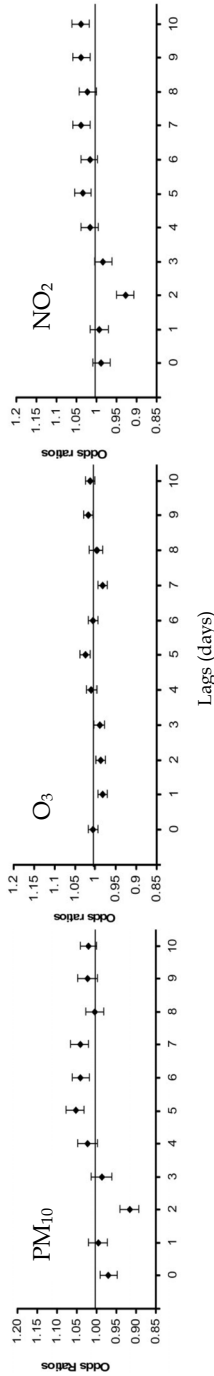
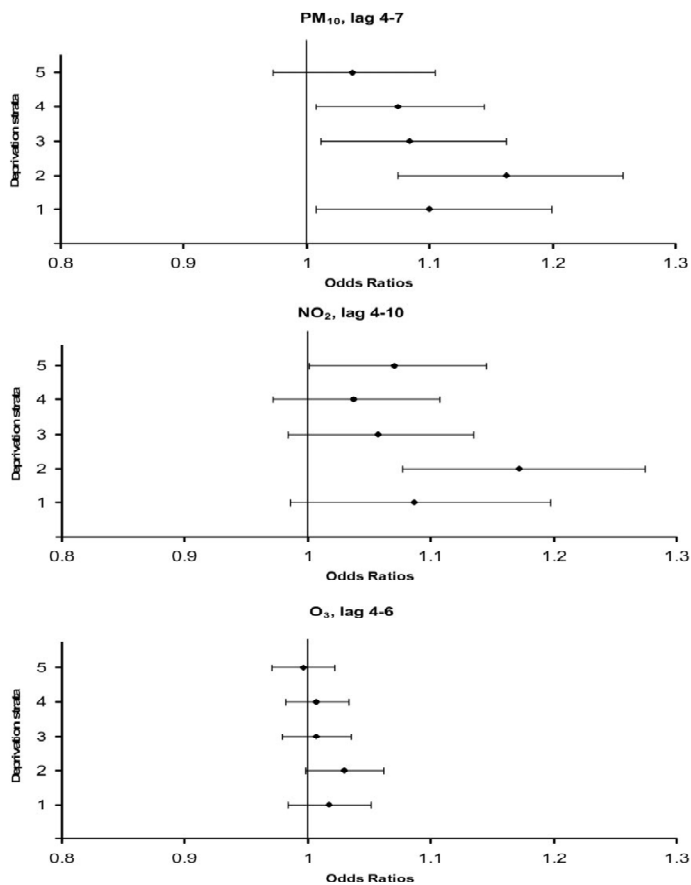


Fig. 9. Odds ratios for an increase of 10  $\mu\text{g}/\text{m}^3$  in the pollutants concentration, subjects <40 years old; for various lags.



**Fig. 10. Interactions by socioeconomic level in those aged < 40 years: associations for the five different strata of socioeconomic levels.**

Stratum 1 is the most advantaged and stratum 5 the most deprived. Associations were estimated for “optimal” lags defined according to the associations reported for individual lags, see Figure 7. For example, for PM<sub>10</sub> among those younger than 40 years, 4-7 corresponds to the mean concentrations for day D4, D5, D6 and D7.

Table VI. Distribution of SABA sales and air pollutant concentrations, Strasbourg Metropolitan Area, 2004

| Deprivation stratum <sup>§</sup> | Population, age groups |        |        |         | SABA sales, age groups |       |       |       | Pollutants (mean, SD)         |                              |                             |                               |                              |                             |
|----------------------------------|------------------------|--------|--------|---------|------------------------|-------|-------|-------|-------------------------------|------------------------------|-----------------------------|-------------------------------|------------------------------|-----------------------------|
|                                  | Total, 0-39            | 0-9    | 10-19  | 20-39   | Total, 0-39            | 0-9   | 10-19 | 20-39 | PM <sub>10</sub> <sup>†</sup> | NO <sub>2</sub> <sup>†</sup> | O <sub>3</sub> <sup>†</sup> | PM <sub>10</sub> <sup>†</sup> | NO <sub>2</sub> <sup>†</sup> | O <sub>3</sub> <sup>†</sup> |
|                                  | 39                     |        |        |         | 39                     |       |       |       |                               |                              |                             |                               |                              |                             |
| <b>Stratum 1</b>                 | 43,674                 | 9,342  | 11,489 | 22,843  | 2,140                  | 733   | 426   | 981   | 19.4                          | 9.9                          | 29.9                        | 10.3                          | 63.1                         | 36.5                        |
| <b>Stratum 2</b>                 | 47,757                 | 9,359  | 11,022 | 27,376  | 2,538                  | 728   | 578   | 1,232 | 20.5                          | 10.4                         | 34.2                        | 10.2                          | 59.3                         | 36.1                        |
| <b>Stratum 3</b>                 | 54,527                 | 9,498  | 9,550  | 35,479  | 2,972                  | 931   | 460   | 1,581 | 21.6                          | 10.6                         | 37.5                        | 10.7                          | 56.0                         | 35.7                        |
| <b>Stratum 4</b>                 | 65,994                 | 10,404 | 11,917 | 43,673  | 3,752                  | 1,192 | 631   | 1,929 | 21.4                          | 10.5                         | 37.0                        | 10.6                          | 57.0                         | 35.8                        |
| <b>Stratum 5</b>                 | 49,111                 | 12,440 | 13,269 | 23,402  | 3,719                  | 1,332 | 763   | 1,624 | 20.7                          | 10.3                         | 35.7                        | 10.2                          | 58.6                         | 35.8                        |
| <b>Overall</b>                   | 261,063                | 51,043 | 52,247 | 152,773 | 15,121                 | 4,916 | 2,858 | 7,347 | 20.8                          | 10.2                         | 35.0                        | 10.3                          | 58.7                         | 36.0                        |

<sup>§</sup> Stratum 1 is the last deprived, and stratum 5 the most deprived

<sup>†</sup> Concentrations averaged for year 2004, in microgram per cubic meter

<sup>‡</sup> Maximum 8-hour daily concentrations, averaged for summer months (April 1 to September 30) of year 2004, in microgram per cubic meter

## 6. References

- Agence de l'Environnement et de la Maîtrise de l'Energie/Institut de Radioprotection et de Sûreté Nucléaire (2003). Ciblex: database of descriptive characteristics of the French population residing near polluted sites (CD-ROM) ref N° 4773. Angers, France/Fontenay-aux-Roses, France.
- Annesi-Maesano, I.; Agabiti, N.; Pistelli, R.; Couilliot, M. F. & Forastiere, F. (2003). Subpopulations at increased risk of adverse health outcomes from air pollution. *Eur Respir J Suppl* 40: 57s-63s.
- Atkinson, R. W.; Anderson, H. R.; Sunyer, J.; Ayres, J.; Baccini, M.; Vonk, J. M.; Boumghar, A.; Forastiere, F.; Forsberg, B.; Touloumi, G.; Schwartz, J. & Katsouyanni, K. (2001). Acute effects of particulate air pollution on respiratory admissions: results from APHEA 2 project. Air Pollution and Health: a European Approach. *Am J Respir Crit Care Med* 164(10 Pt 1): 1860-6.
- Bard, D.; Laurent, O.; Filleul, L.; Havard, S.; Deguen, S.; Segala, C.; Pedrono, G.; Rivière, E.; Schillinger, C.; Rouil, L.; Arveiler, D. & Eilstein, D. (2007). Exploring the joint effect of atmospheric pollution and socioeconomic status on selected health outcomes: an overview of the PAISARC project. *Environ Res Lett* 2(045003): 7 pp.
- Basagana, X.; Sunyer, J.; Kogevinas, M.; Zock, J. P.; Duran-Tauleria, E.; Jarvis, D.; Burney, P. & Anto, J. M. (2004). Socioeconomic status and asthma prevalence in young adults: the European Community Respiratory Health Survey. *Am. J. Epidemiol.* 160(2): 178-88.
- Beguín, M. & Pumain, D. (1994). *La représentation des données géographiques*. Paris, Armand Colin.
- Benach, J. & Yasui, Y. (1999). Geographical patterns of excess mortality in Spain explained by two indices of deprivation. *J. Epidemiol. Community Health* 53(7): 423-31.
- Benlahrech, N.; Le Ruyet, A.; Livebardon, C. & Dejeammes, M. (2001). The mobility of old people (analysis of the household displacement surveys) [In French]. CERTU. Lyon, France.
- Blanc, P. D.; Yen, I. H.; Chen, H.; Katz, P. P.; Earnest, G.; Balmes, J. R.; Trupin, L.; Friedling, N.; Yelin, E. H. & Eisner, M. D. (2006). Area-level socio-economic status and health status among adults with asthma and rhinitis. *Eur. Respir. J.* 27(1): 85-94.
- Braveman, P. A.; Cubbin, C.; Egerter, S.; Chideya, S.; Marchi, K. S.; Metzler, M. & Posner, S. (2005). Socioeconomic status in health research: one size does not fit all. *JAMA* 294(22): 2879-88.
- Buzzelli, M.; Jerrett, M.; Burnett, R. & Finkelstein, N. (2003). Spatiotemporal perspectives on air pollution and environmental justice in Hamilton, Canada, 1985-1996. *Annals of the Association of American Geographers* 93(3): 557-73.
- Carstairs, V. (1995). Deprivation indices: their interpretation and use in relation to health. *J Epidemiol Community Health* 49 Suppl 2: S3-8.
- Carstairs, V. & Morris, R. (1991). *Deprivation and Health in Scotland*. Aberdeen, Aberdeen University Press.
- Cesaroni, G.; Farchi, S.; Davoli, M.; Forastiere, F. & Perucci, C. A. (2003). Individual and area-based indicators of socioeconomic status and childhood asthma. *Eur. Respir. J.* 22(4): 619-24.
- Challier, B. & Viel, J. F. (2001). [Relevance and validity of a new French composite index to measure poverty on a geographical level]. *Rev Epidemiol Sante Publique* 49(1): 41-50.

- Clifford, P.; Richardson, S. & Hemon, D. (1989). Assessing the significance of the correlation between two spatial processes. *Biometrics* 45(1): 123-34.
- Com-Ruelle, L.; Crestin, B. & Dumesnil, S. (2000). Asthma in France by gravity degrees. IRDES. Paris, CREDES.
- Coste, J.; Fermanian, J. & Venot, A. (1995). Methodological and statistical problems in the construction of composite measurement scales: a survey of six medical and epidemiological journals. *Stat Med* 14(4): 331-45.
- DETR (2000). Measuring deprivation at the small area level: the indices of deprivation 2000. 31, N.
- Diez-Roux, A. V.; Nieto, F. J.; Caulfield, L.; Tyroler, H. A.; Watson, R. L. & Szklo, M. (1999). Neighbourhood differences in diet: the Atherosclerosis Risk in Communities (ARIC) Study. *J Epidemiol Community Health* 53(1): 55-63.
- Diez-Roux, A. V.; Merkin, S. S.; Hannan, P.; Jacobs, D. R. & Kiefe, C. I. (2003). Area characteristics, individual-level socioeconomic indicators, and smoking in young adults: the coronary artery disease risk development in young adults study. *Am J Epidemiol* 157(4): 315-26.
- Eibner, C. & Sturm, R. (2006). US-based indices of area-level deprivation: results from HealthCare for Communities. *Soc Sci Med* 62(2): 348-59.
- Ellison-Loschmann, L.; Sunyer, J.; Plana, E.; Pearce, N.; Zock, J. P.; Jarvis, D.; Janson, C.; Anto, J. M. & Kogevinas, M. (2007). Socioeconomic status, asthma and chronic bronchitis in a large community-based study. *Eur Respir J* 29(5): 897-905.
- Erbas, B.; Kelly, A. M.; Physick, B.; Code, C. & Edwards, M. (2005). Air pollution and childhood asthma emergency hospital admissions: estimating intra-city regional variations. *Int J Environ Health Res* 15(1): 11-20.
- Fermanian, J. (1996). [Evaluating correctly the validity of a rating scale: the numerous pitfalls to avoid]. *Rev Epidemiol Sante Publique* 44(3): 278-86.
- Finkelstein, M. M.; Jerrett, M.; DeLuca, P.; Finkelstein, N.; Verma, D. K.; Chapman, K. & Sears, M. R. (2003). Relation between income, air pollution and mortality: a cohort study. *CMAJ*. 169(5): 397-402.
- Flahault, A.; Blanchon, T.; Dorleans, Y.; Toubiana, L.; Vibert, J. F. & Valleron, A. J. (2006). Virtual surveillance of communicable diseases: a 20-year experience in France. *Stat Methods Med Res* 15(5): 413-21.
- Folwell, K. (1995). Single measures of deprivation. *J Epidemiol Community Health* 49 Suppl 2: S51-6.
- Fukuda, Y.; Nakamura, K. & Takano, T. (2007). Higher mortality in areas of lower socioeconomic position measured by a single index of deprivation in Japan. *Public Health* 121(3): 163-73.
- Galan, I.; Tobias, A.; Banegas, J. R. & Aranguéz, E. (2003). Short-term effects of air pollution on daily asthma emergency room admissions. *Eur Respir J* 22(5): 802-8.
- Gilthorpe, M. & Wilson, R. (2003). Rural/urban differences in the association between deprivation and healthcare utilisation. *Soc Sci Med* 57(2055-63).
- Global Initiative for Asthma (2007). Global strategy for asthma management and prevention.
- Gold, D. R. & Wright, R. (2005). Population disparities in asthma. *Annu. Rev. Public Health* 26: 89-113.

- Gottlieb, D. J.; Beiser, A. S. & O'Connor, G. T. (1995). Poverty, race, and medication use are correlates of asthma hospitalization rates. A small area analysis in Boston. *Chest* 108(1): 28-35.
- Hajat, S.; Haines, A.; Goubet, S. A.; Atkinson, R. W. & Anderson, H. R. (1999). Association of air pollution with daily GP consultations for asthma and other lower respiratory conditions in London. *Thorax* 54(7): 597-605.
- Havard, S.; Deguen, S.; Bodin, J.; Laurent, O. & Bard, D. (2008). A small-area index of socioeconomic deprivation to capture health inequalities in France. *Soc Sci Med* 2008, 67-2007-16.
- Haynes, K.; Lall, S. & Trice, P. (2001). Spatial issues in environmental equity. *Int. J. Environ. Technol. Manag.* 1(1-2): 17 - 31.
- Jalaludin, B.; Khalaj, B.; Sheppard, V. & Morgan, G. (2008). Air pollution and ED visits for asthma in Australian children: a case-crossover analysis. *Int Arch Occup Environ Health* 81(8): 967-74.
- Janes, H.; Sheppard, L. & Lumley, T. (2005). Case-crossover analyses of air pollution exposure data: referent selection strategies and their implications for bias. *Epidemiology* 16(6): 717-26.
- Jarman, B. (1983). Identification of underprivileged areas. *Br Med J (Clin Res Ed)* 286(6379): 1705-9.
- Jerrett, M.; Arain, A.; Kanaroglou, P.; Beckerman, B.; Potoglou, D.; Sahuvaroglu, T.; Morrison, J. & Giovis, C. (2005a). A review and evaluation of intraurban air pollution exposure models. *J. Expo. Anal. Environ. Epidemiol.* 15(2): 185-204.
- Jerrett, M.; Burnett, R.; Kanaroglou, P.; Eyles, J.; Finkelstein, N.; Giovis, C. & Brook, J. (2001). A GIS- environmental justice analysis of particulate air pollution in Hamilton, Canada. *Environ. Planning A* 33 955-73.
- Jerrett, M.; Burnett, R. T.; Ma, R.; Pope, C. A., III; Krewski, D.; Newbold, K. B.; Thurston, G.; Shi, Y.; Finkelstein, N.; Calle, E. E. & Thun, M. J. (2005b). Spatial analysis of air pollution and mortality in Los Angeles. *Epidemiology* 16(6): 727-36.
- Jordan, H.; Roderick, P. & Martin, D. (2004). The Index of Multiple Deprivation 2000 and accessibility effects on health. *J Epidemiol Community Health* 58(3): 250-7.
- Kim, S. Y.; O'Neill, M. S.; Lee, J. T.; Cho, Y.; Kim, J. & Kim, H. (2007). Air pollution, socioeconomic position, and emergency hospital visits for asthma in Seoul, Korea. *Int Arch Occup Environ Health* 80(8): 701-10.
- Kitch, B. T.; Chew, G.; Burge, H. A.; Muilenberg, M. L.; Weiss, S. T.; Platts-Mills, T. A.; O'Connor, G. & Gold, D. R. (2000). Socioeconomic predictors of high allergen levels in homes in the greater Boston area. *Environ Health Perspect* 108(4): 301-7.
- Krieger, N.; Williams, D. R. & Moss, N. E. (1997). Measuring social class in US public health research: concepts, methodologies, and guidelines. *Annu. Rev. Public Health* 18: 341-78.
- Kunst, A. E.; Groenhouf, F.; Mackenbach, J. P. & Health, E. W. (1998). Occupational class and cause specific mortality in middle aged men in 11 European countries: comparison of population based studies. EU Working Group on Socioeconomic Inequalities in Health. *BMJ* 316(7145): 1636-42.

- Kunzli, N.; Kaiser, R.; Medina, S.; Studnicka, M.; Chanel, O.; Filliger, P.; Herry, M.; Horak, F., Jr.; Puybonnieux-Textier, V.; Quenel, P.; Schneider, J.; Seethaler, R.; Vergnaud, J. C. & Sommer, H. (2000). Public-health impact of outdoor and traffic-related air pollution: a European assessment. *Lancet* 356(9232): 795-801.
- Laurent, O.; Bard, D.; Filleul, L. & Segala, C. (2007). Effect of Socioeconomic Status on the Relation between Atmospheric Pollution and Mortality: A Review. *J Epidemiol Community Health*.
- Laurent, O.; Pedrono, G.; Segala, C.; Filleul, L.; Havard, S.; Deguen, S.; Schillinger, C.; Riviere, E. & Bard, D. (2008). Air pollution, asthma attacks, and socioeconomic deprivation: a small-area case-crossover study. *Am J Epidemiol* 168(1): 58-65.
- Lee, J. T.; Son, J. Y.; Kim, H. & Kim, S. Y. (2006). Effect of air pollution on asthma-related hospital admissions for children by socioeconomic status associated with area of residence. *Arch Environ Occup Health* 61(3): 123-30.
- Lin, M.; Chen, Y.; Villeneuve, P. J.; Burnett, R. T.; Lemyre, L.; Hertzman, C.; McGrail, K. M. & Krewski, D. (2004). Gaseous air pollutants and asthma hospitalization of children with low household income in Vancouver, British Columbia, Canada. *Am. J. Epidemiol.* 159(3): 294-303.
- Lorant, V. (2000). [Mortality socio-economic inequalities for small-areas in Belgium: assessing concentration]. *Rev Epidemiol Sante Publique* 48(3): 239-47.
- Marshall, R. J. (1991). Mapping disease and mortality rates using empirical Bayes estimators. *J R Stat Soc Ser C Appl Stat* 40(2): 283-94.
- Maynard, R.; Krewski, D.; Burnett, R. T.; Samet, J.; Brook, J. R.; Granville, G. & Craig, L. (2003). Health and air quality: directions for policy-relevant research. *J Toxicol Environ Health A* 66(16-19): 1891-904.
- McHugh, C.; Carruthers, D. & Edmunds, H. (1997). ADMS-Urban: an air quality management system for traffic, domestic and industrial pollution. *Int. J. Environ Pollution* 8: 437-40.
- Mclure, M. & Mittelman, M. (1991). Should we use a case-crossover design? *Ann Rev Public Health* 21: 193-221.
- Medina, S.; Le Tertre, A.; Quenel, P.; Le Moullec, Y.; Lameloise, P.; Guzzo, J. C.; Festy, B.; Ferry, R. & Dab, W. (1997). Air pollution and doctors' house calls: results from the ERPURS system for monitoring the effects of air pollution on public health in Greater Paris, France, 1991-1995. Evaluation des Risques de la Pollution Urbaine pour la Sante. *Environ Res* 75(1): 73-84.
- Messer, L. C.; Laraia, B. A.; Kaufman, J. S.; Eyster, J.; Holzman, C.; Culhane, J.; Elo, I.; Burke, J. G. & O'Campo, P. (2006). The development of a standardized neighborhood deprivation index. *J Urban Health* 83(6): 1041-62.
- Mielck, A.; Reitmeir, P. & Wjst, M. (1996). Severity of childhood asthma by socioeconomic status. *Int. J. Epidemiol.* 25(2): 388-93.
- Morris, R. & Carstairs, V. (1991). Which deprivation? A comparison of selected deprivation indexes. *J Public Health Med* 13(4): 318-26.
- Nauenberg, E. & Basu, K. (1999). Effect of insurance coverage on the relationship between asthma hospitalizations and exposure to air pollution. *Public Health Rep* 114(2): 135-48.
- Naureckas, E. T.; Dukic, V.; Bao, X. & Rathouz, P. (2005). Short-acting beta-agonist prescription fills as a marker for asthma morbidity. *Chest* 128(2): 602-8.

- Neidell, M. J. (2004). Air pollution, health, and socio-economic status: the effect of outdoor air quality on childhood asthma. *J. Health Econ.* 23(6): 1209-36.
- Niggebrugge, A.; Haynes, R.; Jones, A.; Lovett, A. & Harvey, I. (2005). The index of multiple deprivation 2000 access domain: a useful indicator for public health? *Soc Sci Med* 60(12): 2743-53.
- Norris, G.; YoungPong, S. N.; Koenig, J. Q.; Larson, T. V.; Sheppard, L. & Stout, J. W. (1999). An association between fine particles and asthma emergency department visits for children in Seattle. *Environ. Health Perspect.* 107(6): 489-93.
- O'Neill, M. S.; Jerrett, M.; Kawachi, I.; Levy, J. I.; Cohen, A. J.; Gouveia, N.; Wilkinson, P.; Fletcher, T.; Cifuentes, L. & Schwartz, J. (2003). Health, wealth, and air pollution: advancing the theory and methods. *Environ. Health Perspect.* 111(16): 1861-70.
- Pampalon, R. & Raymond, G. (2000). A deprivation index for health and welfare planning in Quebec. *Chronic Dis Can* 21(3): 104-13.
- Pitard, A.; Zeghnoun, A.; Courseaux, A.; Lamberty, J.; Delmas, V.; Fossard, J. L. & Villet, H. (2004). Short-term associations between air pollution and respiratory drug sales. *Environ Res* 95(1): 43-52.
- Prescott, E.; Godtfredsen, N.; Vestbo, J. & Osler, M. (2003). Social position and mortality from respiratory diseases in males and females. *Eur Respir J* 21(5): 821-6.
- Rabinovitch, N.; Strand, M. & Gelfand, E. W. (2006). Particulate levels are associated with early asthma worsening in children with persistent disease. *Am J Respir Crit Care Med* 173(10): 1098-105.
- Romeo, E.; De Sario, M.; Forastiere, F.; Compagnucci, P.; Stafoggia, M.; Bergamaschi, A. & Perucci, C. A. (2006). [PM 10 exposure and asthma exacerbations in pediatric age: a meta-analysis of panel and time-series studies]. *Epidemiol Prev* 30(4-5): 245-54.
- Salmond, C.; Crampton, P. & Sutton, F. (1998). NZDep91: A New Zealand index of deprivation. *Aust N Z J Public Health* 22(7): 835-7.
- Samet, J. & Krewski, D. (2007). Health effects associated with exposure to ambient air pollution. *J Toxicol Environ Health A* 70(3-4): 227-42.
- Schildcrout, J. S.; Sheppard, L.; Lumley, T.; Slaughter, J. C.; Koenig, J. Q. & Shapiro, G. G. (2006). Ambient air pollution and asthma exacerbations in children: an eight-city analysis. *Am J Epidemiol* 164(6): 505-17.
- Singh, G. K. (2003). Area deprivation and widening inequalities in US mortality, 1969-1998. *Am J Public Health* 93(7): 1137-43.
- Son, J. Y.; Kim, H.; Lee, J. T. & Kim, S. Y. (2006). [Relationship between the exposure to ozone in Seoul and the childhood asthma-related hospital admissions according to the socioeconomic status]. *J. Prev. Med. Pub. Health* 39(1): 81-6.
- Sunyer, J.; Spix, C.; Quenel, P.; Ponce-de-Leon, A.; Ponka, A.; Barumandzadeh, T.; Touloumi, G.; Bacharova, L.; Wojtyniak, B.; Vonk, J.; Bisanti, L.; Schwartz, J. & Katsouyanni, K. (1997). Urban air pollution and emergency admissions for asthma in four European cities: the APHEA Project. *Thorax* 52(9): 760-5.
- Tello, J. E.; Jones, J.; Bonizzato, P.; Mazzi, M.; Amaddeo, F. & Tansella, M. (2005). A census-based socio-economic status (SES) index as a tool to examine the relationship between mental health services use and deprivation. *Soc Sci Med* 61(10): 2096-105.
- Thibaudon, M. (2004). [Report of the activity of RNSA (National Aero-biological Surveillance Network), 2003]. *Eur Ann Allergy Clin Immunol* 36(7): 252-5.

- Tolbert, P. E.; Mulholland, J. A.; MacIntosh, D. L.; Xu, F.; Daniels, D.; Devine, O. J.; Carlin, B. P.; Klein, M.; Dorley, J.; Butler, A. J.; Nordenberg, D. F.; Frumkin, H.; Ryan, P. B. & White, M. C. (2000). Air quality and pediatric emergency room visits for asthma in Atlanta, Georgia, USA. *Am J Epidemiol* 151(8): 798-810.
- Tollier, C.; Fusier, I. & Husson, M. C. (2005). [ATC and EphMRA classifications: evolution from 1996 to 2003 and comparative analysis]. *Therapie* 60(1): 47-56.
- Townsend, P. (1987). Deprivation. *J Soc Pol* 16: 125-46.
- Townsend, P.; Phillimore, P. & Beattie, A. (1988). *Health and Deprivation: Inequality and the North*. London, Croom Helm.
- Urbano, F. L. & Pascual, R. M. (2005). Contemporary issues in the care of patients with chronic obstructive pulmonary disease. *J Manag Care Pharm* 11(5 Suppl A): S2-13; quiz S4-6.
- Viegi, G.; Pistelli, F.; Sherrill, D. L.; Maio, S.; Baldacci, S. & Carrozzi, L. (2007). Definition, epidemiology and natural history of COPD. *Eur Respir J* 30(5): 993-1013.
- von Klot, S.; Wolke, G.; Tuch, T.; Heinrich, J.; Dockery, D. W.; Schwartz, J.; Kreyling, W. G.; Wichmann, H. E. & Peters, A. (2002). Increased asthma medication use in association with ambient fine and ultrafine particles. *Eur Respir J* 20(3): 691-702.
- Ward, D. J. & Ayres, J. G. (2004). Particulate air pollution and panel studies in children: a systematic review. *Occup Environ Med* 61(4): e13.
- Weinmayr, G.; Romeo, E.; De Sario, M.; Weiland, S. K. & Forastiere, F. Short-term effects of PM10 and NO2 on respiratory health among children with asthma or asthma-like symptoms: a systematic review and meta-analysis. *Environ Health Perspect* 118(4): 449-57.
- Wright, R. J. & Subramanian, S. V. (2007). Advancing a multilevel framework for epidemiologic research on asthma disparities. *Chest* 132(5 Suppl): 757S-69S.
- Zeghnoun, A.; Beaudou, P.; Carrat, F.; Delmas, V.; Boudhabhay, O.; Gayon, F.; Guincetre, D. & Czernichow, P. (1999). Air pollution and respiratory drug sales in the City of Le Havre, France, 1993-1996. *Environ Res* 81(3): 224-30.

# A new method for estimation of automobile fuel adulteration

Anil Kumar Gupta and R.K. Sharma

*Department of Electronics and Communication Engineering  
National Institute of Technology Kurukshetra-136 119  
India*

## 1. Introduction

Since the beginning of the industrial revolution, the air pollution has been on the rise due to fast increasing use of fossil fuels. In particular, the automobile sector has emerged as a major consumer of fuel oil and a major contributor to air pollution. In developing countries like India, China, Brazil the automobile industry is expected to grow at a faster rate in coming years (Veloso, Kumar 2002) accompanied by proportional increase in the air pollution. The problem is essentially global in nature as the tail pipe emissions of automobiles result in an increase in the greenhouse gases in the atmosphere leading to global warming.

Adulteration of automobile fuels i.e. gasoline and diesel, leads to increased tailpipe emission and the consequent ill effects on public health. The primary cause of adulteration is the greed fueled by differential tax system (World Bank reports July 2002, September 2001, December 2001, CSE India report March 2002). For example, in south Asia, gasoline is taxed most heavily, followed by diesel, kerosene, industrial solvents and recycled lubricants, in that order. The fact that adulteration of gasoline by diesel and that of diesel by kerosene, is difficult to detect, combined with the differential tax structure makes such adulteration financially alluring, even though it is illegal. Mixing kerosene with diesel does not lead to an increase in tailpipe emission, but contributes to air pollution indirectly in South Asia. The diversion of kerosene for adulteration drastically brings down its availability, to the poor households, who turn to bio-mass for the purpose of cooking. This leads to an increase in the indoor air pollution and consequent ill effects on health. For the prevention of adulteration, monitoring of fuel quality at the distribution point, therefore, is highly essential.

In the Indian context, the gasoline is adulterated by mixing diesel and diesel is adulterated by mixing kerosene. This is because these types of adulterations when limited to small volume percent are difficult to detect by the automobile user. The expected adulteration percentage is 10 % to 30 % by volume in both the cases. Less than (10%) adulteration is financially unattractive, while more than 30% adulteration is likely to be easily detected by the user from the degradation of the engine performance caused by the adulterated fuel.

To check the adulteration effectively, it is necessary to monitor the fuel quality at the distribution point itself. The equipment for this purpose should be portable and the measurement method should be quick, capable of providing test result within a very short

time. The measuring equipment should also be preferably inexpensive (as a large number of such units would need be simultaneously deployed) and easy to use.

## 2. Methods for estimation of Fuel Adulteration

The American Society for Testing and Materials International (ASTM International) has developed and documented the test methods for most of the widely used materials including petroleum products. Many ASTM tests for the gasoline and diesel have been standardized and documented. Some of these tests involve determination of physical and chemical properties while others provide a measure of suitability of the fuel for use in automobiles from the point of engine performance / air pollution generated. Though no test is specifically designed to measure the adulteration of petrol by mixing diesel or diesel by mixing kerosene, some tests namely Density test, Evaporation test, Distillation test, Chemical Marker test, Gas Chromatography may be used to determine the adulteration of fuel also. However, none of these methods are suitable for adulteration test in the context mentioned in section-1, as pointed out below.

Density Test (ASTM D4052):

Hydrometers and digital densitometers are used to measure the density of the fuel sample. The reported densities of gasoline, diesel and kerosene at 15°C are in the ranges 0.74-0.75 Kg./L, 0.835-0.855 Kg./L and 0.79-0.80Kg./L respectively. The adulteration causes a change in the density which can be correlated with the adulteration. The method has the advantage that densitometer provides very good accuracy but suffers from the disadvantages that (i) densitometers are expensive and need a controlled environment (for correct operation) which is unlikely to be available in the field at the distribution point and (ii) the change in density is very small even for high level of adulteration as reported in the literature and reproduced below.

| No. | Diesel and Kerosene Proportions (v/v) | Density at 15°C (g/ml) | Kinematic Viscosity at 40°C (Cst) |
|-----|---------------------------------------|------------------------|-----------------------------------|
| 1   | Pure Diesel                           | 0.8456                 | 2.63                              |
| 2   | Prescribed Level                      | 0.82-0.86              | 2 to 3                            |
| 3   | 85:15                                 | 0.8400                 | 2.33                              |
| 4   | 75:25                                 | 0.8390                 | 2.16                              |
| 5   | 65:35                                 | 0.8321                 | 1.89                              |
| 6   | 50:50                                 | 0.8304                 | 1.83                              |
| 7   | 25:75                                 | 0.8234                 | 1.5                               |

Table 1. Density and kinematic viscosity of diesel fuel and adulterant kerosene at different proportions (reprinted from Sh. R. Yadav, et.al, 2005).

Similar results for density variation in gasoline and diesel as a function of % adulteration by diesel and kerosene respectively has also been reported by Sharma and Gupta-2007. Therefore the overall sensitivity of this method is rather poor if the change in density is used

as an indicator of extent of adulteration. However as evident from Table 1, the viscosity of the fuel shows a considerably stronger dependence on the % adulteration and therefore should be a preferred parameter to be calibrated against % adulteration.

#### **Evaporation Test (ASTM D3810):**

The evaporation techniques are capable of detecting very low concentrations (1-2%) of diesel in gasoline and fairly low concentrations (5%) of kerosene in gasoline. However this is basically a laboratory technique and is not suitable for field use.

#### **Distillation Test (ASTM D86):**

This technique exploits the difference in the boiling points of different liquids comprising the fuel sample. Accurate distillation data for uncontaminated fuel is essential for comparison and precise results. The technique, however, is not suitable for field use as the measurement set up is generally bulky and measurement process is time consuming.

#### **Gas Chromatography (GC):**

GC is powerful laboratory tool which can be used to detect hydrocarbon based adulterants. However it requires an experienced technician to operate the equipment and interpret the results. It is an effective method for detection of adulterants in gasoline and diesel but would require easily portable, robust and user friendly equipment which may be operated by an inexperienced operator also.

#### **Adulteration Estimation/Detection using Optical Fiber Sensor:**

A technique for detection/estimation of adulteration of petrol/ diesel by kerosene using optical fiber sensor has been reported by Roy S. (1999). The technique exploits the change in refractive index and therefore the evanescent absorption of monochromatic light in petrol/ diesel when the same is adulterated by mixing kerosene.

Optical fiber acts as a wave guide for light if the cladding has a lower refractive index than that of fiber material. When the light is reflected from the interface of the fiber and the cladding (or any other material surrounding the fiber), the field associated with the light wave extends beyond the interface into the surrounding medium. The amplitude of this field decreases exponentially with distance from the interface. If the surrounding material absorbs some part of the light propagating through the fiber, the power received at the other end of the fiber would be less by the amount absorbed by the surrounding medium. This idea has been implemented in the experimental set up shown below (Roy S. 1999).

The light source in fig. 1 is a He-Ne laser which is coupled with the optical fiber through a lens. The length of the fiber within the vessel containing the fuel under test is unclad so that the fiber is directly in contact with the absorbing medium that is, the fuel under test. The received power is measured by the power meter.

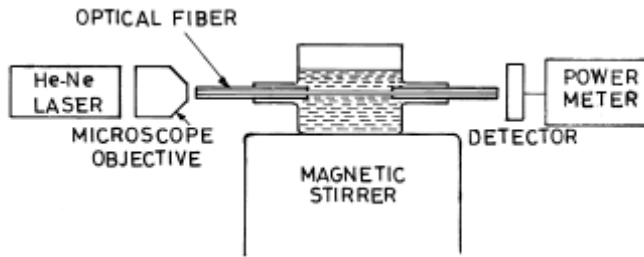


Fig. 1. Optical Fiber Sensor and associated experimental Set up (Reprinted from Roy S., 1999).

The power received by the power meter is reduced by the amount that is absorbed by the fuel through evanescent absorption. The received power at the detector is given by the expression,

$$P(L) = P_0 \cdot \exp(-\alpha \cdot L) \quad (1)$$

where 'L' is length of the unclad optical fiber and 'P<sub>0</sub>' is the power transmitted from the laser source end. The parameter 'α' is evanescent absorption coefficient of the fuel and the factor 'exp(-α.L)' accounts for the power absorbed by the fuel through evanescent absorption. The power P(L) is a sensitive function of 'α' which itself depends upon the refractive index of the fuel.

The dependence of P(L) and 'α' (also refractive index of the fuel) have been experimentally investigated by Roy S. (1999) for petrol and diesel adulterated with kerosene. The method is particularly suitable for adulteration detection in petrol as its refractive index (< 1.42) remains lower than that of core of the optical fiber i.e. silica (refractive index =1.457) even after mixing with 50% kerosene which results in smooth ( and almost linear) variation of received power with % adulteration. The received power normalized with respect to 'P<sub>0</sub>', as observed for petrol adulterated with kerosene are shown in Fig.2. The similar experimental results for diesel adulterated with kerosene are not consistent with the theory and so are not reproduced here.

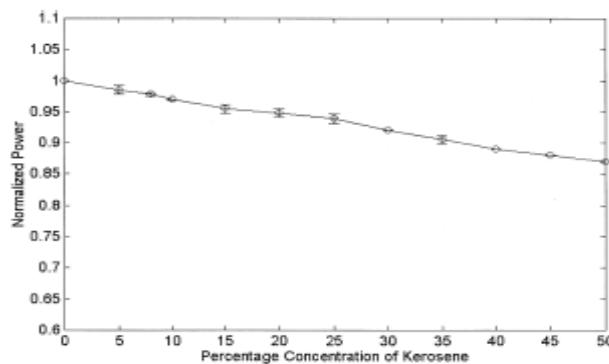


Fig. 2. Normalized power as a function of volume% concentration of kerosene in petrol (Reprinted from Roy S., 1999).

The note worthy feature of this method is that the sensitivity of the sensor can be effectively varied by changing the 'L', the length of unclad fiber because the received power P (L) varies exponentially with 'L'.

### 3. Adulteration Detection using Sound/Ultrasound-A New Method

As mentioned in the previous section, the adulteration leads to the change in density as well as viscosity of the fuel. Since both these parameters influence the speed of sound in a fluid, it is expected that the speed of sound in the adulterated fuel would be different from that in un-adulterated fuel (Thomas K V et.al. 2004). The effect of adulteration of petrol by diesel and diesel by kerosene on the speed of sound in the fuel sample has been investigated by the authors. The experimental method followed is described in following sub-sections.

#### Working Principle:

For determination of speed of sound, the time taken by the sound to travel a known distance (commonly termed as Time of Flight or TOF) is to be determined. There are two basic methods for determination of TOF.

#### (A) Pulse-Echo (PE) Method:

The schematic of the basic experimental set up for this method is shown in Fig. 3. The transmitter TX, excited by an electrical signal of sonic/ultrasonic frequency, emits a pulse of acoustic energy of a short duration.

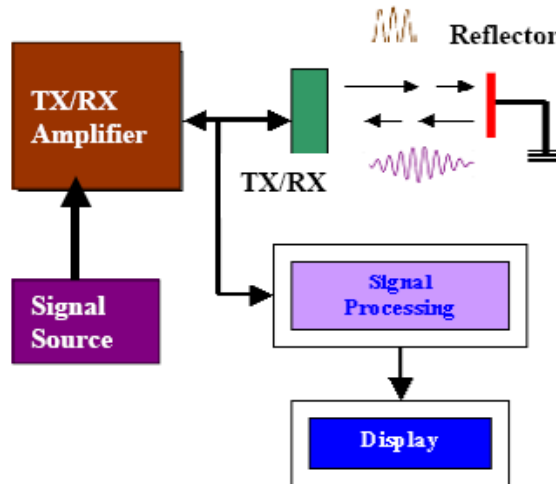


Fig. 3. Basic experimental setup for Pulse-echo method

In general, the transmitting transducer TX also serves as receiving transducer RX (converting received acoustic pulse into electrical signal). The time delay  $T_D$  between the transmitted and the received pulse (after reflection from a target) is measured. The value of  $T_D$  is related with the speed of sound by the equation,

$$\text{Speed of sound, } V_s = 2d / T_D \quad (2)$$

where 'd' is the distance between the TX/TR and the reflector.

This simple principle of measurement gets considerably complicated due to the following:

- The transducer TX / RX (generally ultrasonic piezoelectric crystals) has narrow bandwidth, which causes the long ringing tails in the emitted pulse. So there is no sharply defined start and end point of the pulse emitted.
- The emitted acoustic pulse gets attenuated in the medium. The attenuation is proportional to the square of the frequency. Therefore, the higher frequency components of the pulse get more attenuated than its lower frequency components. As a result, the received pulse is broadened more as compared to the transmitted one.
- Noise also corrupts the received pulse.
- Echoes from other objects make it difficult to identify the echo from the object under study.
- The resolution (for distance measurement) is limited by the width of the acoustic pulse.

Simple threshold technique, for measurement of  $T_D$ , leads to low accuracy in the measurements. Digital Signal Processing (DSP) techniques have been developed to measure  $T_D$  more accurately (Parrilla et.al. 1991). In these techniques, the envelopes of the echoes from a reference object and other echo signals, are extracted and a value of  $T_D$ , for which there is maximum similarity between the reference and echo signals, is determined, using DSP algorithms. The algorithms used for the purpose are norms L1, L2 and correlation. The procedure is computation intensive and requires considerable dedicated hardware. However, the development of FPGAs has made it easy and cost effective to design correlation detector required for the purpose (Urena J et.al 1999). Cross correlation between the transmitted and the received signals has also been used to determine  $T_D$ . More recently the use of wavelet networks, for more accurate measurement of  $T_D$  has been reported (Grimaldi D 2006). An interesting method using self-interference of transmitted pulses has been proposed for accurate measurement of Time of Flight (Cai C et.al. 1993). In this method, transmitter emits two pulse trains which interfere with each other in such a way that the wave envelope becomes zero at certain time instant. The time interval between the two pulse trains is so chosen that the envelope zero is halfway between the two waves. The time instants of zero envelope amplitudes are detected and used for determination of TOF. Analysis of sonar pulses emitted by bats has shown that emissions from each bat are uniquely frequency modulated which enables the bat in distinguishing its own emissions from those of other bats. This principle has been implemented in digital polarity correlation detection method. The cross correlation function for clipped transmitted and received signals has been used for measurement of TOF in digital polarity correlation detection method (Nakahira K et.al 2001). A variation of conventional pulse echo method uses Binary-Frequency- Shift- Keyed (BFSK) signal. The time instant where the transition between each frequency occurs is detected and used for determination of TOF (Webster D 1994). This method offers significant improvement in respect of reduction of measurement errors as compared to correlation-based methods.

## (B) Continuous Wave (CW) Method:

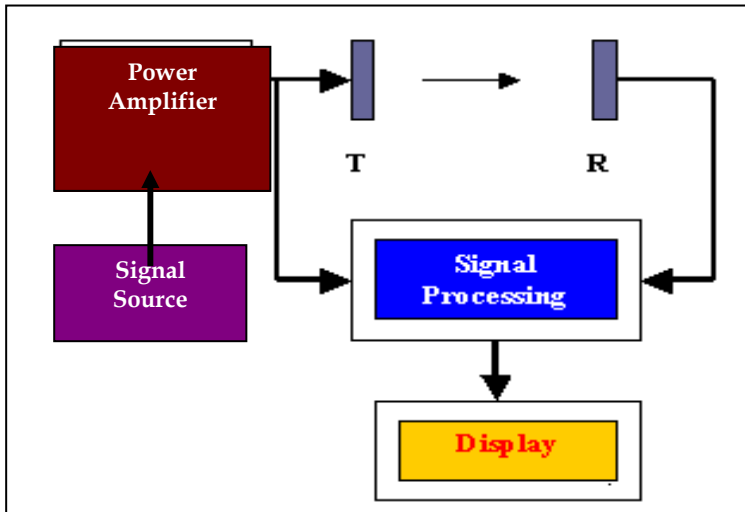


Fig. 4a. Basic Experimental Setup (Continuous Wave Method)

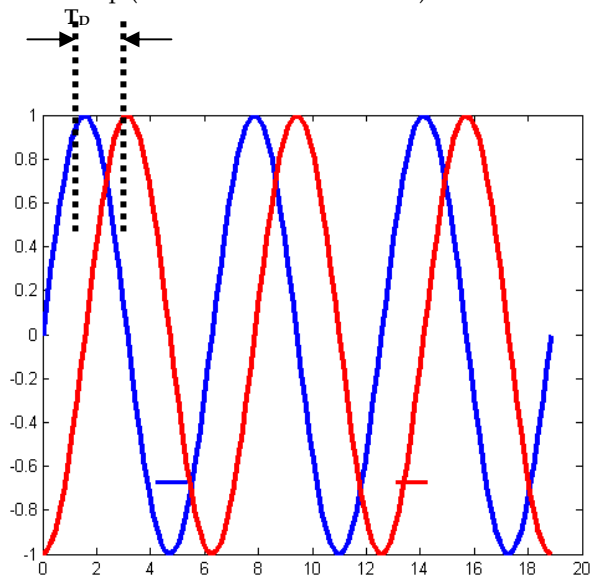


Fig. 4b. Transmitted ( ) and Received ( ) Signals

The typical setup is shown in Fig.4a. The acoustic vibrations of the signal frequency are excited in the medium. The received signal is processed to recover the time-delayed replica of the transmitted signal. The time delay  $T_D$  in Fig.4b is the sum of the transit time of the sound (or TOF) of acoustic radiations and the delay caused by the electronic circuits (including transducers).

The measurement of phase difference between the transmitted and received signal gives transit time (i.e. TOF), if the delay due to electronic circuits is negligible or the necessary correction in the measurement of  $T_D$  has been made. The CW method has found application in fluid flow velocity measurements. This method however does not seem to have attracted much effort possibly because the measurements are more sensitive to external noise, even though it has potential to lead to more accurate measurements.

Experimental Setup for Estimation of Adulteration using Sound Waves:

The authors have studied the effect of adulteration on speed of sound in petrol/diesel, using Continuous Wave (CW) method, with an objective to explore the feasibility of detection/estimation of adulteration of petrol and diesel. The experimental setup (including the electronics part used) is shown in Fig.5. It consists of a 30 cm long metallic cylinder, with inner diameter of 7.62 cm and a base of thin copper foil. The cylinder has a valve-controlled nozzle near its base for controlled removal of fuel contained in the cylinder. The cylinder is placed and locked on a wooden platform which has a circular hole of 3 inch diameter, covered by a speaker (the transmitter- TX) which is fixed on the wooden platform. This ensures that the vibrations of the frame of the speaker do not excite sound waves in the liquid. The pressure waves in the liquid column are excited only by the sound emitted by the speaker, through the copper foil at the base. A glass tube containing the microphone (the receiver- RX) is held vertically inside the cylinder along its axis. The liquid / fuel sample to be tested is contained in the cylinder.

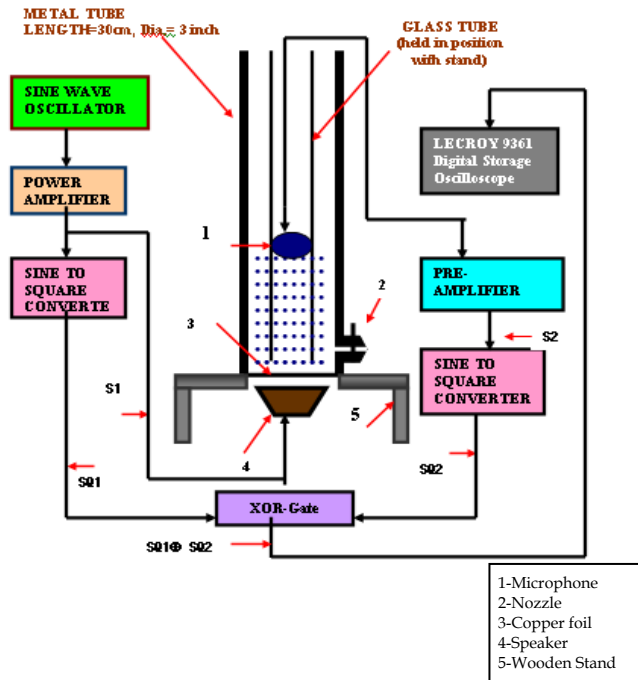


Fig. 5. Experimental setup for measurement of speed of sound in a medium using CW method

Note: The waveforms of the signals S1, S2, SQ1, and SQ2 in Fig. 5 are shown in Fig. 6.

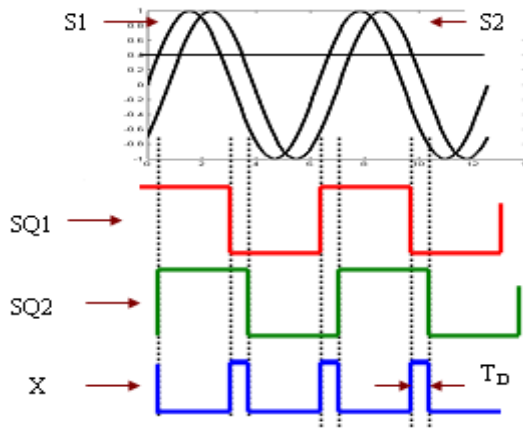


Fig. 6. Signal waveforms

The signal X is Exclusive-OR of signals SQ1 and SQ2 ( $SQ1 \oplus SQ2$ ). The pulse width of 'X',  $T_D$ , is the time delay of the received signal and it is equal to the sum of time taken by the sound to travel through the liquid column of known height plus the delay caused by the circuit.

$$T_D = T_d(\text{circuit}) + \text{TOF} \tag{3}$$

If  $T_{D1}$  and  $T_{D2}$  are measured for path lengths  $h_1$  and  $h_2$  in the medium, then

$$T_{D1} = T_d(\text{circuit}) + \text{TOF}_{h1} \tag{4}$$

$$T_{D2} = T_d(\text{circuit}) + \text{TOF}_{h2} \tag{5}$$

Because the  $T_d(\text{circuit})$  is independent of path length  $h_1$  and  $h_2$  in the medium, therefore

$$\begin{aligned} T_{D1} - T_{D2} &= \text{TOF}_{h1} - \text{TOF}_{h2} \\ &= \text{TOF of sound for path length } h_1 - h_2 \\ &= (h_1 - h_2)/V_s \end{aligned} \tag{6}$$

Or

$$V_s = (h_1 - h_2) / (T_{D1} - T_{D2})$$

Thus, the speed of sound can be determined by measuring the ON- time of signal X (see Fig. 6) for two path lengths  $h_1$  and  $h_2$  in the medium.

In the above experiment, the correct measurement of TOF requires that the received signal S2 is exact replica of transmitted signal S1 because any phase distortion in received signal will lead to shifting of zero crossing point and consequent change in measured value of  $T_D$ .

It was determined experimentally that the preamplifier output remains sinusoidal only in the frequency range 80 Hz to 390 Hz. This was possibly due to the mismatch of acoustic impedance at the speaker output since the speaker output is coupled to the metal diaphragm through air, which provides for rather poor coupling. To ensure accurate measurement of  $T_D$ , all the measurements were taken at 90 Hz. The measurement of time delay  $T_D$  (i.e. ON- time of signal X pulses) was done using digital storage oscilloscope LeCroy 9361A. An average width of signal X in ten successive measurements for the same sample was determined using the built in provision for the same in the oscilloscope.

To test the accuracy of the measurement system described above, the speed of sound in air and water was determined. The average value of speed of sound in air,  $V_s(\text{air})$ , determined using equation (6) is 344.03 m/sec at 23°C which is in very close agreement to the expected value of 344.824 m/sec on the basis of the values of  $V_s(\text{air})$  reported in literature (William M. H 1998). The speed of sound in water at 22°C was determined to be 1486.76 m/sec. The reported value of speed of sound in distilled water is 1482 m/s at 20°C (Benedetto G et.al. 2003). The temperature co-efficient in water being 2.87 m/s/°C, the expected speed of sound in water at 22°C, therefore, is 1488m/s. The value for speed of sound in water determined in our experiment, therefore, is in close agreement with the corresponding reported value (within 1.3 m/sec.).

#### 4. Experimental Results

##### Speed Of Sound In Gasoline And Diesel

The samples of gasoline and diesel used in the experiments (along with the respective test reports) were collected from the local depot of Indian Oil Corporation Limited. The kerosene was obtained from a retail outlet of the public distribution system regulated by Government of India.

The values of  $T_{D1}$  and  $T_{D2}$  in unadulterated gasoline and intentionally adulterated (with diesel) gasoline samples were measured using the experimental setup of Fig. 5 for two different volumes  $V_1$  (= 500ml) and  $V_2$  (= 400ml) contained in the metal cylinder. The corresponding column heights (path lengths)  $h_1$  and  $h_2$  were computed using the equation,

$$h = (\text{Net volume of fuel}) / (\text{Area of cross section}) . \quad (7)$$

The speed of sound was computed using equation (6). The volume percent of diesel in gasoline (i.e. % adulteration) has been plotted against measured speed of sound (in gasoline) in Fig. 7 (labeled as CW).

The experiments, as performed with gasoline, were also carried out with unadulterated diesel and intentionally adulterated (with kerosene) diesel for  $V_1$  (= 500ml) and  $V_2$  (= 300ml). The volume percent of Kerosene in diesel (i.e. % adulteration) has been plotted against measured speed of sound (in diesel) in Fig. 8. (Labeled as CW).

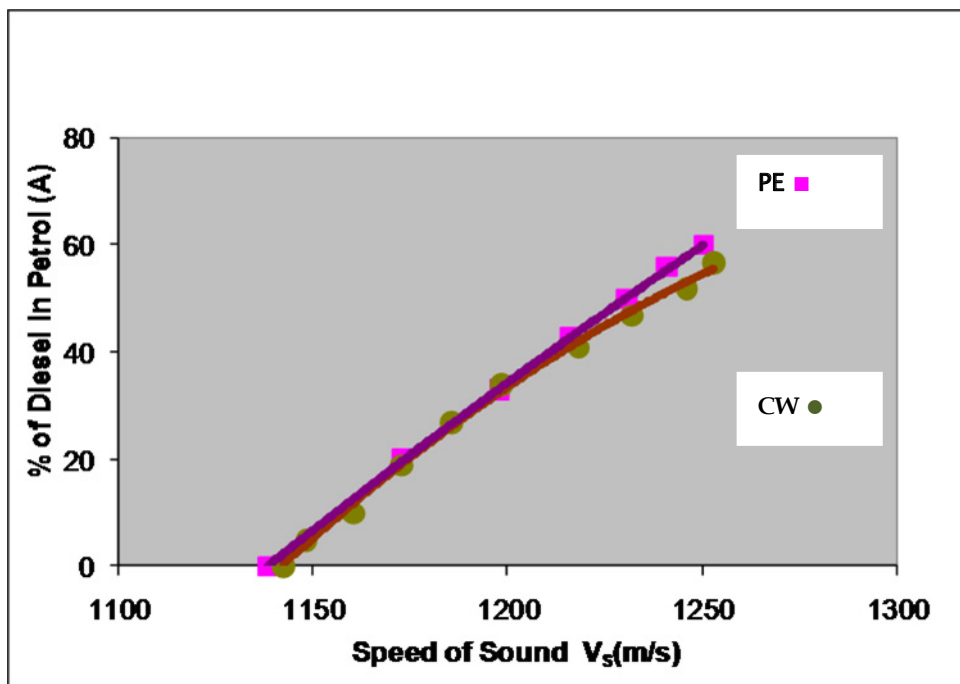


Fig. 7. Speed of Sound in Gasoline Mixed with Diesel

#### Verification of Experimental Results

An extensive search in literature for the speed of sound in gasoline and diesel yielded no result. Therefore to verify the results shown in Figs.7 and 8 (labeled as CW), the speed of sound in gasoline and diesel samples was also determined using equipment, namely NUSONIC model 6080 Concentration Analyzer (manufactured by MAPCO INC. ITALY). The equipment measures the speed of ultrasound (of frequency 4 MHz) in liquids and is based on pulse echo method. The % adulterations vs. speed of sound as measured using this equipment are plotted in Figs. 7 and 8 (labeled as PE). As can be seen, the measured speed of sound by the two methods is in good agreement. In case of gasoline samples the maximum difference between the speeds of sound measured using the two methods is 7.14 m/sec while the same for diesel samples, it is 5.9 m/sec.

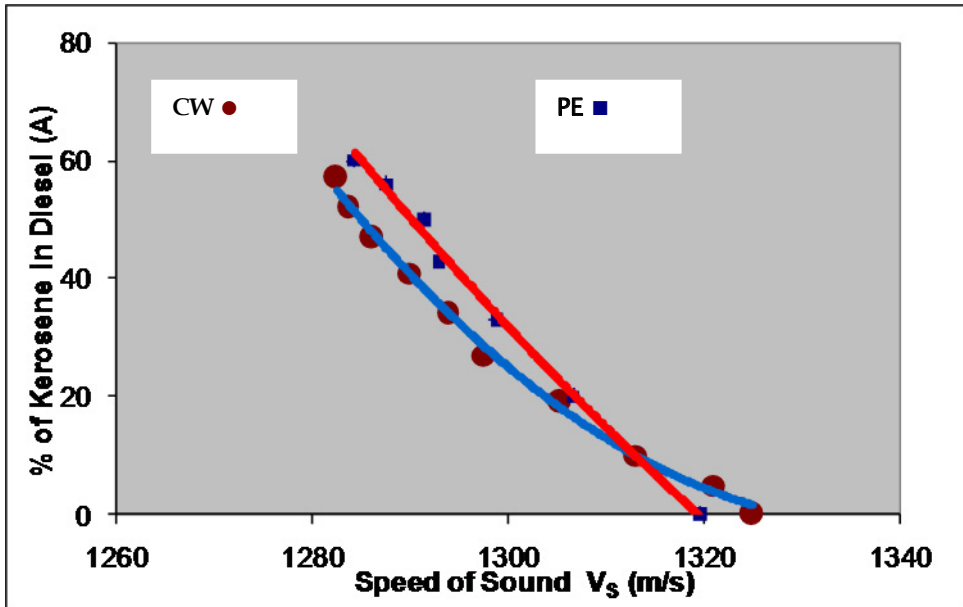


Fig. 8. Speed of Sound in Diesel Mixed with Kerosene

A significant and measurable change in speed of sound in gasoline/diesel samples with change in level of adulteration is seen in Figs. 7 and Fig. 8. This indicates towards the feasibility of calibrating the speed of sound in gasoline/diesel samples in terms of percent adulteration. From the plots of Figs. 7 and 8, the equations of the curves that are the least square fit to the experimental data, have been determined to be:

$$A = -0.0004 * V_s^2 + 1.5014 * V_s - 1184.8 \quad (8)$$

(for gasoline samples using Pulse-echo method)

$$A = -0.001 * V_s^2 + 3.9493 * V_s - 2631.4 \quad (9)$$

(for gasoline samples using CW method)

$$A = 0.0072 * V_s^2 - 20.397 * V_s + 14441 \quad (10)$$

(for diesel samples using Pulse-echo method)

$$A = 0.0184 * V_s^2 - 49.306 * V_s + 32984 \quad (11)$$

(for diesel samples using CW method)

where

$V_s$  = Speed of sound ( m/sec) in fuel under test, and

A = Percent adulteration (by Volume) in the fuel under test.

The equations (8) to (11) can be used for computing percent adulteration when speed of sound in the sample under test is known. Such computations can be easily performed by a micro controller based system with coefficients of the equations stored in its memory. Since the composition and, therefore, the physical properties such as density, viscosity of the gasoline, diesel, and kerosene are not constant and may vary significantly, depending upon the supplier company; the above equations would need to be updated as required. Alternatively, a look-up table of measured speed of sound vs. percent adulteration data for known samples can be used to estimate percent adulteration in the samples under test, by interpolation. However, no attempt has been made to design such a micro controller based system because the commercial equipments (based on Pulse Echo principle) for the purpose are already available for measurement of speed of sound in liquids and these equipments can easily be programmed for detection / estimation of adulteration in gasoline/ diesel using the experimental results obtained in this work.

## 5. Conclusion

The problem of increasing urban air pollution due to fast increasing number of auto mobiles and adulteration of automobile fuel has been pointed out in the context of developing countries. For prevention of the adulteration, the monitoring of fuel quality at the distribution point is essential. For the detection/estimation of the commonly used adulterants (i.e. diesel in petrol and kerosene in diesel), a number of possible methods have been reviewed.

As such there is no standard method/equipment for detection of adulterants. The authors have explored the feasibility of using the speed of sound in the fuel under test to detect/estimate the volume percentage of commonly used adulterants in automobile fuel and have concluded that it is feasible to develop a cheap and easy to operate equipment which measures and uses the measured speed of sound to estimate the adulterants in fuel. A NUSONIC model 6080 Concentration Analyzer (manufactured by MAPCO INC. ITALY), commercially available equipment namely NUSONIC model 6080 Concentration Analyzer (manufactured by MAPCO INC. ITALY) may be used for the purpose with a small modification.

Besides the sound/ultrasound based method proposed by the authors, optical fiber sensor based method needs to be given more research effort. The method of measurement has great advantage of being relatively more insensitive to a number of external disturbances such as acoustic noise, temperature variation etc. and the required measuring equipment can be easily designed at low cost with large sensitivity to adulteration leading to more accurate measurements.

## 6. References

- Benedetto G et.al.,(2003) " Speed of sound in pure water at temperature between 274 and 394K and pressure up to 90 Mpa", 15<sup>th</sup> Symposium on Thermophysical Properties at Boulder, pp. 1-13, June 22-27, Colorado, U.S.A..
- Cai C et.al, (1993) "Accurate digital Time-of-Flight measurement using self-interference", IEEE Transactions on Instrum. and Meas., Vol. 42, No. 6, pp. 990-994.

- CSE India report 'Independent Inspection of Fuel Quality at Fuel Dispensing Stations, Oil tanks and Tank Lorries, prepared by center for Science and Environment, March 2002, available at <http://www.cseindia.org/html/cmp/air/fnladul.pdf>.
- Grimaldi D, (2006) "Time-of-Flight measurement of ultrasonic pulse echo using wavelet networks", IEEE Transactions on Instrum. and Meas., Vol. 55, No. 1, pp. 5-13.
- Nakahira K et.al., (2001) "Distance measurement by an ultrasonic system based on digital polarity correlator", IEEE Transactions on Instrum. and Meas. Vo. 50, No. 6, pp. 1748-1752.
- Parrilla M,et.al. (1991) "Digital signal processing techniques for high accuracy ultrasonic range measurements", IEEE Transactions on Instrum. and Meas.. Vol. 40, No. 4.
- Roy S., (1999)' Fiber optic sensor for determining adulteration of petrol and diesel by kerosene' Sensors and Actuators, B 55, p. 212-216.
- Sh. R. Yadav, et.al. (2005)' Estimation of petrol and diesel adulteration with kerosene and assessment of usefulness of selected automobile fuel quality test parameters', International Journal of Environmental Science & Technology, Vol. 1, No. 4, pp. 253-255.
- Sharma R K, Gupta Anil Kumar, (2007) 'Detection/ Estimation of Adulteration in Gasoline and Diesel using Ultrasonics', IEEE Xplore, p. 509-11.
- Thomas K. V et.al., (2004)' " Measurement of the material properties of Viscous Liquids Using Ultrasonic Guided Waves', IEEE Trans, Ultrason., Ferroelect., Freq. Contr.,Vol. 51, no. 6, pp. 737-747.
- Urena J et.al., (1999) " Correlation detector based on a FPGA for ultrasonic sensors", Elsevier- Microprocessors and Microsystems 23, pp 25-33.
- Vandana Mishra et.al., (2008) 'Fuel Adulteration Detection using Long Period Fiber Grating Sensor Technology' Indian Journal of Pure and Applied Physics, vol. 46, p. 106-110.
- Veloso Fransico, Kumar Rajeev, (2002) 'The Automotive Supply Chain: Global trends and Asian Perspectives', ERD working paper series no. 3, Economics and Research Department, Asian Development Bank.
- Webster D, (1994) "A pulsed ultrasonic distance measurement system based upon phase digitizing", IEEE Transactions on Instrum. and Meas. Vol. 43, No. 4, pp. 578-582.
- Wieldman L.S.M. et.al., (2005) 'Adulteration Detection of Brazilian Gasoline Samples by Statistical Analysis', Elsevier Fuel-84, p. 467-473.
- William M. H, (1998) "Signals, Sound, and Sensation", Springer-Verlag New York.
- World Bank report (July 2002) July 2002 'South Asia Urban Air Quality Management Briefing Note no. 7', available at <http://www.worldbank.org/saurbanair>.
- World bank report (September 2001) "Abuses in Fuel markets", viewpoint note no. 237, available at <http://www.worldbank.org/html/fpd/notes/237/237kojim-831.pdf>.
- World bank report (Dec. 2001) 'Transport Fuel Taxes and Urban Air Quality', Pollution Management in Focus Discussion Note No. 11, available at [http://www.worldbank.org/essd/essd.nsy/GlobalView/In%20Focus%20ll.pdf/\\$File/In%20Focus%20ll.pdf](http://www.worldbank.org/essd/essd.nsy/GlobalView/In%20Focus%20ll.pdf/$File/In%20Focus%20ll.pdf).